



Hashemite Kingdom of Jordan



Jordan Journal of



Biological Sciences

An International Peer-Reviewed Scientific Journal

Financed by the Scientific Research and Innovation Support Fund



<http://jjbs.hu.edu.jo/>

المجلة الأردنية للعلوم الحياتية
Jordan Journal of Biological Sciences (JJBS)

<http://jjbs.hu.edu.jo>

Jordan Journal of Biological Sciences (JJBS) (ISSN: 1995–6673 (Print); 2307-7166 (Online)): An International Peer- Reviewed Open Access Research Journal financed by the Scientific Research and Innovation Support Fund, Ministry of Higher Education and Scientific Research, Jordan and published quarterly by the Deanship of Scientific Research , The Hashemite University, Jordan.

Editor-in-Chief

Professor Atoum, Manar F.
Molecular Biology and Genetics,
The Hashemite University

Editorial Board (Arranged alphabetically)

Professor Amr, Zuhair S.
Animal Ecology and Biodiversity
Jordan University of Science and Technology

Professor Hunaiti, Abdulrahim A.
Biochemistry
The University of Jordan

Professor Khleifat, Khaled M.
Microbiology and Biotechnology
Mutah University

Professor Lahham, Jamil N.
Plant Taxonomy
Yarmouk University

Professor Malkawi, Hanan I.
Microbiology and Molecular Biology
Yarmouk University

Associate Editorial Board

Professor Al-Hindi, Adnan I.
Parasitology
The Islamic University of Gaza, Faculty of Health
Sciences, Palestine

Dr Gammoh, Noor
Tumor Virology
Cancer Research UK Edinburgh Centre, University of
Edinburgh, U.K.

Professor Kasperek, Max
Natural Sciences
Editor-in-Chief, Journal Zoology in the Middle East,
Germany

Professor Krystufek, Boris
Conservation Biology
Slovenian Museum of Natural History,
Slovenia

Dr Rabei, Sami H.
Plant Ecology and Taxonomy
Botany and Microbiology Department,
Faculty of Science, Damietta University, Egypt

Professor Simerly, Calvin R.
Reproductive Biology
Department of Obstetrics/Gynecology and
Reproductive Sciences, University of
Pittsburgh, USA

Editorial Board Support Team

Language Editor
Dr. Shadi Neimneh

Publishing Layout
Eng.Mohannad Oqdeh

Submission Address

Professor Atoum, Manar F
The Hashemite University
P.O. Box 330127, Zarqa, 13115, Jordan
Phone: +962-5-3903333 ext.4147
E-Mail: jjbs@hu.edu.jo

International Advisory Board (Arranged alphabetically)

Professor Ahmad M. Khalil

Department of Biological Sciences, Faculty of Science,
Yarmouk University, Jordan

Professor Anilava Kaviraj

Department of Zoology, University of Kalyani, India

Professor Bipul Kumar Das

Faculty of Fishery Sciences W. B. University of Animal &
Fishery Sciences, India

Professor Elias Baydoun

Department of Biology, American University of Beirut
Lebanon

Professor Hala Gali-Muhtasib

Department of Biology, American University of Beirut
Lebanon

Professor Ibrahim M. AlRawashdeh

Department of Biological Sciences, Faculty of Science, Al-
Hussein Bin Talal University, Jordan

Professor João Ramalho-Santos

Department of Life Sciences, University of Coimbra, Portugal

Professor Khaled M. Al-Qaoud

Department of Biological sciences, Faculty of Science,
Yarmouk University, Jordan

Professor Mahmoud A. Ghannoum

Center for Medical Mycology and Mycology Reference
Laboratory, Department of Dermatology, Case Western
Reserve University and University Hospitals Case Medical
Center, USA

Professor Mawieh Hamad

Department of Medical Lab Sciences, College of Health
Sciences , University of Sharjah, UAE

Professor Michael D Garrick

Department of Biochemistry, State University of New York at
Buffalo, USA

Professor Nabil. A. Bashir

Department of Physiology and Biochemistry, Faculty of
Medicine, Jordan University of Science and Technology,
Jordan

Professor Nizar M. Abuharfeil

Department of Biotechnology and Genetic Engineering, Jordan
University of Science and Technology, Jordan

Professor Samih M. Tamimi

Department of Biological Sciences, Faculty of Science, The
University of Jordan, Jordan

Professor Ulrich Joger

State Museum of Natural History Braunschweig, Germany

Professor Aida I. El Makawy

Division of Genetic Engineering and Biotechnology, National
Research Center. Giza, Egypt

Professor Bechan Sharma

Department of Biochemistry, Faculty of Science University of
Allahabad, India

Professor Boguslaw Buszewski

Chair of Environmental Chemistry and Bioanalytics, Faculty of
Chemistry, Nicolaus Copernicus University Poland

Professor Gerald Schatten

Pittsburgh Development Center, Division of Developmental
and Regenerative Medicine, University of Pittsburgh, School
of Medicine, USA

Professor Hala Khyami-Horani

Department of Biological Sciences, Faculty of Science, The
University of Jordan, Jordan

Professor James R. Bamburg

Department of Biochemistry and Molecular Biology, Colorado
State University, USA

Professor Jumah M. Shakhaneh

Department of Biological Sciences, Faculty of Science, Mutah
University, Jordan

Dr. Lukmanul Hakkim Faruck

Department of Mathematics and Sciences College of Arts and
Applied Sciences, Dhofar, Oman

Professor Md. Yeamin Hossain

Department of Fisheries, Faculty of Fisheries , University of
Rajshahi, Bangladesh

Professor Mazin B. Qumsiyeh

Palestine Museum of Natural History and Palestine Institute for
Biodiversity and Sustainability, Bethlehem University,
Palestine

Professor Mohamad S. Hamada

Genetics Department, Faculty of Agriculture, Damietta
University, Egypt

Professor Nawroz Abdul-razzak Tahir

Plant Molecular Biology and Phytochemistry, University of
Sulaimani, College of Agricultural Sciences, Iraq

Professor Ratib M. AL- Ouran

Department of Biological Sciences, Faculty of Science, Mutah
University, Jordan

Professor Shtaywy S. Abdalla Abbadi

Department of Biological Sciences, Faculty of Science, The
University of Jordan, Jordan

Professor Zihad Bouslama

Department of Biology, Faculty of Science Badji Mokhtar
University, Algeria

Instructions to Authors

Scopes

Study areas include cell biology, genomics, microbiology, immunology, molecular biology, biochemistry, embryology, immunogenetics, cell and tissue culture, molecular ecology, genetic engineering and biological engineering, bioremediation and biodegradation, bioinformatics, biotechnology regulations, gene therapy, organismal biology, microbial and environmental biotechnology, marine sciences. The JJBS welcomes the submission of manuscript that meets the general criteria of significance and academic excellence. All articles published in JJBS are peer-reviewed. Papers will be published approximately one to two months after acceptance.

Type of Papers

The journal publishes high-quality original scientific papers, short communications, correspondence and case studies. Review articles are usually by invitation only. However, Review articles of current interest and high standard will be considered.

Submission of Manuscript

Manuscript, or the essence of their content, must be previously unpublished and should not be under simultaneous consideration by another journal. The authors should also declare if any similar work has been submitted to or published by another journal. They should also declare that it has not been submitted/ published elsewhere in the same form, in English or in any other language, without the written consent of the Publisher. The authors should also declare that the paper is the original work of the author(s) and not copied (in whole or in part) from any other work. All papers will be automatically checked for duplicate publication and plagiarism. If detected, appropriate action will be taken in accordance with International Ethical Guideline. By virtue of the submitted manuscript, the corresponding author acknowledges that all the co-authors have seen and approved the final version of the manuscript. The corresponding author should provide all co-authors with information regarding the manuscript, and obtain their approval before submitting any revisions. Electronic submission of manuscripts is strongly recommended, provided that the text, tables and figures are included in a single Microsoft Word file. Submit manuscript as e-mail attachment to the Editorial Office at: JJBS@hu.edu.jo. After submission, a manuscript number will be communicated to the corresponding author within 48 hours.

Peer-review Process

It is requested to submit, with the manuscript, the names, addresses and e-mail addresses of at least 4 potential reviewers. It is the sole right of the editor to decide whether or not the suggested reviewers to be used. The reviewers' comments will be sent to authors within 6-8 weeks after submission. Manuscripts and figures for review will not be returned to authors whether the editorial decision is to accept, revise, or reject. All Case Reports and Short Communication must include at least one table and/ or one figure.

Preparation of Manuscript

The manuscript should be written in English with simple lay out. The text should be prepared in single column format. Bold face, italics, subscripts, superscripts etc. can be used. Pages should be numbered consecutively, beginning with the title page and continuing through the last page of typewritten material.

The text can be divided into numbered sections with brief headings. Starting from introduction with section 1. Subsections should be numbered (for example 2.1 (then 2.1.1, 2.1.2, 2.2, etc.), up to three levels. Manuscripts in general should be organized in the following manner:

Title Page

The title page should contain a brief title, correct first name, middle initial and family name of each author and name and address of the department(s) and institution(s) from where the research was carried out for each author. The title should be without any abbreviations and it should enlighten the contents of the paper. All affiliations should be provided with a lower-case superscript number just after the author's name and in front of the appropriate address.

The name of the corresponding author should be indicated along with telephone and fax numbers (with country and area code) along with full postal address and e-mail address.

Abstract

The abstract should be concise and informative. It should not exceed **350 words** in length for full manuscript and Review article and **150 words** in case of Case Report and/ or Short Communication. It should briefly describe the purpose of the work, techniques and methods used, major findings with important data and conclusions. No references should be cited in this part. Generally non-standard abbreviations should not be used, if necessary they should be clearly defined in the abstract, at first use.

Keywords

Immediately after the abstract, **about 4-8 keywords** should be given. Use of abbreviations should be avoided, only standard abbreviations, well known in the established area may be used, if appropriate. These keywords will be used for indexing.

Abbreviations

Non-standard abbreviations should be listed and full form of each abbreviation should be given in parentheses at first use in the text.

Introduction

Provide a factual background, clearly defined problem, proposed solution, a brief literature survey and the scope and justification of the work done.

Materials and Methods

Give adequate information to allow the experiment to be reproduced. Already published methods should be mentioned with references. Significant modifications of published methods and new methods should be described in detail. Capitalize trade names and include the manufacturer's name and address. Subheading should be used.

Results

Results should be clearly described in a concise manner. Results for different parameters should be described under subheadings or in separate paragraph. Results should be explained, but largely without referring to the literature. Table or figure numbers should be mentioned in parentheses for better understanding.

Discussion

The discussion should not repeat the results, but provide detailed interpretation of data. This should interpret the significance of the findings of the work. Citations should be given in support of the findings. The results and discussion part can also be described as separate, if appropriate. The Results and Discussion sections can include subheadings, and when appropriate, both sections can be combined

Conclusions

This should briefly state the major findings of the study.

Acknowledgment

A brief acknowledgment section may be given after the conclusion section just before the references. The acknowledgment of people who provided assistance in manuscript preparation, funding for research, etc. should be listed in this section.

Tables and Figures

Tables and figures should be presented as per their appearance in the text. It is suggested that the discussion about the tables and figures should appear in the text before the appearance of the respective tables and figures. No tables or figures should be given without discussion or reference inside the text.

Tables should be explanatory enough to be understandable without any text reference. Double spacing should be maintained throughout the table, including table headings and footnotes. Table headings should be placed above the table. Footnotes should be placed below the table with superscript lowercase letters. Each table should be on a separate page, numbered consecutively in Arabic numerals.

Each figure should have a caption. The caption should be concise and typed separately, not on the figure area. Figures should be self-explanatory. Information presented in the figure should not be repeated in the table. All symbols and abbreviations used in the illustrations should be defined clearly. Figure legends should be given below the figures.

References

References should be listed alphabetically at the end of the manuscript. Every reference referred in the text must be also present in the reference list and vice versa. In the text, a reference identified by means of an author's name should be followed by the year of publication in parentheses (e.g.(Brown,2009)). For two authors, both authors' names followed by the year of publication (e.g.(Nelson and Brown, 2007)). When there are more than two authors, only the first author's name followed by "*et al.*" and the year of publication (e.g. (Abu-Elteen *et al.*, 2010)). When two or more works of an author has been published during the same year, the reference should be identified by the letters "a", "b", "c", etc., placed after the year of publication. This should be followed both in the text and reference list. e.g., Hilly, (2002a, 2002b); Hilly, and Nelson, (2004). Articles in preparation or submitted for publication, unpublished observations, personal communications, etc. should not be included in the reference list but should only be mentioned in the article text (e.g., Shtyawy,A., University of Jordan, personal communication). Journal titles should be abbreviated according to the system adopted in Biological Abstract and Index Medicus, if not included in Biological Abstract or Index Medicus journal title should be given in full. The author is responsible for the scuracy and completeness of the references and for their correct textual citation. Failure to do so may result in the paper being withdraw from the evaluation process. Example of correct reference form is given as follows:-

Reference to a journal publication:

Bloch BK. 2002. Econazole nitrate in the treatment of *Candida vaginitis*. *S Afr Med J.* , **58**:314-323.

Ogunseitan OA and Ndoye IL. 2006. Protein method for investigating mercuric reductase gene expression in aquatic environments. *Appl Environ Microbiol.*, **64**: 695-702.

Hilly MO, Adams MN and Nelson SC. 2009. Potential fly-ash utilization in agriculture. *Progress in Natural Sci.*, **19**: 1173-1186.

Reference to a book:

Brown WY and White SR.1985. **The Elements of Style**, third ed. MacMillan, New York.

Reference to a chapter in an edited book:

Mettam GR and Adams LB. 2010. How to prepare an electronic version of your article. In: Jones BS and Smith RZ (Eds.), **Introduction to the Electronic Age**. Kluwer Academic Publishers, Netherlands, pp. 281–304.

Conferences and Meetings:

Embabi NS. 1990. Environmental aspects of distribution of mangrove in the United Arab Emirates. Proceedings of the First ASWAS Conference. University of the United Arab Emirates. Al-Ain, United Arab Emirates.

Theses and Dissertations:

El-Labadi SN. 2002. Intestinal digenetic trematodes of some marine fishes from the Gulf of Aqaba. MSc dissertation, The Hashemite University, Zarqa, Jordan.

Nomenclature and Units

Internationally accepted rules and the international system of units (SI) should be used. If other units are mentioned, please give their equivalent in SI.

For biological nomenclature, the conventions of the *International Code of Botanical Nomenclature*, the *International Code of Nomenclature of Bacteria*, and the *International Code of Zoological Nomenclature* should be followed.

Scientific names of all biological creatures (crops, plants, insects, birds, mammals, etc.) should be mentioned in parentheses at first use of their English term.

Chemical nomenclature, as laid down in the *International Union of Pure and Applied Chemistry* and the official recommendations of the *IUPAC-IUB Combined Commission on Biochemical Nomenclature* should be followed. All biocides and other organic compounds must be identified by their Geneva names when first used in the text. Active ingredients of all formulations should be likewise identified.

Math formulae

All equations referred to in the text should be numbered serially at the right-hand side in parentheses. Meaning of all symbols should be given immediately after the equation at first use. Instead of root signs fractional powers should be used. Subscripts and superscripts should be presented clearly. Variables should be presented in italics. Greek letters and non-Roman symbols should be described in the margin at their first use.

To avoid any misunderstanding zero (0) and the letter O, and one (1) and the letter l should be clearly differentiated. For simple fractions use of the solidus (/) instead of a horizontal line is recommended. Levels of statistical significance such as: * $P < 0.05$, ** $P < 0.01$ and *** $P < 0.001$ do not require any further explanation.

Copyright

Submission of a manuscript clearly indicates that: the study has not been published before or is not under consideration for publication elsewhere (except as an abstract or as part of a published lecture or academic thesis); its publication is permitted by all authors and after accepted for publication it will not be submitted for publication anywhere else, in English or in any other language, without the written approval of the copyright-holder. The journal may consider manuscripts that are translations of articles originally published in another language. In this case, the consent of the journal in which the article was originally published must be obtained and the fact that the article has already been published must be made clear on submission and stated in the abstract. It is compulsory for the authors to ensure that no material submitted as part of a manuscript infringes existing copyrights, or the rights of a third party.

Ethical Consent

All manuscripts reporting the results of experimental investigation involving human subjects should include a statement confirming that each subject or subject's guardian obtains an informed consent, after the approval of the experimental protocol by a local human ethics committee or IRB. When reporting experiments on animals, authors should indicate whether the institutional and national guide for the care and use of laboratory animals was followed.

Plagiarism

The JJBS hold no responsibility for plagiarism. If a published paper is found later to be extensively plagiarized and is found to be a duplicate or redundant publication, a note of retraction will be published, and copies of the correspondence will be sent to the authors' head of institute.

Galley Proofs

The Editorial Office will send proofs of the manuscript to the corresponding author as an e-mail attachment for final proof reading and it will be the responsibility of the corresponding author to return the galley proof materials appropriately corrected within the stipulated time. Authors will be asked to check any typographical or minor clerical errors in the manuscript at this stage. No other major alteration in the manuscript is allowed. After publication authors can freely access the full text of the article as well as can download and print the PDF file.

Publication Charges

There are no page charges for publication in Jordan Journal of Biological Sciences, except for color illustrations,

Reprints

Ten (10) reprints are provided to corresponding author free of charge within two weeks after the printed journal date. For orders of more reprints, a reprint order form and prices will be sent with article proofs, which should be returned directly to the Editor for processing.

Disclaimer

Articles, communication, or editorials published by JJBS represent the sole opinions of the authors. The publisher shoulders no responsibility or liability what so ever for the use or misuse of the information published by JJBS.

Indexing

JJBS is indexed and abstracted by:

DOAJ (Directory of Open Access Journals)

Google Scholar

Journal Seek

HINARI

Index Copernicus

NDL Japanese Periodicals Index

SCIRUS

OAJSE

ISC (Islamic World Science Citation Center)

Directory of Research Journal Indexing
(DRJI)

Ulrich's

CABI

EBSCO

CAS (Chemical Abstract Service)

ETH- Citations

Open J-Gat

SCImago

Clarivate Analytics (Zoological Abstract)

Scopus

AGORA (United Nation's FAO database)

SHERPA/RoMEO (UK)

المجلة الأردنية للعلوم الحياتية
Jordan Journal of Biological Sciences (JJBS)
ISSN 1995- 6673 (Print), 2307- 7166 (Online)

<http://jjbs.hu.edu.jo>

The Hashemite University
Deanship of Scientific Research
TRANSFER OF COPYRIGHT AGREEMENT

Journal publishers and authors share a common interest in the protection of copyright: authors principally because they want their creative works to be protected from plagiarism and other unlawful uses, publishers because they need to protect their work and investment in the production, marketing and distribution of the published version of the article. In order to do so effectively, publishers request a formal written transfer of copyright from the author(s) for each article published. Publishers and authors are also concerned that the integrity of the official record of publication of an article (once refereed and published) be maintained, and in order to protect that reference value and validation process, we ask that authors recognize that distribution (including through the Internet/WWW or other on-line means) of the authoritative version of the article as published is best administered by the Publisher.

To avoid any delay in the publication of your article, please read the terms of this agreement, sign in the space provided and return the complete form to us at the address below as quickly as possible.

Article entitled:-----

Corresponding author: -----

To be published in the journal: Jordan Journal of Biological Sciences (JJBS)

I hereby assign to the Hashemite University the copyright in the manuscript identified above and any supplemental tables, illustrations or other information submitted therewith (the "article") in all forms and media (whether now known or hereafter developed), throughout the world, in all languages, for the full term of copyright and all extensions and renewals thereof, effective when and if the article is accepted for publication. This transfer includes the right to adapt the presentation of the article for use in conjunction with computer systems and programs, including reproduction or publication in machine-readable form and incorporation in electronic retrieval systems.

Authors retain or are hereby granted (without the need to obtain further permission) rights to use the article for traditional scholarship communications, for teaching, and for distribution within their institution.

- I am the sole author of the manuscript
- I am signing on behalf of all co-authors of the manuscript
- The article is a 'work made for hire' and I am signing as an authorized representative of the employing company/institution

Please mark one or more of the above boxes (as appropriate) and then sign and date the document in black ink.

Signed: _____ Name printed: _____

Title and Company (if employer representative) : _____

Date: _____

Data Protection: By submitting this form you are consenting that the personal information provided herein may be used by the Hashemite University and its affiliated institutions worldwide to contact you concerning the publishing of your article.

Please return the completed and signed original of this form by mail or fax, or a scanned copy of the signed original by e-mail, retaining a copy for your files, to:

Hashemite University
Jordan Journal of Biological Sciences
Zarqa 13115 Jordan
Fax: +962 5 3903338
Email: jjbs@hu.edu.jo

EDITORIAL PREFACE

Jordan Journal of Biological Sciences (JJBS) is a refereed, quarterly international journal financed by the Scientific Research and Innovation Support Fund, Ministry of Higher Education and Scientific Research in cooperation with the Hashemite University, Jordan. JJBS celebrated its 12th commencement this past January, 2020. JJBS was founded in 2008 to create a peer-reviewed journal that publishes high-quality research articles, reviews and short communications on novel and innovative aspects of a wide variety of biological sciences such as cell biology, developmental biology, structural biology, microbiology, entomology, molecular biology, biochemistry, medical biotechnology, biodiversity, ecology, marine biology, plant and animal biology, plant and animal physiology, genomics and bioinformatics.

We have watched the growth and success of JJBS over the years. JJBS has published 11 volumes, 45 issues and 479 articles. JJBS has been indexed by SCOPUS, CABI's Full-Text Repository, EBSCO, Clarivate Analytics- Zoological Record and recently has been included in the UGC India approved journals. JJBS Cite Score has improved from 0.18 in 2015 to 0.58 in 2019 (Last updated on 16 March, 2020) and with Scimago Institution Ranking (SJR) 0.21 (Q3) in 2018.

A group of highly valuable scholars have agreed to serve on the editorial board and this places JJBS in a position of most authoritative on biological sciences. I am honored to have six eminent associate editors from various countries. I am also delighted with our group of international advisory board members coming from 15 countries worldwide for their continuous support of JJBS. With our editorial board's cumulative experience in various fields of biological sciences, this journal brings a substantial representation of biological sciences in different disciplines. Without the service and dedication of our editorial; associate editorial and international advisory board members, JJBS would have never existed.

In the coming year, we hope that JJBS will be indexed in Clarivate Analytics and MEDLINE (the U.S. National Library of Medicine database) and others. As you read throughout this volume of JJBS, I would like to remind you that the success of our journal depends on the number of quality articles submitted for review. Accordingly, I would like to request your participation and colleagues by submitting quality manuscripts for review. One of the great benefits we can provide to our prospective authors, regardless of acceptance of their manuscripts or not, is the feedback of our review process. JJBS provides authors with high quality, helpful reviews to improve their manuscripts.

Finally, JJBS would not have succeeded without the collaboration of authors and referees. Their work is greatly appreciated. Furthermore, my thanks are also extended to The Hashemite University and the Scientific Research and Innovation Support Fund, Ministry of Higher Education and Scientific Research for their continuous financial and administrative support to JJBS.

March, 2020

CONTENTS

Original Articles

- 413 - 418 Evaluation of Pre-treatment Methods and Anaerobic Co-digestions of Recalcitrant Melanised Chicken Feather Wastes with other Wastes for Improved Methane and Electrical Energy Production
Ibrahim Yusuf, Kubra I. Arzai, and Abdulwahid S. Dayyab
- 419 - 429 Characterization of Egyptian durum Wheat Genotypes using Biochemical and Molecular Markers
Samira A. Osman and Walaa A. Ramadan
- 431 - 435 Heat Exposure Affects the mRNA Levels of Antioxidant Enzymes in Embryonic and Adult Broiler Chickens
Amneh H. Tarkhan, Khaled M. M. Saleh and Mohammad B. Al-Zghoul
- 437 - 439 Diet Composition and Prey Selection in the Long-eared Owl, *Asio otus* in Jordan: the Importance of Urban Avifauna
Mohammad A. Abu Baker, Ratib M. Al-Ouran and Zuhair S. Amr
- 441 - 451 Genetic Characterization of Algerian Minor Date Palms (*Phoenix dactylifera* L.) Cultivated in the Oases of Biskra using Nuclear Microsatellite Markers
Ahmed Simozrag and Ziane Laiadi
- 453 - 461 Selenium-Supplemented Diet Influences Histological Features of Liver and Kidney in Tilapia (*Oreochromis niloticus*)
Sonia Iqbal, Usman Atique, Muhammad Sharif Mughal, Muhammad Younus, Muhammad Kamran Rafique, Muhammad Sultan Haider, Hafiza Sundas Iqbal, Shahid Sherzada and Tanveer Ali Khan
- 463 - 468 Inclusion of *Myrmecodia pendens* bulb Extract in the Diet Stimulates Immune Response in *Clarias gariepinus* against *Aeromonas hydrophila*
Rudy A. Nugroho, Yanti P. Sari and Esti H. Hardi
- 469 - 474 *In vitro* Antibacterial Activity of Cell Free Fermentation Supernatant of *Passiflora edulis* forma *flavicarpa* Sims. Fruit Fermented by de Man, Rogosa and Sharp Media
Safarini Marwah, Iif H. Rosyidah, Ni M. Mertaniasih, Muhammad N.S.B. Hamzah, Kholis A. Novianti, Riesta Primaharinastiti, Dian Rahmawaty and Isnaeni Isnaeni
- 475 - 482 Prevalence of Capsular Polysaccharide Genes and Antibiotic Resistance Pattern of *Klebsiella pneumoniae* in Palestine
Ghaleb M. Adwan, Dina M. Owda and Awni A. Abu-Hijleh
- 483 - 492 Prediction of Protein Secondary Structure from Amino Acid Sequences by Integrating Fuzzy, Random Forest and Feature Vector Methodologies
Sivagnanam R. Mani Sekhar, Siddesh G. Matt and Sunilkumar S Manvi
- 493 - 498 Biogenic Silver Nanoparticle Synthesis, Characterization and its Antibacterial activity against Leather Deteriorates
Savita Kate, Madhuri Sahasrabudhe and Archana Pethe
- 499 - 508 Pollen Morphological Variations among some Cultivated *Citrus* species and its Related Genera in Egypt
Wafaa K. Taia, Manaser M. Ibrahim and Mahmoud Abdel-Sattar
- 509 - 518 Direct Somatic Embryogenesis and Regeneration of an Indonesian orchid *Phalaenopsis amabilis* (L.) Blume under a Variety of Plant Growth Regulators, Light Regime, and Organic Substances
Windi Mose, Budi Setiadi Daryono, Ari Indrianto, Aziz Purwantoro and Endang Semiarti
- 519 - 523 Estradiol Affects Ultimobranchial Gland of a Freshwater Catfish, *Heteropneustes fossilis* kept in Different Calcium Environments
Susmita Srivastav, Diwakar Mishra, Sunil K. Srivastav, Nobuo Suzuki and Ajai K. Srivastav
- 525 - 533 Antioxidants Released from *Cichorium pumilum* Jacq. Amendment Mitigate Salinity Stress in Maize
Nadia M El-Shafey and Hamada R AbdElgawad

- 535 – 541 Molecular Identification and Characterization of Parrotfish species from the Farasan Islands, Red Sea-Saudi Arabia
Mohamed M. Hassan , Ayman Sabry and Mohamed Ismail
- 543 – 550 Fungal Endophytes from *Tabernaemontana heyneana* Wall. (Apocynaceae), their Molecular Characterization, L-asparaginase and Antioxidant Activities
Naguvanahally S. Bhavana, Harischandra S. Prakash and Monnanda S. Nalini
- 551 – 557 Responses of *Lantana Camara* Linn. Callus Cultures to Heavy Metals Added to the Culture Media
Reham W. Tahtamouni , Rida A. A .Shibli, Laila S.Younes , Saida Abu-Mallouh and Tamara S. Al-Qudah
- 559 – 565 Synthesis and Characterization of Zinc Nanoparticles by Natural Organic Compounds Extracted from Licorice Root and their Influence on Germination of *Sorghum bicolor* Seeds
Mahmoud A. S. Al-Shaheen, Mustafa N. Owaid and Rasim F. Muslim
- 567 - 574 Assessment of Antimicrobial and Anticancer Activity of Radish Sprouts Extracts
Mahmoud Khalid, Reem Ayayda, Nameer Gheith, Zaidoun Salah, Saleh Abu-Lafi, Amal Jaber, Fuad Al-Rimawi and Ghassab Al-Mazaideh

Evaluation of Pre-treatment Methods and Anaerobic Co-digestions of Recalcitrant Melanised Chicken Feather Wastes with other Wastes for Improved Methane and Electrical Energy Production

Ibrahim Yusuf*, Kubra I. Arzai, and Abdulwahid S. Dayyab

Department of Microbiology, Faculty of Life Sciences, College of Natural and Pharmaceutical Sciences, PMB 3011 BUK Kano, Bayero University Kano state, Nigeria.

Received: October 5, 2019; Revised: November 23, 2019; Accepted: December 8, 2019

Abstract

Poor utilisation of abundant and highly recalcitrant melanised chicken feather (MCF) as a substrate for biological process has led to its accumulation in the environment. This study investigated the possibility of using MCF and its hydrolysates as a substrate for methane and electrical energy (EE) generation. A two-phase system which involves pre-treating MCF and subsequent co-digesting of the pre-treated MCF or its hydrolysates with other wastes was employed for each process. For methane production, MCF hydrolysates obtained from biodegradation of untreated or pre-treated MCF and inocula of cow dung, poultry slaughterhouse and abattoir wastes were used in anaerobic digester (AD). EE was generated through degradation of MCF with and without rice waste water by *Pseudochrobactrum* sp. IY-BUK1 in a microbial fuel cell (MFC). Results showed that pre-treated MCF were degraded about 3 fold faster than untreated, and produced 4 times the amount of keratinase and soluble proteins. MCF pre-treated with $\text{Ca}(\text{OH})_2$ and co-digested with cow dung resulted in significant improvement in biogas production over those pre-treated with NaOH, steam and bacteria and co-digested with poultry slaughterhouse and abattoir wastes. *Pseudochrobactrum* sp. strain IY-BUK1 degraded about 70% of 5% (w/v) pre-treated MCF in MFC with resultant 67.3 U/ml keratinase. Similar to methane yield, $\text{Ca}(\text{OH})_2$ pre-treated MCF were degraded faster in MFC inoculated with IY-BUK1 and produced a maximum voltage, power, and current density corresponding to 350.6mV, $37.77 \times 10^4 \text{mW/m}^2$ and 0.112mA/m^2 respectively in 8 days when compared with un-treated feathers, that produced maximum of 174mV after 13 days. The use of rice water waste in the MFC as supplement produced 167mV more voltage than when only IY-BUK1 was used. The study revealed that recalcitrant MCF pre-treated with $\text{Ca}(\text{OH})_2$ and co digested with cow dung and rice water waste can be successfully employed as a cheap substrate for biogas and electricity production.

Keywords: melanised, feathers, pre-treatment, methane, microbial fuel cells, keratinase, *Pseudochrobactrum* sp. IY-BUK1

1. Introduction

As meat consumption increases globally, generation of wastes from slaughterhouses and abattoirs continues to grow and millions of tons are generated yearly (Peng *et al.*, 2019). In third world countries, especially in Africa, the feather wastes are poorly managed and underutilized and, therefore, serve as source of nuisance to humans, animals, and the environment. They are often burned or deposited to landfill, which are non-ecofriendly means of management (Pandian *et al.*, 2012; Yusuf *et al.*, 2016). The recalcitrant nature of melanised feathers over non-melanised has been the reason for their degradation by soil microbes that utilize feather as substrates to produce enzymes and protein rich hydrolysates (Grande *et al.*, 2004; Gunderson and Frame, 2008; Gurav *et al.*, 2016). Meanwhile, recycling of feather can provide a cheap and alternative source of protein feed stuff, energy, fertilizers, low cost substrates for production of other value added microbial products and can function as a means of clearing the environment of unwanted wastes (Khardenavis *et al.*, 2009; Lasekan *et al.*, 2013; Paul *et al.*, 2013; Yusuf *et al.*, 2015). Cheap and innovative methods within the capacity of our under-equipped research facilities are therefore

needed to reach the objectives of alternative poultry feather utilization.

Furthermore, the persistent release of pollutants to environment by fossil fuels and the frightening rate at which it is getting exhausted has been scientists' great concern over years (Rahimnejad *et al.*, 2012; Parkash, 2016). Searching for cheap and clean alternative sources of energy is currently the biggest challenge for governments and scientists wanting to meet up with the ever increasing demand for cleaner energy (Nair *et al.*, 2013). The use of chicken feather waste (especially the white feather) to produce methane gas has been widely studied by many scientists through anaerobic digestion (AD) (Forgacs *et al.*, 2011; Forgacs *et al.*, 2014; Mézes and Tamás, 2015). In order to improve methane yield from feather protein close to the theoretical methane yield of 0.496 Nm³/kg VS (volatile solids) (Davidsson, 2007), scientists have adopted different pre-treatment methods such as chemical, enzymatic, physical and biological ones to improve feather digestibility and biogas yield. Forgacs *et al.* for instance, reported improved methane yield from 0.18 Nm³/kg VS to 0.40 Nm³/kg VS) from feather pre-treated with recombinant *Bacillus megaterium* strain. Similarly, enzymatic and alkaline pre-treatments of feathers increased the methane by 21% and 32% according to

* Corresponding author e-mail: iyusuf.bio@buk.edu.ng.

Salminen *et al.* (Salminen *et al.*, 2003) through anaerobic digestion. However, pre-treatment of melanised chicken feathers (MCF), which is believed to be more recalcitrant to microbial or enzymatic degradation, as well as co-digesting it with other wastes for improved biogas production has not been documented yet.

Microbial fuel cell (MFC) approaches employ use of microorganisms, specific substrates and conditions for electricity generation (Zhou *et al.*, 2013; Parkash, 2016). In each waste, the organic compound is harnessed and utilised by single or groups of microorganism to produce useful products (Reiche and Kirkwood, 2012; Chaturvedi and Verma, 2014). The high content of different organic compounds including varying amount of carbon and nitrogen compounds in chicken feathers has made them a suitable substrate for electricity generation. Studies have attempted various types of organic compounds and wastes (both industrial and agricultural) as substrate in MFC (Zhou *et al.*, 2013; Parkash, 2016), but only few have reported the use of feathers to produce electrical energy through MFCs (Chaturvedi and Verma, 2014). A study by Chaturvedi and Verma (2014) employed the use of *P. aeruginosa* strain SDS3 in MFC to degrade white feather to generate maximum voltage of 141 mV in 14 days. However, no study has attempted to use MCF to generate electricity. Due to their melanin pigment content and fibrous and insoluble structural proteins joint by disulphide bond linkage, hydrogen bond and hydrophobic interaction, direct usage in MFC and AD may take longer period. Since feather hydrolysates is the efficient substrate to use for biogas production in AD, pre-treating the MCF with either heat, chemical and/or biological agents may improve feather hydrolysate productions by suitable feather degrading bacteria. Similarly, pre-treating MCFs may also improve the potentiality of the feathers of being an easy-to-use substrate for microbes involved in electrical energy production. *Pseudochrobactrum* sp. IY-BUK1 is a novel keratinolytic bacteria that shows profound proteolytic activity against both melanised and non-melanised feathers (Yusuf *et al.*, 2019b).

The aim of this study was, therefore, to evaluate the possibility of using raw MCFs and hydrolysates produced from its biodegradation as a substrate for electrical energy and biogas generation. Furthermore, the study aimed to assess the effectiveness of different pre-treatment methods on MCFs for suitable utilisation by single (*Pseudochrobactrum* sp. IY-BUK1) or groups of bacteria as substrate for improved production of biogas and electrical energy.

2. Materials and Method

2.1. Sample Collection and Processing

Black (melanised) chicken feather (MCF) wastes were procured from chicken abattoir in Kano, Nigeria. The collected feathers were spread on clean surface and other non-feather parts were handpicked. The feathers were then washed with water and detergent extensively, followed by defatting in solution containing 200ml of deionizer water, methanol and chloroform in ratio 1:1:10 and finally rinsed in distilled water. The washed feathers were oven dried at 80°C for 6 h until constant weight was obtained (Yusuf *et al.*, 2016; Yusuf *et al.*, 2019a).

2.2. Isolation of feather degrading bacterium and preparation of culture media

The melanised feather degrading bacterium (MFDB) used in this study was isolated from chicken manure of local chickens reared in a wooden cage. Isolation was carried out in feather meal agar and broth as previously described by (Yusuf *et al.*, 2016, 2019b). The identity of the bacterium was identified as *Pseudochrobactrum* sp. IY-BUK1 (Genbank accession number: MK024282) using morphological, biochemical and molecular characteristics (Yusuf *et al.*, 2019b). The strain showed an enhanced preference for biodegradation of black feathers than white feathers with enhanced production of keratinase and protein hydrolysates.

Feather meal broth (FMB) which contained 10.0 g/L of feather, 0.5 g/L of NaCl, 0.7 g/L of K₂HPO₄, 1.4 g/L of KH₂PO₄, and 0.001 g/L of MgSO₄·6H₂O pH 7.5 was prepared as described by Yusuf *et al.* (2016, 2019a,b) and was used for propagation of the bacterium in an orbital shaker operated at 150 rpm at 30 °C.

2.3. Pre-treatment of melanised chicken feathers using physical, chemical and biological methods

MCFs were pre-treated using physical (steam and boiling), biological (bacteria) and chemical methods. Steam (thermal) pre-treatment was performed by autoclaving 5 g of whole MCFs suspended in 100 ml of distilled water at 121°C, 21psi for 30 min. MCF preheated with boiled water for 30 min was also used. Chemical pre-treatments were carried out using three chemicals, NaOH, Na₂SO₃, and Ca(OH)₂. Pre-treatment of MCFs with NaOH and Na₂SO₃ was carried out according to method of Laba and Szczekala, (2013) using 100mM concentrations. In brief, MCFs were suspended in solutions of 100mM (1 g feathers per 100ml) Na₂SO₃ and NaOH. Pre-treatment with Ca(OH)₂ employed the method of Fargacs *et al.*, 2013, where 1.0 g of MCF (TS) was suspended in 2 % Ca(OH)₂ solution for 1 hour to give a final concentration of 100 g TS_{feather}/L. The MCFs in both cases were then separated, precipitated (in case of Ca(OH)₂), and washed several times with distilled water. Biological pre-treatment was carried out according to the method of Laba and Szczekala, (2013) by exposing 5 g of MCFs to short-term culture of *Pseudochrobactrum* sp. IY-BUK1 in 250ml flask containing 100 ml FMB. After 5 days of continual shaking at 150 rpm at 30 °C, the partially digested raw MCFs were filtered using Whatman no.1 filter paper. The partially digested MCFs were then washed with distilled water and allowed to dry.

Five grams of different pre-treated MCFs were then placed in 100mL of FMB and autoclaved at 121°C, 21psi for 15 min. Untreated raw MCFs were used as control. Inoculation of the FMB containing appropriate MCFs was done with 5 ml (3.15 x 10⁶ cell/mL) of *Pseudochrobactrum* sp. IY-BUK1 except for the control experiments. Volatile solid (VS), and Total solid (TS) of the feathers were determined according to APHA standard methods (APHA, 2005).

2.4. Determination of the Protein Concentration, keratinase activity and feather degradation

An aliquot of 10ml of culture was collected from FMB every 24 h and centrifuged at 10,000 rev/min for 15 min. The cell-free supernatant fluid was used for the

measurement of soluble protein by spectrophotometer (Schimazhu, Japan) with Lowry method (Lowry and Rosebrough, 1951). 1 absorbance was considered as 1 mg/mL protein using bovine serum albumin as standard. Similarly, an aliquot of the cell-free supernatant was used to determine the level of keratinase produced using azokeratin as a substrate as described by *Joshi et al.* (Joshi et al., 2007). Feather degradation (%) was estimated by subtracting the final weight of MCFs in the flask from the final weight of the MCFs from the control. Degradation degree (%) calculation was based on method described by Yusuf et al. (2016).

2.5. Methane digester design and batch anaerobic digestion assay

Methane production using pre-treated and untreated MCFs were carried out in batch digestion experiments in duplicates using feather hydrolysates. The AD was constructed similar to the type employed by Forgács et al. (2014) but with some modifications. ADs were constructed using 150 ml plastic containers. Each of the containers was channeled tightly to a gas collection unit (reservoir) (Fig. 1).

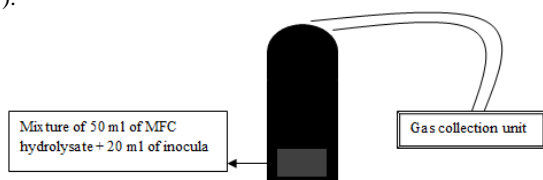


Figure 1. Anaerobic digester setup for methane production by the various pre-treatment melanised feathers

For each AD, 50 mL of hydrolysates obtained from either untreated or pre-treated MCFs were placed as a substrate. The inocula used were cow dung, poultry slaughterhouse waste, and abattoir wastes. Twenty millilitre (20 ml) of the inocula was placed in each AD. Each reactor was then capped and sealed with butyl rubber props, and anaerobic condition was ensured by flushing with a gas mixture and incubated at 50 °C for 30 days. The plastic bottles were shaken in the incubator every day. Gas samples of 0.25 ml were regularly taken from the headspace using a pressure-tight syringe. Geo tech 5000 Biogas analyser was used for the analysis of the biogas harvested. The analyser computes the percentage composition of methane (CH₄).

2.6. MFC construction and its operation

The MFC was constructed as described by Chaturvedi and co-worker (Chaturvedi and Verma, 2014) with slight modifications. A dual chambered H-type locally made MFC was designed consisting of two identical plastic containers (700ml each with an operating volume of 500ml and a head space of 200ml). The cathode and anode were connected by a salt bridge. The salt bridge was prepared by adding 3% NaCl (w/v) into 100ml of dH₂O and mixed properly. Then, 1.6% Agar (w/v) was added to the salt solution and was boiled for 3 min. It was then filled into a half inch PVC pipe sealed with an aluminium foil paper from one side. Two identical carbon rod electrodes and copper wires, with an apparent surface area of 49.2cm², were used as anode and cathode, to which a copper wire was connected and fixed with PVC gum, and the copper wires were passed through a thin hole on the plastic container cover, respectively (Fig. 2). An external circuit

of 66Ω was used in the experiment. The anolyte solution was FMB which contains 0.5% (w/v) of appropriate pre-treated MCF at pH 8.0. Additional sources of carbon (sucrose, glucose, rice wastewater) were added at 1% concentration in another MFC setup. The catholyte solution is 100mM phosphate buffer (pH 7.0).

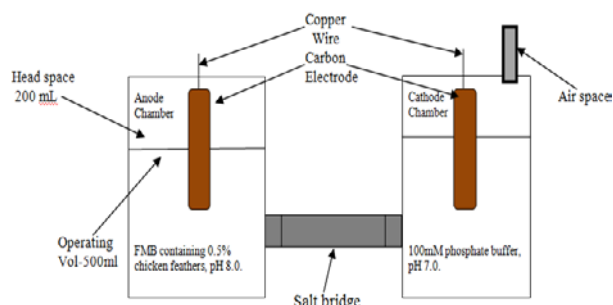


Figure 2. Schematic design of MFC connected with salt bridge

The experiment was carried out in batch mode. During the start up the anolyte was inoculated with 25ml of 18 h old culture of *Pseudochrobactrum* sp. IY-BUK1. The voltage reading was taken after 24 h time interval with digital multi meter (DT-830 model).

2.7. Statistical analysis

Results were presented in Tables and Figures. Statistical analysis was performed using SPSS statistical package (SPSS Inc., Chicago, IL, USA). Chi-square test was used to compare differences between different pre-treatment methods. Statistical significance was set at $p < 0.05$.

3. Results

3.1. Effect of pre-treatment methods of MCF on Protein Concentration, keratinase activity and feather degradation

Different pre-treatments were applied to the MCFs to enhance their digestibility prior to methane and bio-energy production by strain IY-BUK1.

The results of effect of each pre-treatment method on the overall rate of degradation, keratinase production and soluble protein yield are summarized in Table 1. It was found that MCF pre-treated with Ca(OH)₂ resulted in faster feather degradation and highest keratinase yield, followed by NaOH, then bio-thermal method ($p < 0.05$). In line with this, MCFs pre-treated with Ca(OH)₂ resulted in about 4 fold increase in soluble protein concentration when compared with untreated MCF in 5 days. Pre-treating MCFs with strain IY-BUK1 for 5 days was less effective in increasing MCF digestibility by the strain after final incubation, as only 64% of MCF was degraded and only 98.2 U/ml keratinase was released. While degradation of Ca(OH)₂ treated MCF started after 2 days of incubation, that of boiled MCF was observed only after 4 days (data not shown). As degradation progressed from day 2, MCF residues decreased considerably, resulting in a colour change in the FMB from colourless medium to completely black fermentation broth at the end of 5 days of incubation in flask containing Ca(OH)₂, NaOH and bio-thermal treated MCFs. Bacterial hydrolysis of Na₂SO₃ treated MCF generated a lower amount of keratinase and soluble proteins when compared with other chemicals [NaOH and

Ca(OH)₂]. Feather hydrolysates obtained by centrifuging the FMB at 4°C and 15,000 ×g for 15 min was stored at -20 °C and used for biogas production.

Table 1. Comparing effects of different pre-treatment methods on feather degradation, keratinase production and soluble protein released by *Pseudochrobactrum* sp. IY-BUK1 after 5 days of incubation

Type of pre-treated MCF (N=5g/L)	Degradation (%)	Keratinase activity (U/ml)	Concentration of soluble protein (mg/ml)
Values in parenthesis are % difference from untreated MCF			
Untreated MCF	26	32.6±1.0	86.2±14.6
Bio-thermal	100 (74)	122.3±0.3	321.0±11.2
Boiled	64 (38)	98.2±1.8	195.4±2.3
Steam	96 (70)	114.4±1.4	295.3±9.8
Chemical (Na ₂ SO ₃)	89 (63)	84.3±1.2	245.8±10.1
Chemical (NaOH)	100 (74)	133±0.1	302.4±12.1
Chemical Ca(OH) ₂	100 (74)	148.2±2.2	333.5±7.5

3.2. Batch anaerobic digestion assays

In the batch anaerobic digestion experiment, biogas production from protein rich hydrolysates obtained from the selected pre-treated MCFs and that of untreated MCFs were compared, and the result was shown in Fig. 3. After 30-days incubation, CaOH₂ treated MCF produced 0.26 Nm³/kg VS methane which is slightly higher when compared with other treated MCFs and untreated samples (0.125 Nm³/kg VS).

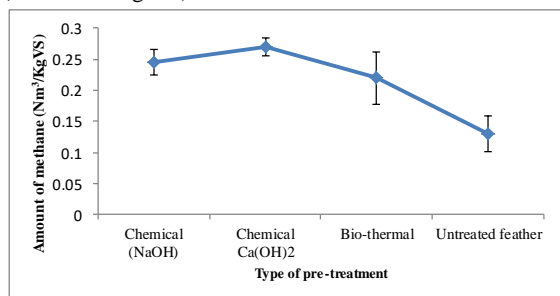


Figure 3. Methane production using untreated and pre-treated melanised feathers after 30 days of incubation

The methane produced in untreated MCF co-digested with cow dung, poultry manure and abattoir waste was 0.195 ± 0.021, 0.105 ± 0.021, and 0.121 ± 0.021 Nm³/kg VS respectively, while that pre-treated chemically with Ca(OH)₂ and as well co-digested with cow dung produced the highest methane of 0.396 Nm³/kg VS which is equivalent to 79.8% of the theoretical value from feather proteins (Davidsson, 2007) (Fig. 4).

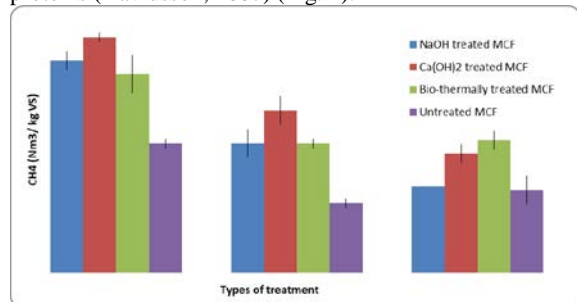


Figure 4. Methane production using hydrolysates co-digested with cow dung, poultry slaughterhouse and abattoir wastes after 12 days of incubation.

In contrast, pre-hydrolysed MCF by poultry slaughterhouse waste showed the least methane yield after

12 days of incubation. Bio-thermally treated MCF yielded 0.195 Nm³/kg VS methane when it was co-digested with cow dung, the amount that is significantly higher than the methane yield from hydrolysates collected in the same MCFs but co-digested with poultry and abattoir wastes.

3.3. Electrical energy generation in MFC fed with pre-treated MCF

Voltage generation in MFC fed with three types of pre-treated MCF showed no significant difference but showed marked difference with untreated MCF. However, Ca(OH)₂ treated MCF yielded maximum voltage of 355mV in 8 days and was relatively stable up to 14th day. The MCF pre-hydrolysed with IY-BUK1 fed into MFC recorded an initial potential of 38mV within 24 h, and after 8 days of incubation, a voltage of 315mV was achieved; the voltage reached its peak (347mV) at 11th days of incubation, and it was stable up to 15th day and thereafter showed gradual decrease (Fig. 5).

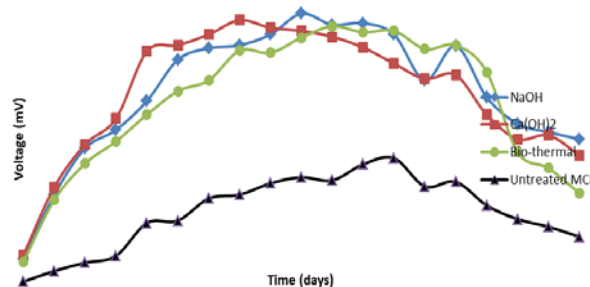


Figure 5. Voltage/day generation in MFC using pre-treated and untreated MCFs in 19 consecutive days

Only approximately 100mV of voltage was produced when hydrolysates obtained from the MCFs after 30 days was used (data not shown). The current and power densities recorded in MFC treated with Ca(OH)₂ followed same pattern with voltage, and reached maximum of 0.112mA/m² and 37.77x10⁴mW/m² respectively after 9 days of incubation (Fig. 6).

Addition of rice water waste to the FMB as extra source of carbon significantly improve the voltage to 467mV in 7 days (Fig. 7)

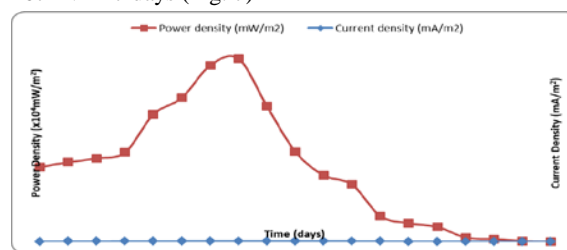


Figure 6. Power and current densities per day in MFC using MCF pre-treated with Ca(OH)₂

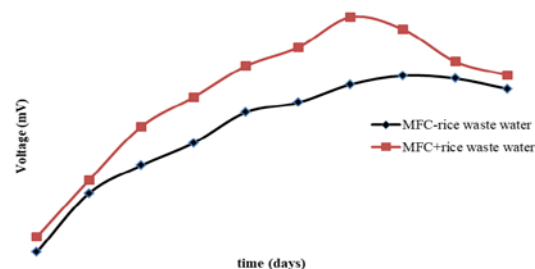


Figure 7. Effect of rice waste water on voltage generation in MFC containing Ca(OH)₂ treated MCF.

4. Discussion

This study has dealt with evaluating the effectiveness of different pre-treatment and co-digestion methods in improving degradability and subsequent utilization of melanised chicken feather waste by microbes for methane and electrical energy production. Prior studies have confirmed that presence of melanin together with compact and resistible structure of melanised feathers are responsible for its low degradability by microbes or their proteases (Gunderson and Frame, 2008; Okoroma *et al.*, 2012) as well as low methane production (Salminen *et al.*, 2003; Forgács *et al.*, 2014). However, degradability of white (non-melanised) feathers has been reported to have improved when pre-treated with either chemical, heat or microbes (Salminen *et al.*, 2003; Łaba *et al.*, 2013; Forgács *et al.*, 2014; Sinkiewicz *et al.*, 2017) prior to anaerobic digestion and has also been proved to improve methane yield (Forgacs *et al.*, 2011; Forgács *et al.*, 2014). Reports of pre-treatment of melanised feathers for any purpose is scarce. In this study, biodegradation of pre-treated MCFs by *Pseudochrobactrum* sp. IY-BUK1 was approximately 75% higher than untreated feathers and feathers pre-treated with microwave-alkali (Lee *et al.*, 2016). In addition to weakening keratin bonds in feather, involvement of heat in all the pre-treatments is done in order to eliminate any pathogenic microbe that might be present in the feathers, in fulfilment of EU legislation of handling of slaughterhouse waste prior to use in anaerobic digestion (EC by-product regulation, 2002). The pre-treatments resulted in cracking the stabilizing disulfide bonds in MCFs in similar way to non- MCFs, which resulted in faster degradation and earlier and higher production of keratinase and hydrolysates rich in soluble proteins. Complete degradation of 5 g/L (w/v) MCF pre-treated with Ca(OH)₂ was completed in 8 days and 333.5±7.5 mg/mL soluble proteins was obtained, which is one and half times higher than that obtained using MCF pre-treated with boiling. This agrees with the findings of Junoh *et al.* (2016) who reported efficiency of Ca(OH)₂ pre-treatment of biological waste. The higher soluble protein in hydrolysates that resulted from MCFs pre-treated with Ca(OH)₂, NaOH over or compared with white feathers indicated its suitability as substrate for biogas production.

Higher concentration of soluble proteins in FMB containing MCFs in comparison with FMB containing equal amount of non-MCF may be partly due to melanin residue, and may indicate its suitability as substrate for biogas production. Use of feather hydrolysates resulting from microbial degradation of non-MCFs in biogas production has been reported (Forgacs *et al.*, 2011). In addition, several studies have reported that co-digesting the substrate with other organic wastes (mostly animal waste) has successfully improved gas yield. In this study, there is no significant difference ($p>0.05$) in amount of methane produced in ADs containing hydrolysates from Ca(OH)₂, NaOH and bio-thermal treated MCFs which have close concentration of soluble proteins. However, the pre-treatments resulted in improved biogas production to 43% over the theoretical methane yield from proteins. This is comparable to results reported by Forgacs *et al.* who reported rapid increase in rate of degradation and

subsequent biogas production when non-melanised feathers were pre-treated biologically with a recombinant *Bacillus megaterium* strain prior to biogas production. Biogas produced in ADs supplemented by cow dungs improved methane production by 52.7% over non-supplemented ADs and about 40% and 30% over hydrolysates supplemented with poultry manure and abattoir wastes respectively.

Higher and faster yield of soluble protein and keratinase from chicken feather biodegradation has been reported in the presence of additional sources of carbon and nitrogen (Thangam and Rajkumar, 2000; Bernal *et al.*, 2003; Lo *et al.*, 2012; Yusuf *et al.*, 2016). Complete degradation of 5g/L of treated and untreated MCFs by strain IY-BUK1 in FMB supplemented by 1g/L of sucrose and rice waste water was achieved in significantly lesser time than non-supplemented FMBs (data not shown) in similar way with feather degrading bacterium *Alcaligenes* sp AQ05-001 (Yusuf *et al.*, 2016). This was applied in MFC by feeding the anodic chamber with FMB containing 0.5% of MCF and 1% of additional carbon source (rice water waste). The overall effect of MCF pre-treatment was also remarkable in MFC, where untreated MCF produced highest voltage of 174mV much later (13th day), compared with pre-treated MCF which produced an average of 175mV in day 3. The slight efficiency of Ca(OH)₂ pre-treatment over NaOH and bio-thermal treatment was also expressed in MFC, where the highest voltage of approximately 355mV was achieved in 8th days but achieved in the 11th day with MCF fed with NaOH treated MCF.

The highest amount of voltage generated in this study was higher than 141mV reported by Chaturvedi and Verma, 2014 when white feathers were degraded by feather degrading bacterium-*P. aeruginosa* strain SDS3 (Chaturvedi and Verma, 2014). The early rise of voltage, current and power densities and subsequent stability of voltage prior to decline indicated the feasibility of electricity generation using MCF, as success of MFC depended partly on rapid onset and duration of stationary phase (Chaturvedi and Verma, 2014). While stationary phase was more prolonged in MFC fed with untreated MCF than pre-treated, supplementation with rice waste water further reduced the ascending and stationary phases, which resulted in higher power generation that lasted for short time. The slow rate of degradation of untreated MCF in MFC as compared to rapid degradation of pre-treated MCFs may then have some advantage, since slow rate of feather degradation will prolong stationary phase of MFC, but with lower voltage.

In summary, biogas and electric energy production from MCF was possible in amount comparable with non-MCF and other wastes especially when pre-treated with Ca(OH)₂. The use of MCFs in biogas and MFC will help in fulfilling the need for achieving hygiene conditions in environment and also offering an environmental, friendly, and economically feasible method for the utilization of MCF waste to produce renewable energy.

Acknowledgement

The authors acknowledged the support of Biochemistry, Microbiology Departments and Central

laboratory complex of Bayero University Kano, for providing space and some equipment for the study.

Conflict of Interest:

The authors declare that they have no conflict of interest

References

- APHA 2005. Standard methods for the examination of water and wastewater, 21th edn. Wasington, DC
- Bernal C, Vidal L, Valdivieso E and Coello N. 2003. Keratinolytic activity of *Kocuria rosea*. *World J Microbiol Biotechnol*, **19**:255–261. doi: 10.1023/A:1023685621215
- Chaturvedi V and Verma P. 2014. Metabolism of Chicken Feathers and Concomitant Electricity Generation by *Pseudomonas aeruginosa* by Employing Microbial Fuel Cell (MFC). *J. Waste Manag*, **9**
- Davidsson Å. 2007. Increase of Biogas Production at Wastewater Treatment Plants Addition of urban organic waste and pre-treatment of sludge. Lund University
- Forgacs G, Alinezhad S, Mirabdollah A, Feuk-Lagerstedt E and Horváth IS. 2011. Biological treatment of chicken feather waste for improved biogas production. *J Environ Sci*, **23**:1747–1753.
- Forgács G, Niklasson C, Sárvári Horváth I and Taherzadeh MJ. 2014. Methane Production from Feather Waste Pretreated with Ca(OH)₂: process development and economical analysis. *Waste Biomass Valor*, **5**:65–73.
- Grande JM, Negro JJ and Torres MJ. 2004. The Evolution of bird plumage colouration: a role for feather-degradation bacteria? *Ardeola*, **51**:375–383.
- Gunderson A and Frame A. 2008. Resistance of melanized feathers to bacterial degradation: is it really so black and white? *J Avian Biol*, **39**:539–545.
- Gurav RG, Tang J, Jadhav JP. 2016 Sulfitolytic and keratinolytic potential of *Chryseobacterium* sp. RBT revealed hydrolysis of melanin containing feathers. *3 Biotech* **6**:145.
- Joshi S, Tejashwini M and Revati N. 2007. Isolation, identification and characterization of a feather degrading bacterium. *Int J Poult Sci*, **6**:689–693.
- Junoh H, Yip C and Kumaran P. 2016. Effect on Ca(OH)₂ pretreatment to enhance biogas production of organic food waste. *IOP Conf Ser Earth Environ Sci*, **32**:012013.
- Khardenavis AA, Kapley A and Purohit HJ. 2009. Processing of poultry feathers by alkaline keratin hydrolyzing enzyme from *Serratia* sp. HPC 1383. *Waste Manag*, **29**:1409–1415.
- Laba W and Szczekala KB. 2013. Keratinolytic Proteases in Biodegradation of Pretreated Feathers. *Polish J Environ Stud*, **22**:1101–1109.
- Lasekan A, Abu F and Hashim D. 2013. Potential of chicken by-products as sources of useful biological resources. *Waste Manag*, **33**(3):552–565.
- Lee, Y.S., Phang, LY., Ahmad, S.A and Ooi PT. 2016. Microwave-alkali treatment of chicken feathers for protein hydrolysate production. *Waste Biomass Valor*, **7**(5): 1147–1157
- Lo W-H, Too J-R and Wu JY. 2012. Production of keratinolytic enzyme by an indigenous feather-degrading strain *Bacillus cereus* Wu2. *J Biosci Bioeng*, **114**:640–7.
- Lowry OC, Rosebrough N. 1951. Protein measurement with the Folin phenol reagent. *J biol chem* **193**:265.
- Mézas L and Tamás J. 2015. Feather Waste Recycling for Biogas Production. *Waste Biomass Valor*, **6**(5):899–911.
- Nair R, Renganathan K, Barathi S and Venkatraman K. 2013. Concentrations using hostel sewage waste as substrate. *Int J Advance Res Technol*, **2**(5):326–330.
- Okoroma EA, Garelick H, Abiola OO and Purchase D. 2012. Identification and characterisation of a *Bacillus licheniformis* strain with profound keratinase activity for degradation of melanised feather. *Int Biodeter Biodegrad*, **74**:54–60.
- Pandian S, Sundaram J, Panchatcharam P, Pandian S. 2012. Isolation, identification and characterization of feather degrading bacteria. *Eur J Exp Biol*, **2**:274–282.
- Parkash A. 2016. Microbial Fuel Cells: A Source of Bioenergy. *J Microb Biochem Technol*, **8**:247–255.
- Paul T, Halder SK, Das A, Paul T, Halder SK, Das A, Bera S, Maity C, Mandal A, Das PS, Mohapatra, PKD, Pati BR and Mondal KC. 2013. Exploitation of chicken feather waste as a plant growth promoting agent using keratinase producing novel isolate *Paenibacillus woosongensis* TKB2. *Biocatal Agric Biotechnol*, **2**:50–57.
- Peng Z, Mao X, Zhang J, Guocheng D and Jian C. 2019. Effective biodegradation of chicken feather waste by co-cultivation of keratinase producing strains. *Microb Cell Fact*, **18**: doi:10.1186/s12934-019-1134-9
- Rahimnejad M, Najafpour GD, Ghoreyshi AA, Talebnia F, Premier GC, Bakeri G, Kim JR and Oh SE. 2012. Thionine Increases Electricity Generation from Microbial Fuel Cell Using *Saccharomyces cerevisiae* and Exoelectrogenic Mixed Culture. *J Microbiol*, **50**:575–576.
- Reiche A and Kirkwood KM. 2012. Comparison of *Escherichia coli* and anaerobic consortia derived from compost as anodic biocatalysts in a glycerol-oxidizing microbial fuel cell. *Bioresour Technol*, **123**:318–23.
- Salminen E, Einola J. and Rintala J. 2003. The methane production of poultry slaughtering residues and effects of pre-treatments on the methane production of poultry feather. *Environ Technol*, **24**:1079–1086.
- Sinkiewicz I, Śliwińska A, Staroszczyk H, Kołodziejaska I. 2017. Alternative methods of preparation of soluble keratin from chicken feathers. *Waste Biomass Valor*, **8**:1043–1048.
- Thangam EB and Rajkumar GS. 2000. Studies on the production of extracellular protease by *Alcaligenes faecalis*. *World J Microbiol Biotechnol*, **16**:663–666.
- Yusuf I, Ahmad S, Phang L and Syed M. 2016. Keratinase production and biodegradation of polluted secondary chicken feather wastes by a newly isolated multi heavy metal tolerant bacterium-*Alcaligenes* sp. *J Environ Manage*, **183**:182–195.
- Yusuf I, Aqlima S, Lai PY, Yasid NA, and Shukor MY. 2019a. Effective production of keratinase by gellan gum-immobilised *Alcaligenes* sp. AQ05-001 using heavy metal-free and polluted feather wastes as substrates. *3 Biotech*, **9**:04–12.
- Yusuf I, Garba L, Shehu MA, Oyiza AM, Kabir MR and Haruna M. 2019b. Selective biodegradation of recalcitrant black chicken feathers by a newly isolated thermotolerant bacterium *Pseudochrobactrum* sp. IY-BUK1 for enhanced production of keratinase and protein-rich hydrolysates. *Int Microbiol*, **1**–12. doi: 10.1007/s10123-019-00090-4
- Yusuf I, Shukor M, Syed M, Yee P. 2015. Investigation of keratinase activity and feather degradation ability of immobilised *Bacillus* sp. khayat in the presence of heavy metals in a semi continuous. *J Chem Pharm Sci*, **8**(2): 342-347.
- Zhou M, Wang H, Hassett J, Gu T. 2013. Recent advances in microbial fuel cells (MFCs) and microbial electrolysis cells (MECs) for wastewater treatment, bioenergy and bioproducts. *J Chem Technol Biotech*, **88**: 508-518

Characterization of Egyptian durum Wheat Genotypes using Biochemical and Molecular Markers

Samira A. Osman and Walaa A. Ramadan*

Genetics and Cytology Department, Genetic Engineering and Biotechnology Division, National Research Centre, Giza, P.O. 12622, Egypt.

Received: November 16, 2019; Revised: December 4, 2019; Accepted: December 8, 2019

Abstract

Landraces are considered an important sources of genetic variations. These variations are extremely important in the programs of plant breeding. Five, eight and twelve oligonucleotide primers of Random amplified polymorphic DNA (RAPD), Simple Sequence Repeats (SSRs), and Inter-Simple Sequence Repeats (ISSRs), respectively and protein marker (SDS-PAGE) were used in durum wheat samples analysis (eight cultivars and four landraces). Compared to molecular markers used, proteins fingerprint gave the highest polymorphism (81.8%) with two specific bands, while RAPD analyses revealed the lowest percentage of polymorphism 50% with no specific bands, the numbers of alleles ranged from 3 to 5 per primer, with an average of 4 per primer. On the other hand, ISSRs markers gave the highest number of unique bands (7 bands), 40 of 68 bands were polymorphic with 58.8% polymorphism. The numbers of alleles ranged from 3 to 9 per primer, with average of 5.6 per primer. However, SSRs displayed two specific bands and the highest polymorphism, 31 out of 50 bands were polymorphic with 62% polymorphism and the numbers of alleles ranged from 1 to 10 per primer, with average of 6.2 per primer. Among the different types of molecular markers, SSRs is a more accurate and informative marker. The similarity matrix of collective data differs from the similarity matrix of each studied markers (protein, RAPD, ISSRs and SSRs); and the similarity of each studied marker differs from each other. This indicates that each studied marker has a specific characterization in discrimination of studied genotypes depending on the site of genomic DNA amplified. Finally, it can also be said that biochemical and molecular markers could be used either separately or together for genetic diversity studies in wheat. This study could also be helpful in the future for genomic mapping and breeding programs of wheat genotypes.

Keywords: *Triticum Durum*, Landraces, Protein Marker, SSRs, ISSRs, RAPD.

1. Introduction

Durum wheat is one of the leading cereals in the world and the most important human food crop. Two-thirds of the world populations live on wheat grain, and production has to be increased significantly in the next decades. Data from FAOSTAT indicates that the need is still growing, as indicated by the steadily increasing yield since 1961. Therefore, introducing modern cultivars is necessary for the food production of world populations. The logical treatment of this problem is the conservation of cultivars and landraces of these native resources.

The genetic variation of wheat cultivars and landraces has been affected by various factors throughout their evolutionary history. The need for improved wheat production coupled with stagnation in the cultivated area leads to a more efficient and more productive demand for wheat production. Traditional breeding depends on the genetic selection of genotypes obtained from crosses. Genotype \times environment interaction is a common problem including time-consumption and costly procedures of phenotyping.

Molecular markers are unaffected by environmental conditions and are detectable in all stages of the plant growth (Dubcovsky, 2004). Genetic markers are important developments in the field of plant breeding (Kebriyae et

al., 2012). Molecular genetic markers are widely used tools in genotyping and species identification. These molecular markers had been used in wheat for detecting genetic diversity, genotype identification, and genetic mapping (Tanyolac, 2003; Malik et al. 2010). Genetic diversity of wheat genotypes is very critical in reducing genetic vulnerability during plant breeding efforts. So, molecular markers provided excellent tools to evaluate the genetic variability (Sofalianet al., 2008). Molecular markers are classified into various groups on the basis of mode of gene action: co-dominant markers as SSRs or dominant markers RAPD and ISSRs. RAPD analysis has been efficient and extensively used to document genetic variation in *Triticum* (Cao et al., 1998; Czaplicki et al., 2000; Tahir, 2008), suggesting a narrow genetic base. ISSRs marker have been used in studies of genetic kinship, for resolving intra- and intergenomic relationships, genetic diversity of plant populations, and cultivars (Khurana-Kaul et al., 2012; Verma et al., 2013; Velasco-Ramirez et al., 2014). ISSRs markers are highly polymorphic and repeatable even for intra-specific purposes in durum wheat genotypes and could be used for genotypes identification. SSRs provide highly informative markers because they are co-dominant (Gupta et al., 1996; Agrama and Tuinstra, 2003; Muhammad et al., 2017). The microsatellite markers have utility in detecting polymorphism and estimating genetic diversity of cultivars (Parvin et al.,

* Corresponding author e-mail: walaanrc70@yahoo.com; walaanrc70@gmail.com.

laboratory complex of Bayero University Kano, for providing space and some equipment for the study.

Conflict of Interest:

The authors declare that they have no conflict of interest

References

- APHA 2005. Standard methods for the examination of water and wastewater, 21th edn. Wasington, DC
- Bernal C, Vidal L, Valdivieso E and Coello N. 2003. Keratinolytic activity of *Kocuria rosea*. *World J Microbiol Biotechnol*, **19**:255–261. doi: 10.1023/A:1023685621215
- Chaturvedi V and Verma P. 2014. Metabolism of Chicken Feathers and Concomitant Electricity Generation by *Pseudomonas aeruginosa* by Employing Microbial Fuel Cell (MFC). *J. Waste Manag*, **9**
- Davidsson Å. 2007. Increase of Biogas Production at Wastewater Treatment Plants Addition of urban organic waste and pre-treatment of sludge. Lund University
- Forgacs G, Alinezhad S, Mirabdollah A, Feuk-Lagerstedt E and Horváth IS. 2011. Biological treatment of chicken feather waste for improved biogas production. *J Environ Sci*, **23**:1747–1753.
- Forgács G, Niklasson C, Sárvári Horváth I and Taherzadeh MJ. 2014. Methane Production from Feather Waste Pretreated with Ca(OH)₂: process development and economical analysis. *Waste Biomass Valor*, **5**:65–73.
- Grande JM, Negro JJ and Torres MJ. 2004. The Evolution of bird plumage colouration: a role for feather-degradation bacteria? *Ardeola*, **51**:375–383.
- Gunderson A and Frame A. 2008. Resistance of melanized feathers to bacterial degradation: is it really so black and white? *J Avian Biol*, **39**:539–545.
- Gurav RG, Tang J, Jadhav JP. 2016 Sulfitolytic and keratinolytic potential of *Chryseobacterium* sp. RBT revealed hydrolysis of melanin containing feathers. *3 Biotech* **6**:145.
- Joshi S, Tejashwini M and Revati N. 2007. Isolation, identification and characterization of a feather degrading bacterium. *Int J Poult Sci*, **6**:689–693.
- Junoh H, Yip C and Kumaran P. 2016. Effect on Ca(OH)₂ pretreatment to enhance biogas production of organic food waste. *IOP Conf Ser Earth Environ Sci*, **32**:012013.
- Khardenavis AA, Kapley A and Purohit HJ. 2009. Processing of poultry feathers by alkaline keratin hydrolyzing enzyme from *Serratia* sp. HPC 1383. *Waste Manag*, **29**:1409–1415.
- Laba W and Szczekala KB. 2013. Keratinolytic Proteases in Biodegradation of Pretreated Feathers. *Polish J Environ Stud*, **22**:1101–1109.
- Lasekan A, Abu F and Hashim D. 2013. Potential of chicken by-products as sources of useful biological resources. *Waste Manag*, **33**(3):552–565.
- Lee, Y.S., Phang, LY., Ahmad, S.A and Ooi PT. 2016. Microwave-alkali treatment of chicken feathers for protein hydrolysate production. *Waste Biomass Valor*, **7**(5): 1147–1157
- Lo W-H, Too J-R and Wu JY. 2012. Production of keratinolytic enzyme by an indigenous feather-degrading strain *Bacillus cereus* Wu2. *J Biosci Bioeng*, **114**:640–7.
- Lowry OC, Rosebrough N. 1951. Protein measurement with the Folin phenol reagent. *J biol chem* **193**:265.
- Mézas L and Tamás J. 2015. Feather Waste Recycling for Biogas Production. *Waste Biomass Valor*, **6**(5):899–911.
- Nair R, Renganathan K, Barathi S and Venkatraman K. 2013. Concentrations using hostel sewage waste as substrate. *Int J Advance Res Technol*, **2**(5):326–330.
- Okoroma EA, Garelick H, Abiola OO and Purchase D. 2012. Identification and characterisation of a *Bacillus licheniformis* strain with profound keratinase activity for degradation of melanised feather. *Int Biodeter Biodegrad*, **74**:54–60.
- Pandian S, Sundaram J, Panchatcharam P, Pandian S. 2012. Isolation, identification and characterization of feather degrading bacteria. *Eur J Exp Biol*, **2**:274–282.
- Parkash A. 2016. Microbial Fuel Cells: A Source of Bioenergy. *J Microb Biochem Technol*, **8**:247–255.
- Paul T, Halder SK, Das A, Paul T, Halder SK, Das A, Bera S, Maity C, Mandal A, Das PS, Mohapatra, PKD, Pati BR and Mondal KC. 2013. Exploitation of chicken feather waste as a plant growth promoting agent using keratinase producing novel isolate *Paenibacillus woosongensis* TKB2. *Biocatal Agric Biotechnol*, **2**:50–57.
- Peng Z, Mao X, Zhang J, Guocheng D and Jian C. 2019. Effective biodegradation of chicken feather waste by co-cultivation of keratinase producing strains. *Microb Cell Fact*, **18**: doi:10.1186/s12934-019-1134-9
- Rahimnejad M, Najafpour GD, Ghoreyshi AA, Talebnia F, Premier GC, Bakeri G, Kim JR and Oh SE. 2012. Thionine Increases Electricity Generation from Microbial Fuel Cell Using *Saccharomyces cerevisiae* and Exoelectrogenic Mixed Culture. *J Microbiol*, **50**:575–576.
- Reiche A and Kirkwood KM. 2012. Comparison of *Escherichia coli* and anaerobic consortia derived from compost as anodic biocatalysts in a glycerol-oxidizing microbial fuel cell. *Bioresour Technol*, **123**:318–23.
- Salminen E, Einola J. and Rintala J. 2003. The methane production of poultry slaughtering residues and effects of pre-treatments on the methane production of poultry feather. *Environ Technol*, **24**:1079–1086.
- Sinkiewicz I, Śliwińska A, Staroszczyk H, Kołodziejaska I. 2017. Alternative methods of preparation of soluble keratin from chicken feathers. *Waste Biomass Valor*, **8**:1043–1048.
- Thangam EB and Rajkumar GS. 2000. Studies on the production of extracellular protease by *Alcaligenes faecalis*. *World J Microbiol Biotechnol*, **16**:663–666.
- Yusuf I, Ahmad S, Phang L and Syed M. 2016. Keratinase production and biodegradation of polluted secondary chicken feather wastes by a newly isolated multi heavy metal tolerant bacterium-*Alcaligenes* sp. *J Environ Manage*, **183**:182–195.
- Yusuf I, Aqlima S, Lai PY, Yasid NA, and Shukor MY. 2019a. Effective production of keratinase by gellan gum-immobilised *Alcaligenes* sp. AQ05-001 using heavy metal-free and polluted feather wastes as substrates. *3 Biotech*, **9**:04–12.
- Yusuf I, Garba L, Shehu MA, Oyiza AM, Kabir MR and Haruna M. 2019b. Selective biodegradation of recalcitrant black chicken feathers by a newly isolated thermotolerant bacterium *Pseudochrobactrum* sp. IY-BUK1 for enhanced production of keratinase and protein-rich hydrolysates. *Int Microbiol*, 1–12. doi: 10.1007/s10123-019-00090-4
- Yusuf I, Shukor M, Syed M, Yee P. 2015. Investigation of keratinase activity and feather degradation ability of immobilised *Bacillus* sp. khayat in the presence of heavy metals in a semi continuous. *J Chem Pharm Sci*, **8**(2): 342-347.
- Zhou M, Wang H, Hassett J, Gu T. 2013. Recent advances in microbial fuel cells (MFCs) and microbial electrolysis cells (MECs) for wastewater treatment, bioenergy and bioproducts. *J Chem Technol Biotech*, **88**: 508-518

2014; Ayman and Mohamed, 2019). The aim of this research was to investigate the discrimination capacity chemical marker and molecular markers (dominant markers (RAPDs and ISSRs) and co-dominant markers (SSRs) and their effectiveness in establishing genetic variation and relationships among Egyptian durum wheat genotypes (eight Cultivars and four Landraces).

2. Materials and Methods

2.1. Plant Materials:

Twelve tetraploid durum wheat genotypes (Triticum durum) $2n = 4X = 28$, eight cultivars and four landraces were provided by the Wheat Research Section and Egyptian National Gene Bank, respectively, Agricultural Research Center, Ministry of Agriculture, Giza, Egypt as are shown in Table (1).

Table (1). The twelve tetraploid wheat genotypes and their origins used in this study.

No.	Genotypes	Genotype
1	Baniswef 3	Cultivar
2	Baniswef 4	Cultivar
3	Baniswef 5	Cultivar
4	Baniswef 6	Cultivar
5	Sohag 1	Cultivar
6	Sohag 3	Cultivar
7	sohag 4	Cultivar
8	sohag 5	Cultivar
9	Sohagalmanseah 33	Landraces
10	Sohagalmanseah 34	Landraces
11	Sohagalmanseah 35	Landraces
12	Sohagalmanseah 41	Landraces

2.2. Methods

2.2.1. Biochemical markers (Protein electrophoresis using SDS-PAGE technique):

Samples of 0.5 g seeds of each genotype were used for protein analyses. Sodium Dodecyl Sulfate Polyacrylamide Gel Electrophoresis (SDS-PAGE) was performed for protein analysis according to Laemmli, 1970. Sample preparation and extraction of seed storage proteins were performed. The marker of the used protein was BLUltraPrestained Protein Ladder (Gene Direct, Cat No. PM001-0500). In this method, 15% Protein separating gel was used. Protein fractionations were performed using the electrophoresis apparatus manufactured by Cleaver, UK. The images were captured by a digital camera (Sony, made in Japan) and transferred directly to the computer and then the protein bands were analyzed by Total Lab program to find out the molecular weight of each band then compare the presence and absence of the band among studied genotypes, and these data were imported in MVSP (Multi-Variant Statistical Package) (Kovach, 1998) to find the similarity matrix and dendrogram (UPGMA, using Nei & Li's coefficient) which reflect the relationships among the studied genotypes.

2.2.2. Molecular markers

2.2.2.1. DNA extraction

The plant genomic DNA was isolated from 12 genotypes wheat by using Gene Jet Plant Genomic DNA purification Mini Kits (Thermo scientific K0791).

2.2.2.2. ISSRs analysis

Twelve ISSRs primers were used to characterize the twelve wheat Genotypes depending upon the literature, Table (2). PCR technique was performed in 25 μ l volume containing: master mix (Thermo scientific K1081), 10 μ l buffer (10 X), 1 μ l primer (100 pmol), 1 μ l DNA template (50 ng) and 13 μ l water (nuclease-free). The amplification was carried out in a thermocycler programmed as follows: 1 cycle of 94°C/2min, 35 cycles of (94°C/1min, annealing temperatures as are shown in Tables (2), /2 min and 72°C/2 min), 1 cycle 72°C/7 min. The primer annealing degrees varied according to the melting point of each primer. Agarose gel was used for separating the PCR products of amplified DNA fragments by electrophoresis. The agarose gel was prepared by dissolving 1.2 g agarose in 100 ml buffer including 40 mM Tris-acetate and 2 mM Na EDTA. The gel was stained with ethidium bromide, photographed under UV light, scanned using Gel-Documentation system (Bio-Rad).

Table (2) represents twelve ISSRs primers names, sequences and melting temperatures to characterize the twelve durum wheat genotypes:

Primer	Sequence (5'-3')	(Tm)
ISSR-2	(AG)8C	50°C
ISSR-3	(GA)8T	55°C
ISSR-4	(CT)8G	52°C
ISSR-5	(CA)6ACAG	46°C
ISSR-6	BDB(TCC)5	48°C
HB12	(CAC)3GC	52°C
844A	5'(CT)8GC 3'	48°C
844B	5'(CT)7A 3'	48°C
17889A	(CA)6 AC	52°C
17889B	(CA)6 GT	41°C
17898BS5	(CA)GA	43°C
HBS11	(GT)6 CC	44°C

* Y=G/C; B=T/G/C; D=A/T/G (Tm): Melting Temperature

2.2.2.3. SSRs analysis

Eight SSRs primers were used to identify the twelve wheat Genotypes, as shown as in Table (3). PCR technique was performed in 25 μ l volume containing: master mix (Thermo scientific K1081), 10 μ l buffer (10 X), 1 μ l primer (100 pmol), 1 μ l DNA template (50 ng) and 13 μ l water (nuclease-free). The amplification was carried out in a thermocycler programmed as follows: 1 cycle of 94°C/2min, 35 cycles of (94°C/1min, annealing temperatures as are shown in Tables (3), /2 min and 72°C/2 min), 1 cycle 72°C/7 min. The primer annealing degrees varied according to the melting point of each primer. Agarose gel was used for separating the PCR products of amplified DNA fragments by electrophoresis. The agarose gel was prepared by dissolving 1.2 g agarose in 100 ml buffer including 40 mM Tris-acetate and 2 mM

Na EDTA. The gel was stained with ethidiumbromide, photographed under UV light, scanned using Gel-Documentation system (Bio-Rad).

Table 3. Represents eight SSRs primers names, sequences and Melting temperatures to characterize the twelve durum wheat genotypes

Primer	Sequence	Melting Temperature
Bmag13	Forward 5'-AAGGGGAATCAAATGGGAG-3'	54°C
	Reverse 5'-TCGAATAGGTCTCCGAAGAAA-3'	
MGB391	Forward 5'-AGCTCCTTCCCTCCCTCC-3'	54°C
	Reverse 5'-CCAACATCTCCTCTCTGA-3'	
GMS1	Forward 5'-CTGACCCCTTGCTTAACATGC-3'	55°C
	Reverse 5'-TCAGCGTGACAAACAATAAAGG-3'	
EBmac624	Forward 5'-AAAAGCATTCACCTCATAAGA-3'	54°C
	Reverse 5'-CAACGCCATCACGTAATA-3'	
Bmag210	Forward 5'ACCTACAGTTCAATAGCTAGTACC-3'	54°C
	Reverse 5'-GCACAAAACGATTACATCATA-3'	
Bmag149	Forward 5'-CAAGCCAACAGGGTAGTC-3'	55°C
	Reverse 5'-ATTGGTTTCTAGAGGAAGAA-3'	
HVITR1	Forward 5'-CCACTTGCCAAACACTAGACCC-3'	55°C
	Reverse 5'-TTCATGCAGATCGGGCCAC-3'	
Bmac0576	Forward 5'-CAATTGTAGCTAGTGGTGC -3'	54°C
	Reverse 5'-GGGTGTATGCAAGTGGGC-3'	

2.2.2.4. RAPD analysis

Five random, 10-mer primers were used for RAPD analysis depending upon the literature (Table 4) to characterize the twelve wheat Genotypes. PCR technique was performed in 25 µl volume containing: master mix (Thermo scientific K1081), 10 µl buffer (10 X), 1µl primer (100 pmol), 1µl DNA template (50 ng) and 13 µl water (nuclease-free). The amplification was carried out in a thermocycler programmed as follows: 1 cycle of 94°C/2min, 35 cycles of (94°C/1min, annealing temperatures as shown in Tables (4), /2 min and 72°C/2 min), 1 cycles 72°C/7 min. The primer annealing degrees varied according to the melting point of each primer. Agarose gel was used for separating the PCR products of amplified DNA fragments by electrophoresis. The agarosegel was prepared by dissolving 1.2 g agarose in 100 ml buffer including 40 mM Tris-acetate and 2 mM Na EDTA. The gel was stained with ethidiumbromide, photographed under UV light, scanned using Gel-Documentation system (Bio-Rad).

Table (4): Represent five RAPD primers sequence to characterize the twelve durum wheat.

Primer	Sequence (5'-3')	Melting Temperature
OPA1	CAGGCCCTTC	50°C
OPA4	AATCGGGCTG	55°C
OPB3	CATCCCCCTG	52°C
OPB10	CTGCTGGGAC	46°C
OPA11	CAATCGCCGT	48°C

2.2.2.5. Statistical analysis

The data were analyzed using total lab Programs. MVSP (Multi-Variant Statistical Package, Kovach 1998) program was used to find the similarity matrix and dendrogram (UPGMA, using Nei&Li's coefficient), which reflects the relationships among the studied genotypes.

3. Results

3.1. Protein analysis:

SDS-PAGE recorded the differences in the seed storage protein depending on the number of bands among twelve durum wheat Genotypesasare shown in Figure (1) and Table (5). The electrophoresis was estimated based on the molecular weight (Mw) of each band represented with a unit of KiloDaltons (kDa). A total number of the band was 22 bands, four of which were monomorphic (18.2%) and 18 were polymorphicbands with 81.8% polymorphism, including two unique bands at MWs 62kDa and 17 kDa appeared in Sohag almansheah 41 and Sohag almansheah 33 genotypes, respectively. The five genotypes Baniswef 3, Baniswef 4, Baniswef 5, Baniswef 6 and Sohag 1 gave the highest number of bands (18 bands) at the same loci in their protein patterns, indicating similar genetic background,while Sohag almansheah 34 exhibited the lowest number of bands (6 bands).

Table 5 . Densitometric analysis represents seed storage protein electrophoretic patterns using SDS-PAGE for characterization of twelve durum wheat genotypes

Band number	Molecular weight	Baniswef 3	Baniswef 4	Baniswef 5	Baniswef 6	Sohag 1	Sohag 3	sohage 4	sohag 5	Sohag almansheah 33	Sohag almansheah 34	Sohag almansheah 35	Sohag almansheah 41
1	110	-	-	-	-	-	-	-	-	+	-	+	+
2	78	+	+	+	+	+	-	-	+	+	-	+	+
3	71	+	+	+	+	+	-	-	+	+	-	+	+
4	62	-	-	-	-	-	-	-	-	-	-	-	+
5	60	+	+	+	+	+	-	+	+	+	-	+	+
6	58	+	+	+	+	+	-	+	+	+	-	+	-
7	56	+	+	+	+	+	+	+	+	+	+	+	+
8	49	+	+	+	+	+	+	+	+	+	+	+	+
9	41	+	+	+	+	+	-	-	+	-	-	+	+
10	35	+	+	+	+	+	+	+	+	+	+	+	+
11	31	+	+	+	+	+	-	-	+	-	-	-	+
12	29	+	+	+	+	+	-	-	+	-	-	-	-
13	26	+	+	+	+	+	-	+	+	-	-	-	-
14	25	+	+	+	+	+	-	-	-	+	+	+	+
15	24	+	+	+	+	+	+	+	+	-	+	-	-
16	19	-	-	-	-	-	+	+	-	-	-	-	-
17	17	-	-	-	-	-	-	-	-	+	-	-	-
18	13	+	+	+	+	+	+	+	+	+	+	+	+
19	9	+	+	+	+	+	-	-	+	+	-	-	-
20	8	+	+	+	+	+	-	-	-	+	-	-	-
21	7	+	+	+	+	+	+	+	+	-	-	-	-
22	5	+	+	+	+	+	+	+	+	+	-	-	-
Total bands		18	18	18	18	18	8	10	16	14	6	11	12

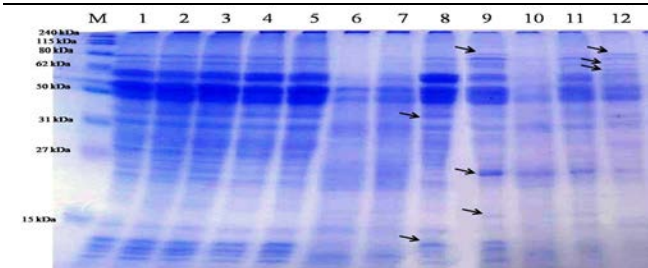
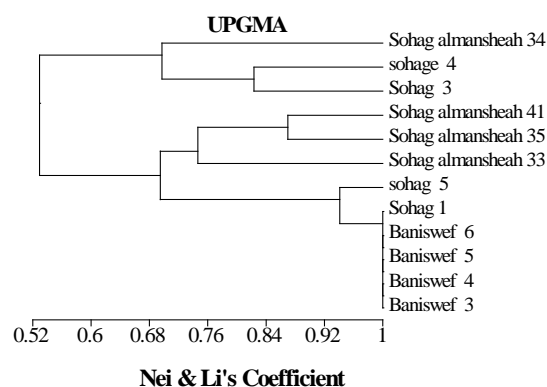


Figure 1. SDS-PAGE of seed storage proteins fingerprint for twelve durum wheat genotypes.

Genetic Similarity: The genetic similarity index and dendrogram tree of the studied twelve durum wheat genotypes were performed using Nei&Li's similarity index on based on proteins electrophoresis as shown in Table (6) and Figure (2). The genetic similarity among 12 the durum wheat genotypes ranged from 42% to 100%, with an average of 71%. Some distinctive genotypes showed identical genetic similarity with others, such as Sohag 1, Baniswef 3, Baniswef 4, Baniswef 5 and Baniswef 6 (100%), Sohag5 and (Sohag 1, Baniswef 3, Baniswef 4, Baniswef 5, and Baniswef 6) with similarity 94%, while some varieties displayed low genetic similarity such as Sohag almansheah 41 and Sohag 3 revealed 42% similarity, Sohag almansheah 41 and Sohag4 (46%), Sohag almansheah 34 and Sohag 5 (46%). The dendrogram showed that the twelve durum wheat genotypes could be divided into two main clusters. The first cluster was classified into two sub-clusters, the first sub-cluster contained only one genotype Sohag almansheah 34. The second sub-cluster contained two genotypes sohag 3 and sohag 4 with similarity index 82%. The second cluster was divided into two sub-clusters; the first sub-cluster contained two main groups; the first group included Sohag almansheah 41 and Sohag almansheah 35 with similarity 87%, while the second group contained the

only one genotypes Sohag almansheah 33. However, the second sub-cluster contained two main groups; the first group included one genotype Sohag5, the second group contained the five genotypes Sohag 1, Baniswef 3, Baniswef 4, Baniswef 5, and Baniswef 6 with a similarity



of 100%.

Figure 2. Dendrogram representing the genetic relationship among the twelve durum wheat genotypes using UPGMA cluster analysis of Nei&Li's similarity coefficient generated from seed storage proteins pattern.

Table (6): Genetic similarity percentages of the twelve durum wheat genotypes based on protein banding patterns.

	Baniswef 3	Baniswef 4	Baniswef 5	Baniswef 6	Sohag 1	Sohag 3	sohage 4	sohag 5	Sohag almansheah 33	Sohag almansheah 34	Sohag almansheah 35	Sohag almansheah 41
Baniswef 3	1.00											
Baniswef 4	1.00	1.00										
Baniswef 5	1.00	1.00	1.00									
Baniswef 6	1.00	1.00	1.00	1.00								
Sohag 1	1.00	1.00	1.00	1.00	1.00							
Sohag 3	0.48	0.48	0.48	0.48	0.48	1.00						
sohage 4	0.64	0.64	0.64	0.64	0.64	0.82	1.00					
sohag 5	0.94	0.94	0.94	0.94	0.94	0.52	0.69	1.00				
Sohag almansheah 33	0.75	0.75	0.75	0.75	0.75	0.38	0.58	0.67	1.00			
Sohag almansheah 34	0.50	0.50	0.50	0.50	0.50	0.77	0.63	0.46	0.50	1.00		
Sohag almansheah 35	0.69	0.69	0.69	0.69	0.69	0.44	0.57	0.67	0.80	0.59	1.00	
Sohag almansheah 41	0.67	0.67	0.67	0.67	0.67	0.42	0.46	0.64	0.69	0.56	0.87	1.00

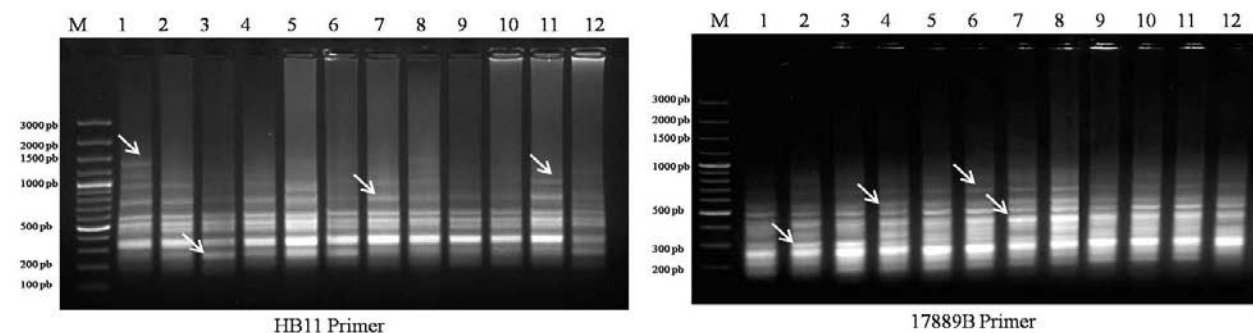
3.2. Identification of durumwheat genotypes by ISSRs analysis:

Twelve ISSR primers were used to characterize the twelve durum wheat genotypes. Figure (3) shows the banding patterns produced from each primer for the twelve genotypes. The amplification results indicated distinct differences for the identification of these genotypes as shown in Table (7). A total of 68 amplified DNA fragments ranging in size from 173–1452bp, and 28 fragments out of 68 loci, 41.2% were monomorphic and 58.8% were polymorphic with average of 3.3 polymorphisms per primer. The number of DNA fragments for each primer varied from 3 (ISSR-5 and HBS11) to 9 (17889B) with average of 5.6 fragments per primer. On the other hand, the primer 17889B gave the highest number of amplified fragments (72 fragments) for

all studied genotypes, while the primer 844B showed the lowest number of bands (24 fragments). Two specific amplicons with molecular size 1452 and 900 bp were detected in the electrophoretic patterns of genotype Sohag almansheah 41 by ISSR2 marker; one specific marker of MW with molecular size 1500 bp was detected in genotype Baniswef 3 by HB12 marker. In addition, two specific fragments at molecular sizes 517 and 313 pb revealed in Sohag 1 and Sohag almansheah 41, respectively by 844B marker. Two specific bands with molecular sizes 210 and 500 bp were detected in the genotype Sohag almansheah 41 by 17889B and 1789BS5 markers, respectively. DNA primer 17889B out of twelve used in ISSR-PCR analysis succeeded to give the high rate of polymorphism between wheat genotypes.

Table 7. The polymorphic loci amplified by the twelve ISSRs primers

Primer	Loci	range sizes of loci	Polymorphic	Monomorphic	Polymorphism%	Specific bands	Total Bands in all genotypes
ISSR-2	6	800-1452	5	1	83%	2	31
ISSR-3	7	180-650	4	3	57.1%	-	61
ISSR-4	7	183-714	4	3	57%	-	71
ISSR-5	3	173-400	-	3	0%	-	36
ISSR-6	6	219-813	3	3	50%	-	63
HB12	8	383-1519	4	4	50%	1	66
844A	6	200-603	2	4	33.3%	-	59
844B	4	250-512	4	-	100%	2	24
17889A	4	295-718	2	2	50%	-	41
17889B	9	213-715	7	2	77.7%	1	72
17898BS5	5	200-700	4	1	80%	1	35
HBS11	3	291-405	1	2	33.3%	-	28
Total loci	68	173-1452	40	28	58.8 %	7	

**Figure 3.** An example of ISSRs banding pattern obtained using HB11 and 17889B primers with 12 Egyptian wheat cultivars and landraces. M: ladder. (1) Baniswef 3; (2) Baniswef 4; (3) Baniswef 5; (4) Baniswef 6; (5) Sohag 1; (6) Sohag 3; (7) Sohag 4; (8) Sohag 5; (9) Sohag almansheah 33; (10) Sohag almansheah 34; (11) Sohag almansheah 35; (12) Sohag almansheah 41.

Genetic Similarity: The genetic similarity index and dendrogram tree of studied twelve durum wheat genotypes were performed using Nei&Li's similarity index on the basis ISSR markers in Table (8) and Figure (4). The genetic similarity values ranged from 73 to 98%, with an average of 85.2%. Some distinctive genotypes showed high genetic similarity, while others such as Sohag almansheah 33 and Sohag almansheah 34 gave the highest genetic similarity (98%), Sohagalmansheah 33 and Sohag almansheah 35 (96%). However, some genotypes displayed low genetic similarity such as Sohag almansheah 41 and (Baniswef 3 and Baniswef 4) revealed 73%, Sohag almansheah 41 and Baniswef 5 (75%), Baniswef 6 and Baniswef 3 (73%). The dendrogram resulting from UPGMA cluster analysis showed that the twelve durum wheat genotypes could be divided into two main clusters. The first cluster contained only one genotype Sohagalmansheah41. The second cluster could be divided into two sub-clusters; the first sub-cluster contained two main groups; the first group was classified into two sub-group; the first sub-group included Sohagalmansheah33, Sohagalmansheah34 with similarity (98%), Sohag almansheah 35 and Sohag 5 with similarity (96%), while the second sub-group contained only one genotype Sohag 4. The Second-group was divided into two sub-groups; the first sub-group included Sohag1 and Sohag 3 with similarity 93%, the second sub-group had one genotype Baniswef 6. The second sub-cluster consisted of two main groups; the first group included only one genotype Baniswef 5, the second group was composed of the two

genotypes Baniswef 3, and Baniswef4 with similarity 85%.

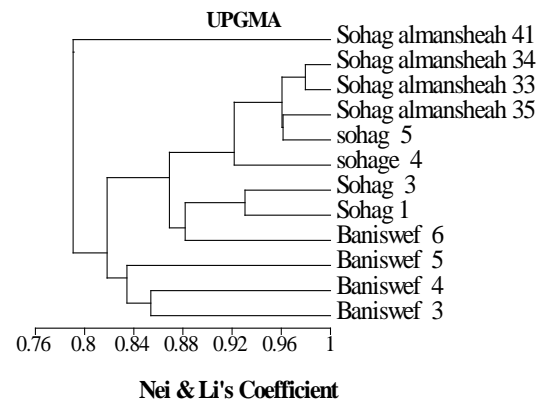
**Figure 4.** Dendrogram representing the genetic relationship among the twelve durum wheat genotypes using UPGMA cluster analysis of Nei-Lis similarity coefficient generated from ISSRs markers.

Table 8. Genetic similarity percentages of the twelve durum wheat genotypes based on ISSRs banding patterns.

	Baniswef 3	Baniswef 4	Baniswef 5	Baniswef 6	Sohag 1	Sohag 3	sohag 4	sohag 5	Sohag almansheah 33	Sohag almansheah 34	Sohag almansheah 35	Sohag almansheah 41
Baniswef 3	1.00											
Baniswef 4	0.85	1.00										
Baniswef 5	0.84	0.83	1.00									
Baniswef 6	0.73	0.82	0.80	1.00								
Sohag 1	0.82	0.90	0.86	0.89	1.00							
Sohag 3	0.80	0.84	0.84	0.87	0.93	1.00						
sohag 4	0.84	0.86	0.84	0.85	0.90	0.87	1.00					
sohag 5	0.81	0.85	0.81	0.84	0.89	0.84	0.93	1.00				
Sohag almansheah 33	0.76	0.84	0.80	0.85	0.91	0.88	0.91	0.96	1.00			
Sohag almansheah 34	0.78	0.82	0.80	0.83	0.89	0.86	0.91	0.96	0.98	1.00		
Sohag almansheah 35	0.77	0.82	0.79	0.86	0.89	0.86	0.93	0.96	0.96	0.96	1.00	
Sohag almansheah 41	0.73	0.73	0.75	0.78	0.78	0.77	0.82	0.82	0.83	0.83	0.85	1.00

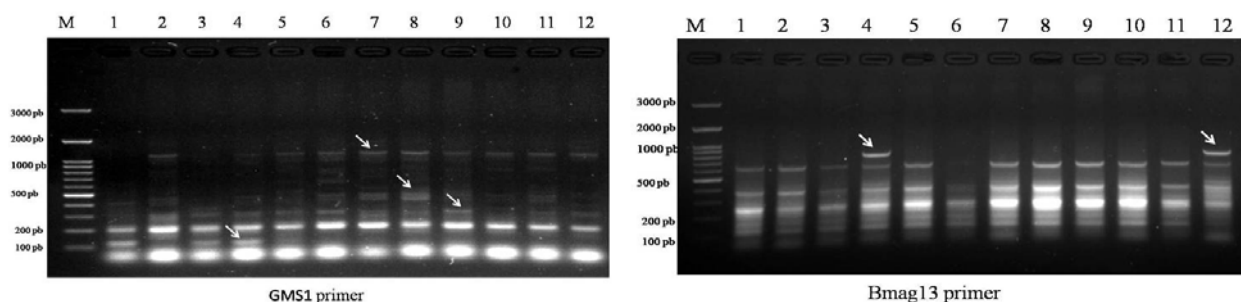
3.3. Identification of durum Wheat genotypes by SSRs analysis:

Figure (5) shows the banding patterns produced from each SSRs primer for the twelve durum genotypes. Table (9) illustrates the amplification results by PCR for the studied wheat genotypes with eight SSR primers indicated distinct differences for identification of these genotypes. A total of 50 amplified DNA fragments ranging from 50-1217bp were presented, whereas 19 fragments out of 50 loci, 38 % were monomorphic and 62% were polymorphic with an average of 3.9 polymorphisms per primer. The number of DNA fragments for each primer varied from 1

band (MGB391) to 10 (Bmag149) with average of 6.2 fragments per primer. On the other hand, the primer Bmag149 gave the highest number of amplified fragments (90 bands) for all investigated genotypes, while the primer MGB391 showed the lowest number of amplified fragments (12 amplicons). Two specific bands with molecular sizes (1000 and 359 bp) were recorded in genotype Sohag almansheah 41, using primers Bmag149 and Bmag13, respectively. Two DNA primers (Bmag13 and Bmag 210) out of eight gave the highest rate of polymorphism.

Table (9): The polymorphic loci amplified by the eight SSRs primers.

Primer	Loci	Range Sizes of loci	Polymorphic	Monomorphic	Polymorphism%	Specific bands	Total Bands in all genotypes
Bmag13	9	123 -803 pb	7	2	77.7%	1	66
MGB391	1	112pb	0	1	0%	-	12
GMS1	8	79 -1217 pb	6	2	75%	-	66
EBmac624	6	147-509 pb	3	3	50%	-	54
Bmag210	9	63-300 pb	6	3	77.7%	-	75
Bmag149	10	51-1000pb	7	3	70%	1	90
HVITR1	3	59-210 pb	-	3	0%	-	36
Bmac0576	4	50-490 pb	2	2	50%	-	43
Total loci	50	50-1217 pb	31	19	62%	2	442

**Figure 5.** An example of SSRs banding pattern obtained using GMS1 and Bmag 13 primers with 12 Egyptian wheat cultivars and landraces. M: ladder. (1) Baniswef 3; (2) Baniswef 4; (3) Baniswef 5; (4) Baniswef 6; (5) Sohag 1; (6) Sohag 3; (7) Sohag 4; (8) Sohag 5; (9) Sohag almansheah 33; (10) Sohag almansheah 34; (11) Sohag almansheah 35; (12) Sohag almansheah 41.

Genetic Similarity: The genetic similarity index and dendrogram tree of the studied wheat genotypes were

performed using Nei-Li's similarity index on the basis SSRs markers in Table (10) and Figure (6). The similarity

values among studied durum wheat genotypes ranged from 64 to 96%, with average 81.5%. Genotypes Sohag3 and Sohag5 gave the highest genetic similarity (96%), Sohag 4 and Sohag 5 (94%). On other hand, Sohag almansheah 41 and Baniswef 3 displayed the lowest genetic similarity (64%), Sohagalmansheah33 and Baniswef 3 (67%). The dendrogram resulting from UPGMA cluster analysis showed that the twelve studied durum wheat genotypes could be divided into two main clusters. The first cluster contained two genotypes Baniswef 3 and Baniswef 5 with similarity 85%, the second cluster was divided into two

sub-clusters; the first sub-cluster contained only one genotype, Sohag almansheah 41. The second sub-cluster consisted of two main groups; the first group contained two genotypes, Sohag almansheah 34 and sohag almansheah 35 with similarity 92%. The second group was Classified into two sub-groups: The first sub-group: hasone genotype Sohagalmansheah 33, the second sub-group: involved Sohag 1 and Baniswef 6 with similarity 90%, sohag 3 and sohag 5 (96%), Baniswef 4 and sohag4 (92%).

Table 10. Genetic similarity percentages of the twelve durum wheat genotypes based on SSRs banding patterns.

	Baniswef 3	Baniswef 4	Baniswef 5	Baniswef 6	Sohag 1	Sohag 3	sohag 4	sohag 5	Sohag almansheah 33	Sohag almansheah 34	Sohag almansheah 35	Sohag almansheah 41
Baniswef 3	1.00											
Baniswef 4	0.76	1.00										
Baniswef 5	0.85	0.83	1.00									
Baniswef 6	0.76	0.86	0.80	1.00								
Sohag 1	0.74	0.90	0.81	0.90	1.00							
Sohag 3	0.72	0.90	0.75	0.89	0.88	1.00						
sohag 4	0.74	0.92	0.81	0.89	0.88	0.90	1.00					
sohag 5	0.73	0.91	0.77	0.88	0.90	0.96	0.94	1.00				
Sohag almansheah 33	0.67	0.84	0.74	0.84	0.86	0.82	0.88	0.87	1.00			
Sohag almansheah 34	0.73	0.84	0.77	0.83	0.88	0.85	0.87	0.89	0.79	1.00		
Sohag almansheah 35	0.75	0.81	0.73	0.83	0.84	0.84	0.81	0.83	0.72	0.92	1.00	
Sohag almansheah 41	0.64	0.78	0.70	0.85	0.84	0.79	0.83	0.83	0.76	0.86	0.8	1.00

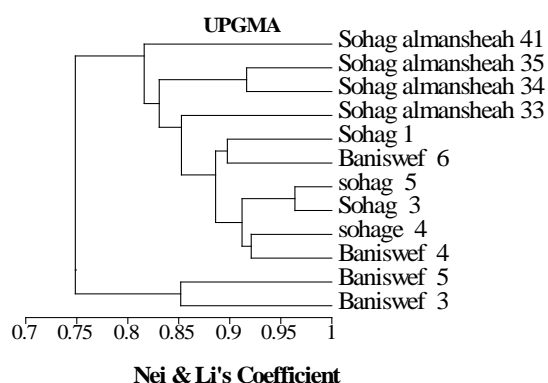


Figure 6. Dendrogram representing the genetic relationship among the twelve durum wheat genotypes using UPGMA cluster analysis of Nei-Lis similarity coefficient generated from SSRs markers

3.4. Identification of durum Wheat Varieties by RAPD analysis:

Characterization of the twelve durum wheat genotypes was performed by five RAPD primers. Figure (7) shows the banding patterns produced from each primer for the twelve genotypes. The amplification results by PCR for the studied wheat genotypes are illustrated in Table (11). A total of 20 amplified DNA fragments ranged from 189– 853bp, whereas ten fragments out of 20 loci, were monomorphic 50 % and 10bands were polymorphic (50%) with average of 2polymorphic fragments per primer. However, the primer OPB10 gave the highest number of amplified fragments (44 bands) for all studied genotypes, while the primer OPA3 showed the lowest number of amplified fragments. (30amplicons). No specific markers were detected in the electrophoretic patterns of all genotypes. The number of DNA fragments for each primer varied from 3 (OPA3) to 5 (OPB10) with average of 4 fragments per primer.

Table 11. The polymorphic loci amplified by the five RAPD primers.

Primer	Loci	range sizes of Loci	Polymorphic	Monomorphic	Polymorphism%	Specific bands	Total Bands in all genotypes
OPA1	4	200-700pb	3	1	75%	-	35
OPA4	3	300-700 pb	1	2	33.3%	-	30
OPB3	4	312-853 pb	3	1	75%	-	34
OPB10	5	789-189pb	2	3	60%	-	44
OPA11	4	208 -500 pb	1	3	25%	-	41
Total loci	20	189-853pb	10	10	50%	-	184

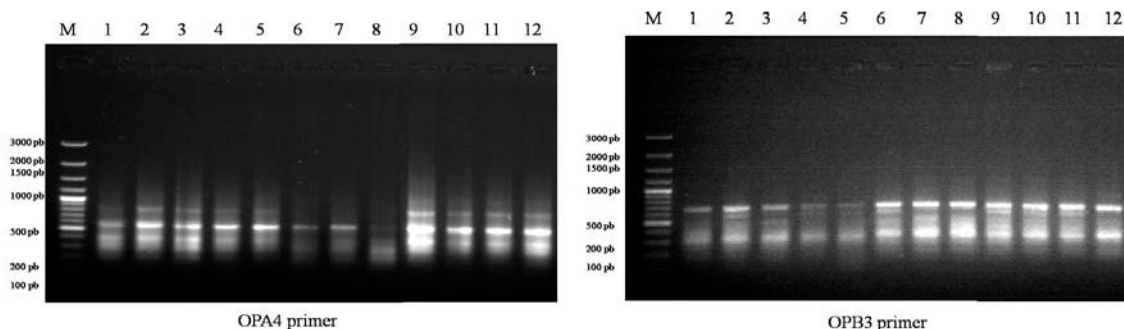


Figure (7): An example of RAPD banding pattern obtained using OPA4 and OPB3 primers with 12 Egyptian wheat cultivars and landraces. M: ladder. (1) Baniswef 3; (2) Baniswef 4; (3) Baniswef 5; (4) Baniswef 6; (5) Sohag 1; (6) Sohag 3; (7) Sohag 4; (8) Sohag 5; (9) Sohag almansheah 33; (10) Sohag almansheah 34; (11) Sohag almansheah 35; (12) Sohag almansheah 41.

Genetic Similarity: The genetic similarity index and dendrogram tree of the studied genotypes were performed using Nei-Li's similarity index depend on RAPD markers as shown in Table (12) and Figure (8). The genetic similarity ranged from 54 to 100%, with an average 77%. Sohag almansheah 33 and almansheah 34 showed identical genetic similarity (100%), Sohag1 and Baniswef 4 revealed high genetic similarity (94%), Sohag 4 and Baniswef 6 (94%), Baniswef 6 and Baniswef 5 (91%), while some genotypes revealed low genetic similarities such as Sohag3 and Baniswef 3 (54%), Sohag1 and Sohag 3 (54%), Sohag almansheah 35 and Baniswef 3 (59%), Sohag almansheah 41 and Sohag 3 (59%).

The dendrogram resulting from UPGMA cluster revealed that the twelve durum wheat genotypes could be divided into two main clusters. The first cluster contained only one genotype Sohag 3, the second cluster was divided into two sub-clusters; the first sub-cluster contained only one genotype Baniswef 3. The second sub-cluster contained two main groups; the first group was composed of three genotypes, Sohag almansheah 33 and Sohag almansheah 34 with similarity 100% and Sohag almansheah 35. The second group was divided into two sub-groups; the first sub-group included one genotype sohag 5, the second sub-group involved the rest of genotypes.

Table (12): Genetic similarity percentages of the twelve durum wheat varieties based on RAPD banding patterns.

	Baniswef 3	Baniswef 4	Baniswef 5	Baniswef 6	Sohag 1	Sohag 3	sohag 4	sohag 5	Sohag almansheah 33	Sohag almansheah 34	Sohag almansheah 35	Sohag almansheah 41
Baniswef 3	1.00											
Baniswef 4	0.81	1.00										
Baniswef 5	0.8	0.89	1.00									
Baniswef 6	0.77	0.92	0.91	1.00								
Sohag 1	0.80	0.94	0.88	0.97	1.00							
Sohag 3	0.54	0.57	0.61	0.59	0.54	1.00						
sohag 4	0.76	0.86	0.85	0.94	0.91	0.64	1.00					
sohag 5	0.71	0.82	0.81	0.85	0.81	0.58	0.84	1.00				
Sohag almansheah 33	0.74	0.85	0.84	0.81	0.84	0.70	0.73	0.76	1.00			
Sohag almansheah 34	0.74	0.85	0.84	0.81	0.84	0.70	0.73	0.76	1	1.00		
Sohag almansheah 35	0.59	0.85	0.71	0.81	0.84	0.70	0.73	0.76	0.86	0.80	1.00	
Sohag almansheah 41	0.71	0.92	0.86	0.89	0.86	0.59	0.82	0.85	0.81	0.81	0.81	1.00

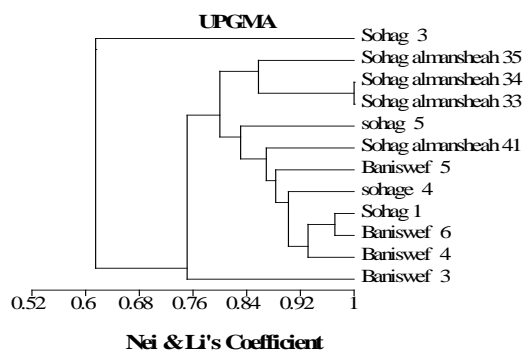


Figure 8. Dendrogram representing the genetic relationship among the twelve durum wheat genotypes using UPGMA cluster analysis of Nei-Lis similarity coefficient generated from RAPD markers.

3.5. Combined results of protein, ISSRs, SSRs and RAPD markers:

The genetic similarity coefficient and dendrogram tree were gathered between the twelve durum wheat cultivars after protein pattern, ISSRs, SSRs, and RAPD markers as illustrated in Table (13) and Figure (9). The genetic similarity ranged from 70 to 92 %, with average 81%. Sohag1, and Baniswef4 and Baniswef 6 showed the highest genetic similarity (92%), Sohag 4 and Sohag 5 (90%), Sohag almansheah 34 and Sohag almansheah 35 (90%). On the other hand, Sohag almansheah 41 and Baniswef 3 revealed the lowest genetic similarity (70%).

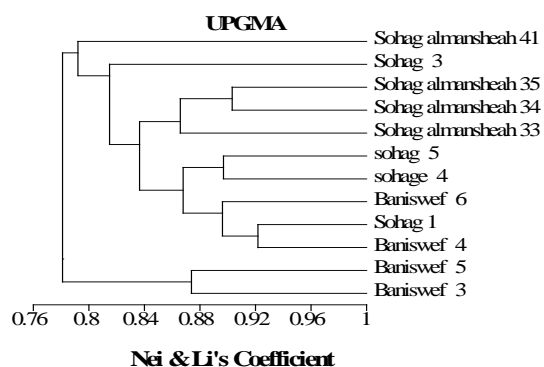
The dendrogram revealed that the twelve durum wheat genotypes could be divided into two main clusters. The first cluster contained only two cultivar Baniswef 3

and Baniswef 5 with similarity 80, the second cluster was divided into two sub-clusters; the first sub-cluster contained only one Landress Sohag almansheah 41. The second sub-cluster contained two main groups; the first group included only one genotype sohage 3, the second

group divided into two sub group; the first sub-group included three landraces Sohag almansheah 35, Sohag almansheah 34 and Sohag almansheah 33, the second sub-group included the rest of genotypes.

Table (13): Genetic similarity percentages of the twelve durum wheat varieties based on combination o proteins, ISSRs, SSRs and RAPD markers.

	Baniswef 3	Baniswef 4	Baniswef 5	Baniswef 6	Sohag 1	Sohag 3	Sohag 4	sohag 5	Sohag almansheah 33	Sohag almansheah 34	Sohag almansheah 35	Sohag almansheah 41
Baniswef 3	1.00											
Baniswef 4	0.84	1.00										
Baniswef 5	0.87	0.87	1.00									
Baniswef 6	0.79	0.87	0.85	1.00								
Sohag 1	0.82	0.92	0.87	0.92	1.00							
Sohag 3	0.71	0.79	0.74	0.80	0.82	1.00						
sohag 4	0.77	0.85	0.81	0.85	0.87	0.85	1.00					
sohag 5	0.80	0.88	0.82	0.87	0.89	0.83	0.90	1.00				
Sohag almansheah 33	0.73	0.83	0.78	0.83	0.86	0.79	0.84	0.87	1.00			
Sohag almansheah 34	0.73	0.80	0.76	0.80	0.84	0.83	0.85	0.86	0.88	1.00		
Sohag almansheah 35	0.73	0.80	0.75	0.82	0.85	0.80	0.83	0.86	0.86	0.90	1.00	
Sohag almansheah 41	0.70	0.77	0.74	0.81	0.80	0.73	0.79	0.80	0.79	0.81	0.83	1.00



Figure(9): Dendrogram generated from the combined results of proteins, ISSRs, SSRs, and RAPD markers among the twelve durum wheat genotypes using UPGMA cluster analysis of Nei-Lis similarity coefficient.

Regarding the collective data of proteins, ISSRs, SSRs and RAPD markers are shown in Table (14), the proteins fingerprint performs the highest percentage of polymorphism 81.8% with two specific bands. On the other hand, RAPD revealed the lowest percentage of polymorphism 50% with no specific bands. ISSRs markers gave (58.8 %) the percentage of polymorphism and gave the highest number of unique bands (7 bands), while SSRs displayed two specific bands and 62% polymorphism.

Table (14): Comparison of the genetic parameter between protein, ISSRs, SSRs and RAPD analysis for the twelve durum wheat genotypes.

Molecular Parameter	Value			
	Protein	ISSR	SSR	RAPD
Total Bands	22	68	50	20
Monomorphic Bands	4	28	19	10
Polymorphic Bands	18	40	31	10
% of Polymorphism	81.8%	58.8%	62%	50%
Unique Bands	2	7	2	-

4. Discussion

We study the genetic diversity of twelve durum genotypes depending on different types of markers, total seed storage protein as a biochemical marker and three types of molecular markers (SSRs, ISSRs, and RAPD markers). The biochemical markers reflect the genetic information of DNA. So, genetic diversity could be efficiently studied using either DNA markers (Mohammadi and Prasanna, 2003) and/or biochemical markers (Nagy *et al.*, 2009). In this study, we observed that the proteins fingerprint provided the highest polymorphism 81.8% with two specific bands, These results were in an agreement with those of (Tahir *et al.*, 1996) who found the high level of polymorphism detected in Pakistani wheat cultivars analyzed with protein markers and (Tahir, 2009) who indicated that protein fingerprint may be useful for selection aims in breeding programs of wheat varieties. Seed storage protein electrophoresis succeeded to identify barley cultivars (El-Rabey *et al.*, 2009b) in maize (Kamal and Yehia, 2010)

On the other hand, RAPD analyses revealed the lowest percentage of polymorphism 50% with no specific bands detected; this percentage of polymorphism was closely related with an earlier study by (Tahir, 2008) who detected the level of polymorphism for bread wheat (40%) and (35%) for durum wheat by RAPD analysis. In RAPD analyses, the number of alleles ranged from 3 to 5 per primer, with average of 4 per primer. The average of polymorphic band (PB) per primer (P) is 2 PB/P; this average was closely related with earlier studies in various plant species such as, 3.58 PB/P in *Cucumis sativus* (Manoharet *et al.*, 2013), 2.9 PB/P in bread wheat (Khaled *et al.*, 2015).

However, molecular markers gave different polymorphism average, ISSRs markers represented the highest number of unique bands (7 bands), 40 of 68 bands

were polymorphic with 58.8% polymorphism. The number of alleles ranged from 3 to 9 per primer, with an average of 5.6 per primer. ISSRs markers are highly polymorphic and repeatable even for intra-specific purposes in wheat varieties and could be used for cultivar identification. These results agreed with those of (Abou-Deif *et al.*, 2013) who used Eight ISSRs primers to characterize wheat genotypes including hexaploid, tetraploid and diploid in relation to their genetic background and geographical origin. ISSRs primers produced 112 amplified DNA fragments ranging in size from 127–1857 base pairs, 17 fragments were monomorphic (15.2%) and 95 fragments were polymorphic (84.8%) with average of 11.87 polymorphisms per primer. According to (Fang and Roose, 1997 and Naik *et al.*, 2017), ISSRs markers were found to be more effective in diversity study than RAPD markers. The present investigation clearly supported that view. The variation evidenced by ISSRs markers was due to selective amplification. They amplified conserved regions existing between the microsatellite repeat sequences, but RAPD markers are not selective; rather, they amplified any regions within the entire genome (Zietkiewicz *et al.* 1994). Although major bands from RAPD reactions were highly reproducible, minor bands could pose difficult to repeat due to the random priming nature of this PCR reaction and potential confounding effects associated with co-migration with other markers (Tessier *et al.*, 1999).

SSRs displayed two specific bands and the highest polymorphism, 31 out of 50 bands were polymorphic with 62% polymorphism. The number of alleles ranged from 1 to 10 per primer, with average of 6.2 per primer. This result agreed with previous study of (Li *et al.*, 2006) who reported that total of 97 alleles were detected at 16 SSR loci. At each locus, the number of alleles ranged from two to fourteen, with an average of 6.1. In wheat, SSRs markers showed a much higher level of polymorphism and informativeness than any other molecular marker (Prasad *et al.*, 2000; Wei *et al.*, 2003). Therefore, Usefulness Technical in detecting polymorphism and highly variable able to distinguish closely genetically related plant genotypes (Hanaan *et al.*, 2013; Ayman and Mohamed, 2019). Highly mutable loci of SSRs may be present at many sites in a genome (Morgante *et al.*, 1998). As the flanking sequence of these sites may be unique, primers can be designed to the flanking sequence (Jones *et al.*, 1997).

In this study, three of the polymerase chain reaction (PCR)-based systems (RAPD, ISSRs and SSRs). Each system is different in principle, type and amount of polymorphism detected. The level of polymorphism was the highest in SSRs analysis 62% compared with 50% of RAPDs and 58.8% of ISSR (Table 14). These results are in harmony with those of (El-Assal and Gaber, 2012) who found that the highest level of polymorphism appeared by SSRs 83% polymorphism compared with RAPD and ISSR analyses.

Among the different types of molecular markers, SSRs is a more accurate and informative marker because of its co-dominance and stability of results (Gupta *et al.*, 1996; Muhammad *et al.*, 2017). The co-dominant nature of SSR markers also permits the detection of a high number of alleles per locus and contributes to higher levels of expected heterozygosity being reached than would be possible with RAPD markers. However, this result also

depends on species under study (Belaj *et al.*, 2003). The highest levels of polymorphism for SSRs system compared to other systems was also reported in previous studies (Russel *et al.*, 1997; Rajora and Rahman, 2003; Parvin *et al.*, 2014; Ayman and Mohamed, 2019).

The similarity matrix of collective data differs from the similarity matrix of each studied marker (protein, RAPD, ISSRs and SSRs); and the similarity of each studied marker is different. This indicates that each studied marker has a specific characterization in discrimination of studied genotypes depending on the site of genomic DNA amplified. Finally, it can also be said that biochemical and molecular markers could be used either separately or together for genetic diversity studies in wheat.

5. Conclusion

Study the genetic diversity of twelve durum genotypes depending on biochemical (SDS-PAGE) marker and three types of molecular markers (SSRs, ISSRs, and RAPD markers). These markers discriminated most genotypes very effectively, whereas, SSRs markers were more discriminating than RAPD and ISSRs markers. The three molecular markers used in this study have shown an aptitude in the differentiation of the cultivars, the congruence between RAPD, ISSR and SSR data sets suggested that either methods, or a combination of all, are applicable to expand the diversity studies in wheat cultivars. There are different strengths and limitations for marker systems, and knowledge of these may be used to guide the choice of techniques.

Finally it can also be said that molecular and biochemical markers could be used either together or separately for studying the genetic relationships among wheat genotypes.

References

- Abou-Deif MH, Rashed MA, Sallam MAA, Mostafa EAH and Ramadan WA. 2013. Characterization of Twenty Wheat Varieties by ISSR Markers. *Middel-East J. Scientific Research*, **15** (2): 168-175.
- Agrama HA and Tuinstra MR. 2003. Phylogenetic diversity and relationships among sorghum accessions using SSRs and RAPDs. *African. J. Biotechnology*, **2**: 334-340.
- Ayman EF and Mohamed A. 2019. Molecular Characterization and Genetic Diversity In Some Egyptian Wheat (*Triticum Aestivum* L.) Using Microsatellite Markers. *Potra-Slovak J. Food Sciences*, **13** (1): 100-108.
- Belaj A, Satovic Z, Cipriani G, Baldoni L, Testolin R, Rallo L and Trujillo I. 2003. Comparative study of the discriminating capacity of RAPD, AFLP and SSR markers and of their effectiveness in establishing genetic relationships in olive. *Theor. Appl. Genet.*, **107**: 736-744.
- Cao WG, Hucl PSG and Chibbar RN. 1998. Genetic diversity within spelta and machawheats based on RAPD analysis. *Euphytica*, **104**: 181-189.
- Czaplicki A, Borsuk P and Moraczewski I. 2000. Molecular methods of identification of wheat varieties. *J. Biomol. Struc. Dynam.*, **17**(6): 2-13.
- Dubcovsky J. 2004. Marker-assisted selection in public breeding programs: The wheat experience. *Crop. Sci.*, **44**(6): 1895-1898.
- El-Assal SED and Gaber A. 2012. Discrimination capacity of RAPD, ISSR and SSR markers and their effectiveness in

- establishing genetic relationship and diversity among Egyptian and Saudi wheat cultivars. *American J. Applied Sci.*, **9**: 724-735.
- El-Rabey HA, Abdellatif KF and KhidrYA. 2009b. Cytogenetic and biochemical study on some barley (*Hordeum vulgare* L.) cultivars. *Aust. J. Basic Appl. Sci.*, **3**: 644-651.
- Fang DQ and Roose ML. 1997. Identification of closely related citrus cultivars with inter-simple sequence repeat markers. *Theor. Appl. Genet.*, **95**:408-417.
- Gupta PK, Balyan HS, Sharma PC and Ramesh B. 1996. Microsatellites in plants: a new class of molecular markers. *Curr. Sci.*, **70**:45-54.
- Hanaa MA, Samah MME and Kamal FA. 2013. SSR- Based Genetic Diversity Assessment in Tetraploid and Hexaploid Wheat Populations. *British Biotechnology Journal*, **13** (3): 390-404.
- Jones J, Edwards KJ, Castaglione S, Winfield MO, Sala F, van de Wiel C, Bredemeijer G, Vosman B, Matthes M, Daly A, Bretschneider R, Bettini P, Buiatti M, Maestri E and Malcevski A. 1997. Reproducibility testing of RAPD, AFLP and SSR markers in plants by a network of European laboratories. *Mol. Breed.*, **3**: 381-390.
- Kamal FA and Yehia AK. 2010. Genetic Diversity of New Maize Hybrids Based on SSR Markers as Compared with Other Molecular and Biochemical Markers. *J. Crop Sci. Biotechnology*, **13** (3) : 139 – 145.
- Kebriyae D, Kordrostami M, Rezadoost MH and Lahiji HS. 2012. QTL analysis of agronomic traits in rice using SSR and AFLP markers. *Not. Sci. Biol.*, **4**(2): 116-123.
- Khaled AGA, Motawea MH and Said AA. 2015. Identification of ISSR and RAPD markers linked to yield traits in bread wheat under normal and drought conditions. *J. Genet. Eng. Biot.*, **13**(2):243-252.
- Khurana KV, Kachhwaha S and Kothari SL. 2012. Characterization of genetic diversity in *Jatropha curcas* L. germplasm using RAPD and ISSR markers. *Indian. J. Biot.*, **11**(1):54-61.
- Kovach WL. 1998. MVSP_ Multi-Variant Statistical Package for windows, ver. 3.0 Kovach computing services: Pentraeth, Wales.
- Laemmli UK. 1970. Cleavage of structural proteins during the assembly of the head of bacteriophage T4. *Nature*, **227**: 680-685.
- Li W, Zhang DF, Wei YM, Yan ZH and Zheng YL. 2006. Genetic Diversity of *Triticum turgidum* L. Based on Microsatellite Markers. *Rus. J. Genet.*, **42**(3) 311-316.
- Malik R, Sareen S, Kundu S. and Shoran J. 2010. The use of SSR and ISSR markers for assessing DNA polymorphism and genetic diversity among Indian bread wheat cultivars. *Prog. Agri.*, **12**: 82-89.
- Manohar SH, Murthy HN and Ravishankar KV. 2013. Genetic diversity in a collection of *Cucumis sativus* L. assessed by RAPD and ISSR markers. *J. Plant. Bioch. Biot.*, **22**(2):241-244.
- Mohammadi SA and Prasanna BM. 2003. Analysis of genetic diversity in crop plants-salient statistical tools and considerations. *Crop. Sci.*, **43**: 1235-1248.
- Muhammad AN, Muhammad AN, Muhammad QS, Yıldız D, Gonul C, Mehtap Y, Rüştü H, Fiaz A, Ahmad A, Nitin L, Hakan Ö, Gyuhwa C and Faheem SB. 2017. DNA molecular markers in plant breeding: current status and recent advancements in genomic selection and genome editing. *Biot. Equipment*, **32** (2): 261-285.
- Nagy E, Spitko T and Marton LC. 2009. Applicability of biochemical and genetic markers in the polymorphism analysis of maize lines. *Cereal. Res. Commun.*, **37**: 373-381.
- Naik A, Prajapat P, Krishnamurthy R and Pathak JM. 2017. Assessment of genetic diversity in *Costus pictus* accessions based on RAPD and ISSR markers. *Biotechnology*, **3**: 7:70.
- Parvin G, Reza T and Fatemeh K. 2014. Genetic diversity and geographical differentiation of Iranian landrace, cultivars, and exotic chickpea lines as revealed by morphological and microsatellite markers. *Phys. Mol. Biol. Plant*, **20**(2):225-233.
- Prasad M, Varshney RK, Roy JK, Balyan HS and Gupta PK. 2000. The Use of Microsatellites for Detecting DNA Polymorphism, Genotype Identification and Genetic Diversity in Wheat. *Theor. Appl. Genet.*, **100**: 584-592.
- Rajora O and Rahman . 2003. Microsatellite DNA and RAPD fingerprinting, identification and genetic relationships of hybrid poplar (*Populus x canadensis*) cultivars. *Theor. Appl. Genet.*, **106**: 470-477.
- Russell JR, Fuller JD, Macaulay M, Hatz BG, Jahoor A, Powell W and Waugh R. 1997. Direct comparison of levels of genetic variation among barley accessions detected by RFLPs, AFLPs, SSRs and RAPDs. *Theor. Appl. Genet.*, **95**: 714-7
- Sofalian O, Chaparzadeh N, Javanmard A and Hejazi MS. 2008. Study the genetic diversity of wheat landraces from northwest of Iran based on ISSR molecular markers. *International. J. Agric. Biol.*, **10**: 466-468.
- Tahir M, Turchetta T, Anwar R and Lafiandra D. 1996. Assessment of genetic variability in hexaploid wheat landraces of Pakistan based on polymorphism for HMW glutenin subunits. *Genet. Res. Crop.*, **43**: 221-220.
- Tahir NA. 2009. Polymorphism of Protein Fractions as Biochemical Markers for Identification of Wheat Varieties. *Jordan Journal of Biological Sciences*, **2**(4): 159-166
- Tahir NA. 2008. Assessment of genetic diversity among wheat varieties in Sulaimanyah using random amplified polymorphic DNA (RAPD) analysis. *Jordan. Journal of Biological Sciences*, **1**(4): 159-164
- Tanyolac B. 2003. Inter-simple sequence repeats (ISSR) and RAPD variation among wild barley (*Hordeum vulgare* subsp. spontaneum) populations from west Turkey. *Genet. Res. Crop.*, **50**: 611-614.
- Tessier C, David J, This P, Boursiquot JM and Charrier A. 1999. Optimization of the choice of molecular markers for varietal identification in *Vitis vinifera* L. *Theor. Appl. Genet.* **98**:171-178.
- Velasco-Ramirez A P, Torres-Moran M I, Molina-Moret S, Sanchez-Gonzalez JJ and Santacruz-Ruvalcaba F, 2014. Efficiency of RAPD, ISSR, AFLP and ISTR markers for the detection of polymorphisms and genetic relationships in camote de cerro (*Dioscorea* spp.) *Electronic Journal of Biotechnology*, **17**(2):65-71.
- Verma KS, Kachhwaha S and Kothari SL. 2013. In vitro plant regeneration of *Citrullus colocynthis* (L.) Schard. and assessment of genetic fidelity using ISSR and RAPD markers. *Ind. J. Biotechnology*, **12**:409-414.
- Wei YM, Zheng YL, Yan Z, W W, Zhang ZQ and Lan XJ. 2003. Genetic Diversity in Chinese Endemic Wheats Based on STS and SSR Markers. *Wheat Information Service*, **97**: 9-15.
- Zietkiewicz E, Rafalski A and Labuda D. 1994. Genome fingerprinting by Simple Sequence Repeat (SSR) anchored polymerase chain reaction amplification. *Genomics*, **20**: 176-183.

Heat Exposure Affects the mRNA Levels of Antioxidant Enzymes in Embryonic and Adult Broiler Chickens

Amneh H. Tarkhan¹, Khaled M. M. Saleh¹ and Mohammad B. Al-Zghoul^{2,*}

¹Department of Applied Biological Sciences, Faculty of Science and Arts, ²Department of Basic Medical Veterinary Sciences, Faculty of Veterinary Medicine, Jordan University of Science and Technology, P.O. Box 3030, Irbid 22110, Jordan

Received: October 14, 2019; Revised: December 2, 2019; Accepted: December 8, 2019

Abstract

Artificial selection pressures utilized by the poultry industry have resulted in broilers capable of fast growth but possessing poor thermoregulatory capacity. Modern broiler strains are, therefore, especially vulnerable to heat exposure during the incubation, rearing, and transport processes. The objective of the present study was to investigate the effects of heat exposure (HE) during embryonic and adult life on catalase, NADPH oxidase 4 (*NOX4*), and superoxide dismutase 2 (*SOD2*) expression. Briefly, the experimental design involved two phases: HE during embryonic development as well as HE during adult life. For the first phase, Ross eggs were divided into control (n=268) and HE (n=270) groups that were incubated under standard (37.8°C and 56% relative humidity (RH)) and HE (39°C and 65% RH for 18 h/day from embryonic day (ED) 10 to 18) conditions, respectively. At ED 18, embryos (n=6) from each group were randomly selected and euthanized to obtain heart, liver, and spleen samples. For the second phase, 28 day-old adult Cobb chickens were exposed to an elevated temperature of 40°C for 7 hours, and, at 0, 1, 3, 5, and 7 hours of HE, 5 chickens were randomly selected and euthanized to obtain liver samples. Embryonic heat exposure resulted in dysregulated catalase, *NOX4*, and *SOD2* mRNA expression. Catalase mRNA expression was significantly higher in the hearts (p=0.014) and spleens (p=0.0299) but significantly lower in the livers (p=0.002) of heat-exposed embryos. Likewise, in heat-exposed embryos, *SOD2* mRNA expression was significantly higher in the hearts (p=0.0002) and spleens (p=0.041) but significantly lower in the livers (p=0.009). Although *NOX4* mRNA levels were significantly higher in the hearts (p=0.003) and significantly lower in the livers (p=0.03) of heat-exposed controls, this expression did not change in the spleens (p=0.79). In contrast, heat stress during adult life affected only the catalase mRNA levels during certain time points, namely after 7 hours of heat exposure (p=0.0001). Since the aforementioned genes play essential roles in the prevention of oxidative stress, the present study could help elucidate the mechanism behind heat-induced oxidative stress in the context of broiler chickens.

Keywords: heat stress; broiler; antioxidant; liver; catalase; superoxide dismutase.

1. Introduction

The broiler industry is the fastest-growing meat industry on a global scale (Chang and Hui-Shung, 2007). Over the past half-century, artificial selection pressures have increased the growth rates of broiler chickens by more than 400% (Zuidhof *et al.*, 2014). Despite these advances, broiler growth is still dependent upon environmental rearing conditions such as feed and water provision, flock density, and ambient temperature, the latter of which can seriously impact broiler welfare (Lara and Rostagno, 2013). In fact, it has been suggested that artificially selecting for increased growth rates has compromised the thermoregulatory capacity of broilers, making them especially susceptible to heat stress (Sandercock *et al.*, 2006). Heat stress is a major cause of broiler mortality during rearing and transportation, resulting in major economic losses and reduced meat quality (St-Pierre *et al.*, 2003; dos Santos *et al.*, 2017).

In broilers, heat stress often manifests in the form of oxidative stress, which occurs as a result of the imbalance

between an organism's antioxidant defence system and its reactive oxygen species (ROS) (Estévez, 2015). NADPH oxidase 4 (*NOX4*) is a constitutionally active membrane-bound complex that helps maintain oxidative homeostasis by acting as an oxygen sensor (Nisimoto *et al.*, 2014). In the process, *NOX4* generates superoxide (O_2^-) radicals and hydrogen peroxide (H_2O_2), and their unchecked production contributes to damage of cellular DNA, lipids, and proteins (Mujahid *et al.*, 2005; Mishra and Jha, 2019). Although they are damaging in excess, both superoxide and hydrogen peroxide play an essential role in innate immune defence mechanisms, and *NOX4* under-expression increases an organism's susceptibility to microbial infection (Rada and Leto, 2008). A plethora of mechanisms are involved in the prevention of oxidative stress in the case of elevated *NOX4* expression, the most notable of which are superoxide dismutase 2 (*SOD2*) and catalase (Al-Zghoul *et al.*, 2019).

Serving as the first line of defence against heat-induced oxidative stress, the antioxidant enzymes *SOD2* and catalase dismutate superoxide and disproportionate hydrogen peroxide, respectively (Matsumoto *et al.*, 2009;

* Corresponding author e-mail: alzghoul@just.edu.jo.

Ighodaro and Akinloye, 2018). As can be seen from Figure 1, SOD2 and catalase are essential to the prevention of oxidative damage in the aftermath of NOX4 expression. Furthermore, heat-stressed broiler chickens were reported to have modulated levels of SOD2 and catalase expression that differed between different types of tissues (Surai, 2016; Del Vesco *et al.*, 2017; Kikusato and Toyomizu, 2019). Compared to other organs, the liver is especially vulnerable to the effects of oxidative stress because of its key role in maintaining homeostasis (Bonkovsky, 2015; Li *et al.*, 2015). It has been previously shown that the liver of broiler chickens is more susceptible than the heart during periods of acute heat stress (Lin *et al.*, 2006).

The optimum incubation temperature for a chicken embryo is $37.8^{\circ}\text{C} \pm 0.3^{\circ}\text{C}$; higher temperatures accelerate growth while lower temperatures inhibit it (Yalcin and Siegel, 2003). To combat the effects of heat stress, thermal manipulation (TM), which is the increase of incubation temperature for a certain period of time during embryonic development, enhances a broiler's ability to tolerate heat stress as an adult (Moraes *et al.*, 2003; Morita *et al.*, 2016; Nariç *et al.*, 2016; Al-Zghoul *et al.*, 2019; Saleh and Al-Zghoul, 2019; Al-Zghoul *et al.*, 2019). Such thermal manipulation should be intermittent and not continuous, as the latter negatively affected the hatchability and overall performance parameters of broilers (Piestun *et al.*, 2008). Although there are previous reports of the post-hatch benefits of embryonic thermal manipulation, the exact effect on embryo physiology and metabolic function is not well-understood.

Despite warming global temperatures and a rapidly growing broiler industry, there is only a small number of studies on the effect of heat-induced oxidative stress on broiler liver function. Similarly, there is a dearth of information on the effects of oxidative stress on the embryonic cardiac, hepatic, and splenic antioxidant function of broilers. Therefore, the main objectives of the present study are to investigate the effects of embryonic heat exposure and the impact of post-hatch heat stress on the cardiac, hepatic and splenic expression of the catalase, NOX4, and SOD2 genes in broiler chickens.

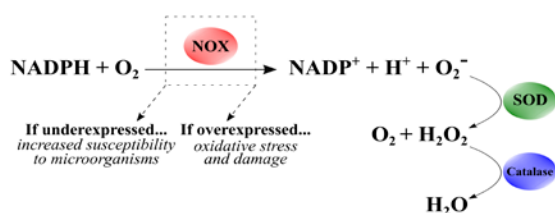


Figure 1. NOX4 acts as an oxygen sensor to protect against oxidative damage. However, its activity generates superoxide and hydrogen peroxide, which must then be dismutated and disproportionated by superoxide dismutase 2 (SOD2) and catalase, respectively.

2. Material and methods

All experimental procedures employed in the current study were approved by the Animal Care and Use Committee at Jordan University of Science and Technology. **Figure 2** illustrates the details of the experimental design described in this section.

2.1. Heat exposure during embryonic development

Fertile Ross eggs ($n=600$) were acquired from Al-watannia poultry certified breeder in Amman, Jordan, and thoroughly examined for any abnormalities. After excluding damaged eggs ($n=17$), the remaining eggs were incubated in two Type I HS-SF commercial incubators (Masalles, Spain) under standard conditions (37.8°C and 56% relative humidity (RH)) until embryonic day (ED) 10. The viability of the incubated eggs was checked on embryonic day (ED) 7 by candling, in which infertile eggs and eggs with dead embryos were excluded from the present study ($n=35$). On ED 10, the eggs in the first incubator were considered as the control group ($n=268$), and the eggs in the other incubator were considered as the heat-exposed (HE) group ($n=280$). The eggs of the control group were maintained at 37.8°C and 56% RH for the entirety of the incubation period, while those in the HE group were incubated at 39°C and 65% RH for 18 h/day during ED 10 to 18. On ED 18, six embryos were randomly selected from each group and their hearts, livers, and spleens were collected.

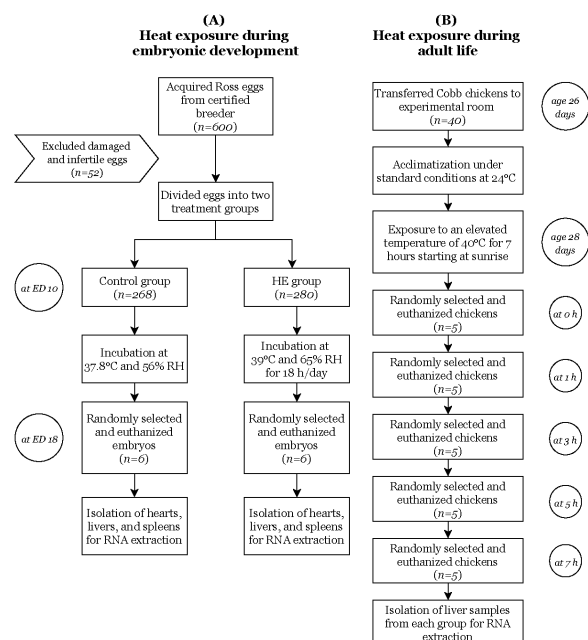


Figure 2. Summary of the experimental procedures employed in the present study. ED: embryonic day; HE: heat-exposed; RH; relative humidity.

2.2. Heat exposure during adult life

At the age of 26 days, healthy Cobb chickens ($n=40$) were transferred to the experimental room in order to acclimate under standard conditions and at a room temperature of 24°C . At the age of 28 days, the chickens were exposed to an elevated temperature of 40°C for 7 hours starting at sunrise. After 0, 1, 3, 5, and 7 hours of heat exposure, 5 chickens were randomly selected and euthanized in order to extract liver samples. The chickens euthanized at 0 hours of heat exposure were considered as the control group to be compared with all other time intervals.

2.3. Total RNA extraction and reverse transcription

Total RNA was extracted using the Direct-zol™ RNA MiniPrep Kit (Zymo Research, USA) alongside a TRI

Reagent Kit (Zymo Research, USA). RNA concentrations were determined using the PowerWave XS2 microplate spectrophotometer (BioTek, USA). 2 µg of total RNA from each sample was used to carry out reverse transcription by means of the Power cDNA Synthesis Kit (iNtRON Biotechnology, South Korea).

2.4. Relative quantification via real-time RT-PCR

The QuantiFast SYBR Green PCR Kit (Qiagen, USA) was used on the Rotor-Gene Q MDx 5plex HRM instrument (Qiagen, USA). Briefly, the 20 µl reaction mix was prepared from 10 µl of master mix, 1.2 µl of forward primer, 1.2 µl of reverse primer, 1 µl of sample cDNA, and 6.6 µl of nuclease-free water. The PCR process involved a single cycle of 95°C for 5 mins, 40 cycles of 95°C for 10s followed by 30s at 55°C, and 72°C for 10s with final melting at 95°C for 20s. The fluorescence emission detection was carried out during the extension step. 28S rRNA was used as an internal control to which the fold changes in mRNA levels were normalized. The single target amplification specificity was assessed using the generated melting curve. The relative quantitation was calculated automatically. Table 1 shows the primer sequences that were used in the real-time RT-PCR analysis (Al-Zghoul *et al.*, 2019).

2.5. Statistical analysis

IBM SPSS Statistics v. 23 was utilized for all statistical analyses. Catalase, *NOX4*, and *SOD2* mRNA levels were expressed as means ± SD. One-way analysis of variance (ANOVA) was used to compare between the control and HE groups during embryonic development. However, ANOVA followed by the all-pairs Bonferroni test was used to compare the difference between time intervals of heat exposure (0, 1, 3, 5, and 7 h). Parametric differences were considered to be statistically significant at $P < 0.05$.

Table 1. Primer sequences used in the PCR analysis.

Gene	Forward (5' to 3')	Reverse (5' to 3')
<i>NOX4</i>	CCAGACCAACTTAGAGGA ACAC	TCTGGGAAAGGCTCAGTA GTA
<i>SOD2</i>	CTGACCTGCCTTACGACT ATG	CGCCTCTTGTATTCTCC TCT
Catalase	GAAGCAGAGAGTTCCCA TTTA	CATACGCCATCTGTTCTAC CTC
28S rRNA	CCTGAATCCCGAGGTAA CTATT	GAGGTGCGGCTTATCATCT ATC

3. Results

3.1. Effect of embryonic heat exposure

The effects of embryonic heat exposure on the mRNA levels of *NOX4*, *SOD2*, and catalase in broiler hearts, livers, and spleens are shown in **Figure 3**. Catalase and *SOD2* mRNA levels were significantly higher in hearts ($p=0.014$; $p=0.0002$) and spleens ($p=0.0299$; $p=0.041$) but significantly lower in the livers of HE embryos compared to controls ($p=0.002$; $p=0.009$). In addition, *NOX4* mRNA levels were significantly higher in the hearts ($p=0.003$) and significantly lower in the livers of HE embryos compared to controls ($p=0.03$). However, the splenic mRNA levels of *NOX4* were not significantly different between the two groups ($p=0.79$).

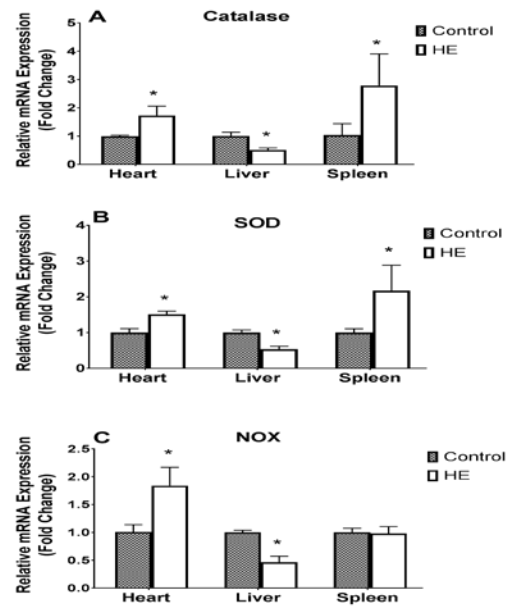


Figure 3. mRNA expression levels of the catalase, *NOX4*, and *SOD2* genes in broilers exposed to heat during embryonic development. In panels A and B, cardiac and splenic catalase and *SOD2* expression is significantly higher in the HE group, while hepatic expression is significantly lower. In panel C, there was no difference in splenic *NOX4* expression between the control and HE groups, but cardiac and hepatic expressions were respectively higher and lower in the HE group. * mean ± SD of HE group is significantly different with control group.

3.2. Effect of adult heat exposure

The effects of heat exposure on the mRNA levels of *NOX4*, *SOD2*, and catalase in the livers of 28 day old chickens are shown in **Figure 4**. Heat exposure did not result in significant changes in the mRNA levels of *NOX4* and *SOD2* in broilers ($p>0.05$). Moreover, heat exposure did not significantly change catalase mRNA levels after 1, 3, and 5 h ($p>0.05$). In contrast, the mRNA levels of catalase were significantly higher after 7 h of heat exposure compared to 0 h ($p=0.0001$).

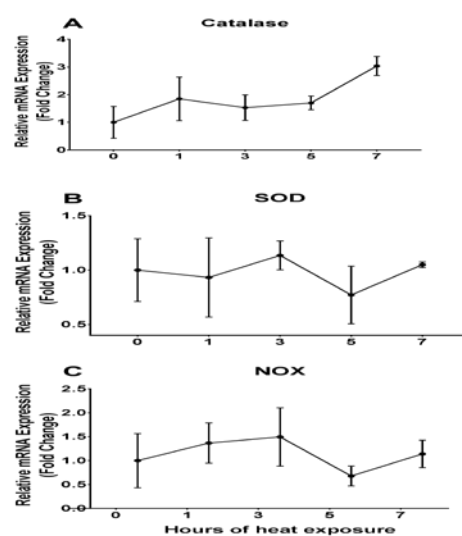


Figure 4. Hepatic mRNA expression levels of the catalase, *NOX4*, and *SOD2* genes in broilers exposed to heat during adult life. In panel A, catalase expression was significantly higher only after 7 h of HE compared to 0 h. In panels B and C, HE did not significantly affect *SOD2* and *NOX4* expression.

4. Discussion

Due to artificial selection pressures imposed by the commercial poultry industry, modern broiler breeds possess significantly enhanced weight gain and feed efficiency rates compared to their predecessors (Zuidhof *et al.*, 2014). However, these selection pressures did not result in similar improvements to the cardiovascular, immune, and respiratory systems, all of which contain organs that play essential roles in broiler thermoregulation (Havenstein *et al.*, 2003). Heat exposure during adult life poses a serious and imminent threat to the global poultry industry, resulting in substantial commercial losses (St-Pierre *et al.*, 2003). Therefore, the aim of the present study was to investigate the effects of heat exposure during the embryonic and adult lives of broiler chickens on the mRNA levels of certain antioxidant enzymes, mainly with regard to the catalase, *NOX4*, and *SOD2* genes.

Catalase mRNA levels were elevated in the heart and spleen but reduced in the liver of embryos exposed to heat. Likewise, catalase mRNA levels significantly increased in the livers of adult broilers after 7 hours of heat exposure. Previously, catalase expression has been reported to increase in heat-stressed broilers in response to heat-induced oxidative stress (Ismail *et al.*, 2013; Del Vesco *et al.*, 2017). Moreover, catalase activity in heat-stressed broilers can be enhanced by means of dietary supplementation (Kumbhar *et al.*, 2018). However, it was found that heat stress during embryonic and adult life resulted in reduced catalase mRNA expression levels in the livers of Cobb and Hubbard breeds (Al-Zghoul *et al.*, 2019).

After heat exposure, *NOX4* mRNA levels were found to significantly increase and decrease in embryo hearts and livers, respectively, although splenic *NOX4* expression remained the same. Contrastingly, *NOX4* mRNA expression levels decreased in the livers of heat-stressed broilers exposed to embryonic thermal manipulation (Al-Zghoul *et al.*, 2019). In adult broilers, heat exposure did not result in significant changes to hepatic *NOX4* expression (Habashy *et al.*, 2018). Nevertheless, *NOX4* mRNA expression levels increased in avian skeletal muscle cells upon exposure to heat stress (Kikusato and Toyomizu, 2019).

Our findings show that heat exposure caused *SOD2* mRNA levels to increase in the hearts and spleens and decrease in the livers of broiler embryos. In contrast, heat exposure during adulthood did not significantly alter *SOD2* expression in broilers. Increased *SOD2* expression in certain types of skeletal muscle was reported in 21-day-old broilers exposed to heat stress (Kikusato and Toyomizu, 2019). In contrast, thermally manipulated Cobb and Hubbard broilers exposed to heat stress exhibited reduced hepatic *SOD2* mRNA expression levels compared to controls (Al-Zghoul *et al.*, 2019).

Differences between antioxidant gene expression in embryos and adults could be due to the fact that embryos are poikilothermic and, therefore, highly sensitive to temperature changes (Yalcin and Siegel, 2003; Noiva *et al.*, 2014). In fact, TM during embryonic development results in lower plasma triiodothyronine concentrations and reduced oxygen consumption, both of which control metabolism and the production of heat in fast-growing

chickens (Loyau *et al.*, 2014). Moreover, the liver has a chief role in the metabolic function and homeostatic maintenance of broilers, particularly in response to cyclic heat stress (Jastrebski *et al.*, 2017).

5. Conclusions

The present findings indicate that heat exposure during embryonic and adult broiler life can have significant effects on a broiler's response to oxidative stress. Of special importance is the catalase gene, as its expression was dysregulated during heat challenge in both the embryonic and adult phases of a broiler's life. Limitations of the present study include the fact that it only utilized one broiler breed (Cobb or Ross) for each experimental phase. In the future, different broiler strains should also be investigated in the context of antioxidant mRNA expression after embryonic and post-hatch heat exposure.

Conflict of Interest

The authors declare no conflict of interest.

Acknowledgements

The authors would like to express their deep appreciation and thanks to the Deanship of Research at Jordan University of Science & Technology for its financial support of this work (Grant#: 44/2019). The authors would also like to thank Eng. Ibrahim Alsukhni for his excellent technical assistance and valuable comments.

References

- Al-Zghoul Mohammad Borhan, Alliftawi ARS, Saleh KMM, Jaradat ZW. 2019. Expression of digestive enzyme and intestinal transporter genes during chronic heat stress in the thermally manipulated broiler chicken. *Poult Sci.* **98**:4113–4122.
- Al-Zghoul Mohammad Borhan, Saleh KM, Ababneh MMK. 2019. Effects of pre-hatch thermal manipulation and post-hatch acute heat stress on the mRNA expression of interleukin-6 and genes involved in its induction pathways in 2 broiler chicken breeds. *Poult Sci.* **98**:1805–1819.
- Al-Zghoul M B, Sukker H, Ababneh MM. 2019. Effect of thermal manipulation of broilers embryos on the response to heat-induced oxidative stress. *Poult Sci* [Internet]. [cited 2019 Nov 29]; 98:991–1001. Available from: <https://academic.oup.com/ps/article/98/2/991/5075983>
- Bonkovsky HL. 2015. On stress and the liver: a chicken and egg conundrum. *Gastroenterology.* **148**:894–7.
- Chang, Hui-Shung. 2007. Overview of the World Broiler Industry: Implications for the Philippines. *Asian J Agric Dev.* **04**:1–16.
- Estévez M. 2015. Oxidative damage to poultry: from farm to fork. *Poult Sci.* **94**:1368–1378.
- Habashy WS, Milfort MC, Rekaya R, Aggrey SE. 2018. Expression of genes that encode cellular oxidant/antioxidant systems are affected by heat stress. *Mol Biol Rep.* **45**:389–394.
- Havenstein G, Ferket P, Qureshi M. 2003. Growth, livability, and feed conversion of 1957 versus 2001 broilers when fed representative 1957 and 2001 broiler diets. *Poult Sci.* **82**:1500–1508.
- Ighodaro OM, Akinloye OA. 2018. First line defence antioxidants-superoxide dismutase (SOD), catalase (CAT) and glutathione peroxidase (GPX): Their fundamental role in the entire antioxidant defence grid. *Alexandria J Med.* **54**:287–293.

- Ismail IB, Al-Busadah KA, El-Bahr SM. 2013. Oxidative Stress Biomarkers and Biochemical Profile in Broilers Chicken Fed Zinc Bacitracin and Ascorbic Acid under Hot Climate. *Am J Biochem Mol Biol.* **3**:202–214.
- Jastrebski SF, Lamont SJ, Schmidt CJ. 2017. Chicken hepatic response to chronic heat stress using integrated transcriptome and metabolome analysis. *PLoS One* [Internet]. [cited 2019 Nov 30]; **12**:e0181900. Available from: <https://dx.plos.org/10.1371/journal.pone.0181900>
- Kikusato M, Toyomizu M. 2019. Differential effects of heat stress on oxidative status of skeletal muscle with different muscle fibre compositions in broiler chicken. *J Anim Feed Sci.* **28**:78–82.
- Kumbhar S, Khan AZ, Parveen F, Nizamani ZA, Siyal FA, El-Hack MEA, Gan F, Liu Y, Hamid M, Nido SA, Huang K. 2018. Impacts of selenium and vitamin E supplementation on mRNA of heat shock proteins, selenoproteins and antioxidants in broilers exposed to high temperature. *AMB Express.* **8**:112.
- Lara LJ, Rostagno MH. 2013. Impact of Heat Stress on Poultry Production. *Anim an open access J from MDPI.* **3**:356–69.
- Li S, Tan H-Y, Wang N, Zhang Z-J, Lao L, Wong C-W, Feng Y. 2015. The Role of Oxidative Stress and Antioxidants in Liver Diseases. *Int J Mol Sci.* **16**:26087–124.
- Lin H, Decuypere E, Buyse J. 2006. Acute heat stress induces oxidative stress in broiler chickens. *Comp Biochem Physiol Part A Mol Integr Physiol.* **144**:11–17.
- Loyau T, Métayer-Coustard S, Berri C, Crochet S, Cailleau-Audouin E, Sannier M, Chartrin P, Praud C, Hennequet-Antier C, Rideau N, et al. 2014. Thermal Manipulation during Embryogenesis Has Long-Term Effects on Muscle and Liver Metabolism in Fast-Growing Chickens. *Wu S-B, editor. PLoS One* [Internet]. [cited 2019 Nov 30]; **9**:e105339. Available from: <https://dx.plos.org/10.1371/journal.pone.0105339>
- Matsumoto H, Silverton SF, Debolt K, Shapiro IM. 2009. Superoxide dismutase and catalase activities in the growth cartilage: Relationship between oxidoreductase activity and chondrocyte maturation. *J Bone Miner Res.* **6**:569–574.
- Mishra B, Jha R. 2019. Oxidative Stress in the Poultry Gut: Potential Challenges and Interventions. *Front Vet Sci.* **6**:60.
- Moraes VMB, Malheiros RD, Bruggeman V, Collin A, Tona K, Van As P, Onagbesan OM, Buyse J, Decuypere E, Macari M. 2003. Effect of thermal conditioning during embryonic development on aspects of physiological responses of broilers to heat stress. *J Therm Biol.* **28**:133–140.
- Morita VS, Almeida VR, Matos Junior JB, Vicentini TI, van den Brand H, Boleli IC. 2016. Incubation temperature alters thermal preference and response to heat stress of broiler chickens along the rearing phase. *Poult Sci.* **95**:1795–1804.
- Mujahid A, Yoshiki Y, Akiba Y, Toyomizu M. 2005. Superoxide radical production in chicken skeletal muscle induced by acute heat stress. *Poult Sci.* **84**:307–314.
- Narınç D, Erdoğan S, Tahtabiçen E, Aksoy T. 2016. Effects of thermal manipulations during embryogenesis of broiler chickens on developmental stability, hatchability and chick quality. *animal.* **10**:1328–1335.
- Nisimoto Y, Diebold BA, Cosentino-Gomes D, Lambeth JD, Lambeth JD. 2014. Nox4: A Hydrogen Peroxide-Generating Oxygen Sensor. *Biochemistry.* **53**:5111–5120.
- Noiva RM, Menezes AC, Peleteiro MC. 2014. Influence of temperature and humidity manipulation on chicken embryonic development. *BMC Vet Res.* **10**.
- Piestun Y, Shinder D, Ruzal M, Halevy O, Brake J, Yahav S. 2008. Thermal Manipulations During Broiler Embryogenesis: Effect on the Acquisition of Thermotolerance. *Poult Sci.* **87**:1516–1525.
- Rada B, Leto TL. 2008. Oxidative innate immune defenses by Nox/Duox family NADPH oxidases. *Contrib Microbiol.* **15**:164–87.
- Saleh KMM, Al-Zghoul MB. 2019. Effect of Acute Heat Stress on the mRNA Levels of Cytokines in Broiler Chickens Subjected to Embryonic Thermal Manipulation. *Animals.* **9**:499.
- Sandercock† DA, Hunter RR, Mitchell MA, Hocking PM. 2006. Thermoregulatory capacity and muscle membrane integrity are compromised in broilers compared with layers at the same age or body weight. *Br Poult Sci.* **47**:322–329.
- dos Santos VM, Dallago BSL, Racanicci AMC, Santana ÂP, Bernal FEM. 2017. Effects of season and distance during transport on broiler chicken meat. *Poult Sci.* **96**:4270–4279.
- St-Pierre NR, Cobanov B, Schnitkey G. 2003. Economic Losses from Heat Stress by US Livestock Industries. *J Dairy Sci.* **86**:E52–E77.
- Surai F P. 2016. Antioxidant Systems in Poultry Biology: Superoxide Dismutase. *J Anim Res Nutr.* **01**.
- Del Vesco AP, Khatlab AS, Goes ESR, Utsunomiya KS, Vieira JS, Oliveira Neto AR, Gasparino E. 2017. Age-related oxidative stress and antioxidant capacity in heat-stressed broilers. *animal.* **11**:1783–1790.
- Yalcin S, Siegel P. 2003. Exposure to cold or heat during incubation on developmental stability of broiler embryos. *Poult Sci.* **82**:1388–1392.
- Zuidhof MJ, Schneider BL, Carney VL, Korver DR, Robinson FE. 2014. Growth, efficiency, and yield of commercial broilers from 1957, 1978, and 20051. *Poult Sci.* **93**:2970–2982.

Diet Composition and Prey Selection in the Long-eared Owl, *Asio otus* in Jordan: the Importance of Urban Avifauna

Mohammad A. Abu Baker^{1,*}, Ratib M. Al-Ouran² and Zuhair S. Amr³

¹Department of Biology, The University of Jordan, Amman, ²Department of Biology, Mutah University, Karak, ³ Department of Biology, Jordan University of Science and Technology, Irbid, Jordan

Received: September 24, 2019; Revised: November 23, 2019; Accepted: December 8, 2019

Abstract

The diet composition of a resident pair of the Long-eared Owl (*Asio otus*) was investigated from a pine stand in southern Jordan. 111 intact and 40 fragmented pellets yielded a total of 181 individual prey items representing at least 3 rodents and 4 urban birds. Prey items were dominated by house sparrows (43.65%), greenfinches (18.78%) and rodents (15.5%) which were found in 40, 16 and 26 pellets, respectively. The results suggest that the Long-eared Owl is an opportunistic feeder preying on a wide spectrum of small vertebrates. Contrary to several reports elsewhere -including the Mediterranean region- where small mammals dominated the diet of the Long-eared Owl, birds were the most frequent prey item found in this study. The fact that the Long-eared Owl roosting in a pine plantation in Jordan depends so heavily on House Sparrows indicates the importance of forest fragments and urban avifauna for survival of this raptor at the southern edge of its distribution range.

Keywords: Diet, *Asio otus*, Jordan, birds.

1. Introduction

The analysis of owl pellets for prey remains provides a useful tool for augmenting biodiversity inventories and gaining insights into the abundance and distribution of small vertebrates (Askew, 2007; Avenant, 2005; Heisler *et al.*, 2015; Torre *et al.*, 2004). Additionally, owls (order Strigiformes) make an ideal group for studying prey selection due to the relative ease of collecting pellets and identifying prey remains. Prey selection and intake in owls are influenced by several factors including: predator and prey size, prey availability, the environment (i.e. vegetation), and intensity of competition (e.g. Herrera and Hiraldo, 1976; Comay and Dayan, 2018).

The Long-eared Owl (*Asio otus*) is a medium-sized nocturnal species with distinct erect, blackish ear-tufts. It has a broad distribution across the northern latitudes of North America, Europe, Eurasia, and the Levant (Cramp and Simmons, 1985). It prefers forests close to open country, edges of semi-open woodland and urban areas (Cramp and Simmons, 1985). It is known as an opportunistic feeder and takes a high diversity of small-sized prey (Birrer, 2009). This owl is considered as an uncommon winter visitor in Jordan (Andrews, 1995). Along with global distribution, diet has been extensively studied in North America and Europe, yet reports on its ecology and diet within the most southern limits of its distribution are under-represented and far from satisfactory (Birrer, 2009). Only recently, Obuch (2018) reported on the diet of this owl in Jordan.

Jordan sits at the most southern edge of distribution of the Long-eared Owl, yet no studies have been conducted on its distribution and ecology. The present study reports

on the diet of a Long-eared Owl from southern Jordan over a period of four months.

2. Methods

Regurgitated pellets (111 in total in addition to 40 broken pellets) from a Long-eared Owl roost site on the edge of Mutah University campus (31° 5.792' N, 35° 43.091' E) in southern Jordan were collected during July - October of 2018. The owls were seen within a plantation of pine trees overlooking open steppe vegetation (Fig. 1). The area sits within the non-forest, dry Mediterranean vegetation. The area is highly degraded by overgrazing and accommodates a suite of urban areas, agricultural farms, and open areas. The majority of the open area is barren and rarely covered by vegetation with a few water run-off-systems (wadis) vegetated by bushes and shrubby microsystems.



Figure 1. A Long-eared Owl seen in the study near Mutah University in southern Jordan.

* Corresponding author e-mail: Ma.Abubaker@ju.edu.jo.

Each pellet was soaked in warm water and teased using a pair of forceps and a needle to separate prey remains for identification. For each species, lower and upper jaws were cleaned and preserved. Prey remains were identified using distinctive morphological characteristics of body and/or skull parts (e.g. mouthparts, mandibles, dentaries) described based on previous collections from the region (Harrison and Bates, 1991; Ujhelyi, 2016; www.skullsite.com).

Diet composition was expressed by frequency of occurrence of each prey item in the pellets (number of pellets with in which a prey item occurred), the total number of individuals (minimum number of individuals, MNI), percentage (number of individuals divided by the total number of prey individuals), and the percentage of mass taken using estimates of prey body weight. The total number of prey individuals in a pellet was determined using the total number of mandibles and/or skulls that were found (Yalden and Morris, 1990).

3. Results

Pellets were dark and cylindrical in shape with an average length of 35.78 ± 0.9 mm (mean \pm standard error) and 21.1 ± 0.3 mm in width. The sample of 111 pellets and fragments contained an average of 1.26 ± 0.05 prey items per pellet that were estimated to belong to a total of 181 prey individuals including, at least three species of small mammals, four species of birds, and additional unidentified species of passerine birds (Table 1). 84 pellets contained one prey item (69 only birds and 15 only rodents), the rest contained two (22 with two birds and three with a bird and a rodent) or three (one with birds only and one with two birds and a rodent) prey items. The 153 individual remains of birds were comprised of House Sparrows (*Passer domesticus*) 43.65% (N=79), Greenfinches (*Chloris chloris*) 17.78% (N=34), Warblers (*Sylvia* sp.) 5.52% (N=10), Common Blackbird (*Turdus merula*) 1.1% (N=2), and unidentified bird limbs (15.47%, N=28). The pellets also contained 28 remains of three rodent species including remains of one mole rat. Although the total frequency of prey items contained 84.5% birds and 15.5% rodents, the total mass intake was 73.7% birds and 26.3% rodents.

Table 1. Food composition of the long-eared owl in Jordan in terms of frequencies and percentages of prey items.

	Occurrence in pellets	MNI	percentage	prey weight	Percent weight
Birds, Aves					
House Sparrow (<i>Passer domesticus</i>)	40	79	43.65	27	34.65
Greenfinch (<i>Chloris chloris</i>)	16	34	18.78	25	13.81
Warbler (<i>Sylvia</i> sp.)	10	10	5.52	17	2.76
Common Blackbird (<i>Turdus merula</i>)	2	2	1.10	100	3.25
Unidentified birds (feathers and limb bones)	26	28	15.47	42.25	19.22
Mammals, Rodentia					
Mole Rat (<i>Nannospalax ehrenbergi</i>)	1	1	0.55	150	2.44
House Mouse (<i>Mus musculus</i>)	4	4	2.21	14	0.91
Tristram's Jird (<i>Meriones tristrami</i>)	14	16	8.84	70	18.19
Unidentified rodents (fur and limb bones)	7	7	3.87	42	4.78
		181	100		

4. Discussion

This is the first report on the diet composition of the Long-eared Owl (*Asio otus*) in its southern most limit of distribution. The diet composition of the Long-eared Owl contained a wide variety of small vertebrate prey items. Bird remains occurred the most in the pellets and comprised the highest frequency at about 84.5% (of which House Sparrows made 43.65%), whereas rodents made up the remaining 15.5% of the diet remains. However, rodents made up 26.3% of the total prey intake compared to birds (73.7%). The remains of nocturnal rodents suggest that hunting for food was mostly done during the night, while birds were hunted at their roost sites within the trees and bushes (Cramp and Simmons, 1985, Leader *et al.*, 2010).

Contrary to several reports elsewhere -including the Mediterranean region and the Levant- where small mammals dominated the diet of the Long-eared Owl (Yosef, 1997; Seçkin and Coşkun, 2005, Seçkin and Coşkun, 2006; Leader *et al.*, 2008; Birrer, 2009), birds were the most frequent prey item in this study. In other parts in the Middle East, Field Voles (*Microtus guentheri*) were the main prey item (Yosef, 1997; Charter *et al.*,

2012). Diet composition in other parts of the Long-eared Owl's distribution revealed a higher percentage of small mammals followed by birds (Birrer, 2009). Rodents accounted for the largest prey class among the biomass of mammalian prey taken (Birrer, 2009). In the Negev Desert, the diet of Long-eared Owl consisted mainly of small mammals (71.3%) and birds (26.5%) birds, of which migratory birds formed a significantly larger part of the total birds consumed during migration than during the non-migratory months (Leader *et al.*, 2008). The diet of wintering Long-eared Owls in Zabol, Iran, was predominantly larger rodents (c. 150 g) including the Indian Gerbil (*Tatera indica*), whereas birds made up 25.6% of prey items (Khaleghizadeh *et al.*, 2009). In Diyarbakir, Turkey, Long-eared Owl pellets were composed mostly of Rodentia (95.48% of the identified remains), with Field Voles (*M. guentheri*) representing 71.29% of the prey remains.

Our results are consistent with Obuch (2018), in which the diet of *A. otus* consisted mainly of birds in urban areas (78.3%). Obuch (2018) found that House Sparrow, *P. domesticus*, was most common prey item reaching 40.1%. Long-eared Owls in this study most probably consumed more birds because of the abundance of passerines and the

lack of small mammals. In a city park in Jerusalem, the diet of the Long-eared Owl was composed of 13 species of birds which accounted for the most common prey group (91% by number) (Kiat *et al.*, 2008). House Sparrows (*Passer domesticus*) and Blackcaps (*Sylvia atricapilla*) were the most frequent prey species (22% and 17% by number). Göçer (2016) also found that all prey items from an urban park were Passeriformes and consisted of two species belonging to Passeridae and Hirundinidae. 78 of the 86 prey items (90.7%) were House Sparrow (*Passer domesticus*) and the other eight (9.3%) were House Martin (*Delichon urbicum*).

The fact that the Long-eared Owl roosting in a pine plantation in Jordan depends so heavily on House Sparrows indicates the importance of forest fragments and urban birds for the survival of this raptor at the southernmost edge of its distribution range (Kiat *et al.*, 2008; Göçer, 2016). Our results and those of others strongly suggest that *A. otus* has opportunistic feeding habits. While most energy-yielding prey were nocturnal small mammals (e.g. *M. tristrami*), smaller to avian prey (e.g. *P. domesticus*) were also hunted. Feeding and prey selection by *A. otus* within the urban areas of Jordan is likely influenced by the abundance and availability of prey species (Village, 1981; Yosef, 1997; Pirovano *et al.*, 2000). The results suggest that owls in general are able to adjust their diet to urban environments (see also Amr *et al.* 2016).

References

- Amr ZS, Handal EN, Bibi F, Najajreh MH and Qumsiyeh MB. 2016. Change of diet of the Eurasian Eagle Owl, *Bubo bubo*, suggest decline in biodiversity in Wadi Al Makhrou, Bethlehem Governorate, Palestinian Territories. *Slovak Raptor J.*, **10**: 75–79.
- Andrews IJ. 1995. **The Birds of the Hashemite Kingdom of Jordan**. Andrews IJ, Musselburgh.
- Askew NP, Searle JP and Moore NP. 2007. Prey selection in a Barn Owl *Tyto alba*. *Bird Study*, **54**: 130–132.
- Avenant NL. 2005. Barn owl pellets: A useful tool for monitoring small mammal communities? *Belg J Zool.*, **135**: 39–43.
- Birrer S. 2009. Synthesis of 312 studies on the diet of the Long-eared Owl *Asio otus*. *Ardea*, **97**: 615–624.
- Charter M, Izhaki I, Leshem Y and Roulin A. 2012. Diet and breeding success of long-eared owls in a semi-arid environment. *J Arid Environ.*, **85**: 142–144.
- Comay O. and Dayan T. 2018. What determines prey selection in owls? Roles of prey traits, prey class, environmental variables, and taxonomic specialization. *Ecol. Evol.*, **8**: 3382–3392.
- Cramp S and Simmons KEL. 1985. **Handbook of the birds of Europe, the Middle East, and North Africa. The birds of the Western Palearctic. Volume IV. Terns to woodpeckers**. Oxford University Press, Oxford.
- Göçer E. 2016. Diet of a nesting pair of Long-eared Owls, *Asio otus*, in an urban environment in southwestern Turkey (Aves: Strigidae). *Zool Middle East*, **62**: 25–28.
- Harrison DL and Bates PJ. 1991. **The Mammals of Arabia**. Harrison Zoological Museum, Sevenoaks.
- Heisler LM, Somers CM and Poulin RG. 2016. Owl pellets: a more effective alternative to conventional trapping for broad-scale studies of small mammal communities. *Methods Ecol. Evol.*, **7**: 96–103.
- Herrera CM and Hiraldo F. 1976. Food niche and trophic relationships among European owls. *Ornis Scand.*, **7**: 29–41.
- Khaleghizadeh A, Arbabi T, Noori G, Javidkar M and Shahriari A. 2009. Diet of wintering Long-eared Owl *Asio otus* in Zabol, southeastern Iran. *Ardea*, **97**: 631–633.
- Kiat Y, Perlman G, Balaban A, Leshem Y, Izhaki I and Charter M. 2008. Feeding specialization of urban Long-eared Owls, *Asio otus* (Linnaeus, 1758), in Jerusalem, Israel. *Zool Middle East*, **43**: 49–54.
- Leader Z, Yom-Tov Y and Motro U. 2008. Diet of the Long-eared Owl in the Northern and Central Negev Desert, Israel. *Wilson J Ornithol.*, **120**: 641–645.
- Leader Z, Yom-Tov Y and Motro U. 2010. Diet comparison between two sympatric owls-*Tyto alba* and *Asio otus*-in the Negev Desert, Israel. *Isr J Ecol Evol.*, **56**: 207–216.
- Obuch J. 2018. On the diet of owls (Strigiformes) in Jordan. *Slovak Raptor J.*, **12**: 9–40.
- Pirovano A, Rubolini D, Brambilla S and Ferrari N. 2000. Winter diet of urban roosting Long-eared Owls *Asio otus* in northern Italy: the importance of the Brown Rat *Rattus norvegicus*. *Bird Study*, **47**: 242–244.
- Seçkin S and Coşkun Y. 2005. Small mammals in the diet of the Long-eared Owl, *Asio otus*, from Diyarbakır, Turkey. *Zool Middle East*, **35**: 102–103.
- Seçkin S and Coşkun Y. 2006. Mammalian Remains in the Pellets of Long-eared Owls (*Asio otus*) in Diyarbakır Province. *Turk J Zool.*, **30**: 271–278.
- Torre I, Arrizabalaga A and Flaquer C. 2004. Three methods for assessing richness and composition of small mammal communities. *J Mammal.*, **85**: 524–530.
- Ujhely P. 2016. Cranial morphology of European passerine bird families (Aves, Passeriformes). *Ornis Hungarica*, **24**: 54–77.
- Village A. 1981. The diet and breeding of Long-eared Owls in relation to vole numbers. *Bird Study*, **28**: 214–224. www.skullsite.com.
- Yalden DW and Morris PA. 1990. The Analysis of Owl Pellets. *Occasional publication of the Mammal Society*, **13**: 1–24.
- Yosef R. 1997. Diet of Long-eared Owls *Asio otus* wintering in the Khula valley, Israel. *Sandgrouse*, **19**: 148–149.

Genetic Characterization of Algerian Minor Date Palms (*Phoenix dactylifera* L.) Cultivated in the Oases of Biskra using Nuclear Microsatellite Markers

Ahmed Simozrag and Ziane Laiadi*

Laboratory of Genetic, Biotechnology and Valorization of Bioresources (LGBVB), University of Biskra, BP 145RP, Biskra 07000, Algeria.

Received: September 17, 2019; Revised: November 24, 2019; Accepted: December 11, 2019

Abstract

In this study, minor and neglected cultivars of *Phoenix dactylifera* L. previously not reported were discriminated by molecular analysis using thirteen SSR markers in order to evaluate their genetic diversity and the relationships among them. The used set of markers could distinguish all eighty genotypes analyzed here according to the uniqueness of genotypes, and no similarity was found among the cultivars. A total of 101 polymorphic alleles were identified with an average of 7.77 alleles per locus, indicating the high level of polymorphism existing among the cultivars. The most informative loci was mPdCIR085, with the highest number of effective alleles ($N_e=5.88$) and had the lowest probability of identical genotypes ($PI=0.052$). The cumulative probability for genotype sharing among unrelated cultivars combining the 13 loci was 5.95×10^{-13} ; this value is low was enough to allow the check for synonymies in the samples. The study of genetic relationships among cultivars from different areas in Biskra oases showed the existence of close relatedness within some groups of cultivars. These facts suggest a common origin of them due to potential paternity relationships or easy exchange of plant materials by virtue of neighbor lines and mutual social relations between farmers.

Keywords: Biskra oases, date palm, genetic diversity, relationship.

1. Introduction

Date palm (*Phoenix dactylifera* L., $2n = 36$) is a dioecious perennial monocotyledon belonging to the family Arecaceae or Palmaceae (Munier, 1973). Palm trees are the most visible and undisputed trees of the populations in oases and arid regions; through germplasm exchange, date palm agriculture has expanded to Australia, Southern Africa, South America, Mexico and the United States of America (Jain *et al.*, 2011), and where considered of great socio-economic importance in the Arabian region (Khierallah *et al.*, 2011). It has a halo of holiness for all Muslims because it is mentioned in the Quran and Sunnah, as dates constitute the favorite meal during Ramadan and Muslims generally break their fast by eating them. Algeria is characterized by a rich, complex and diversified date palm heritage, for according to recent statistics in 2015. Algerian date palm groves contained 18 million trees occupying 169,380 ha (Al-Khayri *et al.*, 2015; Moussouni *et al.*, 2017). Existing cultivars in all oases result from an empirical selection carried out traditionally by the farmers whereby the process of selection is done independently in every oasis (Elhoumaizi *et al.*, 2002). However, date palm production has shifted from traditional cultivation in rich and diverse agrosystems to intensive monocultures (Jain *et al.*, 2011). As a consequence, cultivars of minor economic interest have been abandoned favouring international varieties such as Deglet Nour, Ghers, Mech degla. The

identification of date palm cultivars has been traditionally carried out by morphological markers, where the most common characters used are the morphology of leaves, spines and fruit characters, features which require a large set of phenotypic data that are sensitive to environmental factors and can be observed only in mature trees (Nixon, 1950; Sedra *et al.*, 1998; Elshibli and Korpelainen, 2008) as well as the developmental stages of the plant (Elhoumaizi *et al.*, 2002).

Data based on molecular markers such as RFLPs, RAPDs and ISSRs have been performed to characterize date palm genotypes (Zehdi *et al.*, 2004b) or other molecular markers like AFLP (Cao and Chao, 2002; El-Assar *et al.*, 2005; Adawy *et al.*, 2006).

During the last decades, microsatellite markers have demonstrated to be a powerful tool for plant diversity analysis due to their high level of polymorphism, codominant behavior, relative abundance, Mendelian inheritance, specific location and amenability to automation, and high throughput genotyping (Kalia *et al.*, 2011). Therefore, data become easier to exchange among laboratories (Udupa and Baum, 2001), which allows direct comparison and use of common databases. For date palms, Microsatellite markers were initially used for the investigation of genetic diversity in date palm by Billotte *et al.* (2004), and have thereafter been extensively used for genotype and cultivar characterization in different producing countries (Zehdi *et al.*, 2004a,b; Al-Ruqaishi *et al.*, 2008; Elshibli and Korpelainen, 2008; Ahmed and Al-

* Corresponding author e-mail: ziane.laiadi@univ-biskra.dz; zlayadi@yahoo.fr.

Qaradawi,2009; Johnson *et al.*,2009; Akkak *et al.*,2009; Pintaud *et al.*,2010; Elmeir *et al.*,2011; Khierallah *et al.*,2011; Zehdi *et al.*,2012; Zehdi *et al.*,2015; Guettouchi *et al.*,2017; Huda *et al.*,2019). In this study, we focus on cultivars which have been mostly neglected in research and economic commercialization in spite of being traditionally important until now and common for their quality of sub-products. We report the first data on the genetic diversity and putative genetic relationships among 80 Algerian date palm cultivars of Biskra oases, using 13 microsatellite markers.

2. Materials and methods

2.1. Plant material

Plant material consisted of eighty samples, given in Supplementary Table 1, collected from cultivars traditionally cultivated in different locations in Biskra (Tolga, Biskra center, Mchounech), some of which were collected in border areas in the state (Oued Righ), and several of which are believed to be endangered autochthonous cultivars (Figure 1). Young leaves were collected from mature, randomly sampled trees, dried in silica gel and stored at room temperature until DNA extraction.

Table 1. Alleles sizes (bp) and their frequencies (%) for the thirteen loci studied.

mPdCIR010		mPdCIR015		mPdCIR016		mPdCIR025		mPdCIR035		mPdCIR044		mPdCIR048	
Allele	Freq												
121	4.80	122	2.17	128	40.91	200	13.89	162	0.63	299	64.38	158	20.67
123	13.70	124	51.45	130	53.90	213	31.94	164	1.27	301	26.71	159	0.67
126	1.37	126	10.15	132	0.65	215	3.47	165	8.23	307	1.37	175	12.67
127	2.06	130	1.45	137	4.55	217	1.39	170	1.27	317	7.53	193	27.33
132	3.43	131	0.73			219	0.69	172	6.33			195	38.67
133	13.70	136	7.25			227	22.92	175	32.28				
135	52.74	138	23.19			231	25.69	177	10.76				
138	3.43	157	3.62					182	1.90				
159	0.69							188	6.96				
163	4.11							189	26.58				
								193	1.90				
								198	0.63				
								199	0.63				
								206	0.63				

cont. Table 1

mPdCIR057		mPdCIR063		mPdCIR070		mPdCIR078		mPdCIR085		mPdCIR090	
Allele	Freq										
250	36.08	122	19.74	186	7.38	117	25.69	149	6.72	141	42.57
252	6.33	140	60.53	190	0.82	120	2.08	157	11.19	148	3.38
254	28.48	155	17.11	192	21.31	121	6.94	161	0.75	150	2.03
256	11.39	166	2.63	193	0.82	123	14.58	165	0.75	161	5.41
263	5.70			194	29.51	134	2.78	167	2.99	166	5.41
269	10.76			195	12.30	136	9.72	169	17.91	167	4.05
274	1.27			196	0.82	146	16.67	171	20.90	168	24.32
				197	16.39	152	21.53	177	17.16	169	9.46
				199	2.46			179	21.64	171	2.70
				207	1.64					172	0.68
				209	6.56						

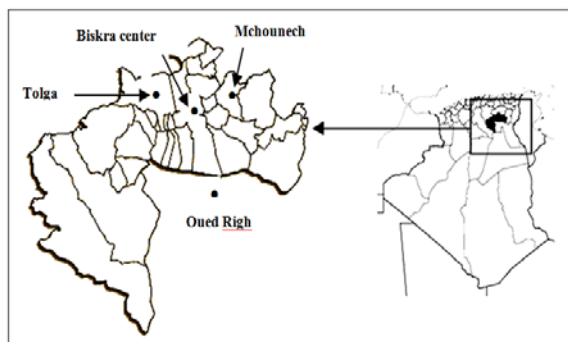


Figure 1. Map showing four Algerian oasis date palms referred in the text.

2.2. DNA isolation and microsatellite analysis

DNA isolation and microsatellite analysis was carried out according to procedure described by Saro *et al.* (2014). Total genomic DNA was extracted from 1 g of silica-dried leaf tissue from each sampled adult following Dellaporta *et*

al. (1983), after grinding plant material with a Mixer Mill MM300 (RETSCH, Haan, Germany).

The obtained DNA solution was purified using GenElute™ PCR Clean-Up Kit (SIGMA-ALDRICH, St. Louis, MO, USA).

The DNA concentration was checked on a spectrophotometer “Eppendorf BioPhotometer® D30” to confirm a minimum of 20 ng/μL. We amplified 13 dinucleotide (GA) microsatellite loci previously developed for *P. dactylifera* (Billotte *et al.*, 2004): mPdCIR010, mPdCIR015, mPdCIR016, mPdCIR025, mPdCIR035, mPdCIR044, mPdCIR048, mPdCIR057, mPdCIR063, mPdCIR070, mPdCIR078, mPdCIR085 and mPdCIR090. DNA fragments were amplified in two PCR multiplex reactions with four loci each, using the Qiagen Multiplex PCR kit (QIAGEN, Valencia, CA, USA) and following the manufacturer's instructions, but accommodating reagent's proportions to a final volume of 15μL. Amplified PCR products were run on an ABI3730 capillary sequencer using an internal size standard (GS500 (-250) LIZ), and

fragment sizes were manually scored using GENEMAPPER software (Applied Biosystems, Foster City, CA, USA).

2.3. Data analysis

We used « IDENTITY 1.0 » software (Wagner and Sefc, 1999) to detect all possibilities of identical genotypes, where genetic diversity was measured by estimating the average number of alleles per locus (N_a), the average number of effective alleles (N_e) and the gene diversity or expected heterozygosity (H_e), the average probability of identity per locus (PI), the cumulative PI , using GENALEX 6.41 (Peakall and Smouse, 2006). Genetic distances between cultivars were calculated as the allele sharing distance (DAS) (Jin and Chakraborty, 1994). Phylogenetic tree based on the distance matrix was constructed using the neighbour-joining method (Saitou and Nei, 1987) by POPULATIONS v.1.2.30 (<http://bioinformatics.org>, LANGELLA, unpubl.) while MEGA5.2 (Tamura *et al.* 2011) was used to display it.

3. Results and discussion

3.1. Microsatellite analysis

The thirteen SSR markers were chosen for this study to identify different genotypes in the eighty analyzed samples (Supplementary Table 1). Allele sizes and frequencies of the analyzed loci are shown in Table 1. The distribution of allele frequencies for each locus allows assessing the identification ability of the markers, being more informative if this distribution is equitable (Sefc *et al.*, 1999; Santana *et al.*, 2007). In this study, the most frequent alleles were mPdCIR044-299, mPdCIR063-140, mPdCIR016-130 and mPdCIR010-135 with high percentage values of 64.38%, 60.53%, 53.90% and 52.74% respectively. The number of alleles per locus (Table 2) varied from 4 (mPdCIR016, mPdCIR044, mPdCIR063) to 14 (mPdCIR035). A microsatellite preferably should have at least 4 alleles to be useful for the evaluation of genetic diversity as per the standard selection of microsatellites loci (Barker, 1994). Total of 101 alleles were identified with an average of 7.77 alleles per locus, which agrees with the results of previous works on 49 cultivars collected from three main oases in Tunisia (Zehdi *et al.*, 2004b), who detected 7.14 alleles per locus when analyzing 46 Tunisian date palm accessions by using 14 microsatellite loci where Elshibli and Korpelainen (2008) in Sudan identified a high number of alleles per locus (21.4), which is more than the number of alleles per locus detected in this study. Expected heterozygosity for each locus ranged from 50.80% (mPdCIR044) to 82.33% (mPdCIR078 and 83% (mPdCIR085), with a mean of 70.71%, while observed heterozygosity varied between 23.30% (mPdCIR044) and 86.11% (mPdCIR025), with a mean of 67.40% in global H_o value is higher than expected for 9 loci vs 4 loci. Thus the higher value of H_o in the majority of loci observed in this study under Hardy-Weinberg conditions suggests high genetic variability in this population. Despite the four loci analyzed (mPdCIR044, mPdCIR035, mPdCIR070 and mPdCIR090) showed observed heterozygosity lower than Hardy-Weinberg expectations, as in previous works especially for last primers (Zehdi *et al.*, 2004b ; Elshibli and Korpelainen,

2008). The most informative loci was mPdCIR085 with nine alleles ($N_e=5.88$) and had the lowest probability of identical genotypes ($PI=0.052$), followed by mPdCIR078 ($N_e=5.65$; $PI = 0.055$) and mPdCIR070 ($N_e=5.40$; $PI = 0.058$), while the opposite was the case for mPdCIR016 ($N_e = 2.17$) and mPdCIR044 ($N_e = 2.03$), both of which with four alleles and had the highest probability of identity ($PI=0.31$), for the mPdCIR044 was found to be the least informative locus. Originally, Billotte *et al.* (2004) have signalled this case as locus which produced erratic amplification and possibly referred to a mutational polymorphism at an annealing site. The probability for genotype sharing among unrelated cultivars combining the 13 loci was 5.95×10^{-13} , lower enough to allow the check for synonymies in the sample.

Table 2. Genetic parameters obtained with thirteen SSR markers for eighty distinct cultivars.

	N	N_a	N_e	I	H_o	H_e	F	PI
mPdCIR010	73	10	3.099	1.563	0.795	0.677	-0.173	0.130
mPdCIR015	69	8	2.976	1.404	0.710	0.664	-0.070	0.153
mPdCIR016	77	4	2.174	0.872	0.558	0.540	-0.034	0.311
mPdCIR035	79	14	4.920	1.912	0.633	0.797	0.206	0.067
mPdCIR025	72	7	4.144	1.536	0.861	0.759	-0.135	0.099
mPdCIR044	73	4	2.034	0.890	0.233	0.508	0.542	0.307
mPdCIR048	75	5	3.533	1.343	0.720	0.717	-0.004	0.130
mPdCIR057	79	7	4.111	1.606	0.772	0.757	-0.020	0.094
mPdCIR063	76	4	2.298	1.022	0.579	0.565	-0.025	0.242
mPdCIR070	61	11	5.397	1.891	0.590	0.815	0.276	0.058
mPdCIR078	72	8	5.653	1.851	0.847	0.823	-0.029	0.055
mPdCIR085	67	9	5.880	1.873	0.836	0.830	-0.007	0.052
mPdCIR090	74	10	3.859	1.701	0.622	0.741	0.161	0.098
mean	72.846	7.769	3.852	1.497	0.674	0.707	0.053	0.138
Cumulative								5.95×10^{-13}

Statistical results for 13 microsatellite markers used in the present study, namely: sample size N, observed number of alleles (N_a), effective number of alleles (N_e), Shannon's Information index (I), observed heterozygosity (H_o), expected heterozygosity (H_e) and Probability of identity.

3.2. Cluster analysis

The dendrogram based on genetic distance measure (Figure 2) was constructed using the weighted neighbour-joining method for the evaluation of genetic diversity and relatedness between the investigated cultivars. The dendrogram clustered the eighty cultivars into three major groups (I, II and III).

The first minor cluster grouped ten genotypes. A first subdivision contained the well-known cultivars in Mchounech called 'Tbsrithe' closely linked to 'Lamari' and 'Abdelazaz', and were cultivated near to Biskra center. The three cultivars showed common morphological features like the color of fruit and their softness, but these two cultivars were closely linked in the color of the fruit 'brown to black', although distinct in the appearance of outer skin, smooth for the first and wrinkled skin for the second. The remaining cultivars in this group were very

interesting as five cultivars shared a significant number of alleles, and they all appeared in a homogeneous color and fruit softness: 'Bajamil', 'Arelou Oued Souf', 'Melk Lahcen', 'Loulou' and 'Charka' cultivated in the same area in south of the region called "Still" or "Oued Rhig" which in the border of the state (Figure 1), are very close with two other cultivars 'DGuel Litima' and 'Jaouzia', in brown color and half softness fruits. Traditionally cultivated in central areas of the region, this fact suggests that central area is a common origin of them. The second cluster contained 23 accessions representing three sub-clusters. This cluster grouped the majority of cultivars belonging to 'Mchounech' area, and the closest relationships were detected between the following pairs of genotypes: "Hathourite, Tamazoute", "Takarboucht, Taourekht" and "Noyet Arechti, Takerbrateth". It should also be noted that most of them were named by using terms to refer to the color of fruit locally in chaoui dialects as one characteristic of the region. On the other hand, one sub-cluster includes "Mech degla" famous cultivar with dry fruits characterized by their resistance and low cost in terms of cultural practice, conservation and marketing of their dates which has high nutritional value; unfortunately, they are considered as secondary quality date varieties

which run the risk to disappear in favor of Deglet-Nour soft variety (Amellal and Benamara, 2008). "Mech degla" shared a significant alleles with two cultivars which are closely related to each other 'Arelou Biskra' in Oued Righ and 'Saout Bghal' from Mechnouch. These last cultivars (Simozrag *et al.*, 2016) showed common morphological features as the fruit color, and their leaves with Mech degla and Hamrayet hamlaoui in the same sub-cluster. The third cluster showed signs of likely genetic relationships among the largest gatherings of cultivars, including 47 cultivars which spread over three areas of oases: East (Mechounech), west (Tolga) and south of Biskra (Oued Righ). As in all date-growing areas of Sudan as reported by Elshibli and Korpelainen (2008), the farmers are using a few selected males for the pollination of female trees. In addition, they sometimes mixed the pollen grains of more than one male for pollination and finally new cultivars are a result of a continuous selection process carried out by farmers in their fields following sexual reproduction.

Altogether, these facts suggest a common origin of cultivars due to potential paternal relationships or easy exchange of plant materials among farmers by virtue of geographical zones and social well-being.

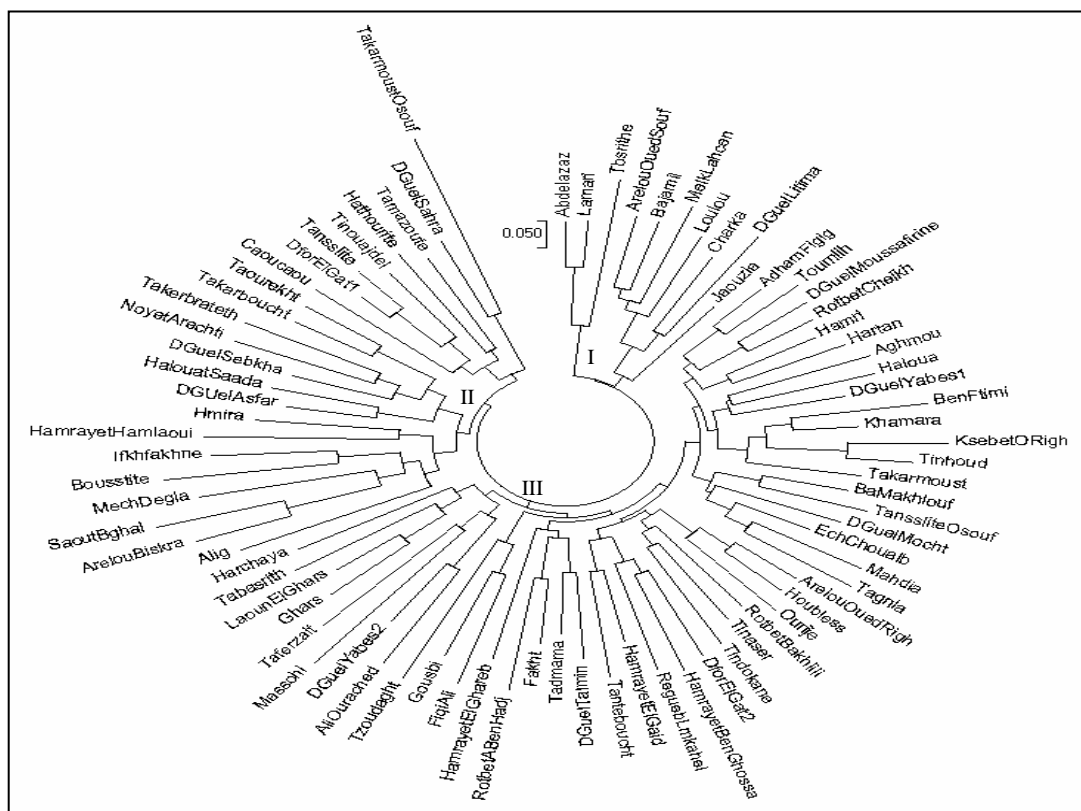


Figure 2. Neighbor-joining tree of individual genotypes based on 13 microsatellites loci. (Dendrogram generated with Populations software using shared allele distance).

4. Conclusion

Genetic relationships among cultivars from different areas in Biskra oases showed the existence of close relatedness within some groups of cultivars.

Results of the present work constitute the first study of minor varieties which are characterized by a low trade value but are still traditionally important and common for

their quality of sub-products; they showed here a high genetic diversity across their traditional cultivation area.

These informations make it necessary to develop breeding strategies for economically and agronomically interesting cultivars with important traits such as fruit quality; furthermore, it is recommended to select tolerant varieties against biotic and abiotic stresses and to enrich the germplasm collections.

Acknowledgements

We want to thank Professor Pedro.A.SOSA and his group from Universidad de Las Palmas de Gran Canaria, ULPGC, Canary Islands (Spain) for their invaluable help and contribution to this work through molecular analysis and other methods..

Funding

This work was supported by Algerian Ministry of Higher Education and Scientific Research to Z. Laiadi and A. Simozrag.

Authors' contribution

Both authors have read the manuscript and agreed to its content.

Conflict of interest

The authors declare that they have no conflict of interest.

References

- Ahmed TA and Al-Qaradawi AY.2009. Molecular phylogeny of Qatari date palm genotypes using simple sequence repeats markers. *Biotechnology*, **8**:126–131.
- Adawy SS, Hussein EHA, Ismail SEME and El-Itriby HA. 2006. Genomic diversity in date palm (*Phoenix dactylifera* L.) as revealed by AFLPs in comparison to RAPDs and ISSRs. In: Abstracts of 3rd international date palm conference, Abu Dhabi, United Arab Emirates, 19–21 February.
- AkkakA, Iscarriot V,Torello-Marinoni D, Boccaccio P, Bertram C and Beta R.2009. Development and evaluation of microsatellite markers in *Phoenix dactylifera*L. and their transferability to other Phoenix species. *Biol Plantarum*,**53**:164–166.
- Al-Khayri JM, Jain SM and Johnson DV.2015.**Date Palm Genetic Resources and Utilization. Volume 1: Africa and the Americas.** Springer Dordrecht Heidelberg, New York London.
- Al-Ruqaishi IA, DaveyM, Alderson P andMayes S.2008.Genetic relationships and genotype tracing in date palms (*Phoenix dactylifera* L.) in Oman based on microsatellite markers. *Plant Genet Resour*,**61**:70–72.
- AmellalH and Benamara S.2008. Vacuum drying of common date pulp cubes. *Dry technol*,**26**:378–382.
- Barker PSF.1994. A global protocol for determining genetic distance among domestic livestock breeds. Proceeding of 5th world congress on genetic application of livestock production, Guelph and Ontario, Canada,**21**:501–508.
- Bedjaoui H and Benbouza H. 2018. Assessment of phenotypic diversity of local Algerian date palm (*Phoenix dactylifera* L.) cultivars.*J Saudi Soc Agric Sci*, doi.org/10.1016/j.jssas.2018.06.002.
- Billotte N, Marseillac N, Brittner P, Noyer JL, jacquemoud-Collet JP, Moreau C, Couvreur T, Chevallier MH, Pintaud JC and Risterucci AM. 2004. Nuclearmicrosatellite markers for the date palm (*Phoenix dactylifera* L.): characterizationand utility across the genus Phoenix and in other palm genera. *Mol Ecol Notes*, **4**: 256–258.
- Cao BR and Chao CT. 2002. Identification of date cultivars in California using AFLP markers. *Hortic Sci*, **37**:966–968.
- Dellaporta SL, Wood J and Hicks JB. 1983. A plant DNA minipreparation: version II.*Plant Mol Biol Report*,**1**:19-21.
- El-Assar AM, Krueger RR, Devanad PS and Chao CT. 2005. Genetic analysis of Egyptian date (*Phoenix dactylifera* L.) accessions using AFLP markers. *Genet Resour Evol*, **52**:601–607.
- Elhoumaizi MA, Saaidi M, Oihabi A and Cilas C. 2002.Phenotypic diversity of datepalm cultivars (*Phoenix dactylifera* L.) from Morocco. *Genet Resour Crop Evol*, **49**:483–490.
- ElmeerK, Sarwath H, Malek J, Baum M and Hamwiah A.2011. New microsatellite markers for assessment of genetic diversity in date palm (*Phoenix dactylifera* L.). *3 Biotech*,**1**:91-97.
- ElmeerK and Mattat I.2015. Genetic diversity of Qatari date palm using SSR markers. *Genet Mol Res*,**14**: 1624-1635.
- Elshibli S and Korpelainen H. 2008.Microsatellite markers reveal high genetic diversity in date palm (*Phoenix dactylifera* L.) germplasm from Sudan. *Genetica*,**134**: 251–260.
- Guettouchi A, Haider N, NabulsiI and YkhlefN. 2017. Molecular characterization of Algerian date palm cultivars using circular plasmid-like DNAs. *Indian J Genet Plant Breed*,**77**(1):170.
- Huda MN, Hasan M, Abdullah HM and Sarker U. 2019. Spatial distribution and genetic diversity of wild date palm (*Phoenix sylvestris*) growing in coastal Bangladesh. *Tree Genet Genomes*,**15**:3.
- Jain SM, Al-Khayri JM and Johnson DV. 2011. **Date palm biotechnology.** Springer Dordrecht Heidelberg, New York, London.
- Jin L and Chakraborty R. 1994. Estimation of genetic-distance and coefficient of gene diversity from single-probe multilocus DNA-fingerprinting data. *Mol Biol Evol*,**11**: 120-127.
- Johnson C, Cullis TA, Cullis MA and Cullis CA. 2009.DNA markers for variety identification in date palm (*Phoenix dactylifera* L.). *J Hortic Sci Biotechnol*,**84**: 591–594.
- Kalia RK, Rai MK, Kalia S, Singh R and Dhawan AK. 2011.Microsatellite markers: an overview of the recent progress in plants. *Euphytica*,**177**:309–334.
- Khierallah HSM, Bader SM, Baum M and Hamwiah A.2011. Genetic diversity of Iraqi Date palms revealed by microsatellite polymorphism. *J Am Soc Hortic Sci*,**136**: 282-287.
- Moussouni S, Pintaud J-C, Vigouroux Y and Bouguedoura N.2017.Diversity of Algerian oases date palm (*Phoenix dactylifera* L., *Arecaceae*): Heterozygote excessand cryptic structure suggests farmer management had a major impact on diversity. PLOS ONE [https://doi.org/10.1371/journal.pone.0175232.
- Munier P.1973. **Le palmier dattier.** Ed. Maisonneuve et Larose, Paris .
- Nixon RW. 1950. Imported cultivars of dates in the United States. USDA 834,144
- Peakall R and SmousePE.2006. Genalex 6: Genetic analysis in Excel. Population genetic software for teaching and research. *Mol Ecol Resour*,**6**:288-295.
- Pintaud JC, Zehdi S, Couvreur T, Barrow S, Henderson S, Aberlenc-Bertossi F,Tregear J and Billotte N. 2010. Species delimitation inthe genus Phoenix (*Arecaceae*) based on SSR markers, with emphasis on the identity of the date palm (*Phoenix dactylifera* L.). In: Seberg O., Petersen G., Barfod A., Davis J. (eds) **Diversity, phylogeny, and evolution in the monocotyledons.** Arhus University Press, Denmark 267–286.
- Saitou N and Nei M.1987.The neighbor-joining method - a new method for reconstructing phylogenetic trees.*Mol Biol Evol*, **4**: 406-425.

- Santana JC, Hidalgo E, de Lucas AI, Recio P, Ortiz JM, Martin JP, Yuste J, Arranz C and Rubio JA. 2007. Identification and relationships of accessions grown in the grapevine (*Vitis vinifera* L.) Germplasm Bank of Castilla y León (Spain) and the varieties authorized in the VQPRD areas of the region by SSR-marker analysis. *Genet Resour Crop Evol*, **55**: 573-583.
- Saro I, Robledo-Arnuncio JJ, González-Pérez MA and Sosa PA. 2014. Patterns of pollen dispersal in a small population of the Canarian endemic Palm (*Phoenix canariensis*). *Heredity*, **113**: 215-223.
- Sedra MH, Lashermes P, Trouslot M and Hamon S.1998. Identification and genetic diversity analysis of date palm (*Phoenix dactylifera* L.) varieties of Morocco using RAPD markers. *Euphytica*,**103**:75–82.
- Sefc KM, Regner F, Turetschek E, Glossl J and Steinkellner H. 1999. Identification of microsatellite sequence in *Vitis riparia* and their applicability for genotyping of different *Vitis* species. *Genome*, **42**: 367-373.
- Simozrag A, Chala A, Djerouni A and Bentchikou ME. 2016. Phenotypic diversity of date palm cultivars (*Phoenix dactylifera* L.) from Algeria. *Gayana Bot*,**73** (1), 42-53.
- Tamura K, Peterson D, Peterson N, Stecher G, Nei M and Kumar S.2011. MEGA5: Molecular evolutionary genetics analysis using maximum likelihood, evolutionary distance, and maximum parsimony methods. *Mol Biol Evol*,**28**: 2731-2739.
- Udupa SM and Baum M. 2001. High mutation rate and mutational bias at (TAA)_n microsatellite loci in chickpea (*Cicerarietinum* L.). *MolGenet Genomics*, **265** :1097-1103.
- Wagner HW and SefcKM.1999. Identity 1.0. Centre for Applied Genetics, University of Agricultural Science, Vienna.
- Zehdi S, Sakka H, Rhouma A, Salem, AOM, Marrakchi M and Trifi M.2004a. Analysis of Tunisian date palm germplasm using simple sequence repeat primers. *Afr J Biotechnol*, **3**:215–219.
- Zehdi S, Trifi M, Billotte N, Marrakchi M and Pintaud JC.2004b. Genetic diversity of Tunisian date palms (*Phoenix dactylifera* L.) revealed by nuclear microsatellite polymorphism. *Hereditas*,**141**:278–287.
- Zehdi S, Cherif E, Rhouma S, Santoni S, Salhi HAand Pintaud JC.2012. Molecular polymorphism and genetic relationships in date palm (*Phoenix dactylifera* L.): The utility of nuclear microsatellite markers. *Sci Horticult*, **148**:255-263.
- Zehdi S, Cherif E, Moussouni S, Gros-Balthazard M, Abbas-Naqvi Sand Ludeña B. 2015. Genetic structure of the date palm (*Phoenix dactylifera* L.) in the Old World reveals a strong differentiation between eastern and western populations. *Ann Bot*,**116**: 101-112.

Supplementary Table 1. some morphological characters and genetic profiles of eighty Algerian date palm (*Phoenix dactylifera* L.) cultivars analyzed at 13 microsatellite loci

N°	Cultivar	Origine	Fruit color	Fruit shape	Fruit consistency	mPdCIR010		mPdCIR015		mPdCIR016		mPdCIR035		mPdCIR025		mPdCIR044		mPdCIR048	
1	Abdelazaz	Biskra center	black	straight	soft	133	135	122	126	130	130	175	175	227	231	299	299	158	195
2	Adham Figig	Oued Righ	brown	oval	soft	133	135	124	124	128	130	164	175	227	231	299	299	158	193
3	Aghmou	Oued Righ	brown	oval	semi-dry	135	135	124	138	128	128	175	188	/	/	299	299	158	193
4	Ali Ourached	Oued Righ	brown	triangular	semi-dry	127	/	/	/	128	137	175	175	227	227	317	317	193	195
5	Alig	Oued Righ	yellow	oval	semi-dry	135	163	/	/	128	130	172	175	231	231	299	301	158	175
6	Arelou Oued Righ	Oued Righ	amber	oval	soft	/	/	124	138	128	130	175	177	200	213	299	299	195	195
7	Arelou Oued souf	Oued Righ	amber	oval	soft	126	135	124	130	130	130	189	189	213	231	301	301	193	195
8	Arelou Biskra	Biskra center	brown	oval	soft	/	/	/	/	130	130	172	188	213	227	301	301	158	175
9	Ba Makhlouf	Oued Righ	red	triangular	semi-dry	123	135	124	157	128	130	175	188	227	231	299	299	158	193
10	Bajamil	Oued Righ	amber	oval	soft	121	135	124	126	130	130	189	189	213	231	301	301	193	195
11	Ben Ftimi	Oued Righ	brown	oval	soft	133	135	124	126	130	130	172	177	215	227	299	299	158	195
12	Bousstite	Oued Righ	brown	straight	semi-dry	135	135	126	138	128	130	189	189	200	217	301	301	175	175
13	Caoucaou	Biskra center	brown	oval	semi-dry	/	135	/	/	130	130	175	182	213	213	299	301	/	/
14	Charka	Oued Righ	amber	straight	semi-dry	135	135	136	138	128	130	189	189	213	231	301	301	195	195
15	Dfor El Gat1	Oued Righ	yellow	oval	semi-dry	/	135	/	/	130	130	175	175	213	215	299	299	193	195
16	Dfor El Gat2	Oued Righ	black	straight	semi-dry	123	135	131	138	128	128	172	175	213	227	299	317	158	195
17	DGuel Mocht	Oued Righ	//	//	//	133	135	/	/	130	130	175	175	213	227	299	301	193	195
18	DGuel Sahara	Oued Righ	//	//	//	121	135	124	124	130	130	175	177	213	213	299	299	175	195
19	DGUel Asfar	Oued Righ	amber	straight	soft	133	135	124	138	128	130	175	175	/	/	299	301	/	/
20	DGuel Litima	Biskra center	amber	straight	semi-dry	163	135	136	138	130	130	165	172	215	231	301	301	195	195
21	DGuel Moussafirine	Oued Righ	brown	oval	semi-dry	133	135	124	157	128	130	162	175	200	213	299	299	158	193
22	DGuel Sebkhah	Oued Righ	brown	straight	semi-dry	133	135	124	124	128	130	175	188	200	231	299	299	158	193
23	DGuel Talmin	Oued Righ	brown	triangular	semi-dry	135	135	/	/	130	137	188	188	/	/	299	301	193	195
24	DGuel Yabes1	Oued Righ	yellow	triangular	dry	135	135	124	138	128	130	172	175	213	231	299	299	158	175
25	DGuel Yabes2	Oued Righ	yellow	triangular	dry	123	135	124	124	128	137	165	175	227	231	299	317	193	195
26	Ech Chouaib	Tolga	yellow	straight	semi-dry	123	135	124	138	130	137	/	/	/	/	299	317	175	193
27	Fakht	Oued Righ	brown	straight	dry	123	135	124	126	128	137	175	177	213	231	299	299	193	195
28	Fiqi Ali	Oued Righ	brown	straight	soft	123	135	124	138	128	137	175	188	200	227	301	301	195	195
29	Ghars	Biskra center	brown	triangular	soft	132	135	124	126	128	130	189	189	200	231	299	301	195	195
30	Gousbi	Oued Righ	yellow	straight	semi-dry	123	135	124	138	128	128	165	175	200	227	299	299	195	195
31	Haloua	Tolga	yellow	oval	semi-dry	135	135	124	138	128	130	189	189	213	213	299	299	195	195
32	Halouat Saada	Tolga	amber	oval	semi-dry	132	135	124	138	128	130	189	189	213	227	299	299	159	193

33	Hamrayet Ben Ghossa	Oued Righ	black	ovoid	soft	135	135	136	138	128	128	175	177	213	227	301	301	158	195
34	Hamrayet El Gaid	Oued Righ	black	triangular	semi-dry	135	135	124	124	/	/	175	177	213	227	299	301	158	195
35	Hamrayet El Ghareb	Oued Righ	black	triangular	soft	121	135	124	138	/	/	165	177	213	231	299	299	195	195
36	Hamrayet Hamlaoui	Oued Righ	black	straight	semi-dry	121	135	124	124	128	130	172	175	200	231	307	307	175	193
37	Hamri	Tolga	black	oval	dry	123	135	124	138	128	130	175	177	213	231	299	299	158	193
38	Harchaya	Biskra center	brown	straight	dry	132	135	124	124	128	128	189	189	213	213	299	301	193	195
39	Hartan	Oued Righ	brown	oval	semi-dry	135	135	124	138	128	128	189	189	213	231	299	299	158	193
40	Hathourite	M'chouneche	brown	triangular	soft	123	135	124	126	130	130	170	175	213	231	/	/	195	195
41	Hmira	Biskra center	amber	straight	soft	123	135	124	136	128	130	189	193	231	231	299	301	175	193
42	Houbless	Oued Righ	brown	oval	semi-dry	133	135	124	124	128	130	175	177	227	227	299	299	195	195
43	Ifkhfakhne	M'chouneche	brown	oval	semi-dry	135	135	122	138	128	130	165	172	213	217	301	317	158	175
44	Jaouzia	Biskra center	brown	oval	semi-dry	123	135	124	124	128	130	165	175	227	231	301	301	158	195
45	Khamara	Oued Righ	black	oval	soft	133	135	124	138	128	130	172	177	/	/	299	299	158	195
46	Ksebet ORigh	Oued Righ	amber	oval	semi-dry	133	135	/	/	128	130	189	189	227	231	299	299	158	175
47	Lamari	M'chouneche	brown	oval	semi-dry	135	/	122	126	130	130	189	189	227	231	299	299	158	195
48	Laoun El Ghars	Biskra center	brown	straight	soft	133	135	/	/	128	130	165	175	200	231	299	299	195	195
49	Loulou	Oued Righ	black	oval	soft	132	135	124	136	130	130	189	189	213	231	301	301	158	193
50	Mahdia	Oued Righ	yellow	oval	dry	135	138	124	136	130	130	189	189	200	227	299	299	158	193
51	Massohi	Oued Righ	red	oval	dry	123	123	124	126	130	130	189	206	227	231	299	317	175	193
52	Mech Degla	Biskra center	yellow	straight	dry	/	/	124	/	130	130	170	182	213	231	/	/	175	175
53	Melk Lahcen	Oued Righ	brown	triangular	semi-dry	123	126	124	124	130	130	189	189	215	231	301	301	193	195
54	Noyet Arechti	Biskra center	brown	oval	semi-dry	133	138	124	124	128	128	175	175	200	231	/	/	193	193
55	Ourije	Oued Righ	brown	straight	semi-dry	133	135	138	138	128	130	175	177	200	227	299	301	/	/
56	Regueb Lmkahel	Oued Righ	amber	straight	dry	123	135	138	138	128	128	177	182	213	227	299	299	175	195
57	Rotbet ABenHadj	Biskra center	yellow	oval	semi-dry	123	127	124	126	128	137	165	175	213	231	317	317	175	193
58	Rotbet Bakhlili	Biskra center	brown	oval	semi-dry	135	135	124	138	130	130	175	175	200	213	299	299	195	195
59	Rotbet Cheikh	Biskra center	amber	straight	soft	133	135	124	124	128	130	175	177	200	213	299	299	158	193
60	Saout Bghal	M'chouneche	black	straight	semi-dry	123	163	126	138	128	130	189	199	213	227	301	301	158	175
61	Tansslite Osouf	Oued Righ	black	straight	soft	121	123	124	157	128	130	175	175	213	227	299	299	158	193
62	Tabasrith	M'chouneche	brown	straight	soft	135	163	124	126	128	128	189	193	227	231	299	301	195	195
63	Tadmama	Oued Righ	red	oval	soft	133	135	124	157	128	130	175	188	200	213	299	299	193	195
64	Taferzait	Oued Righ	brown	oval	semi-dry	135	163	124	138	128	130	189	193	215	227	301	301	193	193
65	Tagnia	M'chouneche	brown	oval	semi-dry	123	135	138	138	130	130	189	189	200	213	299	299	158	193
66	Takarbout	Biskra center	black	round	semi-dry	133	135	124	136	128	130	165	175	/	/	/	/	193	193
67	Takarmoust	Biskra center	black	round	soft	132	135	124	138	128	130	189	189	213	231	299	299	158	195
68	Takarmoust	Oued	black	round	soft	127	127	124	136	/	/	175	188	/	/	299	301	175	195

	Osouf	Righ																		
69	Takerbrateth	M'chouneche	black	round	semi-dry	138	159	124	124	128	128	175	177	200	231	299	299	/	/	
70	Tamazoute	M'chouneche	amber	oval	dry	123	135	124	124	130	130	165	165	200	213	299	299	/	/	
71	Tansslite	Oued Righ	black	straight	soft	121	135	124	136	130	130	189	189	213	213	299	299	193	195	
72	Tanteboucht	M'chouneche	black	round	soft	135	163	124	130	130	130	189	189	213	227	299	299	158	195	
73	Taourekht	M'chouneche	brown	oval	soft	133	135	124	124	128	130	175	188	200	213	/	/	193	193	
74	Tbsrithe	M'chouneche	brown	straight	semi-dry	135	138	126	138	128	130	165	165	227	231	317	317	158	195	
75	Tinaser	M'chouneche	amber	oval	soft	121	135	/	/	128	130	172	175	213	231	299	299	193	195	
76	Tindokane	Oued Righ	black	round	soft	135	135	136	138	128	130	175	177	219	227	299	299	195	195	
77	Tinhoude	Oued Righ	yellow	oval	semi-dry	133	135	126	138	128	130	175	177	227	231	299	299	158	175	
78	Tinouajdel	Oued Righ	brown	straight	semi-dry	135	135	124	157	130	130	175	189	/	/	/	/	193	195	
79	Toumlih	Oued Righ	brown	oval	soft	133	135	124	124	128	128	164	177	213	213	299	299	158	193	
80	Tzoudaght	M'chouneche	black	straight	soft	133	138	124	124	128	132	188	198	200	227	/	/	195	195	

Supplementary Table 1. some morphological characters and genetic profiles of eighty Algerian date palm (*Phoenix dactylifera* L.) cultivars analyzed at 13 microsatellite loci

N°	Cultivar	Origine	Fruit color	Fruit shape	Fruit consistency	mPdCIR05 7	mPdCIR063 63	mPdCIR070 70	mPdCIR078 78	mPdCIR085 85	mPdCIR090 090						
1	Abdelazaz	Biskra center	black	straight	soft	254	254	140	140	194	199	/	/	157	169	141	166
2	Adham Figig	Oued Righ	brown	oval	soft	250	254	122	140	192	194	117	123	/	/	168	168
3	Aghmou	Oued Righ	brown	oval	semi-dry	250	252	140	155	194	195	120	152	157	171	161	168
4	Ali Ourached	Oued Righ	brown	triangular	semi-dry	250	256	140	140	/	/	121	123	179	179	141	168
5	Alig	Oued Righ	yellow	oval	semi-dry	252	254	155	155	/	/	134	146	167	179	141	169
6	Arelou Oued Righ	Oued Righ	amber	oval	soft	250	250	122	140	194	/	152	152	157	179	168	168
7	Arelou Oued souf	Oued Righ	amber	oval	soft	254	269	140	140	192	192	117	136	169	177	141	171
8	Arelou Biskra	Biskra center	brown	oval	soft	250	252	122	140	209	209	117	146	167	169	148	166
9	Ba Makhlouf	Oued Righ	red	triangular	semi-dry	250	254	140	155	193	195	152	152	171	177	141	168
10	Bajamil	Oued Righ	amber	oval	soft	254	256	140	140	186	197	136	146	169	177	141	141
11	Ben Ftimi	Oued Righ	brown	oval	soft	250	250	155	155	/	/	117	123	171	179	148	168
12	Bousstite	Oued Righ	brown	straight	semi-dry	250	254	122	122	192	192	134	146	149	165	/	/
13	Caoucaou	Biskra center	brown	oval	semi-dry	254	269	140	140	/	/	146	146	177	179	150	167
14	Charka	Oued Righ	amber	straight	semi-dry	250	263	122	140	192	192	117	152	177	179	141	141
15	Dfor El Gat1	Oued Righ	yellow	oval	semi-dry	254	263	140	140	/	/	136	146	169	179	141	141
16	Dfor El Gat2	Oued Righ	black	straight	semi-dry	250	254	140	155	/	/	117	123	149	161	168	168
17	DGuel Mocht	Oued Righ	//	//	//	250	254	140	155	/	/	134	152	171	177	141	150
18	DGuel Sahara	Oued Righ	//	//	//	252	256	122	140	192	197	117	136	169	171	141	148
19	DGUel Asfar	Oued Righ	amber	straight	soft	250	274	122	140	195	209	117	146	171	177	141	166
20	DGuel Litima	Biskra center	amber	straight	semi-dry	250	269	140	140	197	197	136	152	177	179	141	141

21	DGuel Moussafirine	Oued Righ	brown	oval	semi-dry	250	254	155	155	194	194	/	/	/	/	141	161
22	DGuel Sebkha	Oued Righ	brown	straight	semi-dry	269	269	122	140	/	/	117	117	/	/	141	166
23	DGuel Talmin	Oued Righ	brown	triangular	semi-dry	250	254	140	140	194	195	117	152	177	179	/	/
24	DGuel Yabes1	Oued Righ	yellow	triangular	dry	250	250	122	140	/	/	152	152	171	177	141	168
25	DGuel Yabes2	Oued Righ	yellow	triangular	dry	250	256	140	166	186	194	123	152	179	179	168	168
26	Ech Chouaib	Tolga	yellow	straight	semi-dry	250	254	140	155	/	/	/	/	/	/	/	/
27	Fakht	Oued Righ	brown	straight	dry	250	254	140	140	192	192	117	152	177	179	141	172
28	Fiqi Ali	Oued Righ	brown	straight	soft	256	269	/	/	192	/	117	117	149	171	/	/
29	Ghars	Biskra center	brown	triangular	soft	263	269	122	140	194	194	121	123	157	179	141	167
30	Gousbi	Oued Righ	yellow	straight	semi-dry	256	269	140	140	192	195	120	152	157	179	161	168
31	Haloua	Tolga	yellow	oval	semi-dry	250	250	122	140	/	/	117	152	157	171	161	169
32	Halouat Saada	Tolga	amber	oval	semi-dry	250	274	140	140	195	209	117	146	171	177	141	171
33	Hamrayet Ben Ghossa	Oued Righ	black	ovoid	soft	250	269	140	155	197	197	123	136	/	/	141	168
34	Hamrayet El Gaid	Oued Righ	black	triangular	semi-dry	250	254	140	155	194	197	152	152	169	179	141	168
35	Hamrayet El Ghareb	Oued Righ	black	triangular	soft	254	256	140	140	/	/	123	152	/	/	168	168
36	Hamrayet Hamlaoui	Oued Righ	black	straight	semi-dry	263	263	140	140	186	192	146	152	169	169	141	171
37	Hamri	Tolga	black	oval	dry	254	256	140	155	194	194	117	123	171	177	141	166
38	Harchaya	Biskra center	brown	straight	dry	256	269	122	140	194	195	117	123	177	179	141	167
39	Hartan	Oued Righ	brown	oval	semi-dry	250	254	140	155	186	194	123	146	171	177	141	167
40	Hathourite	M'chouneche	brown	triangular	soft	254	254	122	140	190	195	146	152	169	179	141	166
41	Hmira	Biskra center	amber	straight	soft	250	263	140	140	192	192	117	146	169	177	141	141
42	Houbless	Oued Righ	brown	oval	semi-dry	250	250	140	140	194	194	/	/	/	/	168	168
43	Ifkhfakhne	M'chouneche	brown	oval	semi-dry	254	254	122	140	192	192	117	146	/	/	141	141
44	Jaouzia	Biskra center	brown	oval	semi-dry	250	269	122	140	/	/	117	152	/	/	141	168
45	Khamara	Oued Righ	black	oval	soft	250	252	/	/	192	194	/	/	171	179	141	141
46	Ksebet ORigh	Oued Righ	amber	oval	semi-dry	250	252	155	155	/	/	123	136	171	171	169	169
47	Lamari	M'chouneche	brown	oval	semi-dry	254	254	122	140	194	199	117	152	157	169	141	167
48	Laoun El Ghars	Biskra center	brown	straight	soft	263	269	140	140	/	/	121	123	157	179	/	/
49	Loulou	Oued Righ	black	oval	soft	250	256	140	140	197	197	136	152	169	171	141	141
50	Mahdia	Oued Righ	yellow	oval	dry	250	254	140	155	192	192	117	152	171	177	169	169
51	Massohi	Oued Righ	red	oval	dry	256	263	166	166	194	207	117	146	171	179	141	171
52	Mech Degla	Biskra center	yellow	straight	dry	250	252	122	140	192	209	146	146	169	171	168	168
53	Melk Lahcen	Oued Righ	brown	triangular	semi-dry	254	256	122	140	197	197	117	136	157	169	141	169
54	Noyet Arehti	Biskra center	brown	oval	semi-dry	250	269	122	140	194	195	121	146	157	177	141	166
55	Ourije	Oued Righ	brown	straight	semi-dry	250	250	140	155	194	194	123	123	171	179	141	168
56	Regueb Lmkahel	Oued Righ	amber	straight	dry	250	269	140	140	197	197	121	152	/	/	141	168

57	Rotbet ABenHadj	Biskra center	yellow	oval	semi-dry	250	254	140	140	/	/	117	146	171	177	141	161
58	Rotbet Bakhlili	Biskra center	brown	oval	semi-dry	250	269	140	140	/	/	121	136	/	/	141	168
59	Rotbet Cheikh	Biskra center	amber	straight	soft	250	269	140	155	194	194	117	123	149	149	141	168
60	Saout Bghal	M'choune che	black	straight	semi-dry	250	252	122	122	209	209	117	146	167	167	150	167
61	Tansslite Osouf	Oued Righ	black	straight	soft	250	254	/	/	196	197	/	/	169	171	141	168
62	Tabasrith	M'choune che	brown	straight	soft	250	254	122	140	194	194	121	123	169	179	169	169
63	Tadmama	Oued Righ	red	oval	soft	250	254	140	140	192	194	/	/	177	179	168	168
64	Taferzait	Oued Righ	brown	oval	semi-dry	256	256	140	166	186	194	123	152	171	179	141	169
65	Tagnia	M'choune che	brown	oval	semi-dry	250	254	140	155	194	195	121	152	157	171	161	169
66	Takarboucht	Biskra center	black	round	semi-dry	254	256	140	140	186	195	117	146	157	177	141	161
67	Takarmoust	Biskra center	black	round	soft	250	252	140	155	192	195	123	152	171	179	141	141
68	Takarmoust Osouf	Oued Righ	black	round	soft	256	256	122	122	197	197	120	136	157	169	148	148
69	Takerbrateth	M'choune che	black	round	semi-dry	250	/	/	/	195	195	117	117	/	/	168	168
70	Tamazoute	M'choune che	amber	oval	dry	254	256	122	140	186	192	117	146	169	179	141	168
71	Tansslite	Oued Righ	black	straight	soft	254	263	140	140	197	209	136	146	169	179	141	141
72	Tanteboucht	M'choune che	black	round	soft	250	250	140	155	197	197	152	152	169	179	141	169
73	Taourekht	M'choune che	brown	oval	soft	254	254	140	140	186	195	/	/	177	177	141	166
74	Tbsrith	M'choune che	brown	straight	semi-dry	254	254	122	140	194	207	117	134	169	169	169	169
75	Tinaser	M'choune che	amber	oval	soft	250	269	122	140	194	194	117	121	149	149	141	141
76	Tindokane	Oued Righ	black	round	soft	250	254	122	140	192	194	123	136	149	149	141	141
77	Tinhoud	Oued Righ	yellow	oval	semi-dry	250	252	140	155	194	199	123	136	171	171	168	168
78	Tinouajdel	Oued Righ	brown	straight	semi-dry	254	254	140	155	186	197	117	146	/	/	141	141
79	Toumlih	Oued Righ	brown	oval	soft	250	254	122	140	192	194	117	152	157	171	/	/
80	Tzoudaght	M'choune che	black	straight	soft	250	254	140	155	192	194	117	121	157	169	161	168

Selenium-Supplemented Diet Influences Histological Features of Liver and Kidney in Tilapia (*Oreochromis niloticus*)

Sonia Iqbal^{1†}, Usman Atique^{1,2,†*}, Muhammad Sharif Mughal³, Muhammad Younus⁴, Muhammad Kamran Rafique⁴, Muhammad Sultan Haider⁵, Hafiza Sundas Iqbal⁶, Shahid Sherzada¹ and Tanveer Ali Khan⁷

¹Department of Fisheries and Aquaculture, University of Veterinary and Animal Sciences, Lahore, Pakistan; ²Department of Bioscience and Biotechnology, Chungnam National University, South Korea; ³Department of Zoology, Government College University (GCU), Lahore, Pakistan; ⁴College of Veterinary and Animal Sciences, Jhang, University of Veterinary and Animal Sciences, Lahore, Pakistan; ⁵Department of Zoology, University of Lahore, Pakistan; ⁶Department of Zoology, Lahore College for Women University, Lahore, Pakistan; ⁷Department of Zoology, University of Punjab, Lahore, Pakistan

Received: October 21, 2019; Revised: November 15, 2019; Accepted: December 15, 2019

† Indicates equal author contributions.

Abstract

Selenium is considered as an eco-toxicological paradox owing to its antioxidant and toxic properties. This study aimed at exploring the potential impacts of selenium supplemented in feed on the histology of vital organs of tilapia (*Oreochromis niloticus*). During this study, neither behavioural abnormalities nor any fish mortalities recorded in fish subjected to different selenium levels during this trial. The results revealed significant histological changes in liver and kidney tissues, mainly linked in a dose-dependent manner. The resultant histological changes exhibited mild or no alterations in fish that consumed the diet having 2 mg Se/kg. However, the intensity of histopathological alterations manifested more in the liver and kidney tissues of fish, having fed on a higher dose of selenium (8 mg Se/kg) as compared to control, 2, and 4 mg Se/kg in the feed. In the case of the liver, there were severe cytoplasmic vacuolations of hepatocytes and central vein dilation, erythrocytes haemolyzed, prominent vascular hypertrophy, and fibrosis of perivascular parts conspicuously noticeable leading to loss of characteristic architecture of hepatic tissues. However, in kidney tissues, renal tubules were seen atrophied and degenerative vacuolar changes in the renal tubular epithelial cells, pyknotic nuclei, as well as a thin layer of fibrous connective tissue (FCT), observed which were swiftly proliferating in peritubular parts of the medulla. In conclusion, selenium incorporated in higher concentrations damaged the vital organs in a dose-dependent manner resulting in histological alterations and proved to be harmful to the fish. However, lower level (2 mg/kg) did not influence or have the least affected histological changes in vital organs.

Keywords: Selenium; Liver; Kidney; Histological changes; Tilapia; Hepatocytes

1. Introduction

Tilapia (*Oreochromis niloticus*) has emerged as a model organism gaining attention from researchers for a variety of biological investigations such as immunology, growth, and histological inferences, i.e. the microscopic examination of different vital organs/tissue (Galman and Avtalion, 1989; Coward and Bromage, 1998; Benli and Özkul, 2010; Iqbal *et al.*, 2017; Guerreiro *et al.*, 2018). Exploring the chronic and acute toxic effects of varying selenium levels in the aquatic ecosystem and organisms has recently gained more attention (Lemly, 2004; Han *et al.*, 2011). Histological studies of kidney, liver, and muscles have been performed to investigate the influence of different micro-additives in the tilapia diet (Ramesh *et al.*, 2014; Obirikorang *et al.*, 2018; Kokou *et al.*, 2019; Ismail *et al.*, 2019) when used for beneficial purposes like growth enhancer.

Selenium (Se) is a non-metallic element and occurs in nature in different combinations such as selenite, selenate, and selenomethionine (Takayanagi 2001; Mechora *et al.*, 2013; Iqbal *et al.*, 2017). The primary natural sources of this element for fish are the water bodies and alluvial sediments (Patterson *et al.*, 2010; Younus *et al.*, 2015). It is a well-proven antioxidant as well as an indispensable part of numerous biological molecules like DNA and proteins (Han *et al.*, 2011; Moon *et al.*, 2020; Bae *et al.*, 2020). Therefore, it is recognized for its critical physiological role and is a prerequisite for the standard functioning of various enzymes and the immune system (Patterson *et al.*, 2010; Ramesh *et al.*, 2014; Sarkar *et al.*, 2015; Iqbal *et al.*, 2020). Selenite and selenate are prevailing compounds of selenium existing in the aquatic environment due to higher water solubility. Selenium concentrations (0.1 - 0.5 mg/kg dry weight of feed) recommended for normal physiological activities of fish (Hilton and Hodson, 1983; Gatlin and Wilson, 1984; Han *et al.*, 2011). However, excessive accumulation of

* Corresponding author e-mail: physioatique@gmail.com.

selenium in aquatic organisms caused rare haematological, histopathological, teratogenic, and reproductive disorders (Lemly, 2002) due to its persistent nature, bio-accumulative properties, and toxicity.

Recent studies confirming higher doses of selenium (8 mg/kg) resulted in inducing histopathological modifications and damaged the characteristic structure of liver cells. Studies in tilapia highlighted haemosiderin pigments, haemolysis of cells, and fatty degenerations, whereas lower concentrations (e.g., 2 mg/kg) induced necrotic changes (Morrison and Wright, 1999; Lemly, 2002) around blood vessels and caused haemolysis of cells. Similarly, lower selenium concentrations enhanced glutamate oxaloacetate transaminase (GOT) level, glutamate pyruvate transaminase (GPT) secretions, and lactate dehydrogenase concentration (LDH) in the target fishes (El-Hammady *et al.*, 2007; Wang *et al.*, 2018).

In most of the studies, using liver tissues as primary reference organs while assessing the selenium effects was due to the reported preferential selenium accumulation in the case of examined exposed fish specimens (Hodson *et al.*, 1980). Selenium compounds were also capable of protecting the internal organs from the toxicity of heavy metals such as cadmium and mercury and palm oil (Watanabe *et al.*, 1997; Zulfahmi *et al.*, 2018). Selenium is reported as an integral component of the enzyme glutathione peroxidase, which assumes the role in catalysis reactions that can protect the cell membranes against potential oxidative damages (Rotruck *et al.*, 1973). The use of different forms of organic selenium, for instance, selenomethionine and seleno-yeast to improve the bioavailability of selenium, also examined due to elevated potentially and higher bioavailability than ordinary inorganic selenium forms (Watanabe *et al.*, 1997; Schram *et al.*, 2008).

Very interestingly, several authors reported a fine line of difference between the edible (positive) and toxic (harmful) role of selenium. The disparity renders it as an existing contradiction in the field of aquatic toxicology since it is well established as an eco-toxicological paradox to act like both as essential micro-nutrient as well as a toxin depending upon its level in the environment (Schram *et al.*, 2008; Iqbal *et al.*, 2017). Therefore, it became critical to ascertain its role in changing the natural terrain of liver and kidney tissues when used as micronutrients to reveal a distinguishable line between constructive nutrient concentration and destructive toxic limits.

Considering the grander importance of selenium, the present study was conducted to investigate the potential role of selenium in the histopathological changes in vital organs in tilapia. We studied kidney and liver to witness the possible effects of different levels of selenium dispensed to tilapia incorporated in fish feed under laboratory conditions.

2. Materials and Methods

2.1. Experimental site

The 90 days long study about the potential effect of selenium on histology of selected vital organs of tilapia (*O. niloticus*) was conducted in Research and Training Facilities at the Department of Fisheries and Aquaculture,

University of Veterinary and Animal Sciences (Ravi Campus, Pattoki), Lahore, Pakistan.

Table 1. Selected Feed Ingredients (dry weight), inclusion level and chemical composition of experimental and basal diets

Sr. #	Ingredients	Inclusion level (g/100g)			
		Basal diet (Control)	Treatment 1	Treatment 2	Treatment 3
1	Fish meal	8	8	8	8
2	Guar meal	30	29.998	29.996	29.992
3	Soya bean meal	9	9	9	9
4	Wheat bran	18	18	18	18
5	Canola meal	8	8	8	8
6	Rice polish	24	24	24	24
7	Vitamin Premix ^a	2	2	2	2
8	Selenium free mineral premix ^b	1	1	1	1
9	Selenium dose ^c	0.00	0.002	0.004	0.008
Total		100 g			
Chemical composition					
1	Crude protein	30.2	30.2	30.2	30.1
2	Crude lipid	7.3	7.2	7.3	7.3
3	Dry matter	86.4	86.4	86.3	86.5
4	Ash	6.8	6.7	6.6	6.9

a: Vitamin premix (IU or g/kg diet): vitamin A, 16000 IU; vitamin D, 8000 IU; vitamin K, 14.72; thiamin, 17.8; riboflavin, 48; pyridoxine, 29.52; cyanocobalamin, 0.24; tocopherols acetate, 160; ascorbic acid (35%), 800; niacinamide, 79.2; Calcium-D-pantothenate, 73.6; folic acid, 6.4; biotin, 0.64; inositol, 320; choline chloride, 1500; L-carnitine, 100; **b:** Selenium free mineral premix; (g /kg of diet): calcium, 5.5; phosphorus, 17.5; iron, 10; magnesium, 2.8; copper, 1.5; iodine, 0.15; manganese, 9.5; zinc, 25; cobalt, 0.13; **c:** Sodium selenite (Na_2SeO_3) in milligrams

2.2. Fish management and experimental plan

Healthy tilapia fish were collected from the nursery ponds at the training facilities and were acclimated to laboratory conditions in indoor cemented rectangular-shaped tanks for two weeks duration before the experiment. The given feed compositions were based on selenium-graded inclusion levels along with respective chemical composition given in table 1. Three doses of formulated fish feed were prepared on the basis of selenium supplementation level viz., 2 mg/kg (Treatment-1), 4 mg/kg (Treatment-2) and 8 mg/kg (Treatment-3) of selenium in fish feed and were properly mixed followed by extrusion, drying and finally storage at -20°C while considering each dose as a distinctive treatment. The controlled diet did not receive selenium supplementation. This trial was executed in four fixed cemented rectangular fish tanks constructed with dimensions as 2.896 × 0.762 × 0.914 m (length × width × depth) and with 2.018 cubic meters total water capacity. Tank 1, 2, and 3, were designated as treatment tanks, whereas the fourth one as selenium deficient (control). There were three replicates in each treatment tank, as well as in the selenium-deficient treatment tank. The stocking density fixed to 15 fish per tank having weight ranges 10 – 25 g and fed on 30% crude protein feed dispensed at the rate of 3% body weight thrice per day. The physicochemical water quality was monitored daily to manage the potential water quality stressors on histopathological changes. We ensured continuous supply of fresh and well-oxygenated turbine water while the optimal water levels were maintained by discharges via overflow pipes.

2.3. Histopathological assessments

Samples from the excised tissues of selected vital organs of interest viz., liver, being major detoxifying organ and kidney, being the excretion factory, procured after euthanizing the fishes (by using MS222) followed by anesthesia. The removed organ samples were properly preserved in neutrally buffered formalin solution for 24 hours, followed by dehydration of the tissues as per the method of Lille and Fullmer (1976). The clearing, infiltration and embedding, section cutting (5 μ), and stretching of tissues were performed after that. Hematoxylin was the staining reagent used for tissues nucleic acid staining. On the other hand, eosin used as staining reagent for cytoplasm and extracellular matrix as established by Luna (1968) and Bernet *et al.* (1999). Slides were stained by using the method described by Lille and Fullmer (1976). Then, coverslips were mounted by using DPX followed by coding and stochastic analysis. These slides were analyzed quantitatively to explore the histopathological alterations including degenerated vacuoles, necrosis, apoptosis as well as the general health of cells that are visible by hematoxylin and eosin (H & E).

Table 2. Records of selected physicochemical parameters in treatment and control Tanks

Water Quality Parameters	Treatments				Permissible limits
	Control	Treatment 1	Treatment 2	Treatment 3	
pH	8.58 \pm 0.020	8.56 \pm 0.028	8.58 \pm 0.017	8.57 \pm 0.018	7-9
D.O.	6.20 \pm 0.150	6.04 \pm 0.167	6.14 \pm 0.289	6.26 \pm 0.274	>5
Temperature ($^{\circ}$ C)	30.35 \pm 0.022	30.35 \pm 0.026	30.33 \pm 0.030	30.34 \pm 0.022	15-35
TDS	396.92 \pm 26.88	378.06 \pm 23.378	441.81 \pm 37.648	430.19 \pm 32.532	500-1200
EC (μ S/cm)	649.09 \pm 14.776	659.27 \pm 34.58	663.29 \pm 30.429	697.79 \pm 23.835	300-1500
Hardness	18.1 \pm 0.012	18.2 \pm 0.014	18.03 \pm 0.018	17.9 \pm 0.015	>20
Nitrates	0.83 \pm 0.13	0.84 \pm 0.15	0.83 \pm 0.14	0.84 \pm 0.20	0-100
Chlorides	6.5 \pm 0.11	6.9 \pm 0.19	7.0 \pm 0.13	7.0 \pm 0.18	4-160
Salinity	0.8 \pm 0	0.8 \pm 0.001	0.8 \pm 0.01	0.8 \pm 0.02	--
Ammonia	N.D.	0.011 \pm 0.0034	0.012 \pm 0.0051	0.010 \pm 0.0032	0-0.05

D.O.: Dissolved oxygen, TDS: Total dissolved solids, EC: Electrical conductivity, T.A. Total alkalinity, N.D.: Not detected. All values are mentioned in mg/L (ppm) except pH, temperature, and electrical conductivity. Our results displayed that the central vein was dilated in the liver of control treatment fish. Moreover, mild vacuolation was also seen in hepatocytes cytoplasm. However, portal areas were not distinctly observed. In the case of kidney tissues from control group fish, tubules were seen with the empty lumen. Haematopoietic tissues were also present (Figure 1 a,b).

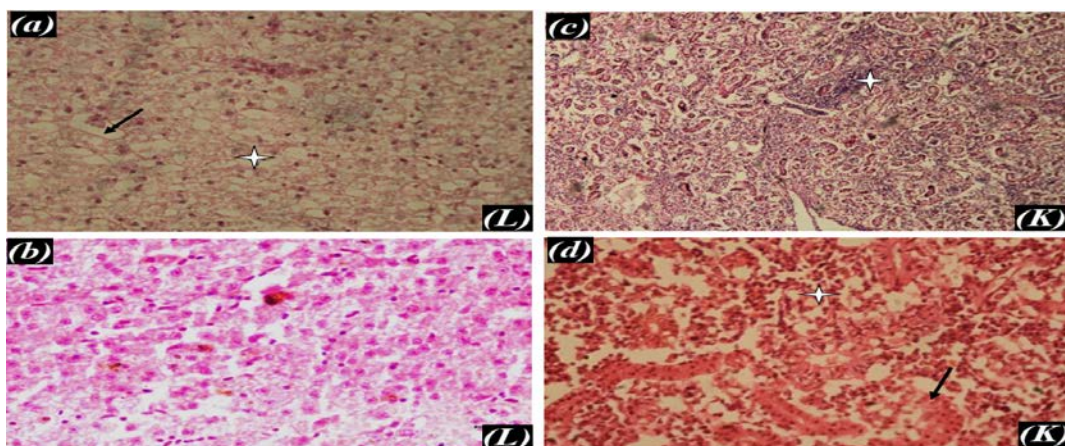


Figure 1. Comparison between Liver (L) and Kidney (K) histological changes in control and 2 mg/kg treatments. (a) T. S. of liver control group (Central vein seems to be dilated (represented by a thin black arrow). Mild vacuolation (indicated by a star) is seen in hepatocytes cytoplasm. Portal areas are not seen distinctly here (H&E 40X); (b) T. S. of Liver Se 2mg/ kg feed (Treatment-1) Mild degenerative changes are seen (Less histological alterations seen); (c) T. S. of kidney control group (Tubules are seen with empty lumen (indicated by thin arrow). Hematopoietic tissue is also present (represented by a star) (H&E 10x); (d) T.S. of kidney treated with Se 2mg/ kg feed (Treatment-1) (Mild infiltration of mononuclear cells, vacuolation in tubular epithelial cells seen with pyknotic nuclei (represented by an arrow). Some renal tubules are completely collapsed with their obliterated lumen (designated by a star) (H&E 40x).

Three views per fish were conducted at 10 \times and 40 \times and analysis was tabulated by using the scoring system as described by Bernet *et al.* (1999). Photographs were accomplished with a trinocular microscope using a Nikon digital camera (Bancroft and Gamble, 2007).

3. Results

The physicochemical quality of the experimental culture environment maintained around the optimal ranges (Table 2). No apparent disease symptoms, slow movements, morbid, or moribund fish samples were noticed during the study duration. Before histological sample processing, systematic macroscopic observation of fish, including internal and external morphology, was performed with the help of lens and naked eye, and it did not reveal any macroscopic abnormalities, attaching parasites on gills and skin and no injuries were noticed. The comparative details of histopathological alterations in liver and kidney of tilapia (*O. niloticus*) fed on selenium graded diets are mentioned in table 1.

Mild degenerative changes were seen in the liver of tilapia (*O. niloticus*) fish exposed to selenium (2 mg Se/kg). Slight histopathological changes were observed in the liver and kidney of fish exposed to 2 mg Se/kg. We observed mild infiltration of mononuclear cells found in the kidney of fish exposed to selenium supplemented feed (2 mg Se/kg). Vacuolation in tubular epithelial cells seen with pyknotic nuclei. Some renal tubules completely collapsed with their obliterated lumen (Figure 1 c,d).

Table 3. Comparative details of histopathological alterations in liver and kidney of tilapia (*Oreochromis niloticus*) fed on control and selenium graded diets

Dose Range	Histopathological changes in selected vital organs	
	Liver	Kidney
Control	Central vein dilated Mild vacuolations in hepatocytes cytoplasm.	No distinct portal areas Tubules with the empty lumen Hematopoietic tissues present
Treatment 1 (2 mg Se/Kg)	Mildly degenerated	Mild infiltration of mononuclear cells Pyknotic nuclei Vacuolations in tubular epithelial cells Renal tubules collapsed with the obliterated lumen
Treatment 2 (4 mg Se/Kg)	Infiltration of fat in the vacuoles of the hepatocyte cytoplasm Thickening of blood vessels leading to dilation Fatty degeneration in parenchymal cells Peripherally displaced nuclei Hemosiderin pigments in blood vessels Vascular congestion in blood vessels	Degeneration Fibrosis The lumen of renal tubules filled with an eosinophilic proteinaceous mass Degenerative changes in epithelial cells Congestion of blood vessels
Treatment 3 (8 mg Se/Kg)	Fibrosis in the perivascular area Severe vacuolations in hepatocytes cytoplasm Fibrous connective tissue tracts indicate fibrosis Vascular hypertrophy Central vein dilated Haemolysed erythrocytes Dilated central vein with the empty lumen Hemosiderin pigment in a central vein Nuclei elongated and pushed towards periphery	Renal tubules undergoing atrophy Degenerative vacuolar changes in renal tubules Pyknotic changes in epithelial cells nuclei Hyaline casts in the tubular lumen Sloughing of tubular epithelial cells The thin layer of fibrous connective tissue in peritubular areas

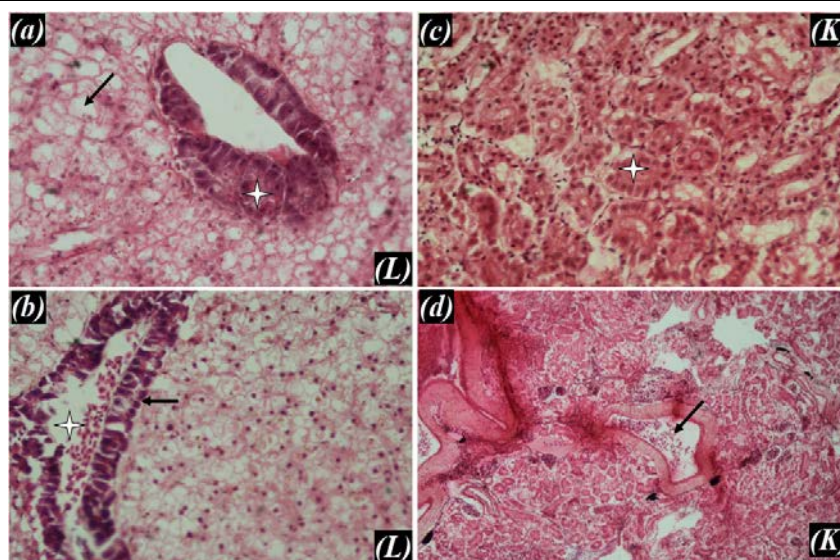


Figure 2. Comparison between Liver (L) and Kidney (K) histological changes treated by Se 4 mg/kg. (a) T. S. of Liver treated with Se 4mg/kg (Treatment-1) (Blood vessel is extremely dilated with thickening in its wall (represented by a star). Fatty degeneration is also present in parenchymal cells with peripherally displaced nuclei seen clearly (represented by arrow) 40x H&E Stain); (b) T.S. of Liver treated with Se 4mg/kg (Treatment-2) (Vascular congestion is seen with degenerative changes in blood vessel wall (represented by arrow). At some places hemosiderin pigment is also visible, 40x H&E.); (c) T. S. of Kidney treated with Se 4mg/kg (treatment-2) (Lumen of renal tubules is filled with eosinophilic proteinaceous mass (represented by star). Degenerative changes are evident in lining epithelial cells are also seen. 40x H&E); (d) T. S. of Kidney treated with 4mg/kg (Treatment-2) (Lumen of blood vessel is dilated with congestion (represented by arrow) H&E 40x).

Table 4. A histopathological score of the liver of tilapia fed on control and selenium graded diets (n=5)

Histopathological Change	Control	Treatment 1	Treatment 2	Treatment 3
Focal necrosis	-	-	+	+
Vacuolation	+	-	++	+++
Hemorrhage	-	-	++	+
Pyknotic hepatocytes	-	-	+	+++
Hypertrophy	-	-	-	++
Congested blood cells	-	-	++	+++
Fibrosis	+	-	+	+++
Inflammatory cell infiltration	+	-	++	+
Tumor (Benign/malignant)	-	-	-	-

Where - Symbolizes no significant histopathological alterations; + Mild alterations; ++ Moderate alterations; +++ Severe alterations

Table 5. A histopathological score of the kidney of tilapia fed on control and selenium graded diets (n=5)

Histopathological Change	Control	Treatment 1	Treatment 2	Treatment 3
General necrosis	-	-	++	++
Pyknotic nuclei	+	+	-	+++
Vacuolations	-	+	+	+++
Fibrosis	-	-	+++	+++
Congested blood cells	+	-	+++	++
Atrophy	-	-	+	+++
Hemorrhage	-	-	++	++
Tumor (benign/malignant)	-	-	-	-

Where - Symbolizes no significant histopathological alterations; + Mild alterations; ++ Moderate alterations; +++ Severe alterations

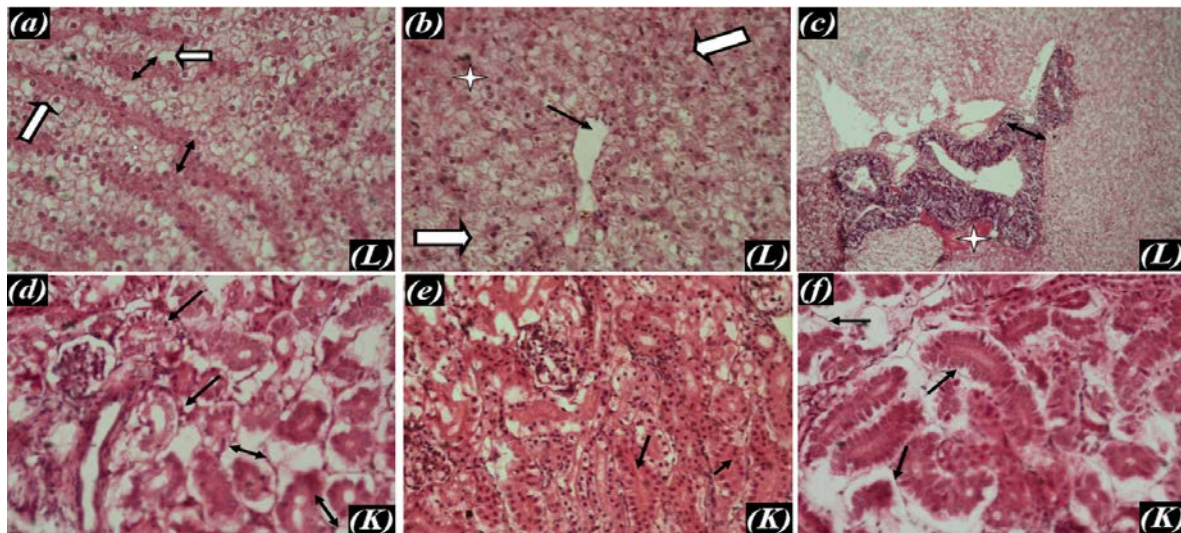


Figure 3. Comparison between Liver (L) and Kidney (K) histological changes under Se 8 mg/kg treatment. (a) T. S. of Liver treated with Se 8mg/kg (Treatment-3) (Severe vacuolation is present in hepatocytes cytoplasm indicate fatty change (represented by arrowhead). Fibrous connective tissue tracts are also present indicates fibrosis (black arrow) 40x; H&E); (b) T. S. of Liver treated with Se 8mg/kg (Treatment-3) (Dilated central vein with empty lumen is seen (indicated through black arrow). Haemosiderin pigment is also present (represented by arrowhead). Unstained fat vacuoles seen in hepatocyte cytoplasm (represented through star) (H&E 40x); (c) T. S. of Liver treated with Se 8mg/kg (Treatment-3) (Vascular hypertrophy (represented through double arrow) with thickened wall is seen. In perivascular area fibrosis is also seen) (H&E 40x); (d) T. S. of Kidney treated with Se 8mg/kg (Treatment-3) (Renal tubules are undergoing atrophy (represented by double arrow). Degenerative vacuolar changes are seen in many renal tubules (indicated through thin arrow) (H&E; 40x); (e) T. S. of Kidney treated with Se 8mg/kg (Treatment-3) (Hyaline casts are present in tubular lumen (indicated by thin arrow). Pyknotic changes are seen in epithelial cells nuclei) (H&E; 40x); (f) T. S. of Kidney treated with Se 8mg/kg (Treatment-3) (Thin layer of fibrous connective tissue (FCT) is seen in peritubular areas at many places (indicated through thin arrow). Tubular epithelial cells are also undergoing sloughing) (H&E; 40x).

The occurrence of histopathological modifications was much evident in the kidney of the fish exposed to selenium dose of 8 mg/kg supplemented in the feed as compared to the control, 2, and 4 mg Se/kg. However, the liver of fish exposed to 8 mg/kg Se, vascular hypertrophy with thickened wall was also seen. In the perivascular area, fibrosis was also seen. In the kidney of fish exposed to 8 mg Se/kg, renal tubules were undergoing atrophy. Degenerative vacuolar changes were also seen in many renal tubules (Figure 3 a-f). The histopathological scores of liver and kidney of tilapia fed on control and selenium

graded diets are presented in Tables 4 and 5. The results indicated moderate to severe alterations in the liver and kidney of *O. niloticus* in the 2 mg/Kg and 8 mg/Kg selenium treatments. Critical changes in pyknotic hepatocytes, blood cells, and Fibrosis were predominant in the liver in 8 mg/Kg selenium treatment while severe vacuolations, fibrosis, and atrophy were observed in the kidney in the same treatment.

4. Discussion

Histopathological studies are accomplished to explore the preliminary effects or responses as well as acute exposure results to environmental chemical stressors because of the ability of fish to respond to the direct impact as well as secondary effects caused by the mounting stress (Atique *et al.*, 2020a; Khanom *et al.*, 2020; Saeed *et al.*, 2020). The liver and kidney are the vital organs that can respond to such changes (Bernet *et al.*, 2004; El-Hammady *et al.*, 2007). The liver is also one of the essential digestive glands in fish and is the largest extramural organ. Liver in fish is supposed to carry out the essential physiological activities including but not limited to homeostatic maintenance, plasma protein synthesis, storage (e.g., energy, vitamins, and trace metals), nutrient assimilation, bile production, and detoxification. The fish liver may or may not contain pancreatic tissues. The kidney is the principal excretory organ for water elimination, particularly vital to freshwater fishes due to its reabsorption mechanisms for water-salt maintenance. The water quality holds the key of the balanced regulatory functions in fish in controlled (Haider *et al.*, 2016; Batool *et al.*, 2018; Haider *et al.*, 2018; Khan *et al.*, 2018) and natural waters (Atique and An, 2018; Atique *et al.*, 2019; Atique *et al.*, 2020b; Atique and An, 2020; HaRa *et al.*, 2020). The teleost kidney is partly comprised of haematopoietic, excretory parts, phagocytic, and endocrine tissues. The fish kidney may or may not be fused in the structural arrangement. During response generation to the uncomplimentary developments in or outside of the body, they can be studied as indicative organs as they undergo various histological changes.

Mild degenerative changes were observed in liver and kidney tissues of tilapia (*O. niloticus*) fed on 2 mg/kg diet. Our results of the present study are corroborating with El-Hammady *et al.* (2007), who revealed less or negligible histopathological modifications in fish exposed to a lower dose of selenium, i.e., 2 mg/kg in the feed. Noticeably, the colour of the liver in fish exposed to 2 mg/kg was of dull grey-red when matched to other selenium graded treatment tilapias, i.e. 4 mg/kg and a higher dose of 8mg/kg of feed. It may have been caused by the mild degenerative alterations linked to selenium dose (Gatlin and Wilson, 1984). It is imperative to consider that a healthy fish is not only categorized based on absence or presence of histopathological changes because it may exhibit mild or moderate histological alterations or inflammatory responses owing to physical reactions (Bernet *et al.*, 2004). In this study, slight infiltrations of the mononuclear cells in the kidney of fish were witnessed in the lower level of selenium-supplemented treatment, i.e., 2 mg/kg of feed. Our results conform with Peebua *et al.* (2008), who discovered vacuolations in many tubules as well as nuclear pyknosis in the fish kidney.

To the next level of selenium-graded diet effects, the liver in fish devouring the 4 mg/kg feed resulted in the dilation of the lumen of blood vessels and thickening in their walls. Fatty degeneration was also noticed in the parenchymal cells with clearly displaced peripheral nuclei. The kidney of the same treated group denoted degeneration and fibrosis. The lumen in renal tubules was observed to be filled with eosinophilic proteinaceous mass. Also, several degenerative changes were marked in the

lining of epithelial cells. Similar results were corroborated by the application of Bernet *et al.* (1999) protocol that supported our conclusions. The outcomes were in a match with the findings of El-Hammady *et al.* (2007), who also recorded the degenerative variations as well as fibrosis in fish kidney fed on similar diet regimes.

Moreover, hepatic cells degeneration and hemorrhages were also distinguishable. The blood vessels dilation was noticed very prominently (Hilton *et al.*, 1980). In the previous studies, renal tubular degeneration as well as the perturbed circulatory mechanism like hemorrhages observed in the cultured fish have been concomitant of an antibiotic treatment (Smith *et al.*, 1973; Roberts, 2012), whereas, the necrosis of renal haematopoietic tissues, which are indeed very sensitive, may arise due to various biotic and toxic situations or medications (Roberts, 2012).

Frequency and histopathological alterations score recorded in our study were very conspicuous in the liver and kidney tissues processed from 8 mg/kg selenium incorporated feed. Tilapia (*O. niloticus*), when fed on a high dose of selenium (8 mg/kg), different sections of liver exhibited hemosiderin pigments along with hemolysis of cells and fatty degenerations. Such abnormal deposition of fat in the fish liver from treatment 3 resulted due to the excessive fat production as well as its utilization (Lemly, 2002). Desai *et al.* (1984) put forth similar observations having said that the fatty degenerative changes in the liver of tilapia linked with the reduction of an energy consumption level or on the contrary, argued at the enhanced amount of fat synthesis.

In the same pattern, uptake and increase of selenium levels in trout (*Salmo gairdneri*) tissues inhabited for a prolonged duration while feeding at supplemented selenium dose (3µg/kg) diet may result in toxicity (Hilton *et al.*, 1980). If trout are exposed to selenium added feed (4.29 and 15.00 µg/g), its detoxification into methyl derivatives and seleno-proteins inside the liver.

Our findings also corroborate with Peebua *et al.* (2008), who confirmed that hepatocytes indicate necrosis, accumulated lipid vacuoles, hydropic swelling as well as the vacuolation present in the liver. It further argued that tubular cells go through hydropic blisters, the lipid vacuoles accumulate in the cytoplasm of the tubular epithelial cells along with pyknotic nuclear alterations (Morrison and Wright, 1999). Therefore, such histopathological changes of hepatocytes indicated towards the hydropic degeneration, as well as the accumulation of lipid vacuoles and necrotic changes in the liver, are essential. On the other hand, the histopathological changes in kidney tissues included the mass of vacuoles in tubular cells and stark necrotic areas and tubular degeneration. Our findings corroborate with the observations of Oulmi *et al.* (1995) in the case of *O. mykiss* and Gupta and Kumar (2006) in *C. mrigala*. Both groups observed small granules in the cytoplasmic region, haemolysis of cells in addition to nuclear deformations of the epithelium in the proximal tubules.

The overall findings of our study corroborate with the investigations of Hilton *et al.* (1980), who published his observations conveying that when selenium level exceeded the limit of 0.38 µg/g, escalated uptake of selenium in liver witnessed. Ramesh *et al.* (2014) and El-Hammady *et al.* (2007) both identified that the liver damages could be seen in case of excessive accumulation of sodium selenite that

ultimately leads to liver toxicity (Lemly, 2002). The liver is so definitely prone to selenium toxicity being the main selenium storage organ, as well as for detoxification (Hodson *et al.*, 1980). Also, degenerative structural changes in tissues of the liver occur when the fish is exposed to an increased concentration of selenium (Sorensen *et al.*, 1984). Besides, toxicants lead to liver cell necrosis and vascular degeneration (Malarvizhi *et al.*, 2012).

5. Conclusion

It is concluded that dietary selenium could inflict tissue damages if fed to juvenile tilapia in considerably higher concentrations. However, it inflicted minimal tissue damages when fed at lower levels incorporated in fish feed. Such significant variations in selenium toxicity in vital organ tissues suggested a higher degree of complexity in the selenium toxicity mechanism. However, the present study paved the way towards the recommendation of lower levels of selenium supplemented in the fish feed for tilapia, which could be very useful for fish health.

Author Contributions

SI and UA equally contributed to this study and conducted the experiment, collected the samples, and analyzed the data and prepared the manuscript under the supervision of MSM and MY. MKR helped in image processing while MSH, HSI, SS, and TAK helped in manuscript preparation.

Funding

This research received no external funding.

Acknowledgements

We thankfully acknowledge the management of the Department of Fisheries and Aquaculture for providing logistic support in completing this study.

Conflict of Interests

The authors declare no conflict of interest.

References

Atique U and An K-G. 2018. Stream Health Evaluation Using a Combined Approach of Multi-Metric Chemical Pollution. *Water*, **10**: 661. <https://doi.org/https://doi.org/10.3390/w10050661>

Atique U, Byungjin L, Johee Y and An K-G. 2019. Biological Health Assessments of Lotic Waters by Biotic Integrity Indices and their Relations to Water Chemistry. *Water*, **11**: 436. <https://doi.org/10.3390/w11030436>

Atique U and An, K-G. 2020. Landscape heterogeneity impacts water chemistry, nutrient regime, organic matter and chlorophyll dynamics in agricultural reservoirs. *Ecol. Indic.*, **110**: 105813. doi:10.1016/j.ecolind.2019.105813

Atique U, Iqbal S, Khan N, Qazi B, Javeed A, Anjum KM, Haider MS, Khan TA, Mahmood S and Sherzada S. 2020a. Multivariate Assessment of Water Chemistry and Metals in a River Impacted by Tanning Industry. *Fresenius Environ. Bull.*, **29**(04): 3013–3025.

Atique U, Kwon S-K and An, K-G. 2020b. Linking weir imprints with riverine water chemistry, microhabitat alterations, fish assemblages, chlorophyll-nutrient dynamics, and ecological health assessments. *Ecol. Indic.*, **117**: 106652. doi:10.1016/j.ecolind.2020.106652

Bae D-Y, Atique U, Yoon J, Lim B and An K-G. 2020. Ecological Risk Assessment of Urban Streams Using Fish Biomarkers of DNA Damages and Physiological Responses. *Polish J Environ Stud.*, **29**:1–10. doi:10.15244/pjoes/104660

Bancroft JD and Gamble M. 2007. **Theory and Practice of Histological Techniques** (5th Ed) Churchill Livingstone London, 125-138 pp.

Batool SS, Khan N, Atique U, Azmat H, Iqbal KJ, Mughal DH, Ahmad MS, Batool S, Munawar S, Dogar S, Nawaz M and Amjad S. 2018. Impact of Azomite Supplemented Diets on the Growth and Body Composition of Catfish (*Pangasius hypophthalmus*). *Pak J Zool.*, **Suppl. Ser**: 08–12. doi:http://dx.doi.org/10.17582/journal.pjz/2018.SuppSer13

Benli AÇK and Özkul A. 2010. Acute toxicity and histopathological effects of sublethal fenitrothion on Nile tilapia, *Oreochromis niloticus*. *Pestic Biochem Physiol.*, **97**: 32–35. doi:10.1016/j.pestbp.2009.12.001

Bernet D, Schmidt H, Meier W, Burkhardttholm P and Wahli T. 1999. Histopathology in fish: Proposal for a protocol to assess aquatic pollution. *J Fish Dis.*, **22**: 25-34. <https://doi.org/10.1046/j.1365-2761.1999.00134.x>

Bernet D, Schmidt-Posthaus H, Wahli T and Burkhardt-Holm P. 2004. Evaluation of two monitoring approaches to assess effects of wastewater disposal on histological alterations in fish. *Hydrobiologia*, **524**: 53–66. <https://doi.org/10.1023/B:HYDR.0000036196.84682.27>

Coward K and Bromage NR. 1998. Histological classification of oocyte growth and the dynamics of ovarian recrudescence in *Tilapia zillions*. *J Fish Bio.*, **53**: 285–302. <https://doi.org/10.1111/j.1095-8649.1998.tb00981.x>

Desai AK, Joshi MM and Ambadhori PA. 1984. Histological observations on the liver of *Tilapia mossambica* after exposure to monocrotophos, an organophosphorus insecticide. *Toxicol Lett.*, **27**: 325-331. [https://doi.org/10.1016/0378-4274\(84\)90092-4](https://doi.org/10.1016/0378-4274(84)90092-4)

El-Hammady AKI, Ibrahim SA and El-Kasheif MA. 2007. Synergistic reactions between vitamin E and Selenium in diets of hybrid tilapia (*Oreochromis niloticus* x *Oreochromis aureus*) and their effect on the growth and liver histological structure. *Egyptian J Aquat Biol Fish.*, **30**: 53-58.

Galman OR and Avtalion OR. 1989. Further study of the embryonic development of *Oreochromis niloticus* (Cichlidae, Teleostei) using scanning electron microscopy. *J Fish Biol.*, **34**: 653-664. <https://doi.org/10.1111/j.1095-8649.1989.tb03347.x>

Gatlin DM and Wilson RP. 1984. Dietary selenium requirement of fingerling channel catfish. *J Nutr.*, **114**: 627–633. <https://doi.org/10.1093/jn/114.3.627>

Guerreiro I, Oliva-Teles A and Enes P. 2018. Prebiotics as functional ingredients: focus on Mediterranean fish aquaculture. *Rev Aquac.*, **10**(4): 800-832. doi:10.1111/raq.12201

Gupta AK and Kumar A. 2006. Histopathological lesions in the selected tissues of *Cirrhinus mrigala* (Ham.) fingerlings exposed to a sublethal concentration of mercury. *J Environ Biol.*, **27**: 235-240.

Haider MS, Ashraf M, Azmat H, Khaliq A, Javid A, Atique U, Zia M, Iqbal KJ, and Akram S. 2016. Nutritive evaluation of fish acid silage in *Labeo rohita* fingerlings feed. *J Appl Anim Res.*, **44**: 158–164. doi:10.1080/09712119.2015.1021811

Haider MS, Javid A, Azmat H, Abbas S, Ashraf S, Altaf M, Atique U, Iqbal S, Iqbal KJ, and Baool M, 2018. Effect of

- Processed Fish Waste on Growth Rate and Digestive Enzymes Activities in *Cyprinus carpio*. *Pak J Zool., Suppl. Ser:* 191–198. doi:http://dx.doi.org/10.17582/journal.pjz/2018.SupplSer13
- Han D, Xie S, Liu, M, Xiao X, Liu H, Zhu X and Yang Y. 2011. The effects of dietary selenium on growth performances, oxidative stress and tissue selenium concentration of gibel carp (*Carassius auratus gibelio*). *Aquac Nutr.*, **17**: 741-749. doi:10.1111/j.1365-2095.2010.00841.x
- HaRa J, Atique U and An K-G. 2020. Multiyear Links between Water Chemistry, Algal Chlorophyll, Drought-Flood Regime, and Nutrient Enrichment in a Morphologically Complex Reservoir. *Int. J. Environ. Res.*, **17**(9): 3139. doi:10.3390/IJERPH17093139
- Hilton JW, Hodson PV and Slinger SJ. 1980. The requirement and toxicity of selenium in rainbow trout (*Salmo gairdneri*). *Nutrition*. **770**: 2527-2535. doi:10.1093/jn/110.12.2527
- Hilton TW and Hodson PV. 1983. Effect of increased dietary carbohydrate on selenium metabolism and toxicity in rainbow trout (*salmo gairdneri*). *J Nutr.*, **113**: 1241-1248. https://doi.org/10.1093/jn/113.6.1241
- Hodson PV, Spray DJ and Blunt BR. 1980. Effects of rainbow trout (*Salmo gairdneri*) of a chronic exposure to water-born selenium. *Can J Fish Aquat Sci.*, **37**: 233-40. https://doi.org/10.1139/f80-030
- Iqbal S, Atique U, Mughal MS, Khan N, Haider MS, Iqbal KJ and Akmal M. 2017. Effect of Selenium Incorporated in Feed on the Hematological Profile of Tilapia (*Oreochromis niloticus*). *J Aquac Res Development.*, **8**: 513. doi: 10.4172/2155-9546.1000513
- Iqbal S, Atique U, Mahboob S, Haider MS, Iqbal HS, Al-Ghanim KA, Al-Misned F, Ahmed Z and Mughal MS. 2020. Effect of Supplemental Selenium in Fish Feed Boosts Growth and Gut Enzyme Activity in Juvenile Tilapia (*Oreochromis niloticus*). *J. King Saud Univ. Sci.*, **35**(5): 2610–2616. doi: 10.1016/j.jksus.2020.05.001
- Ismail M, Wahdan A, Yusuf MS, Metwally E and Mabrok M. 2019. Effect of dietary supplementation with a synbiotic (Lacto Forte) on growth performance, haematological and histological profiles, the innate immune response and resistance to bacterial disease in *Oreochromis niloticus*. *Aquac Res.*, **50**(9): 2545-2562. doi:10.1111/are.14212
- Khan N, Atique U, Ashraf M, Mustafa A, Mughal MS, Rasool F, Azmat H, Tayyab M, and Iqbal KJ. 2018. Effect of Various Protein Feeds on the Growth, Body Composition, Hematology and Endogenous Enzymes of Catfish (*Pangasius hypophthalmus*). *Pak J Zool., Suppl. Ser:* 112–119. doi:http://dx.doi.org/10.17582/journal.pjz/2018.SupplSer13
- Khanom DA, Nesa A, Jewel MAS, Haque MA, Paul AK, Iqbal S, Atique U and Alam L. 2020. Muscular Tissue Bioaccumulation and Health Risk Assessment of Heavy Metals in Two Edible Fish Species (*Gudusia chapra* and *Eutropiichthys vacha*) in Padma River, Bangladesh. *Punjab Univ. J. Zool.*, **35**(1): 81–89. doi:10.17582/journal.pujz/2020.35.1.81.89
- Kokou F, Henry M, Nikoloudaki C, Kounna C, Vasilaki A and Fountoulaki E. 2019. Optimum protein-to-lipid ratio requirement of the juvenile shi drum (*Umbrina cirrosa*) as estimated by nutritional and histological parameters. *Aquac Nutr.*, **25**: 444–455. doi:10.1111/anu.12870
- Lemly AD. 2004. Aquatic selenium pollution is a global environmental safety issue. *Ecotoxicol Environ Saf.*, **59**: 44–56. doi:10.1016/S0147-6513(03)00095-2
- Lemly D. 2002. Symptoms and implications of selenium toxicity in fish: the Belews Lake case example. *Aquat Toxicol.*, **57**: 39–49. https://doi.org/10.1016/S0166-445X(01)00264-8
- Lille RD, and Fullmer HM. 1976. **Histopathological techniques and practical histochemistry** (4th Ed), Mac Graw Hill Book Co., Newyork, USA.
- Luna GL. 1968. **Manual of histopathological staining methods of the Armed Force Institute of Pathology**, (3rd Ed). McGraw–HillCo, New York, USA.
- Malarvizhi M, Kavitha C, Saravanan M and Ramesh M. 2012. Carbamazepine (CBZ) induced enzymatic stress in gill, liver and muscle of a common carp, *Cyprinus carpio*. *JKSUS.*, **24**: 179–186. https://doi.org/10.1016/j.jksus.2011.01.001
- Mechora S, Stibilj V and Germ M. 2013. The uptake and distribution of selenium in three aquatic plants grown in Se (IV) solution. *Aquat Toxicol.*, **128–129**: 53-59. doi:10.1016/j.aquatox.2012.11.021
- Moon W-K, Atique U, An K-G. 2020. “Ecological risk assessments and eco-toxicity analyses using chemical, biological, physiological responses, DNA damages and gene-level biomarkers in Zebrafish (*Danio rerio*) in an urban stream” *Chemosphere.*, **239**: 124754. doi:10.1016/j.chemosphere.2019.124754
- Morrison CM and Wright Jr JR. 1999. A study of the histology of the digestive tract of the Nile tilapia. *J Fish Biol.*, **54**: 597–606. https://doi.org/10.1111/j.1095-8649.1999.tb00638.x
- Obirikorang KA, Mensah NE and Asiamah EA. 2018. Growth, feed utilization, and liver histology of juvenile Nile tilapia (*Oreochromis niloticus*) fed diets containing increasing levels of swine fat. *J Appl Aquac.*, **30**: 366–381. doi:10.1080/10454438.2018.1493017
- Oulmi Y, Negele RD and Braunbeck T. 1995. Cytopathology of liver and kidney in rainbow trout (*Oncorhynchus mykiss*) after long-term exposure to sublethal concentrations of linuron. *Dis Aquat Org.*, **21**: 35-52
- Patterson JMM, Paige GB and Reddy KJ. 2010. Selenium in surface and irrigation water in the Kendrick irrigation district, Wyoming. *Environ Monit Assess.*, **171**: 267–280. https://doi.org/10.1007/s10661-009-1277-y
- Peebua P, Maleeya K, Prayad P and Sombat S. 2008. Histopathological alterations of Nile tilapia, *Oreochromis niloticus* in acute and subchronic alachlor exposure. *J Environ Biol.*, **29**(3): 325-331.
- Ramesh M, Marimuthu S, Velusami VG and Rama KP. 2014. Hematological, biochemical and enzymological responses in an Indian major carp *Labeo rohita* induced by sublethal concentration of water borne selenite exposure. *Chem Biol Interact.*, **207**: 67-73. DOI: 10.1016/j.cbi.2013.10.018
- Roberts RJ. 2012. **Fish Pathology**, Blackwell Publishing Ltd (590 pp).
- Rotruck JT, Pope AL, Ganther HE, Swanson AB, Haefeman DG and Hoelstra WG. 1973. Selenium: biochemical role component of glutathione peroxidase. *Science*, **179**: 588–590. DOI: 10.1126/science.179.4073.588
- Saeed F, Iqbal, KJ, Atique U, Javid A, Khan N, Iqbal S, Majeed H, Azmat H, Khan BYA, Baboo I, Shahid MT and Afzal G. 2020. Toxic trace metals assessment in selected organs of edible fish species, sediment and water in Head Punjnad, Punjab, Pakistan. *Punjab Univ. J. Zool.*, **35**(1): 43–50. doi: 10.17582/journal.pujz/2020.35.1.43.50
- Sarkar B, Bhattacharjee S, Daware A, Tribedi P, Krishnani KK and Minhas PS. 2015. Selenium Nanoparticles for Stress-Resilient Fish and Livestock. *Nanoscale Res Lett.*, **10**, 371. doi:10.1186/s11671-015-1073-2
- Schram E, Pedrero Z, Cámara C, Van der Heul JW and Luten JB. 2008. Enrichment of African catfish with functional selenium originating from garlic. *Aqua Res.*, **39**: 850-860. https://doi.org/10.1111/j.1365-2109.2008.01938.x
- Smith CE, Holway JE and Hammer GL. 1973. Sulphamerazine toxicity in cut-throat trout brood fish *Salmo clarki* (Richardson). *J*

- Fish Biol.*, **5**: 97–101. <https://doi.org/10.1111/j.1095-8649.1973.tb04434.x>
- Sorensen EMB, Cumbie M, Bauer TL, Bell HS and Harlan CW. 1984. Histopathological, hematological, condition-factor and organ weight changes associated with selenium accumulation in “fish from Belews Lake, North Carolina. *Arch Environ Contam Toxicol.*, **13**: 153–162. <https://doi.org/10.1007/BF01055872>
- Takayanagi K. 2001. Acute toxicity of waterborne Se (IV), Se (VI), Sb (III), and Sb (V) on red seabream (*Pagrus major*). *Bull Environ Contam Toxicol.*, **66**(6): 808–813. <https://doi.org/10.1007/s001280080>
- Wang KZ, Xu WN, Zhou M, Zhang DD, Sun CX, Qian Y and Liu WB. 2018. Effects of fishmeal replacement with cottonseed meal protein hydrolysate on growth, digestion and intestinal histology of juvenile Chinese soft-shelled turtle, *Pelodiscus sinensis*. *Aquac Nutr.*, **24**: 1406–1415. doi:10.1111/anu.12677
- Watanabe T, Kiron V and Satoh S. 1997. Trace Minerals in fish nutrition. *Aquaculture*, **151**: 185-207. [https://doi.org/10.1016/S0044-8486\(96\)01503-7](https://doi.org/10.1016/S0044-8486(96)01503-7)
- Younus M, Iqbal S, Mughal MS, Javid A, Rafique MK, Khan AU, Khan N and Atique U. 2015. Effect of Selenium Incorporated in Feed on the Hematological Profile of *Oreochromis Niloticus*. *Abstract of Applied Sciences and Engineering*, 1–22.
- Zulfahmi I, Muliari M, Akmal Y and Batubara AS. 2018. Reproductive performance and gonad histopathology of female Nile tilapia (*Oreochromis niloticus* Linnaeus 1758) exposed to palm oil mill effluent. *Egypt J Aquat Res.*, **44**: 327–332. doi:10.106/j.ejar.2018.09.003

Inclusion of *Myrmecodia pendens* bulb Extract in the Diet Stimulates Immune Response in *Clarias gariepinus* against *Aeromonas hydrophila*

Rudy A. Nugroho^{1,2,*}, Yanti P. Sari³ and Esti H. Hardi⁴

¹Animal Physiology, Development, and Molecular Laboratory, Department of Biology, Faculty of Mathematics and Natural Sciences, Mulawarman University, Jl. Barong Tongkok No 4. Gn Kelua, Samarinda, 75123, ²Research Center of Medicine and Cosmetic from Tropical Rainforest Resources, PUI PT OKTAL, ³Tissue Culture Laboratory, Department of Biology, Faculty of Mathematics and Natural Sciences, ⁴Department of Aquaculture, Faculty of Fisheries and Marine Sciences, Mulawarman University, East Kalimantan, Indonesia

Received: November 5, 2019; Revised: November 29, 2019; Accepted: December 15, 2019

Abstract

To evaluate the effects of *Myrmecodia pendens* bulb extract (MBE) inclusion on the growth and blood profile of catfish (*Clarias gariepinus*), a group of fish were fed with 1% MBE (T) and compared with a control (C). After 30 days of feeding, the growth, survival and blood profiles were compared between the two groups. Surviving fish from each group were distributed into five subgroups: C without injection (CG1), C with *Aeromonas hydrophila* injection (CG2), C injected with *A. hydrophila* and antibiotics (CG3), T without injection (TG4) and T with *A. hydrophila* injection (TG5). Survival and blood profile post-injection were evaluated for 48 h. After 30 days of feeding, the growth, survival and blood profiles of fish fed MBE was higher than the control. Meanwhile, 24 h post-bacterial injection, fish CG2 showed significantly reduced survival (70%), erythrocytes ($2.15 \times 10^6 \mu\text{L}^{-1}$), platelets ($39.48 \times 10^3 \mu\text{L}^{-1}$) and haemoglobin (4.24 g dL^{-1}). However, increases in leucocytes ($49.55 \times 10^3 \mu\text{L}^{-1}$) and lymphocytes ($49.32 \times 10^3 \mu\text{L}^{-1}$) were found in fish TG5. This finding demonstrated the usefulness of MBE inclusion in the diet of *C. gariepinus* for improving growth, survival, blood profile and resistance to *A. hydrophila*.

Keywords: *Clarias gariepinus*, *Myrmecodia pendens*, survival, blood profile, *Aeromonas hydrophila*

1. Introduction

One of the most significant pathogens in many fish cultures, causing mass mortality, is *Aeromonas* species (Hoai et al., 2019). *Aeromonas hydrophila*, an opportunistic Gram-negative pathogen living in freshwater, has been identified as one of the *Aeromonas* species that causes mass disease outbreaks in fish such as *Siniperca chuatsi* (Chen et al., 2018) and *Carassius auratus* (Linnaeus 1758) (Dharmaratnam et al., 2018). Previous research has revealed that *A. hydrophila* intramuscular injection into *Pangasianodon hypophthalmus* (Sauvage) resulted in a virulent reaction and decreased immune response (Tamam dusturi and Yuhana, 2016).

To tackle mass mortalities of fish cultures, some fish farmers use antibiotics to prevent virulent reactions to *A. hydrophila* (Sinclair et al., 2016), as commonly used for haemorrhagic septicaemia disease in *Pangasianodon hypophthalmus* (Xuan et al., 2018). Nevertheless, antibiotics are expensive, and their inappropriate application may induce environmental deterioration and negatively affect farming bio-environments (Sinclair et al., 2016). In addition, the increasing market demand for eco-friendly fish products is necessary. As an alternative, researchers

have attempted to use various plant extracts as a natural antimicrobial agent.

A potential plant that can be used as an antimicrobial agent source to increase survival and immunocompetence in fish is the ant nest plant (*Myrmecodia* sp). The *Myrmecodia* species, which has been taxonomically determined as *M. tuberosa* and *M. pendens*, is widely used in West Papua, East Kalimantan and several regions in Indonesia as a herb with significant therapeutic value (Hertiani et al., 2010). Local people have used this species as part of herbal remedies for several medicinal applications, such as ulcers, haemorrhoids, nosebleeds, backaches, allergies, uric acid disorders, strokes, coronary heart problems, Tuberculosis, tumours, cancers and lactagogum (Soeksmanto et al., 2010). *M. pendens*, an epiphyte plant, attaches to large trees and can be found in bubbles underneath the rod (Hamsar and Mizaton, 2012). Previous studies have reported that qualitatively, *Myrmecodia* contains several important secondary metabolite compounds, namely phenolics, flavonoids, alkaloids, saponins and steroid/triterpenoids (Sari et al., 2017) that are potentially beneficial for medical purposes.

According to Gartika et al. (2018), *M. pendens* bulb extract (MBE) can inhibit and eradicate *Streptococcus mutans* biofilms. Hertiani et al. (2010) also found that *M. tuberosa* Jack's quorum-sensing has a relationship with the pathogenicity of *Pseudomonas aeruginosa* and

* Corresponding author e-mail: rudyagung.nugroho@fmipa.unmul.ac.id.

Staphylococcus aureus. Meanwhile, an ethyl acetate fraction of methanolic extracts of *Myrmecodia tubers* reduced the growth of *Streptococcus sanguis* ATCC 10566 (Fatriadi et al., 2018), and a previous study of *Myrmecodia* species in fish also found that 0.5–1% *Myrmecodia* extract is useful for enhancing the growth and blood profile status of *P. hypophthalmus* (Nugroho et al., 2019).

Although there has been a significant amount of research regarding *Myrmecodia* species, there has been relatively little focus on the aquaculture field. Thus, it is necessary to perform in-depth research on the application of *M. pendens* in fish, particularly with respect to its role as a therapeutic agent for tackling bacterial pathogens. This study investigated the effects of MBE on the survival and blood profile (including erythrocytes, leucocytes, haemoglobin value (Hb) and platelets (PLT) in *C. gariepinus* when challenged with *A. hydrophila*. Differential leucocytes such as lymphocytes, monocytes and granulocytes, all of which are pivotal blood indices in the immune system of *C. gariepinus*, were also determined during pre- and post-challenge tests.

The immune status of catfish is related to their blood profiles, which are important in monitoring the health status of fish (Shen et al., 2018). Blood profiles such as erythrocytes, leucocytes, Hb, and PLT in fish are pivotal tools that can be used to determine physiological and pathological status in fish (Aliko et al., 2018). Leucocytes or white blood cell counts are generally used as fish health status indicators; they relate to components of the innate immune system and involve immunological function regulation in fish (Velazquez-Carriles et al., 2018). Immunological function related to physiological responses in fish can also be measured by alterations in both total and differential leucocyte counts. These counts have been used as regular indicators in the health status and immune competence of various fish (Jaafar et al., 2016; Aliko et al., 2018).

2. Materials and Methods

2.1. Plant materials

M. pendens bulbs were purchased from a local market. To make a powder, bulbs were dried, cut into small pieces and ground into a powder. This powder was extracted using 95% ethanol for two days, filtrated, evaporated and stored at 4 °C until it was used as a crude extract (MBE). Every 75 g of *M. pendens* bulb powder in 1 L of 95% ethanol produced 18 g crude extract.

2.2. Control and treatment diet preparation

The control diet was a commercial pellet and was obtained from a local commercial market (Hi Pro Vite FF-888). The control diet contained 36–38% protein, 2% lipid, 2% crude fibre, 10% ash and 12% moisture. The treatment diet was prepared by adding 1% MBE to the control diet. The optimum MBE addition (1%) was determined from previous experiments. Both control and treatment diets were repelletised using a mincer, dried in an oven at 50 °C and allowed to cool to room temperature. All diets were stored in a dark plastic bag prior to being given to fish.

2.3. Fish preparation and experimental setup

Six-hundred fish (average initial weight 27.36 g) were obtained from a local breeding fish farm in Samarinda,

East Kalimantan, Indonesia. All fish were acclimated at the Animal Physiology, Development, and Molecular Laboratory, Mulawarman University, East Kalimantan for five days. The fish were then randomly distributed into two groups (C and T) with triplicate groups of 40 fish per replicate group. Each fish was then placed in an individual plastic tank (60 L capacity, 40 L of freshwater in each tank). For 30 days (pre-challenge), fish in each group were fed with control or treatment diets at a rate of 3% of body weight three times per day. Temperature, pH, and dissolved oxygen (DO) were checked once a week with a routine thermometer and an HM-7 pH meter (TOA-DKK Corporation, Japan). Nitrate, nitrite and ammonium were also checked weekly using chemical test kits (Salifert test kit™). Siphoning was carried out daily to remove uneaten food and faeces before renewing the water. Forty percent of the water volume was renewed every day and maintained at 40 L of water in every plastic tank.

2.4. Challenge test

On the final day of the feeding trial (day 30), all surviving fish in both control and treatment groups were distributed as follows: the control group was randomly divided into triplicates of three subgroups (30 fish per subgroup): control (C) subgroup fish without bacterial injection (CG1), control subgroup fish with bacterial injection (CG2) and control subgroup fish with bacteria and antibiotic (Gentamycin sulphate 0.1%) injection (CG3). The treatment group of fish was randomly distributed into triplicates of two subgroups (30 fish per subgroup): treatment (T) fish group with no injection (TG4) and with bacterial injection (TG5). All bacterial injections were performed with 20 µL of *A. hydrophila* at 10^6 cfu mL⁻¹ intraperitoneally.

2.5. Sampling and analytical procedure

On the first and final days of pre-challenge, the weight of all fish was measured to calculate the initial weight, final weight, body weight gain (BWG), daily weight gain (DWG), average weekly gain (AWG) and specific growth rate (SGR). Feed properties such as feed conversion ratio (FCR) were also determined. At the end of the pre-challenge test, blood profile, such as the number of erythrocytes (10^6 µL⁻¹) and leucocytes (10^3 µL⁻¹), haemoglobin (g dL⁻¹), lymphocytes (10^3 µL⁻¹), monocytes (10^3 µL⁻¹), granulocytes (10^3 µL⁻¹) and PLT (10^3 µL⁻¹) was determined. The survival rate of the fish in each group was noted every week during the pre-challenge test. During the challenge test, the survival and blood profile of fish (N = 3 fish per subgroup) was taken and measured every 24 h interval until 48 h. Blood profile measurement was performed using a Mindray BC2800 Auto Haematology Analyser (Mindray@Shenzhen, China).

2.6. Statistical analysis

Data are expressed as means ± standard error (SE) and were analysed using SPSS version 22 (SPSS, Inc., USA). Survival data were firstly transformed to arcsine. Blood parameters such as erythrocytes, leucocyte, Hb and differential leucocytes before the challenge test were analysed with a t-test to determine the significance of differences between control and treatment groups. Meanwhile, two-way ANOVA was used to evaluate survival, erythrocytes, leucocytes, Hb, PLT as well as data regarding the number of lymphocytes, monocytes and

granulocytes in the post-challenge test. A Duncan Multiple Range post hoc test was used to determine significant differences. All test results were reported as significant if P values were less than 0.05.

3. Results

During the pre-challenge test, the temperature, pH and DO value were noted as follows: $28.1 \text{ }^\circ\text{C} \pm 0.3$, 7.17 ± 0.2 and $8.1 \pm 0.3 \text{ mg L}^{-1}$. The nitrate, nitrite and ammonia values in all tanks were below the limits of detection. The growth of both control and treatment groups of fish fed 1% MBE in the diet are presented in Table 1.

Table 1. Growth parameters and Survival of *Clarias gariepinus* fed 1% of *Myrmecodia pendens* bulb extract for 30 days

Parameters	Groups	
	Control	Treatment
Initial weight (g)	27.36±0.11 ^a	27.72±0.18 ^a
Final weight (g)	50.52±1.00 ^a	67.11±0.81 ^b
BWG (g)	23.16±0.97 ^a	39.38±0.80 ^b
AWG (g/week)	2.89±0.12 ^a	4.92±0.10 ^b
DWG (g/day)	0.41±0.01 ^a	0.70±0.01 ^b
SGR	1.19±0.03 ^a	1.61±0.02 ^b
FCR	2.00±0.09 ^a	1.18±0.02 ^b

Note: Control group = group of fish without *Myrmecodia pendens* bulb extract in the diet. Treatment group = group of fish with *Myrmecodia pendens* bulb extract supplementation in the diet. Mean±Standard error (SE) followed by different letter superscript (a, b) at the same row indicate significantly different ($P < 0.05$). BWG = Body weight gain, AWG = Average weekly gain, DWG = Daily weight gain, SGR = Specific growth rate, FCR = Feed conversion ratio.

After 30 days of the feeding trial, the growth of fish fed MBE in the diet was significantly higher ($P < 0.05$) compared to the control group, as shown in the final weight, BWG, AWG, DWG and SGR. The FCR of fish fed 1% MBE in the diet (1.18 ± 0.02) was significantly better than the control group. Significantly higher survival (t-test, $P < 0.05$) (Figure 1) and erythrocytes, leucocytes, Hb, PLT, lymphocytes and granulocytes (Table 2) were also found in fish fed MBE in the diet. However, monocytes were not affected by 1% MBE inclusion in the diet.

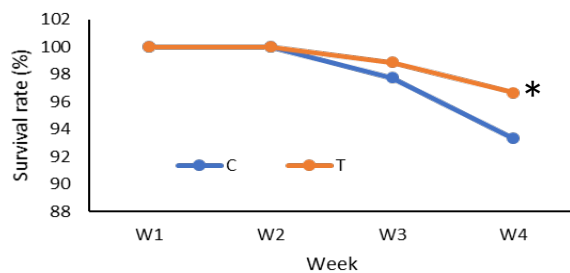


Figure 1. Survival of *Clarias gariepinus* fed 1% *Myrmecodia pendens* bulb extract in the diet for 30 days. * = significantly difference at $P < 0.05$. C = control group of fish without *Myrmecodia pendens* bulb extract supplementation. T = Treatment group of fish with *Myrmecodia pendens* extract supplementation in the diet for 30 days.

Table 2. Blood parameters of *Clarias gariepinus* fed 1% of *Myrmecodia pendens* bulb extract for 30 days

Parameters	Groups	
	Control	Treatment
Erythrocyte ($10^6 \mu\text{L}^{-1}$)	2.11±0.02 ^a	3.34±0.08 ^b
Leucocyte ($10^3 \mu\text{L}^{-1}$)	38.51±0.06 ^a	48.48±0.14 ^b
PLT ($10^3 \mu\text{L}^{-1}$)	40.84±0.02 ^a	41.80±0.05 ^b
Hb (g dL ⁻¹)	5.75±0.03 ^a	6.55±0.03 ^b
Lymphocyte ($10^3 \mu\text{L}^{-1}$)	33.09±0.03 ^a	43.39±0.16 ^b
Monocyte ($10^3 \mu\text{L}^{-1}$)	1.06±0.01 ^a	1.20±0.02 ^a
Granulocyte ($10^3 \mu\text{L}^{-1}$)	1.04±0.005 ^a	2.32±0.085 ^b

Note: Control group = group of fish without *Myrmecodia pendens* bulb extract in the diet. Treatment group = group of fish with *Myrmecodia pendens* bulb extract supplementation in the diet. Mean±Standard error (SE) followed by different letter superscript (a, b) at the same row indicate significantly different ($P < 0.05$). PLT = Platelets, Hb = Haemoglobin.

In the challenge test, fish in the control subgroup injected with *A. hydrophila* (CG2) showed significantly reduced survival (Figure 2). As can be seen in Table 3, there was a significant decrease in the number of erythrocytes ($2.15 \times 10^6 \mu\text{L}^{-1}$), platelets ($39.48 \times 10^3 \mu\text{L}^{-1}$) and Hb (4.24 g dL^{-1}) in the control subgroup injected with *A. hydrophila* (CG2) at 48 h post challenge. However, increases of leucocytes ($49.55 \times 10^3 \mu\text{L}^{-1}$) and lymphocytes ($49.32 \times 10^3 \mu\text{L}^{-1}$) were found in fish TG5. Meanwhile, fish in the control subgroup injected with *A. hydrophila* and antibiotic (CG3) had relatively constant erythrocytes and monocytes, whereas an increase of leucocytes and granulocytes was observed 24 h post challenge. The Hb of fish in the subgroup CG3 was also gradually reduced until 48 h post challenge. Nevertheless, lymphocytes increased 24 h post challenge. Further, fish fed 1% MBE in the diet and injected with *A. hydrophila* (TG5) showed relatively constant erythrocytes and Hb values. The leucocytes, lymphocytes, monocytes and granulocytes were increased at 24 h post injection.

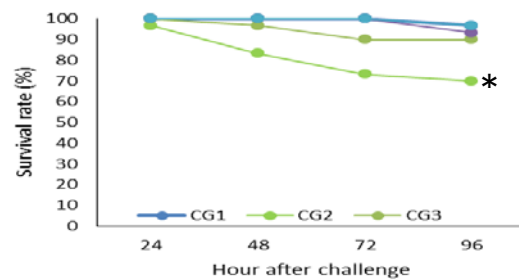


Figure 2. Survival rate of *Clarias gariepinus* in challenge test. Significantly decreased (*) of survival was found in fish groups without *Myrmecodia pendens* extract supplementation and injected with *Aeromonas hydrophila*. CG1 = subgroups fish without bacterial injection, CG2 = control subgroups fish with bacterial injection, CG3 = control subgroups fish with bacteria and antibiotic injection. TG4 = subgroups MBE-fed fish with no injection. TG5 = Subgroups of MBE-fed fish with bacterial injection.

Table 3. Blood parameters and differential leucocyte of *Clarias gariepinus* during challenge test

Parameters	Time	Control groups			Treatment groups	
		CG1	CG2	CG3	TG4	TG5
Erythrocyte (10 ⁶ µL ⁻¹)	0	1.209±0.030 ^a	1.213±0.03 ^a	1.228±0.02 ^a	1.341± 0.166 ^b	1.328±0.0541 ^b
	24	1.217±0.018 ^a	2.222±0.19 ^b	2.242±0.03 ^{ab}	1.374±0.028 ^c	2.352±0.008 ^c
	48	1.226±0.008 ^a	1.215±0.02 ^b	2.210±0.05 ^b	1.374±0.038 ^c	1.23.38±0.067 ^d
Leucocyte (10 ³ µL ⁻¹)	0	1.38.58±0.071 ^a	1.38.43±0.11 ^a	1.37.94±0.664 ^a	1.48.35±0.270 ^b	1.48.62±0.084 ^b
	24	1.38.44±0.2631 ^a	2.45.39±0.89 ^b	2.43.51±0.301 ^c	1.48.78±0.029 ^d	1.48.48±0.35 ^b
	48	1.38.06±0.3781 ^a	2.46.53±0.86 ^b	3.45.84±0.031 ^b	1.48.79±0.042 ^c	3.49.55±0.33 ^b
PLT (10 ³ µL ⁻¹)	0	1.40.84±0.014 ^a	1.40.83±0.045 ^a	1.41.33±0.335 ^{ab}	1.42.83±0.110 ^b	1.41.76±0.020 ^b
	24	1.40.83±0.037 ^a	2.39.15±0.282 ^{ab}	1.241.84±0.054 ^c	1.42.74±0.063 ^d	2.42.67±0.013 ^a
	48	1.40.75±0.029 ^a	2.39.48±0.384 ^{ab}	2.341.53±0.280 ^c	1.42.91±0.023 ^c	2.42.38±0.247 ^a
Hb (g dL ⁻¹)	0	1.5.79±0.02 ^a	1.5.72±0.07 ^a	1.5.66±0.04 ^a	1.6.55±0.035 ^b	1.6.56±0.059 ^b
	24	1.5.49±0.06 ^a	2.5.47±0.05 ^a	2.5.63±0.07 ^a	1.6.72±0.067 ^b	1.26.53±0.015 ^c
	48	1.5.46±0.06 ^a	3.4.24±0.08 ^b	3.4.68±0.03 ^c	1.6.76±0.011 ^d	1.6.56±0.028 ^e
Lymphocyte (10 ³ µL ⁻¹)	0	1.33.15±0.013 ^a	1.33.04±0.04 ^b	1.33.10±0.07 ^c	1.43.16± 0.056 ^d	1.43.63±0.26 ^e
	24	1.33.15±0.017 ^a	2.43.80±0.66 ^b	2.44.47±0.24 ^c	1.43.53±0.065 ^d	2.49.00±0.01 ^e
	48	2.33.24±0.031 ^a	2.43.19±0.60 ^b	3.48.17±0.30 ^c	1.43.56±0.008 ^d	2.49.32±0.28 ^e
Monocyte (10 ³ µL ⁻¹)	0	1.1.05±0.017 ^a	1.1.08±0.015 ^a	1.1.20±0.034 ^a	1.1.24±0.035 ^b	1.1.17±0.03 ^b
	24	1.1.03±0.0006 ^a	1.1.18±0.017 ^a	1.1.08±0.012 ^a	1.1.37±0.037 ^b	1.1.44±0.23 ^b
	48	1.1.03±0.0009 ^a	1.1.17±0.005 ^a	1.1.14±0.052 ^a	1.1.47±0.018 ^b	1.1.21±0.02 ^b
Granulocyte (10 ³ µL ⁻¹)	0	1.1.04±0.006 ^a	1.1.05±0.068 ^b	1.1.03±0.005 ^{ab}	1.2.21±0.147 ^b	1.2.44±0.021 ^c
	24	2.1.03±0.001 ^a	2.2.71±0.095 ^b	2.2.78±0.031 ^b	2.2.10±0.063 ^b	2.1.86±0.088 ^c
	48	3.1.02±0.0009 ^a	3.2.84±0.062 ^b	3.2.91±0.014 ^b	3.2.31±0.056 ^b	3.1.80±0.025 ^c

Note: Mean±Standard error (SE) follow by different letter superscript (a, b,c,d,e) at the same row indicate significantly different ($P < 0.05$). Meanwhile, different letter subscript (1,2,3) follow by Mean±Standard error (SE) at the same column indicate significantly different ($P < 0.05$). CG1 = subgroups fish without bacterial injection, CG2 = control subgroups fish with bacterial injection, CG3 = control subgroups fish with bacteria and antibiotic injection. TG4 = subgroups MBE-fed fish with no injection. TG5 = Subgroups of MBE-fed fish with bacterial injection. PLT = Platelets, Hb = Haemoglobin.

4. Discussion

Plant extracts containing active phytochemicals and various bioactive ingredient activities such as such as flavonoids, alkaloids, saponins, quinones, triterpenoids, tannins and phenolics have been claimed to be beneficial as a supplementation in the diet of aquaculture species (Afzali and Wong, 2019). The present findings revealed that the supplementation of 1% MBE can significantly enhance the growth at pre-challenge and survival of *Clarias gariepinus*, either pre or post challenge with *A. hydrophila*. Similarly, survival rate of *A. hydrophila*-infected silver catfish (*Rhamdia quelen*) bath with *Hesperozygis ringens* (Benth.) has also been reported (Rosa et al., 2019). According to Nugroho et al. (2019) and Nugroho et al. (2017), the phytochemicals from *Myrmecodia* may boost the innate immune system and improve survival rates of Siamese fighting fish (*Betta* sp) against *A. hydrophila*. Tilapia (*Oreochromis niloticus*) injected with *Boesenbergia pandurata*, *Solanum ferox*, *Zingiber zerumbet* also had significantly higher survival than controls with no injection (Hardi et al., 2018).

The *Myrmecodia pendens* is abundant in secondary metabolite plant ingredients such as flavonoids (Lestari et

al., 2019). Maulida et al. (2018) found that flavonoids have a strong antioxidant property that enhanced superoxide dismutase (SOD), catalase (CAT) and glutathione peroxidase (GSH-Px) activity, and reduced malondialdehyde (MDA) levels (Xie et al., 2018). Increases in such antioxidant enzymes may be useful for tackling free radical formation and decreasing lipidic superoxide damage, further increasing the growth and survival of *C. gariepinus*. Besides flavonoids, the biological properties of tannins for boosting fish survival have also been widely reported. For example, tannins from *Terminalia catappa* leaves improved the survival of *A. hydrophila*-infected *Betta* sp (Nugroho et al., 2016; Nugroho et al., 2017). Ashraf and Bengtson (2007) revealed that tannin can reduce harmful chemicals and improve the survival and growth of striped bass (*Morone saxatilis*) larvae. Further, phenolics found in the bulbs of *M. pendens* may also improve survival and immune function stimulation in *C. gariepinus*, while the application of phenolics from liquorice roots (*Glycyrrhiza glabra* L) in diets of Nile tilapia (*Oreochromis niloticus*) improved their survival (El Mesallamy et al., 2015).

The current findings demonstrated that there were significantly reduced erythrocytes and Hb counts

following *A. hydrophila* injection. This result is similar to Ayik (2009), who reported reduced erythrocytes and Hb in rainbow trout (*Oncorhynchus mykiss*) infected with *Pseudomonas putida*. The decreased count of erythrocytes and Hb in both control and treatment subgroups may be due to haemolytic activity caused by *A. hydrophila* infection (dos Santos et al., 2017). According to Yu et al. (2005) and Janda and Abbott (2010), *A. hydrophila* can produce several haemolytic toxins with virulence activities, causing haemolytic anaemia. In contrast, fish leucocytes were found to increase gradually following injection with bacteria. The improvement of leucocytes post injection could be due to their ability to combat bacteria invading the fish immune system. These findings are similar to a past study, which found increased leucocyte levels in juvenile and adult Victoria Labeo (*Labeo victorianus*) challenged with *A. hydrophila* (Ngugi et al., 2015). The biochemical mechanism(s) that lead to MBE-fed fish leucocytes being increased during infection is(are) yet to be clearly determined. Nevertheless, Sujatha et al. (2019) observed that flavonoids have antibacterial properties and can inhibit bacterial growth, reduce the erythrocyte haemolysis counts that are caused by bacterial infection, protect erythrocyte membranes (Asgary et al., 2005), cause erythropoiesis and maintain the heme iron (Shatoor, 2011).

Activated platelets can release cytokines and chemokines, modulating the immune function that relates to pathogenesis (Faggio et al., 2017). The current study found that the PLT of subgroups of MBE-fed fish (TG5) in the challenge test had increased significantly. However, decreased PLT was observed in the control subgroup (CG2) following 48 h post injection. This finding is in accordance with a previous study revealing that *Clarias gariepinus* injected with 2.00 ppm aqueous extracts of *Lepidagathis alopecuroides* leaves showed the highest value of PLT (Gabriel et al., 2009). Phytochemicals from bulb extracts of *M. pendens* containing flavonoids were reported to have various benefits, such as platelet function modulation (Vallance et al., 2019) and provision of antioxidants with positive effects against pathogens. In addition, some flavonoids possess anti-platelet aggregation effects (Faggio et al., 2017).

The lymphocytes, monocytes and granulocytes lead to the production of antibodies and respond to antigens that act as mediators both in cellular and humoral immune processes (Soltanian and Fereidouni, 2016). Fish with and without MBE in the diet were found in the present work to significantly increase lymphocytes, monocytes and granulocyte following 24 h post *A. hydrophila* injection. The lymphocyte counts of all fish subgroups stabilised after 24 h, whereas the granulocytes of the subgroups of MBE-fed fish were constant 48 h post challenge. Based on Sivagurunathan et al. (2011) report, monocytes which play an important role in protecting fish against bacteria via the immune defence system, can transform into macrophages, which phagocytose pathogens at the first recognition site and subsequent infections. Meanwhile, Neutrophils, one of the granulocyte types, are also involved in bacterial phagocytosis activity during initial infections.

5. Conclusion

Myrmecodia pendens bulb extract inclusion in the diet of *Clarias gariepinus* is beneficial for enhancing blood indices and improving immune function. A diet containing 1% *Myrmecodia pendens* bulb extract in the feed of *Clarias gariepinus* is recommended for protecting fish against *Aeromonas hydrophila*. However, further research is required to determine the role of the active phytochemical ingredient in the MBE that is involved in immune function system in fish, including cellular and molecular responses. Finally, field research is also necessary before applying MBE extract as an immunostimulant to tackle bacterial disease in fish cultures.

Acknowledgement

The current project is funded by Kemenristekdikti (Ministry of Research and Technology General Higher Education) through Penelitian Dasar Unggulan Perguruan Tinggi (PDUPT) 2019, contract number 179/UN.17.41/KL/2019. All authors also thank the Research Center of Medicine and Cosmetic from Tropical Rainforest Resources, PUI PT OKTAL, Mulawarman University for its support, and the Faculty of Mathematics and Natural Sciences, Mulawarman University, East Kalimantan, Samarinda for the various facilities provided.

References

- Afzali S and Wong W. 2019. Effects of dietary supplementation of *Sonneratia alba* extract on immune protection and disease resistance in goldfish against *Aphanomyces invadans*. *Trop Biomed.*, **36**: 274-288.
- Aliko V, Qirjo M, Sula E, Morina V and Faggio C. 2018. Antioxidant defense system, immune response and erythron profile modulation in gold fish, *Carassius auratus*, after acute manganese treatment. *Fish Shellfish Immunol.* **76**: 101-109.
- Asgary S, Naderi G and Askari N. 2005. Protective effect of flavonoids against red blood cell hemolysis by free radicals. *Exp Clin Cardiol.* **10**: 88.
- Ashraf M and Bengtson DA. 2007. Effect of tannic acid on feed intake, survival and growth of striped bass (*Morone saxatilis*) larvae. *Int J Agric Biol.* **9**: 751-754.
- Ayik SB. 2009. Hematological parameters and erythrocyte osmotic fragility in rainbow trout, *Oncorhynchus mykiss*, experimentally infected with *Pseudomonas putida*. *JFAS.* **4**: 246-253.
- Chen N, Jiang J, Gao X, Li X, Zhang Y, Liu X, Yang H, Bing X and Zhang X. 2018. Histopathological analysis and the immune related gene expression profiles of mandarin fish (*Siniperca chuatsi*) infected with *Aeromonas hydrophila*. *Fish Shellfish Immunol.*, **83**: 410-415.
- Dharmaratnam A, Swaminathan TR, Kumar R and Basheer V. 2018. *Aeromonas hydrophila* associated with mass mortality of adult goldfish *Carassius auratus* (Linnaeus 1758) in ornamental farms in India. *Indian J Fish.*, **65**: 116-126.
- dos Santos AC, Sutuli FJ, Heinzmann BM, Cunha MA, Brusque ICM, Baldissarroto B and Zeppenfeld CC. 2017. *Aloysia triphylla* essential oil as additive in silver catfish diet: Blood response and resistance against *Aeromonas hydrophila* infection. *Fish Shellfish Immunol.*, **62**: 213-216.

- El Mesallamy AM, El-Marakby HI, Souleman AM and El-Naby FSA. 2015. Evaluation of phenolic extract of licorice roots in diets of Nile tilapia (*Oreochromis niloticus*). *Egypt Pharmaceut J.*, **14**: 117.
- Faggio C, Sureda A, Morabito S, Sanches-Silva A, Mocan A, Nabavi SF and Nabavi SM. 2017. Flavonoids and platelet aggregation: a brief review. *Eur J Pharmacol.*, **807**: 91-101.
- Fatriadi F, Kurnia D and Satari MH. 2018. Antibacterial activity of ethyl acetate fraction from methanolic extracts of ant-plant tubers towards *Streptococcus sanguis* ATCC 10566. *Padjadjaran J Dentistry.*, **30**: 190-193.
- Gabriel U, Obomanu F and Edori O. 2009. Haematology, plasma enzymes and organ indices of *Clarias gariepinus* after intramuscular injection with aqueous leaves extracts of *Lepidagathis alopecuroides*. *Afr J Biochem Res.* **3**: 312-316.
- Gartika M, Pramesti HT, Kurnia D and Satari MH. 2018. A terpenoid isolated from sarang semut (*Myrmecodia pendans*) bulb and its potential for the inhibition and eradication of *Streptococcus mutans* biofilm. *BMC Complement Altern Med.*, **18**: 151.
- Hamsar MN and Mizaton HH. 2012. Potential of ant-nest plants as an alternative cancer treatment. *J Pharm Res.*, **5**: 3063-3066.
- Hardi E, Saptiani G, Kusuma I, Suwinarti W and Nugroho R. 2018. Evaluation of traditional plant extracts for innate immune mechanisms and disease resistance against fish bacterial *Aeromonas hydrophila* and *Pseudomonas* sp. In: IOP Conference Series: Earth and Environmental Science., p 012003.
- Hertiani T, Sasmito E, Sumardi and Ulfah M. 2010. Preliminary study on immunomodulatory effect of sarang-semut tubers *Myrmecodia tuberosa* and *Myrmecodia pendens*. *Online J Biol Sci.*, **10**: 136-141.
- Hoai TD, Trang TT, Van Tuyen N, Giang NTH and Van Van K. 2019. *Aeromonas veronii* caused disease and mortality in channel catfish in Vietnam. *Aquaculture.*, 734425.
- Jaafar RM, Ohtani M, Kania PW and Buchmann K. 2016. Correlation between leukocyte numbers and body size of rainbow trout. *Open J Immunol.*, **6**: 101.
- Janda JM and Abbott SL. 2010. The genus *Aeromonas*: taxonomy, pathogenicity, and infection. *Clin Microbiol Rev.*, **23**: 35-73.
- Lestari W, Yusry WN, Iskandar SH, Ichwan SJ, Irfan NI and Suriyah WH. 2019. Gene expression of selected apoptotic markers in human oral squamous carcinoma HSC-3 cell line treated with *Myrmecodia pendans* plant extract. *Makara J Health Res.*, **23**: 10.
- Maulida NF, Yanuaritamala B, Yanuar A, Saputri FC and Mun'im A. 2018. Optimization of Microwave-Assisted extraction to obtain optimum antioxidant activity and anthocyanin concentration from *Myrmecodia pendens* tubers using response surface methodology. *Pharm Res.*, **10**: 253.
- Ngugi CC, Oyoo-Okoth E, Mugo-Bundi J, Orina PS, Chemoiwa EJ and Aloo PA. 2015. Effects of dietary administration of stinging nettle (*Urtica dioica*) on the growth performance, biochemical, hematological and immunological parameters in juvenile and adult Victoria Labeo (*Labeo victorianus*) challenged with *Aeromonas hydrophila*. *Fish Shellfish Immunol.*, **44**: 533-541.
- Nugroho RA, Hardi EH, Sari YP, Aryani R and Rudianto R. 2019. Growth performance and blood profiles of striped catfish (*Pangasianodon hypophthalmus*) fed leaves extract of *Myrmecodia tuberosa*. *Nusantara Bioscience.*, **11**: 89-96.
- Nugroho RA, Manurung H, Nur FM and Prahastika W. 2017. *Terminalia catappa* L. extract improves survival, hematological profile and resistance to *Aeromonas hydrophila* in *Betta* sp. *Arch Pol Fisheries.*, **25**: 103-115.
- Nugroho RA, Manurung H, Saraswati D, Ladyescha D and Nur FM. 2016. The effects of *Terminalia catappa* leaf extract on the haematological profile of ornamental fish *Betta splendens*. *Biosaintifika: Journal of Biology and Biology Education.*, **8**: 241-248.
- Rosa I, Rodrigues P, Bianchini A, Silveira B, Ferrari F, Bandeira Junior G, Vargas A, Baldisserotto B and Heinzmann B. 2019. Extracts of *Hesperozygis ringens* (Benth.) Epling: in vitro and in vivo antibacterial activity against fish pathogenic bacteria. *J Appl Microbiol.*, **126**: 1353-1361.
- Sari YP, Kustiawan W, Sukartiningsih S and Ruchaemi A. 2017. The potential of secondary metabolites of *Myrmecodia tuberosa* from different host trees. *Nusantara Bioscience.*, **9**: 170-174.
- Shatoor AS. 2011. Acute and sub-acute toxicity of *Crataegus aronia* syn. *azarolus* (L.) whole plant aqueous extract in wistar rats. *Am J Pharmacol Toxicol.*, **6**: 37-45.
- Shen Y, Wang D, Zhao J and Chen X. 2018. Fish red blood cells express immune genes and responses. *Aquaculture Fisheries.*, **3**: 14-21.
- Sinclair HA, Heney C, Sidjabat HE, George NM, Bergh H, Anuj SN, Nimmo GR and Paterson DL. 2016. Genotypic and phenotypic identification of *Aeromonas species* and CphA-mediated carbapenem resistance in Queensland, Australia. *Diagn Microbiol Infect Dis.*, **85**: 98-101.
- Sivagurunathan A, Amila Meera K and Xavier Innocent B. 2011. Investigation of immunostimulant potential of *Zingiber officinale* and *Curcuma longa* in *cCrrhinus mrigala* exposed to *p. Aeruginosa*-haematological assessment. *IJRAP.*, **2**: 899-904.
- Soeksmanto A, Subroto M, Wijaya H and Simanjuntak P. 2010. Anticancer activity test for extracts of sarang semut plant (*Myrmecodya pendens*) to HeLa and MCM-B2 cells. *PJBS.*, **13**: 148.
- Soltanian S and Fereidouni MS. 2016. Effect of Henna (*Lawsonia inermis*) extract on the immunity and survival of common carp, *Cyprinus carpio* infected with *Aeromonas hydrophila*. *IAR.*, **8**: 247-261.
- Sujatha R, Siva D and Nawas P. 2019. Screening of phytochemical profile and antibacterial activity of various solvent extracts of marine algae *Sargassum swartzii*. *WSN.*, **115**: 27-40.
- Tamamduhuri R and Yuhana M. 2016. Administration of microencapsulated probiotic *Bacillus* sp. NP5 and prebiotic mannan oligosaccharide for prevention of *Aeromonas hydrophila* infection on *Pangasianodon hypophthalmus*. *JFAS.*, **11**: 67.
- Vallance TM, Ravishankar D, Albadawi DA, Osborn HM and Vaiyapuri S. 2019. Synthetic Flavonoids as Novel Modulators of Platelet Function and Thrombosis. *Int J Mol Sci.*, **20**: 3106.
- Velazquez-Carriles C, Macias-Rodríguez ME, Carbajal-Arizaga GG, Silva-Jara J, Angulo C and Reyes-Becerril M. 2018. Immobilizing yeast β -glucan on zinc-layered hydroxide nanoparticle improves innate immune response in fish leukocytes. *Fish Shellfish Immunol.*, **82**: 504-513.
- Xie J, Wang W, Dong C, Huang L, Wang H, Li C, Nie S and Xie M. 2018. Protective effect of flavonoids from *Cyclocarya paliurus* leaves against carbon tetrachloride-induced acute liver injury in mice. *Food Chem Toxicol.*, **119**: 392-399.
- Xuan T, Hoang HA and Tam L. 2018. Stability and activity of TG25P phage in control of *Aeromonas hydrophila* in striped catfish pond water. *AJSTD.*, **21**: 64-70.
- Yu H, Zhang Y, Lau Y, Yao F, Vilches S, Merino S, Tomas J, Howard S and Leung K. 2005. Identification and characterization of putative virulence genes and gene clusters in *Aeromonas hydrophila* PPD134/91. *Appl Environ Microbiol.*, **71**: 4469-4477.

In vitro Antibacterial Activity of Cell Free Fermentation Supernatant of *Passiflora edulis forma flavicarpa* Sims. Fruit Fermented by de Man, Rogosa and Sharp Media

Safarini Marwah.^{1,2}, Iif H. Rosyidah^{1,3}, Ni M. Mertaniasih⁴, Muhammad N.S.B. Hamzah⁵, Kholis A. Novianti¹, Riesta Primaaharinastiti¹, Dian Rahmawaty⁴ and Isnaeni Isnaeni¹,

¹Department of Pharmaceutical Chemistry, ²Magister student of Magister Program, Faculty of Pharmacy, ³Doctoral student of Doctoral Program, Faculty of Pharmacy, Universitas Airlangga, Mulyorejo, Surabaya 60115, ⁴Department of Microbiology, Faculty of Medicine, Universitas Airlangga, Mayjen Prof. DR. Moestopo 6-8, Surabaya 60268, Indonesia; ⁵PAPRSB Institute of Health Sciences, Universiti Brunei Darussalam, Tungku Link, Gadong BE1410, Brunei

Received: September 25, 2019; Revised: December 9, 2019; Accepted: December 21, 2019

Abstract

Antibacterial activities of cell free fermentation supernatant (CFFS) of passion fruit (*Passiflora edulis forma flavicarpa* Sims.) fermented in de Man-Rogosa and Sharpe (MRS) broth media against *Staphylococcus spp.*, Methicillin-Resistant *Staphylococcus aureus* (MRSA), and Extended Strain Methicillin-Resistant (ESBL) *Escherichia coli* have been investigated. The fermentation broth was derived from 24 and 48 hours cultures collection after rotary shaking incubation at 37°C. A bioassay was performed using well diffusion agar method on nutrient agar media, incubated at 37°C for 24 hours. Minimum inhibitory concentration and potency of the CFFS were determined using kanamycin, streptomycin, vancomycin, erythromycin, and amoxicillin as standards. It was found that the fermentation broth containing 32×10^4 CFU/g exhibited inhibitory activity against *S. Aureus* ATCC 25923 and *S. epidermidis* FN-6 after 24 hours similar to 48 hours fermentation. The anti-bacterial activities of 24 hours fermentation supernatant against all the test bacteria were almost similar. The characteristic of the CFFS indicated the acid property with pH of 3 ± 0.1 . Lactic acid bacteria were detected by biochemical identification based on catalase, Gram staining, motility, H₂S, indol, Simon citrate, and Voges Proskauer tests. Thin layer chromatography-contact bioautography was developed by KH₂PO₄ solution as eluent and *E. coli* as a test bacterium showed two spots by which two clear inhibition zones were obtained. The prospective of CFFS passion fruit as a potential antibacterial substance source is recommended for future development.

Keywords: Antibacterial activity, passion fruit, fermentation supernatant, *Staphylococcus spp.*, ESBL, MRSA.

1. Introduction

Nowadays, the use of natural ingredients as raw materials in drug development is beginning to be in demand among the pharmaceutical industry communities. According to World Health Organization (WHO) data, about 80% of the world population are using products based on medicinal herbs. Plants, especially those with ethnopharmacological uses, have been the primary sources of medicine for early drug discovery (Sofija, 2017). During the last 10 years, the discovery of new antibiotic drugs is not considered comparable with the prevalence of antibacterial resistance, so research for the discovery of antibiotic raw materials began to be directed at natural sources (Asirvathamdos, *et al.*, 2008).

Passion fruit (*Passiflora edulis*), a member of the Passifloraceae family, is also well-known as markisa fruit. It has more than 500 species (Paull and Duarte, 2012; Reis *et al.*, 2018). The plant originated from Brazil and has

scattered to other countries in Asia, Australia, Africa, India, South America, and the Caribbean. It has other variants that can be identified by the color of their fruits such as yellow which is *P. edulis forma flavicarpa*, purple which is *P. edulis forma edulis*, and orange which is *P. edulis* var. *caerulea* (Reis *et al.*, 2018). The plant parts (flower, leaves, stem, fruits, and roots) have several medicinal effects and have been used traditionally. The flower is the part that is used mostly for its calming effect, anticonvulsant and antihypertensive properties, which are useful for patients with anxiety and insomnia. However, it is not as potent as *Passiflora carnata* flower (Ramaiya *et al.*, 2014). Meanwhile, the fruits are almost round or oval in shape; about 4cm to 8cm in diameter, and mainly used as food since they have a juicy orange pulp. The pulp is sweet-sour in flavicarpa variant and sweeter in both *edulis* and *caerulea* variant. The skin is tough, smooth, and waxy but wrinkles when it is ripe. The seed is numerous, hard, small, and pitted inside the fruit. It has many common names according to the country they are grown in such as

* Corresponding author e-mail: isna.yudi@gmail.com; isnaeni@ff.unair.ac.id.

'markisa' in Indonesia and Malaysia, 'limangkan' in Laos, 'maracuya peroba' in Portugal, 'maracuja-do-campo' in Brazil (Paull and Duarte, 2012; Aziz, 2016).

The fruits contain good amount of nutrients which are good for dietary consumption and have numerous phytochemicals such as glycosides including flavonoids (Ingale and Hivrale, 2010), e.g. luteolin-6-C-chinovoside, luteolin-6-C-fucoside, cyanogenic glycosides, e.g. passibiflorin, epipassibiflorin, passicapsin, passicoriacin, epipassicoriacin, cyanogenic-b-rutinoside, epitetraphyllin B, amygdalin, prunasin, triterpenoid glycosides, e.g. passiflorine), and salicylate glycosides. Other chemicals such as b-carboline alkaloids harman, harmine, harmaline and harmalol, phenols, carotenes, and g-lactones are also found in the fruit (Bernes *et al.*, 2007). Passion fruit is a fruit that has a high nutritional value where there are many multimineral contents and various vitamins, as well as high carbohydrates and water (Zibadi and Watson, 2004). These compounds may become the prospect of antimicrobial, antioxidant, anticancer, and anticarcinogenic (Ramaiya *et al.*, 2014; Oliveira *et al.*, 2016). Reis *et al.* (2018) mention that the compound is also associated with antiplatelet, antiviral, antiallergic, and anti-inflammatory activities. Furthermore, the plant parts of the passion fruit including the peel extract and the pulp are positively tested for antibacterial and antifungal activity on certain microbial tested (4). It has been reported that antibacterial and antifungal compound has been isolated by Birner and Nicolls as cited by Ramaiya *et al.* (2014).

In recent years, there have been many studies on the antimicrobial activity of the *Passiflora edulis* plant by which is strong to moderate inhibition both in Gram-positive and Gram-negative has been exhibited. Extracts from the leaves and flowers of the plant *Passiflora edulis* are able to inhibit the growth of pathogenic bacteria such as *V. Cholerae*, *Pseudomonas aeruginosa*, *Escherichia coli*, *Bacillus subtilis* (Ingale and Hivrale, 2010), *Salmonella typhi*, *Staphylococcus aureus*, *Streptococcus pyrogens*, and *Bacebuspenilis* (Asirvathamdoss, *et al.*, 2008).

There have been numerous studies of passion fruit for its phytochemical properties; however, there are no reports concerning the antibacterial activities of the pulp of fruit fermented by de Man Rogose and Sharp (MRS) media against pathogenic bacteria. Zahroh (2014) has reported lactic acid bacteria (LAB) isolated from the passion fruit *Passiflora edulis* var. Sims. Some LAB have been known as sources of bioactive substances included antimicrobial. This study has performed antibacterial activities of cell-free fermentation supernatant (CFFS) of *Passiflora edulis* forma *flavicarpa* fruit against ESBL *Escherichia coli*, MRSA, and some species of *Staphylococcus* and non-ESBL *Escherichia coli*. Screening active substances by Thin Layer Chromatography-contact bioautography have also been reported.

2. Materials and Method

2.1. Plant source and determination

The yellow passion fruits (Figure 1) were collected freshly from a local farm in Sidoarjo, harvested in April 2019. The passion fruit plant was identified and determined based on the taxonomy character of leaf, flower, fruit, stem plant, and recommended by

Herbarium Malangensis, Department of Biology, Faculty of Math and Science, Universitas Negeri Malang as *Passiflora edulis* forma *flavicarpa*, Sims.

2.2. Sample preparation, fermentation, and characterization

The passion fruits were washed and dried before they were divided into two parts and the 5 gram of fruit pulps were weighed and put into 50 mL of MRS broth media to be fermented with rotary shaker at 150 rpm and at 37°C for 48 hours. The fermentation broth was taken after 24 hours of fermentation, centrifuged, and the supernatant was collected for characterization and bioassay.

2.3. Determination of Total Plate Count (TPC)

The supernatant was then made into a serial dilution of 1:10 until 10⁷ using sterile normal saline solution. Each of the serial dilutions was inoculated on the MRS (Oxoid, UK) agar and incubated at 37°C for 24 hours. Cell growth was observed and the plating colonies were counted using bacteria colony counter.

2.4. Inoculum preparation.

The selected bacteria strain was transferred aseptically to sterile saline water, vortex, and then the turbidity was measured using spectrophotometer against the sterile saline water to obtain 25% Transmittance (about 10⁹ CFU/ml of bacteria) turbidity or optical density at 580nm (Isnaeni *et al.*, 2019).

2.5. Bacterial inhibitory activity.

Screening inhibitory activity of the passion fruit was performed after 24 and 48 hours fermentation. The bioassay was done by well agar diffusion method using NA media and *Staphylococcus aureus* ATCC 25923, *Escherichia coli* ATCC 8739, ESBL and MRSA bacteria obtained from RSUD Dr. Soetomo as test bacteria. The test media were prepared by pour plate method. 10-12 mL of melted NA (45-50°C) were poured into the empty sterile petri disk, used as a base layer. The seed layer was prepared by adding 3-5 µL of 25 % transmittance of the test bacteria inoculum into 8 mL of the melted NA, mixed well with vortex, poured on the surface of the base layer, and allowed it to solidify. The well was made by bored with 7 mm in diameter. Each well reservoir was filled with 50 µL of the solution test. Incubation was performed at 37°C for 24 hours. Growth inhibitory zone diameter was measured by digital caliper (Isnaeni, 2019).

2.6. Thin Layer Chromatography-contact bioautography

The developing chamber used was CAMAG Chamber (10x10) with lid and was prepared aseptically. Hence, the size of the TLC plate used was 6cm x 10cm and it was dried at 100°C for 20 minutes before developing. The solvent used was 7.5% of KH₂PO₄ solution. The samples used were 20µL for each spot and "overspot" loading was used to concentrate the samples on one spot over again after the previous spot has dried. The samples were CFFS of passion fruit of 24-hour fermentation, streptomycin (100ul/ml), and kanamycin (100uL/ml) used as standard.

The Contact Bioautography was performed after the developed TLC plate had completely dried from the residual solvent and contacted, silica gel side down, onto the *Escherichia coli* seed layer as the test bacterium in the petri dish. The agar plate and the contacted plate were stored in the refrigerator for 1 hour to allow the diffusion

of the active substances in the chromatogram into the seed layer. Furthermore, the plate was removed from the agar plate, then incubated for 24 hours at 37°C. The growth of the *E. coli* and the inhibition zone were observed.

2.7. Minimum Inhibitory Concentration.

Determination of the minimum inhibitory concentration (MIC) of the passion fruit CFFS was done using the agar dilution method, where a number desired volume of the supernatant (1ml, 2ml, and 3ml) were mixed with the NA media. Then it was inoculated with six test bacteria by streaking using Öse needle about 1cm on the surface of the NA medium. Multiple replicates were performed on the same agar plate. The agar plates were then incubated at 37°C for 20-24 hours. An agar plate without the passion fruit CFFS was performed as the negative control. Serial dilution of CFFS had been applied from 100%, 75%, 50%, 25%, 12.5%, and 6.25% of concentration on the paper disk with volume capacity of 10µL, placed on the surface of NA agar inoculated by *E. coli* as a test bacterium. Zone of growth inhibitory activity was observed after 20-24 hours of incubation.

3. Results

3.1. Characteristic of Free Cell Fermentation Supernatant

Performance of the fermentation broth of passion fruit in MRS media (Table 1) was brownies in color, pH value 6 ± 0.1 before and decreased to 3 ± 0.1 after 24 and 48 hours fermentation. Total plate count in MRS and NA media was 133×10^3 and 32×10^4 CFU / mL respectively. Several colonies suspected Lactobacilli and Streptococci were found, based on the identification of the isolates with

biochemical reactions (Gram staining, catalase, and motility test, conformed to vitek-2).

Table 1. Characteristic of CFFS passion fruit fermented in MRS media

Parameters	Characteristics
Organoleptic	Liquid, browns colour
Odor	Specific smell of passion fruit
pH	6 ± 0.1 (0 hours), 3 ± 0.1 (24 hours)
Total plate count in MRS and NAMedia	133×10^3 and 32×10^4 CFU/ml
Inhibitory activity at 0 hour incubation	- (<i>S. aureus</i> and <i>E. coli</i>)
Inhibitory activity at 24 hours incubation	+ (<i>S. aureus</i> and <i>E. coli</i>)
Inhibitory activity at 48 hours incubation	+ (<i>S. aureus</i> and <i>E. coli</i>)
Lactic acid bacteria screening	+ based on Gram staining, morphology, catalase and motility test, conformed to VITEK-2

3.2. Antibacterial activity

The CFFS of passion fruit screening growth inhibitory activity against *S. aureus* ATCC 25923 showed that the potency of the CFFS after 24 hours and 48 hours fermentation was almost similar (Table 2 and Figure 1), as well as the activity against *S. epidermidis* FN-6 (Figure 2), ESBL, and non-ESBL *E. coli* after 24 hours of fermentation (Figure 3). Subsequent tests were carried out for fermented broth after incubation for 24 hours on several *Staphylococcus spp.* and *E. coli* (Table 2). The agar well diffusion test performed to 5 different strains of *E. coli* showed that the CFFS of passion fruit presented inhibitory activity against five different strains of *E. coli* with the zone of inhibition diameter from 13.80 mm to 22.05 mm (Figure 4).

Table 2. Inhibitory activities of CFFSpassion fruit after 24 hours fermetation againts various test bacteria

Bacteria	Zone of growth Inhibition (mm)					
	CFFS	Van 8ppm	Cefat 8 ppm	Strep 8 ppm	Am 16 ppm	Ery 8 ppm
<i>Exteded Spectrum Beta Lactamase</i>	$17,78 \pm 0,60$					
<i>Escherichia coli</i> ATCC 8739	$17,47 \pm 0,57$					
ESBL <i>E. coli</i> 6110	$15,10 \pm 1,17$					
ESBL <i>E. coli</i> 6024	$16,33 \pm 0,31$					
ESBL <i>E. coli</i> 5949	$20,65 \pm 0,69$					
<i>Staphylococcus aureus</i> ATCC 25923	$17,76 \pm 1,12$	16.63 ± 0.05	20.00 ± 0.00	22.98 ± 3.15	19.88 ± 0.65	21.35 ± 0.00
MRSA	15.13 ± 1.03					
<i>Staphylococcus epidermidis</i> FNG-1	$15,68 \pm 0,86$					
<i>Staphylococcus epidermidis</i> FNG- 2	$16,83 \pm 0,47$					
<i>Staphylococcus epidermidis</i> FNG- 3	$15,80 \pm 0,68$					
<i>Staphylococcus epidermidis</i> FNG-4	$16,48 \pm 0,41$					
<i>Staphylococcus epidermidis</i> FNG-5	$16,99 \pm 0,39$					
<i>Staphylococcus epidermidis</i> FNG-6	$15,43 \pm 0,44$					
<i>Staphylococcus epidermidis</i> FNG-7	$16,16 \pm 0,59$					
<i>Staphylococcus epidermidis</i> FNG-8	$17,03 \pm 0,24$					
<i>Staphylococcus epidermidis</i> FNG-9	$17,06 \pm 0,24$					
<i>Staphylococcus epidermidis</i> FNG-10	$17,80 \pm 1,12$					

Diameter of agar hole = 7 mm. Van= Vancomycin, Cefad= Cefadorxil, Strep= Streptomycin, Am = Amoxycilin, Ery = Erythromycin

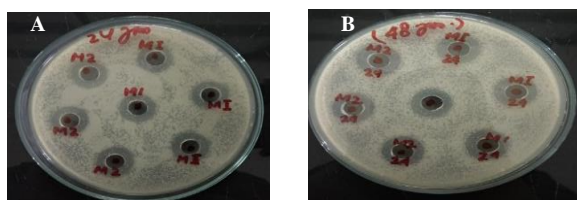


Figure.1. Growth inhibitory activity of passion fruit CFFS in MRS media against *S. aureus* ATCC 25923 after incubation at 37°C for 24 hours (A) and 48 hours (B).

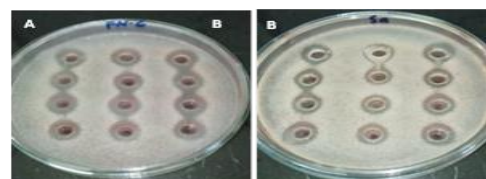


Figure.2. Growth inhibitory activity of passion fruit CFFS in MRS media against *S. epidermidis* FN-6 (A) and *S. aureus* ATCC 25923 (B) after incubation at 37°C for 24 hours.

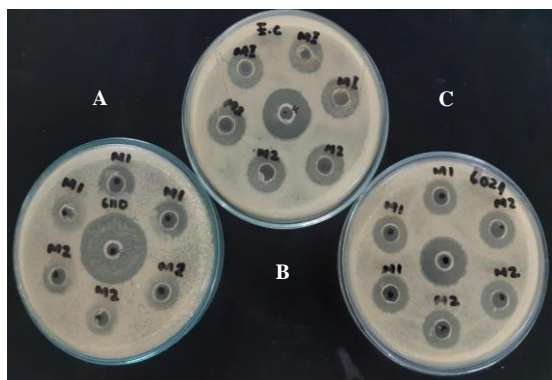


Figure.3. Growth inhibitory activity of passion fruit CFFS in MRS media against ESBL 6110 (A), non-ESBL *E.coli* (B), and ESBL 6024 (C) after incubation at 37°C for 24 hours.

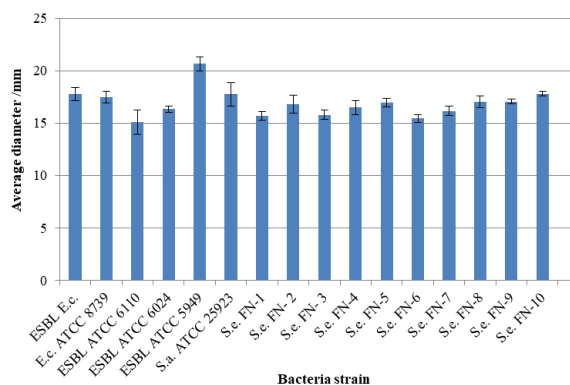


Figure 4. Average diameter (mm) of zone inhibition of CFFS against test bacteria

3.3. Minimum inhibitory concentration

The MIC of CFFS passion fruit was performed after antibacterial sensitivity was done. Figure 5 depicted the sensitivity of CFFS against six test bacteria. The agar dilution test of the CFFS had shown that the negative control agar plate (without CFFS addition) was covered with full growth of all test bacteria, while the agar plate with 1mL of the CFFS had shown inhibition to most of the inoculated area with few insignificant bacterial growths. Furthermore, the agar plate with 2mL and 3 ml of the CFFS had completely inhibited all microbial growth (Table 3). Table 3 showed the susceptibility test of the agar dilution test against the test bacteria. In addition, determination of MIC using serial dilution of 10 µL CFFS 100%, 75%, 50%, 25%, 12.5%, and 6.25 % applied on the sterile paper disk indicated that 75% of exhibited zone of growth inhibitory activity were less than 13 mm, meanwhile the 50% CFFS solution did not exhibit inhibitory activity.

3.4. Statistical analysis

Statistical analysis using Kruskal Wallis test was performed to evaluate the significant difference of inhibitory activity of the CFFS against bacterial tests. From the analysis results, it was obtained Asymp sig value that was 0,000. CFFS provided the greatest inhibitory activity on ESBL *E. coli* 5949 and the smallest one in *Staphylococcus epidermidis* FNG-6.

Table 3. Sensitivity test of six test microbial against passion fruit CFFS after 24 hours using streak method

Bacteria	Volume of CFFS added to 10 ml nutrient agar media											
	Positive Control (Without CFFS)			1mL			2mL			3 mL		
	R1	R2	R3	R1	R2	R3	R1	R2	R3	R1	R2	R3
ESBL	+	+	+	+	-	-	-	-	-	-	-	-
E ESBL6110	+	+	+	-	-	-	-	-	-	-	-	-
E ESBL6024	+	+	+	-	-	-	-	-	-	-	-	-
E ESBL5949	+	+	+	-	-	-	-	-	-	-	-	-
E ESBL8739	+	+	+	-	-	+	-	-	-	-	-	-
SA ATCC 25923	+	+	+	-	-	+	-	-	-	-	-	-

R = Replicate

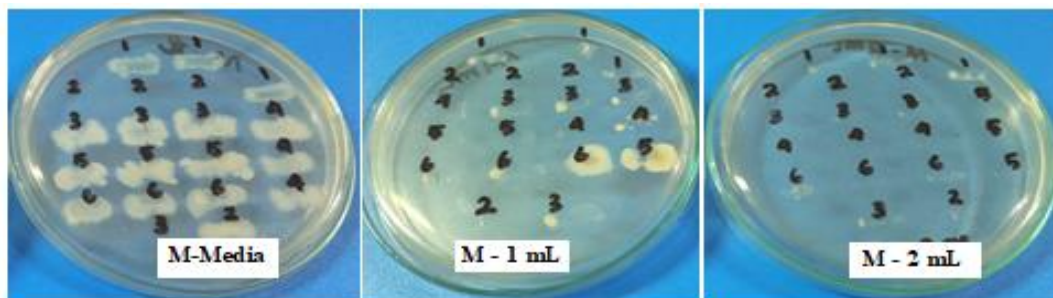


Figure 5. Sensitivity of six test bacteria against CFFS on Nutrient Agar mediaESBL *E. coli*, 2. NA-broth, 3. ESBL 6024, 4. ESBL 5949, non-ESBL *E.coli* ATCC 8739, *S.aureus* ATCC 25923, M-Media: media without CFFS, M-1 mL: NA Media + 1 mL of CFFS, M-2 mL: NA Media + 2 mL of CFFS.

4. Discussion

Passion fruit, as well as other fruits, is a suitable habitat for the growth of lactic acid bacteria (Askari *et al.*, 2012) and even probiotics, due to their adequate nutritional content. White and Sharareh (2018) have reported the results of their research on the fermentation process of *Lactobacillus rhamnosus* GR-1 using apple, orange, and grape juice. The main fermentation products that can be directly detected and dominant are lactic acids and other organic acids, thereby reducing the pH value in the fermentation process. In this study, pH value of the CFFS decreased at 24 hours of evaluation from 6 to 3. It was reported that passion fruit by-product stimulates the growth and folate production by starters and probiotic cultures in fermented soymilk (Mac *et al.*, 2017). The fermentation process using inulin apparently accelerates growth by up to 10 times compared to being stored in a refrigerator. The potential of the CFFS passion fruit as lactic acid bacteria by which many useful substances produced by fermentation processes might prospectively develop.

In this study, it has also been proven that before the fermentation process, the viability of the cell colonies in MRS media was less than 30×10^4 CFU / mL after 24 hours of incubation. The MRS is a selective medium for the growth of lactic acid bacteria (Askari *et al.*, 2012). Before the fermentation process, CFFS passion fruit also did not show inhibitory activity against all test bacteria (Table 1). Antimicrobial activity of dried fruit has been widely reported (Aziz *et al.*, 2006). This phenomenon proves the importance of the presence of active compounds in fruit (Ingale and Hivrale, 2010; Reis *et al.*, 2018) as antimicrobial. Asirvathamdos *et al.* (2008) have reported in-vitro antimicrobial activity of passion fruit extract, but the effect of the fermentation process in selective media MRS for probiotic growth and antibacterial activities has not yet been reported. Fermentation with MRS media leads to increase the population of lactic acid bacteria that are able to produce lactic acid and other organic acids, as well as other active ingredients that can act as anti-bacterial. Therefore, the CFFS passion fruit was not only effective as a source of active compounds, but also a source of lactic acid bacteria that have various activities. The accumulation of inhibitory activity against pathogenic microbes is very interesting to be further studied in order to detect the dominant component contributing as an antibacterial.

Pathogenic bacteria used as test bacteria ESBL, MRSA, and non-ESBL *E.coli* and *Staphylococcus spp.* are usually resistant bacteria group against methicillin and beta lactam antibiotics, in which in this research was represented by vancomycin, meropenem, cefadroxil, amoxicillin, streptomycin, kanamycin, and erythromycin. The antibiotics standard solutions used at the CFFS passion fruit showed intermediate until sensitive against some test bacteria at 100%/50 μ L with MIC of 10% (Table 2, Figures 5 and 6). Antibacterial activity data from CFFS compared with various bacteria test were analyzed using the IBM SPSS ver 24 program. From the results of normality testing requiring one group of samples that had a sig value <0.05, we could obtain abnormal data distribution results.

Statistical analysis was using the non parametric Kruskal Wallis method with a confidence degree of 0.95 ($\alpha = 0.05$). From the analysis results, it was obtained Asymp sig value of 0,000, so that the p value was <0.05. It can be said that there were significant differences between the antibacterial activity of CFFS with the type of bacteria test. CFFS provides the greatest inhibitory activity on ESBL *E. coli* 5949 and the smallest one on *Staphylococcus epidermidis* FNG-6. However, this phenomenon cannot prove the inhibitory potential of bacteria based on their Gram bacteria. The CFFS has a broad spectrum activities, but its inhibitory potential will depend on these individual bacterial strains. Therefore, further research is needed for this matter. In the future, it is interesting to examine the passion fruit CFFS activities on *Mycobacterium tuberculosis* (MTB) and Multi Drugs Resistant (MDR)-TB and other MDRs. On the other hand, the CFFS has potential opportunity to improve as an antimicrobial instant preparation.

The results of active substances identification by TLC-contact bioautography showed that CFFS contained two active compounds and the TLC chromatograms could be detected by UV lamps (Figure 7), but the Rf value of active compound on the TLC-bioautograms was still needed to be further investigated, whether it was derived from the same compounds as detected with UV lights. Based on the TLC chromatogram developed by a single eluent of KH_2PO_4 solution with a pH of 6.5, which was able to eluate the active compound with Rf 0.4-0.5 (tailing), the active compound was predicted to be polar. The TLC-bioautography method was very suitable for screening active compounds for both identification and separation through eluent system optimization. A very simple method can separate the active compound components from natural ingredients, two or more compounds from the same class, for example, the antibiotic streptomycin aminoglycosides and kanamycin (Febri *et al.*, 2019) that have been validated (Isnaeni *et al.*, 2019).



Figure 6. Determination of MIC of 10 μ L CFFS on the paper disk against *S. aureus* (A) and *E. coli* (B) on NA media at 100%, 75%, 50%, 25%, 12.5%, and 6.25% concentration.

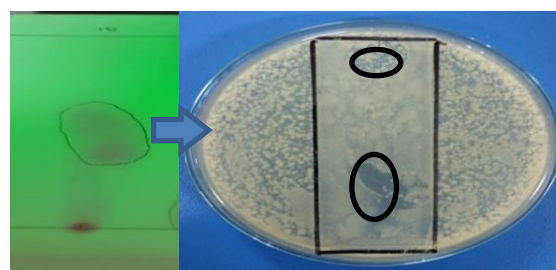


Figure 7. TLC-Chromatogram of CFFS on Silica Gel GF₂₅₄ using 7.5% KH_2PO_4 solution as eluent under UV lamp detection (A) and TLC-contact bioautogram using *E. coli* as a test bacterium (B).

5. Conclusion

Cell-free fermentation supernatant of passion fruit (*Passiflora edulis forma. flavicarpa* Sims.) is recommended to be developed as a source of active substances for antibacterial against pathogenic bacteria event for multi drugs resistant. The active substance might be a polar compound. Furthermore, isolation, separation, and purification to obtain the active isolates or novel substances are very interesting to be studied in the future.

References

- Asirvathamdoss, Doss PA, Rangasamydhanabalan. 2008. In-vitro antimicrobial activity of extracts of passiflora edulis (Passifloraceae) and sphaeranthus indicus (Asteraceae). *Ethnobot leaflets.*, **12**: 728-733.
- Askari GA, Azzeddine K, Khadija K, Reda C, and Zakaria M. 2012. Screening of lactic acid bacteria isolated from dried fruits and study of their antibacterial activity. *Middle East JSci Res.*, **11(2)**: 209-215.
- Aziz N'A. 2016. A review of the antimicrobial properties of three selected underutilized fruits of Malaysia. *IJPCR.*, **8** : 1278–1283.
- Bernes J, Anderson LA, Phillipson JD. 2007. **Passion flower. In: Herbal Medicines**, third ed. Pharmaceutical Press, United Kingdom
- Febri A, Iftitahatur R, Asri D, and Isnaeni. 2020. Method validation of contact and immersion TLC-bioautography for determination of streptomycin sulfate shrimp. *Turk J Pharm Sci.*, (ahead of print)
- Ingale AG and Hivrale AU. 2010. Pharmacological studies of Passiflora sp. and their bioactive compounds. *Afr J Plant Sci.*, **4(10)**: 417-426.
- Isnaeni, Andri A, and Muhammad.Y. 2017. Validation of thin-layer-chromatography-bioautographic method for determination of streptomycin. *JFIKI.*, **4(1)**: 32-38.
- Mac A, Bedani R, LeBlanc JG, and Saad SMI. 2017. Passion fruit by-product and fructooligosaccharides stimulate the growth and folate production by starter and probiotic cultures in fermented soymilk. *Int J Food Microbiol.*, **261**: 35-41.
- Oliveira CF, Gurak PD, Cladera-Olivera F, and Marczak LDF. 2016. Evaluation of physicochemical, technological and morphological characteristics of powdered yellow passion fruit peel. *Int Food Res J.*, **23(4)**:1653–1662.
- Paul RE and Duarte O. (Eds.) 2012. **Tropical fruits, Volume 2**. Available at: <https://www.cabi.org/isc/datasheet/38799> (accessed on 5 November, 2019).
- Ramaiya SD, Bujang JS, and Zakaria MH. 2014. Assessment of total phenolic, antioxidant, and antibacterial activities of passiflora species. *Sci World J.*, pp.1-10.
- Reis RLC, Facco EMP, Salvador M, Flôres SH, and de Oliveira Rios A. 2018. Antioxidant potential and physicochemical characterization of yellow, purple and orange passion fruit. *J Food Sci Technol.*, **55(7)**:2679–2691
- Sofija MD. (Eds.) 2017. **From medicinal plant raw material to herbal remedies**. Available at: <https://www.intechopen.com/books/aromatic-and-medicinal-plants-back-to-nature/from-medicinal-plant-raw-material-to-herbal-remedies> (accessed on 5 November, 2019).
- White J and Sharareh H. 2018. Development of probiotic fruit juice using *Lactobacillus rhamnosus* GR-1 fortified with short chain and long chain fiber. *Fermentation.*, **4(27)**: 1-12.
- Zibadi S, and Watson, RR. 2004. Passion fruit (*Passiflora edulis*) composition, efficacy, and safety. *JEBIM.*, **1(3)**: 183-187
- Zahro, F. 2014. Isolasi dan identifikasi bakteri asam laktat asal fermentasi Markisa Ungu (*Passiflora edulis* var. Sims) sebagai penghasil eksopolisakarida. Undergraduate thesis, Universitas Islam Negeri Maulana Malik Ibrahim, Malang.

Prevalence of Capsular Polysaccharide Genes and Antibiotic Resistance Pattern of *Klebsiella pneumoniae* in Palestine

Ghaleb M. Adwan^{*}, Dina M. Owda and Awni A. Abu-Hijleh

Department of Biology and Biotechnology, An-Najah National University, P. O. Box (7)-Nablus, Palestine.

Received: October 17, 2019; Revised: November 29, 2019; Accepted: December 21, 2019

Abstract

Klebsiella pneumoniae (*K. pneumoniae*) is a pathogenic bacteria responsible for a wide spectrum of infections in both hospital and community settings. A total of 66 isolates of *K. pneumoniae* were collected from different clinical sources in Palestine. The aim of this study was to determine the frequency of virulence genes in *K. pneumoniae* isolates using PCR technique, hypermucoviscosity (HMV) phenotype and antibiotic resistance profile. Rate of resistance to antibiotics was as follows: Trimethoprim/sulphamethoxazole (89%), Amoxicillin/clavulanic acid (82%), Aztreonam (77%), Tetracycline (71%), Ceftriaxone (67%), Imipenem (59%), Kanamycin (58%), Ceftazidime (56%), Levofloxacin (44%) and Ciprofloxacin (40%). In addition, isolates recovered from urine samples showed higher resistance ($P < 0.05$) against Imipenem, Ceftriaxone, Ceftazidime and Amoxicillin/clavulanic acid than isolates recovered from throat swabs. The prevalence of multidrug resistant *K. pneumoniae* isolates was 90.9%. Moreover, 5% of isolates were positive for HMV phenotype test. The prevalence of capsular polysaccharide genes among *K. pneumoniae* isolates was as follows: *cps* (100%), *K1* serotype (21.1%), *K2* serotype (11.7%), *p-rmpA2* (15.2%), *c-rmpA* (7.6%), *P-rmpA* (12.1%), and *magA* (0.0%). The results of this study showed that 87% of *rmpA* genes are detected in non *K1/K2* isolates and approximately 25% of tested isolates carried *K1* serotype or *K2* serotype or both serotype genes. Based on distribution of virulence factors, 3 (4.5%) strains were identified as probable hypervirulent *K. pneumoniae*. The presence of *K1* or *K2* or both serotype genes in these isolates together with other genes such as *rmpA* and high level of drug resistance should make bacteria a highly infectious agent, which leads to failure of treatment. Overall, this study demonstrates the significant role of rapid diagnosis and proper treatment of infections caused by this pathogen.

Keywords: *K. pneumoniae*, virulence factor, *rmpA* genes, *K1* serotype gene, *K2* serotype gene, *magA* gene, capsule polysaccharide synthesis (*cps*) gene, Palestine.

1. Introduction

Klebsiella pneumoniae is considered as a widespread human pathogen that is responsible for a broad spectrum of infections in both hospital and community settings. *Klebsiella pneumoniae* is also considered as a common animal pathogen associated with multiple infections, including mastitis in dairy cows (Janda and Abbot, 2009; Pan *et al.*, 2015). Pathogenicity of *K. pneumoniae* depends on different virulence factors including lipopolysaccharide antigen (O-antigen), fimbriae, capsular polysaccharides (K antigen) and siderophores (Schembri *et al.*, 2005; Vuotto *et al.*, 2017). Each of these factors plays a particular function in the pathogenesis depending on the mode of infectivity and the type of infection (Janda and Abbott, 2006).

The incidence of bacterial infections has been increasing in the past few decades. This has led to the continuous and uncontrolled use of antibiotics for prevention and treatment in most parts of the world. Consequently, the emergence of multidrug resistance (MDR) among different strains of pathogens including *K. pneumoniae* has increased. One of these mechanisms used

for transmitting multi-drug resistance among microbial pathogens is horizontal spread of antibiotic resistance genes among bacteria. The efflux pump systems are among the most important causes of MDR (Wasfi *et al.*, 2016).

The capsule is considered one of the most essential virulence factors in *K. pneumoniae*, which is associated with biofilm formation and protection of the pathogen from phagocytosis, serum bactericidal activity and antimicrobial peptides (Struve and Krogfelt, 2003; Lin *et al.*, 2013; Pan *et al.*, 2015). Currently, there are about 79 capsular types recognized in different *Klebsiella* sp. strains (Pan *et al.*, 2015). Some of these types are *K1* and *K2* serotypes, which are considered as the most virulent from non-*K1/K2* strains (Lin *et al.*, 2004). Another gene, which is known as mucoviscosity associated gene A (*magA*) is restricted to the capsule gene cluster serotype *K1* and the chromosomal *K2* capsule associated gene A (*k2A*) for the *K2* serotype (Yu *et al.*, 2006; Doud *et al.*, 2009). This gene is more prevalent in strains isolated from human liver abscesses (Fang *et al.*, 2004; Lee *et al.*, 2006). Existence of this gene in these strains is associated with hypermucoviscosity (HMV) phenotype and eradication resistance by human serum and phagocytosis (Fang *et al.*,

^{*} Corresponding author e-mail: adwang@najah.edu.

2004; Lee *et al.*, 2006). The *rmp* (regulator of the mucoid phenotype) genes play a pivotal role in hyper-production of mucoid phenotype in *K. pneumoniae* strains. The *rmpA* gene is plasmid-mediated (*p-rmpA*) or chromosomal-mediated (*c-rmpA*), which gives the strains a highly enhanced mucoviscous phenotype, regulates the capsular polysaccharide synthesis and participates in neutrophilic phagocytosis resistance (Yeh *et al.*, 2007; Cheng *et al.*, 2010; Ko *et al.*, 2017). In addition, it was shown that *rmpA* gene is associated with strains related to invasive infections (Yu *et al.*, 2006).

Molecular detection of capsule polysaccharide genes and other associated genes has been reported in different countries. A recent study conducted in Brazil showed that the prevalence of K2 serotype and K1 serotype genes among *K. pneumoniae* isolates was 4% and 0%, respectively (Ferreira *et al.*, 2019). Several studies carried out in Iran showed that the prevalence of virulence factors in *K. pneumoniae* isolated from different clinical samples was 6.9%-27.82%, 6.96%-32.9%, 13.91%-20.2% and 3.8% for of K1 serotype, K2 serotype, *rampA* and *magA* genes, respectively (Ranjbar *et al.*, 2019; Moghadas *et al.*, 2018; Zamani *et al.*, 2013; Feizabadi *et al.*, 2013). In Iraq, it was found that 100% of clinical isolates of *K. pneumoniae* had capsule polysaccharide synthesis (*cps*) gene, 18.6% had K1 serotype, 32.6% had K2 serotype, 7% had K1/K2 serotypes and 41.9% were non-K1/K2 serotypes. Other genes were also detected such as *magA*, *rmpA*, *rmpA1* and *rmpA2* and the prevalence was 25.6%, 48.8%, 44.2% and 44.2%, respectively (Abdul-Razzaq *et al.*, 2014). Also, it was shown that 57.5% *K. pneumoniae* had K1 capsular serotype, 27.5% had K2 serotype and 15% had non-K1/K2 serotype. In addition, the prevalence of *magA*, *k2A* and *rmpA* genes was 57.5%, 27.5% and 27.5%, respectively (Al-Jailawi *et al.*, 2014).

A recent study from China, the hypermucoviscosity, as well as *magA*, K1 and K2 serotypes in *K. pneumoniae* isolates accounted to 30.7%, 45.4%, 40.5%, and 19.0%, respectively (Zhang *et al.*, 2019). In another study carried out in China, the hypervirulent *K. pneumoniae* was recognized in 31.4% of the infected patients with bacteremia, and in this study 4 serotypes K1, K2, K20, and K57 were identified (Liu *et al.*, 2014). In Taiwan, it was found that 98% of *K. pneumoniae* strains recovered from liver abscess were *magA*⁺ (Fang *et al.*, 2004). Additionally, it was shown that 38.5% of tested *K. pneumoniae* isolates had a HMV phenotypes. The existence of *rmpA* and/or *rmpA2* gene was confirmed in approximately 91% of these isolates, while these genes found only in about 18% of the isolates did not show HMV phenotype. The K1 and/or K2 serotypes were present in 16.5% of the isolates, the *rmpA* and/or *rmpA2* gene were detected in 46.2% of the isolates, with *rmpA* found in 38.5% and *rmpA2* in 45.1% of the isolates. The *magA* gene was shown to coexist in 8.8% isolates with K1 serotype (Lee *et al.*, 2010). Another study conducted in Taiwan showed that the frequency of K1 and K2, *rampA* and HMV phenotype was 0.0% and 7.7%, 0.0% and 0.0% respectively, from *K. pneumoniae* peritoneal dialysis-related peritonitis, while the frequency was 5.6%, 9.3%, 29.6% and 27.8% for K1, K2, *rampA* and HMV phenotype, respectively, from *K. pneumoniae* isolated from urinary tract infection (Lin *et al.*, 2015). In Spain, 53 of invasive and hypermucoviscous phenotypic *K.*

pneumoniae isolates, 30.2% of these isolates had a genotype *magA*⁺/*rmpA*⁺, 22.6% *magA*⁻/*rmpA*⁺, and the remaining 47.2% *magA*⁻/*rmpA*⁻. Results of this study showed that all isolates had a genotype *magA*⁺/*rmpA*⁺ were K1 serotype, while 75% of the isolates that had a genotype *magA*⁻/*rmpA*⁺ were K2 serotype (Cubero *et al.*, 2016).

This study aimed to determine the frequency of virulence factor encoding genes in *K. pneumoniae* isolates, such as *cps*, K1 serotype and K2 serotype genes, *magA*, *p-rmpA*, *c-rmpA*, and *p-rmpA2* using PCR technique, from patients in Northern West Bank-Palestine. Additionally, we wanted to determine the phenotypic characterization including HMV and antibiotic resistant phenotypes for these isolates. This report based on detection of these virulence genes using PCR seems to be the first report from Palestine.

2. Materials and Methods

2.1. Bacterial Strains Collection and Identification

A total of 66 non-duplicate isolates of *K. pneumoniae* were collected from clinical sources as shown in Table 1. These isolates were recovered from in-patients and out-patients from different hospitals in Northern West Bank-Palestine during 2019 (Table 1). Duplicate isolates were excluded. Identification of these isolates was carried out in laboratories of these hospitals by API 20 E system and confirmed using conventional methods in microbiology research laboratory, at An-Najah National University.

Table 1. Source of 66 of *K. pneumoniae* isolates collected from different hospitals.

Hospital	Sample source (n)					Total
	wound	urine	Sputum Trap	swab	Blood	
N	5	5	1	0	1	12
W	0	3	0	0	0	3
T	0	1	0	1	0	2
J	0	6	0	2	0	8
TH	0	2	0	0	0	2
R	0	23	0	10	0	33
S	0	3	2	1	0	6
Total =	5	43	3	14	1	66

N: An-Najah National University Hospital; W: Alwatany Hospital; T: Al-Turk Hospital; J: Jenin Governmental Hospital; TH: Thabet Hospital; R: Rafidia Hospital; S: Nablus Specialist Hospital.

2.2. Antibacterial Resistance

Antimicrobial susceptibility was determined according to the Clinical and Laboratory Standard Institute (CLSI) using the disk diffusion method (CLSI, 2017). All *K. pneumoniae* isolates were examined for resistance to Cefazidime (CAZ, 30µg), Ciprofloxacin (CIP, 5µg), Aztreonam (ATM, 30µg), Imipenem (IPM, 10 µg), Levofloxacin (LEV, 10µg), Ceftriaxone (CFX, 30µg), Trimethoprim/Sulphamethoxazole (SXT, 1.25/23.75µg), Tetracycline (TE, 30µg), Kanamycin (K, 30µg) and Amoxicillin/Clavulanic acid (AMC, 20/10 µg). The plates were incubated at 37°C for 18-24 hrs. The inhibition zones were measured, and isolates were classified as resistant, intermediate or susceptible according to the criteria recommended by CLSI guidelines (CLSI, 2017). The *K. pneumoniae* isolates resistant to three or more classes of antimicrobial agents were considered MDR strains. The

reference strain of *K. pneumoniae* ATCC 13883 was used as a quality control in all of the experiments of antimicrobial susceptibility testing.

2.3. String Test for Hypermucoviscosity

The string test for HMV detection was carried out as described previously (Fang *et al.*, 2004). The tested strains were inoculated on 5% sheep blood agar plates and incubated at 37°C overnight. A standard bacteriologic loop was used to stretch a mucoviscous string from the colony. Hypermucoviscosity was defined by the formation of viscous string, which has a length of ≥ 5 mm, when a loop was used to stretch the colony on blood agar plate (positive string test).

2.4. DNA Isolation and PCR Amplification

2.4.1. DNA isolation

Genome of *K. pneumoniae* was prepared for PCR according to the method described previously (Adwan *et al.*, 2013). Briefly, the cells were scraped off an overnight MHA plate, washed with 800 μ L of 1X Tris-EDTA buffer (10 mM Tris-HCl, 1 mM EDTA [pH 8]), centrifuged, and the pellet was resuspended in 400 μ L of sterile double distilled H₂O, and boiled for 10-15 minutes. The cells were incubated on ice for ten minutes. The debris were pelleted by centrifugation at 11,500 X g for five minutes.

Table 2. Target genes for PCR amplification, primer sequences, size of amplicons and annealing temperatures used.

gene	Primer sequence 5'→3'	Ta*	Amplicon size	
<i>cps</i>	cpsF GCT GGT AGC TGT TAA GCC AGG GGC GGT AGC G	59°C	398	Brisse <i>et al.</i> , 2004
	cpsR TGT ACA AGA TCC ATT TTC AGC CCC GCT GTC G			
<i>K1</i> serotype	K1F GTA GGT ATT GCA AGC CAT GC	50°C	1046	Lin <i>et al.</i> , 2015
	K1R GCC CAG GTT AAT GAA TCC GT			
<i>K2</i> serotype	K2F GGA GCC ATT TGA ATT CGG TG	50°C	1121	Lin <i>et al.</i> , 2015
	K2R TCC CTA GCA CTG GCT TAA GT			
<i>p-rmpA2</i>	prmpA2F CTT TAT GTG CAA TAA GGA TGT T	50°C	451	Lee <i>et al.</i> , 2010
	prmpA2R CCT CCT GGA GAG TAA GCA TT			
<i>c-rmpA</i>	crmpAF TGG CAG CAG GCA ATA TTG TC	53°C	1006	Fang <i>et al.</i> , 2007
	crmpAR GAA AGA GTG CTT TCA CCC CCT			
<i>p-rmpA</i>	prmpAF TAC TTT ATA TGT AAC AAG GAT GTA AAC ATA G	56°C	441	Fang <i>et al.</i> , 2007
	prmpAR CAG TAG GCA TTG CAG CAC TGC			
<i>magA</i>	magAF TAG GAC CGT TAA TTT GCT TTG T	52°C	795	Struve <i>et al.</i> , 2005
	magAR GAA TAT TCC CAC TCC CTC TCC			

*Ta: Annealing temperature

2.5. Statistical Analysis

Generated data was analyzed by Z-test using SPSS software version 20. A $P < 0.05$ values were considered statistically significant.

3. Results

3.1. Antibacterial Resistance

In general, the results of this study showed that bacterial isolates had high resistance rate to most antimicrobial agents tested. These isolates showed high resistance rate against Trimethoprim/sulphamethoxazole (89%), Amoxicillin/clavulanic acid (82%), Aztreonam (71%) and Tetracycline (71%), while these isolates showed resistance rate 44% and 40% against Levofloxacin and Ciprofloxacin, respectively. The antimicrobial resistance profile of these isolates is presented in Table 3. Also, results showed that about 91% of the isolates were

The DNA concentration was determined using a nanodrop spectrophotometer (Genova Nano, Jenway). The DNA samples were stored at -20°C.

2.4.2. PCR Amplification

The presence of 7 virulence genes was investigated using uniplex PCR. Primer sequences, size of amplicons and the annealing temperatures for detection these genes are presented in Table 2. For detection of these genes, each PCR reaction consisted of 12.5 μ L of PCR premix with MgCl₂ (ReadyMix™ Taq PCR Reaction mix with MgCl₂, Sigma), 0.2 μ M of each primer, 3 μ L (50-100 ng) of DNA template. A negative control without a DNA template and a positive control strain (department collection) possessing a tested genes were used during PCR. The cycling conditions were: initial denaturation for 3 minutes at 94°C; followed by thirty-five cycles of denaturation at 94°C for fifty seconds, annealing temperature for each pair of primers is mentioned in Table 2 for fifty seconds, and extension at 72°C for two minutes, followed by a single final extension step at 72°C for five minutes. The PCR products were resolved by electrophoresis on 1.5 % agarose gel to determine the size of amplified fragments after staining with a final concentration of 0.5 μ g/ml ethidium bromide.

MDR. In addition, isolates recovered from urine samples showed higher resistance ($P < 0.05$) against Imipenem, Ceftriaxone, Ceftazidime and Amoxicillin/clavulanic acid than isolates recovered from throat swabs. Data are presented in Table 4. However, the prevalence of antibiotic resistance was not significant ($P < 0.05$) between isolates recovered from males and females. Data are presented in Table 5.

Table 3. Antibiotic resistance profile of 66 *K. pneumoniae* isolates recovered from different clinical samples.

Antibiotic	Antibiotic resistance n (%)*		
	S	I	R
Imipenem	20 (30)	7 (11)	39 (59)
Ceftriaxone	17 (26)	5 (8)	44 (67)
Ceftazidime	26 (39)	3 (5)	37 (56)
Aztreonam	13 (20)	2 (3)	51 (77)
Ciprofloxacin	28 (42)	11 (17)	27 (41)
Levofloxacin	36 (54)	1 (2)	29 (44)
Kanamycin	13 (20)	15 (22)	38 (58)
Trimethoprim/sulphamethoxazole	7 (11)	0 (0)	59 (89)
Amoxicillin/clavulanic acid	7 (11)	5 (8)	54 (81)
Tetracycline	19 (29)	0 (0)	47 (71)

*n: number of isolates; S: Susceptible; I: Intermediate; R: Resistant

Table 4. Antibiotic resistance rates according to the source of isolates.

Antibiotic	Sample source (n)**					Total
	Urine n=43	Throat swab n=14	Wound n=5	Sputum trap n=3	Blood n=1	
Imipenem	27 (62.8)*	4 (28.6)*	5 (100)	2 (66.7)	1 (100)	39 (59)
Ceftriaxone	31 (72.1)*	6 (42.9)*	3 (60)	3 (100)	1 (100)	44 (67)
Ceftazidime	26 (60.5)*	4 (28.6)*	3 (60)	3 (100)	1 (100)	37 (56)
Aztreonam	34 (79.1)	10 (71.4)	3 (60)	3 (100)	1 (100)	51 (77)
Ciprofloxacin	16 (37.2)	5 (35.7)	2 (40)	3 (100)	1 (100)	27 (41)
Levofloxacin	20 (46.5)	4 (28.6)	1 (20)	3 (100)	1 (100)	29 (44)
Kanamycin	25 (58.1)	6 (42.9)	3 (60)	3 (100)	1 (100)	38 (58)
Trimethoprim/ Sulphamethoxazole	39 (90.7)	12 (85.7)	5 (100)	2 (66.7)	1 (100)	59 (89)
Amoxicillin/ clavulanic acid	39 (90.7)*	6 (42.9)*	5 (100)	3 (100)	1 (100)	54 (81)
Tetracycline	31 (72.1)	9 (64.2)	4 (80)	2 (66.7)	1 (100)	47 (71)

*significant at $p < 0.05$; **n: number of isolates

Table 5. Antibiotic resistance rates according to the to patients' gender.

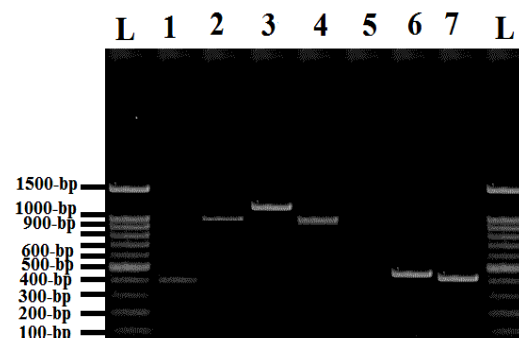
Antibiotic	Gender		Total
	Male (38)	Female (28)	
Imipenem	21 (55.2)	18 (64.2)	39 (59)
Ceftriaxone	23 (60.5)	21 (75)	44 (67)
Ceftazidime	18 (47.3)	19 (67.8)	37 (56)
Aztreonam	27 (71)	24 (85.7)	51 (77)
Ciprofloxacin	12 (31.5)	15 (53.5)	27 (41)
Levofloxacin	14 (36.8)	15 (53.5)	29 (44)
Kanamycin	22 (57.8)	16 (57.1)	38 (58)
Trimethoprim/ Sulphamethoxazole	34 (89.3)	25 (89.2)	59 (89)
Amoxicillin/clavulanic acid	31 (51.5)	23 (82.1)	54 (81)
Tetracycline	27 (71)	20 (71.4)	47 (71)

3.2. Hypermucoviscosity Testing

Results of the current study showed that among 66 of *K. pneumoniae* isolates, only 3 (5%) isolates recovered from urine, sputum trap and throat swab displayed hypermucoviscous phenotype. These isolates showed multidrug resistance to different tested antibiotics. In addition to *cps* gene, these isolates carried *K1/K2* (urine sample), *p-rmpA2* (sputum trap sample); however, the third isolate (throat swab) was negative for other tested genes.

3.3. Detection of Virulence Genes

Virulence related genes were studied by uniplex PCR. The prevalence of *cps*, *K1*, *K2*, *p-rmpA2*, *c-rmpA*, *P-rmpA* and *magA* genes among *K. pneumoniae* isolates was 100%, 21.1%, 11.7%, 15.2%, 7.6%, 12.1% and 0.0%, respectively. Data are presented in Figure 1 and Table 6. Results in Table 6 indicate the presence of statistically significant difference ($p < 0.05$) in the prevalence of *p-rmpA2* and *P-rmpA* genes between isolates recovered from urine and throat swab samples in favor of throat swab samples.

**Figure 1.** Uniplex PCR profile specific for genes responsible for capsular polysaccharides production. Lanes L represent 100-bp ladder; lane 1 represents *cps* gene (398-bp); lane 2 represents *K1* serotype gene (1046-bp); lane 3 represents *K2* serotype gene (1121-bp); lane 4 represents *c-rmpA* gene (1006-bp); lane 5 represents *magA* gene (795-bp); lane 6 represents *p-rmpA2* gene (451-bp) and lane 7 represents *P-rmpA* gene (441-bp).**Table 6.** Virulence gene profiles of 66 *K. pneumoniae* recovered from different sample sources.

Virulence gene	Sample source (n)					Total
	Urine n (43)	Throat swab (14)	Wound (5)	Sputum trap (3)	Blood (1)	
<i>cps</i>	43 (100)	14 (100)	5 (100)	3 (100)	1 (100)	66 (100)
<i>K1</i>	10 (23.2)	3 (21.4)	1 (20.0)	0 (0.0)	0 (0.0)	14 (21.2)
<i>K2</i>	9 (20.9)	1 (7.1)	1 (20.0)	0 (0.0)	0 (0.0)	11 (11.7)
<i>p-rmpA2</i>	3 (7)*	5 (35.7)*	1 (20)	1 (33.3)	0 (0.0)	10 (15.2)
<i>c-rmpA</i>	5 (16.7)	0 (0.0)	0 (0.0)	0 (0.0)	0 (0.0)	5 (7.6)
<i>P-rmpA</i>	2 (4.7)*	6 (42.9)*	0 (0.0)	0 (0.0)	0 (0.0)	8 (12.1)
<i>magA</i>	0 (0.0)	0 (0.0)	0 (0.0)	0 (0.0)	0 (0.0)	0 (0.0)

*significant at $p < 0.05$; **n: number of isolates

The findings of the current study showed that 32 (48.5%) *K. pneumoniae* isolates carried 2 or more virulence genes. The most predominant patterns were *cps*, *K1* serotype, *K2* serotype (10.6%) and *cps*, *p-rmpA2* (7.5%). The data presented in Table 7 indicate the presence of statistically significant difference ($p < 0.05$) in

the prevalence of *cps*, *p-rmpA*, *p-rmpA2* pattern between isolates recovered from urine and throat swab samples in favor of throat swab samples. Also, results showed that 87% of *p-rmpA*, *c-rmpA*, *p-rmpA2* genes are detected in non K1/K2 isolates and approximately 25% of tested *K. pneumoniae* carried K1 serotype or K2 serotype or both serotype genes. In addition, distribution of these virulence genes between MDR isolates and non-MDR isolates showed the presence of statistically significant difference ($p < 0.05$) in the distribution of *p-rmpA* gene between isolates recovered from urine and throat swab samples in favor of throat swab samples. Data are presented in Table 8. While distribution of virulence genes according to patients' gender, results showed the presence of statistically significant difference ($p < 0.05$) in the distribution of *p-rmpA* gene between isolates recovered from males and females in favor of isolates recovered from females. Data are presented in Table 9.

Table 7. Virulence patterns identified among 66 *K. pneumoniae* recovered from different sample sources.

Virulence gene pattern n (%)**	Sample source (n)					Total
	Urine (43)	Throat swab (14)	Wound (5)	Sputum trap (3)	Blood (1)	
<i>cps</i> , K1, K2	5 (11.6)	1 (7.1)	1 (20)	0 (0.0)	0 (0.0)	7 (10.6)
<i>cps</i> , <i>p-rmpA</i>	2 (4.6)	2 (14.3)	0 (0.0)	0 (0.0)	0 (0.0)	4 (6.1)
<i>cps</i> , <i>p-rmpA</i> , <i>p-rmpA2</i>	0 (0.0)*	4 (28.6)*	0 (0.0)	0 (0.0)	0 (0.0)	4 (6.1)
<i>cps</i> , K1	2 (4.6)	2 (14.3)	0 (0.0)	0 (0.0)	0 (0.0)	4 (6.1)
<i>cps</i> , <i>p-rmpA2</i>	2 (4.6)	1 (7.1)	1 (20)	1 (33.3)	0 (0.0)	5 (7.5)
<i>cps</i> , <i>c-rmpA</i>	3 (7.0)	0 (0.0)	0 (0.0)	0 (0.0)	0 (0.0)	3 (4.5)
<i>cps</i> , K1, K2, <i>c-rmpA</i>	2 (4.6)	0 (0.0)	0 (0.0)	0 (0.0)	0 (0.0)	2 (3.0)
<i>cps</i> , K2	2 (4.6)	0 (0.0)	0 (0.0)	0 (0.0)	0 (0.0)	2 (3.0)
<i>cps</i> , K1, <i>p-rmpA2</i>	1 (2.3)	0 (0.0)	0 (0.0)	0 (0.0)	0 (0.0)	1 (1.5)
<i>Cps</i>	24 (55.8)	4 (28.6)	3 (60)	2 (66.7)	1 (100)	34 (51.5)
Total	43 (100)	14 (100)	5 (100)	3 (100)	1 (100)	66 (100)

*significant at $p < 0.05$; **n: number of isolates

Table 8. Distribution of virulence genes in MDR isolates and non-MDR isolates.

Virulence genes	MDR isolates n (%)	Non-MDR isolates n (%)	Total
<i>cps</i>	60 (100)	6 (100)	66 (100)
K1	12 (20)	2 (33.3)	14 (21.1)
K2	10 (16.7)	1 (16.7)	11 (16.7)
<i>p-rmpA2</i>	8 (13.3)	2 (33.3)	10 (15.2)
<i>c-rmpA</i>	5 (8.3)	0 (0.0)	5 (7.6)
<i>p-rmpA</i>	5 (8.3)*	3 (50)*	8 (12.1)

n: number of isolates; *significant at $p < 0.05$

In addition, in this study 3 (4.5%) strains were identified as probable hypervirulent *K. pneumoniae*. These strains carried *cps*, K1, K2, *c-rmpA* (n=1) and *cps*, K1, *p-rmpA2* (n=1). All these probable hypervirulent strains were MDR.

Table 9. Virulence gene profiles of 66 *K. pneumoniae* isolates distributed according to patients' gender

Virulence gene n (%)	Gender (n)**		Total
	Male (38)	Female (28)	
<i>CPS</i>	38 (100)	28 (100)	66 (100)
K1	9 (23.6)	5 (17.8)	14 (21.2)
K2	6 (15.7)	5 (17.8)	11 (11.7)
<i>p-rmpA2</i>	2 (5.2)*	8 (28.5)*	10 (15.2)
<i>c-rmpA</i>	4 (10.5)	1 (3.5)	5 (7.6)
<i>p-rmpA</i>	3 (7.8)	5 (17.8)	8 (12.1)
<i>magA</i>	0 (0.0)	0 (0.0)	0 (0.0)

*significant at $p < 0.05$; **n: number of isolates

4. Discussion

Klebsiella pneumoniae is a major pathogen that can cause nosocomial and community acquired infections. This pathogen harbors numerous virulence factors, which help this microorganism to cause infections. The isolates of *K. pneumoniae* had high-level of resistance rate against most antimicrobial agents tested and most of them were MDR isolates. This may be due to misuse of antibiotics at clinical settings. This is also influenced by the deficiency of a clear national antibiotic policy and over-the-counter antibiotic availability in this country (Adwan *et al.*, 2014, 2016a; 2016b). Additionally, rates as high as 84% of MDR *K. pneumoniae* isolates were detected in other studies (Ferreira *et al.*, 2019). Antibiotic efflux pumps are considered as one of the most important antimicrobial resistance mechanisms used by this pathogen. Existence of the multidrug efflux pump system is significantly correlated with the MDR pattern (Wasfi *et al.*, 2016; Ferreira *et al.*, 2019).

The results of this study indicate that all tested *K. pneumoniae* isolates carried the *cps* gene, which agrees with previously published research (Abdul-Razzaq *et al.*, 2013; 2014). The presence of capsule in *K. pneumoniae* is considered one of the most vital virulence determinants. It helps in biofilm formation and enhances resistance to antibiotics by minimizing the binding of antimicrobial peptides to bacterial surface. In addition, it is an important factor that contributes in protecting the pathogen from phagocytosis process as well as serum bactericidal activity (Struve and Krogfelt, 2003; Chung *et al.*, 2008; Lin *et al.*, 2013; Pan *et al.*, 2015; Theophano *et al.*, 2017).

In this study, among the 66 *K. pneumoniae* isolates collected from different clinical specimens, 3 (5%) isolates showed HMV phenotype. One of these isolates carried K1/K2 serotype genes, and the other carried *p-rmpA2* gene. However, the third isolate was negative for all tested genes. Two of these 3 isolates, which showed HMV phenotype, were *magA*^{-ve}/*rmpA*^{-ve}. This may be due to these strains having mutations in these genes, which might have a potential effect on the primer annealing sites. Our findings agree with Cubero *et al.*, 2016, who found that 47.2% of hypermucoviscous isolates were *magA*^{ve}/*rmpA*^{ve}. However, this result is in conflict with previous studies carried out in Taiwan (Yu *et al.*, 2006) and Iran (Zamani *et al.*, 2013; Shakib *et al.*, 2018) which showed that 38.5% of *K. pneumoniae* isolates in Taiwan were positive to HMV phenotype, and 14.3% and 60.95% of *K. pneumoniae* isolates were positive to HMV phenotype in Iran. In a

study carried out by Shakib *et al.*, (2018), only 30% of isolates which had HMV phenotypes were *rmpA*⁺ or *magA*⁺. Another study in Iran showed that 33.48% of *K. pneumoniae* isolates were positive to HMV phenotype (Nahavandinejad and Asadpour, 2017). In Taiwan, most of the strains which showed positive HMV phenotype (91.4%) were *rmpA*⁺ or *rmpA2*⁺, while these genes were found only in 17.9% of the isolates without HMV phenotype (Yu *et al.*, 2006). In another study in Taiwan, it was found that the frequency of both *rampA* and HMV phenotype was 0.0% from *K. pneumoniae* peritoneal dialysis-related peritonitis. However, the frequency of both *rampA* and HMV phenotype was 29.6% and 27.8%, respectively, from *K. pneumoniae* isolated from urinary tract infection (Lin *et al.*, 2016). In a recent study in China, 45.7% of *K. pneumoniae* showed HMV phenotype (Liu and Guo, 2019). Furthermore, *K. pneumoniae* isolates exhibited the hypermucoviscosity phenotype were not limited to *magA* gene (Nahavandinejad and Asadpour, 2017). These confusions in results could be related to the sample source. In most of those studies, *K. pneumoniae* isolates were invasive and collected from liver abscess and meningitis infections.

According to K markers, *K. pneumoniae* can be grouped into 4 serotypes including K1 group, K2 group, K1/K2 group, and non K1/K2 group. Results of this study showed that the prevalence of K1 serotype was higher than K2 serotype. These results were consistent with a previously published reports (Lee *et al.*, 2010; Al-Jailawi *et al.*, 2014; Cubero *et al.*, 2016; Akbari *et al.*, 2017; Thonda and Oluduro, 2018; Ranjbar *et al.*, 2019; Zhang *et al.*, 2019). However, these were in contrast to other studies (Lin *et al.*, 2004; Feizabadi *et al.*, 2013; Abdul-Razzaq *et al.*, 2014; Lin *et al.*, 2015; Moghadas *et al.*, 2018; Ferreira *et al.*, 2019). In a recent study in Iran carried out by Shakib *et al.*, (2018), 70 *K. pneumoniae* isolates collected from different clinical sources, demonstrated that the incidence of K2 serotype gene among these isolates was 0.0% (Shakib *et al.*, 2018). In another study in Iran, the frequency of K1, K2 and non-K1/K2 serotypes was 10.77%, 6.15%, 83.07%, respectively (Akbari *et al.*, 2017). In the current research, approximately 25% of the isolates carried the K1 or K2 or K1/K2 serotype genes, which gives an indication that these isolates are more virulent than other isolates.

Outcomes of this research showed that the prevalence of *magA* gene was 0.0% among *K. pneumoniae* isolates recovered from different sources. This result was in contrast to other studies which showed that the prevalence of this gene ranged from 1.4%-98% (Fang *et al.*, 2004; Struve *et al.*, 2005; Zamani *et al.*, 2013; Nahavandinejad and Asadpour, 2017; Shakib *et al.*, 2018; Thonda and Oluduro, 2018). The presence of *magA* gene in clinical isolates of *K. pneumoniae* plays an important role in serious infections such as septicemia, bacteremia, and pneumonia as well as lung and liver abscesses (Chung *et al.*, 2007), HMV, protecting the pathogen from phagocyte and serum bactericidal activity (Lee *et al.*, 2006). This gene is considered as a diagnostic marker of invasive *K. pneumoniae* strains. Numerous studies have shown that *magA* is more prevalent among K1 serotype strains (Struve *et al.*, 2005; Yu *et al.*, 2006; Lin *et al.*, 2006; Abdul-Razzaq *et al.*, 2014). This may be due to that this gene is

located in *cps* gene cluster K1 of *K. pneumoniae* (Yu *et al.*, 2006; Hsueh *et al.*, 2013).

Results of the current study showed that the frequency of *p-rmpA*, *c-rmpA*, *p-rmpA2* with the prevalence of (12.1%), (7.6%) and (15.2%) respectively. Most *p-rmpA*, *c-rmpA* and *p-rmpA2* genes are detected in non K1/K2 isolates. This result is consistent with a previously published study (Abdul-Razzaq *et al.*, 2014), which showed that *rmpA* genes were more prevalent in non K1/K2 serotype isolates. Results of our study were in contrast to previously published report (Al-Jailawi *et al.*, 2014), which showed that *rmpA* genes were more prevalent in serotype K2. In this study, the frequency of *rmpA* genes among isolates was 28.8%, while the frequency of these genes in literature ranged from 15%-46.2% (Lee *et al.*, 2010; Al-Jailawi *et al.*, 2014; Nahavandinejad and Asadpour, 2017; Thonda and Oluduro, 2018). The *rmpA* genes are plasmid or chromosomal-mediated (*prmpA* or *crmpA*), which confers highly enhanced mucoviscous phenotype and participates in neutrophilic phagocytosis resistance (Yeh *et al.*, 2007; Ko *et al.*, 2017). The coexistence of *magA* and the *rmpA* or *rmpA2* genes in the *K. pneumoniae* isolates increased the occurrence of expression of the HMV phenotype in these isolates (Lee *et al.*, 2010). In addition, it was shown that *rmpA*⁺ extended-spectrum β -lactamases (ESBL-) *K. pneumoniae* strains had greater pathogenic potential than *rmpA*⁻ ESBL-K. pneumoniae and non-ESBL-K. pneumoniae strains (Lin *et al.*, 2016).

It is important to note that genes encoding *rmpA*, K1, or K2 were highly associated with the hypervirulent variant of *K. pneumoniae* (Ferreira *et al.*, 2019), which can cause serious community acquired infection. In this study, 3 (4.5%) strains were identified as probable hypervirulent *K. pneumoniae*. These strains carried *cps*, K1, K2, *c-rmpA* (n=2) and *cps*, K1, *p-rmpA2* (n=1). All these probable hypervirulent strains were MDR. This result is consistent with a recent report from Egypt, which showed that 6.2% strains were identified as probable hypervirulent *K. pneumoniae* (EL-Mahdy *et al.*, 2018). However, this result was in contrast to another study from Brazil, which showed that there was no strains with molecular characteristics of the hypervirulent *K. pneumoniae* (Ferreira *et al.*, 2019).

According to the results obtained in this study, approximately 25% of isolates were found to be positive for either K1 serotype or K2 serotype or both K1 and K2 serotype genes. In addition, the presence of *rmpA* genes in these isolates gave an indication that some of these isolates may be more highly virulent than others. The presence of these virulence factors accompanied by high level of drug resistance should make bacteria a highly infectious agent and lead to failure of treatment. This study explained the significance and the value of rapid diagnosis and proper treatment of infections caused by *K. pneumoniae* in order to achieve prevention of complicated infections.

Acknowledgment

The authors are grateful to Prof. Saleh A. Naser, University of Central Florida, College of Medicine, for language revision.

References

- Abdul Razzaq MS, Trad JK and Khair-Alla Al-Maamory EH. 2013. Genotyping and detection of some virulence genes of *Klebsiella pneumoniae* isolated from clinical cases. *Med J Babylon*, **10**(2): 387-399.
- Abdul-Razzaq MS, Al-Khafaji JKT and Al-Maamory EHK. 2014. Molecular characterization of capsular polysaccharide genes of *Klebsiella pneumoniae* in Iraq. *Int J Curr Microbiol App Sci*, **3**(7): 224-234.
- Adwan G and Abu Jaber A. 2016a. Frequency and molecular characterization of β -lactamases producing *Escherichia coli* isolated from North of Palestine. *Br Microbiol Res J*, **11**(5): 1-13, Article no.BMRJ.22631.
- Adwan G, Abu Hasan N, Sabra I, Sabra D, Al-butmah S, Odeh S, Abd Albake Z and Badran H. 2016b. Detection of bacterial pathogens in surgical site infections and their antibiotic sensitivity profile. *Int J Med Res Health Sci*, **5**(5): 75-82.
- Adwan G, Adwan K, Jarrar N and Salameh Y. 2013. Prevalence of *seg*, *seh* and *sei* genes among clinical and nasal swab of *Staphylococcus aureus* isolates. *Br Microbiol Res J*, **3**(2): 139-149.
- Adwan K, Jarrar N, Abu-Hijleh A, Adwan G and Awwad E. 2014. Molecular characterization of *Escherichia coli* isolates from patients with urinary tract infections in Palestine. *J Med Microbiol*, **63**: 229-234.
- Akbari R and Asadpour L. 2017. Identification of capsular serotypes K1 and K2 in clinical isolates of *Klebsiella pneumoniae* in North of Iran. *Med Lab J*, **11**(1): 36-39.
- Al-Jailawi MH, Zedan TH and Jassim KA. 2014. Multiplex-PCR assay for identification of *Klebsiella pneumoniae*. *Int J Pharm Sci Rev Res*, **26**(1): 112-117.
- Brisse S, Issenhuth-Jeanjean S and Grimont PAD. 2004. Molecular serotyping of *Klebsiella* species isolates by restriction of the amplified capsular antigen gene cluster. *J Clin Microbiol*, **42**: 3388-3398.
- Cheng HY, Chen YS, Wu CY, Chang HY, Lai YC and Peng HL. 2010. *RmpA* regulation of capsular polysaccharide biosynthesis in *Klebsiella pneumoniae* CG43. *J Bacteriol*, **192**(12): 3144-3158.
- Chung DR, Lee HR, Lee SS, Kim SW, Chang HH, Jung SI, Oh MD, Ko KS, Kang CI, Peck KR and Song JH. 2008. Evidence for Clonal Dissemination of the Serotype K1 *Klebsiella pneumoniae* Strain Causing Invasive Liver Abscesses in Korea. *J Clin Microbiol*, **46**(12): 4061-4063.
- Chung DR, Lee SS, Lee HR, Kim HB, Choi HJ, Eom JS, Kim JS, Choi YH, Lee JS, Chung MH, Kim YS, Lee H, Lee MS and Park CK. 2007. Emerging invasive liver abscess caused by K1 serotype *Klebsiella pneumoniae* in Korea. *J Infect*, **54**: 578-583.
- Clinical and Laboratory Standards Institute (CLSI). 2017. Performance standards for antimicrobial susceptibility testing. 27th ed. CLSI supplement. M100. Wayne, PA, USA.
- Cubero M, Grau I, Tubau F, Pallarés R, Dominguez MA, Linares J and Ardanuy C. 2016. Hypervirulent *Klebsiella pneumoniae* clones causing bacteraemia in adults in a teaching hospital in Barcelona, Spain (2007-2013). *Clin Microbiol Infect*, **22**: 154-160.
- Doud M, Zeppegno R, Molina E, Miller N, Balachandar D, Schnepfer L, Poppiti R and Mathee K. 2009. A k2A-positive *Klebsiella pneumoniae* causes liver and brain abscess in a Saint Kitt's man. *Int J Med Sci*, **6**(6): 301-304.
- El-Mahdy R, El-Kannishy G and Salama H. 2018. Hypervirulent *Klebsiella pneumoniae* as a hospital-acquired pathogen in the intensive care unit in Mansoura, Egypt. *Germes*, **8**(3): 140-146.
- Fang CT, Chuang YP, Shun CT, Chang SC and Wang JT. 2004. A novel virulence gene in *Klebsiella pneumoniae* strains causing primary liver abscess and septic metastatic complications. *J Exp Med*, **199**(5): 697-705.
- Fang CT, Lai SY, Yi WC, Hsueh PR, Liu KL and Chang SC. 2007. *Klebsiella pneumoniae* genotype K1: An emerging pathogen that causes septic ocular or central nervous system complications from pyogenic liver abscess. *Clin Infect Dis*, **45**(3): 284-293.
- Feizabadi M M, Raji N and Delfani S. 2013. Identification of *Klebsiella pneumoniae* K1 and K2 capsular types by PCR and Quellung test. *Jundishapur J Microbiol*, **6**(9): e7585. doi: 10.5812/ijm.7585.
- Ferreira RL, da Silva BCM, Rezende GS, Nakamura-Silva R, Pitondo-Silva A, Campanini EB, Brito MCA, da Silva EML, Freire CCM, da Cunha AF and Pranchevicius MDS. 2019. High prevalence of multidrug-resistant *Klebsiella pneumoniae* harboring several virulence and β -lactamase encoding genes in a Brazilian intensive care unit. *Front Microbiol*. **9**: 3198. doi: 10.3389/fmicb.2018.03198.
- Hsueh K-L, Yu L-K, Chen Y-H, Cheug Y-H, Hsieh Y-C, Chu ke S-C, Hung K-W, Chen C-J and Huang T-H. 2013. Feoc from *K.pneumoniae* contains 4Fe -4s cluster. *J Bacteriol*, **195**: 4726-4734.
- Janda JM and Abbot SL. The Family *Enterobacteriaceae*. 2009. In: Goldman E and Green LH (Eds.), **Practical Handbook of Microbiology**. 2nd edition CRC Press, Taylor and Francis group, Boca Raton, FL, USA, p 853.
- Janda JM and Abbott SL. 2006. **The Genera *Klebsiella* and *Raoultella*, The Enterobacteria**. 2nd ed. ASM Press, Washington, USA, pp. 115-129
- Ko K. 2017. The contribution of capsule polysaccharide genes to virulence of *Klebsiella pneumoniae*. *Virulence*, **8**(5): 485-486.
- Lee CH, Liu JW, Su LH, Chien CC, Li CC and Yang KD. 2010. Hypermucoviscosity associated with *Klebsiella pneumoniae*-mediated invasive syndrome: a prospective cross-sectional study in Taiwan. *Int J Infect Dis*, **14**(8): e688-92. doi: 10.1016/j.ijid.2010.01.007.
- Lee HC, Chuang YC, Yu WL, Lee NY, Chang CM, Ko NY, Wang LR and Ko WC. 2006. Clinical implications of hypermucoviscosity phenotype in *Klebsiella pneumoniae* isolates: association with invasive syndrome in patients with community-acquired bacteraemia. *J Int Med*, **259**: 606-614.
- Lin HA, Huang YL, Yeh KM, Siu LK, Lin JC and Chang FY. 2016. Regulator of the mucoid phenotype A gene increases the virulent ability of extended-spectrum beta-lactamase-producing serotype non-K1/K2 *Klebsiella pneumoniae*. *J Microbiol Immunol Infect*, **49**(4): 494-501.
- Lin JC, Chang FY and Fung CP. 2004. High prevalence of phagocytic-resistant capsular serotypes of *Klebsiella pneumoniae* in liver abscess. *Microbes Infect*, **6**: 1191-1198.
- Lin TH, Huang SH, Wu CC, Liu HH, Jinn TR, Chen Y and Lin CT. 2013. Inhibition of *Klebsiella pneumoniae* growth and capsular polysaccharide biosynthesis by *Fructus mume*. *Evid Based Complement Alternat Med*, **2013**: 621701. doi: 10.1155/2013/621701.
- Lin WH, Tseng CC, Wu AB, Yang DC, Cheng SW, Wang MC and Wu JJ. 2015. Clinical and microbiological characteristics of peritoneal dialysis-related peritonitis caused by *Klebsiella pneumoniae* in southern Taiwan. *J Microbiol Immunol Infect*, **48**(3): 276-283.
- Lin YC, Chen TL, Chen HS, Wang FD and Liu CY. 2006. Clinical characteristics and risk factors for attributable mortality in *K. pneumoniae* bacteremia. *J Bacteriol*, **39**(1): 67-72.

- Liu C and Guo J. 2019. Hypervirulent *Klebsiella pneumoniae* (hypermucoviscous and aerobactin positive) infection over 6 years in the elderly in China: antimicrobial resistance patterns, molecular epidemiology and risk factor. *Ann Clin Microbiol Antimicrob*, **18**(1): 4. doi: 10.1186/s12941-018-0302-9.
- Liu YM, Li BB, Zhang YY, Zhang W, Shen H, Li H and Cao B. 2014. Clinical and molecular characteristics of emerging hypervirulent *Klebsiella pneumoniae* bloodstream infections in Mainland China. *Antimicrob Agents Chemother*, **58**(9): 5379-5385.
- Moghadas AJ, Kalantari F, Sarfi M, Soroush Shahhoseini S and Mirkalantari S. 2018. Evaluation of virulence factors and antibiotic resistance patterns in clinical urine isolates of *Klebsiella pneumoniae* in Semnan, Iran. *Jundishapur J Microbiol*, **11**(7): e63637. doi: 10.5812/jjm.63637.
- Nahavandinejad M and Asadpour L. 2017. Mucoviscosity determination and detection of *magA* and *rmpA* genes in clinical isolates of *Klebsiella pneumoniae* in Northern Iran. *Crescent J Med Biol Sci*, **4**: 104–107.
- Pan YJ, Lin TL, Chen CT, Chen YY, Hsieh PF, Hsu CR, Wu MC and Wang JT. 2015. Genetic analysis of capsular polysaccharide synthesis gene clusters in 79 capsular types of *Klebsiella* spp. *Sci Rep*, **5**: 15573. doi: 10.1038/srep15573.
- Ranjbar R, Fatahian Kelishadrokh A and Chehelgerdi M. 2019. Molecular characterization, serotypes and phenotypic and genotypic evaluation of antibiotic resistance of the *Klebsiella pneumoniae* strains isolated from different types of hospital-acquired infections. *Infect Drug Resist*, **12**: 603-611.
- Schembri MA, Blom J, Krogfelt KA and Klemm P. 2005. Capsule and fimbria interaction in *Klebsiella pneumoniae*. *Infect Immun*, **73**(8): 4626-4633.
- Shakib P, Kalani M, Ramazanzadeh R, Ahmadi A and Rouhi S. 2018. Molecular detection of virulence genes in *Klebsiella pneumoniae* clinical isolates from Kurdistan Province, Iran. *Biomed Res Ther*, **5**(8): 2581-2589.
- Struve C and Krogfelt KA. 2003. Role of capsule in *Klebsiella pneumoniae* virulence: lack of correlation between *in vitro* and *in vivo* studies. *FEMS Microbiol Lett*, **218**(1): 149-154.
- Struve C, Bojer M, Nielsen EM, Hansen DS and Krogfelt KA. 2005. Investigation of the putative virulence gene *magA* in a worldwide collection of 495 *Klebsiella* isolates: *magA* is restricted to the gene cluster of *Klebsiella pneumoniae* capsule serotype K1. *J Med Microbiol*, **54**(Pt 11): 1111-1113.
- Theophano PE, George AS, Leonidas ST and George LD. 2017. *Klebsiella pneumoniae*: virulence, biofilm and antimicrobial resistance. *Ped Infect Dis J*, **36**(10): 1002-1005.
- Thonda OA and Oluduro AO. 2018. Capsular typing and analysis of virulence genes of multidrug resistant *Klebsiella pneumoniae* and *Klebsiella oxytoca* from hospital-associated specimen in Nigeria. *Nat Sci*, **16**(3): 79-85.
- Vuotto C, Longo F, Pascolini C, Donelli G, Balice MP, Libori MF, Tiracchia V, Salvia A and Varaldo PE. 2017. Biofilm formation and antibiotic resistance in *Klebsiella pneumoniae* urinary strains. *J Appl Microbiol*, **123**(4): 1003-1018.
- Wasfi R, Elkhatib WF and Ashour HM. 2016. Molecular typing and virulence analysis of multidrug resistant *Klebsiella pneumoniae* clinical isolates recovered from Egyptian hospitals. *Sci Rep*, **6**: 38929. doi: 10.1038/srep38929.
- Yeh KM, Kurup A, Siu LK, Koh YL, Fung CP, Lin JC, Chen TL, Chang FY and Koh TH. 2007. Capsular serotype K1 or K2, rather than *magA* and *rmpA*, is a major virulence determinant for *Klebsiella pneumoniae* liver abscess in Singapore and Taiwan. *J Clin Microbiol*, **45**: 466-471.
- Yu WL, Ko WC, Cheng KC, Lee HC, Ke DS, Lee CC, Fung CP and Chuang YC. 2006. Association between *rmpA* and *magA* genes and clinical syndromes caused by *Klebsiella pneumoniae* in Taiwan. *Clin Infect Dis*, **42**: 1351-1358.
- Zamani A, Yousefi Mashouf R, Ebrahimzadeh Namvar A and Alikhani MY. 2013. Detection of *magA* gene in *Klebsiella* spp. isolated from clinical samples. *Iran J Basic Med Sci*, **16**: 173-176.
- Zhang S, Zhang X, Wu Q, Zheng X, Dong G, Fang R, Zhang Y, Cao J and Zhou T. 2019. Clinical, microbiological, and molecular epidemiological characteristics of *Klebsiella pneumoniae*-induced pyogenic liver abscess in southeastern China. *Antimicrob Resist Infect Control*, **8**: 166. doi: 10.1186/s13756-019-0615-2.

Prediction of Protein Secondary Structure from Amino Acid Sequences by Integrating Fuzzy, Random Forest and Feature Vector Methodologies

Sivagnanam R. Mani Sekhar^{1,2,*}, Siddesh G. Matt² and Sunilkumar S Manvi¹

¹School of Computing & Information Technology, Reva University, Bengaluru, Karnataka, ²Department of Information Science & Engineering, Ramaiah Institute of Technology, Bengaluru, India.

Received: October 17, 2019; Revised: November 27, 2019; Accepted: December 28, 2019

Abstract

The study of protein structure is an important research area in computational biology. Several algorithms have been used to predict the structure of the protein, but still it is a time consuming and challenging task as the dataset is increased day by day. The Proposed Work Enhanced Fuzzy Random Forest (EFRF) scrapes information from various websites allowing us to get class labels for our unsupervised data set. Afterward, Feature Vectors have been used to generate a transformed view of the protein sequences, which are then used as input to the proposed EFRF classifiers for prediction of secondary structure like alpha, Beta sheet, and Coil. Subsequently, Nave Bayers (NB), Support Vector Machine (SVM) classifiers have been used to compare and contrast precision and accuracy. The experiment shows that the proposed solution EFRF achieves an accuracy of 96% compared to the SVM 75 % and NB 41%.

Keywords: Protein, Machine learning, Protein secondary structure, Random forest, Fuzzy, Bioinformatics and Feature Vector.

1. Introduction

Proteins are the multifaceted and essential building blocks for living organisms. They show a vital role in the development of cell body, structure, and functions. Different Proteins are made up of different structures, resulting in unique functionality. They are made from peptide bonds and amino acids sequence. Amino acid is made up of the carboxylic and amino groups. They help in the formation of a peptide bond by releasing H₂O. Mainly, proteins are formed from twenty different amino acids, and each twenty amino acids have been represented by a Universal coding scheme. When each of these amino acids joins together, they form a chain called polypeptide chain. Out of twenty different amino acids, nine are marked as vital for the human body, as nine of these amino acids need to be taken as supplements. As drug development requires a particular knowledge of the binding sites of candidate compounds, a well-predicted structure helps in the computational screening and optimizing candidate compounds. Identifying the mechanism by which a protein functions and how it folds is of great curiosity for researchers and developers.

Prediction of protein function and structure is a challenging task in bioinformatics (Kumar, 2015). A suitable structure prediction mechanism helps the researcher in finding the essential functions. In the past, different computation techniques have been developed for prediction of primary, secondary, tertiary, and quaternary structure (Quan et al., 2016; Brender and Zhang, 2015; Carnevali et al., 2003; Lee et al., 1996; Mandal and Jana,

2012; Benítez and Lopes, 2010). While extracting protein secondary structure, selection of the right algorithm and feature extraction techniques are very important. Many statistical methods have been proposed, but their computation performance is not sufficient for huge and multifaceted biological datasets. Meanwhile, as the data size is increasing by date, still it is a challenging task for prediction of protein secondary structure, resulting in incessant growth of high throughput analytical model. However, identification of protein secondary structure helps in the understanding of protein tertiary structure and also offers perception of protein function.

Currently, researchers are working on Machine learning and template-based learning methodologies for structure prediction. A multi-classifier can perform quite better than the single classifier and allows it to handle a complex and huge dataset. Subsequently, extend its support in handling missing data and reducing noise level Bonissone et al.(2008a, 2008b).

Random Forest works on the principle of the decision tree. It is one of the most popular algorithms in bioinformatics, as it is comparatively easy to use and robust against imperfect records for experimental biological problems (Yang, 2010; Smolarczyk and Stapor, 2018; Cao et al., 2016; Jo and Cheng, 2014). In (Bankapur and patil, 2018), authors have used SXGbg and CE approaches for feature extraction. After successful retrieval of the essential features, the author has used different machine learning for classification like KNN, SVM, and RF for structure prediction. As sequence finding and resolution play an important role in protein structure, prediction author (Hu, et al., 2018) used loop with 2-15

* Corresponding author e-mail: manisekharsr@gmail.com.

amino acids and matrix score to cover more area for protein structure computation. (Li et al., 2011) has used RF algorithm for secondary structure prediction. They have developed a method called ProC_S3, working on an RR contact map, and with top 600 features. (Jai and Hu, 2011) Proposed a method for predicting β -hairpin motifs using the RF algorithm by incorporating several properties. Their result shows that RF performs better compared to other algorithms.

In proposed work author has presented a method called EFRF for the identification of protein secondary structure. The work focuses on the creation of multi-classifier by incorporating random forest (RF) technique (Breiman, 2001), subsequently feature vector has been generating. For inadequate values, random forest is constructed using fuzzy techniques. The integration of Random forest with fuzzy logic makes system more dynamic and helps in overcoming ambiguous data (Bonissone et al., 2010), but the accuracy of system also depends upon the selected features; if the selected features are not effective even the good algorithm can result in poor accuracy. In this work we have selected features which have direct correlation with 3D structure of the protein; later, these features are combined in a matrix to improve the efficiency of the vector.

This paper is organized as follows: section II provides a brief discuss about the different approaches used in protein structure prediction. In section III, a proposed EFRF methodology and its architecture for protein secondary structure are proposed and discussed. Section IV illustrates the implementation of the proposed work. Later, Dataset and achieved result are discussed in section V. Finally, section VI discusses the conclusion part.

2. Related Work

As evolutionary and syntactical based evidence is not adequate for extraction of valuable feature from the protein sequences, (Sudha et al., 2018) proposed an Enhanced Artificial Neural Network (ANN) for prediction of protein Structural Class and Fold Recognition. They have used physic chemical information and FCS technique for feature extraction by integrating FCS methodology. The result shows that Enhanced ANN performs well in RDD, EDD, TG, DD datasets. Here computation is based on the limited features. Performance can be further increased by introducing evolutionary and syntactical feature and also by latest feature extraction techniques.

A bio-inspired computing approach for prediction of protein secondary structure is presented in (Yavuz et al., 2018). Here the computation is performing in two different stages; in first stage, they used clonal selection algorithm (CSA) for data training. Later in the second stage, they used a deep learning technique called multilayer perceptron for classification. The result shows that dataset trained from CSA performs well. The proposed solution aims to improve by introducing fuzzy logic in classification.

(Hasic et al., 2017) uses a multi neural network method and consensus function for prediction of proteins secondary structure. These methods result in lowering the hypothesis space, which in turn helps in finding the best result. They have focused more on identifying and

prediction of alpha helices and beta sheets from the CB513 and 25PDB datasets. (Kathuria et al., 2018) uses a machine learning techniques for identification of unknown protein structures. They used Amide frequencies and RF classifier for prediction of protein secondary structure. The result shows that the model performs better in amides dataset. ROC curve and area have been used for validation of model. Multi classification techniques can be involved during secondary protein structure prediction to achieve more accuracy.

The work of (Zhang et al., 2016) used chaos game concept for prediction of protein secondary structure from the given sequence of proteins. The accuracy of structure is depending upon the likeness of protein data. This issue can lead to the unwanted structure prediction. They used a time series technique, feature vector of 36 dimension and CGR to overcome this issue. The prediction accuracy can be further increased by incorporating Random tree learning techniques.

3. Proposed Solution

Machine learning techniques have been universally used in Bioinformatics domain and other related areas. They provide a platform for developers in creation of automatically learning system with the capability of improvement from experience. Decision Tree is one of the most widely used analytic methods in Machine learning. Collection of Decision trees is known as a Random Forest. However, RF can work effectively when applied to large dataset, whereas they can be unstable when training value deals with small distribution. To overcome this issue, fuzzy logic has been incorporated in tree construction (Bonissone et al., 2010).

Steps followed in the proposed approach to predict secondary protein structure are as follows:

Step 1: Parallelized collection and analysis of data:

Protein Data is collected parallel and stored in local driver for structure prediction. Later cleaning and optimization procedure is applied by removing DNA and RNA from the stored dataset.

Step 2: Design and generation of feature vectors: This step illustrates the process of identification & selection of necessary features; subsequently it combines in a matrix to improve the efficiency of vector.

Step 3: Prediction of protein secondary structure using EFRF techniques: The classifier takes a vector as an input, subsequently integrating fuzzy concept and RF for protein structure prediction.

The steps given above are showed in Figure 1. Here data is extracted from protein data bank parallel. Later, the protein dataset is cleaned and analysis for efficient computation of the model. Subsequently, feature vector is computed from the given sequence data by incorporating 3 compositions, 3 to 15 transition values with the given frequency and protein length. Finally, the protein structure is predicted using proposed EFRF, SVM & NB.

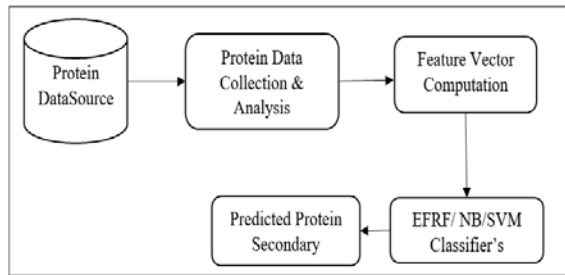


Figure 1. Proposed EFRF Architecture for protein structure prediction

3.1. Parallelized collection and analysis of data

Selenium is used for extracting protein data from websites by processing the HTML Web Page and extracting data for manipulation to a local storage. Once the protein sequences are stored locally, the application can run without an internet connection. Protein Data Banks contain millions of sequences and the whole process was parallelized using Java and multithreading to increase computational performance. The sequence data that is collected from the internet had a mix of protein and non-protein data (such as DNA and RNA) which was filtered and cleansed as per requirement. Figure 2, describes the Data preprocessing stages. Here the unstructured data is extracted from protein data bank, subsequently cleaned with required attributes using parallel computation and drives. Later Post processed data is stored in a local machine with features and labels.

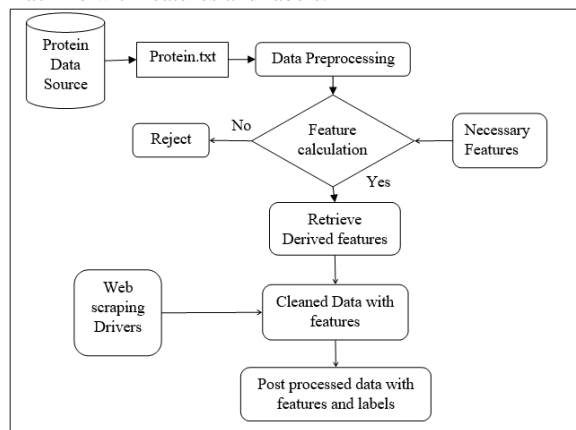


Figure 2. Proposed parallelized data proposing system design in EFRF

3.2. Design and Generation of feature vectors

Design and Development of Feature Vector is a measurable entity that is used to describe a feature of the objects. Selection of feature vectors is key factor in improving the performance of the predictor algorithm. For structure prediction, the features selected need to have direct correlation to the 3D structure of the protein. Here, four different features are selected for structure prediction: these are Hydrophobicity, Polarizability, Polarity and Van der Waals Volume. These features are combined in a matrix to improve the efficiency of the vector.

3.2.1. Generating Feature Vector:

The proposed work involves a single dimensional feature vector that is unique to each protein sequence. A vector of length 105 is generated for each protein sequence based on values of certain physical and chemical

properties. Here, sequence of protein is converted from a heterogeneous size to a feature vector of homogeneous size.

The twenty amino acids are segregated into three different categories based on their values corresponding to the properties. The physical and chemical properties taken into account are Hydrophobicity, Polarizability, Polarity, and Van Der Waals Volume. These 20 amino acids are categories into three clusters (Chinnasamy et al., 2005) corresponding to their values and properties, as shown in Table 1.

Table 1. Secondary structure classes attribute with corresponding classes

Attribute	Cluster 1	Cluster 2	Cluster 3
Class	Coil	Helix	Strand
Hydrophobicity	C, F, I, L, M, V, W	D, E, K, N, Q, R	A, G, H, P, S, T, Y
Polarizability	F, H, K, M, R, W, Y	A, C, D, G, P, S, T	E, I, L, N, V, Q
Polarity	D, E, H, K, N, Q, R	C, F, I, L, M, V, W, Y	A, G, S, T, P
Van der Waals Volume	F, H, K, M, R, W, Y	A, D, G, S, T	C, E, I, L, N, P, Q, V

The feature vectors 23 made up of separate individual feature vectors that are as follows:

Composition Feature Vector (Comp_i): The composition feature vector is computed as follows

$$\text{Comp}_i = (\text{Tg}_i / \text{SeqLen})100; \quad (1)$$

In equation 1, "Comp_i" represents the percent composition of each group, "Tg" tells group total and "SeqLen" denotes the sequence length

Transition Feature Vector (Trs_{ij}): Trs_{ij} shows the group occurrence percentage for group i to j for the value of one, two, and three.

Transition Feature Vector (Tij): Tij is characterized by the t frequency per cent with which group i is followed by group j or vice versa where i, j takes the values 1, 2 or 3 respectively.

Distribution Feature Vector (DFV): The DFV comprises five values from three groups that represent the sections of the given sequence value, also specify the first residue of a given group is located, and where other are located.

Percentage Frequency Feature Vector (PFFV): The PFFV defines the length as 20 and lists out the different percentage of these 20 amino acids in the given protein sequence data.

3.2.2 Calculations for Feature Vectors:

This section shows the computation of feature vector values based on their properties. A property can have 3 compositions, 3 to 15 transition values with the given frequency and protein length. The section below elucidates the calculation of the feature vector.

- 3 composition values with 4 properties: $3 \times 4 = 12$
- 3 transition values with 4 properties: $3 \times 4 = 12$
- 15 transition values with 4 properties: $15 \times 4 = 60$
- Percentage frequency of each amino acid: $20 \times 1 = 20$
- Length of protein: 1
- Feature Vector: $12 + 12 + 60 + 20 + 1 = 105$

3.3. Prediction of protein secondary structure using Enhanced Fuzzy Random Forest methodology

The proposed EFRF system architecture is shown in Figure 3; it illustrates the process of protein secondary structure prediction. The stored dataset is converted from amino acid sequence to feature vector by using selected features and feature vector algorithm. Subsequently in parallel, protein data is extracted in FASTA format with amino acid sequence & feature vector. Then, these optimized values are given as an input with required features. Afterwards, proposed EFRF, SVM, & NB classifiers are applied on it for protein secondary class prediction. The workflow of the system is a monolithic architecture. The data set comprises eight thousand cleansed sequences stored locally. The user interface takes a protein sequence as input and based on the feature vectors a scoring matrix is generated. Subsequently, the Feature Vector is used as input for the classifiers.

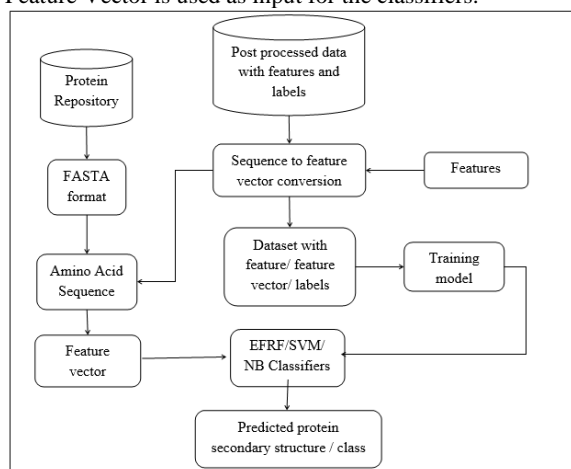


Figure 3. Proposed EFRF Data Post-Processing System Design for secondary structure prediction

(Jang, 1994; Janikow, 1998; K M Lee et al., 1999; Pulkkinen and Koivisto, 2008) illustrate the different methodologies in which fuzzy logic is combined positively with decision tree. According to RF (Breiman, 2001) progression of each node step by step and subsequently during the tree construction process each node will get split randomly with the available attributes. Finally, new process of split will perform based on random selection.

Fuzzy Random forest (FRF) (Bonissone et al., 2010) can be used for protein structure prediction; the proposed work uses fuzzy partition method for each inner node (INod) of the trees (Cadenas, Garrido and Martinez, 2009). $INod_1, INod_2, INod_3, \dots, INod_f$, are the state values generated from membership method (μ_{INodi}) as shown in equation 2. Here the construction of the tree size is a key point.

$$\forall x \in E \sum_{i=1}^{INodf} \mu_{INodi}(x) = 1 \quad (2)$$

According to (Bonissone, 2010; Chinnasamy, 2005) split of tree depends on numerical values and membership values ($\chi_{Tr, Nd}$); these values help in finding the tree (Tr) with node (Nd). The membership value helps in the splitting process of the tree (Tr). If the membership degree value is more than zero, the split will happen according to equation 3. Here 'CN' is represented as child node, 'Tr' is represented as tree

$$\chi_{(Tr, CN)}(\text{sample}) * \chi_{(Tr, node)}(\text{sample}) * \mu_{fuzz_set_prt}(\text{sample}) \quad (3)$$

Fuzzy random forest matrix (MFRF) 11 is used in classification problems; it classifies data to a given class and also generates the state of the node leaf (Le) and tree (Tr), subsequently also supporting in decision making 11 as shown in equation 4

$$\text{FuzzyAggre}(\text{class}_i, \text{MFRF}) = \sum_{tree=1}^{\text{Total tree}} \sum_{leaf_index=1}^{\text{no_of leafnode}} (MFRF)_{tree, leaf_index, class} \quad (4)$$

4. Implementation

In this work, two different classified NB (Robles et al., 2004) and SVM (Cortes and Vapnik, 1995; Cai et al. 2002) are compared with the proposed EFRF algorithm. The proposed model accepts primary protein sequences from the user; subsequently, Feature Vectors are generated from the entered sequence and then analyzed to predict class labels for each entered sequence. The protein sequences vary in length and can be categorized based on various physical and stereo chemical properties; these properties determine the feature vector generation. The attributes used to describe the sequence in the article include Polarity, Hydrophobicity, Polarizability and Van der Waals Volume.

The proposed EFRF model is categorized into three sub modules: *initial, intermediate and final modules*

Initial sub-Module: Initially used an unsupervised data set from the Protein Data bank which needed a lot of data preprocessing before actually using the data present in the data set. The data set contained about four hundred thousand sequences which were a mixture of DNA, RNA and Protein sequences. Firstly, extract the protein sequences from the data set since those records were the only meaningful records for this project. The other parameters were Sequence ID, Sequence Type, Sequence Length, Sequence Name and the Primary Sequence itself. This model requires the Class Label, the Secondary Structure of Protein. This unsupervised dataset had to be converted into a supervised dataset.

Intermediate Sub-Module: It displayed the results of the sequence with their frequency percentages. The percentage in the output is responsible for categorizing them into the final secondary structure.

The dataset (PDB) used had about eight thousand protein sequences to handle. So, this manual process took around two hours for two hundred sequences. Further, Selenium driver is used for web scraping. This allowed us to automate the retrieval process and increase efficiency of the conversion. The total time it took to retrieve and analyze all the sequence and to create a class label for each and every sequence out of the eight thousand protein sequences was about seven hours. Since this was not optimal performance, we converted the script so as to run on six different threads on six different Google Chrome tabs so as to achieve parallelization. The whole retrieval and data aggregation process took about two hours.

Final Module: After the conversion of the unsupervised dataset into a supervised data set, three classifiers namely NB, SVM and EFRF were used for predicting the secondary structure of protein. These classifiers are operating extremely differently from each other.

The attributes sent to these classifiers were the feature vectors and the class label with the classifiers for prediction. These classifiers take up to 75% of the dataset for training, and the rest for testing to provide an insight of how accurate the predictions turn out to be. Here, Feature Vector is used to create a Vector having consistent values to the chemical properties of the protein sequence. Algorithm 1 focuses on overall protein secondary structure prediction; the algorithm takes protein primary sequence as an input and generates corresponding protein secondary structure. Lines 2 to 4 compute the necessary feature vector score by incorporating secondary structure attributes as shown in algorithm 2. Finally, feature vector score is input to the classifier for protein secondary prediction as shown in line 5 to 7.

Algorithm 1: Proposed EFRF with Feature Vector Scoring

```

Input: Primary Protein Sequence
Output: Protein secondary structure
1. begin
2.     Compute feature vector score
3.         Apply Algorithm 2
4.     return vector score
5.     Generate protein secondary structure
6.         Apply Algorithm 3
7.     return protein class
8. end

```

Algorithm 2 shows the proposed Feature Vector Scoring process. The algorithm takes Protein sequence as an input and subsequently computes Composition, Transition and distribution values are as shown in line number 2 to 7. Line 8 computes the frequency of the given sequence of each array. Finally, line 12 to 14 computes the vector score for the given sequence of array. Similarly, the process is applied to the different amino acid sequences.

Algorithm 2: Proposed Feature Vector Scoring process

```

Input: Primary Protein Sequence
Output: A vector score for the Sequence
1. Procedure find Feature Vector (sequenceSQ)
2. begin
3.     for each property do
4.         divideAA --> 3Groups
5.         calcComposition(SQ) --> return compArr
6.         calcTransition(SQ) --> return transArr
7.         calcDistribution(SQ) --> return distArr
8.     for each AA do
9.         calc frequencyof AAinSQ
10.    return PFarr
11.    for each in array do
12.        fv[]+ = array
13.        return fv
14.    end
15. end

```

Algorithm 3 discusses the procedure for protein structure prediction such as Helix, Coil and strand class. Here features vector is given as an input; subsequently for the corresponding feature vector and protein sequence a necessary structure will be predicted. Line 1 focuses on the calling part of the training model for protein class prediction; subsequently random features is selected in line 3. Next, line 4 stores the node split values to a variable called "d". Later, line 6 performs the node split using fuzzy; afterwards, line 8 builds a RF using fuzzy concept, consequently predicting the class using training model. The predicted Helix, Coil, & Strand is stored in a target as

shown in line 9. Further, for each outcome of the random tree, vote is calculated as show in line 11. Finally lines 12 to 17 compute the votes for each attributes resulting in protein structure prediction.

Algorithm 3: Enhanced Fuzzy Random Forest

```

Input: Feature Vector of size 1 x 105
Output: Predicted Protein Structure
1. TrainingModel ()
2. begin
3.     k =RandomSelectFeatures() (From m features, k << m)
4.     d = FuzzyBestSplit(k)
5.     i = 0
6.     while ((i < n) && (n != 1)) do
7.         d = FuzzyBestSplit(d)
8.         BuildFuzzyForest(d, i)
9.         PredictionFromTrainedModel()
10.        targetOutcome[n] =
RandomDecisionTree(k) {AlphaHelix, RandomCoil,
    EtendedStrand}
11.        votes[m] ==>
CalculateVotes(targetOutcome[i]){i = 0, 1, n =size}{m <<
n}
12.        max = 0
13.        i = 0
14.        while (i < n) do
15.            if (max < votes[j] {j = 0, 1, ..m})
16.                max = votes[j]
17.        return max
18. end

```

5. Results and Discussions

5.1. Dataset

A sample dataset of protein sequence extracted from the protein data bank (PDB) is shown in Figure 4. The dataset is split into three parts: Initial Dataset, Intermediate Supervised Dataset, and Supervised Dataset. The section below illustrates the step by step process of data conversion.

5.1.1. Initial Dataset

This data is directly obtained from the data bank. It requires preprocessing in order to be useful in sequence prediction. The files "pdbseq.res.txt" and "pdbNS.txt" focus on the necessary sequences after removing RNA and DNA sequences.

```

>101m_A mol:protein length:154 MYOGLOBIN
MVLSEGENQLVHLVWAKVEADVAGHGQDILIRLFKSHPETLEKFDVRFKHLKTEAMKASEDLKKHGVT
>1021_A mol:protein length:165 T4 LYSOZYME
MNIIFEMLRIDEGLRLKIYKDTEGYTTIGIGHLLTKSPSLNAAKSELDKAIGRNTNGVITKDEAEKLF
>102m_A mol:protein length:154 MYOGLOBIN
MVLSEGENQLVHLVWAKVEADVAGHGQDILIRLFKSHPETLEKFDVRFKHLKTEAMKASEDLKKAGVT
>1031_A mol:protein length:167 T4 LYSOZYME
MNIIFEMLRIDEGLRLKIYKDTEGYTTIGIGHLLTKSPSLNSLDAKSELDKAIGRNTNGVITKDEAEK
>103m_A mol:protein length:154 MYOGLOBIN
MVLSEGENQLVHLVWAKVEADVAGHGQDILIRLFKSHPETLEKFDVRFKHLKTEAMKASEDLKKAGVT
>1041_A mol:protein length:166 T4 LYSOZYME
MNIIFEMLRIDEGLRLKIYKDTEGYTTIGIGHLLTKSPSLNAAKSELDKAIGRNTNGVITKDEAEK
>1041_B mol:protein length:166 T4 LYSOZYME

```

Figure 4. Sample Protein dataset from PDB (Protein Data Bank)

pdb seqres.txt: It contains the following information: Protein Sequence ID, Class, Molecule Type, Protein, Length of the sequence, Name of the sequence, Primary Protein Sequence as displayed in figure 5.

```
101m_A mol: protein length: 154 MYOGLOBIN
MVLSEGEWQLVLHVWAKVEADVAGHGQDILIRLFKSHPETLEKFDVRVKHLK
TEAMKASEDLKKHGVTVTALGAILKKKGHHEAELKPLAQSHATKHKIPIK
YLEFISEAIIHVLHSRHPGNFGADAQGAMNKALELFRKDIAAKYKELGYQG
```

Figure 5. pdb sequence.txt file

Useful attributes: Protein Sequence ID, Type, Primary Protein Sequence

Cleansed Dataset : Considers only Protein Sequence after discarding RNA and DNA sequences from the data bank.

pdb NS.txt: It contains the following information: Name of the sequence, Primary Protein Sequence as showed in figure 6.

```
MYOGLOBIN
MVLSEGEWQLVLHVWAKVEADVAGHGQDILIRLFKSHPETLEKFDVRVKHLKTE
AEMKASEDLKKHGVTVTALGAILKKKGHHEAELKPLAQSHATKHKIPIKYLEFI
SEAIHVLHSRHPGNFGADAQGAMNKALELFRKDIAAKYKELGYQG
```

Figure 6. Sample pdb NS.txt file

5.1.2. Intermediate Supervised Dataset:

Intermediate dataset is an unsupervised dataset obtained directly from the Protein Data Bank. It does not have a class label for the sequence of amino acids and various other parameters as shown in "contenttest.txt" file.

ContentTest.txt : It contains the following information: Name of the sequence, Primary Protein Sequence, Class Label (Secondary Structure Prediction), Percentage of the Secondary Structure Percentage in the Sequence as displayed in figure 7.

```
MYOGLOBIN
MVLSEGEWQLVLHVWAKVEADVAGHGQDILIRLFKSHPETLEKFDVRVKHLKTE
AEMKASEDLKKHGVTVTALGAILKKKGHHEAELKPLAQSHATKHKIPIKYLEFI
SEAIHVLHSRHPGNFGADAQGAMNKALELFRKDIAAKYKELGYQG
Alpha helix: 75.32
```

Figure 7. Sample ContentTest.txt file

5.1.3. Supervised Dataset:

The supervised dataset has been created by web scraping from enter here the website from where we scraped and the class label obtained is used as the class label for the amino acid sequence which along with the sequence length forms our supervised dataset. As shown in "contentTest.csv" file.

ContentTest.csv : It contains the following information: Name of the sequence, Primary Structure Sequence, Class Label (Secondary Structure Prediction) as presented in figure 8.

```
MYOGLOBIN,MVLSEGEWQLVLHVWAKVEADVAGHGQDILIRLFKSHPETLEKFD
VKHLKTEAE
MKASEDLKKHGVTVTALGAILKKKGHHEAELKPLAQSHATKHKIPIKYLEFISEAII
HVLHSRHPGNFGADAQGAMNKALELFRKDIAAKYKELGYQG, Alpha helix
```

Figure 8. Sample ContentTest.csv file

5.2. Feature Vector Input

The feature vector of length 105 is constructed by taking into the properties of the amino acid sequence which includes Hydrophobicity, Polarity, Polarizability and Van Der Waals Volume. Individual Composition, Transition and Distribution values for each of the properties are generated and together with the sequence length and percentage frequency of each amino acid are combined to constitute the feature vector. An array of floating point values that are fed as attributes to the classifiers are displayed in Figure 9.

```
[0.25609756, 0.42682928, 0.31707317, 0.40243903, 0.34146342, 0.25609756,
0.37804878, 0.3292683, 0.29268292,..., 0.085365854, 0.085365854, 0.0121951215,
0.0121951215, 0.024390243, 82.0]
```

Figure 9. An array of floating point values

Now the sequence, after validation, is converted into a vector which consists of floating point values. This vector is called a feature vector. The feature vector is then provided as input to the classifiers for prediction purposes. The use of Feature Vector is to generate a Vector containing corresponding values to the chemical properties of the protein sequence.

5.3. Classifier's for prediction of protein secondary structure

In this work, authors use three different classifiers for prediction of protein secondary structure. Initially, NB (Chinnasamy et al., 2005) classifier is used for structures prediction, as it performs well in multi class environment. Subsequently, as the dataset contains large dimension feature vector; authors have also used a SVM (Cortes and Vapnik, 1995; Cai, 2002) for prediction of structures. Finally, the proposed model EFRF is integrated using Fuzzy concept, RF and Feature vector concepts for prediction of protein structures. This section focuses on the accuracy measures, precision measures and Normalized Confusion Matrix for Proposed EFRF, SVM & NB.

5.3.1. Accuracy-Measures for Proposed EFRF, SVM & NB

Figure 10 & Figure 11 shows the two graphs generated from the dataset with splits of 60% of the dataset used for training in the first case and 75% of the dataset used for training in the other case. The Accuracy of NB classifier varies within the range size of approximate 0.27 with the variation in the size of datasets from 1000 to 8000. The observed variations are against the expected behavior that the increase in size of training dataset should lead to increase in accuracy. This concludes that our Feature Vector does not work well for the NB Classifier.

The Accuracy of SVM varies within range size of 0.02 with the variation in the size of dataset. This behavior is

parallel to the expected behavior as accuracy increases with the increase in size of dataset. Although there may be a slight decrease in the values of accuracy with the increase in the dataset size, this may be neglected due to the reason that this small variation can sometimes occur as a result of overfitting. Overall, the classifier has a good accuracy of 76%. Thus, SVM is a suitable classifier for the feature vector.

The Accuracy of proposed EFRF varies within range size of 0.03 with the variation in the size of dataset. The graphs show almost a linear relationship. This behavior sharply coincides with our expected behavior as accuracy increases with the increase in size of dataset. As a result, the classifier does an excellent work in predicting all the three structures. Overall, the classifier has a good accuracy of 96%. Thus, EFRF is the most suitable classifier for the feature vector.

Table 2 and figure 10 show the dataset of size 1000, 2000, 3000,4000, 5000, 6000, 7000, 8000 with 60:40 data split proposed EFRF give an accuracy of 92.9%, 95.2%, 94.4%,95.0%,95.0%, 96.5%, 95.7%, 95.5% whereas SVM give an accuracy of 77.3%, 76.9%, 75.8%, 75.5%, 78.0%, 77.6%, 76.0%, 75.8% and NB gives an accuracy of 77.5%, 49.8%, 48.5%, 45.1%, 45.3%, 46.5%, 46.5%, 41.8%. The result show that proposed EFRF perform better compare to other algorithms.

Table 2. Accuracy-Measure: Comparative Results among SVM, NB & the proposed methods EFRF with 60:40 Data split.

Dataset size	Enhanced Fuzzy		
	Random Forest (EFRF)	Support Vector machine (SVM)	Naïve Baye's (NB)
1000	93	77.3	77.5
2000	95	76.9	49.8
3000	94.4	75.8	48.5
4000	95.1	75.5	45.1
5000	95	78	45.3
6000	96.5	77.6	46.5
7000	95.7	76	46.5
8000	95.5	75.8	41.8

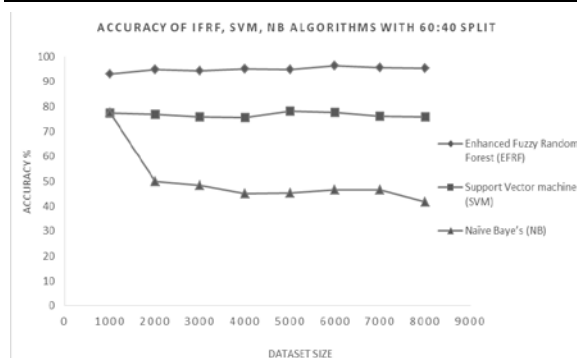


Figure 10. Graph with Accuracy-Measure: Outcomes Among SVM, NB & proposed methods EFRF with 60:40 Data split.

Similarly, table 3 and figure 11 illustrate the dataset of size 1000, 2000, 3000,4000, 5000, 6000, 7000, 8000 with 75:25 data split the proposed EFRF give an accuracy of 92.9%, 96.0%, 97.0%, 96.1%, 96.8%, 96.2%, 96.1%, 96.2% whereas SVM give an accuracy of 76.0%, 78.8%, 75.3%, 76.7%, 77.5%, 78.0%, 75.5%, 75.3% and finally NB gives an accuracy of 74.8%, 49.0%, 44.1%, 42.6%, 45.4%, 49.9%, 49.0%, 41.5%. The result show that proposed EFRF performs better compare to other algorithms.

Table 3. Accuracy-Measure: Comparative Results among SVM, NB & proposed methods EFRF with 75:25 Data split.

Dataset size	Enhanced Fuzzy		
	Random Forest (EFRF)	Support Vector machine (SVM)	Naïve Baye's (NB)
1000	92.8	76	74.8
2000	96	78.8	49
3000	96.9	75.3	44.1
4000	96.1	76.7	42.6
5000	96.8	77.5	45.4
6000	96.2	78	49.9
7000	96.2	75.5	49
8000	96.3	75.3	41.5

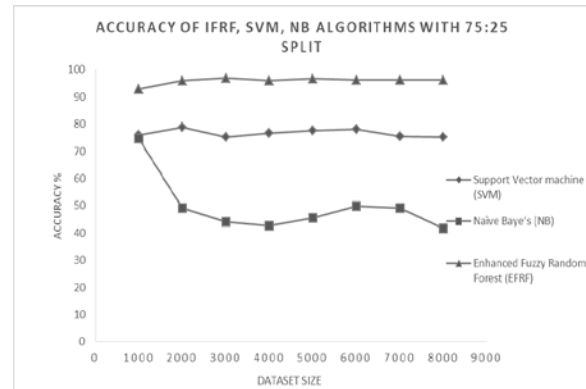


Figure 11. Graph with Accuracy-Measure: Outcomes Among SVM, NB & proposed methods EFRF with 75:25 Data split.

The section 5.3.1 provides a brief discussion on how the accuracy and results varied across the classifiers. In this NB, classifier yielded an accuracy of approximately 47%. This low accuracy is the consequence of poor prediction of sequences which are Random Coil. In order to find a better classifier which suits the given feature vector, SVM is incorporated. SVM produced an overall accuracy of 78%, hence showing competence with our developed feature vector. But still, the classifier fails when predicting the structure of most of the Alpha Helix sequences. Finally, the EFRF classifier gives an excellent accuracy of 96% showing a strong capability of success with the Feature Vector.

5.3.2. Precision-Measures for Proposed EFRF, SVM & NB

The precision measures for the Proposed EFRF, SVM & NB are shown in table 4. The Precision value of the proposed EFRF system is 96.2% whereas for the SVM and NB is 72.9% & 41.5% for the dataset of size 8000. This shows that proposed EFRF performs well when compared with SVM & NB. Similarly, Table 4 and figure 12 illustrate the dataset of size 1000, 2000, 3000,4000, 5000, 6000, 7000, 8000 with 60:40 data split the proposed EFRF give a precision of 92.9%, 95.2%, 94.4%, 95%, 95%, 96.5%, 95.7%, 95.5% whereas SVM give a precision of 74.5%, 75.7%, 73%, 72.6%, 75.7%, 74.7%, 72.7%, 73.7% and later NB gives a precision of 77.5%, 49.8%, 48.5%, 45.1%, 45.3%, 46.5%, 46.5%, 41.8%. The result tells that proposed EFRF performs well compared to other algorithms.

Table 4. Precision -Measure: Comparative Results among SVM, NB & proposed methods EFRF with 60:40 Data split.

Dataset size	Enhanced Fuzzy Random Forest (EFRF)	Support Vector machine (SVM)	Naïve Baye's (NB)
1000	92.9	74.5	77.5
2000	95.2	75.7	49.8
3000	94.4	73	48.5
4000	95	72.6	45.1
5000	95	75.7	45.3
6000	96.5	74.7	46.5
7000	95.7	72.7	46.5
8000	95.5	73.7	41.8

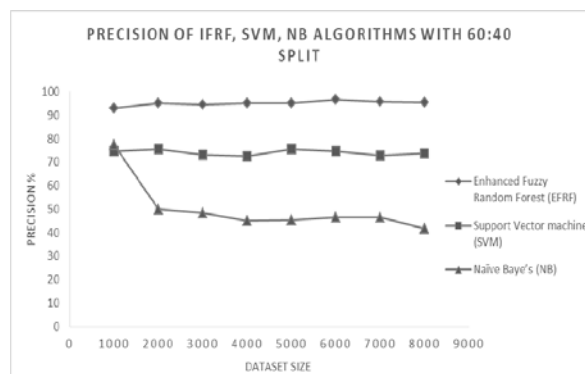


Figure 12. Graph with Precision -Measure: Outcomes Among SVM, NB & proposed methods EFRF with 60:40 Data split.

Table 5 and figure 13 discuss the dataset of size 1000, 2000, 3000, 4000, 5000, 6000, 7000, 8000 with 75:25 data split the proposed EFRF give a precision of 92.9%, 96%, 97%, 96.1%, 96.8%, 96.2%, 96.1%, 96.2, % whereas SVM give a precision of 73.8%, 78.3%, 72.9%, 74.2%, 75.1%, 75.8%, 71.9%, 72.9% and later NB gives a precision of 74.8%, 49%, 44.1%, 42.6%, 45.4%, 49.9%, 49%, 41.5%. The result tells that proposed EFRF performs well compared to other algorithms.

Table 5. Precision -Measure: Comparative Results Among SVM, NB & proposed methods EFRF with 75:25 Data split. Best Results Are Bolded Per Row

Dataset size	Enhanced Fuzzy Random Forest (EFRF)	Support Vector machine (SVM)	Naïve Baye's (NB)
1000	92.9	73.8	74.8
2000	96	78.3	49
3000	97	72.9	44.1
4000	96.1	74.2	42.6
5000	96.8	75.1	45.4
6000	96.2	75.8	49.9
7000	96.1	71.9	49
8000	96.2	72.9	41.5

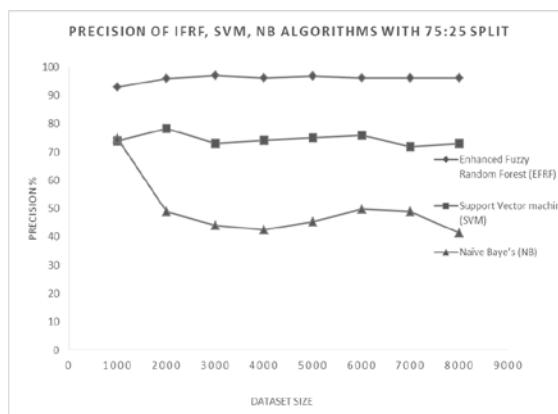


Figure 13. Graph with Precision -Measure: Outcomes among SVM, NB & the proposed methods EFRF with 75:25 Data split.

5.3.3. Normalized Confusion Matrix for Proposed EFRF, SVM & NB

The Confusion Matrix for the NB Classifier 25 with the predicted values normalized between 0 and 1 is shown in Figure 14. From the matrix, it can be concluded that the classifier does a good work in predicting 87% of Alpha helix structure correctly. Also, the classifiers performance in predicting the Extended Strand sequences correctly is above average at 69%. However, when it comes to predicting the Random Coil sequences, the classifier Performance is very bad with only 3 percent of the testing sequences predicted correctly.

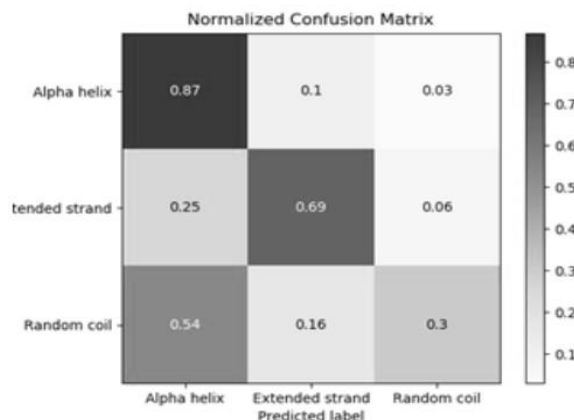


Figure 14. Normalized Confusion Matrix for Naive Bayes

SVM is very effective in cases when the number of dimensions is very large. The Confusion Matrix for the SVM Classifier with the predicted values normalized between 0 and 1 is shown in Figure 15. From the matrix, it can be analyzed that the classifier does an excellent work in predicting the structure of Extended Strand and Random Coil correctly for almost all the testing sequences. However, the performance of the classifier fails when it comes in predicting the structure of Alpha helix sequences. Consequently, only 28% of the testing sequences are predicted correctly as Alpha helix. With an overall accuracy of 76%, SVM was a good classifier for the feature vector.

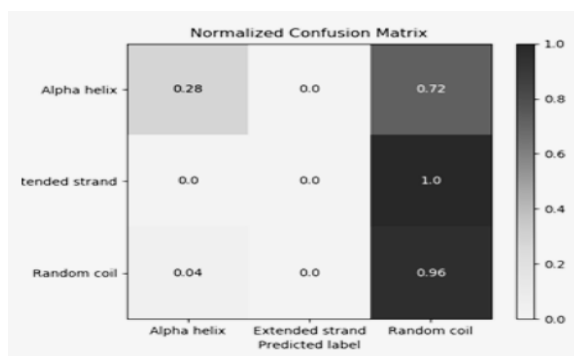


Figure 15. Normalized Confusion Matrix for Support Vector Machines

In the prospect for a better classifier to improve the accuracy, the proposed work EFRF integrates Fuzzy concept with RF Classifier. The Confusion Matrix for the EFRF Classifier with the predicted values normalized between 0 and 1 is shown in Figure 16. From the confusion matrix, it can be inferred that the classifier does an excellent work in correctly predicting all the three structures for almost all the testing sequences.

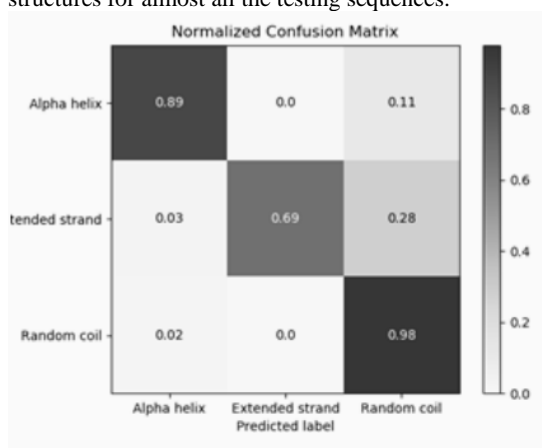


Figure 16. Normalized Confusion Matrix for Enhanced Fuzzy Random Forest

5.4. Evaluation of models

There are different measures used in the validation of predicted values. The section below discusses the performance measure using Root Mean squared error, and Correlation.

Root Mean squared error (RMSE): RMSE is used to compute the error rate of a model. It calculates the difference between expected result (ER) and observed result (OR) with its square root of the same. RMSE computation process is showed in equation 5, here 'ER' expected result, 'OR' observed result and 'k' is the number of instance.

$$RMSE = \sqrt{\frac{\sum_{i=1}^k (OR_i - ER_i)^2}{k}} \quad (5)$$

Correlation: Correlation helps in computation of statistical relation between expected result (ER) and observed result (OR). Correlation computation process is shown in equation 6, here 'ER' expected result, 'OR' observed result and 'k' is the number of instance.

$$\text{Correlation} = \frac{\sum_{i=1}^k (ER_i - \text{Mean } ER_i)(OR_i - \text{Mean } OR_i)}{\sqrt{\sum_{i=1}^k (ER_i - \text{Mean } ER_i)^2 \sum_{i=1}^k (OR_i - \text{Mean } OR_i)^2}} \quad (6)$$

Table 6 shows the computed RMSE, correlation and predicted accuracy for the proposed model EFRF, NB and SVM. The result shows that EFRF outperform when compared with the NB and SVM for the value of RMSE and Correlation. Here the proposed EFRF model has the lowest RMSE value of 0.33 whereas for SVM is 0.99 and NB is 1.5. Similarly, EFRF has the highest correlation value of 0.95 whereas for SVM is 0.55 and NB is 0.38.

Table 6. Performance Measure among NB, SVM, & proposed method EFRF

Model	RMSE	Correlation	Accuracy %
Naïve Baye's (NB)	1.5	0.38	41.5
Support Vector Machine (SVM)	0.99	0.55	75.3
Enhanced Fuzzy Random Forest (EFRF)	0.33	0.95	96.3

6. Conclusion

The proposed work EFRF uses a Machine Learning model in prediction of the two-dimensional structures of the protein from their amino acid sequences. The model takes the primary protein sequence as input and outputs the structural class through which the protein folds. These can be used in various Drug developments, which in particular requires knowledge of the binding sites of the candidate compounds, a well-predicted structure helps in the computational screening and optimizing candidate compound. The unsupervised dataset to train our Machine Learning model is a linear chain of amino acids that forms the primary structure of the protein. The extracted information from various websites allows us to get class labels for our unsupervised data set. Subsequently generates a unique Feature Vectors for each protein sequence based on Polarity, Hydrophobicity, Polarizability, and Van der Waals Volume. Later, various classification models are used to analyze and predict class labels for each sequence. For the given dataset, NB classifier yielded an accuracy of approximately 47%. This low accuracy is the consequence of poor prediction of sequences, which are Random Coil. Whereas SVM produced an overall accuracy of 78%, hence shows competence with our developed feature vector. But still, the classifier fails when predicting the structure of most of the Alpha Helix sequences. Later, the proposed EFRF classifier gives an accuracy of 96%, showing a strong capability of success with the developed Feature Vector. Finally, the model is further validated using RMSE and correlation. The computed result shows that the EFRF model has the lowest RMSE value of 0.33, whereas for SVM is 0.99, and NB is 1.5. Similarly, EFRF has the highest correlation value of 0.95, whereas for SVM is 0.55, and NB is 0.38.

References

- Bankapur, S. and Patil, N., 2018, October. Protein Secondary Structural Class Prediction Using Effective Feature Modeling and Machine Learning Techniques. In 2018 IEEE 18th International Conference on Bioinformatics and Bioengineering (BIBE) (pp. 18-21). IEEE.
- Benítez C M V and Lopes H S. 2010. Protein structure prediction with the 3D-HP side-chain model using a master-slave parallel genetic algorithm. *Journal of the Brazilian Computer Society*, 16(1), 69-78.
- Bonissone P P, Cadenas J M, Garrido M C, and Diaz-Valladares R A. 2008b. Combination methods in a fuzzy random forest. In 2008 IEEE International Conference on Systems, Man and Cybernetics (pp. 1794-1799). IEEE.
- Bonissone P P, Cadenas J M, Garrido M C, and Diaz-Valladares R A. 2008a. A fuzzy random forest: Fundamental for design and construction. In *Proceedings of the 12th International Conference on Information Processing and Management of Uncertainty in Knowledge-Based Systems (IPMU'08)* (pp. 1231-1238).
- Bonissone P, Cadenas J M, Garrido M C, and Díaz-Valladares R A. 2010. A fuzzy random forest. *International Journal of Approximate Reasoning*, 51(7), 729-747.
- Breiman L. 2001. Random forests. *Machine learning*, 45(1), 5-32.
- Brender J R, and Zhang Y. 2015. Predicting the effect of mutations on protein-protein binding interactions through structure-based interface profiles. *PLoS computational biology*, 11(10), e1004494.
- Cadenas, J. M., Garrido, M. C., & Martinez, R. (2009). Una estrategia de particionamiento fuzzy basada en combinación de algoritmos. In *Proceedings in XIII Conferencia de la Asociación Española para la Inteligencia Artificial, Sevilla, Spain* (pp. 379-388).
- Cai Y D, Liu X J, Xu X B and Chou K C. 2002. Prediction of protein structural classes by support vector machines. *Computers & chemistry*, 26(3), 293-296.
- Cao, R., Jo, T. and Cheng, J., 2016. Evaluation of protein structural models using random forests. arXiv preprint arXiv:1602.04277.
- Carnevali P, Tóth G, Toubassi G, and Meshkat, S N. 2003. Fast protein structure prediction using Monte Carlo simulations with modal moves. *Journal of the American Chemical Society*, 125(47), 14244-14245.
- Chinnasamy A, Sung W K, and Mittal A. 2005. Protein structure and fold prediction using tree-augmented naive Bayesian classifier. *Journal of Bioinformatics and computational Biology*, 3(04), 803-819.
- Cortes C and Vapnik V. 1995. Support-vector networks. *Machine learning*, 20(3), 273-297.
- Hasic H, Buza E, and Akagic A. 2017. A hybrid method for prediction of protein secondary structure based on multiple artificial neural networks. In *2017 40th International Convention on Information and Communication Technology, Electronics and Microelectronics (MIPRO)* (pp. 1195-1200). IEEE.
- Hu, X.Z., Long, H.X., Ding, C.J., Gao, S.J. and Hou, R., 2018. Using random forest algorithm to predict super-secondary structure in proteins. *The Journal of Supercomputing*, pp.1-12.
- Jang J S. 1994. Structure determination in fuzzy modeling: a fuzzy CART approach. In *Proceedings of 1994 IEEE 3rd International Fuzzy Systems Conference* (pp. 480-485). IEEE.
- Janikow C Z. 1998. Fuzzy decision trees: issues and methods. *IEEE Transactions on Systems, Man, and Cybernetics, Part B (Cybernetics)*, 28(1), 1-14.
- Jia, S.C. and Hu, X.Z., 2011. Using random forest algorithm to predict β -hairpin motifs. *Protein and peptide letters*, 18(6), pp.609-617.
- Jo, T. and Cheng, J., 2014, December. Improving protein fold recognition by random forest. In *BMC bioinformatics* (Vol. 15, No. 11, p. S14). BioMed Central.
- Kathuria C, Mehrotra D, and Misra N K. 2018. Predicting the protein structure using random forest approach. *Procedia computer science*, 132, 1654-1662.
- Kumar M. 2015. An enhanced algorithm for multiple sequence alignment of protein sequences using genetic algorithm. *EXCLI journal*, 14, 1232.
- Lee B, Kurochkina N and Kang H S. 1996. Protein folding by a biased Monte Carlo procedure in the dihedral angle space. *The FASEB journal*, 10(1), 119-125.
- Lee K M, Lee K M, Lee J H and Lee-Kwang H. 1999. A fuzzy decision tree induction method for fuzzy data. In *FUZZ-IEEE'99. 1999 IEEE International Fuzzy Systems. Conference Proceedings (Cat. No. 99CH36315)* (Vol. 1, pp. 16-21). IEEE.
- Li, Y., Fang, Y. and Fang, J., 2011. Predicting residue-residue contacts using random forest models. *Bioinformatics*, 27(24), pp.3379-3384.
- Mandal S, and Jana N D. 2012. Protein structure prediction using 2D HP lattice model based on integer programming approach. In *Proceedings of 2012 International Congress on Informatics, Environment, Energy and Applications* (pp. 17-18).
- Protein Data bank (2018). Retrieved from: <https://pdb101.rcsb.org/learn/guide-to-understanding-pdb-data/primary-sequences-and-the-pdb-format>.
- Pulkkinen P, and Koivisto H. 2008. Fuzzy classifier identification using decision tree and multiobjective evolutionary algorithms. *International Journal of Approximate Reasoning*, 48(2), 526-543.
- Quan L, Lv Q, and Zhang Y. 2016. STRUM: structure-based prediction of protein stability changes upon single-point mutation. *Bioinformatics*, 32(19), 2936-2946.
- Robles V, Larrañaga P, Peña J M, Menasalvas E, Pérez M S, Herves V and Wasilewska A. 2004. Bayesian network multi-classifiers for protein secondary structure prediction. *Artificial Intelligence in Medicine*, 31(2), 117-136.
- Smolarczyk, T. and Stapor, K., 2018. Random Forest Classifier for Early-Stage Protein Structure Prediction. *Studia Informatica*, 39.
- Sudha P, Ramyachitra D, and Manikandan P. 2018. Enhanced artificial neural network for protein fold recognition and structural class prediction. *Gene Reports*, 12, 261-275.
- Yang, P., Hwa Yang, Y., B Zhou, B. and Y Zomaya, A., 2010. A review of ensemble methods in bioinformatics. *Current Bioinformatics*, 5(4), pp.296-308
- Yavuz B Ç, Yurtay N, and Ozkan O. 2018. Prediction of protein secondary structure with clonal selection algorithm and multilayer perceptron. *IEEE Access*, 6, 45256-45261.
- Zhang L, Kong L, Han X, and Lv J. 2016. Structural class prediction of protein using novel feature extraction method from chaos game representation of predicted secondary structure. *Journal of theoretical biology*, 400, 1-10.

Biogenic Silver Nanoparticle Synthesis, Characterization and its Antibacterial activity against Leather Deteriorates

Savita Kate^{1,*}, Madhuri Sahasrabudhe² and Archana Pethe³

¹Department of Biotechnology, Shivchhatrapati College, ²Department of Microbiology Maulana Azad College, Aurangabad-431001,

³Department of Microbiology, Shivaji College of Arts, Commerce and Science, Akola-444001, M.S., India

Received: October 26, 2019; Revised: December 25, 2019; Accepted: December 31, 2019

Abstract

Biogenic Silver Nanoparticles (AgNPs) were synthesized using aqueous plant extract of *Portulaca oleracea* L.(Portulacaceae) at 75°C in 20min. AgNPs were confirmed by UV-visible spectra. Highest absorbance peak was found at 420nm; FTIR showed the peaks at 515.24 cm⁻¹ with significant changes upon reduction, biogenic AgNPs. Dmean number was found to be 52.26 nm and zeta potential -29.1mV. AgNPs crystalline particle size was found in range of 28.8 nm to 30.08 nm by XRD. Scanning Electron Microscopy (SEM) analysis confirms AgNPs were spherical in shape. The biogenic synthesized AgNPs showed distinct zone of inhibition against all bacterial leather isolates ranging from 14.66±1 to 20.33±1.52 mm. Minimum inhibitory concentration (MIC) values of the biosynthesized silver nanoparticles against bacterial isolates ranged from 4-20 µg/ml. Experimental outcomes propose that the biogenic silver nanoparticles showed efficient antibacterial activity against leather deteriorates and can be used for preservation of leather.

Keywords: leather deteriorates, MIC, SEM, Zeta potential

1. Introduction

Nanotechnology is a recent field that is used in research nowadays, creating an impression in all domains of human life. Biogenic synthesis of nanoparticles has proven to be better methods over physical and chemical methods due to slower kinetics and their stabilization. There are multiple opportunities to develop greener processes for the manufacture of nanoparticles. Due to involvement of hazardous chemical, low material conversions, high energy requirement, and difficult, wasteful purification in physical and chemical methods, biosynthesis of silver nanoparticles using plant extract and microorganism has been practiced. The most predominant method for the synthesis of silver nanoparticles is using plant extract owing to easy availability, cost efficiency, eco-friendliness, and non-toxicity (Firdhouse et al., 2012). *Argimone mexicana*, *Tridax procumbens* L., *Jatropha curcas* L., *Calotropis gigantea* L., *Solanum melongena* L., *Datura metel* L., *Carica papaya* L. and *Citrus aurantium* L. leaf extracts were involved in green synthesis of silver nanoparticles, and evaluations of their antimicrobial activities were studied for *Aspergillus flavus*, *Escherichia coli* and *Pseudomonas aeruginosa* and were found to be highly effective ((Khandelwal et al.,2010; Rajasekharreddy et al.,2010). Plants extracts usually include various polyphenols, such as flavonoids, which act as the best reducing agent useful in the synthesis of silver nanoparticles. Luteolin or rosmarinic acid reducing substances are found in *Ocimum sanctum*, *Portulaca oleracea*. Reducing agents are most conceivably responsible for the conversion of Ag⁺ to Ag⁰ which occurs

during the formation of enol/keto form of those substances. The resulting forms revealed promising antibacterial properties against microorganism such as *Escherichia coli*, *Staphylococcus aureus* and *S. typhi*, *Proteus* spp. (Muthumary et al. 2011).

The leather is a richest source of nutrients for microorganisms. The fibrous proteins present in leather are collagen (98%), elastin (1%) and keratin (1%) (Tissier and Chensais, 2000). Leather making is an important socio-economic activity for several countries throughout the world and used everywhere in daily life. The decomposition of collagen, the major component of leather, has been studied more extensively. Raw hides deteriorated easily and their deterioration depends on a number of factors: time, temperature, moisture content, and the state of the hide. Collagenase activity by *Clostridium* spp., *Bacteriodes* spp., and *Staphylococcus aureus* had earlier been reported (Jaouadi et al. 2013). During the manufacture processes of finished leather from raw hide, the bacterial flora of leather was found to be changed. *Bacillus* spp. was the most prevalent, and was found in nearly all steps of the tanning process. Not surprisingly, *Bacillus* spp., especially *Bacillus cereus* and *Bacillus subtilis*, have been correlated with the majority of cases of deterioration of hides and skins (Baird, 1998). However, not much previous research has been done to inhibit growth of bacterial leather isolates (leather bacterial growth) using pure biogenic silver nanoparticles. Therefore, the present work was undertaken to study biogenic silver nanoparticles synthesis and its antibacterial effect against bacteria isolated indigenously from leather samples.

* Corresponding author e-mail: savitaakate@gmail.com.

2. Materials and Methods

2.1. Isolation and identification of bacteria:

In the present study deteriorated leather samples were collected from Kedar leather industry, Aurangabad, M.S. in sterilized polythene bags and were brought to the laboratory. Leather deteriorating bacteria were screened by inoculating collected deteriorated leather samples into peptone solution (1% peptone water) incubated at 37°C for 24h and isolation of bacteria was carried out on nutrient agar M002-Hi-Media (Mozotto et al. 2010). To check the ability of different leather isolates to hydrolyze main leather protein collagen, collagen agar plates (1% collagen peptide type I, TC343-Hi-Media and 2% agar Hi-Media) were used and incubated at 37°C for 48h. Bacterial leather isolates showing collagenolytic activity were screened with larger transparent circle around the bacterial colony after incubation by adding a drop of mercuric chloride precipitation reagent (Lili et al. 2010). As per Bergey's manual of systematic bacteriology second edition process, the bacterial leather isolates were identified. The isolates were further subjected for genetic analysis by 16s rDNA sequencing. The sequences obtained were deposited to GenBank for accession number.

2.2. Biogenic silver nanoparticles (AgNPs) synthesis

Portulaca oleracea L. aqueous extract (10%) was prepared by boiling fresh washed leaves in sterile distilled water for 10 mins then filtered through whatmann filter paper No.1. To 10 ml of silver nitrate solution (1mM) 1ml of aqueous extract of *Portulaca oleracea* L. was added then incubated at 75°C for various time intervals 20-35 min. The colour change from yellowish to reddish brown in the reaction mixture was confirmed biosynthesis of nanoparticles (Firdhouse et al., 2013; Mittal, 2012).

2.3. Characterization of Silver Nanoparticles

Characterization of synthesized biogenic silver Nanoparticles was carried out by Ultraviolet-visible spectrophotometry (Elico), Fourier transform infrared spectroscopy (FTIR) measurements (Bruker Corporation), Scanning electron microscopy (SEM), Nanoparticles size analysis, Zeta potential determination (Malvern Zetasizer Nano-ZS) and X-ray diffraction studies (XRD) (D8 advance Bruker axs) (Alzahrani et al., 2015; Khushboo Singh, 2014; Lilyprava Dash, 2013 and Sumitra Chanda, 2013).

2.4. Antibacterial activity of synthesized biogenic AgNPs

2.4.1. Agar well diffusion method

0.1 ml (O.D.₆₀₀ 1.0) of selected bacterial leather isolates was added in different soft agar and mixed well. Seeded soft agar was then plated on basal agar (Muller Hilton agar) plates. After 30 minutes of cooling incubation, inoculated plates were punched using cork borer for obtaining 6mm wells. In one well, 25µl of biogenic silver nanoparticles (0.1g/L) were added. These cultures were also tested against Streptomycin (300mcg), Chloramphenicol (25mcg), Fusidic acid (10mcg), Erythromycin (5mcg), Methicillin (10mcg) and Novobiocin (5mcg) discs (Hi media Pvt. Ltd., India). All inoculated plates were incubated at 37°C for 24h. Diameter of zone of inhibition was measured in mm; the

experiments were carried out in triplicates and mean values of zone diameter were determined (Bauer and Kirby, 1966; Awad et al., 2014).

2.5. Minimum inhibitory concentration (MIC) of biogenic silver Nanoparticles for bacteria:

In the present work, minimum inhibitory concentration was determined by standard broth dilution method (Sushmita Deb, 2014 and Zohresh Majidnia, 2012). The MIC was performed in 2ml Muller-Hinton broth (MH) using AgNPs in varying concentrations ranging from 1-10-20µg/ml in test tubes, while one was maintained as blank with AgNPs, not having bacterial suspension (negative control) and second tube having only bacterial suspension, not AgNPs. 0.5 MacFard standard bacterial inoculums were prepared in sterile saline which was equals 10⁶ Cfu/ml. The tubes were then incubated at 37°C for 24 h. After incubation, the MIC was determined by measuring the growth density of test organisms at 600nm on spectrophotometer (Sushmita Deb, 2014; Zohresh Majidnia et al., 2012). MIC is the lowest concentration of an antimicrobial that will inhibit the visible growth of a microorganism after overnight incubation.

2.6. Leather preservation:

Leather preservation was carried out using biogenic silver nanoparticles as per protocol mentioned by Petical (2013) with some modification. Leather samples with the control sample size of 1 × 2 cm² were sterilized using 70% ethanol for 20 minutes, then leather samples were washed for 30 min with sterile distilled water and were immersed three times in biogenic silver nanoparticles 0.1 g/L at 30°C for 1h, followed by free drying. Treated and untreated samples were exposed to leather isolates then kept in incubator and checked for the efficiency of biogenic AgNPs in the form of bacteria growth on samples.

3. Result and Discussion

3.1. Isolation, screening and identification of leather deteriorates

From collected fifty deteriorated leather samples, twenty seven bacteria were found to be hydrolyzing keratin, collagen (leather main protein), gelatin and casein at 37°C after 24-48h of incubation. Most proficient five bacterial leather isolates were further identified by morphological, biochemical, 16srDNA sequences (Om gene bio, Pune) submitted to GenBank with accession number: *Arthrobacter creatinolyticus* KJ009396, *Bacillus pumilus* KP015747 (H4.9/8), *Bacillus megaterium* KM369985 strain SAK, *Bacillus amyloliquefaciens* KP015745 (strain JS518) and *Bacillus cereus* KP015746 (Lr3/2). *Staphylococcus* sp. and *Brevibacterium* sp. *Pseudomonas* sp. and *Bacillus* sp. from some deteriorated footwear samples reported by Sanchez-Navarro (2013). *Bacillus subtilis*, *A. awamori*, *Pseudomonas aeruginosa* were reported from soaking of animal skins (Zambare et al., 2013), Jaouadi et al., (2013) isolated *B. licheniformis* PWD-1, *Brevibacillus brevis*. We isolated *Arthrobacter creatinolyticus* KJ009396 from deteriorated leather sample which is the first report.

3.2. Biogenic Silver nanoparticles (AgNPs) synthesis

Biogenic AgNPs were synthesized by using *Portulaca oleracea L.* in 20 mins at 75°C at 1:10 ratio of plant extract to 1mM of silver nitrate solution, formation reddish brown colour in reaction mixture after incubation indicates biogenic AgNPs synthesis. Formation of AgNPs at different time intervals may be due to variation in secondary metabolites present in the plant extracts (Firdhouse, 2012). Secondary metabolites play an important role in reduction of silver nitrate to AgNPs and for capping of synthesized AgNPs (P. Lalitha, 2015). Singha (2014) reported AgNPs synthesis at 100°C in 15 mins using *Neptunia oleraceae* plant extract of 1:10 ratio, by using aqueous extract of *Brassica oleracea*, *capitata*, and *Phaseolus vulgaris* silver nanoparticles were synthesized in dark after 24h (Sushmita Deb, 2014). Silver nanoparticles synthesis was reported by Vanaja (2013) from stem extract of *C. aromaticus* in 4 h time of incubation and observed that colour intensity was increased while increasing the time incubation which confirmed increased silver nanoparticles synthesis.



Figure 1. AgNPs synthesis by using *Portulaca oleracea L.*

3.3. Characterization of Silver Nanoparticles

UV-Vis Spectroscopy

Formation of silver nanoparticles was confirmed by UV-visible spectra, and highest absorbance peak was found at 420 nm (Fig. 2). UV-visible spectra show no evidence of absorption in the range of 400–800 nm for the plant extract. Singha (2014) reported the UV absorption peaks of AgNPs by *N. oleraceae* from 400 to 440 nm clearly indicating the formation of spherical AgNPs by using plants extract. Creation of peak at this range is owing to the phenomenon of surface plasmon resonance, i.e. excitement of surface plasmon present on the outer surface of the metal nanoparticles by applying electromagnetic field; progressively reduced in the peaks specifies no further formation nanoparticles. Higher absorbance spectra is directly proportional to the increasing particle size. Also, it is well recognized that the absorbance of Ag NPs depends mainly upon size and shape. The characteristics of Ag nanoparticles normally appear at a wavelength interval of 400–600nm. UV-Vis spectra of Ag nanoparticles synthesized using the *I. balsamina* aqueous extract evince the blue shift of the absorption band with increasing AgNO₃ concentration. This information shows that the Ag nanoparticles have formed in the extract, where the Ag⁺ has been reduced to Ag⁰.

Proteins and all secondary metabolites of extract play a critical role in both the reducing and capping mechanism for nanoparticle formation (Aritonang F. et al., 2019). The position and shape of the plasmon absorption depends on the particle size and shape (Chanda, 2013). Our biogenic AgNPs showed UV-Vis spectra with highest absorbance peak at 420 nm indicating the formation of spherical AgNPs by using *Portulaca oleracea L.* plants extract.

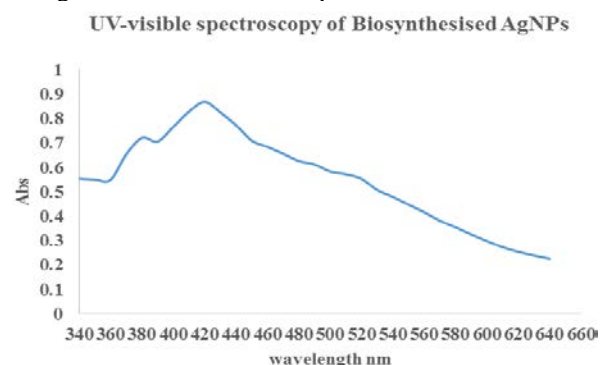


Figure 2. UV-visible spectroscopy of biosynthesized silver nanoparticles

3.4. Fourier transform infrared spectroscopy (FTIR)

FTIR measurements were carried out to identify the possible biomolecules responsible for reduction, capping and efficient stabilization of silver nano particles and the local molecular environment of the capping agents on the nanoparticles (Chandra, 2013). Fig.3 represents the FT-IR spectra recorded for biosynthesized silver nanoparticle from aqueous extract of *Portulaca oleracea L.* at 75°C conditions to know the functional group responsible for the reduction and stabilization of biogenic silver nanoparticles. The strong peak was observed at 3225.33cm⁻¹ may be due to presence of –OH or –NH group. The peak at 1636cm⁻¹ and 2114 cm⁻¹ revealed the presence of carbonyl and –CN triple bond stretching in proteins respectively. The peaks at 515.24 cm⁻¹ showed significant changes upon reduction. Hence, the presence of these functional groups was responsible for the stabilization of synthesized AgNPs and also acts as reducing and capping agent; the results obtained are in agreement with the result of the Firdhouse et al.(2012). FTIR measurements of biogenic AgNPs by using plant extract in present work as well as the literature cited revealed carboxylic groups and amines from proteins play an important role in stabilization, reduction and capping for AgNPs.

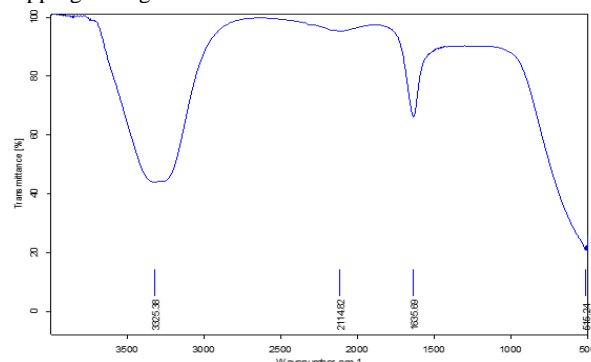


Figure 3. FT-IR spectra of biosynthesized silver nanoparticles at 75°C from aqueous extract of *Portulaca oleracea L.*

3.5. Particle size Analysis and Zeta potential

Biogenic AgNPs Dmean number 52.26 nm and in master curve distribution Dmean number 134.53 nm (Fig. 4&5) were analyzed at 25 °C with an average rate count of 1505 kcps at wavelength 657 nm. Asghari Gholamreza (2014) reported, Statistical distribution of biogenic AgNPs by the *Portulaca oleracea* L. plant part extract form nanoparticles with different sizes; 146 nm, 136 nm and 175 nm for root, leaf, and stem extracts, respectively and the fresh leaves aqueous extract of the plant synthesized silver nanoparticles with particle size less than 60 nm (Fridhouse et al., 2012). Shankar et al. (2003) found 50-100 nm size biogenic AgNPs by using *Azadirachta indica*. The present work reported the results obtained are in agreement with the size of the silver nanoparticle cited in literature. Zeta potential of biogenic AgNPs was found to be -29.1mV by Malvern Instruments (Fig. 6) indicates stable AgNPs while Colloidal silver solution (CSS) Zeta potential was -51.46 mV reported by Aurora et al. (2013).

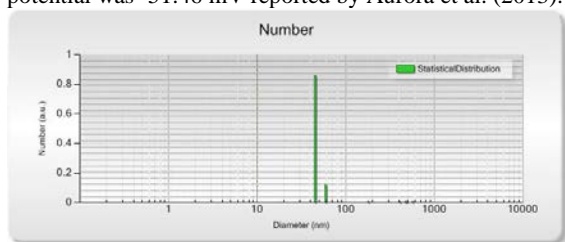


Figure 4. Particle size Analysis: Statistical distribution

Results			
	Mean (mV)	Area (%)	Width (mV)
Zeta Potential (mV): -29.1	Peak 1: -29.1	100.0	5.58
Zeta Deviation (mV): 5.58	Peak 2: 0.00	0.0	0.00
Conductivity (mS/cm): 0.110	Peak 3: 0.00	0.0	0.00

Result quality : Good

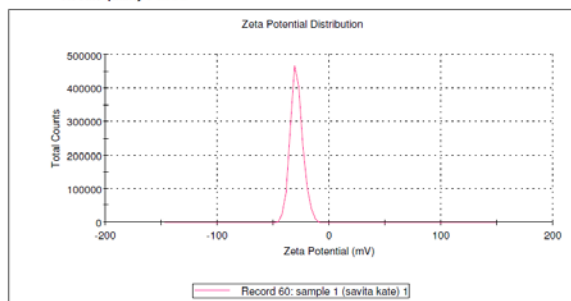


Figure 5. Zeta potential analysis of Biogenic AgNPs

3.6. X-ray Diffraction Method (XRD)

To calculate the crystalline particle size, crystal structure and formation of silver nano particles was confirmed by using XRD valuable research tool (Bindhu et al., 2013). The XRD pattern silver nanoparticles synthesized from aqueous extract of *Portulaca oleracea* L. (Fig 6) showed the presence of sharp and intense peak at $2\theta = 32.20^\circ$; according to Scherrer's formula, $D_p = 0.94\lambda / \beta_{1/2} \cdot \cos\theta$, an average crystal size of the silver nanoparticles can be estimated from the X- ray wavelength of the Cu Ka radiation ($\lambda = 1.54\text{Å}$), the Bragg angle (θ) and the width of the peak at half height (maximum) (β) in radians. The particle size of the synthesized nanoparticles can be calculated using Debye- Scherrer's equation $D_p = 0.94\lambda / \beta_{1/2} \cdot \cos\theta$ (nm), AgNPs size was found in range of 28.8 nm to 30.08 nm which was smaller in size than the reported nanoparticle size 32.24 nm (Firdhouse et al.2012).

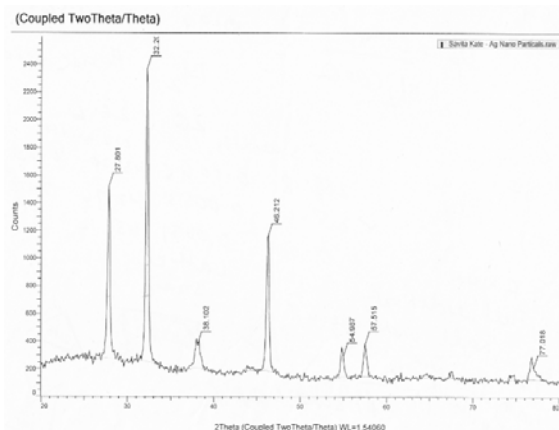


Figure 6. X-ray diffraction of Biosynthesized Silver nanoparticles

3.7. Scanning Electron Microscop

The SEM analysis gives a brief idea about the morphology and size of the nano particles. For SEM analysis synthesized silver nanoparticles was coated on a glass substrate. The micrograph showed well separated silver nanoparticles with little agglomeration. The particle size of the synthesized silver nanoparticles varied compared to that of the size obtained from XRD analysis. The analysis confirms the shape AgNPs to be spherical. Similarly, spherical shape silver nanoparticle was reported by using the leaf extract of *Coleus aromaticus* (Vanaja, 2013).

3.8. Antibacterial activity of synthesized biogenic AgNPs

The antibacterial properties of the biogenic synthesized AgNPs were studied, and distinct zone of inhibition was found against all bacterial leather isolates and zone of inhibition ranges from $14.66 \pm 1.15 - 20.33 \pm 1.52$ mm in diameter as shown in Table 1; also compared with the diameter of zone of inhibition of known antibiotics such as Streptomycin (300mcg), Chloramphenicol (25mcg), Fusidic acid (10mcg), Erythromycin (5mcg), Methicillin (10mcg) and Novobiocin (5mcg) were used as the positive control. K. Roy et al., (2015) reported antibacterial activity of biogenic silver nanoparticles synthesized by using extract of *Cucumis sativus* and was studied against three bacterial strains *Staphylococcus aureus* (10mm), *Klebsiella pneumoniae* (14mm) and *Escherichia coli* (12mm). They found that antibacterial activity of AgNPs against gram negative was more as compared to gram positive bacteria, and this is due to the release of Ag^+ ions from silver nanoparticles. Singh et al. (2015) did the antibacterial assays on *Escherichia coli* (16 ± 0.5 mm) and *Pseudomonas aeruginosa* (13 ± 0.5 mm) using biogenic AgNPs synthesized by green *Phyllanthus niruri* leaves. In the present study, biogenic AgNPs showed highest zone of inhibition against *Bacillus amyloliquefaciens* KP015745 ($20.33 \text{mm} \pm 1.52 \text{mm}$) which was equal to Erythromycin (5mcg), Methicillin (10mcg) antibiotics followed by *Bacillus megaterium* KM369985 strain SAK (17 ± 1.73 mm) which was higher than Streptomycin (300mcg), Fusidic acid (10mcg), Erythromycin (5mcg) and *Bacillus pumilus* KP015747 showed complete resistance against Chloramphenicol (25mcg), Erythromycin (5mcg) and Methicillin (10mcg) but biogenic AgNPs showed inhibition (14.66 ± 1.15 mm) (Fig.7&8).

Table 1. Zone of inhibition shown by different Inhibitors

Sr. No.	Name of the organism	Zone of inhibition shown by different Inhibitors (mm)						
		A	B	C	D	E	F	G
01	<i>Bacillus megaterium</i> KM369985 strain SAK	17±1.73	14	24	23	18	15	21
02	<i>Bacillus cereus</i> KP015746	15±1	20	25	28	20	25	25
03	<i>Bacillus pumilus</i> KP015747	14.66±1.15	20	-	24	-	-	18
04	<i>Bacillus amyloliquefaciens</i> KP015745	20.33±1.52	36	25	27	20	20	26
05	<i>Arthrobacter creatinolyticus</i> KP015744	16.33±1.52	24	20	22	21	25	22

Where, A- Biosynthesized silver nanoparticles (20µl), B- Streptomycin (300mcg), C- Chloramphenicol (25mcg), D- Fusidic acid (10mcg), E- Erythromycin (5mcg) F- Methicillin (10mcg) G- Novobiocin (5mcg)

**Figure 7.** Zone of inhibition *B. megaterium***Figure 8.** Zone of inhibition *B. pumilus*

3.9. MIC of Silver Nanoparticles for bacteria

The antibacterial effects of the biogenic silver nanoparticles were measured by determining the minimum concentration needed to inhibit the growth of leather isolates. MIC values of the biosynthesized silver nanoparticles against leather isolates were given in Table 2. Leather bacterial isolates in the present study were inhibited at the concentration of 4-20 µg/ml of AgNPs. Chan Yen San et al. (2013) reported the MIC of AgNPs were between 1.6–47, 0.25–7.03, 0.4–30 and 0.4–4.7 µg/ml for *S. aureus*, *S. epidermidis*, *E. coli* and *C.*

albicans, respectively. Minimum Inhibitory Concentration (MIC) of AgNPs against *Staphylococcus aureus* was 800 µg/ml and for *E. coli* was 300 µg/ml reported by Vivekanandan et al. (2012) in their study, while Ruparelia et al. (2008) found MIC for *E. coli* was 40 µg/ml, for *S. aureus* 120 µg/ml, for *B. subtilis* 40 µg/ml in his work. Kim et al., (2011) the MIC of AgNPs against *S. aureus* and *E. coli* was 100 µg/ml. In the current work, the biogenic AgNPs was found to be more effective than the literature cited presents.

Table 2. MIC of AgNPs against the selected isolates

Sr. No.	Name of the isolate	MIC (µg/ml)
1	<i>Bacillus megaterium</i> KM369985 strain SAK	20
2	<i>Bacillus cereus</i> KP015746	5
3	<i>Bacillus pumilus</i> KP015747	5
4	<i>Bacillus amyloliquefaciens</i> KP015745	10
5	<i>Arthrobacter creatinolyticus</i> KP015744	4

4. Conclusion:

Preservation of leather by application of biogenic AgNPs was studied, and it was found that there was no growth of leather isolates on treated leather samples while untreated samples started to deteriorate by the isolates. Even after six months, there was no deterioration of leather samples, showing the efficiency of biogenic AgNPs in preservation of leather. Hence, biogenic AgNPs obtained in the present study can be effectively used for leather preservation.

Acknowledgements

Authors thank The Principal Dr. P.V. Ashtekar for providing infrastructure facilities to carry out present study.

Conflict of interest

Authors declare no conflict of interest.

References

- Firdhouse M. and Lalitha P. 2012. Green Synthesis of Silver Nanoparticles Using the Aqueous Extract of *Portulaca oleracea* (L.). *Asian J Pharm Clin Res.*, **6** (1):92-94.
- Khandelwal N., Singh A., Jain D., Upadhyay M. K. and Verma H.N. 2010. Green synthesis of silver nanoparticles using Argimone mexicana leaf extract and evaluation of their antimicrobial activities. *Digest Journal of Nanomaterials and Bio structures.*, **5** (2): 483 – 489.
- Rajasekharreddy P., Rani P.U. and Sreedhar B. 2010. Qualitative assessment of silver and gold nanoparticle synthesis in various plants: a photobiological approach. *J. Nanopart. Res.*, **12**: 1711–1721.
- Kaviya S, Santhanalakshmi J, Viswanathan B, Muthumary J, Srinivasan K. 2011. Biosynthesis of silver nanoparticles using citrus sinensis peel extract and its antibacterial activity. *Spectrochim Acta - Part A Mol Biomol Spectrosc.*, **75**: 594-598.
- Tissier C. and Chensais M. 2000. Biocides used as preservatives in the leather industry, Product type 9: fibre, leather, rubber and polymerized materials preservatives. *Emission scenario Documents.*, 1-14.

- Nadia Zarai Jaouadi and Hatem Rekik et al. 2013. Biochemical and molecular characterization of a serine keratinase from *Brevibacillus brevis* US575 with promising keratin biodegradation and Hide dehairing activities. *PLoS One*, **8** (10):1-17.
- Baird D. H. 1998. The Microbial Decomposition of Chromium. Master of Science in Microbiology, University of Canterbury.
- Lili Liu, Meihu Ma, Zhaoxia Cai Xieli Yang and Wentao Wang. 2010. Purification and Properties of a Collagenolytic Protease Produced by *Bacillus cereus* MBL13 Strain. *Food Technol. Biotechnology*, **48** (2): 151-160.
- Lalitha P. and Firdhouse M. Jannathul. 2015. Biocidal potential of biosynthesized silver nanoparticles against fungal threats. *J Nanostructure Chem.*, **5**: 25-33.
- Mittal Subhangi. 2012. Biosynthesis of Silver Nanoparticles (AgNPs) using waste fruit Peel as an antimicrobial drug agent. Department of Botany, Faculty science, Dayalbagh Educational Institute Dayalbagh Agra-28110.
- Alzahrani Eman. 2015. Eco-Friendly Production of Silver Nanoparticles from Peel of Tangerine for Degradation of Dye. *World Journal of Nano Science and Engineering*, **5**:10-16.
- Singh K, Panghal M, Kadyan S, Chaudhary U and Yadav P. 2014. Antibacterial Activity of Synthesized Silver Nanoparticles from *Tinospora cordifolia* against Multi Drug Resistant Strains of *Pseudomonas aeruginosa* Isolated from Burn Patients. *J Nanomed Nanotechnol.*, **5**(2): 1-6.
- Dash L. 2013. Biological Synthesis and Characterization of Silver Nanoparticles using *Bacillus thuringiensis*. Department of Life Science National Institute of Technology Rourkela-769008, Orissa, India.
- Aritonang H., Koleangan H. and Wuntu A. 2019. Synthesis of Silver Nanoparticles Using Aqueous Extract of Medicinal Plants* (*Impatiens balsamina* and *Lantana camara*) Fresh Leaves and Analysis of Antimicrobial Activity. *International Journal of Microbiology* Volume 2019, Article ID 8642303, 8 pages <https://doi.org/10.1155/2019/8642303>.
- Chanda S. 2013. Silver nanoparticles (medicinal plants mediated): A new generation of antimicrobials to combat microbial pathogens- a review. *FORMATEX*, 1314-1323.
- Bauer A.W, Kirby W.M., Sherris J.C. and Turck M. 1966. Antibiotic susceptibility testing by a standardized single disk method. *Am J Clin Pathol.*, **45**:493-496.
- Awad A., Hendi A., Khalid M., Ortashi O., Dalia F., Elradi A., Lamia E., Eisa., Shorog-lahieb A., Al-Otiby, Merghani M. and Awad A. G. 2014. Silver nanoparticles biogenic synthesized using an orange peel extract and their use as an anti-bacterial agent. *International Journal of Physical Sciences*, **9**(3):34-40.
- Deb S. 2014. Synthesis and Characterization of Silver Nanoparticles Using *Brassica oleracea capitata* (Cabbage) and *Phaseolus vulgaris* (French Beans): A Study on their Antimicrobial Activity and Dye Degrading Ability. *International Journal of Chem Tech Research*, **6**(7):3909-3917.
- Idris A., Majidnia Z. and Valipour P. 2013. Antibacterial Improvement of Leather by Surface Modification using Corona Discharge and Silver Nanoparticles Application. *Journal of Science and Technology*. 1-15.
- Petica A., Gaidau Ma C. J., Simion D. and Niculescu M. 2013. Antimicrobial Electrochemically Obtained Nanosilver Solutions for Leather and Furskin Treatment. *REV. CHIM. (Bucharest)*, **64**(11): 1329-1334.
- Sanchez-Navarro M. M., Pérez-Liminana M. A., Cuesta-Garrote N., Maestre-Lopez M. I., Bertazzo M., Martinez-Sanchez M. A., Orgiles-Barcelo C. and Aran-Ais F. 2013. Latest Developments in Antimicrobial Functional Materials for Footwear. *FORMATEX*. 102-113.
- Zambare V.P., Nilegaonkar S.S. and Kanekar P.P. 2013. Protease Production and Enzymatic Soaking of Salt-Preserved Buffalo Hides for Leather Processing. *IIOAB Letters*, **3**: 2161-3702.
- Singha Sumita., Neog Kundal., Kalita Partha Pratim., Talukdar Nayan and Sarma Manash Pratim. 2014. Biological synthesis of silver nanoparticles by *Neptunia oleraceae*. *International Journal of Basic and Applied Biology*, **2**(2):55 – 59.
- Vanaja M., Rajeshkumar S., Paulkumar K., Gnanajobitha G., Malarkodi C. and Annadurai G. 2013. Phytosynthesis and characterization of silver nanoparticles using stem extract of *Coleus aromaticus*. *International Journal of Materials and Biomaterials Applications*, **3**(1): 1-4.
- Asghari Gholamreza., Jaleh Varshosaz and Nafiseh Shahbazi. 2013. Synthesis of silver nanoparticle using *Portulaca oleracea* L.L. extracts. *Nanomedicine Journal*, **1**(2):94-99.
- Shankar S. S., Ahmad A., Sastry M. 2003. Geranium Leaf Assisted Biosynthesis of Silver Nanoparticles. *Biotechnology Progress*, **19** (6): 1627-1631.
- Bindhu M. R. and Umadevi M. 2013. Synthesis of monodispersed silver nanoparticles using *Hibiscus cannabinus* leaf extract and its antimicrobial activity. *Spectrochimica Acta Part A: Molecular and Biomolecular Spectroscopy*, **101**:184-190.
- Roy K., Sarkar C.K. and Ghosh C.K. 2015. Single-Step Novel Biosynthesis of Silver Nanoparticles Using *Cucumis Sativus* Fruit Extract and Study of its photocatalytic and antibacterial Activity. *Digest Journal of Nanomaterials and Biostructures*, **10**(1):107 – 115.
- Singh A. and Dhaliwal H. 2015. Green Synthesis of Silver Nanoparticles Using *Phyllanthus Niruri* Leaf Extract and Evaluation of Their Antimicrobial Activities. *European Journal of Environmental Ecology*, **2**(1):9-13.
- San Chan Yen and Don Mashitah Mat. 2013. Biosynthesis of Silver Nanoparticles from *Schizophyllum Commune* and in-vitro Antibacterial and Antifungal Activity Studies. *Journal of Physical Science*, **24**(2):83-96.
- Vivekanandan K.Ea., Rajb K. Gokul., Kumaresana S. and M. Pandib. 2012. Biosynthesis of silver nanoparticle activity against bacterial strain, cephalixin antibiotic synergistic activity. *INT J CURR SCI*, **4**:1-7.
- Kim, Soo-Hwan., Hyeong-Seon Lee., Deok-Seon Ryu., Soo-Jae Choi and Dong-Seok Lee. 2011. Antibacterial Activity of Silver-nanoparticles Against *Staphylococcus aureus* and *Escherichia coli*. *Korean J. Microbiol. Biotechnol.*, **39**(1):77-85.

Pollen Morphological Variations among some Cultivated *Citrus* species and its Related Genera in Egypt

Wafaa K. Taia¹, Manaser M. Ibrahim^{1,*} and Mahmoud Abdel-Sattar^{2,3}

¹Botany and Microbiology Department, Faculty of Science, ²Pomology Department, Faculty of Agriculture, Alexandria University, Alexandria, Egypt; ³Department of plant production, College of Food Science and Agriculture, King Saud University, P. O. 2640, Riyadh, 11451, Saudi Arabia.

Received: November 8, 2019; Revised: December 16, 2019; Accepted: January 3, 2020

Abstract

The present investigation aims to study the pollen morphology and ultra-structure of pollen grain characteristics for nine *Citrus* species and three related genera cultivated in Egypt. The pollen grains were photographed by using both light (LM) and scanning electron microscopy (SEM). Twelve qualitative and quantitative pollen morphological characters were used to differentiate among the studied taxa. Statistical analysis of palynological data indicated that the pollen size, shape, colpi length, apertures number and type, ora size, amb shape, mesocolpium diameter and exine ornamentation were the most distinguished characters in the circumscription of the studied taxa and were of taxonomic value. But the characters of P/E, ora shape and exine thickness were of less taxonomic value among the closely related taxa of *Citrus*, *Fortunella margarita*, *X Citrofortunella floridana* and *Poncirus trifoliata*.

Keywords: *Citrus*, *Fortunella margarita*, *X Citrofortunella floridana*, pollen morphology, *Poncirus trifoliata*, Rutaceae

1. Introduction

According to Engler, (1931), Rutaceae is divided into seven subfamilies, primarily by gynoeceum characters especially the fruit type. *Citrus* species and its related genera (i.e. *Fortunella*, *Poncirus*, *Eremocitrus*, *Microcitrus* and *Clymenia*) all belong to subtribe Citrinae, tribe Citreae, of the orange subfamily Aurantioideae. *Citrus* (Rutaceae), characterized by having different life forms as trees and shrubs. It contains aromatic compounds with pellucid glands on the stems, leaves and fruits. The leaves are usually opposed, compound and without stipules, sometimes with thorns (Sharma, 1993). The *Citrus* fruit is berry or hesperidium with a leathery rind or hard shell and often with pulp formed by juicy or sappy emergencies that arise on the carpellary walls. Species within the genus *Citrus* are highly economic and medicinal plants distributed all over the world (Swingle and Reece, 1967). Several taxonomists have classified various kinds of *Citrus* species into groups and given them valid names (Roxburgh, 1832; Brandis, 1874; Marcovitch, 1926; Swingle, 1943; Swingle and Reece, 1967; Hodgson, 1965 and Tanaka, 1936 and 1977). Swingle's system appears to be the most useable all over the world (Nicolosi, 2007).

Distinguishing of *Citrus* species and related genera according to morphological and geographical distribution are very difficult because *Citrus* contains an enormous degree of genetic variation, with abundant natural hybridization (Moore, 2001). The classifications of the genus *Citrus* are complex and the precise number of natural species is unclear, as many of the named species

are hybrids clonally propagated through seeds (by apomixes) and there is genetic evidence that even some wild, true-breeding species are of hybrid origin (Swingle and Reece, 1967 and Chase *et al.*, 1999). Mandarins, Pomelo, Citrons, Kumquats, Papedas, Australian and New Guinean species are considered as the ancestral or original *Citrus* species and all the rest are hybrids of them (Barett and Rodes, 1976; Scora, 1975 and Nicolosi, 2007).

In Egypt, there are no wild *Citrus* species (Täckholm 1974 and Boulos, 1999). All the present species (about 7 including 9 varieties) are introduced and cultivated in a cultivation area representing about 29% of the total fruit area in Egypt (Hamza and Tate, 2017 and Abobatta, 2019).

The use of pollen morphological characters are important in plant taxonomy. As Davis and Heywood (1973) pointed out, these characters can be highly significant at the species and generic levels of taxa or among higher levels. The use of pollen morphology in solving taxonomic problems has been used since a long time ago where Erdtman, (1952) studied the pollen characters of different Angiosperm and Gymnosperm families, while both Saad and Taia, (1988) and Taia and Sheha, (2001) used pollen characters in the differentiation among *Astragalus* and *Atriplex* species, respectively. Moreover, Taia, (2004) revealed the differences among the genera of tribe Trifolieae (Leguminosae) using pollen characters. Besides, Avci *et al.*, (2013) and Inyama *et al.*, 2015 were able to differentiate among the members of *Onobrychis* (Fabaceae), and *Citrus* (Rutaceae) species, respectively, using palynological characters. Recently in (2018), Mary and Gopal studied the pollen morphological characters of the two genera (*Ehretia pubescens* and

* Corresponding author e-mail: manaser99@yahoo.com.

Cormona retusa) Ehretiaceae, and proved that it is an important tool in the identification between them. This work is considered as a step in finding the way in differentiating among nine *Citrus* species and their related genera.

Therefore, this study aims to investigate and assess the relationships among nine *Citrus* species as well as three related genera cultivated in Egypt using pollen morphological characters.

2. Materials and Methods

The present investigation was carried out on mature trees of nine *Citrus* species and three related genera; *Citrus aurantifolia* (Christm.) Swing. [Mexican lime], *Citrus aurantium* L. [Sour orange], *Citrus grandis* (L.) Osbeck. [Pummelo], *Citrus latifolia* Tanaka [Persian "Tahiti" lime], *Citrus limetta* Risso. [Sweet lime], *Citrus paradisi* Macf. [Marsh grapefruit], *Citrus reshni* Hort. ex Tanaka [Cleopatra mandarin], *Citrus reticulata*-Blanco [Clementine tangerine], *Citrus sinensis* (L.) Osbeck. [Succari orange], *Fortunella margarita* (Lour.) Swing. [Oval Kumquat], and *X Citrofortunella floridana* J. W. Ingram & H. E. Moore, which is a hybrid between *Citrus aurantifolia* (Christm.) Swing. [Mexican lime], and *Fortunella japonica* (Thunb.) Swing. [Round Kumquat], and *Poncirus trifoliata* (L.) Raf. [Trifoliolate orange] grown in a private orchard. This orchard is located 120 Km away from Alexandria on Alexandria-Cairo desert road (GPS co-ordinates: 30°44'47.8"N, 30°09'15.2"E). These species were collected by Dr. Mahmoud Abdel-Sattar in the year 2017 and identified at Pomology Department, Faculty of Agriculture, Alexandria University, and vouchers of the studied taxa were allocated there.

Four uniform trees were selected from each *Citrus* species and related genera, from which mature anthers were taken from the upper most flowers of the branches to obtain the mature pollen grains used in this investigation.

Pollen grain samples of all studied taxa were acetolyzed according to Erdtman's technique (Erdtman, 1952). The acetolyzed samples were used for both light

and scanning electron microscopy. Slides were prepared from acetolyzed portion of pollen grains for light microscope examination by mounting in glycerin jelly, examined and measured using Zeiss light microscope with a pre-calibrated eye-piece micrometer. Measurements given are the means of 40 acetolyzed well developed pollen grains from each taxa.

Pollen grains of the acetolyzed portion were dehydrated in ethanol series placed onto coverslips, left for ethanol evaporation then attached to copper stubs by double sided tape, coated with 30 nm gold using fine coat ion sputter JEOL JFC 1100E, examined and photographed at 30 KV using JEOL JSM-3500 scanning electron microscope present in the Faculty of Science, Alexandria University. The terminology used in the present study is according to Faegri, (1956) and Erdtman, (1952).

Statistical analysis

For all the studied taxa, the mean values of the pollen characters were separated and calculated then compared using the least significant difference (L.S.D) test at 0.05 level of probability (Snedecor and Cochran, 1990). The statistical analysis was performed using SAS (Statistical Analysis System) version 9.13, (2008).

3. Results

The results obtained from the twelve studied taxa are summarized in table 1 and illustrated in plates 1-12. The pollen grains of all taxa were monads, radially symmetrical, isopolar and were different in size. The pollen shape varied from prolate-spheroidal (P/E 1.02) to sub-prolate (P/E 1.20) except in *F. margarita* (Plate 10), where it was oblate-spheroidal (P/E 0.97). The mean polar axis length ranged from 26 μ m (*F. margarita* and *X Citrofortunella floridana*) to 34.48 μ m in *C. grandis*. Moreover, the mean equatorial diameter ranged from 26 μ m (*F. margarita* and *X Citrofortunella floridana*) to 33.44 μ m in *C. grandis*.

Table 1. Pollen morphological characters of the studied *Citrus* species and its related taxa

Characters → Taxa ↓	Common name	P. L.	E. D.	P/E	Pol. Sh.	Ap.	C. L.
<i>C. aurantifolia</i> (Christm.) Swing.	Mexican lime	28.00 - 34.40	23.20 - 32.00	1.17	3	2	22.40 - 30.40
		31.32	27.54				26.96
<i>C. aurantium</i> L.	Sour orange	25.60 - 36.00	24.80 - 32.00	1.09	2	5	22.40 - 30.40
		30.72	28.27				25.36
<i>C. grandis</i> (L.) Osbeck	Pummelo	31.20 - 37.60	30.40 - 36.80	1.03	2	4	30.21 - 34.40
		34.48	33.44				31.80
<i>C. latifolia</i> Tanaka	Tahiti lime	27.20 - 36.00	24.00 - 31.20	1.20	3	5	22.40 - 31.20
		31.58	26.42				26.44
<i>C. limetta</i> Risso	Sweet lime	28.80 - 40.00	27.20 - 37.60	1.07	2	1	24.00 - 35.20
		33.72	31.76				28.38
<i>C. paradisi</i> Macf.	Marsh grapefruit	28.00 - 39.20	24.00 - 35.20	1.09	2	5	22.40 - 33.60
		33.14	30.64				27.85
<i>C. reshni</i> Hort. ex Tanaka	Cleopatra mandarin	26.40 - 32.80	24.00 - 31.20	1.09	2	1	20.00 - 27.20
		29.80	27.46				24.48
<i>C. reticulata</i> Blanco	Clementine tangerine	25.60 - 35.20	25.60 - 35.20	1.09	2	2	19.20 - 29.60
		30.46	28.14				24.84
<i>C. sinensis</i> (L.) Osbeck	Succari orange	28.80 - 36.00	25.60 - 33.60	1.10	2	4	24.00 - 30.00
		32.20	29.58				27.60
<i>Fortunella margarita</i> (Lour.) Swing.	Oval Kumquat	23.20 - 29.60	24.00 - 29.60	0.97	1	3	18.40 - 24.00
		26.04	26.22				20.96

<i>X Citrofortunella floridana</i> J. W. Ingram & H. E. Moore	Limequat	24.00 - 28.00 26.56	23.20 - 28.80 26.12	1.02	2	1	18.40 - 23.20 21.02
<i>Poncirus trifoliata</i> (L.) Raf.	Trifoliolate orange	28.80 - 36.00 32.26	28.80 - 36.00 31.19	1.04	2	2	23.20 - 30.4 26.44
<i>LSD</i> _{0.05}		<i>0.93</i>	<i>0.89</i>	<i>0.03</i>			<i>0.94</i>

P. L. = Mean Polar Length, E. D. = Mean Equatorial Diameter, P/E = Mean Polar length/ Mean Equatorial diameter, Pol. Sh. = Pollen Shape (1. Oblate-spheroidal, 2. Prolate-spheroidal, 3. Sub-prolate), Ap. = Aperture number and type (1. Tri- and tetra-colporate, 2. Tetra- and penta-colporate, 3. Tri-, tetra- and penta- colporate, 4. tri- and tetra-colpate and tri- and tetra-colporate, 5. Tetra- and penta-colpate and tetra- and penta-colporate), C. L. = Mean Colpi Length. Bold Numbers = Mean of means, Italic numbers = Least Significant difference values.

Table 1 (Cont.) Pollen morphological characters of the studied *Citrus* species and its related taxa

Characters → Taxa ↓	Common name	Meso. D.	Ora L.	Ora W.	Amb Sh.	Ex. Th.	Ex. Or.
<i>C. aurantifolia</i> (Christm.) Swing.	Mexican lime	8.00 - 12.80 9.70	1.60 - 2.40 2.08	7.20 - 8.80 7.71	2	2.40	4
<i>C. aurantium</i> L.	Sour orange	8.00 - 12.00 9.36	2.40 - 4.00 3.20	8.00 - 8.80 8.30	2	2.70	3
<i>C. grandis</i> (L.) Osbeck	Pummelo	8.00 - 13.60 11.22	2.40 - 4.00 3.06	7.20 - 8.80 7.90	1	2.40	1
<i>C. latifolia</i> Tanaka	Tahiti lime	8.00 - 12.00 9.36	2.40 - 3.20 2.97	7.20 - 8.80 7.69	2	2.40	4
<i>C. limetta</i> Risso	Sweet lime	8.00 - 18.40 12.72	2.40 - 4.00 3.20	6.40 - 8.00 7.30	1	2.40	4
<i>C. paradisi</i> Macf.	Marsh grapefruit	6.40 - 15.20 10.54	1.60 - 4.00 3.30	6.40 - 8.00 6.90	2	2.40	1
<i>C. reshni</i> Hort. ex Tanaka	Cleopatra mandarin	8.00 - 12.00 9.78	3.20 - 4.00 4.20	7.20 - 9.60 8.10	1	2.40	2
<i>C. reticulata</i> Blanco	Clementine tangerine	8.00 - 12.80 10.30	1.60 - 3.20 2.90	6.40 - 7.20 6.80	2	2.40	2
<i>C. sinensis</i> (L.) Osbeck	Succari orange	6.40 - 14.40 10.40	2.40 - 4.00 3.60	7.20 - 8.00 7.20	1	2.40	1
<i>Fortunella margarita</i> (lour.) Swing.	Oval Kumquat	8.00 - 12.00 9.82	2.40 - 4.00 3.50	4.80 - 7.20 6.08	3	2.40	3
<i>X Citrofortunella floridana</i> J. W. Ingram & H. E. Moore	Limequat	8.00 - 12.80 9.82	2.40 - 3.20 3.00	5.60 - 7.20 6.40	1	2.40	3
<i>Poncirus trifoliata</i> (L.) Raf.	Trifoliolate orange	8.80 - 12.00 10.72	3.20 - 3.40 3.20	4.80 - 7.20 6.40	2	2.40	3
<i>LSD</i> _{0.05}		<i>0.71</i>	<i>0.44</i>	<i>0.83</i>		<i>0.04</i>	

Meso. D. = Mean Mesocolpi Diameter, Ora L. = Mean Ora Length, Ora W. = Mean Ora Width, Amb Sh. = Amb Shape (1. Rounded, triangular and squared, 2. Squared and rounded, 3. Rounded-triangular, squared and rounded), Ex. Th. = Mean Exine thickness, Ex. Or. = Exine Ornamentation (1. Tectate-perforate, 2. Tectate-perforate to microreticulate, 3. Foveolate, 4. Reticulate). **Bold Numbers** = Mean of means, *Italic numbers* = Least Significant difference values.

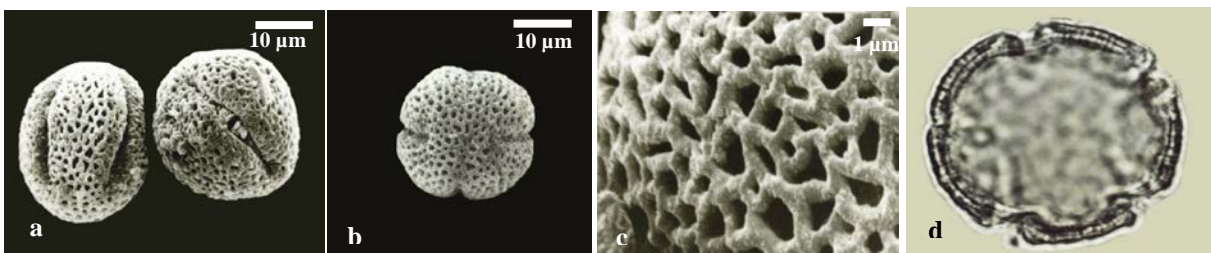


Plate 1. SEM (a-c) and LM (d) photomicrographs of *C. aurantifolia* pollen grains; **a:** Equatorial view (colporate), **b:** Polar view (aperture number), **c:** Exine ornamentation, **d:** Polar view (aperture number).

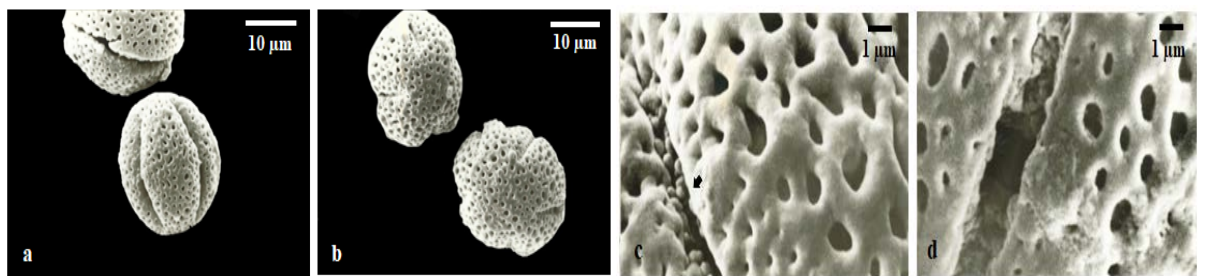


Plate 2. SEM (a-d) photomicrographs of *C. aurantium* pollen grains; **a:** Equatorial view (colporate), **b:** Polar view (aperture number), **c:** Exine Ornamentation (colpate - **arrow**), **d:** Exine ornamentation (colporate).

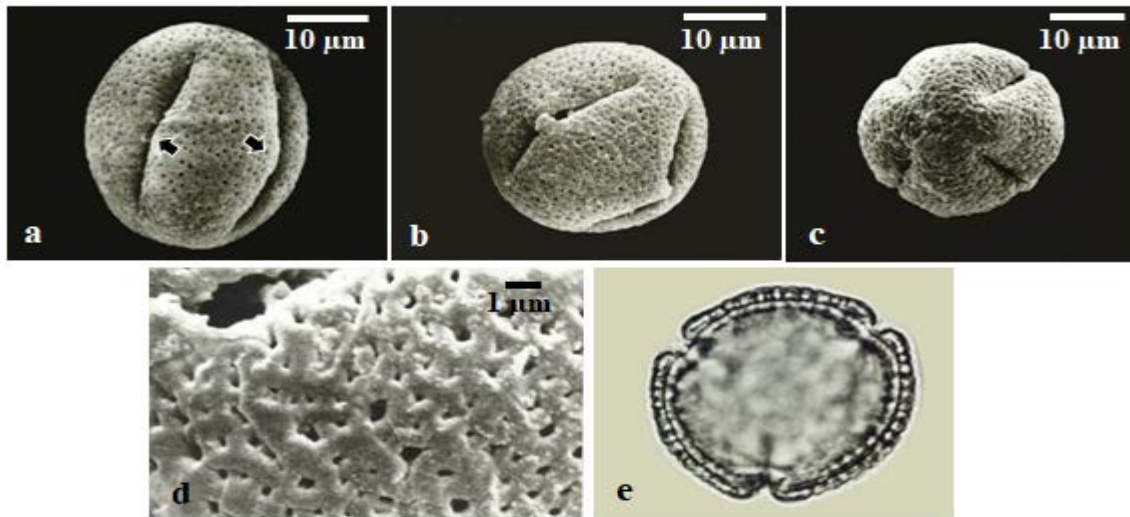


Plate 3. SEM (a-d) and LM (e) photomicrographs of *C. grandis* pollen grains; **a:** Equatorial view (colpate - **arrows**), **b:** Equatorial view (colporate), **c:** Polar view (aperture number), **d:** Exine ornamentation, **e:** Polar view (aperture number)

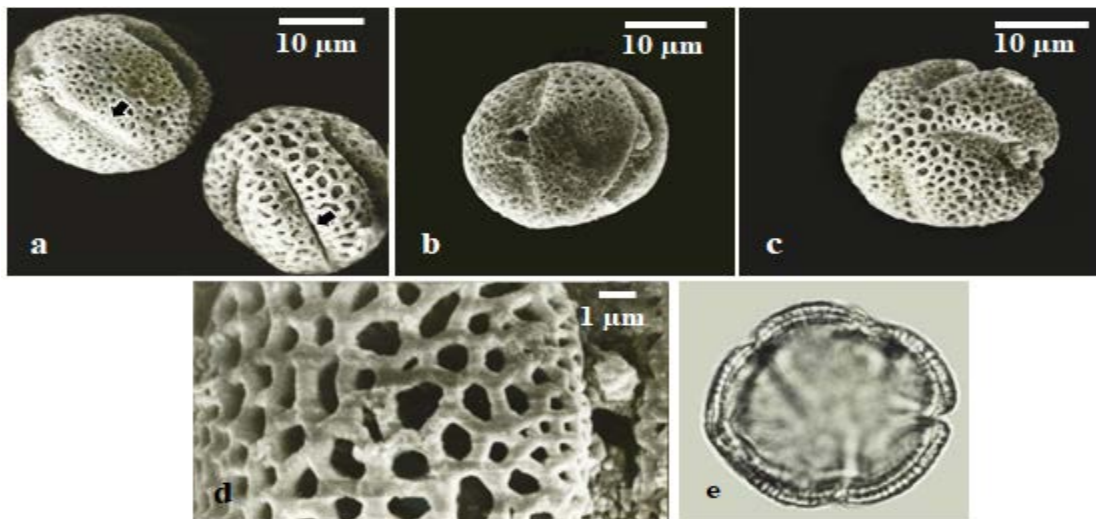


Plate 4. SEM (a-d) and LM (e) photomicrographs of *C. latifolia* pollen grains; **a:** Equatorial view (colpate - **arrows**), **b:** Equatorial view (colporate), **c:** Polar view (aperture number), **d:** Exine ornamentation, **e:** Polar view (aperture number)

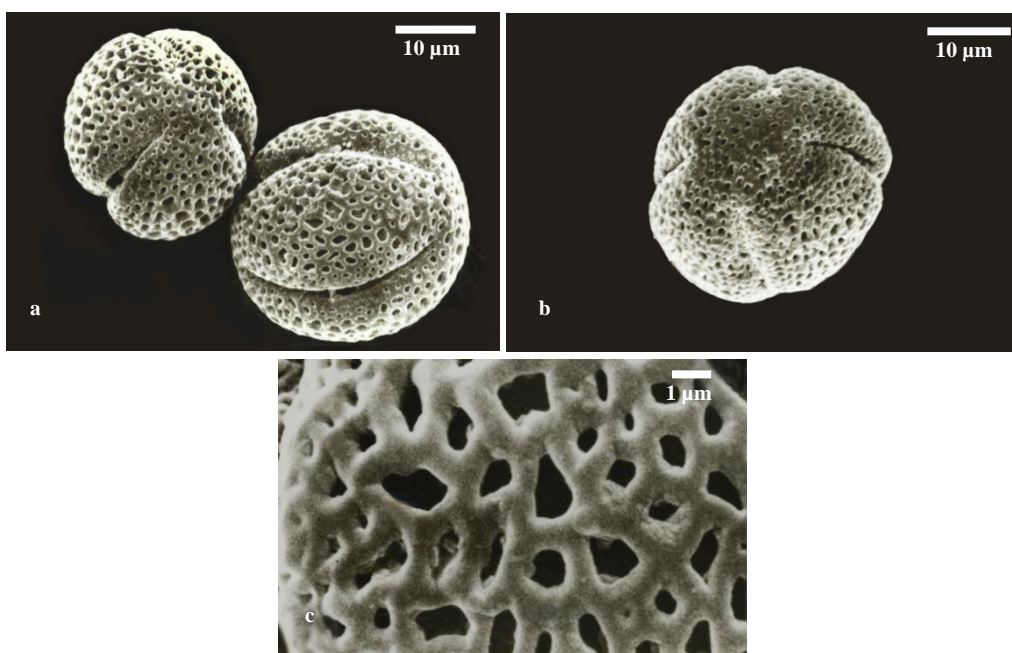


Plate 5. SEM (a-c) photomicrographs of *C. limetta* pollen grains; **a:** Equatorial and polar views (colporate, aperture number), **b:** Polar view (aperture number), **c:** Exine ornamentation

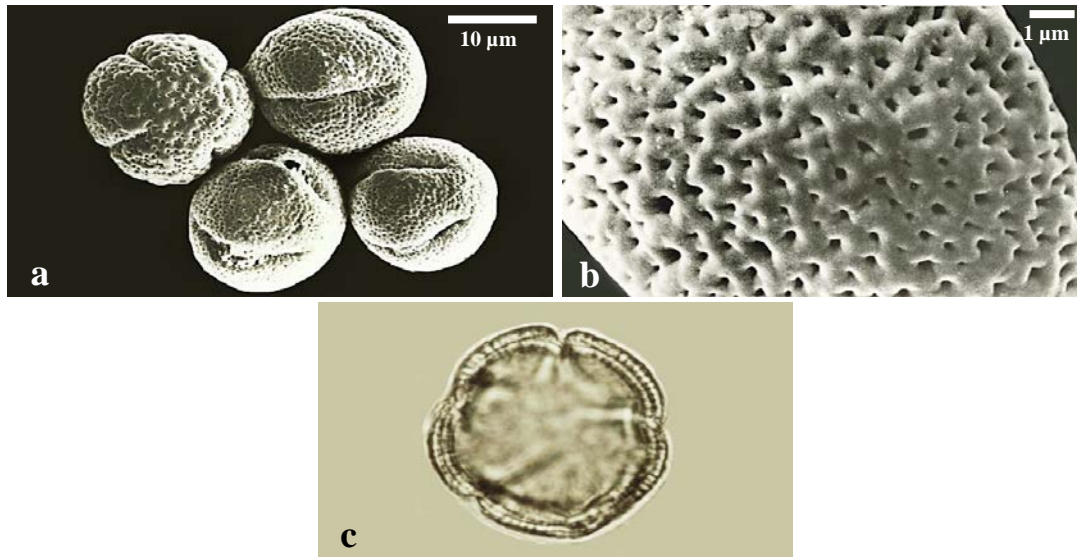


Plate 6. SEM (a-b) and LM (c) photomicrographs of *C. paradisi* pollen grains; **a:** Equatorial and polar views (colpate - arrow, colpate, aperture number), **b:** Exine ornamentation, **c:** Polar view (aperture number)

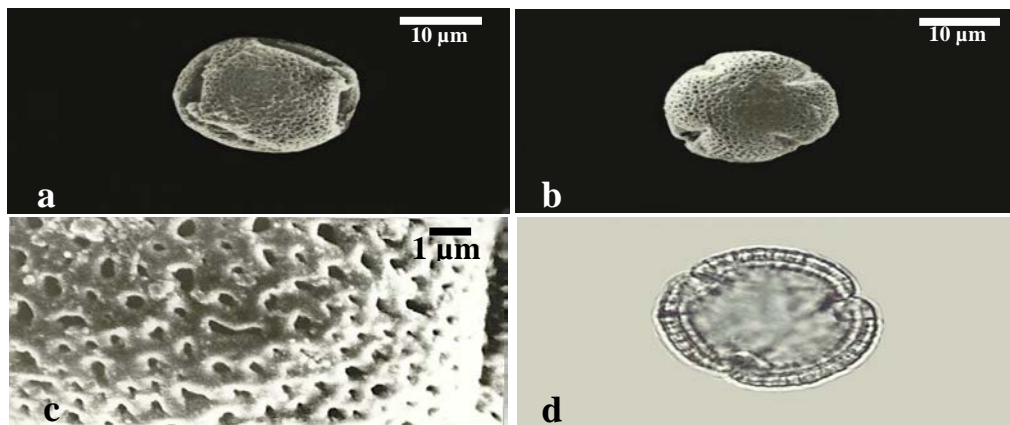


Plate 7. SEM (a-c) and LM (d) photomicrographs of *C. reshni* pollen grains; **a:** Equatorial view (colporate), **b:** Polar view (aperture number), **c:** Exine ornamentation, **d:** Polar view (aperture number).

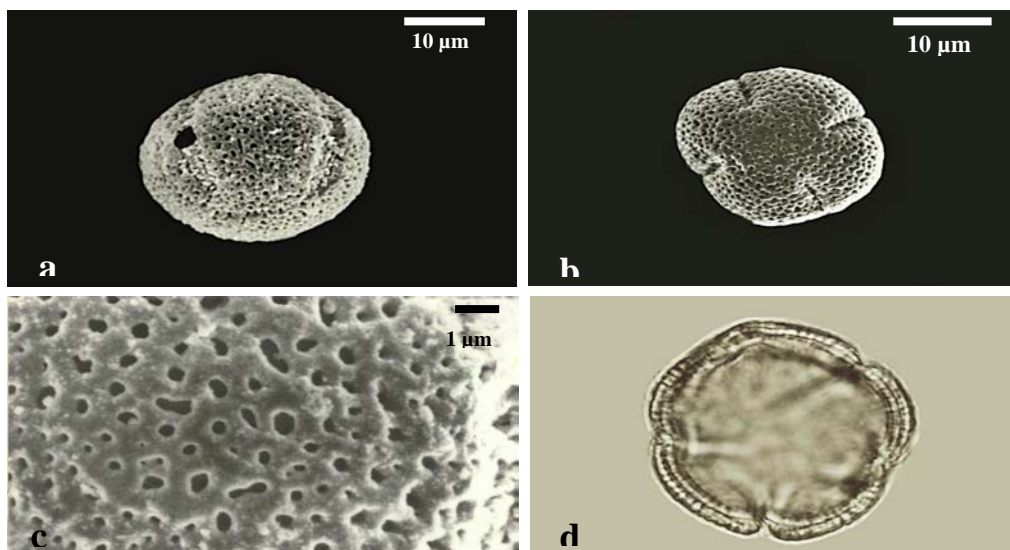


Plate 8. SEM (a-c) and LM (d) photomicrographs of *C. reticulata* pollen grains; **a:** Equatorial view (colporate), **b:** Polar view (aperture number), **c:** Exine ornamentation, **d:** Polar view (aperture number).

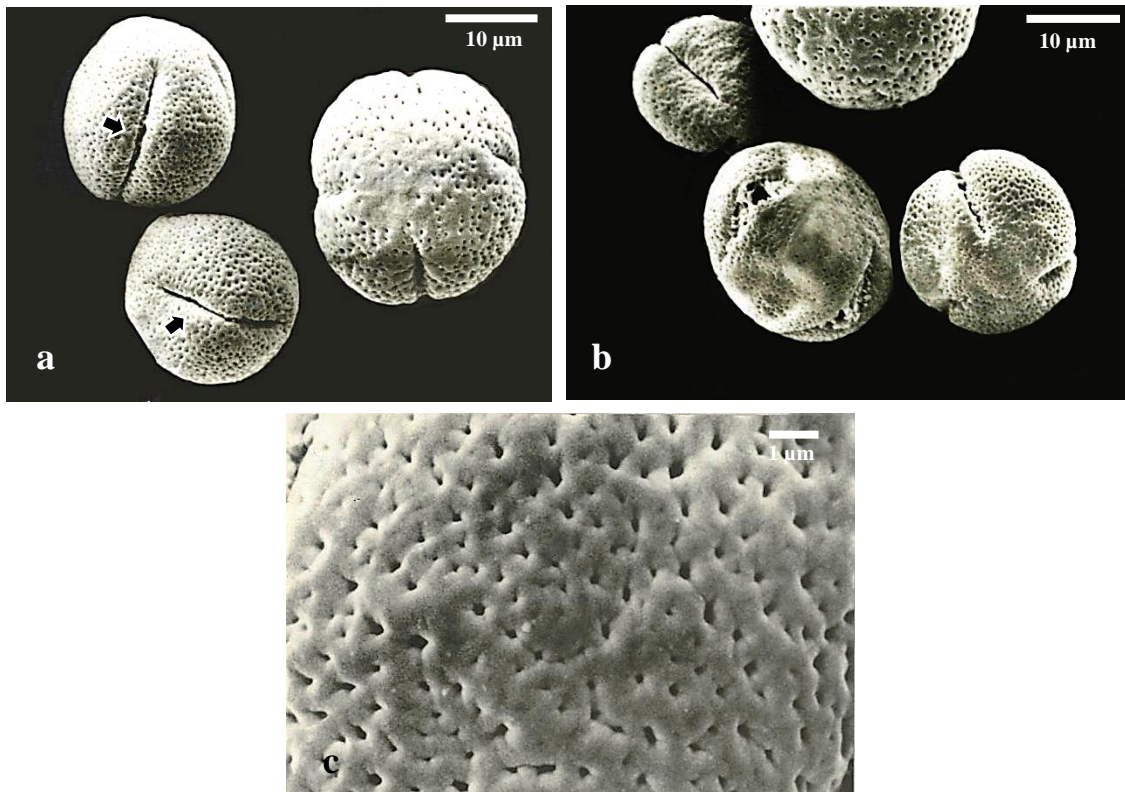


Plate 9. SEM (a-c) photomicrographs of *C. sinensis* pollen grains; **a:** Equatorial and polar views (colpate - **arrows**, aperture number), **b:** Equatorial and polar views (colporate, aperture number), **c:** Exine ornamentation

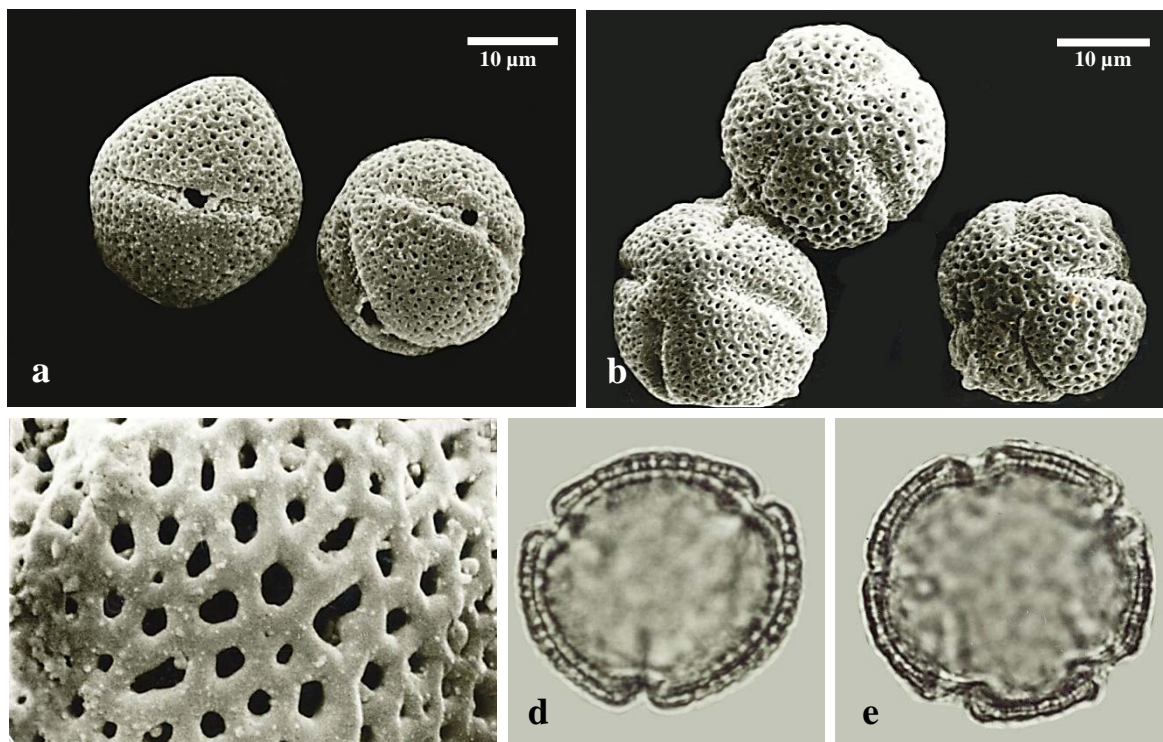


Plate 10. SEM (a-c) and LM (d and e) photomicrographs of *Fortunella margarita* pollen grains; **a:** Equatorial view (colporate), **b:** Equatorial and polar views (aperture number), **c:** Exine ornamentation, **d:** Polar view (aperture number), **e:** Polar view (aperture number)

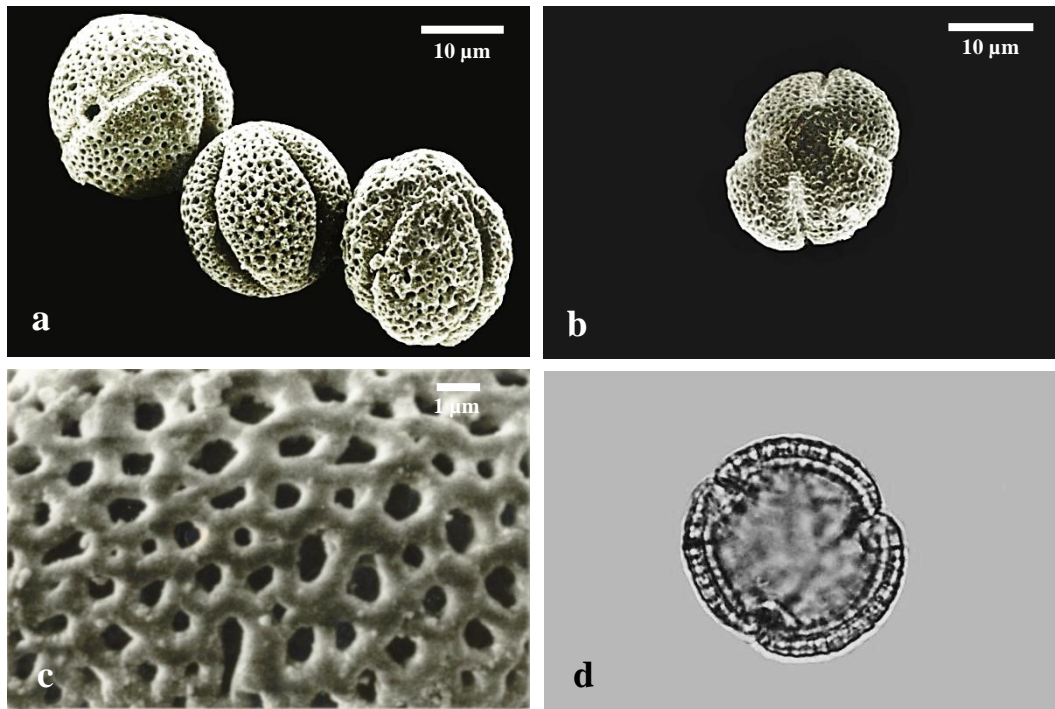


Plate 11. SEM (a-c) and LM (d) photomicrographs of *X Citrofortunella floridana* pollen grains; **a:** Equatorial view (colporate), **b:** Polar view (aperture number), **c:** Exine ornamentation, **d:** Polar view (aperture number)

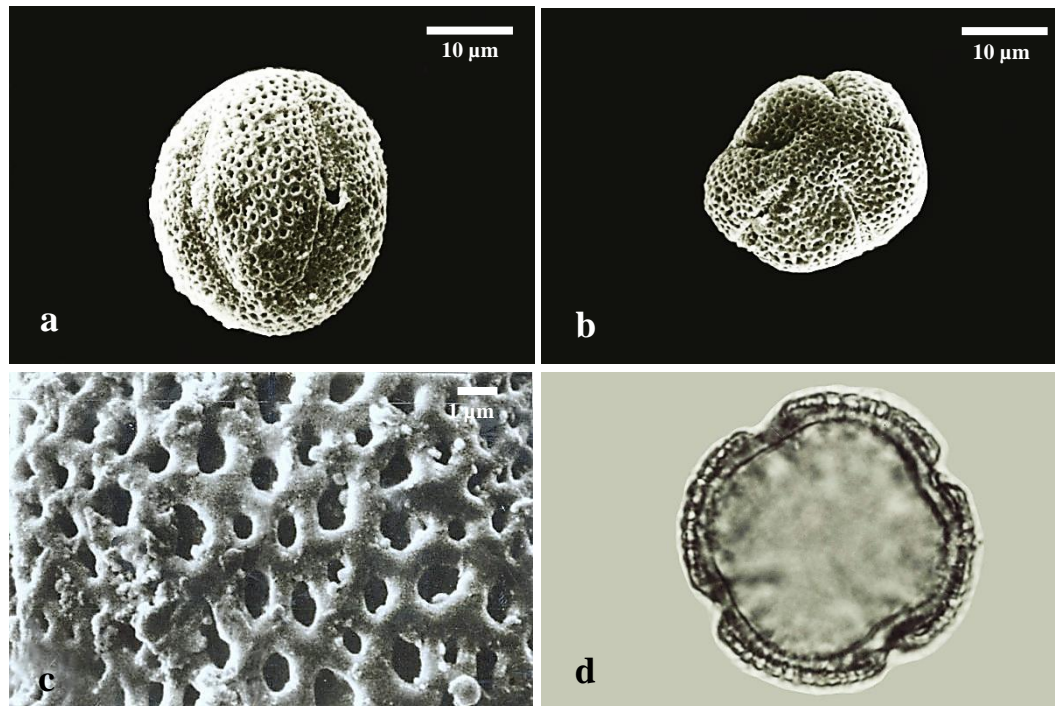


Plate 12. SEM (a-c) and LM (d) photomicrographs of *Poncirus trifoliata* pollen grains; **a:** Equatorial view (colporate), **b:** Polar view (aperture number), **c:** Exine ornamentation, **d:** Polar view (aperture number)

Apertures types

The types of apertures were either colpate or colporate and ranged from three to five in number. The variations in the type and number of apertures were found to be within the same taxa and the same anther as well. Five groups of aperture types were found; 1) the first group included three taxa characterized by tri-tetra-colporate aperture types, *C. limetta* (Plate 5a and b), *C. reshni* (Plate 7a, b and d) and *X Citrofortunella floridana* (Plate 11a, b and d). 2). The

second group also included three taxa characterized by tetra-penta-colporate aperture types in *C. aurantifolia* (Plate 1a, b and d), *C. reticulata* (Plate 8 a, b and d) and *P. trifoliata* (Plate 12a, b and c). 3). The third group has only *F. margarita* which included the tetra-penta-colporate types, in addition to the tri-colporate ones (Plate 10a, b, d and e). 4) The taxa in the fourth group were characterized by tri-tetra-colpate and tri-tetra-colporate aperture types in *C. grandis* (Plate 3a, b, c and e) and *C. sinensis* (Plate 9a and b). 5) Finally, group five comprised *C. aurantium*, *C. latifolia* and *C. paradisi* with pollen grains that have tetra-

penta-colpate and tetra-penta-colporate types of apertures (Plate 2a, b, c and d; Plate 4a, b, c and e and Plate 6a and c), respectively.

The ecto-aperture colpi, in all the studied taxa were long, wide, with rounded or pointed ends, equally spaced around the equator. They were characterized by uneven margins and covered with granular membranes. The mean colpi length varied within the studied taxa from a minimum of 20.00 μm in both *F. margarita* and *X Citrofortunella floridana* to a maximum of 31.80 μm in *C. grandis*. Moreover, the mean mesocolpium diameter varied from 9.36 μm in *C. aurantium* and *C. latifolia* to 12.72 μm in *C. limetta*. The endo-apertures pori were lalongate in all the studied taxa, where the ora width ranged from 6.08 to 6.40 μm in *F. margarita*, *X Citrofortunella floridana* and *P. trifoliata*; slightly wider from 6.80 to 7.30 μm in *C. reticulata*, *C. paradisi*, *C. sinensis* and *C. limetta* and more than 7.30 μm in the rest of the taxa. The amb shapes are mostly rounded- triangular or square, and sometimes both shapes are found in the same taxon. The pollen amb was of two shapes; rounded-triangular and square in *C. grandis* (Plate 3c and e), *C. limetta* (Plate 5a and b), *C. reshni* (Plate 7b and d), *C. sinensis* (Plate 9a and b), and *X Citrofortunella floridana* (Plate 11b and d), while it was also of another two shapes; rounded and square in *C. aurantifolia* (Plate 1b and d), *C. aurantium* (Plate 2b), *C. latifolia* (Plate 4c and e), *C. paradisi* (Plate 6a and c), *C. reticulata* (Plate 8b and d) and *P. trifoliata* (Plate 12b and d). Besides, the amb was of three shapes; rounded-triangular, rounded and square in *F. margarita* (Plate 10b, d and e).

Exine ornamentations

The exine is considerably thin; it was 2.40 μm thick in all the studied taxa, except in *C. aurantium* as it was 2.70 μm . The exine ornamentation of the pollen grains of the studied taxa, as observed by the scanning electron microscope, appeared in four different types. The first type was tectate perforate with smooth tectum, which is provided by more or less rounded pores in *C. grandis* (Plate 3d), *C. paradisi* (Plate 6b) and *C. sinensis* (Plate 9c). The second type was tectate perforate to microreticulate with latimurate reticulum, which is characterized by more or less straight and smooth muri and rounded to oval small sized lumina in *C. reshni* (Plate 7c), and *C. reticulata* (Plate 8c). The third type was foveolate with latimurate reticulum, which is characterized by more or less straight and smooth muri and nearly rounded large-sized lumina in *C. aurantium* (Plate 2c and d), *F. margarita* (Plate 10c), *X Citrofortunella floridana* (Plate 11c) and *P. trifoliata* (Plate 12c). The fourth type was reticulate with angustimurate reticulum, which is characterized by straight and rough muri and the lumina were different in size and shape in *C. aurantifolia* (Plate 1c), *C. latifolia* (Plate 4d) and *C. limetta* (Plate 5c).

Pollen types

Accordingly, the studied taxa can be classified into three different groups according to their pollen characters. The first group included five taxa; *C. grandis*, *C. limetta*, *C. paradise*, *C. sinensis* and *P. trifoliata*. These five taxa were characterized by the biggest pollen size, where the

polar axis length was more than 32.20 μm , with prolate-spheroidal pollen, colpi length more than 26.44 μm and mesocolpium diameter exceed 10.30 μm . The second group included five taxa viz. *C. aurantifolia*, *C. aurantium*, *C. latifolia*, *C. reshni* and *C. reticulata*. These taxa have medium polar axis length, ranged from 29.80 to 31.58 μm with prolate-spheroidal and sub-prolate pollen, colpi length ranged from 24.48 to 26.44 μm and mesocolpium diameter ranged from 9.36 to 10.30 μm . Meanwhile, the third group included *F. margarita* and *X Citrofortunella floridana*. Both species have the polar axis length ranging from 26.00 to 26.60 μm , oblate-spheroidal or prolate-spheroidal pollen, with shorter colpi ranging from 20.96 to 21.02 μm and mesocolpium diameter of about 9.82 μm .

In summary, by using pollen morphological characters, it is very difficult to construct pollen key for the studied *Citrus* species, and its related genera, because of the great similarities among them in shape, aperture, and exine ornamentation

4. Discussion

The pollen morphological characters and ultrastructure have been used to identify and distinguish between species and cultivars of fruit trees (Asma, 2008; Gilani *et al.*, 2010 and Nikolić and Milatović, 2016). *Citrus* and its related two genera, *Fortunella* and *Poncirus*, are considered one of the important economic and medicinal fruits in the world; they are rich plants in vitamin C and volatile oils (Scora, 1988). However, there are no reports on pollen morphology of *Citrus* species in Egypt. Inyama *et al.*, (2015) found that palynological characters were useful in delimiting six studied *Citrus* species. They could be exploited in conjunction with other evidence in species identification and characterization, while they were insignificant in the reclassification of the investigated taxa.

In the present study, palynological investigations indicated that variations in pollen morphological characters were of taxonomic significance. In particular, the twelve studied taxa were found to be significantly different from each other in six quantitative pollen characters; this includes polar length, equatorial diameter, colpi length, ora length, ora diameter, mesocolpi diameter. While the mean ratio of the polar length and the equatorial diameter (P/E) and the exine thickness were insignificantly different from each other. These results were in agreement with those reported by Breis *et al.*, (1993) and Mohammad *et al.*, (1999). The pollen shape varies from oblate-spheroidal, prolate-spheroidal to subprolate in all the studied taxa. This finding agrees with that found by Ye *et al.*, (1981) and Mohammad *et al.*, (1999). The variations of pollen size were suggested by Kozaki and Hirai, (1986) and Mohammad *et al.*, (1999) where they reported that pollen grain of *C. grandis* and *P. trifoliata* had larger pollen than *C. latifolia*, *C. limetta* and *F. margarita*, while those of *C. aurantium*, *C. sinensis* and *C. reshni* were intermediate in size. These suggestions were in agreement with the results of the present study where the studied taxa were classified into three different groups according to their pollen size. The first group included *C. grandis*, *C. limetta*, *C. paradise*, *C. sinensis* and *P. trifoliata*, which have the largest pollen grains, where the polar axis length ranged from 32.20 to 34.48 μm , while the equatorial

diameter ranged from 29.58 to 33.44 μm . The second group which included *C. aurantifolia*, *C. aurantium*, *C. latifolia*, *C. reshni* and *C. reticulata* had medium sized pollen grains, where the polar axis length ranged from 29.80 to 31.58 μm , while the equatorial diameter ranged from 26.42 to 28.27 μm . Moreover, the third group included two taxa *F. margarita* and *X Citrofortunella floridana* with the smallest pollen grains, where the polar axis length ranged from 26.04 to 26.56 μm , while the equatorial diameter ranged from 26.12 to 26.22 μm . On the contrary, these groups did not coordinate with Al-Anbari *et al.*, (2015), who recognized four groups in the Iraqi pollen grains based on pollen size and exine ornamentation.

Meanwhile, the most variable characters found in the present investigation were within the number and type of apertures, exine ornamentations, ora width as well as mesocolpium diameters. This was in line with Ye *et al.*, (1981) and Mohammad *et al.*, (1999).

Grant *et al.*, (2000) found considerable variation in pollen morphology of subfamily Aurantioideae, which divided the studied taxa into five pollen types. The differences include aperture number, ecto-colpus shape and size, exine ornamentation and wall structure. When designating pollen types for the subfamily Aurantioideae, the principal characters used were the aperture number and exine ornamentation. These characters were in harmony with the obtained results and as a conclusion, the aperture type and ora size were the most distinguished characters in the circumscription of the studied taxa. According to the type and number of apertures, five types were observed in the studied taxa. Type (1) Tri-tetra-colporate was found in *C. limetta*, *C. reshni* and *X Citrofortunella floridana*. Type (2) Tetra-penta-colporate was found in *C. aurantifolia*, *C. reticulata* and *P. trifoliata*. Type (3) Tri-tetra-penta-colporate was found in *F. margarita*. Type (4) included both "tri-tetra-colpate and tri-tetra-colporate" and was found in *C. grandis* and *C. sinensis*. Finally, type (5) included both "tetra-penta-colpate and tetra-penta-colporate" and was found in *C. aurantium*, *C. latifolia* and *C. paradisi*. These multi types of pollen apertures were found in the studied species from the same anther which may be due to chromosomal abnormalities as mentioned by Stace *et al.*, (1993).

Moreover, the exine thickness was the same in all the studied taxa and considered as an insignificant character, while the exine ornamentations showed great variations in the sculpturing types and have taxonomic value in the classification of the studied taxa, where it was diversified from tectate-perforate, tectate-perforate to microreticulate, foveolate or reticulate. According to the exine ornamentations, four different types were observed. Type (1) was tectate-perforate in *C. grandis*, *C. paradisi* and *C. sinensis*. Type (2) was tectate-perforate to microreticulate in *C. reshni* and *C. reticulate*, while Type (3) was foveolate with latimurate reticulum in *C. aurantium*, *F. margarita*, *X Citrofortunella floridana* and *P. trifoliata*. Type (4) was reticulate with angustimurate reticulum, in *C. aurantifolia*, *C. latifolia* and *C. limetta*. These findings agree with those found by Ye *et al.*, (1981) and Mohammad *et al.*, (1999), while disagreeing with the results of Kozaki and Hirai (1986) who stated that the exine patterns were sub-reticulate in the species of *Citrus*, *Poncirus*, *X Citrofortunella floridana* and *Fortunella*.

5. Conclusions

In the present investigation, the pollen size, pollen shape, colpi length, the apertures number and type, ora size, amb shape, mesocolpium diameter, and exine ornamentation were the most distinguished characters in the circumscription of the studied taxa. All the studied pollen grain characters except ora shape and exine thickness could be considered as of taxonomic value in the differentiation among the closely related taxa of *Citrus*, *Fortunella*, *X Citrofortunella floridana* and *Poncirus* in the present study.

References

- Abobatta WF. 2019. *Citrus* Varieties in Egypt: An Impression. *Int. Res. J. Applied Sci.*, 1:63-66.
- Al-Anbari AK, Barusux S, Pornponggrueng P and Theerakulpisut P. 2015. Pollen grain morphology of *Citrus* (Rutaceae) In: Iraq. International Conference on Plant, Marine and Environmental Sciences (PMES-2015) Jan. 1-2, 2015 Kuala Lumpur (Malaysia), pp. 8-13.
- Asma BM. 2008. Determination of pollen viability, germination ratios and morphology of eight apricot genotypes. *Afr. J. Biotechnol.*, 7:4269-4273.
- Avci S, Sancak C, Can A, Acar A and Pinar N. 2013. Pollen morphology of the genus *Onobrychis* (Fabaceae) in Turkey. *Turk J Bot.*, 37(4):669-681. DOI: 10.3906/bot-1207-52.
- Barrett HC and Rhodes AM. 1976. A numerical taxonomic study of affinity relationships in cultivated *Citrus* and its close relatives, *Syst Bot*, 1:105-136. <http://dx.doi.org/10.2307/2418763>.
- Boulos L. 1999. **Flora of Egypt**. Vol. 2, Al Hadara Publishing, Cairo, Egypt.
- Brandis D. 1874. **Rutaceae: The forest flora of north-west and central India**. A. Constable St Company, Limited edition, London, pp. 50-56.
- Breis FB, Sanchez CP, Gilabert CE and Castillo MEC. 1993. The pollen morphology of *Citrus limon* cv. "Verna" from the Murcia region. *S.E. Anales de Biología*, 19:63-69.
- Chase MW, Morton CM and Kallunki JA. 1999. Phylogenetic relationships of Rutaceae: A cladistic analysis of the subfamilies using evidence from RBC and ATP sequence variation. *Am. J. Bot.*, 86(8):1191-1199.
- Davis PH and Heywood VH. 1973. **Principles of Angiosperm Taxonomy**. Robert E. Krieger Publishing Company, Huntington, New York.
- Engler A. 1931. Rutaceae. In: Engler A, and Prantl k, (editors). **Die Natürlichen Pflanzenfamilien**, Second edition, Engelmann, Leipzig, 19a:187-359.
- Erdtman G. 1952. **Pollen morphology and plant taxonomy of angiosperms**. Almqvist and Wiksell, Stockholm.
- Faegri K. 1956. Recent trends in Palynology. *Bot Rev*, 22:639-664.
- Gilani SA, Qureshi RA, Khan AM and Potter D. 2010. Morphological characterization of the pollens of the selected species of genus *Prunus* Linn. from northern Pakistan. *Afr. J. Biotechnol.*, 9:2872-2879.
- Grant M, Blackmore S and Morton C. 2000. Pollen morphology of the sub-family Aurantioideae (Rutaceae). *Grana*, 39:8-26.
- Hamza M and Tate B. 2017. Egyptian Orange Exports Thrives Thanks to Currency Devaluation. United States Department of Agriculture, Foreign Agricultural Service. Gain Report, Global Agricultural Information Network.

- Hodgson RW. 1965. Taxonomy and Nomenclature in *Citrus* fruits. In: Advances in Agricultural Science and their application. *The Madras Agr. J.*, Coimbatore, 317-333.
- Inyama CN, Osuoha VUN, Mbagwu FN and Duru CM. 2015. Systematic Significance of Pollen Morphology of *Citrus* (Rutaceae) from Owerri. *Med Aromat Plants*, 4-191 DOI:10.4172/2167-0412.1000191.
- Kozaki I and Hirai M. 1986. **Pollen ultrastructure of *Citrus* for taxonomic identification.** In: Development of new technology for identification and classification of tree crops and ornamentals (edited by Kitaura K Akihama T; Kukimura H; Nakajima K; Rori M and Kozaki I). Fruit tree Research Station, Ministry of Agriculture, Forestry and Fisheries, Japan pp 11-17.
- Mohammad P, Shirraishi M, Toda J, Aguja SE and Ohmine Y. 1999. Characterization with scanning electron microscope of the pollen of *Citrus* plant. *Sarhad Journal of Agriculture*, **15**(1):29-35 [Cited from Horticultural Science Abstracts **69**(8)].
- Marcovitch VV. 1926. Indeeing van het geslacht *Citrus*, Landbouw, **2**(4).
- Mary A and Gopal GV. 2018. Pollen Morphology of selected taxa of Ehretiaceae from Western Ghats, India. *Ann. Plant Sci.*, **7**(11):2446-2450 <http://dx.doi.org/10.21746/aps.2018.7.11.1>.
- Moore GA. 2001. Oranges and lemons: Clues to the taxonomy of *Citrus* from molecular markers. *Trends Genet.*, **17**(9):536-40.
- Nicolosi E. 2007. **Origin and taxonomy.** In: Khan IA (editor). *Citrus* Genetics, Breeding and Biotechnology. CAB International, Wallingford, United Kingdom, pp. 19-44.
- Nikolić D, and Milatović D. 2016. Pollen morphology of some sweet cherry cultivars observed by scanning electron microscopy. *Acta Hortic.*, **1139**:369-374 DOI:10.17660/ActaHortic.2016.1139.64.
- Roxburgh W. 1832. **Flora Indica.** 2nd ed. by Carey W 3. Thacker and Company, Calcutta and Parbury, Allen and Company, London.
- Saad SI and Taia WK. 1988. Palynological studies of some species in the genus *Astragalus* L. (Leguminosae) in *Egypt. Arab Gulf J Sci Res*, **B6**(2):227-243.
- Singh Z and Singh L. 2008. **The SAS System for Windows**, Version 9.13, SAS Institute Inc., Cary, NC, USA.
- Scora RW. 1975. On the history and origin of *Citrus*. *Bulletin of the Torrey Botanical Club.*, **102**:369-375. <http://dx.doi.org/10.2307/2484763>.
- Scora RW. 1988. Biochemistry. Taxonomy and evolution of modern cultivated *Citrus*. Proceeding of International Society of Citriculture, **1**:277-289.
- Sharma OP. 1993. **Plant Taxonomy.** Tata McGraw-Hill. Publishing Company. New Delhi-New York, pp. 244-247.
- Snedecor GW and Cochran WG. 1990. **Statistical methods** 7th Ed. The Iowa State Univ. Press Ames Iowa U.S.A., pp. 593.
- Stace HM, Armstrong JA and James SH. 1993. Cytoevolutionary patterns in Rutaceae. *Plant Syst Evol*, **187**:1-28.
- Swingle WT. 1943. The botany of *Citrus* and its wild relatives in the orange subfamily. In: **The *Citrus* industry.** Webber, HJ and Batchelor, LD (editors), University of California Press, Berkeley **1**:128-474.
- Swingle WT and Reece PC. 1967. The botany of *Citrus* and its wild relatives. In: **The *Citrus* industry.** Reuther W, Webber HJ and Batchelor LD (editors). University of California Press, Berkeley, **1**:190-430.
- Taia WK. 2004. Palynological Study within Tribe *Trifolieae* (Leguminosae). *Pak J Biol Sci*, **7**(7):1303-1315.
- Taia WK and Sheha MA. 2001. Palynological study within some *Atriplex* species. *Bio Sci. Res. Bull.*, **17**(2):91-97.
- Täckholm V. 1974. **Students Flora of Egypt.** Cairo University, Beirut, **2**:334-335.
- Tanaka T. 1936. The taxonomy and nomenclature of Rutaceae-Aurantioideae. *Blumea - Biodiversity, Evolution and Biogeography of Plants*, **2**(2):101-110.
- Tanaka T. 1977. Fundamental discussion of *Citrus* classification. *Stud Citrol*, **14**:1-6.
- Ye YM; Kong Y; Zheng XH. 1981. Studies on Pollen Morphology of *Citrus* Plants. In: Matsumoto K. (ed.) Proc. Int. Soc., Citriculture, Vol. 1. I.S.C. Printing Co., Misaki-cho, Japan, pp. 23-25.

Direct Somatic Embryogenesis and Regeneration of an Indonesian orchid *Phalaenopsis amabilis* (L.) Blume under a Variety of Plant Growth Regulators, Light Regime, and Organic Substances

Windi Mose¹, Budi Setiadi Daryono¹, Ari Indrianto¹, Aziz Purwantoro² and Endang Semiarti^{1,*}

¹Graduate School, Faculty of Biology, Universitas Gadjah Mada, Teknika Selatan, ² Faculty of Agriculture, Universitas Gadjah Mada, Bulaksumur, Yogyakarta 55281, Indonesia

Received: September 3, 2019; Revised: December 29, 2019; Accepted: January 31, 2020

Abstract

Phalaenopsis amabilis is an Indonesian native orchid often used as parent to produce various orchid hybrids. However, this natural orchid is increasingly difficult to find growing naturally in the forest due to over-harvesting and destruction of its natural habitat. The objectives of this study were to investigate the effect of plant growth regulators (PGRs), light regime, and organic substances on the induction and regeneration of somatic embryos (SEs) of *P. amabilis* orchid. Root, stem, leaf, and protocorm explants were cultured on New Phalaenopsis (NP) medium supplemented with thidiazuron (TDZ) (0.0, 1.0, 2.0, 3.0 mg L⁻¹) in combination with α -naphthalene acetic acid (NAA), 2,4-dichlorophenoxyacetic acid (2,4-D), and indole acetic acid (IAA) with concentrations of 1.0, 2.0, and 3.0 mg L⁻¹. Light and dark conditions were tested for their effectiveness to induce the formation of SEs, and the resulting SEs were cultured on NP medium supplemented with various organic substances (banana, bean sprout, tomato, and potato extracts) with concentrations of 50, 100, 150, 200, and 250 g L⁻¹. Results showed that the highest number of SEs (36.45 \pm 0.26 embryos) was found in stem explants cultured in NP medium supplemented with 3.0 mg L⁻¹ TDZ and 1 mg L⁻¹ NAA. When explants were cultured in dark conditions, the number of SEs significantly increased with the highest number of SEs achieved in stem explants culture in 3.0 mg L⁻¹ TDZ and 1.0 mg L⁻¹ NAA. NP medium supplemented with 150 g L⁻¹ tomato extract was the most effective medium for growth of SEs-derived plants. Seedlings of this treatment produced an average of 4.20 \pm 0.17 leaves and 3.20 \pm 0.11 roots after 12 weeks of culture. In conclusion, SEs can be produced effectively from stem explants with a combination of 3.0 mg L⁻¹ TDZ and 1.0 mg L⁻¹ NAA, one month early in dark conditions, and regenerated on NP medium with addition of tomato extract.

Keywords Organic substances, plant growth regulators, *Phalaenopsis amabilis*, somatic embryogenesis

1. Introduction

Orchidaceae is one of the largest and diverse families of flowering plants. About 5000 of 20,000 species of orchid live naturally and distributed throughout Indonesia (Schuiteman, 2010). *P. amabilis* is one of the most important orchids in Indonesia. This orchid has preeminent flowering characteristics with beautiful flower shape and graceful inflorescence; it also has been used extensively in the breeding program as parent plant to create new superior hybrids (Semiarti *et al.*, 2010). However, the availability of this orchid is hindered due to illegal trade and deforestation; hence, other means of propagation would be required such as tissue culture technique.

Somatic embryogenesis is a powerful system for plant mass propagation through tissue culture technique and has been extensively used for orchid conservation (Bhattacharyya *et al.*, 2016; Moradi *et al.*, 2017). In plant tissue culture systems, the addition of plant growth regulators (PGRs) into the culture medium is the most

preferred way to induce somatic embryogenesis (Borpuzari and Borthakur, 2016; Méndez-Hernández *et al.*, 2019). Usually, the combination of auxin and cytokinin is the most utilized PGRs during the initiation of somatic embryos (SEs) in orchid plants (Shen *et al.*, 2018; Soonthornkalump *et al.*, 2019; Zanello and Cardoso, 2019). Previously, we successfully developed an efficient protocol to induce SEs formation using thidiazuron (TDZ) (Mose *et al.*, 2017).

Structurally, TDZ is different from natural purine-based cytokinins which have a typical 5-carbon side chains (Tarkowski *et al.*, 2009). However, TDZ's action in development is much closed to cytokinin metabolism and associated with isopentenyl adenine that lead to rapid cell division and initiation of organogenesis (Guo *et al.*, 2011). TDZ is widely used in plant somatic embryogenesis, either alone or conjugated with other PGRs (Hong *et al.*, 2010; Guo *et al.*, 2011). Jainol and Gansau (2017) reported that combination of TDZ and α -naphthalene acetic acid (NAA) successfully induced high number of SEs from leaf tip explants of *Dimorphorchis lowii* orchid. Moreover, Moradi

* Corresponding author e-mail: endsemi@ugm.ac.id.

et al. (2017) reported that combination of TDZ and 2,4-D induced SEs formation from single node, crown, apical bud, and protocorm explants of *Epipactis veratrifolia* orchid.

It has been found that incubation of explants with NAA or 2,4-D during somatic embryogenesis induction produces an increase of endogenous auxin in some species (Pasternak *et al.*, 2002; Vondráková *et al.*, 2011). Ayil-Gutiérrez *et al.* (2013) reported that the addition of NAA in the culture medium during somatic embryogenesis induction increased the free IAA and IAA amide conjugates levels in *Coffea canephora* explants, where part of the increase of the auxin content is due to de novo synthesis. Ceccarellil *et al.* (2000) reported that 2,4-D induced tryptophan-dependent synthesis of IAA in *Daucus carota* suspension culture during the induction of SEs. Furthermore, considerable efforts have been made to identify light conditions that are needed to optimize the protocol for somatic embryogenesis induction in plants (Baharan *et al.*, 2015). Light is one of the crucial factors affecting plant tissue culture (Hew and Yong, 2004). The intensity and condition of light has been reported to affect somatic embryogenesis induction in *Cattleya* and *Oncidium* orchids (Cueva-Agila *et al.*, 2016; Sampaio *et al.*, 2010). In *Phalaenopsis* orchid, low intensity of light is known to accelerate *in vitro* shoot formation (Tanaka *et al.*, 1988).

Various kinds of organic substances have also been used in large-scale for orchid tissue culture including banana pulp, potato extract, coconut water, corn extract, and beef extract (Nambiar *et al.*, 2012). Yong *et al.* (2009) reported that certain organic substances contain growth factors such as cytokinin and auxin which were found to have potential for promoting growth of tissue cultured plants. *Trans*-zeatin riboside (ZR) and *trans*-zeatin (Z) which are cytokinins contained in banana pulp (Ge *et al.*, 2008), auxin and gibberellin in tomato extract (Shuiying *et al.*, 2016) and bean sprout extract (Sanjaya *et al.*, 2019), and cytokinin in potato extract (Anstis and Northcote, 1975; Lomin *et al.*, 2018) are very beneficial for balancing nutrient availability in the culture medium.

Organic substances promote growth of orchid seeds, increase the size of protocorm-like bodies (PLBs), and help regeneration of plantlets (Abbaszadeh *et al.*, 2018; Chew *et al.*, 2018; Dulić *et al.*, 2018). It was reported in Abbaszadeh *et al.* (2018) that organic substances contained not only PGRs, but also vitamins, inorganic ions, amino acids, and sugars. Hence, the present investigation was to know the effect of PGRs and light regime on the induction of SEs, and the effect of organic substances on the regeneration of SEs in *P. amabilis* orchid.

2. Materials and Methods

2.1. Plant materials, growth conditions, and culture medium

Green siliques were collected from *P. amabilis* potted plants following 120 days of self-pollination. The siliques were dipped in 70% ethanol, passed over a Bunsen gas burner fire and waited until the fire went out. This process was repeated three times. After being sterilized and cut open the seeds were taken out and sown on New Phalaenopsis (NP) solid medium (Islam *et al.*, 1998;

Semiarti *et al.*, 2010). Cultures were maintained at a temperature of $25 \pm 1^\circ\text{C}$ with $14 \mu\text{mol m}^{-2} \text{s}^{-1}$ intensity of continuous light.

2.2. PGRs treatment to induce SEs formation

To evaluate the effect of PGRs on SEs formation, we performed a test with 144 combinations of four kinds of explants (protocorm, leaf, stem, and root), three different kinds of auxins (NAA, 2,4-D, and IAA), and 12 combinations of TDZ concentrations (0.0, 1.0, 2.0, 3.0 mg L⁻¹) and NAA or 2,4-D or IAA concentrations (1.0, 2.0, 3.0 mg L⁻¹).

Roots, stems, and leaves of 6-month-old *in vitro* plantlets and 4-week-old protocorms were used as explants (Figure 4a, f, k, and p). Explants were cut transversely (± 0.5 cm) and planted on NP solid medium supplemented with the combination of PGRs. Cultures were maintained at a temperature of $25 \pm 1^\circ\text{C}$ in dark conditions for the first 14 days of culture and then transferred to 16 h light conditions. Subcultures were conducted every two weeks and observed every day using dissecting microscope (Eschenbach, Germany). Photographs were taken once a week for eight weeks using digital camera (Canon Power Shot A2400, Japan).

2.3. Light treatment for SEs formation

In order to determine the role of light and dark conditions in the formation of SEs in *P. amabilis* orchid, we selected the best combination of TDZ and NAA, or 2,4-D, or IAA in all types of explants and repeated the assays culturing the explants in the dark or in 16 h light photoperiod for the first month of culture. After one month, cultures in dark conditions were transferred to 16 h light conditions. Cultures were maintained with a temperature of $25 \pm 1^\circ\text{C}$. Observations were conducted every day using dissecting microscope and photographed once a week for eight weeks using digital camera.

2.4. Histological analysis of SEs development

Histological sections of SEs were prepared using paraffin method according to Ruzin (1999). The sections were examined under light microscope (Olympus, Japan) and photographed using Optilab Microscope Camera (Miconos, Indonesia).

2.5. Additional organic substances in the culture media for plant regeneration

Four different organic substances (banana, bean sprout, tomato, and potato extracts) with five different concentrations (50, 100, 150, 200, 250 g L⁻¹) were evaluated for SEs regeneration. Banana (*Musa paradisiaca* var. *sapientum*), bean sprout from mung bean (*Vigna radiata*), tomato (*Lycopersicon esculentum*) cultivar 'Arthaloka', and potato (*Solanum tuberosum*) cultivar 'Granola' was obtained from local markets. Banana, tomato, and potato were separately prepared by cutting them into 1 cm³ cubes, while bean sprout was cut into two parts. Each material was homogenized, and homogenate was filtered through a steel mesh with a 150 μm pore size. Each organic substance was added into the media prior to autoclaving. Mature SEs produced from the best combination of PGRs in all types of explants (experiment 2.2) that have formed leaf primordia were planted on NP solid medium supplemented with organic substances. NP basal medium without addition of organic substances was

used as control. Cultures were maintained at a temperature of $25 \pm 1^\circ\text{C}$ with $14 \mu\text{mol m}^{-2} \text{s}^{-1}$ intensity of continuous light. Observations were conducted using dissecting microscope and photographed once a week for 12 weeks using a digital camera.

2.6. Experimental design and data analysis

In the experiments, each explant and plant were referred to as one replicate. Twenty replicates for SEs induction and regeneration were used in each experiment. For SEs induction, explants were cultured in Petri dishes ($\text{Ø}100 \text{ mm} \times 15 \text{ mm}$). Each Petri dish contained five explants. For regeneration of SEs, 100 mL culture flasks were used. Each flask contained 3 – 4 plantlets. Data were subjected to analysis of variance (ANOVA) and comparisons between the mean values of treatment made by the Duncan's Multiple Range Test calculated at the confidence level of $p \leq 0.05$. The statistical package SPSS (Version-22) was used for the analysis.

3. Results

3.1. Effect of PGRs on direct SEs formation

The results showed that among the treatments, the highest number of SEs (36.45 ± 0.26) was observed in stem explants cultured on NP medium supplemented with 3 mg L^{-1} TDZ and 1.0 mg L^{-1} NAA (Figure 1). Furthermore, we found that the combination of TDZ and 2,4-D highly inhibited SEs formation in all types of explants. SEs failed to form in root explants cultured at all concentrations of 2,4-D alone with no TDZ (Figure 2). In addition, root and leaf explants cultured on NP medium supplemented with 1.0 mg L^{-1} TDZ and 3.0 mg L^{-1} 2,4-D, and root explants cultured on NP medium supplemented with 1.0 mg L^{-1} TDZ and 2.0 mg L^{-1} 2,4-D did not form any embryos. In combination of TDZ and IAA, the highest number of SEs was found in stem explants cultured on NP medium supplemented with 3.0 mg L^{-1} TDZ and 1.0 mg L^{-1} IAA, resulted in 25.20 ± 1.96 embryos per explant (Figure 3).

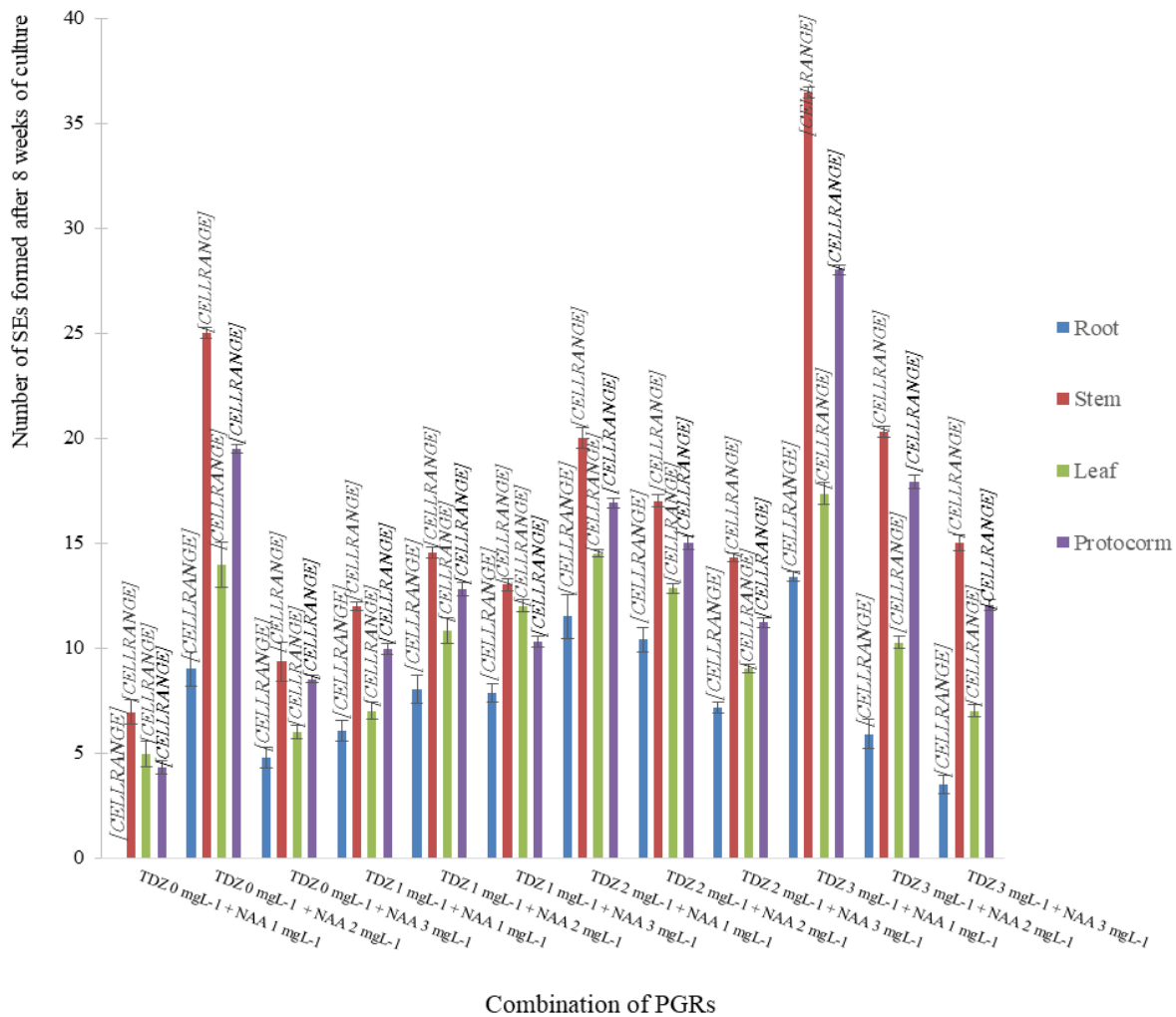


Figure 1. Effects of combination of TDZ and NAA on the formation of SEs from various types of explants in *Phalaenopsis amabilis*. Data in the bars followed by the same letters are not significantly different by Duncan's multiple range test at $p \leq 0.05$.

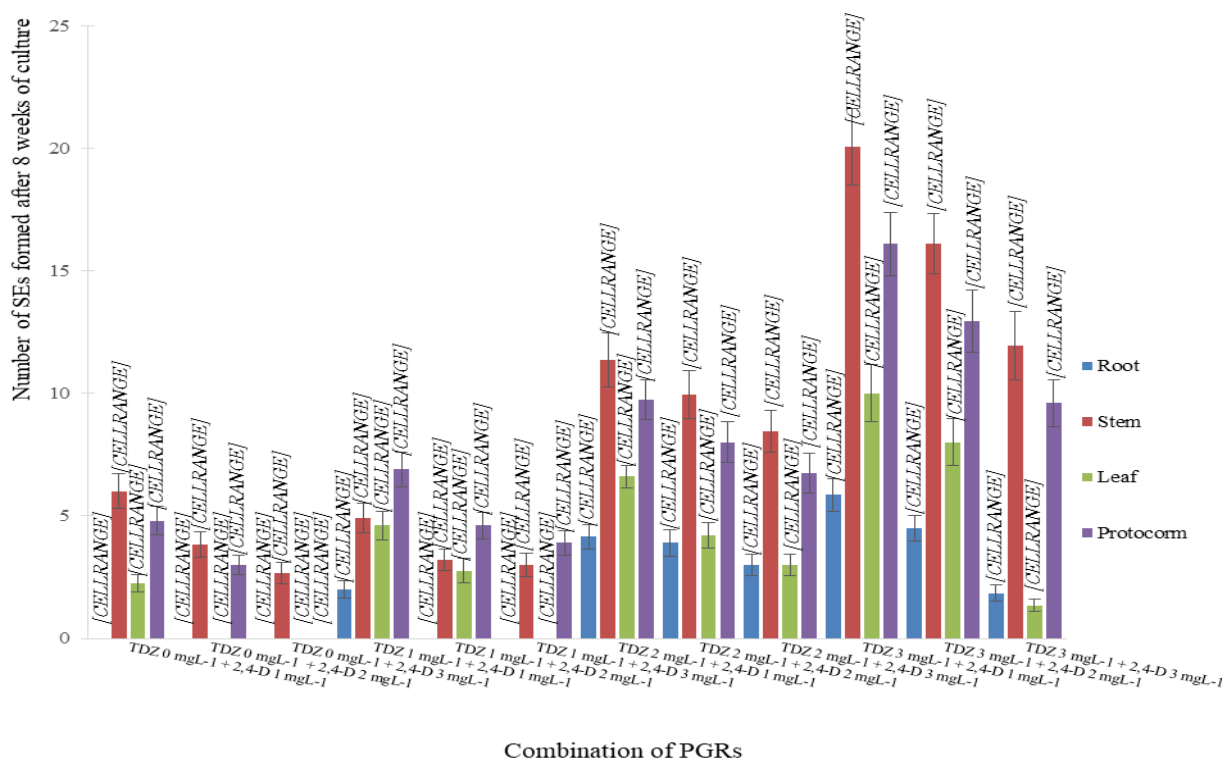


Figure 2. Effects of combination of TDZ and 2,4-D on the formation of SEs from various types of explants in *Phalaenopsis amabilis*. Data in the bars followed by the same letters are not significantly different by Duncan's multiple range test at $p \leq 0.05$.

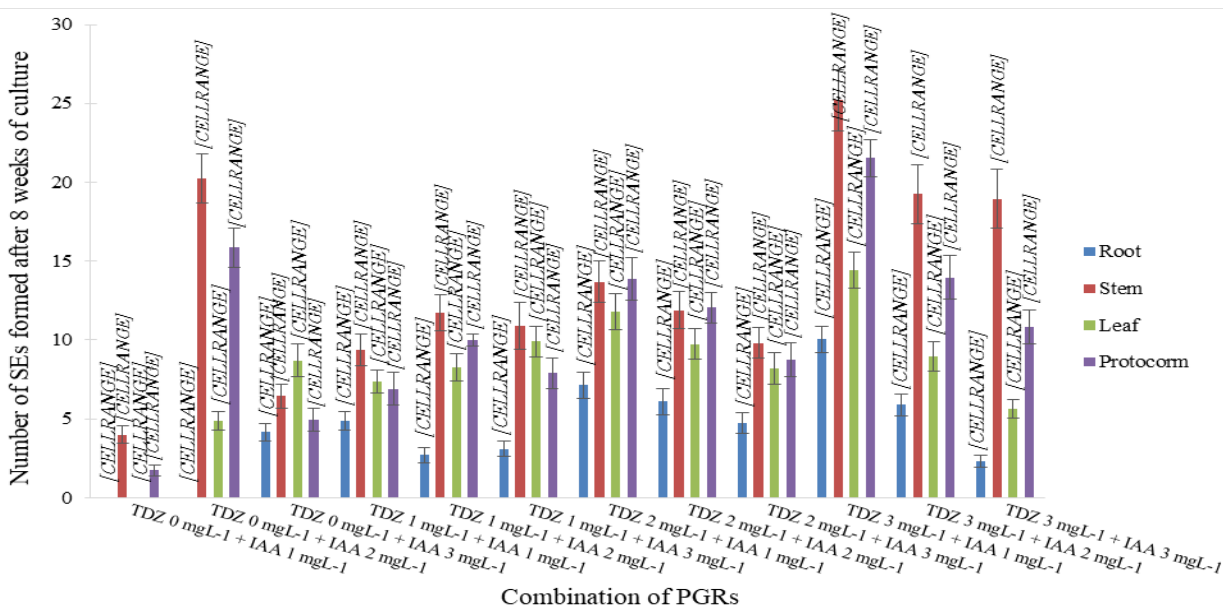


Figure 3. Effects of combination of TDZ and IAA on the formation of SEs from various types of explants in *Phalaenopsis amabilis*. Data in the bars followed by the same letters are not significantly different by Duncan's multiple range test at $p \leq 0.05$.

Histological analysis showed that pro-embryos consisted of small, thick-walled cells, and clearly distinguishable from the surrounding cells by the dense cytoplasm and conspicuous nucleus (Figure 5a). Pro-embryos enlarged and subsequently formed globular embryos with suspensor at the basal region (Figure 5b-c). Globular embryos developed into scutellar embryos with notch at the apical region of embryo (Figure 5d). Shoot apical meristem (SAM) eventually formed from the notch, surrounded by two leaf primordia, coleoptile, and procambium in the middle part of embryo (Figure 5e), marked the development of a mature embryo.

The present results showed that direct somatic embryogenesis was achieved in all treatments. After first subculture, pro-embryos emerged from the wounding site of protocorm and stem explants (Figure 4h and r), and from the tissue near the cut side of root and leaf explants (Figure 4c and m). These embryos further developed, progressively enlarged, became globular and eventually formed a distinctive feature on the apical region (Figure 4d, i, n, s) before forming leaf primordia (Figure 4e, j, o, and t).



Figure 4. Developmental stages of SEs of *Phalaenopsis amabilis* from various explants. (a-e) Root (f-j) stem (k-o) leaf and (p-t) protocorm explants, (b, g, l, q) Section of explants were cultured in the treatment medium, Pro-embryos appeared from the wounding area of stem (h) and protocorm (r) explants, and near the cut side of root (c) and leaf (m) explants, and subsequently formed globular structure (arrows), (d, i, n, s) Embryos formed a distinctive feature on the apical region (arrows), (e, j, o, and t) Embryos with leaf primordia (arrows). Scale bars (a, f, k, p – t): 100 μ M, Scale bars (b – e, g – j, l – o): 200 μ M.

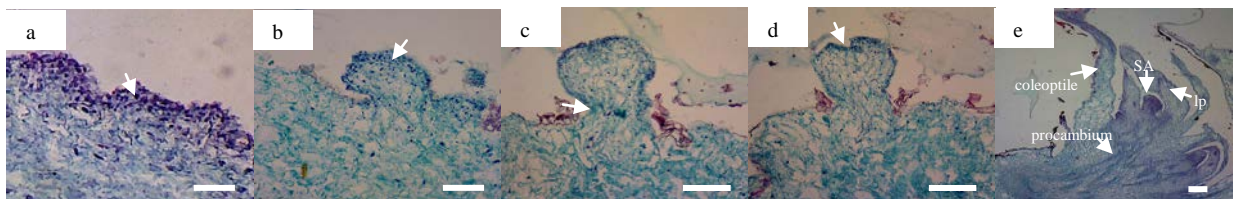


Figure 5. Anatomy of SEs development in *Phalaenopsis amabilis*. (a) Pro-embryos consisted of cells with large and densely-stained nuclei (arrow); (b) Pro-embryo developed into globular embryo (arrow) and formed suspensor (arrow) at the basal region (c); (d) Scutellar embryo with notch at the apical region (arrow); (e) Mature embryo consisted of SAM, leaf primordia (lp), coleoptile, and procambium. Scale bars: 200 μ m.

3.2. Effect of light regime during SEs formation

When explants were cultured in dark conditions for the first month of culture, higher number of SEs were obtained (Figure 6). The highest number of SEs was found in stem explants cultured on NP medium supplemented with 3 mg L⁻¹ TDZ and 1 mg L⁻¹ NAA, which gives values of 40.12 \pm 0.31 embryos per explant. Meanwhile, light conditions highly retarded SEs formation in all explants. Explants

formed whitish to yellow-green SEs in darkness (Figure 7a), and turned green after one week transferred to light conditions (Figure 7b). On the other hand, explants easily become browned and eventually necrotic in light conditions, and the SEs formation rate was reduced (Figure 7c-d). In both treatments, stem explants had the best embryogenic response than other types of explants.

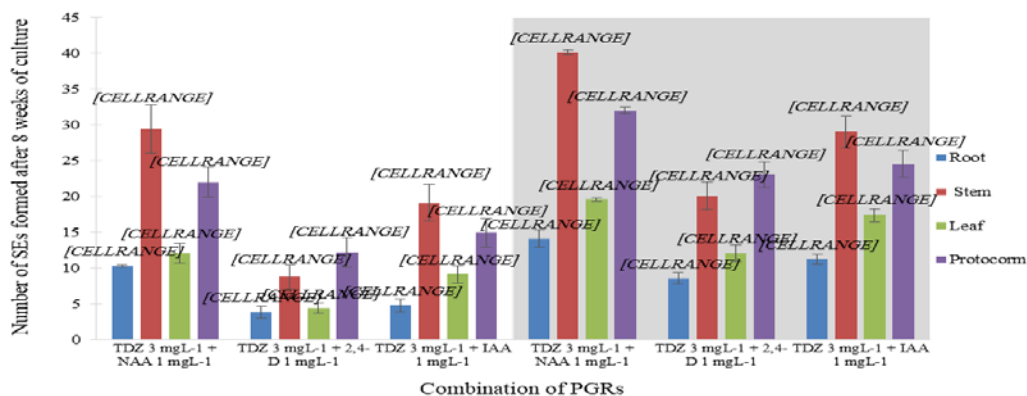


Figure 6. Effects of light regime on the formation of SEs from various types of explants in *Phalaenopsis amabilis*. Data in the bars followed by the same letters are not significantly different by Duncan's multiple range test at $p \leq 0.05$.

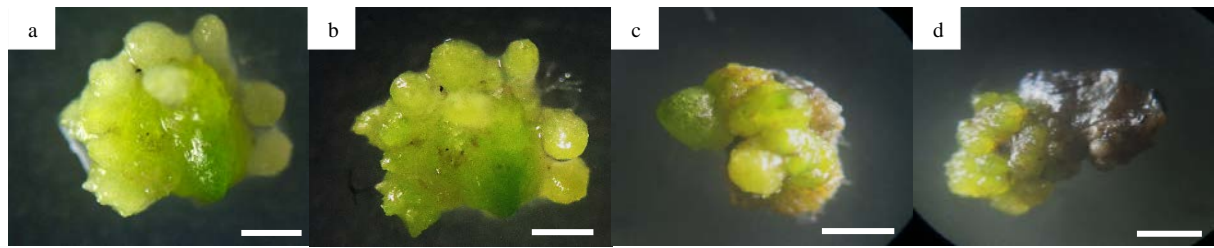


Figure 7. Growth of SEs after cultured in dark and light conditions for one month. SEs from stem explant cultured in dark conditions appeared whitish to yellow-green in color (a) and turned green after one week transferred to light conditions (b); Explant cultured in light conditions turned into brown and the number of embryos decreased (c-d). Scale bars: 500 μ m.

3.3. Effect of additional various organic substances on regeneration of SEs

SEs of *P. amabilis* responded variably when cultured on different organic substances. The seedling development process began with the formation of leaf primordia at the apical region of SEs (Figure 8a). First leaf initiated after 2

weeks of subculture (Figure 8b), followed by a formation of second leaf and first root one month later (Figure 8c). The formation of second root started after 8 weeks, and it was followed by the elongation of roots (Figure 8d). After 12 weeks of culture, a seedling could produce up to two leaves and two roots (Figure 8e).



Figure 8. Growth of SEs into plantlets on NP basal medium. (a) Eight-week-old mature SEs; (b) Leaf primordia fully grown into leaves after 2 weeks of subculture; (c) After 4 weeks, the second leaf and root has formed; (d) Plantlet after 8 weeks and (e) 12 weeks of culture. Scale bars: 0.5 cm.

The effects of organic substances on the regeneration of SEs into seedlings are shown in Table 1 and Figure 9. The results revealed that the regeneration of SEs had significantly enhanced by the addition of organic substances. Among the different organic substances, tomato extract was found to be the most effective. It was observed that SEs treated in NP medium containing 150 g

L^{-1} tomato extract successfully produced 4.20 ± 0.17 leaves after 12 weeks of culture with an average length of leaves at 25.21 ± 0.31 mm, and the average width of leaves at 8.06 ± 0.05 mm per responsive explant. Moreover, the addition of $150 \text{ mg } L^{-1}$ of tomato extract also promoted the highest number of roots (3.20 ± 0.11 roots) with an average length of roots at 25.03 ± 0.19 mm.

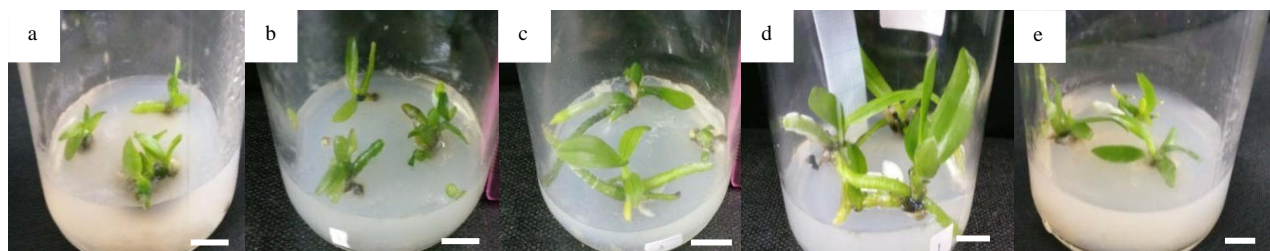


Figure 9. SE-derived plantlets after 12 weeks of culture on NP media supplemented with different organic substances. (a) Control; (b) Banana extract; (c) Bean sprout extract; (d) Tomato extract; (e) Potato extract. Scale bars: 1 cm.

Table 1. Effect of additional organic substances on regeneration of SEs after 12 weeks of culture

Organic substances (g L ⁻¹)	Number of leaves	Leaf length (mm ±SE)	Leaf width (mm ±SE)	Number of roots	Root length (mm ±SE)
Control	2.00 ±0.14 ^a	5.73 ±0.09 ^a	3.71 ±0.07 ^a	1.70 ±0.12 ^a	8.33 ±0.49 ^a
Banana					
50	2.15 ±0.16 ^{abc}	6.31 ±0.22 ^b	4.08 ±0.08 ^{bc}	1.90 ±0.12 ^{ab}	10.61 ±0.92 ^b
100	2.40 ±0.22 ^{abcd}	10.88 ±0.16 ^c	4.88 ±0.07 ^{de}	2.00 ±0.12 ^{abcd}	13.28 ±0.50 ^d
150	2.70 ±0.23 ^{def}	13.38 ±0.12 ^e	5.91 ±0.14 ^{hi}	2.40 ±0.11 ^{defghi}	16.29 ±0.78 ^{hi}
200	3.40 ±0.19 ^{gh}	11.26 ±0.18 ^{ef}	5.69 ±0.09 ^{gh}	2.35 ±0.13 ^{cdefgh}	14.56 ±0.50 ^{ef}
250	3.10 ±0.24 ^{fgh}	9.06 ±0.23 ^d	5.28 ±0.07 ^f	2.20 ±0.13 ^{bcdef}	11.03 ±0.11 ^{bc}
Bean sprout					
50	2.10 ±0.13 ^{ab}	11.00 ±0.11 ^c	3.92 ±0.03 ^b	2.10 ±0.14 ^{abcde}	14.34 ±0.85 ^e
100	2.30 ±0.17 ^{abcd}	14.57 ±0.11 ^b	4.21 ±0.05 ^c	2.25 ±0.14 ^{bcdefg}	17.51 ±0.62 ^d
150	3.15 ±0.19 ^{fgh}	19.04 ±0.18 ^k	4.86 ±0.06 ^{de}	2.50 ±0.13 ^{efghi}	20.39 ±0.13 ^m
200	3.55 ±0.17 ^h	17.35 ±0.17 ^j	5.33 ±0.05 ^f	2.70 ±0.10 ^{hi}	16.62 ±0.26 ^d
250	3.35 ±0.24 ^{gh}	15.81 ±0.10 ⁱ	5.00 ±0.05 ^e	2.30 ±0.14 ^{bcdefgh}	15.24 ±0.12 ^{fg}
Tomato					
50	3.00 ±0.17 ^{efgh}	17.80 ±0.25 ^j	6.68 ±0.03 ^j	2.10 ±0.12 ^{abcde}	19.69 ±0.18 ^l
100	3.55 ±0.22 ^h	21.00 ±0.32 ^l	7.44 ±0.06 ^l	2.50 ±0.11 ^{efghi}	22.00 ±1.02 ^o
150	4.20 ±0.17 ⁱ	25.21 ±0.31 ⁿ	8.06 ±0.05 ⁿ	3.20 ±0.11 ^j	25.03 ±0.19 ^p
200	3.60 ±0.11 ^h	23.09 ±0.26 ^m	7.64 ±0.02 ^m	2.80 ±0.13 ⁱ	21.26 ±0.13 ⁿ
250	3.45 ±0.18 ^h	18.57 ±0.15 ^k	7.06 ±0.07 ^k	2.70 ±0.12 ^{hi}	18.06 ±0.99 ^{jk}
Potato					
50	2.60 ±0.16 ^{bcdef}	7.36 ±0.14 ^c	4.69 ±0.05 ^d	1.95 ±0.15 ^{abc}	12.70 ±0.60 ^d
100	2.80 ±0.17 ^{defg}	11.61 ±0.15 ^f	5.04 ±0.04 ^e	2.40 ±0.13 ^{defghi}	16.58 ±0.40 ⁱ
150	3.20 ±0.15 ^{fgh}	15.31 ±0.13 ⁱ	5.66 ±0.04 ^g	2.65 ±0.13 ^{sh}	18.68 ±0.44 ^k
200	3.00 ±0.19 ^{efgh}	17.32 ±0.18 ^j	6.01 ±0.05 ⁱ	2.55 ±0.11 ^{fghi}	15.66 ±0.65 ^{sh}
250	2.45 ±0.15 ^{abcde}	14.69 ±0.18 ^h	5.80 ±0.04 ^{gh}	2.35 ±0.15 ^{cdefgh}	11.60 ±0.58 ^c

Note: Data in the same column followed by the same letters are not significantly different by Duncan's multiple range test at $p \leq 0.05$.

4. Discussion

4.1. Effect of PGRs on SEs formation

PGRs are key in impacting somatic embryogenesis (Mujib *et al.*, 2016). In most investigated cases, SEs induction initially requires auxin and cytokinin added together in the culture medium. In orchids, various classes of auxins have been widely employed and reported in a number of species like *Cymbidium* Twilight Moon 'Day Light' (Teixeira da Silva and Tanaka, 2006), *Malaxis densifolia* (Mahendran and Bai, 2016), *E. veratrifolia* (Moradi *et al.*, 2017), *P. aphrodite* (Gow *et al.*, 2018), and *Paphiopedilum niveum* (Soonthornkalump *et al.*, 2019). In this study, TDZ in combinations with various auxins (NAA, 2,4-D, IAA) were incorporated in NP medium to evaluate their effects on SEs formation in various types of explants of *P. amabilis* orchid. Among the combination of PGRs, 3.0 mg L⁻¹ TDZ and 1.0 mg L⁻¹ NAA produced the highest number of SEs from stem explants. It is worth noting that Khoddamzadeh *et al.* (2011) reported a high level of direct SEs induction (72%) when *P. bellina* leaf tissues were cultured on the same medium. Nevertheless,

Zanello and Cardoso (2019) reported low SEs formation when using lower concentration of TDZ and high concentration of NAA (0.125 mg L⁻¹ TDZ and 1.0 mg L⁻¹ NAA) on leaf tissues of *Phalaenopsis* hybrid 'RP3' and 'Ph908'.

In other reports, combination of 2,4-D with TDZ at appropriate concentrations was effective for SEs induction in *Oncidium* 'Gower Ramsey' (Chen and Chang, 2000), *Cattleya maxima* (Cueva Agila *et al.*, 2013), and *E. veratrifolia* (Moradi *et al.*, 2017). On the contrary, we found that the use of 2,4-D and TDZ highly retarded the formation of SEs in *P. amabilis* orchid. In accordance with our results, Shen *et al.* (2018) also reported the inhibitory effect of 2,4-D and TDZ on SEs formation in *Tolumnia Louise Elmore* 'Elsa' orchid. No globular embryos were found at this combination that resulted in high percentage of browning (100%). Yam and Arditti (2017) stated that the effects of the same auxin may differ in respect to one species and may not be the same with another orchid. In line with this, Naranjo *et al.* (2016) reported that different genetic makeup plays a role in tissue culture responsiveness. Moreover, we also anticipate the difference between the basal medium in each research. Oyamada and Takano (1985) found that the response of

SEs to certain PGRs depended on the particular chemical level in the basal solution.

Apart from the kind of PGRs, explant types also affect the formation of SEs in orchid (Chugh *et al.*, 2009). Leaves are the most common target tissue used for SEs induction in orchid (Jainol and Gansau, 2017). Different protocols have been developed for a number of orchid species through somatic embryogenesis using leaf explants (De Conti *et al.* 2018; Shen *et al.*, 2018, Zanello and Cardoso, 2019). However, orchid leaves are known to be recalcitrant to regeneration and possessed high oxidation rate (Temjensangba and Deb, 2005; Kaur and Bhutani, 2009). Recently, SEs were regenerated from seed-derived protocorm and stem explants (Mose *et al.*, 2017; Soonthornkalump *et al.*, 2019). Here, we found that stem explants successfully produced high number of SEs in all PGRs combinations. Consistent with our results, Kanjilal *et al.* (1999) also reported that SEs were effectively induced from stem disc culture of *Dendrobium moschatum* orchid.

4.2. Effect of light regime during SEs formation

Light is known to affect induction and maturation of somatic embryogenesis (Meneses *et al.*, 2005; Chung *et al.*, 2007). In some orchid plants, somatic embryogenesis induction is more effective in the absence of light (Gow *et al.*, 2009; Sampaio *et al.*, 2010). Cueva-Agila *et al.* (2016) reported that light inhibits the formation of SEs in leaf explants of *Cattleya maxima* orchid. In the present research, it was perceived that explants cultured in light conditions for the first 30 days of culture produced lower number of SEs compared to explants cultured in dark conditions. In addition, Gow *et al.* (2009) reported that leaf explants of *P. amabilis* Shimadzu var. *formosa* and *P. nebula* showed high intensity of browning after 60 days of culture in light conditions. Explant browning is greatly affected by light (Patel *et al.*, 2018). Light induced the production and accumulation of phenolic compounds (von Aderkas *et al.*, 2015). North *et al.* (2010) reported that oxidation of phenolic compounds produced quinones that are toxic and causing tissue necrosis and death of explant. In studies on leaf explants of date palm plants (*Phoenix dactylifera*), light stimulated secretion of phenolic compound and inhibited callus formation (Baharan *et al.*, 2015).

4.3. Effect of additional organic substances on regeneration of SEs

Regeneration response of SEs into plantlets are generally slow in many orchid genera including *Phalaenopsis* (Yam and Arditti, 2017). Hence, the media and its formulation are important to maximize orchid's vigour in the tissue culture conditions (Gnasekaran *et al.*, 2010). Chew *et al.* (2018) reported that addition of organic substances in the culture medium increased the percentage of SEs regeneration response. Besides containing hormones, proteins and minerals, organic substances have also become natural carbon source that is needed for orchid development (Nambiar *et al.*, 2012). Carbon sources of culture medium supplement the low CO₂ concentration and light energy deficiency to the plants under *in vitro* conditions (Sarmah *et al.*, 2017). Organic substances such as banana and tomato contain carbon

source in the form of simple or complex sugars (Gnasekaran *et al.*, 2010). Sugars enter into the metabolic pathways and breaking down of sugar produces the required energy for *in vitro* orchid germination, growth of cells, buds, and even plantlets growth (Zahara *et al.*, 2017).

In this study, medium supplemented with 150 g L⁻¹ of tomato extract gave the highest plantlet growth rate. Our result is also in agreement with a study on the growth enhancement effect of tomato extract in *Dendrobium* hybrids (Hapsoro *et al.*, 2018), *Vanda helvola* (David *et al.*, 2015), and *Vanda* Kasem's Delight (Gnasekaran *et al.*, 2012). Furthermore, Gnasekaran *et al.* (2010) reported that tomato extract serves to promote cell division through cytokinin and increased the percentage of *Phalaenopsis violacea* PLBs proliferation rate.

According to Semiarti *et al.* (2010), tomato (*L. esculentum* 'Arthaloka') extract contained 3.70% total sugars, 1.78% total proteins, 1.05% crude fibre, 1.84% total carotene, 0.042% vitamin C, 0.024% antioxidants (DPPH: 1,1-diphenyl-2-picrylhydrazyl), and other components. Gnasekaran *et al.* (2012) reported that the presence of antioxidants in the culture medium successfully prevented browning of PLBs of *Vanda* Kasem's Delight orchid. Moreover, Cunningham *et al.* (1996) reported that carotenoids with cyclic end-groups were essential components of photosynthetic membranes and play a role in preventing photo-oxidation. Apart from carotenoid and DPPH, tomato also contains lycopene. Lycopene served as strong antioxidant which inhibits free radical formation, assists wound cells repairing process, and inhibits DNA oxidation (Halliwell, 1996). The presence of these antioxidants successfully prevented browning of culture and maximized the growth of SEs into plantlets.

5. Conclusion

Direct somatic embryogenesis in *P. amabilis* orchid can be effectively induced from various explants by using a combination of auxin and cytokinin, with the best combination being 3.0 mg L⁻¹ TDZ and 1.0 mg L⁻¹ NAA. Stem of *in vitro* seedlings was the best explant to be used to induce direct somatic embryogenesis in *P. amabilis*. Dark condition was needed for SEs formation, and addition of tomato extract has effectively increased the regeneration rate of SEs. These findings provided efficient protocols for commercial propagation and conservation of *P. amabilis* orchids.

Acknowledgements

This work was supported by the Ministry of Research, Technology and Higher Education of the Republic of Indonesia in part with scheme of PUPT UGM research grant (2017-2018) to ES, and in part with the scheme of PMDSU research grant (2017-2018) to ES as PI. We thank Mrs. Hj. Sri Suprih Lestari the owner of TITI Orchids Nursery for the gift of *P. amabilis* parental plants used in this research.

References

- Abbaszadeh SM, Miri SM and Naderi R. 2018. An effective nutrient medium for asymbiotic seed germination and *in vitro* seedling development of *Phalaenopsis* 'Bahia Blanca'. *Jornamental*, **8**: 183-192.
- Anstis PJP and Northcote DH. 1975. Cytokinin activity in potato tuber extracts. *Z Pflanzenphysiol*, **75**: 273-275.
- Ayil-Gutiérrez B, Galaz-Ávalos RM, Peña-Cabrera E and Loyola-Vargas VM. 2013. Dynamics of the concentration of IAA and some of its conjugates during the induction of somatic embryogenesis in *Coffea canephora*. *Plant Signal Behav*, **8**: e26998.
- Baharan E, Mohammadi PP, Shahbazi E and Hosseini SZ. 2015. Effects of some plant growth regulators and light on callus induction and explants browning in date palm (*Phoenix dactylifera*) *in vitro* leaves culture. *Iranian Journal of Plant Physiology*, **5**: 1473-1481.
- Bhattacharyya P, Kumaria S, Job N and Tandon P. 2016. *En-masse* production of elite clones of *Dendrobium crepidatum*: A threatened, medical orchid used in Traditional Chinese Medicine (TCM). *J Appl Res Med Aromat Plants*, **3**: 168-176.
- Borpuzari PP and Borthakur M. 2016. Effect of plant growth regulators and explants sources on somatic embryogenesis of matured tissue of the anticancerous medicinal plant *Plumbago rosea*. *J Med Plants Stud*, **4**: 165-170.
- Ceccarellil N, Monding A, Curadi M, Lorenzi R and Schiavo FL. 2000. Auxin metabolism and transport in an embryogenic cell line of *Daucus carota* L. *J Plant Physiol*, **157**: 17-23.
- Chen J and Chang W. 2000. Efficient plant regeneration through somatic embryogenesis from callus cultures of *Oncidium* (Orchidaceae). *Plant Sci*, **160**: 87-93.
- Chew Y-C, Halim MHA, Abdullah WMANW, Abdullah JO and Lai K-S. 2018. Highly efficient proliferation and regeneration of protocorm-like bodies (PLBs) of the threatened orchid, *Phalaenopsis bellina*. *Sains Malays*, **47**: 1093-1099.
- Chugh S, Guha S and Rao IU. 2009. Micropropagation of orchids: A review on the potential of different explants. *Sci Hortic*, **122**: 507-520.
- Chung HH, Chen JT and Chang WC. 2007. Plant regeneration through direct somatic embryogenesis from leaf explants of *Dendrobium*. *Biol Plant*, **51**: 346-350.
- Cueva Agila AY, Guachizaca I and Cella R. 2013. Combination of 2,4-D and stress improves indirect somatic embryogenesis in *Cattleya maxima* Lindl. *Plant Biosystem – An International Journal Dealing with all Aspects of Plant Biology: Plant Biosyst*, **149**: 235-241.
- Cueva-Agila AY, Medina J, Concia L and Cella R. 2016. Effects of plant growth regulator, auxin polar transport inhibitors on somatic embryogenesis and CmSERK gene expression in *Cattleya maxima* (Lindl.). In: Mujib A (ed). **Somatic Embryogenesis in Ornamentals and Its Applications**, 1st ed. Springer, India, pp. 255-267.
- Cunningham FX Jr, Pogson B, Sun Z, McDonald KA, Dellapenna D and Gantt E. 1996. Functional analysis of the B and E lycopene cyclase enzymes of *Arabidopsis* reveals a mechanism for control of cyclic carotenoid formation. *Plant Cell*, **8**: 1613-1626.
- David D, Jawan E, Marbawi H and Ganzau JA. 2015. Organic substances improves the *in vitro* growth of native orchid *Vanda helvola* Blume. *Not Sci Biol*, **7**: 192-197.
- De Conti D, Corredor-Prado J, Junior DR, Suzuki RM, Guerra MD and Pescador R. 2018. Determination of endogenous IAA and carbohydrates during the induction and development of protocorm-like bodies of *Cattleya trigina* A. Richard. *Acta Sci*, **40**: e37874.
- Dulić J, Ijubojević M, Prlainović I, Barać G, Narandžić T and Ognjanov V. 2018. Germination and protocorm formation of *Ophrys sphegodes* Mill. - *In vitro* protocol for a rare orchid species. *Cont Agri*, **67**: 196-201.
- Ge L, Tan SN, Yong JWH, Hua L and Ong ES. 2008. Separation of cytokinin isomers with a partial filling-micellar electrokinetic chromatography-mass spectrometry approach. *Electrophoresis*, **29**: 2024-2032.
- Gnasekaran P, Poobathy R, Samian MR and Subramanian S. 2012. Effects of complex organic substances on improving the growth of PLBs of *Vanda Kasem's Delight*. *Aust J Crop Sci*, **6**: 1245-1248.
- Gnasekaran P, Rathinam X, Sinniah UR and Subramaniam S. 2010. A study on the use of organic additives on the protocorm-like bodies (PLBs) growth of *Phalaenopsis violacea* orchid. *J Phytol*, **2**: 029-033.
- Gow W-P, Chen J-T and Chang W-C. 2009. Effects of genotype, light regime, explant position and orientation on direct somatic embryogenesis from leaf explants of *Phalaenopsis amabilis* orchids. *Acta Phytol Plant*, **31**: 363-369.
- Gow W-P, Chung H-H, Chen J-T and Chang W-C. 2018. Factors affecting thidiazuron-induced direct somatic embryogenesis of *Phalaenopsis Aphrodite*. In: Ahmad N and Faisal M. (eds). **Thidiazuron: From urea derivative to plant growth regulator**. Springer, Singapore. pp. 317-327.
- Guo B, Abbasi BH, Zeb A, Xu LL and Wei YH. 2011. Thidiazuron: A multi-dimensional plant growth regulator. *Afr J Biotechnol*, **10**: 8984-9000.
- Halliwel B. 1996. Antioxidants. In: Ziegler EE and Filer LJ Jr (eds). **Present Knowledge in Nutrition**, 7th ed. ILSI Press, Washington DC. pp. 596-603.
- Hapsoro D, Septiana VA, Ramadiana S and Yusnita Y. 2018. A medium containing commercial foliar fertilizer and some organic substances could substitute MS medium for *in vitro* growth of *Dendrobium* hybrids seedlings. *Jurnal Floratek*, **13**: 11-22.
- Hew CS and Yong JWH. 2004. **The physiology of tropical orchids in relation to the industry**. World Scientific, Singapore.
- Hong PI, Chen JT and Chang WC. 2010. Shoot development and plant regeneration from protocorm-like bodies of *Zygopetalum mackayi*. *In Vitro Cell & Dev Biol – Plant*, **46**: 306-311.
- Islam MO, Ichihashi S and Matsui S. 1998. Control of growth and development of Protocorm like body derived from callus by carbon source in *Phalaenopsis*. *Plant Biotechnol*, **15**: 183-187.
- Jainol JE and Gansau JA. 2017. Embryogenic callus induction from leaf tip explants and protocorm-like bodies formation and shoot proliferation of *Dimorphochis lowii*: Borneon endemic orchid. *AGRIVITA*, **39**: 1-10.
- Kaur S and Bhutani KK. 2009. *In vitro* propagation of *Vanda testacea* (Lindl.) Reichb.f. -a rare orchid of high medicinal value. *Plant Tissue Cult Biotechnol*, **19**: 1-6.
- Khoddamzadeh AA, Sinniah UR, Kadir MA, Mahmod K and Sreeramanan S. 2011. *In vitro* induction and proliferation of protocorm-like bodies from leaf segments of *Phalaenopsis bellina* (Rchb.f.) Christenson. *Plant Growth Regul*, **65**: 381-387.
- Lomin SN, Myakushina A, Kolachevskaya OO, Getman IA, Arkhipov DV, Savelieva EM, Osolodkin DI and Romanov GA. 2018. Cytokinin perception in potato: new features of canonical players. *J Exp Bot*, **69**: 3839-3853.
- Mahendran G and Bai VN. 2016. Direct somatic embryogenesis of *Malaxis densifolia* (A. Rich.) Kuntze. 2016. *Journal of Genetic Engineering and Biotechnology*, **14**: 77-81.

- Meneses A, Flores D, Muñoz M, Arrieta G and Espinoza AM. 2005. Effect of 2,4-D, hydric stress and light on Indica rice (*Oryza sativa*) somatic embryogenesis. *Rev Biol Trop*, **53**: 361-368.
- Méndez-Hernández HA, Ledezma-Rodríguez M, Avilez-Montalvo RN, Juárez-Gómez YL, Skeete A, Avilez-Montalvo J, De-la-Peña C and Loyola-Vargas VM. 2019. Signaling Overview of Plant Somatic Embryogenesis. *Front Plant Sci*, **10**: 77.
- Moradi S, Daylami SD, Arab M and Vahdati K. 2017. Direct somatic embryogenesis in *Epipactis veratrifolia*, a temperate terrestrial orchid. *J Hort Sci Biotech*, **92**: 88-97.
- Mose W, Indrianto A, Purwantoro A and Semiarti E. 2017. The influence of thidiazuron on direct somatic embryo formation from various types of explant in *Phalaenopsis amabilis* (L.) Blume orchid. *HAYATI J Biosci*, **24**: 201-205.
- Mujib A, Ali M, Tonk D, Isah T and Zafar N. 2016. Embryogenesis in ornamental monocots: Plant growth regulators as signalling element. In: Mujib A (ed). **Somatic Embryogenesis in Ornamentals and Its Applications**. Springer, India. pp. 255-267.
- Nambiar N, Tee CS and Maziah M. 2012. Effects of organic substances and different carbohydrate sources on proliferation of protocorm-like bodies in *Dendrobium* Alya Pink. *Plant Omics*, **5**: 10-18.
- Naranjo EJ, Fernandez Betin O, Urrea Trujillo AI, Callejas Posada R, Atehortúa Garcés L. 2016. Effect of genotype on the *in vitro* regeneration of *Stevia rebaudiana* via somatic embryogenesis. *Acta Biol Colomb*, **21**: 87-98.
- North JJ, Ndakidemi PA and Laubscher CP. 2010. The potential of developing an *in vitro* method for propagating Strelitziaceae. *Afr J Biotechnol*, **9**: 7583-7588.
- Oyamada T and Tanako T. 1985. Investigations on the macroinorganic nutrients in special reference to ratios of $\text{NO}_3^-/\text{SO}_4^{2-}$ and $\text{K}^+/\text{Ca}^{2+}$ in tissue culture media of orchids. *Sci Rep Fac Agr Meijo Univ*, **21**: 1-9.
- Kanjilal B, De Sarker D, Mitra J and Datta KB. 1999. Stem disc culture: Development of a rapid mass propagation method for *Dendrobium moschatum* (Buch.-Ham) Swartz – An endangered orchid. *Curr Sci*, **77**: 497-500.
- Pasternak TP, Prinsen E, Ayaydin F, Miskolczi P, Potters G, Asard H, Van Onckelen HA, Dudits D and Feher A. 2002. The role of auxin, pH, and stress in the activation of embryogenic cell division in leaf protoplast-derived cells of alfalfa. *Plant Physiol* **129**: 1807-1819.
- Patel A, Patil G, Mankad M and Subhash N. 2018. Optimization of surface sterilization and manipulation of *in vitro* conditions for reduced browning in pomegranate (*Punica granatum* L.) variety *Bhagava*. *Int J Chem*, **6**: 23-28.
- Ruzin S. 1999. **Plant Microtechnique and Microscopy**. Oxford University Press, Oxford.
- Sampaio J, Stancato G and Appezzato B. 2010. Direct regeneration of protocorm-like bodies (PLBs) from leaf apices of *Oncidium flexuosum* Sims (Orchidaceae). *Plant Cell Tiss Org*, **103**: 411-416.
- Sanjaya W, Indratmi D and Sufianto. 2019. Applications various extracts of plants on stem growth response of red dragon fruit (*Hylocereus polyrhizus*). *Journal Tropical Crop Science and Technology*, **1**: 33-43.
- Sarmah D, Kolukunde S, Sutradhar M, Singh BK, Mandal T and Mandal N. 2017. A review on: *In vitro* cloning of orchids. *Int J Curr Microbiol App Sci*, **6**: 1909-1927.
- Schuiteman A. 2010. Orchid in Indonesia and their conservation. Proceeding of the 2010 International Seminar on Orchid Conservation and Agribusiness, Yogyakarta, Indonesia.
- Semiarti E, Indrianto A, Purwantoro A, Martiwi INA, Feroniasanti YML, Nadifah F, Mercuriani IS, Dwiyani R, Ikawaka H, Yoshioka Y, Machida Y and Machida C. 2010. High-frequency genetic transformation of *Phalaenopsis amabilis* orchid using tomato extract-enriched medium for preculture of protocorm. *J Hort Sci Biotech*, **3**: 205-210.
- Shen H-J, Chen J-T, Chung H-H and Chang W-C. 2018. Plant regeneration via direct somatic embryogenesis from leaf explants of *Tolumnia* Louise Elmore 'Elsa'. *Bot Stud*, **59**: 4.
- Shuiying R, Hongfei W, Shun F, Jide W and Yi L. 2016. Determination of 21 plant growth regulators in tomatoes using an improved ultrasound-assisted QuEChERS technique combined with a liquid chromatography tandem mass spectrometry method. *Anal Methods*, **8**: 4808-4815.
- Soonthornkalump S, Nakkamong K and Meesawat U. 2019. *In vitro* cloning via direct somatic embryogenesis and genetic stability assessment of *Paphiopedilum niveum* (Rchb.f.) Stein: the endangered Venus's slipper orchid. *In Vitro Cell Dev Biol Plant*, **55**: 265-276.
- Tanaka M, Kumura M and Goi M. 1988. Optimal conditions for shoot production from *Phalaenopsis* flower-stalk cuttings cultured *in vitro*. *Sci Hortic*, **35**: 117-126.
- Tarkowski P, Ge L, Yong JWH and Tan SN. 2009. Analytical methods for cytokinins. *Trends Anal Chem*, **28**: 323-335.
- Teixeira da Silva JA and Tanaka M. 2006. Multiple regeneration pathways via thin cell layers in hybrid *Cymbidium* (Orchidaceae). *J Plant Growth Regul*, **25**: 203-210.
- Temjensangka T and Deb CR. 2005. Regeneration of plantlets from *in vitro* raised leaf explants of *Cleisostoma racimeferum* Lindl. *Indian J Exp Biol*, **43**: 377-381.
- von Aderkas P, Teyssier C, Charpentier J-P, Gutmann M, Pâques L, Le Metté, Ader K, Label P, Kong L and Lelu-Walter M-A. 2015. Effect of light conditions on anatomical and biochemical aspects of somatic and zygotic embryos of hybrid larch (*Larix X marschllinsii*). *Ann Bot*, **115**: 605-615.
- Vondráková Z, Kateřina E, Fischerová L and Vágner M. 2011. The role of auxins in somatic embryogenesis of *Abies alba*. *Cent Eur J Biol*, **6**: 587-596.
- Yam TW and Arditti J. 2017. **Micropropagation of Orchids**. Wiley, New York.
- Yong JWH, Ge L, Ng YF and Tan SN. 2009. The chemical composition and biological properties of coconut (*Cocos nucifera* L.) water. *Molecules*, **14**: 5144-5164.
- Zahara M, Datta A, Boonkorkeaw P and Mishra A. 2017. The effects of different media, sucrose concentrations and natural additives on plantlet growth of *Phalaenopsis* Hybrid 'Pink'. *Braz Arch Biol Technol*, **60**: e160149.
- Zanello CA and Cardoso JC. 2019. PLBs induction and clonal plantlet regeneration from leaf segment of commercial hybrids of *Phalaenopsis*. *J Hort Sci Biotech*, **94**: 627-631.

Estradiol Affects Ultimobranchial Gland of a Freshwater Catfish, *Heteropneustes fossilis* kept in Different Calcium Environments

Susmita Srivastav¹, Diwakar Mishra², Sunil K. Srivastav³, Nobuo Suzuki⁴ and Ajai K. Srivastav^{3*}

¹Department of Zoology, Shiv Harsh Kisan P. G. College, Basti-272001, ²Department of Zoology, Government Girls' P. G. College, Ghazipur-233001, ³Department of Zoology, D.D.U. Gorakhpur University, Gorakhpur-273009, India; ⁴Noto Marine Laboratory, Institute of Nature and Environmental Technology, Kanazawa University, Ogi,Noto-cho, Ishikawa, Japan.

Received: October 11, 2019; Revised: December 29, 2019; Accepted: January 31, 2020

Abstract

Some individuals of a freshwater fish species *Heteropneustes fossilis* were divided into groups A-D. Group A and B were kept in artificial freshwater. Group C and D were maintained in calcium-deficient freshwater. The groups A and C were administered with vehicle and the groups B and D were injected with estradiol. Plasma calcium levels and UBG were studied after 1, 3, 5, 10 and 15 days.

In group B fish, estradiol administration resulted in hypercalcemia from day 3 to 10; however, after day 15 calcium level of plasma slightly decreased. Plasma calcium level of group C exhibited slight decrease from that of the day 1 to 3. Thereafter, the level increased on day 10 and 15. Plasma calcium level of the estradiol treated group D exhibited progressive increase from day 3 to 15.

In group B, the nuclear volume of UBG exhibited progressive increase from day 5 to 10 and displayed weak staining response of cytoplasm. After day 15, few degenerating cells were noticed and nuclear volume of UBG cells exhibited slight decrease. In group C, staining response of the cytoplasm of UBG cells became slightly weak on day 10 and 15. In group D, there is a progressive increase in the nuclear volume from day 10 to 15, and the ultimobranchial cells displayed weak staining response. Moreover, after day 15, few degenerating ultimobranchial cells were observed in group D.

Keywords: Estradiol, Fish, Plasma calcium, Ultimobranchial gland

1. Introduction

The fish possess a unique and more complex system than that of the terrestrial vertebrates as they remain in intimate contact with surrounding water which provides an inexhaustible supply of calcium, thus building calcium gradients across the body surface. In land vertebrates, direct exchange of calcium between body and surrounding medium is not possible and they rely solely on dietary calcium uptake. In this condition, body calcium level is regulated by a balance between intestinal calcium absorption and renal calcium excretion.

The fish regulate their blood calcium level very efficiently, which involves different hormones such as prolactin from pituitary, vitamin D metabolites, calcitonin from ultimobranchial gland (UBG) and stanniocalcin from corpuscles of Stannius (CS) (Srivastav 1983, 1989; Srivastav and Srivastav 1988; Srivastav and Singh 1989, 1992; Srivastav *et al.* 1995, 1998; Prasad *et al.* 2015 and Kumar *et al.* 2017). Different hormones act through various target organs such as skin, fin, gut, gill, bone, and kidney for calcium regulation.

Vitellogenin is released into the circulation after its synthesis from the liver (Baily 1957; Chen 1983; Bjornsson and Haux 1985 and Kwon *et al.* 1993) and

transported to the ovaries where it is conjugated as vitellin and stored as yolk (Persson *et al.* 1994, 1995 and Yeo and Mugiya 1997). Vitellogenin synthesis is induced by estradiol-17 β (Naderi *et al.*, 2015). The increased plasma calcium level during vitellogenesis has been correlated (Bjornsson and Haux, 1985) with the enhanced synthesis of vitellogenin which binds calcium ions. During vitellogenesis, there is an increased calcium demand which has to be taken either from the environment, and intestinal uptake or from the internal calcium reservoirs.

The source of additional calcium needed after estradiol-induced vitellogenesis in fishes is in controversy. Increased calcium uptake from the environment (Fleming *et al.* 1964 and Persson *et al.* 1994), mobilization from scales (Mugiya and Watabe 1977; Carragher and Sumpter 1991 and Persson *et al.* 1994, 1995), muscles (Persson *et al.* 1994) and from bile (Mugiya and Hazama 1994) have been reported after estradiol treatment in fishes. On the contrary, Estradiol treatment to fish has also been reported not to affect the calcium uptake from environment (Mugiya and Ichii 1980), tissues like muscle (Carragher and Sumpter 1991), bone (Mugiya and Watabe 1977; Carragher and Sumpter 1991 and Persson *et al.* 1994), and intestine (Mugiya and Ichii 1980) as well as calcium excretion through kidneys (Carragher and Sumpter 1991 and Persson *et al.* 1994).

* Corresponding author e-mail: ajaiksrivastav@hotmail.com.

In this study, an attempt has been made to investigate the effects of estradiol administration in a freshwater catfish, *Heteropneustes fossilis* maintained either in artificial freshwater or in calcium-deficient freshwater. The experimentally induced changes by this hormone in the plasma calcium level have been correlated with the activity of the ultimobranchial gland.

2. Materials and methods

Live specimens of the freshwater catfish *Heteropneustes fossilis* (both sexes; body wt. 27-39 g) were collected from Gorakhpur, India (26.7606° N, 83.3732° E) and acclimated to laboratory conditions for two weeks in plastic pools (48 inch x 40 inch x 22 inch; capacity 125 gallon). The tank-water was half renewed daily and the fish were fed on dry shrimp powder on alternate days. For experimentation, 12 fish were kept in glass aquaria containing 10 litres of the medium. The water was replaced on alternate days. The Ethical Committee of the Department of Zoology, DDU Gorakhpur University, approved all the experimental protocols.

Experimentation: After acclimation the fish were divided into four groups (A-D) and were given the following treatments:

Group A: The fish from this group were given a single intra-peritoneal injection of groundnut oil as a vehicle (0.1 ml /100 g body wt) and kept in artificial freshwater.

Group B: The fish from this group were given a single intra-peritoneal injection of 0.1 ml of estradiol preparation (1 mg/100 g body wt) and kept in artificial freshwater.

Group C: The fish from this group were given a single intra-peritoneal injection of the vehicle (0.1 ml of ground nut oil/100 g body wt) and kept in calcium-deficient freshwater.

Group D: The fish from this group were given a single intra-peritoneal injection of 0.1 ml of estradiol preparation (1 mg/100 g body wt) and kept in calcium-deficient freshwater.

The preparation of estradiol used for the groups B and D were dissolved in groundnut oil. The doses of estradiol were selected on the basis of experiments done earlier on the same fish species (Singh *et al.*, 2009). Plasma concentrations of E₂ ranged from 0.12±0.04 ng ml⁻¹ to 0.96±0.13 ng ml⁻¹ in males and 1.04±0.19 ng ml⁻¹ to 10.50±0.97 ngml⁻¹ in females from resting phase to spawning phase (Tewary *et al.*, 2001). The fish were not fed for a period from 24 h before to the end of the experimentation.

For experimentation freshwater and calcium-deficient freshwater were prepared with the following compositions:

- Artificial freshwater:** Distilled water containing (in mmol/liter): NaCl 2.10; Na₂SO₄ 0.45; KCl 0.06; CaCl₂ 0.8; MgCl₂ 0.20. pH of the solution was adjusted to 7.6 with NaHCO₃.
- Calcium-deficient freshwater:** same as the artificial freshwater without CaCl₂.

Twelve fishes from each group were anaesthetized with MS 222 and blood samples from caudal peduncle were collected in heparinized tubes on days 1, 3, 5, 10 and 15 following the treatment. The plasma were separated by centrifugation and used to analyse its calcium content with Sigma kits. After collection of the blood samples, the fish

were autopsied and the body parts containing the UBG gland were removed and fixed in aqueous Bouin's fluid. The tissues were routinely processed in graded series of alcohol, cleared in xylene and embedded in paraffin. Serial sections were cut at 6 µm and stained with hematoxylin-eosin (HE).

Nuclear indices (length and width) were determined (300 nuclei were measured from six specimens) with the aid of ocular micrometer, and then nuclear volume was calculated as:

$$\text{Volume} = 4/3 \pi ab^2$$

Where 'a' is the major semiaxis and 'b' is the minor semiaxis.

Data were presented as the mean ± S.E. of six specimens and Student's t-test was used to determine statistical significance, and P value was set at <0.05. Each experimental group was compared to its specific time control group.

3. Results

3.1. Biochemical and histological parameters of Group A and B fish:

Plasma calcium level of the vehicle-injected fish (group A) exhibited almost no change throughout the experiment (Figure 1).

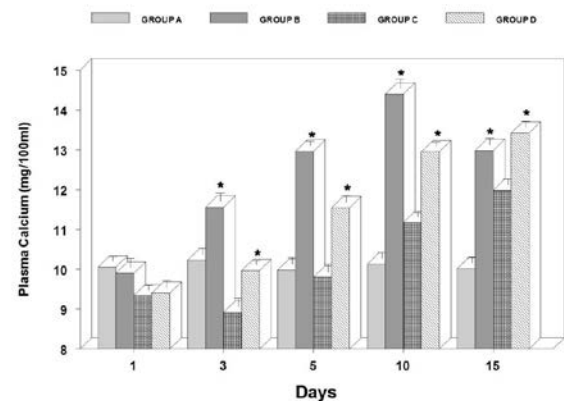


Figure 1. Changes in the plasma calcium levels of *Heteropneustes fossilis* kept under four different experimental conditions. Group A vehicle-injected fish kept in artificial freshwater, Group B estradiol-injected fish kept in artificial freshwater, Group C vehicle-injected fish kept in calcium-deficient freshwater or Group D estradiol-injected fish kept in calcium deficient freshwater. Each value represents mean ± S.E. of six specimens. Asterisk indicates significant differences (P<0.05) with vehicle-injected specimens

No significant change has been noticed in the plasma calcium level in the estradiol treated group B fish up to day 1. However, a progressive increase of calcium level was observed from day 3 to day 10, but after day 15 the level slightly decreased (Figure 1).

The ultimobranchial gland of the vehicle-injected (control; group A) *Heteropneustes fossilis* exists in the interseptum between the pericardial and abdominal cavities. It is not visible with the naked eyes and can only be detected in the serial sections of the interseptum with the aid of an optical microscope. A thick connective tissue sheath envelops the ultimobranchial gland. The ultimobranchial gland consists of follicles and cell cords (Figure 2). All the ultimobranchial cells are alike, having indistinct cell boundaries and eosinophilic cytoplasm. The

gland of the vehicle-injected fish exhibited no change in histological structure throughout the experiment.

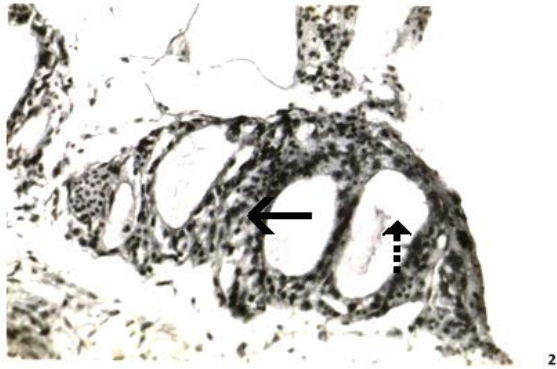


Figure 2. Histomorphograph of ultimobranchial gland of 5 day vehicle-injected *Heteropneustes fossilis* kept in artificial freshwater showing follicles (broken arrow) and cords (arrow). HE x 200.

In estradiol-treated group B fish, there was no change in the nuclear volume of ultimobranchial cells up to day 3. From day 5 to 10 the nuclear volume exhibited a progressive increase (Figure 3). Moreover, the ultimobranchial cells display poor staining response after days 5 and day 10 (Figure 4). After day 15, few degenerating cells were noticed (Figure 5) and the nuclear volume decreased slightly (Figure 3).

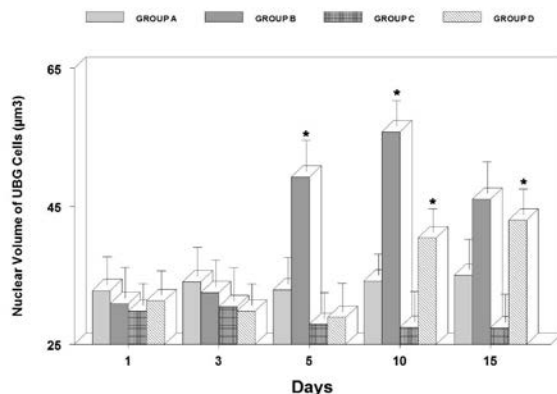


Figure 3. Nuclear volume of ultimobranchial gland of *Heteropneustes fossilis* kept under four different experimental conditions. Group A vehicle-injected fish kept in artificial freshwater, Group B estradiol-injected fish kept in artificial freshwater, Group C vehicle-injected fish kept in calcium-deficient freshwater or Group D estradiol-injected fish kept in calcium deficient freshwater. Each value represents mean \pm S.E. of six specimens. Asterisk indicates significant differences ($P < 0.05$) with vehicle-injected specimens.

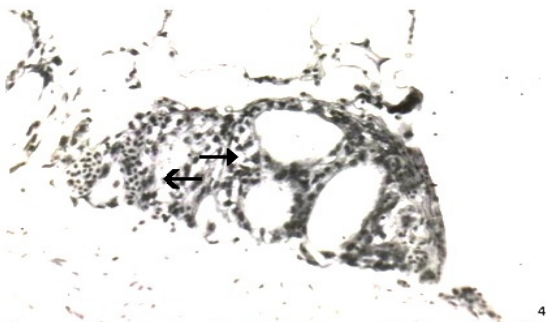


Figure 4. Histomorphograph of ultimobranchial gland of 10 day estradiol treated fish kept in artificial freshwater exhibiting weak staining (arrows) response. HE x 200.



Figure 5. Histomorphograph exhibiting degenerating cells (arrows) in the ultimobranchial gland of 15 days estradiol treated *Heteropneustes fossilis* maintained in artificial freshwater. HE x 200.

3.2. Biochemical and histological parameters of Group C and D fish:

The plasma calcium level of the vehicle-injected group C fish exhibited a slight decrease on days 1 and 3 as compared to fish kept in artificial freshwater. Thereafter, the plasma calcium level had increased on days 5, 10 and 15 resulting in hypercalcemia (Figure 1).

The plasma calcium levels of the estradiol treated group D fish exhibited no change at day 1. Estradiol treatment caused a progressive increase in the plasma calcium level from day 3 to 15 (Figure 1).

There was no change in the ultimobranchial gland of the vehicle-injected group C fish up to day 5. On days 10 and 15, the ultimobranchial cells exhibited slightly less staining intensity (Figure 6). These cells did not exhibit significant change in their nuclear volume throughout the experiment (Figure 3).

The nuclear volume of ultimobranchial cells in estradiol-treated group D fish did not show significant change up to day 5. From day 10 to 15, a progressive increase in the nuclear volume (Figure 3) of the ultimobranchial cells was observed with less staining intensity (Figure 7). Moreover, after day 15, few degenerating cells were noticed in the gland (Figure 8).

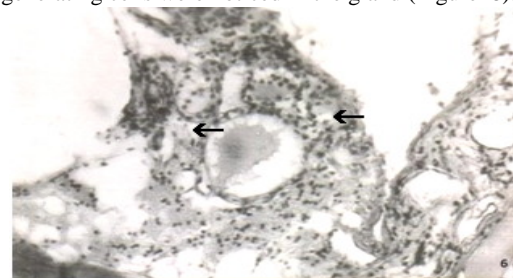


Figure 6. Histomorphograph of ultimobranchial gland of 10 day vehicle-injected fish kept in calcium-deficient freshwater showing decrease staining response of the cytoplasm (arrows). HE x 200.

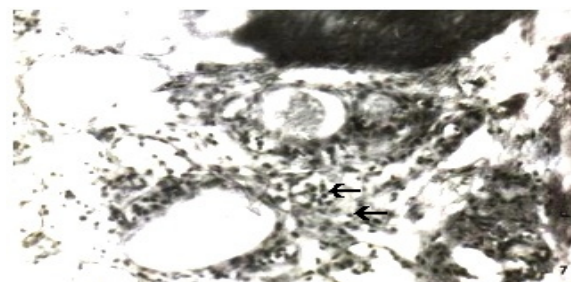


Figure 7. Histomorphograph of ultimobranchial gland of 10 day estradiol treated *Heteropneustes fossilis* kept in calcium-deficient freshwater depicting weak staining (arrows) response of the cytoplasm. HE x 200.



Figure 8. Histomorphograph exhibiting degenerating cells (arrows) in the ultimobranchial gland of 15 day estradiol treated fish maintained in calcium-deficient freshwater. HE x 200.

4. Discussion

In the present study, estradiol treatment caused elevation in the plasma calcium level of the fish kept in artificial freshwater. This derives support from reports of earlier workers, who have also reported an increase in plasma levels of this electrolyte after estradiol treatment (Baily 1957; Fleming *et al.* 1964; Yamada *et al.* 1982; Bjornsson and Haux 1985; Bjornsson *et al.* 1989; Norberg *et al.* 1989; Madsen and Korsgaard 1991; Mugiya and Hazama 1994; Persson *et al.* 1994, 1995 and Srivastav *et al.* 2016, 2017). The increased blood calcium might be due to increased mobilization from internal stores. Calcium mobilization from scales has been noticed in E₂ (estradiol) treated rainbow trout (Carragher and Sumpter 1991 and Persson *et al.* 1994) and goldfish and killifish (Mugiya and Watabe 1977). Muscle calcium mobilization has been reported by Persson *et al.* (1994) in E₂ treated rainbow trout. Mugiya and Watabe (1977) and Carragher and Sumpter (1991) have reported that there was no change in calcium content of muscle, vertebrae, rib bones, jaws or otolith of rainbow trout (*Oncorhynchus mykiss*) after estradiol treatment.

As the fish were not fed in the present study, the increased plasma calcium content in estradiol treated *H. fossilis* could not be attributed to the increased intestinal calcium uptake.

In calcium-deficient freshwater estradiol administration resulted into hypercalcemia. There exists no report of such a study from teleosts. Since calcium is not available in the surrounding media and also the animals were not fed in the present study, the hypercalcemia observed in estradiol treated *H. fossilis* could not be linked to the calcium absorption at intestinal mucosa and/or branchial calcium uptake. Enhanced calcium uptake from the environment after estradiol injection has been reported from other fish species (Fleming *et al.* 1964 and Persson *et al.* 1994). In contrast, Mugiya and Ichii (1980) have noticed no effect of estradiol on the *in situ* branchial calcium uptake.

The ultimobranchial gland of estradiol treated fish kept either in artificial freshwater or calcium deficient freshwater exhibited an increased activity which is evident by increased nuclear volume and degranulation of ultimobranchial cells. Several workers have noticed an increase in the activity of ultimobranchial gland during gonadal maturation (Lopez *et al.* 1968; Yamane and Yamada 1977; Srivastav 1983; Ahmad and Swarup 1988 and Singh 1990). Moreover, it has been reported that

female chum salmon and Japanese eel have higher circulating calcitonin levels during spawning period (Defetos *et al.* 1974; Watts *et al.* 1975 and Yamauchi *et al.* 1978). The observed hyperactivity of ultimobranchial gland may be attributed to the estradiol induced maturation as suggested by these workers. This response of the ultimobranchial gland may also be linked to the protection of skeletal calcium as suggested by Chan *et al.* (1968) and Yamauchi *et al.* (1978).

In vehicle-injected *H. fossilis* kept in calcium-deficient freshwater, the ultimobranchial gland became active on day 10 and 15, which is evident from weak staining response of the ultimobranchial cells. This may be due to the observed hypercalcemia at these intervals.

5. Conclusion

It can be concluded that (i) estradiol caused hypercalcemia in fish kept either in artificial freshwater or in calcium-deficient freshwater, (ii) The ultimobranchial gland of estradiol treated fish kept either in artificial freshwater or calcium deficient freshwater exhibited an increased activity.

Acknowledgements

The authors are thankful to The Head, Department of Zoology, D. D. U. Gorakhpur University, Gorakhpur, India, for providing laboratory facilities for this study.

References

- Ahmad N and Swarup K. 1988. Seasonal changes in the functional morphology of the ultimobranchial body in relation to the reproductive cycle and changes in serum calcium level of a freshwater female catfish, *Mystus vittatus* (Bloch). *Proc Nat Acad Sci*, **58**: 359-363.
- Bailey RE. 1957. The effect of estradiol on serum calcium, phosphorus and protein of goldfish. *J Exp Zool*, **136**: 455-469.
- Bjornsson BTh and Haux C. 1985. Distribution of calcium, magnesium and inorganic phosphate in plasma of estradiol-17 β treated rainbow trout. *J Comp Physiol B*, **155**: 347-352.
- Bjornsson BTh, Haux C, Bern HA and Defetos LJ. 1989. 17 β -estradiol increases plasma calcitonin levels in salmonid fish. *Endocrinol*, **125**: 1754-1760.
- Carragher JF and Sumpter JP. 1991. The mobilization of calcium from calcified tissues of rainbow trout (*Oncorhynchus mykiss*) induced to synthesize vitellogenin. *Comp Biochem Physiol*, **99A**: 169-172.
- Chan DKO, Chester Jones I and Smith RN. 1968. The effect of mammalian calcitonin on the plasma levels of calcium and inorganic phosphate in the European eel (*Anguilla anguilla*). *Gen Comp Endocrinol*, **11**: 243-245.
- Chen TT. 1983. Identification and characterization of estrogen-responsive gene products in the liver of rainbow trout. *Canad J Biochem Cell Biol*, **61**: 802-810.
- Defetos LJ, Watts EG, Copp DH and Potts JT Jr. 1974. A radioimmuno-assay for salmon calcitonin. *Endocrinol*, **94**: 155-160.
- Fleming WR, Stanley JG and Meier AH. 1964. Seasonal effects of external calcium, estradiol, and ACTH on the serum calcium and sodium levels of *Fundulus kansae*. *Gen Comp Endocrinol*, **04**: 61-67.

- Kumar A, Srivastava S and Srivastav SK. 2017. Hypophysectomy induced histological changes in corpuscles of Stannius of a freshwater catfish, *Heteropneustes fossilis*. *Int J Zool Invest*, **03**:129-134.
- Kwon HC, Hayashi S and Mugiya Y. 1993. Vitellogenin induction by estradiol 17 β in primary hepatocyte culture in the rainbow trout, *Oncorhynchus mykiss*. *Comp Biochem Physiol*, **104B**: 381-396.
- Lopez E, Peignoux-Deville J and Bagot E. 1968. Etude histophysiologique du corps ultimobranchial dun teleosteen, *Anguilla anguilla* L. au cours d'hypercalcemia experimentales. *Comptes Rendus de l' Academie des Sciences, Paris* **267D**: 1531-1534.
- Madsen SS, and Korsgaard B. 1991. Opposite effects of 17 β estradiol and combined growth hormone-cortisol treatment on hyposome regulatory performance in sea trout presmolts, *Salmo trutta*. *Gen Comp Endocrinol*, **83**: 276-282.
- Mugiya Y and Hazama K. 1994. Effects of Stannius corpuscles extracts and 17 β estradiol on the concentration of gallbladder calcium in the rainbow trout, *Oncorhynchus mykiss*. *Japan J Ichthyol*, **41**: 117-122.
- Mugiya Y and Ichii T. 1980. Effects of estradiol 17 β on branchial and intestinal calcium uptake in the rainbow trout, *Salmo gairdneri*. *Comp Biochem Physiol*, **70A**: 97-101.
- Mugiya Y and Watabe N. 1977. Studies on fish scale formation and resorption. II. Effect on estradiol on calcium homeostasis and skeletal tissue resorption in the goldfish, *Carassius auratus*, and the killifish, *Fundulus heteroclitus*. *Comp Biochem Physiol*, **57A**: 197-202.
- Naderi M, Safahieh A, Madiseh SD, Zolgharnein H and Ghatrami ER. 2015. Induction of vitellogenin synthesis in immature male yellowfin seabream (*Acanthopagrus latus*) exposed to 4-nonylphenol and 17 β -estradiol. *Toxicol Indus Hlth* **31**: 209-220.
- Norberg B, Bjornsson BTh, Brown CL, Wichardt UP, Deftos LJ and Haux C. 1989. Changes in plasma vitellogenin, sex steroids, calcitonin, and thyroid hormones related to sexual maturation in female brown trout (*Salmo trutta*). *Gen Comp Endocrinol*, **75**: 316-326.
- Persson P, Sundell K and Bjornsson BTh. 1994. Estradiol 17 β induced calcium uptake and resorption in juvenile rainbow trout *Oncorhynchus mykiss*. *Fish Physiol Biochem*, **13**: 379-386.
- Persson P, Takagi Y and Bjornsson BTh. 1995. Tartarate resistant acid phosphatase as a marker for scale resorption in rainbow trout, *Oncorhynchus mykiss*: effects of estradiol 17 β treatment and refeeding. *Fish Physiol Biochem*, **14**: 329-339.
- Prasad M, Kumar A, Suzuki N and Srivastav Ajai K. 2015. Botanical pesticide *Nerium indicum* alters prolactin cells of stinging catfish, *Heteropneustes fossilis*. *Int J Zool Invest*, **01**:77-84.
- Singh S. 1990. Studies of endocrine glands regulating calcium and inorganic phosphorus homeostasis in *Heteropneustes fossilis*. Ph. D. Thesis, University of Gorakhpur, Gorakhpur, India.
- Singh V, Singh PB and Srivastava S. 2009. Testosterone and estradiol-17 beta dependent phospholipid biosynthesis in ovariectomized catfish, *Heteropneustes fossilis* (Bloch). *J Env Biol*, **30**: 633-640.
- Srivastav AK. 1983. Calcemic responses in the freshwater mud eel *Amphipnous cuchia* to vitamin D₃ administration. *J Fish Biol*, **23**: 301-303.
- Srivastav AK. 1989. Effect of 1, 25 dihydroxycholecalciferol administration on prolactin cells of the freshwater catfish *Clarias batrachus*. *Zool Jahr Physiol*, **93**: 241-244.
- Srivastav AK and Singh P. 1989. Response of prolactin cells of the freshwater mud eel, *Amphipnous cuchia* to vitamin D₃ administration. *Zool Jahr Physiol*, **93**: 235-240.
- Srivastav AK and Singh S. 1992. Effect of vitamin D₃ on serum calcium and inorganic phosphate levels of the freshwater catfish, *Heteropneustes fossilis*, maintained in artificial freshwater, calcium-rich freshwater, and calcium-deficient freshwater. *Gen Comp Endocrinol*, **87**: 63-70.
- Srivastav AK and Srivastav SP. 1988. Corpuscles of Stannius of *Clarias batrachus* in response to 1, 25 dihydroxyvitamin D₃ administration. *Zool Sci*, **05**: 197-200.
- Srivastav S, Mishra D, Srivastav SK and Srivastav AK. 2016. Alterations in the Corpuscles of Stannius after Estradiol Administration to Stinging Fish, *Heteropneustes fossilis* Maintained in Different Calcium Environments. *Int J Zool Invest*, **2** (1): 24-34.
- Srivastav AK, Wendelaar Bonga SE and Flik G. 1998. Plasma calcium and stannioalcin levels of male tilapia, *Oreochromis mossambicus* fed with calcium-deficient food and treated with 1, 25(OH)₂D₃. *Gen Comp Endocrinol*, **110**: 290-294.
- Srivastav AK, Singh S and Sasayama Y. 1995. Vitamin D₃ induced changes in the prolactin cells of the fish, *Heteropneustes fossilis* reared in artificial freshwater, calcium-rich freshwater or calcium-deficient freshwater. *J Reprod Biol Comp Endocrinol*, **07**: 72-82.
- Srivastav SK, Srivastava S, Srivastava AK, Mishra D and Prakash C. 2017. Effects of sex Steroids (testosterone and estradiol) on serum calcium and phosphate levels of a freshwater male teleost, *Heteropneustes fossilis*. *Int J Zool Invest*, **03**: 198-202.
- Tewary BK, Kirubakaran R and Ray AK. (2001). Plasma levels of Gonadotropin-II and gonadal sex steroids in triploid catfish, *Heteropneustes fossilis* (Bloch). *Fish Physiol Biochem*, **24**: 9-14.
- Watts EG, Copp, DH and Deftos LJ. 1975. Changes in plasma calcitonin and calcium during the migration of salmon. *Endocrinol*, **96**: 214-218.
- Yamada J, Tomioka J, Yamane S, Iguchi M and Nakamura Y. 1982. In "Comparative Endocrinology of Calcium Regulation", (Oguro, C. and Pang, P.K.T., eds.), p. 143, Japan Sci Soc Press, Tokyo.
- Yamane S and Yamada J. 1977. Histological changes of the ultimobranchial gland through the life history of the masu salmon. *Bull Japan Soc Scient Fish*, **43**: 375-386.
- Yamauchi H, Matsuo M, Yoshida A and Orimo H. 1978. Effect of eel calcitonin on serum electrolytes in the eel *Anguilla japonica*. *Gen Comp Endocrinol*, **34**: 343-346.
- Yeo IK and Mugiya Y. 1997. Effects of extracellular calcium concentrations and calcium antagonists on vitellogenin induction by estradiol-17 β in primary hepatocyte culture in the rainbow trout *Oncorhynchus mykiss*. *Gen Comp Endocrinol*, **105**: 294-301.

Antioxidants Released from *Cichorium pumilum* Jacq. Amendment Mitigate Salinity Stress in Maize

Nadia M El-Shafey^{1*} and Hamada R AbdElgawad^{1,2}

¹Department of Botany and Microbiology, Faculty of Science, Beni-Suef University, Salah Salem Street, Beni-Suef, 62511, Egypt.

²Department of Biology, University of Antwerp, Groenenborgerlaan 171, 2020, Antwerpen, Belgium.

Received: October 25, 2019; Revised: January 3, 2020; Accepted: January 31, 2020

Abstract

Amending soil with weeds, among the organic farming practices, is an innovative approach to improve crop yield and recycle nutrients. A pot experiment was carried out to investigate the impact of amending soil with phenolic rich *Cichorium pumilum* Jacq. leaves (0.0, 10 and 20 g powdered dry matter kg⁻¹ soil) on maize responses to salt stress (0.0, 100 and 200 mM NaCl). Generally, soil amendment enhanced the growth of maize and alleviated the negative stress impact. Amendment at 10 g powdered dry leaves of *C. pumilum* kg⁻¹ soil enhanced the total chlorophyll in severe stressed plant, compared with that grown in unamended stressed soil. Antioxidants such as flavonoids content were increased in all stressed and unstressed samples grown in the amended soil. Consequently, soil amending also induced less oxidative damage (hydrogen peroxide and lipid peroxidation) in stressed plants. Reduced oxidative damage was also associated with the increased catalase and peroxidase activities, and these increases were higher in root explaining the more enhancement in root growth (Pearson correlation). Results indicated that using *C. pumilum* Jacq. amendment, as a way of organic farming, mitigated the harmful effect of salinity on maize plants via its antioxidative potential. Weed amendment, as one of the organic farming methods, contributed via its ability to release antioxidant phenolic compounds.

Keywords: Antioxidant, Organic farming, Phenolic compounds, Salt stress

1. Introduction

Cichorium pumilum Jacq. (synonym: *C. endivia* subsp. *divaricatum* (Schousb.) P.D. Sell, *C. divaricatum* Schousb., *C. endivia* subsp. *pumilum* (Jacq.) Coutinho, *C. intybus* subsp. *pumilum* (Jacq.) Ball) (<http://www.theplantlist.org>) belongs to family Asteraceae. It is one of the annual wild plants growing in Egypt. It also grows as one of the undesired weeds infecting Egyptian fields as well as other fields in some of the Mediterranean countries (Abu-Irmaileh, 1982; Boulet *et al.*, 2002; Gervilla *et al.*, 2019; Qasem, 1992). Previous studies stated that genus *Cichorium* is well defined with the presence of polyphenols including phenolic acids and flavonoids in addition to the presence of sesquiterpenoids (El-Shafey and AbdElgawad, 2012; Kisiel and Michalska, 2006). Also, the antioxidant and antiradical activities of the genus *Cichorium* have been proved (Ghanaatiyan and Sadeghi, 2017; Sahan *et al.*, 2017).

Organic farming as an alternative to conventional agriculture offers solutions to the environmental problems created by some of the practices such as using industrial fertilizers and pesticides. Organic farming is one of the fastest growing agriculture practices over the world, due to providing soil with long-term fertility, supplementing crop with nutrients and reducing adverse impacts of farming systems on the natural habitats and environment (Hassan *et al.*, 2018; Padel and Lampkin, 1994; Peigné *et al.*, 2016). Amending soil with organic wastes and plant residues comes among organic farming practices to enhance soil

fertility, recycling nutrients and biodiversity and microbial populations (Lim *et al.*, 2015). In addition, organic amendment contributes to supply nutrients and enhance plant productivity depending on the quality and quantity of the amendment (Diallo *et al.*, 2006; Roy *et al.*, 2010). Investigating the influence of weed residues on crop productivity has attracted attention, since removing weeds manually, leaving to dry and mixing with soil or ploughing them directly with soil is already still among farming practices (Batish *et al.*, 2007; Hassan *et al.*, 2018). Previous studies recommended utilizing weed residues to enhance crop biomass and yield (Awodun and Ojeniyi, 1999; Awopegba *et al.*, 2016; Falade and Ojeniyi, 1997).

Salt stress is among the main constraints that cause a great loss in crop production. It severely affects plant via inducing osmotic stress and ion toxicity. Moreover, salinity disturbs redox homeostasis in plant cells, causing the burst of reactive oxygen species (ROS). These ROS result in oxidation of lipids, proteins and nucleic acids, leading to membrane damage, enzymatic inhibition and metabolic dysfunction and finally plant death (Hasanuzzaman *et al.*, 2013; Liang *et al.*, 2018). Parallel to production of ROS generally produced from electron transport systems, plant evolved enzymatic antioxidant defense systems including superoxide dismutase (SOD) catalase (CAT) and peroxidase (POD) in addition to nonenzymatic ones such as ascorbate, glutathione, tocopherol, flavonoids and polyphenolic compounds (Liang *et al.*, 2018; Parida and Das, 2005). Plants with more effective employment of their enzymatic and non-enzymatic antioxidants exhibit more enhanced salt

tolerance, as ROS scavenging is very important in salt tolerance (Chinnusamy *et al.*, 2005). There is a worldwide demand for inexpensive and environmentally safe technologies to overcome salinity problem, increase plant tolerance and enhance soil. This makes amending soil with weeds, particularly those rich in phenolics, one of the options that may secure most of these demands.

In the present study, our hypothesis is that *C. pumilum* amendment enhances maize plant growth, especially under stress conditions. To test this hypothesis, the antioxidative potential of *C. pumilum* amendment (10 and 20 g powdered dry leaves kg⁻¹ soil) and its impact on maize growth under different levels of salt stress (0.0, 100 and 200 mM NaCl) were investigated. The biochemical basis of the main effects of amendment (10 g powdered dry leaves kg⁻¹ soil), salinity and their interaction on maize plant were also studied.

2. Materials and Methods

Fresh leaves of the flowering plants of *Cichorium pumilum* Jacq. were collected during winter season from clover and wheat fields in Beni-Suef Governorate, Beni-Suef, Egypt. Samples were identified as reported previously (El-Shafey and Abdelgawad, 2012).

2.1. Extraction of phenolic compounds

The collected leaves were washed under running tap water and then washed three times using distilled water. Leaves were air dried at room temperature and then grinded to fine powder. For preparation of the aqueous extract, about 5 g of the powdered dry leaves were soaked in 100 ml dist. water and agitated on the orbital shaker for 24 hours at 110 rpm and 60°C. The extract was centrifuged at 4000 rpm, filtered through a muslin cloth and then through filter paper Whatman No. 1 by using vacuum and pressure pump (AP-9925 Auto Science). The filtrate was concentrated by using a rotary evaporator (Shanghai Senco Technology Company, Shanghai, China) under reduced pressure at 45°C. Finally, the residue was collected and used for HPLC analysis.

2.2. Analysis of free phenolic compounds

After drying, the residue of aqueous extract was dissolved in HPLC grade MeOH to give 1000 ppm, then 20 µl of methanol dissolved sample were injected into HPLC system (Shimadzu class-LC 10 AD chromatograph supplied with shimadzu SPD-10 AUV-VIS). Phenomenex C18 column (25cm*4.6mm i.d, 5Mm particle size) was used as a stationary phase for HPLC determinations. The retention times of twenty-five highly purified phenolic compounds (Sigma-Aldrich Laborchemikalien, Germany) as well as our sample were detected at 254 nm. Quantitative determinations were carried out using calibration curves of the standards, and values of phenolic compounds were expressed as µg g⁻¹ dry weight.

2.3. Treatments and plant growth analysis

Experiment was repeated twice, giving similar trends, and results of one are shown. Before sowing, pots (15 cm diameter and 15 cm depth) were filled with sandy clay soil (1:3), and the dry powder of *Cichorium* leaves was applied as amendment at 0.0, 10 and 20 g powdered dry leaves kg⁻¹ soil (mixed with 2 cm depth of the surface soil layer). Ten grains of maize (single cross 10; Sc10) were sown per each pot in a random way. Pots with amended and unamended

soil were irrigated with tap water and kept in net house at the Botanical Garden, Botany and Microbiology Department, Faculty of Science, Beni-Suef University, where average high and low temperatures were 32-35 and 20-22°C respectively, during May and June. After emergence, the growing seedlings were thinned to 4 seedlings. After two weeks of sowing, pots were irrigated with salt solutions (0.0, 100 and 200 mM NaCl) and permanently kept at its field capacity level. The experiment was designed in a split-plot design, where the amendment treatments were the main plots and salinity levels were subplots. After two weeks of salinity application, the plants were harvested and used to determine the growth parameters (lengths, and fresh and dry weights of both root and shoot). The biochemical analyses were performed in fresh and dry samples of plants grown in both amended (10 g powdered dry leaves kg⁻¹ soil) and unamended soils.

2.4. Photosynthetic pigments and flavonoids

The photosynthetic pigments were extracted and estimated according to Lichtenthaler (1987). Approximately 0.5 g of fresh leaves was homogenized in 5 ml cold acetone (80%) and the extract was centrifuged for ten minutes at 4000 rpm and 4°C. The optical density of the extract was measured at 663.2, 646.8 and 470 nm using 80% acetone as a blank. The amounts of chlorophyll (Chl) a, Chl b and carotenoids were calculated in µg per ml extract by using the equations given below, and expressed as µg g⁻¹ dry weight.

Concentration of Chl a = $12.25 A_{663.2} - 2.79 A_{646.8}$

Concentration of Chl b = $21.50 A_{646.8} - 5.10 A_{663.2}$

Concentration of carotenoids = $(1000 A_{470} - 1.82 \text{ Chl a} - 85.02 \text{ Chl b}) / 198$

Total flavonoids were extracted in 80% methanol (Sayed *et al.*, 2017). The mixture was agitated overnight at 100 rpm on an orbital shaker and then centrifuged at 6000 rpm at room temperature. Content of total flavonoids was determined in the supernatant by aluminum chloride (Zhishen *et al.*, 1999). The absorbance was read at 510 nm. Quercetin standard curve was used to estimate the concentration of total flavonoids that was expressed as µg g⁻¹ dry weight.

2.5. Enzymatic antioxidants

Frozen samples were homogenized in cold phosphate buffer (67 mM and pH 7.0). The homogenate was centrifuged at 10,000 rpm for 15 min at 4°C, and the supernatant was used as a crude enzyme. Activity of SOD (EC 1.15.1.1) was quantified based on the competitive inhibition of nitroblue tetrazolium chloride (NBT) reduction by the superoxide radical (Beyer, 1987). One unit of SOD activity was calculated as the amount of enzyme required to cause 50% inhibition of the rate of NBT reduction. The activity of catalase (CAT; EC 1.11.1.6) was assayed by following the decomposition of H₂O₂ as a decline in the absorbance at 240 nm (Kato and Shimizu, 1987). Catalase activity was calculated using the extinction coefficient (40 mM⁻¹ cm⁻¹ at 240 nm) and expressed as µM H₂O₂ destroyed min⁻¹ g⁻¹ fresh weight. Peroxidase (POD; EC 1.11.1.7) activity was estimated following the change of catechol absorbance at 430 nm due to oxidation by H₂O₂ (Kar and Mishra, 1976). The enzyme activity was expressed as the change in optical density of catechol min⁻¹ g⁻¹ fresh weight.

2.6. Hydrogen peroxide (H₂O₂) and lipid peroxidation (LPO)

One gram of frozen plant material was homogenized with 10 ml of 0.1% trichloroacetic acid (TCA) and the homogenate was centrifuged at 10,000 rpm for 15 min. The supernatant was used for assaying H₂O₂ and lipid peroxidation. Hydrogen peroxide was estimated by potassium iodide and the absorbance was recorded at 390 nm (Velikova *et al.*, 2000). The concentration of H₂O₂ was calculated from its standard curve and expressed as $\mu\text{M g}^{-1}$ fresh weight. Lipid peroxidation (LPO) was determined by measuring the absorbance of the colored complex formed due to reaction of malondialdehyde (MDA; a principal product of lipid peroxidation) with thiobarbituric acid (TBA) at 532 nm (Jambunathan, 2010). The amount of MDA was calculated using the extinction coefficient of $155 \text{ mM}^{-1} \text{ cm}^{-1}$ and expressed as nmol g^{-1} fresh weight.

2.7. Statistical analysis

All statistical analyses were performed using SPSS 16.0 program for Windows (SPSS, Chicago, IL, USA). Split-plot ANOVA was applied to investigate the effect of amendment, salinity and their interaction. Differences among means were established using Duncan test ($P < 0.05$), and Pearson correlations were determined among variables.

3. Results

3.1. Free phenolic compounds in *C. pumilum*

Nine free phenolic compounds, most of which are phenolic acids, were detected and quantified in the aqueous extract of *C. pumilum* (Table 1). Among these, caffeic acid (18.9%), gallic acid (16.2%), pyrogallol (14.2%), vanillic acid (14.0%) and cinnamic acid (13.6%) were the most abundant phenolic compounds detected in *C. pumilum* aqueous extract. Also, ferulic acid with the proportion 10.7% of the total detected compounds was found in the aqueous extract. Protocatechuic acid, coumarin and apigenin were found in lower proportion (3.0-5.3%).

Table 2. Mean Squares of main effects and interaction for morphological and physiological criteria of maize treated with *C. pumilum* amendment and salinity.

Source	df	Shoot length	Root length	Shoot FW	Root FW	Shoot DW	Root DW
Salinity	2	603***	82***	3.3***	0.022	0.049***	0.002
Amendment	2	1498***	172***	5.5***	0.375*	0.036***	0.01*
Salinity× Amendment	4	134***	34***	0.097	0.113*	0.003	0.002
		Chl a	Chl b	Carotenoids	Total chlorophyll		Chl a/b
Salinity	2	29333	46243***	1812	149173*		0.032
Amendment	1	10850	159795***	1205	87368		2.107***
Salinity× Amendment	2	78504	12330*	9890**	153009*		0.079
		Shoot flav	Root flav	Shoot SOD	Root SOD	Shoot CAT	Root CAT
Salinity	2	648***	305***	29114***	554085*	1802***	6575***
Amendment	1	624***	624***	6277	485253	632**	5036***
Salinity× Amendment	2	10.7	0.106	7230***	357811*	62.3	1044***
		Shoot POD	Root POD	Shoot H ₂ O ₂	Root H ₂ O ₂	Shoot LP	Root LP
Salinity	2	7484***	9603***	3485***	4409*	2066***	3803***
Amendment	1	1661*	2150***	2892***	8916*	3562***	11769***
Salinity× Amendment	2	287*	2176***	14.8	866	99.6	417**

*, **, *** < significant at 0.05, 0.01, and 0.001 probability levels, respectively, Chl a; chlorophyll a, Chl b; chlorophyll b, flav; flavonoids, SOD, superoxide dismutase, CAT; catalase, POD; peroxidase, LP; lipid peroxidation.

Table 1. HPLC analysis of phenolic compounds in aqueous extract of *C. pumilum* Jacq. leaves

Standard phenolic compounds	Retention time min		Concentration $\mu\text{g g}^{-1}$ dry weight
	Standard	Sample	
Gallic acid	8.2	8.2	151.1
Pyrogallol acid	9.2	9.3	132.2
Protocatechuic acid	12.7	12.8	28.0
Caffeic acid	18.0	18.1	176.4
Vanillic acid	18.0	18.1	130.4
Coumarin	22.2	21.6	38.6
Ferulic acid	24.9	25.0	99.6
Cinnamic acid	36.1	36.0	126.7
Apigenin	38.0	38.2	49.0
Total			932.0

3.2. Plant growth

Salinity adversely affected growth parameters of maize, while amendment enhanced these parameters and alleviated their loss exerted by salinity as compared with control (Table 2 and Figure 1). As interaction (salinity×amendment) was significant for shoot and root lengths as well as root fresh weight ($P < 0.001$ and $P < 0.05$, respectively; Table 2), the amendment-induced enhancement in these parameters was more pronounced under stress conditions, particularly the severe one (Figure 1a-b, d). Amendment significantly increased means of shoot ($P < 0.001$; Table 2) and root ($P < 0.05$) dry biomass of both salt stressed and unstressed maize (Figure 1e-f). In most cases, there was no significant difference between the influence of 10 g and that of 20 g of *C. pumilum* amendment; both significantly enhanced shoot and root biomass. However, the dose 10 g of amendment was the most effective in mitigating the adverse effect of salinity on plant growth. For example, shoot and root dry weights treated with 10 g amendment amplified by 2 and 5.7 fold, respectively (Figure 1e-f) as compared with those grown under severe stress without amendment.

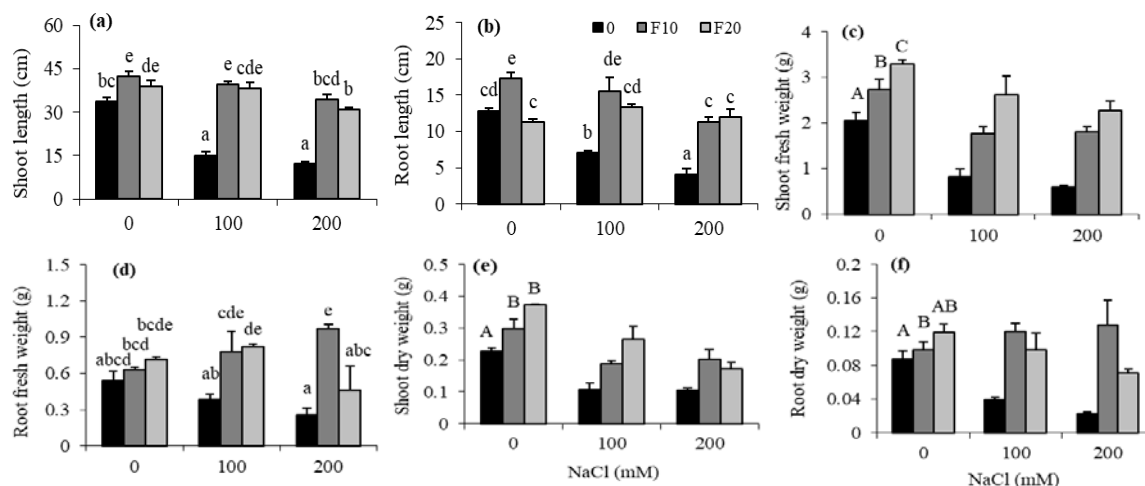


Figure 1. Effect of *C. pumilum* amendment on shoot and root lengths (a-b), fresh weights (c-d) and dry weights (e-f) of maize under different levels of salt stress (0.0, 100 and 200 mM NaCl). Treatments of 0, F10 and F20 are 0.0, 10 and 20 g amendment kg⁻¹ soil. Values are means of 5 replicates ± SE. Values with at least one similar letter are non-significantly different at $P=0.05$. Capital letters are for main effect of amendment, while small letters are for multiple comparison in case of a significant interaction.

3.3. Photosynthetic pigments and flavonoids

Under severe stress, both Chl a and carotenoids as well as total chlorophyll declined below control (Table 3), but that decline was alleviated by applying amendment making the levels of these parameters approach that of control. Amendment mainly augmented Chl b content leading to a significant decrease (Table 2; $P < 0.001$) in Chl a/b ratio. Salinity×amendment interaction was significant for Chl b and total Chlorophyll ($P < 0.05$), as well as for carotenoids ($P < 0.01$). In all these traits, amendment effectively enhanced their levels and alleviated

the loss imposed in them by severe salt stress (Table 3). Means comparison of flavonoids, one of the non-enzymatic antioxidants, revealed a significant decline as affected by salinity ($P < 0.001$; Table 2) and was more apparent at the highest level of stress, while the main effect of amendment significantly increased means of flavonoids of all the stressed and unstressed shoot and root ($P < 0.001$; Table 2-3). Although there was no significant interaction for this parameter in both organs, the increase in flavonoids value as affected with amendment was more pronounced in the stressed organs, particularly roots.

Table 3. Effect of *C. pumilum* amendment (10 g powered dry leaves kg⁻¹ soil) on photosynthetic pigments and contents of shoot and root flavonoids in maize plants under different levels of salt stress (0.0, 100 and 200 mM NaCl).

Treatments	Chl a ($\mu\text{g g}^{-1}$ dry wt)	Chl b ($\mu\text{g g}^{-1}$ dry wt)	Carotenoids ($\mu\text{g g}^{-1}$ dry wt)	Total chlorophyll ($\mu\text{g g}^{-1}$ dry wt)	Chl a/b	Shoot flavonoids ($\mu\text{g g}^{-1}$ dry wt)	Root flavonoids ($\mu\text{g g}^{-1}$ dry wt)
C	592 ± 0	432 ± 18c	217 ± 4c	1024 ± 24b	1.37 ± 0.04	38.5 ± 1.5	31.19 ± 0.7
F	425 ± 4	570 ± 3d	146 ± 20ab	995 ± 30b	0.75 ± 0.07	53.37 ± 0.5	42.73 ± 1.5
100	506 ± 134	313 ± 87b	224 ± 57c	819 ± 221b	1.62 ± 0.02	29.61 ± 1.1	21.9 ± 0.8
F-100	311 ± 98	447 ± 22c	170 ± 17abc	758 ± 120b	0.69 ± 0.18	39.74 ± 0.8	33.65 ± 0.7
200	267 ± 31	184 ± 12a	124 ± 14a	451 ± 43a	1.45 ± 0.08	20 ± 0.7	16.87 ± 0.5
F-200	481 ± 262	477 ± 57c	201 ± 61bc	958 ± 319b	0.96 ± 0.44	30.33 ± 1.0	28.94 ± 0.6

Values are means of 3 replicates ± SE. Values with at least one similar letter are non-significantly different at $P=0.05$, while those with no letters are incase nonsignificant interaction. F; Samples amended with 10 g powered dry leaves per kg soil.

3.4. Enzymatic antioxidants

The effect of salt stress on SOD activity was contrasting to that on CAT and POD enzymes. While salinity amplified the activity of SOD, those of CAT and POD were decreased by increasing NaCl-concentration in both shoot and root of maize (Figure 2). Moreover, amending soil with *C. pumilum* dry powdered leaves significantly inhibited SOD, but stimulated CAT and POD in both parts. Interaction (salinity×amendment) was significant on SOD of both shoot and root ($P < 0.001$ and 0.05, respectively; Table 2). At 200 mM NaCl, amendment kept the activity of shoot SOD nonsignificantly changed relative to the nonamended samples, while declined that of root SOD to the level of control (Figure 2a-b). Salinity

dimensioned CAT and POD activities in shoots grown in both amended and nonamended soils. In all the investigated salinity levels, CAT activity of the amended shoots was higher than that of the nonamended ones, whereas the alleviating effect of amendment on shoot POD was significant only under severe stress ($P > 0.05$; Table 2). Although salinity induced a dramatic decline in CAT and POD of roots grown in the nonamended soil, amendment significantly stimulated these enzymes at 100 mM NaCl to a level over control ($P < 0.001$; table 2, Figure 2d, f). Interestingly, the response of those enzymes to amendment at 200 mM was different, as amendment attenuated the activity of both enzymes.

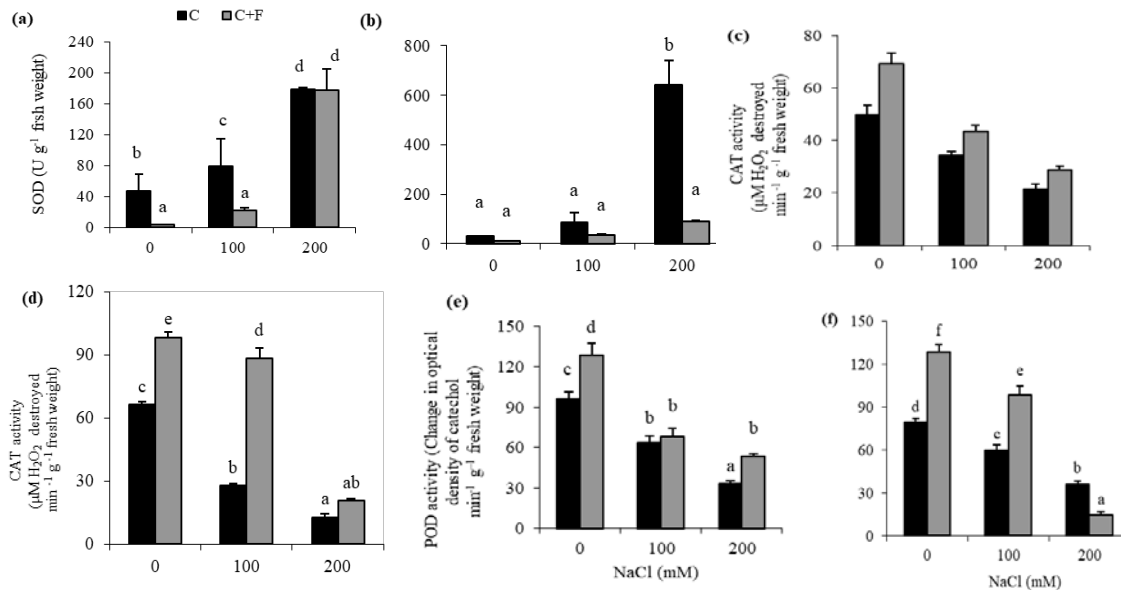


Figure 2. Effect of *C. pumilum* amendment (10 g powered dry leaves kg⁻¹ soil) on SOD; superoxide dismutase (a-b), CAT; catalase (c-d) and POD; peroxidase (e-f) activities in shoot and root of maize plants grown under different levels of salt stress (0.0, 100 and 200 mM NaCl). Treatments of C and C+F; 0.0 and 10 g amendment kg⁻¹ soil. Values are means of 3 replicates ± SE. Values with at least one similar letter are non-significantly different at $P=0.05$, while those with no letters are in case of no significant interaction.

3.5. Hydrogen peroxide (H₂O₂) and lipid peroxidation (LPO)

Salinity main effect significantly increased the accumulation of H₂O₂ in both shoot ($P < 0.001$; Table 2) and root ($P < 0.05$) grown in the amended and nonamended soils as well, and the accumulation was lower in the amended samples across all salinity levels (Figure 3a-b). Similar effect to that of salinity and amendment on

H₂O₂ accumulation was imposed on LPO in shoot (Figure 3c). The decline in lipid peroxidation due to treatment with amendment was more pronounced in stressed roots than stressed shoots. Amendment effectively declined LPO value to the level of control ($P < 0.01$; Table 2, Figure 3d), although it was increased to 1.8-fold of control at severe concentration.

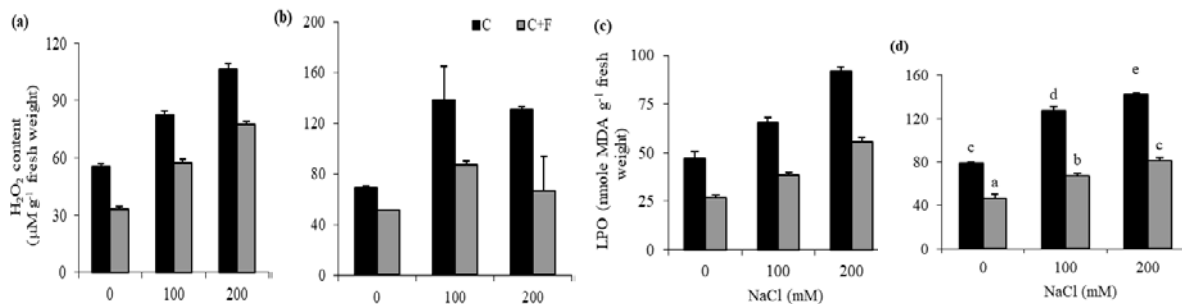


Figure 3. Effect of *C. pumilum* amendment (10 g powered dry leaves kg⁻¹ soil) on H₂O₂; hydrogen peroxide (a-b) content and LPO; lipid peroxidation (c-d) in shoot and root of maize plants grown under different levels of salt stress (0.0, 100 and 200 mM NaCl). Treatments of C and C+F; 0.0 and 10 g amendment kg⁻¹ soil. Values are means of 3 replicates ± SE. Values with at least one similar letter are non-significantly different at $P=0.05$, while those with no letters are in case of no significant interaction.

4. Discussion

Organic amendment is known to supply nutrients to soil and enhance its fertility and physical properties which leads in turn to improvement of plant performance (Ali *et al.*, 2017; Roy *et al.*, 2010). In the current study, amending soil with *C. pumilum* dry powdered leaves enhanced fresh and dry biomass as well as the length of both stressed and unstressed maize plants, and the influence was more pronounced in the stressed samples, particularly root ones. Similar enhancement of maize growth was also reported after applying weed residues to soil (Awodun and Ojieniyi, 1999; Falade and Ojieniyi, 1997; Jabeen and Ahmed, 2009). The positive effect on growth that detected in the present study by applying amendment may be due to the

antioxidative stimulatory and/or protective effect of the components released from *C. pumilum* amendment. Applying weed amendment, particularly that rich in phenolics, may add more advantages to the employment of organic amendment. Recently, it was reported that the productivity of bean plants was increased when soil was amended with the dry residues of the phenolic-rich weed; *Sonchus oleraceus* (Hassan *et al.*, 2018). Most of the phenolic compounds that showed abundance in *C. pumilum* leaves were documented as potential antioxidants (Hussain and Reigosa, 2011; Li *et al.*, 2013; Wan *et al.*, 2014). These phenolic compounds, when leached from *C. pumilum* leaves to soil, could work in a synergistic or antagonistic way that they positively affected the growth and the physiological processes of maize plants. They

might also supply the plant with the defenses effectively employed by the root to counteract the adverse effects of salinity, leading to more pronounced enhancement of root than shoot. The ability of the exogenously applied natural phenolics to improve plant defense mechanisms was documented (El-Shafey and AbdElgawad, 2012; Mohamed *et al.*, 2017).

Both phenolics and salt-stress are known to impact photosynthetic pigments concentration (Hussain and Reigosa, 2011; Khodary, 2004). Due to the imbalance between the generation and detoxification, salt stress excessively generates ROS such as superoxide radicals and singlet oxygen, naturally produced in chloroplasts within the electron transfer chain of photosystem II (PSII) and photosystem I (PSI) (Foyer and Shigeoka, 2011). Thus, presence of integrative and effective enzymatic and nonenzymatic antioxidative system is necessary for maintaining efficient photosynthetic machinery. In addition to dismutases and peroxidases, plant utilizes some antioxidants as carotenoids, flavonoids, ascorbates and glutathione to quench and scavenge the excess generated singlet oxygen, superoxides and hydrogen peroxide (Agati *et al.*, 2007; Gururani *et al.*, 2015). Treating maize plants with 10 g of *C. pumilum* amendment in combination with 200 mM NaCl increased the concentration of Chl a, Chl b, carotenoids and total chlorophyll as compared with plants grown under salt-stress without amendment. Our results support those reported on syringic acid and apigenin, when applied on cowpea (Alsaadawi *et al.*, 1986) and rice (Mekawy *et al.*, 2018), respectively. The positive effect of *C. pumilum* amendment was more obvious in case of Chl b than Chl a, leading in turn to a decline in Chl a/b ratio in all samples that have been subjected to the amendment in presence or absence of salinity. The lower a/b ratio is linked with the increase in size of light-harvesting chlorophyll a/b-binding proteins associated with PSII (LHCII) antenna (Taiz and Zeiger, 2010). Enlargement of the LHCII antenna size may cause excess excitation of chlorophyll which, if not dissipated via non-photochemical quenching (NPQ), may cause excess generation and accumulation of superoxides and H₂O₂; these could cause photoinhibition and damage of PII when not scavenged effectively. It is difficult to precisely explain how amendment enhanced Chl b content, probably by decreasing conversion of Chl b into Chl a, but we believe that photoinhibition did not happen in our investigated plants grown in amended soil. The reason is that amendment alleviated the loss in carotenoids which play an essential role in photoprotection and antioxidant defense (Pessaraki, 2016) and increased their concentration over those in the leaves of nonamended plants under salt stress. Additionally, amending soil with phenolic-rich residues was reported to increase the concentration of phenolics in plant (Batish *et al.*, 2007; Hassan *et al.*, 2018). *Cichorium pumilum* is known to contain high concentrations of not only phenolics (Table 1), but also quinones and quinone precursors (Threlfall and Whistance, 1970). These components, when taken up,

could work as antioxidants or photochemical or nonphotochemical quenchers and hence improve photosynthesis, mainly under stressful conditions (Bukhov *et al.*, 2003; Kościelniak *et al.*, 2011; Zhao and Zou, 2002). Unfortunately, the quenching of chlorophyll inflorescence was not measured in the current study. Nevertheless, exogenous phenolics were found to enhance photochemical efficiency of photosystem PII (F_v/F_m & F_m/F_0), photochemical quenching (qP) and net photosynthetic rate (P_N) and lowered NPQ leading to enhanced photosynthesis (Zhao and Zou, 2002). This role was found to be accomplished via scavenging superoxide species and protecting photosynthetic machinery from the induced oxidative damage. Similar results were reported on salicylic acid when applied to cucumber leaves under high temperature and strong light stress (Sun *et al.*, 2006), but cinnamic acid applied to *Lactuca sativa* at high concentration (1.5 mM) induced oxidative stress. It reduced plant biomass and decreased photochemical efficiency of photosystem PII as well as qP and NPQ (Hussain and Reigosa, 2011). Hence, it is important to take in consideration that the effect of the phenolic compound that would be exogenously applied to plant under stressful condition would be varied according to its structure and concentration. In their study, Bukhov *et al.* (2003) discovered that exogenous artificial quinones could work as photochemical and non-photochemical quenchers of energy in PSII, mimicking the properties of the endogenous plastoquinones that act as an electron carrier between PSII and the cytochrome b6f complex.

Concerning flavonoids, Agati *et al.* (2007) provided a strong evidence that flavonoids located in chloroplast, likely associated with its envelope, have the potential to scavenge singlet oxygen *in vivo*. The increased flavonoids content, in absence or presence of salt stress, might be linked with the amendment-mediated triggering of the biosynthesis of these compounds and/or the uptake by roots of the exogenous flavonoids released from the surrounding amended rhizosphere. The up-regulation of phenylpropanoids pathway, in response to exogenously applied phenolics, resulting in enhanced accumulation of flavonoids was discussed in literatures (El-Soud *et al.*, 2013; Hassan *et al.*, 2018). In the present work, flavonoids were found to be positively correlated ($r = 0.754^{**}$ and 0.787^{**}) with both of fresh and dry weights, respectively (Table 4), while high negative correlations were scored between flavonoids and H₂O₂ ($r = -0.964^{**}$) as well as LPO ($r = -0.908^*$). These correlations indicated that the augmented flavonoids in the salt-stressed samples due to amendment was directly linked with the enhanced tolerance of maize plants, and that enhancement was accomplished by protecting membranes against the stress-induced H₂O₂ and other ROS and their subsequent LPO and membrane damage. In the same context, accumulation of flavonoids due to apigenin application was found to be related to the increased salt tolerance of rice seedlings (Mekawy *et al.*, 2018).

Table 4. Correlations among various parameters of maize plants cultivated in soil amended with (0.0 and 10 g powdered dry leaves kg⁻¹ soil) *C. pumilum* powdered dry leaves under different levels of salt stress (0.0, 100 and 200 mM NaCl).

Criteria	Correlation Coefficient (<i>r</i>)						
	Fresh weight	Dry weight	Flavonoids	Catalase	Peroxidase	Superoxide dismutase	Hydrogen peroxide
Dry weight	0.986**						
Flavonoids	0.754**	0.787**					
Catalase	0.807*	0.817*	0.959**				
Peroxidase	0.830*	0.868*	0.852*	0.920*			
Superoxide dismutase	-0.390	-0.480	-0.659*	-0.590*	-0.530		
Hydrogen peroxide	-0.921*	-0.862*	-0.964**	-0.865*	-0.590*	0.640*	
Lipid peroxidation	-0.770**	-0.838**	-0.908*	-0.578*	-0.628*	0.711**	0.974**

** Correlation is significant at 0.01 level. * Correlation is significant at 0.05 level.

Generating more ROS, such as superoxides and H₂O₂, is among the dangerous effects exerted by salinity on plant cells. Plants utilize SOD to dismutate superoxide radicals and form H₂O₂ and O₂ molecules (Parida and Das, 2005). The scavenging of H₂O₂ in cells is critical to avoid oxidative damage (Yamasaki *et al.*, 1997), as it can generate [•]OH, a highly dangerous ROS, via Fenton reaction (Gill and Tuteja, 2010). In the existing work, increasing salt stress stimulated maize SOD, while inhibited CAT and POD enzymes, and their inhibition could lead to the accumulation of H₂O₂ causing peroxidation of macromolecules and dysfunction of membranes (Parida and Das, 2005). The positive correlation ($r = 0.974^{**}$) that was found between H₂O₂ and LPO and the negative one ($r = -0.862^{*}$) existing between H₂O₂ and dry weight (Table 4) may confirm the harmful effect of the accumulated H₂O₂ in the stressed maize tissues. Compared with the plants grown in nonamended soil, those grown in the amended one exhibited a lower activity of SOD in absence as well as presence of NaCl, indicating lower *de novo* synthesis of SOD that was likely associated with less generation of superoxide radicals or better scavenging with other mechanisms. That situation was obviously exhibited at 200 mM NaCl in maize roots. Meanwhile, at lower salinity levels CAT and POD exhibited higher activity in response to *C. pumilum* amendment. The role of enzymatic antioxidants at lower salt stress appeared more effectively in root, linked with its more enhancement in fresh ($r = 0.807^{*}$ and 0.830^{*}) and dry ($r = 0.817^{*}$ and 0.868^{*}) weights (Table 4).

Since root was the main part that is close to soil, it was reasonable to exhibit a more noticeable inhibition in its dry weight by salinity alone and more alleviation of that inhibition by adding *C. pumilum* amendment than that of shoot (Figure 1e-f). The negative correlation ($r = -0.659^{*}$) that was detected between flavonoids and SOD and the higher increase of root flavonoids at severe salt stress may indicate that flavonoids could have a direct role in scavenging the superoxide radicals induced under salinity. These findings are in parallel with the study of Mekawy *et al.* (2018) who found that pretreatment of rice seeds with apigenine, a flavone aglycone, enhanced seedling growth under salt stress. That enhancement was associated with the increased activities of CAT and ascorbate peroxidase (APX) in root and the accumulation of carotenoids and flavonoids in shoot. Besides flavonoids, other nonenzymatic antioxidants could be involved in alleviation of oxidative stress as a result of amending soil with *C. pumilum*. For example, organic amendment was found to

alleviate salinity-induced oxidative damage in tomato via maintaining the redox states of ascorbate and glutathione, increasing ascorbate (ASC) and glutathione (GSH) concentrations and enhancing the enzymatic antioxidant defenses and photosynthetic machinery (Tartoura *et al.*, 2014). In the present study, *Cichorium pumilum* amendment might directly help via its released antioxidants, or indirectly, by motivating maize antioxidant defenses, in scavenging some of salinity-generated ROS to the level that made increasing SOD activity unrequired, and at the same time enough to trigger the *de novo* synthesis of CAT and POD enzymes. Consequently, all lead to less accumulated H₂O₂ and MDA, more stability and integrity of membranes and macromolecules in the amended samples and more tolerance to salt stress. Confirming this, positive correlations were detected between SOD ($r = 0.640^{*}$ and 0.711^{**}), and negative ones between CAT ($r = -0.865^{*}$ and -0.578^{*}) or POD ($r = -0.590^{*}$ and -0.628^{*}) and both of H₂O₂ and MDA, respectively (Table 4). The results of the current study support the positive correlation reported previously between the ability of exogenously applied phenolics to alleviate stress-induced harmful effects on plant and the enhancement of antioxidant defenses (El-Soud *et al.*, 2013; Saleh and Madany, 2015; Wan *et al.*, 2014). In the same regard, *Corchorus olitorius* and *Urtica pilulifera* seed extract alleviated the oxidative damage induced by copper stress on tomato seed germination. The extracts lowered the levels of MDA and H₂O₂ and enhanced the activities of CAT and ascorbate peroxidase (APX) in the stressed seedlings (İşeri *et al.*, 2018).

In conclusion, amending soil with powdered dry *C. pumilum* leaves, as a way of organic farming, mitigated salt stress in maize via scavenging the evolved ROS. That scavenging came directly by the antioxidants released from the amendment or indirectly by enforcing the enzymatic antioxidant defenses or the non-enzymatic ones, particularly flavonoids, leading consequently to lower level of lipid peroxidation and enhanced productivity. However, prospective large-scale investigations are still needed to validate the application of *C. pumilum* amendment in field and to confirm its positive potential on maize grain yield.

Acknowledgement

The authors are grateful to Dr. Emad Ali Al Sherif and Dr. Walaa Azmy, Department of Botany and Microbiology, Faculty of Science, Beni-Suef University,

Egypt, for their help in identification of *Cichorium pumilum* Jacq. collected samples.

References

- Abu-Irmaileh BE. 1982. **Weeds of Jordan (weeds of crop fields)**, Amman University, Amman, Jordan.
- Agati G, Matteini P, Goti A and Tattini M. 2007. Chloroplast-located flavonoids can scavenge singlet oxygen. *New Phytol*, **174**: 77-89.
- Ali S, Rizwan M, Qayyum MF, Ok YS, Ibrahim M, Riaz M, Arif MS, Hafeez F, Al-Wabel MI and Shahzad AN. 2017. Biochar soil amendment on alleviation of drought and salt stress in plants: a critical review. *Environ Sci Pollut R*, **24**: 12700-12712.
- Alsaadawi IS, Al-Hadithy SM and Arif MB. 1986. Effects of three phenolic acids on chlorophyll content and ions uptake in cowpea seedlings. *J Chem Ecol*, **12**: 221-227.
- Awodun M and Ojeniyi S. 1999. Use of weed mulches for improving soil fertility and maize performance. *Appl Trop Agric*, **2**: 26-30.
- Awopegba M, Awodun M and Oladele S. 2016. Maize (*Zea mays*) biomass and yield as influenced by leguminous and non-leguminous mulch types in southwestern Nigeria. *Bulg J Soil Sci*, **1**: 154-169.
- Batish D, Lavanya K, Singh H and Kohli R. 2007. Phenolic allelochemicals released by *Chenopodium murale* affect the growth, nodulation and macromolecule content in chickpea and pea. *Plant Growth Regul*, **51**: 119-128.
- Beyer W. 1987. Assaying for superoxide dismutase activity: Some large consequences of minor changes in conditions. *Anal Biochem*, **161**: 559-566.
- Boulet C, Labrousse P, Arnaud MC, Zehhar N and Fer A. 2002. Orobanche -weeds relationships: an important aspect of broomrape control. Proceedings of the meeting. Integrated control of broomrape, COST 849 Parasitic Plant Management in Sustainable Agriculture. Obermarchtal, Germany.
- Bukhov NG, Sridharan G, Egorova EA and Carpentier R. 2003. Interaction of exogenous quinones with membranes of higher plant chloroplasts: modulation of quinone capacities as photochemical and non-photochemical quenchers of energy in Photosystem II during light-dark transitions. *Biochim Biophys Acta (BBA)-Bioenergetics*, **1604**: 115-123.
- Chinnusamy V, Jagendorf A and Zhu J-K. 2005. Understanding and improving salt tolerance in plants. *Crop Sci*, **45**: 437-448.
- Diallo MD, Duponnois R, Guisse A, Sall S, Chotte JL and Thioulouse J. 2006. Biological effects of native and exotic plant residues on plant growth, microbial biomass and N availability under controlled conditions. *Eur J Soil Biol*, **42**: 238-246.
- El-Shafey N and AbdElgawad H. 2012. Luteolin, a bioactive flavone compound extracted from *Cichorium endivia* L. subsp. *divaricatum* alleviates the harmful effect of salinity on maize. *Acta Physiol Plant*, **34**: 2165-2177.
- El-Soud WA, Hegab MM, AbdElgawad H, Zinta G and Asard H. 2013. Ability of ellagic acid to alleviate osmotic stress on chickpea seedlings. *Plant Physiol Biochem*, **71**: 173-183.
- Falade I and Ojeniyi S. 1997. Effect of siam weed mulch on soil nutrient contents and maize performance. *Appl Trop Agric*, **2**: 100-113.
- Foyer CH and Shigeoka S. 2011. Understanding oxidative stress and antioxidant functions to enhance photosynthesis. *Plant Physiol*, **155**: 93-100.
- Gervilla C, Rita J and Cursach J. 2019. Contaminant seeds in imported crop seed lots: a non-negligible human-mediated pathway for introduction of plant species to islands. *Weed Res*, **59**: 245-253.
- Ghanaatiyan K and Sadeghi H. 2017. Differential responses of chicory ecotypes exposed to drought stress in relation to enzymatic and non-enzymatic antioxidants as well as ABA concentration. *J Horticult Sci Biotechnol*, **92**: 404-410.
- Gill SS and Tuteja N. 2010. Reactive oxygen species and antioxidant machinery in abiotic stress tolerance in crop plants. *Plant Physiol Biochem*, **48**: 909-930.
- Gururani Mayank A, Venkatesh J and Tran LSP. 2015. Regulation of photosynthesis during abiotic stress-induced photoinhibition. *Mol Plant*, **8**: 1304-1320.
- Hasanuzzaman M, Nahar K and Fujita M. 2013. Plant response to salt stress and role of exogenous protectants to mitigate salt-induced damages. In: Ahmad P, Azooz M and Prasad M (Eds.), **Ecophysiology and Responses of Plants under Salt Stress**. Springer, New York, pp. 25-87.
- Hassan MO, Saleh AM and AbdElgawad H. 2018. *Sonchus oleraceus* residue improves nutritive and health-promoting value of common bean (*Phaseolus vulgaris* L.): A metabolic study. *J Agr Food Chem*, **66**: 2092-2100.
- Hussain MI and Reigosa MJ. 2011. A chlorophyll fluorescence analysis of photosynthetic efficiency, quantum yield and photon energy dissipation in PSII antennae of *Lactuca sativa* L. leaves exposed to cinnamic acid. *Plant Physiol Biochem*, **49**: 1290-1298.
- İşeri ÖD, Körpe DA, Sahin FI and Haberal M. 2018. *Corchorus olitorius* and *Urtica pilulifera* extracts alleviate copper induced oxidative damage and genotoxicity in tomato. *Acta Biol Hung*, **69**: 300-312.
- Jabeen N and Ahmed M. 2009. Possible allelopathic effects of three different weeds on germination and growth of maize (*Zea mays*) cultivars. *Pak J Bot*, **41**: 1677-1683.
- Jambunathan N. 2010. Determination and detection of reactive oxygen species (ROS), lipid peroxidation, and electrolyte leakage in plants. In: Sunkar R (Ed.) **Plant Stress Tolerance: Methods and Protocols**. Humana Press, Totowa, NJ, pp. 291-297.
- Kar M and Mishra D. 1976. Catalase, peroxidase, and polyphenoloxidase activities during rice leaf senescence. *Plant Physiol*, **57**: 315-319.
- Kato M and Shimizu S. 1987. Chlorophyll metabolism in higher plants. VII. Chlorophyll degradation in higher plants. VII. Chlorophyll degradation in senescing tobacco leaves: Phenolic-dependent peroxidative degradation. *Can J Bot*, **65**: 729-735.
- Khodary S. 2004. Effect of salicylic acid on the growth, photosynthesis and carbohydrate metabolism in salt-stressed maize plants. *Int J Agric Biol*, **6**: 5-8.
- Kisiel W and Michalska K. 2006. Sesquiterpenoids and phenolics from roots of *Cichorium endivia* var. *crispum*. *Fitoterapia*, **77**: 354-7.
- Kościełniak J, Ostrowska A, Biesaga-Kościełniak J, Filek W, Janeczko A, Kalaji HM and Stalmach K. 2011. The effect of zearalenone on PSII photochemical activity and growth in wheat and soybean under salt (NaCl) stress. *Acta Physiol Plant*, **33**: 2329-2338.
- Li D-M, Nie Y-X, Zhang J, Yin J-S, Li Q, Wang X-J and Bai J-G. 2013. Ferulic acid pretreatment enhances dehydration-stress tolerance of cucumber seedlings. *Biol Plant*, **57**: 711-717.
- Liang W, Ma X, Wan P and Liu L. 2018. Plant salt-tolerance mechanism: A review. *Biochem Biophys Res Commun*, **495**: 286-291.
- Lichtenthaler HK. 1987. Chlorophylls and carotenoids: Pigments of photosynthetic biomembranes. In: **Methods in enzymology**. Academic Press, pp. 350-382.

- Lim SL, Wu TY, Lim PN and Shak KPY. 2015. The use of vermicompost in organic farming: overview, effects on soil and economics. *J Sci Food Agric*, **95**: 1143-1156.
- Mekawy AMM, Abdelaziz MN and Ueda A. 2018. Apigenin pretreatment enhances growth and salinity tolerance of rice seedlings. *Plant Physiol Biochem*, **130**: 94-104.
- Mohamed MSM, Saleh AM, Abdel-Farid IB and El-Naggar SA. 2017. Growth, hydrolases and ultrastructure of *Fusarium oxysporum* as affected by phenolic rich extracts from several xerophytic plants. *Pestic Biochem Physiol*, **141**: 57-64.
- Padel S and Lampkin N. 1994. **The Economics of Organic Farming: An International Perspective**, CAB International.
- Parida AK and Das AB. 2005. Salt tolerance and salinity effects on plants: a review. *Ecotoxicol Environ Saf*, **60**: 324-349.
- Peigné J, Casagrande M, Payet V, David C, Sans FX, Blanco-Moreno JM, Cooper J, Gascoyne K, Antichi D, Barberi P, Bigongiali F, Surböck A, Kranzler A, Beeckman A, Willekens K, Luik A, Matt D, Grosse M, Heß J, Clerc M, Dierauer H and Mäder P. 2016. How organic farmers practice conservation agriculture in Europe. *Renew Agr Food Syst*, **31**: 72-85.
- Pessaraki M. 2016. (Ed.) **Handbook of Photosynthesis**, CRC press, Boca Raton.
- Qasem J. 1992. Nutrient accumulation by weeds and their associated vegetable crops. *J Horticult Sci*, **67**: 189-195.
- Roy S, Arunachalam K, Dutta BK and Arunachalam A. 2010. Effect of organic amendments of soil on growth and productivity of three common crops viz. *Zea mays*, *Phaseolus vulgaris* and *Abelmoschus esculentus*. *Appl Soil Ecol*, **45**: 78-84.
- Sahan Y, Gurbuz O, Guldas M, Degirmencioglu N and Begenirbas A. 2017. Phenolics, antioxidant capacity and bioaccessibility of chicory varieties (*Cichorium spp.*) grown in Turkey. *Food Chem*, **217**: 483-489.
- Saleh AM and Madany MMY. 2015. Coumarin pretreatment alleviates salinity stress in wheat seedlings. *Plant Physiol Biochem*, **88**: 27-35.
- Sayed M, Khodary SEA, Ahmed ES, Hammouda O, Hassan HM and El-Shafey NM. Elicitation of flavonoids by chitosan and salicylic acid in callus of *Rumex vesicarius* L. *Acta Horticulturae*, **1187**: 165-176.
- Sun Y, Xu W and Fan A. 2006. Effects of salicylic acid on chlorophyll fluorescence and xanthophyll cycle in cucumber leaves under high temperature and strong light. *Ying yong sheng tai xue bao= The Journal of Applied Ecology*, **17**: 399-402.
- Taiz L and Zeiger E. 2010. **Plant Physiology**, 5th ed. Sinauer Associates, Sunderland, Massachusetts U.S.A.
- Tartoura KAH, Youssef SA and Tartoura E-SAA. 2014. Compost alleviates the negative effects of salinity via up-regulation of antioxidants in *Solanum lycopersicum* L. plants. *Plant Growth Regul*, **74**: 299-310.
- Threlfall D and Whistance G. 1970. Biosynthesis of ubiquinone—a search for polyprenyl phenol and quinone precursors. *Phytochemistry*, **9**: 355-359.
- Velikova V, Yordanov I and Edreva A. 2000. Oxidative stress and some antioxidant systems in acid rain-treated bean plants: Protective role of exogenous polyamines. *Plant Sci*, **151**: 59-66.
- Wan Y-Y, Chen S-Y, Huang Y-W, Li X, Zhang Y, Wang X-J and Bai J-G. 2014. Caffeic acid pretreatment enhances dehydration tolerance in cucumber seedlings by increasing antioxidant enzyme activity and proline and soluble sugar contents. *Sci Horticult*, **173**: 54-64.
- Yamasaki H, Sakihama Y and Ikehara N. 1997. Flavonoid-peroxidase reaction as a detoxification mechanism of plant cells against H₂O₂. *Plant Physiol*, **115**: 1405-1412.
- Zhao H and Zou Q. 2002. Protective effects of exogenous antioxidants and phenolic compounds on photosynthesis of wheat leaves under high irradiance and oxidative stress. *Photosynthetica*, **40**: 523-527.
- Zhishen J, Mengcheng T and Jianming W. 1999. The determination of flavonoid contents in mulberry and their scavenging effects on superoxide radicals. *Food Chem*, **64**: 555-559.

Molecular Identification and Characterization of Parrotfish species from the Farasan Islands, Red Sea-Saudi Arabia

Mohamed M. Hassan^{1,2}, Ayman Sabry^{1,3} and Mohamed Ismail^{2,*}

¹ Department of Biology, College of Science, Taif University, P.O. Box 11099, Taif 21944, Saudi Arabia; ² Genetics Department, Faculty of Agriculture, Menoufia University, Shibin El-Kom, 32516, Egypt; ³ Cell Biology Department, National Research Center, 12622, Dokki, Giza, Egypt

Received: Feb 3, 2020; Revised: August 17, 2020; Accepted: August 31, 2020

Abstract

Cheilinus trilobatus, *Cheilinus quinquecinctus*, and *Chlorurus sordidus* specimens from Saudi Arabia's Farasan Islands were collected and genotyped using inter simple sequence repeats (ISSRs) and start codon targeted (SCoT) primers. Mitochondrial cytochrome C oxidase subunit I (COI) gene fragments were used for DNA barcoding. ISSRs and SCoT primers showed moderate polymorphisms: expected heterozygosity (H_{exp}) of 0.470 and 0.435 and average polymorphism information contents (PICs) of 0.359 and 0.339 for ISSRs and SCoT markers were observed, respectively. *Cheilinus quinquecinctus* had the highest genetic diversity from ISSRs (70%) and SCoT (73%). *Chlorurus sordidus* and *C. trilobatus* showed similar genetic diversities of 29% and 39% based on ISSRs, respectively, and 60.32% for both species based on SCoT. *Cheilinus quinquecinctus* had the lowest nucleotide diversity (π) of 0.003, while *C. sordidus* and *C. trilobatus* had π values of 0.065 and 0.103, respectively. Analysis of molecular variance (AMOVA) revealed greater genetic variation among species rather than within them using ISSRs (65% and 67%, respectively) and SCoT (35% and 33%, respectively). COI-based AMOVA showed similar genetic variation among (51.11%) and within (48.89%) species. The current study highlighted outperformance of COI compared to ISSRs and SCoT markers in differentiating among parrotfish species. Also, ISSR outperformed SCoT since it was able to clearly show three distinct groups in principal component analysis. This study also confirmed the presence of three distinct parrotfish species, which will provide an insight into parrotfish diversity. Moreover, the results will contribute to monitoring parrotfish migration between Farasan Islands and different geographic locations which significantly affect species conservation.

Keywords ISSR; SCoT; COI; *Cheilinus trilobatus*, *Cheilinus quinquecinctus*, *Chlorurus sordidus*, Farasan Islands.

1. Introduction

Parrotfish (family Scaridae) are a distinctive group of labroid fish, comprising 10 genera that contain 90 species, including *Scarus niger*, *S. (Chlorurus) sordidus*, *S. frenatus*, and *S. ghobban* (Saad *et al.*, 2013). Meanwhile, the genus *Cheilinus* belongs to the family Labridae and contains wrasses (e.g. *Cheilinus trilobatus* and *Cheilinus quinquecinctus*) that are native to the Indian and Pacific Oceans and the Red Sea (Bogorodsky *et al.*, 2016).

Parrotfish (Scaridae) and wrasse (Labridae) are diverse fish families with an ecologically important role. Feeding activities for both families involve browsing of macroalgae, hence contributing to the maintenance of coral reefs (Bonaldo *et al.*, 2014). Several parrotfish species move across large areas; their movement plays a significant role in connecting different ecosystems (Fox and Bellwood, 2007; Nystrom and Folke, 2001).

Parrotfish include two major clades (*Chlorurus* and *Cheilinus*) that diversified during the Miocene, followed by speciation during the Pliocene (Choat *et al.*, 2012). Both form a noticeable part of the herbivorous fish community. The phenotypic characterization of parrotfish

is challenging due to the presence of a series of coloration changes. For instance, *Sparisoma* species color pattern varies by sex and developmental stage and is only clearly visible in fresh specimens (Bernardi *et al.*, 2000).

Since the species characterization of parrotfish in the Red Sea is poorly investigated due to the difficulties in morphological identification of parrotfish, the use of molecular barcoding is important. Such genetic markers represent effective and reliable alternative in parrotfish identification. Accordingly, COI gene has been established as an efficient species-level DNA barcoding marker for marine fish (Veneza *et al.*, 2013; Ali *et al.*, 2019; Ali *et al.*, 2020). The reliability and accessibility of the COI barcoding enabled them to be extensively used for both fish identification and monitoring of biodiversity (Shen *et al.*, 2017).

In addition to the use of COI as the most common barcode for fish identification, inter simple sequence repeats (ISSRs) and start codon targeted (SCoT) markers have also been applied in the assessment of parrotfish diversity (Sabry *et al.*, 2015). ISSRs markers are useful in genetic divergence estimates among closely related species (Sabry *et al.*, 2015), and many studies have demonstrated the utility of ISSRs markers for monitoring fish genetic

* Corresponding author e-mail: mohamed.ismail@agr.menoufia.edu.eg.

diversity (Paul *et al.*, 2018; Labastida-Estrada *et al.*, 2019). Recently, many alternative markers have been developed. SCoT markers, for instance, are reproducible markers that were developed using short, conserved regions in plant genomes that surround translation initiation codons (Amirmoradi *et al.*, 2012). Subsequently, these markers have been used to evaluate genetic diversity and population structure, and to identify cultivars (Hamidi *et al.*, 2014). However, the use of SCoT markers in animal studies remains relatively limited as compared to its use in plant studies.

The Farasan Islands are considered a high priority for conservation and a destination of annual aggregation of parrotfish to spawn (Gladstone, 2002). Therefore, from a conservation perspective, the assessment of parrotfish species identity and genetic diversity is a priority. In addition, the molecular structure of fish species is crucial for stock identification, improvement, and genetic resources preservation (Bingpeng *et al.*, 2018). However, such studies have yet to be extended to marine populations of the Farasan Islands, as one of the richest biodiversity hotspots in the Red Sea (Pearman *et al.*, 2014). Farasan Island of Saudi Arabia is underrepresented in marine species diversity assessment. In the current study, three different markers ISSRs, SCoT, and COI will be used to determine the genetic diversity and barcode three parrotfish species (*Cheilinus trilobatus*, *C. quinquecinctus*, and *Chlorurus sordidus*) from the Farasan Islands.

2. Materials and Methods

2.1. Fish Sampling and Genomic DNA Extraction

Parrotfish specimens were collected from the commercial fisheries at Farasan Islands (16°40'N, 42°00'E), on the Jeddah coast in Saudi Arabia. Samples were transferred frozen to the laboratory for further analyses. According to the morphological examination of the collected samples, most of the samples belonged to family Scaridae. The collected samples were identified by their morphological characteristics as described in FishBase (Froese and Pauly, 2019). Following morphological identification, three different species were detected: *Chlorurus sordidus*, *Cheilinus trilobatus*, and *Cheilinus quinquecinctus* (Figure 1), 10 specimens were selected from each species for DNA analyses. Approximately, 1 gm of fish muscle tissue was cut and ground in liquid nitrogen. The powdered fish muscle was used for genomic DNA extraction using the DNeasy Blood and Tissue Kit (QIAGEN, Valencia, CA, USA) according to the manufacturer's instructions.

2.2. ISSRs Genotyping

A total of nine ISSR primer pairs were used in PCR (Table 1). DNA amplification was performed in a final volume of 25 µL using a C1000™ Thermo Cycler (Bio-Rad, Germany), Master mix Promega (Promega, Co., Wisconsin, USA) and 1 µL of 10 ng DNA. The PCR reaction was performed according to Hassan *et al.* (2015) using the following protocol: 94°C for 10 min, followed by 40 cycles of denaturation at 94°C for 1 min, annealing at a primer-specific annealing temperature ranging from 48-54°C for 1 min and an extension at 72°C for 2 min, and a final extension at 72°C for 10 min. All PCR products were electrophoresed on 2% agarose gel electrophoresis in

0.5X TAE (20 mM Tris-HCl, 10 mM Acetic acid, 0.5 mM EDTA, pH 8.0); the gel was stained with ethidium bromide and visualized with UV light.



Figure 1. Parrotfish species collected from the Farasan Islands, Saudi Arabia; (a) *Chlorurus sordidus*, (b) *Cheilinus trilobatus*, (c) *Cheilinus quinquecinctus*.

2.3. ISSRs Genotyping

A total of nine ISSR primer pairs were used in PCR (Table 1). DNA amplification was performed in a final volume of 25 µL using a C1000™ Thermo Cycler (Bio-Rad, Germany), Master mix Promega (Promega, Co., Wisconsin, USA) and 1 µL of 10 ng DNA. The PCR reaction was performed according to Hassan *et al.* (2015) using the following protocol: 94°C for 10 min, followed by 40 cycles of denaturation at 94°C for 1 min, annealing at a primer-specific annealing temperature ranging from 48-54°C for 1 min and an extension at 72°C for 2 min, and a final extension at 72°C for 10 min. All PCR products were electrophoresed on 2% agarose gel electrophoresis in 0.5X TAE (20 mM Tris-HCl, 10 mM Acetic acid, 0.5 mM EDTA, pH 8.0); the gel was stained with ethidium bromide and visualized with UV light.

2.4. SCoT Genotyping

A total of 10 SCoT markers were selected for specimen genotyping (Table 1). PCR reactions were performed according to Etminan *et al.*, (2016). Amplification consisted of 94°C for 5 min, followed by 45 cycles of denaturation at 94°C for 45 s, primer annealing at 45°C for 45 s and primer elongation at 72°C for 90 s. The final extension was 10 min at 72°C. All PCR products were analyzed with 1.5% agarose gel electrophoresis in 0.5X TAE (20 mM Tris-HCl, 10 mM Acetic acid, 0.5 mM EDTA, pH 8.0), and the gel was stained with ethidium bromide and visualized with UV light.

Table 1. Inter simple sequence repeat (ISSR) and Start codon targeted (SCoT) markers used in parrotfish species genotyping.

Marker	Primer sequence (5'-3')	Marker	Primer sequence (5'-3')
ISSR-2	(GA) ₈ A	SCoT-1	ACGACATGGCGACCACGC
ISSR-3	(AG) ₈ TG	SCoT-2	ACCATGGCTACCACCGGC
ISSR-4	(GA) ₈ TT	SCoT-5	CAATGGCTACCACTAGCG
ISSR-8	(TG) ₈ AA	SCoT-6	CAATGGCTACCACTACAG
ISSR-9	TAG(CA) ₇	SCoT-7	ACAATGGCTACCACTGAC
ISSR-13	(GA) ₈ C	SCoT-8	ACAATGGCTACCACTGCC
ISSR-18	(AC) ₇ CG	SCoT-10	ACAATGGCTACCACTACC
ISSR-19	(AG) ₈ TT	SCoT-11	AAGCAATGGCTACCACCA
ISSR-28	(GTG) ₆	SCoT-12	ACGACATGGCGACCAACG
		SCoT-14	ACGACATGGCGACCACGC

2.5. DNA Sequencing of COI gene

The COI standard barcoding region (655 bp) was amplified for each of the 30 fish specimens using a pair of forward FishF1 (5'-TCAACCAACCACAAAGACATTG-GCAC-3'), and reverse FishR1 (5'-TAGACTTCTGGGT-GGCCAAAGAATCA-3') universal primers, as previously described in Ivanova *et al.*, (2007). Each amplification reaction contained 2 µL of DNA, 10.5 µL of deionized water, 12.5 µL of Master Mix (Promega, Co., Wisconsin, USA), 0.5 µL of forward primer (10 µM), and 0.5 µL of reverse primer (10 µM) at a total volume of 25 µL. The PCR reactions were performed according to the following profile: initial denaturation at 95°C for 5 min, followed by a total of 35 cycles of 94°C for 45 s, 54°C for 1 min, and 72°C for 45 s, and a final extension at 72°C for 7 min. Successful amplifications were confirmed by 5% agarose gel electrophoresis in 0.5X TAE (20 mM Tris-HCl, 10 mM Acetic acid, 0.5 mM EDTA, pH 8.0), and the gel was stained with ethidium bromide and visualized with UV light. PCR amplicons of the COI gene were purified from gels using an QIAquick PCR Purification Kit (QIAGEN, Valencia, CA, USA) and sequenced on the Applied Biosystems 3500 Genetic Analyzer Sequencer (Hitachi, Japan).

2.6. ISSRs and SCoT Data Analysis

For ISSRs and SCoT analysis, all genotypes were screened based on the presence/absence of a specific band (allele). Following genotype screening, GenAlex v6.5 (Peakall and Smouse, 2006) was used to estimate the percentage of polymorphisms in each species. Additionally, the iMEC program (Amiryousefi *et al.*, 2018) was used to calculate the expected heterozygosity (H_{exp}), polymorphism information content (PIC), discriminating power (D), and resolving power (R). NTSYS-pc v2.01 (Rohlf, 2000) was also used to determine the phylogenetic relationship among the three species. Phylogenetic trees were produced according to the unweighted pair group method with arithmetic mean (UPGMA). Principal component analysis (PCA) was also performed using GenAlex. To determine the level of genetic variation of each species, the analysis of molecular variance (AMOVA) was also obtained using GenAlex with 1000 permutations.

2.7. COI Sequence Analysis

All sequences were aligned and edited using BioEdit, version 7.0.9 (Hall, 1999). Following sequence alignment and editing, genetic polymorphisms of each species were estimated as nucleotide diversity (π) using DnaSP v6 (Rozas *et al.*, 2017). Genetic distance between species was estimated based on Kimura's two-parameter distance model (K2P) (Kimura, 1980), as implemented in MEGA-X (Kumar *et al.*, 2018). To determine genetic differentiation among species, AMOVA was conducted using Arlequin v3.5 (Excoffier and Lischer, 2010) with 1000 permutations. Using the 30 sequences from parrotfish species along with a single COI sequence belonging to Tuna (*Thunnus tonggol*, gene bank accession number JN635369.1) as an outgroup, the phylogenetic tree was constructed according to Neighbor joining (NJ) method based on p-distance (Nei and Kumar 2000). The relative robustness of individual tree branches was estimated by bootstrapping using 1000 pseudoreplicate datasets, with

80% cut-off. PCA was also performed on the K2P genetic distance matrix using GenAlex to determine species grouping. A total of 30 sequences of the COI region were deposited in GeneBank with accession numbers MN692884-MN692913.

3. Results

3.1. Parrotfish Genetic Diversity

The number of alleles at ISSRs ranged between 5 and 17, with an average of 10.77 alleles per locus (Table 2), while the number of alleles at SCoT markers ranged between 9 and 27, with an average of 12.5 alleles per locus. The expected heterozygosity (H_{exp}) was similar for both markers, with an average of 0.470 and 0.435 for ISSRs and SCoT markers, respectively. In contrast, both markers showed a comparable moderate level of PIC, with average of 0.359 and 0.339 for ISSRs and SCoT markers,

Table 2. Polymorphism of ISSR and SCoT markers in parrotfish species.

Marker	No. of alleles	H_{exp}	PIC	D	R
ISSR-2	10	0.499	0.374	0.777	4.933
ISSR-3	13	0.467	0.358	0.862	7.133
ISSR-4	17	0.386	0.311	0.932	8.067
ISSR-8	11	0.5	0.375	0.754	6.933
ISSR-9	12	0.5	0.375	0.762	7.733
ISSR-13	12	0.498	0.374	0.783	9.067
ISSR-18	9	0.42	0.332	0.511	4.467
ISSR-19	5	0.477	0.363	0.847	3.933
ISSR-28	8	0.486	0.368	0.661	3.2
Mean	10.778	0.47	0.359	0.765	6.163

D = discriminating power; H = expected heterozygosity; PIC = polymorphism information content; R = resolving power.

Table 2. Continued.

Marker	No. of alleles	H_{exp}	PIC	D	R
SCoT-1	27	0.352	0.290	0.948	12.33
SCoT-2	15	0.422	0.333	0.909	7.467
SCoT-5	9	0.48	0.365	0.841	5.467
SCoT-6	10	0.349	0.288	0.95	5.867
SCoT-7	12	0.388	0.313	0.931	5.267
SCoT-8	12	0.492	0.371	0.81	7.667
SCoT-10	11	0.442	0.345	0.892	6.2
SCoT-11	9	0.458	0.353	0.874	5.2
SCoT-12	10	0.499	0.375	0.73	3.333
SCoT-14	10	0.468	0.358	0.861	3.6
Mean	12.5	0.435	0.339	0.875	6.24

D = discriminating power; H = expected heterozygosity; PIC = polymorphism information content; R = resolving power.

respectively. SCoT outperformed ISSR in discriminating among the three species, with average discriminating powers (D) of 0.765 and 0.875 for ISSR and SCoT markers, respectively. Both ISSR and SCoT markers showed similar magnitudes of resolving power (R), with average R values of 6.163 and 6.240, respectively.

Using ISSR and SCoT markers, *Cheilinus quinquecinctus* showed the highest genetic diversity, with 70% and 73% for ISSR and SCoT markers, respectively (Table 3). Both *Chlorurus sordidus* and *Cheilinus trilobatus* showed comparable magnitudes of genetic diversity using ISSR and SCoT markers. Using ISSRs, *C. sordidus* and *C. trilobatus* showed a genetic diversity of 29% and 39%, respectively, while both species had a genetic diversity of 60.32% using SCoT markers.

COI showed different patterns of genetic diversity. *Cheilinus quinquecinctus* had the lowest nucleotide diversity of 0.003, while the nucleotide diversity of *Cheilinus trilobatus* was 0.103, 1.5-fold higher than that of *Chlorurus sordidus*. The COI sequence length varied among the species, with averages of 625, 695, and 684 bp for *Chlorurus sordidus*, *Cheilinus trilobatus*, and *Cheilinus quinquecinctus*, respectively.

Table 3. Genetic diversity of parrotfish species based on inter simple sequence repeats (ISSRs), start codon targeted markers (SCoT), and mitochondrial cytochrome C oxidase subunit I (COI).

	Species	% Polymorphism
ISSR	<i>Chlorurus sordidus</i>	29.90
	<i>Cheilinus trilobatus</i>	39.18
	<i>Cheilinus quinquecinctus</i>	70.10
	Mean	46.39
SCoT	<i>Chlorurus sordidus</i>	60.32
	<i>Cheilinus trilobatus</i>	60.32
	<i>Cheilinus quinquecinctus</i>	73.02
	Mean	64.55
COI*	<i>Chlorurus sordidus</i>	0.065
	<i>Cheilinus trilobatus</i>	0.103
	<i>Cheilinus quinquecinctus</i>	0.003
	Mean	0.057

*Genetic diversity at COI estimated as nucleotide diversity (π).

3.2. Analysis of Molecular Variance (AMOVA)

The AMOVA of the three species based on ISSRs showed 65% of the molecular variance occurred between species, while 35% of the molecular variance occurred within species (Table 4). Similarly, using SCoT markers, the amount of molecular variance among species was 67%. However, using COI, the amount of molecular variance showed a similar magnitude among and within species, at 51.11% and 48.89%, respectively.

Table 4. AMOVA of parrotfish species based on inter simple sequence repeats (ISSR), start codon targeted markers (SCoT) and mitochondrial cytochrome C oxidase subunit I (COI).

	df	SS	Est. var.	% V	
ISSR	Among species	2	321.40	15.25	65.00*
	Within species	27	222.60	8.24	35.00
	Total	29	544.00	23.49	
SCoT	Among species	2	192.07	8.006	67.00*
	Within species	27	431.20	15.97	33.00
	Total	29	623.27	23.977	
COI	Among species	2	5.40	0.24	48.89*
	Within species	27	6.90	0.26	51.11
	Total	29	12.30	0.50	

df; degree of freedom, SS; sum of squares, Est. var.; estimated variance; % V; percentage of total variation; *significant at $P < 0.05$ based on 1000 permutations.

3.3. Phylogenetic Relationship and Principal Component Analysis

The phylogenetic relationship between the three species was determined based on ISSRs, SCoT, and COI markers. Phylogenetic trees based on ISSR and SCoT markers are presented in supplementary Figures S1 and S2. The COI-based NJ phylogenetic tree showed three distinct groups representing the three species: *Chlorurus sordidus*, *Cheilinus trilobatus*, and *Cheilinus quinquecinctus* (Figure 2). Using PCA, the parrotfish species formed three distinct groups using ISSRs and COI markers (Figure 3). However, based on SCoT markers, the three species formed three groups, with some individuals shared among groups.

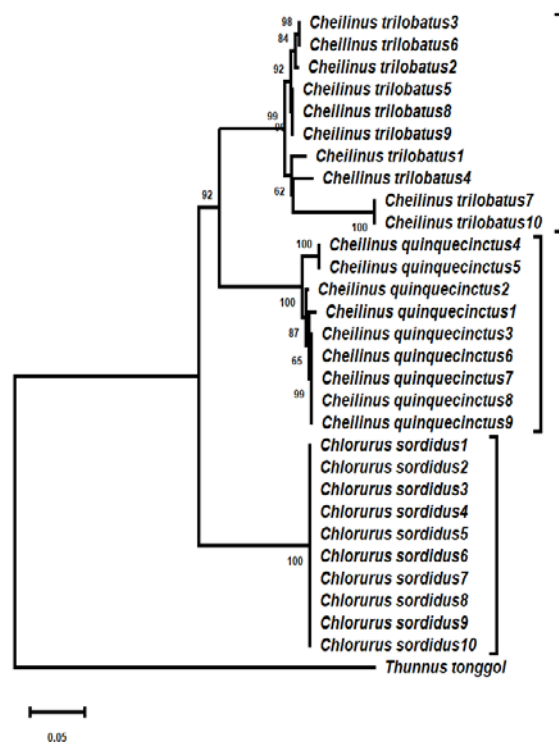


Figure 2. Neighbor-Joining (NJ) phylogenetic tree based on COI sequences for the three parrotfish species (*Chlorurus sordidus*, *Cheilinus trilobatus*, and *Cheilinus quinquecinctus*), numbers above branches are bootstrap values $> 60\%$.

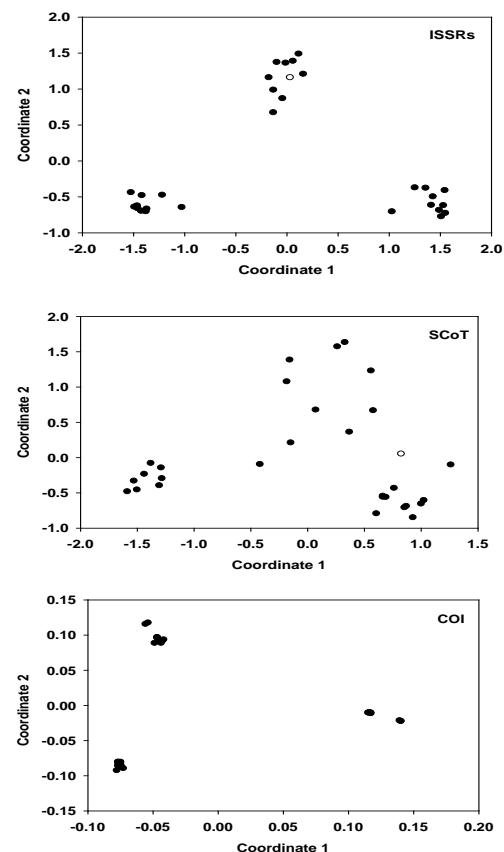


Figure 3. Principal component analysis based on inter simple sequence repeats (ISSRs), start codon targeted markers (SCoT), and cytochrome oxidase subunit I (COI) for three parrotfish species (*Chlorurus sordidus*, *Cheilinus trilobatus*, and *Cheilinus quinquecinctus*).

4. Discussion

The identification of parrotfish species from the Red Sea was modified and redescribed as a distinct group from the parrotfish species mainly found in the western Indian and western Pacific oceans (Bodorodsky *et al.*, 2016). Few studies have addressed the level of genetic diversity of parrotfish species, and mainly focused on their taxonomy and evolution (Almeida *et al.*, 2017). In the present study, the molecular characterization and genetic diversity of three parrotfish species, *Chlorurus sordidus*, *Cheilinus trilobatus*, and *Cheilinus quinquecinctus*, from the Farasan Islands, Saudi Arabia, were studied. The level and pattern of genetic diversity is one of the major factors affecting the biological potential of any species. Since the species under consideration contribute significantly to the Farasan Islands ecosystem, it is crucial to understand its genetic diversity. To better assess the genetic diversity of parrotfish species, three different molecular markers were used; ISSRs, SCoT, and COI that were previously documented in assessing species genetic diversity. Different marker systems have distinctively distributed across the genomes while exhibiting different patterns of genetic diversity (Veneza *et al.*, 2013; Hamidi *et al.*, 2014). Therefore, the combination of different molecular markers in addressing genetic diversity could assist in understanding species biodiversity. The number of SCoT alleles was higher than that of ISSRs; however, both markers had comparable mean *PICs*. The studied ISSRs and SCoT markers were reasonably informative ($0.50 > PIC > 0.25$); however, the discrimination power of SCoT was higher than that of ISSRs, which was previously reported in discriminating among closely related species (Etminan *et al.*, 2016, Etminan *et al.*, 2018). Among the studied species, *Cheilinus quinquecinctus* had the highest genetic diversity based on ISSRs and SCoT markers, whereas *Chlorurus sordidus* and *Cheilinus trilobatus* showed similar magnitudes of genetic diversity. The higher genetic diversity of *Cheilinus quinquecinctus* observed at the two dominant markers might be associated with its life-history characteristics (e.g., early maturity) (Romiguier *et al.*, 2010). In contrast, COI showed a contrasting pattern where *Cheilinus quinquecinctus* had the lowest genetic diversity (i.e., low π). The observed low nucleotide diversity of *Cheilinus quinquecinctus* is a probable sign of genetic bottleneck followed by a sudden expansion (Grant and Bowen, 1998). Moreover, mitochondrial COI lacks recombination as compared to intergenic regions of nuclear DNA (Veneza *et al.*, 2013), while ISSRs and SCoT are highly polymorphic. A similar pattern of low nucleotide diversity was also observed at COI in *Konosirus punctatus*, a coastal marine fish species in China (Liu, 2020). The genetic differentiation among species was apparent, where AMOVA revealed higher genetic differentiation among species compared to that within species, based on ISSR and SCoT markers. However, based on COI, the genetic variance within species was similar to that among species. The discrepancies in genetic variance associated with nuclear genetic markers (i.e., ISSRs and SCoT) as compared to that of mitochondrial genetic markers (COI) has been reported in other fish species and mainly associated with the different recombination rates at nuclear versus

mitochondrial genetic markers. For instance, *Xenophysogobio nudicorpa* populations from Yangtze River showed a six-fold increase in genetic variation among groups using nuclear genetic markers compared to that recorded using mitochondrial genetic markers (Dong *et al.*, 2019). Species grouping was examined using cluster analysis and PCA, which is considered an efficient tool in defining the relationships among individuals of the same and/or different species. The phylogenetic trees of the three species and the PCA showed a comparable grouping pattern. However, the most supported phylogenetic tree and PCA were obtained based on COI, where all the specimens from the same species grouped together with grouping pattern matched species morphological identification.

5. Conclusion

The Farasan Islands, Saudi Arabia, is considered a major aggregation spot of fish species. Hence it is crucial to identify parrotfish (family Scaridae), one of the most common fish species, with significant ecological impacts on coral reefs. The current study is the first to document the identification and assessment of the genetic diversity of three parrotfish species using three different genetic markers. Nuclear genetic markers indicated presence of higher genetic variance between, rather than within, species; however, COI highlighted an equivalent variance within and among species. COI barcoding clearly separated the studied species into three distinct groups based on phylogeny and PCA. Additionally, this study indicated that the genetic diversity of mitochondrial genetic markers is a prevailing tool in discriminating between different parrotfish species even while exhibiting less variability. On the other hand, SCoT performed poorly in differentiating among parrotfish species calling for caution in using SCoT while investigating marine fish genetic diversity.

References

- Ali FS, Ismail M and Mamoon A. 2019. Comparative molecular identification of genus *Dicentrarchus* using mitochondrial genes and internal transcribed spacer region. *Egy J Aquat Biol Fish.*, **23**: 371-384.
- Ali FS, Ismail M and Aly W. 2020. DNA barcoding to characterize biodiversity of freshwater fishes of Egypt. *Mol Biol Rep.*, **47**: 5865-5877.
- Almeida LAH, Nunes LA, Bitencourt JA, Molina WF and Affonso PRAM. 2017. Chromosomal evolution and cytotoxicity in wrasses (Perciformes: Labridae). *J Hered.*, **108**: 239-253.
- Amiryousefi A, Hyvönen J and Poczai P. 2018. iMEC: online marker efficiency calculator. *Appl Plant Sci.*, **6**: e01159.
- Amirmoradi B, Talebi R and Karami E. 2012. Comparison of genetic variation and differentiation among annual *Cicer* species using start codon targeted (SCoT) polymorphism, DAMDPCR, and ISSR markers. *Plant Syst Evol.*, **298**: 1679-1688.
- Bernardi G, Robertson DR, Clifton KE and Azzurro E. 2000. Molecular systematics, zoogeography, and evolutionary ecology of the Atlantic parrotfish genus *Sparisoma*. *Mol Phylogenet Evol.*, **15**: 292-300.
- Bingpeng X, Heshan L, Zhilan Z, Chunguang W, Yanguo W and Jianjun W. 2018. DNA barcoding for identification of fish species in the Taiwan Strait. *PLoS One.*, **13**: 1-13.

- Bogorodsky SV, Alpermann TJ and Mal AO. 2016. Redescription of *Cheilinus quinquecinctus* Rüppell, 1835 (Pisces: Perciformes: Labridae), a valid endemic Red Sea wrasse. *Zootaxa.*, **4158**: 451-472.
- Bonaldo R, Hoey AS and Bellwood DR. 2014. The ecosystem roles of parrotfishes on tropical reefs. *Oceanogr Mar Biol.*, **52**: 81-132.
- Choat JH, Carpenter KE, Clements KD, Rocha LA, Russell B, Myers R, Lazuardi ME, Muljadi A, Pardede S and Rahardjo P. 2012. *Chlorurus sordidus*. The IUCN Red List of Threatened Species. e.T190715A17795228.
- Dong W, Wang D and Tian H. 2019. Genetic structure of two sympatric gudgeon fishes (*Xenophysogobio boulengeri* and *X. nudicarpa*) in the upper reaches of Yangtze River Basin. *Peer J.*, **7**: e7393.
- Etminan A, Pour-Aboughadareh A, Mohammadi R, Ahmadi-Rad A, Noori A, Mahdavian Z and Moradi Z. 2016. Applicability of start codon targeted (SCoT) and inter-simple sequence repeat (ISSR) markers for genetic diversity analysis in durum wheat genotypes. *Biotechnol Biotec Eq.*, **30**: 1075-1081.
- Etminan A, Pour-Aboughadareh A, Noori A, Ahmadi-Rad A, Shooshtari L, Mahdavian Z and Yousefiazar-Khanian M. 2018. Genetic relationships and diversity among wild *Salvia* accessions revealed by ISSR and SCoT markers. *Biotechnol Biotec Eq.* **32**: 610-617.
- Excoffier L and Lischer HEL. 2010. Arlequin suite ver 3.5: A new series of programs to perform population genetics analyses under Linux and Windows. *Mol Ecol Resour.*, **10**: 564-567.
- Froese R, Pauly D (2019) FishBase. World wide web electronic publication. Accessed on 10 Nov. 2019.
- Fox RJ and Bellwood DR. 2007. Quantifying herbivory across a coral reef depth gradient. *Mar Ecol Prog Ser.*, **339**: 49-59.
- Froese R and Pauly D. 2019. FishBase. world wide web electronic publication. Accessed 10/06/2019
- Gladstone W. 2002. Fisheries of the Farasan Islands (Red Sea). Naga, *WorldFish Center Quart.*, **25**: 30-34.
- Grant WAS and Bowen BW. 1998. Shallow population histories in deep evolutionary lineages of marine fishes: insights from sardines and anchovies and lessons for conservation. *J. Hered.*, **89**: 415-426.
- Hall TA. 1999. BioEdit: a user-friendly biological sequence alignment editor and analysis program for Windows 95/98/NT. *Nucleic Acids Symp Ser.*, **41**: 95-98.
- Hamidi H, Talebi R and Keshavarzi F. 2014. Comparative efficiency of functional gene-based markers, start codon targeted polymorphism (SCoT) and conserved DNA-derived polymorphism (CDDP) with ISSR markers for diagnostic fingerprinting in wheat (*Triticum aestivum* L.). *Cereal Res Commun.*, **42**: 558-567.
- Hassan MM, Gaber A and El-Hallous EI. 2015. Molecular and morphological characterization of *Trichoderma harzianum* from different Egyptian soils. *Wulfenia J.*, **21**: 80-96.
- Ivanova N, Zemlak TS, Hanner RH and Hebert PD. 2007. Universal primer cocktails for fish DNA barcoding. *Mol Ecol Notes.*, **7**: 544-548.
- Kimura M. 1980. A simple method for estimating evolutionary rates of base substitutions through comparative studies of nucleotide sequences. *J Mol Evol.*, **16**: 111-20.
- Kumar S, Stecher G, Li M, Knyaz C and Tamura K. 2018. MEGA X: molecular evolutionary genetics analysis across computing platforms. *Mol Biol Evol.*, **35**: 1547-1549.
- Labastida-Estrada E, Machkour-M'Rabet S, Carrillo L, Hénaut Y and Castelblanco-Martínez DN. 2019. Genetic structure of Mexican lionfish populations in the southwest Gulf of Mexico and the Caribbean Sea. *PLoS One.*, **14**: e0222997.
- Liu B, Zhang K, Zhu K, Shafi M, Gong L, Jiang L, Liu L, Muhammad Fand Lü Z. 2020. Population genetics of *Konosirus punctatus* in Chinese coastal waters inferred from two mtDNA genes (COI and Cytb). *Front. Mar. Sci.*, **7**: 534.
- Nei M and Kumar S. 2000. Molecular Evolution and Phylogenetics. Oxford University Press, New York.
- Nystrom M and Folke C. 2001. Spatial resilience of coral reefs. *Ecosystems.*, **4**: 406-417.
- Paul A, Mukhopadhyay T and Bhattacharjee S. 2018. Genetic characterization of *Barilius barna* (Hamilton, 1822) in the Teesta River of Sub-Himalayan West Bengal, India, through RAPD and ISSR fingerprinting. *Proc Zool Soc.*, **71**: 203.
- Peakall R and Smouse PE. 2006. GENALEX 6: genetic analysis in Excel. Population genetic software for teaching and research. *Mol Ecol Notes.*, **6**: 288-295.
- Pearman JK, El-Sherbiny MM, Lanzen A, Al-Aidaros AM and Irigoien X. 2014. Zooplankton diversity across three Red Sea reefs using pyrosequencing. *Front Mar Sci.*, **1**: 1-11.
- Rohlf FJ. 2000. NTSYS-pc: numerical taxonomy and multivariate analysis system version 2.1. Exeter Publishing, Setauket.
- Romiguier J, Ranwez V, Douzery EJP and Galtier N. 2010. Contrasting GC-content dynamics across 33 mammalian genomes: relationship with life-history traits and chromosome sizes. *Genome Res.*, **20**: 1001-1009.
- Rozas J, Ferrer-Mata A, Sánchez-DelBarrio JC, Guirao-Rico S, Librado P, Ramos-Onsins SE and Sánchez-Gracia A. 2017. DnaSP 6: DNA sequence polymorphism analysis of large data sets. *Mol Biol Evol.*, **34**: 3299-3302.
- Saad YM, Abu Zinadah OAH and El-Domyati FM. 2013. Monitoring of genetic diversity in some parrotfish species based on inter simple sequence repeat polymorphism. *Life Sci J.*, **10**: 1841-1846.
- Sabry AM, Hassan MM, Mohamed AA and Awad NS. 2015. Molecular characterization of some popular fish species in Saudi Arabia. *Inter J Appl Sci Biotechnol.*, **3**: 359-366.
- Shen SY, Tian HW, Liu SP, Chen DQ, Hao LV and Wang DQ. 2017. Genetic diversity of *Leptobotia microphthalmia* in the upper Yangtze River inferred from mitochondrial DNA. *Chinese J Ecol.*, **10**: 2824-2830.
- Veneza I, Felipe B, Oliveira J, Silva R, Sampaio I, Schneider H and Gomes GA. 2013. Barcode for the authentication of the snappers (Lutjanidae) of the western Atlantic: rDNA 5S or mitochondrial COI? *Food Control.*, **38**: 116-123.

Supplementary Figures

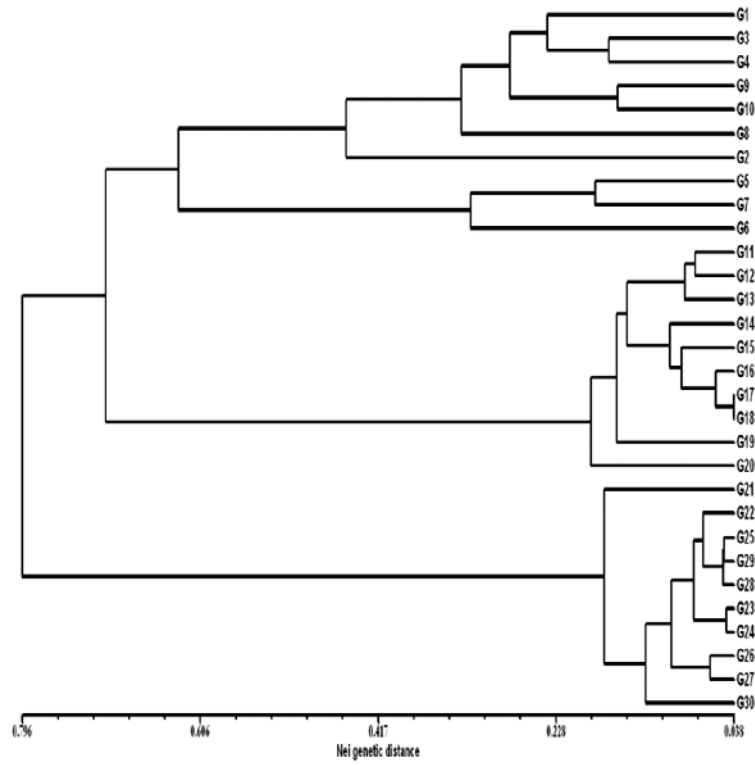


Figure S1. UPGMA phylogenetic tree based on ISSR of the parrotfish species. *Chlorurus sordidus*; G1-G10, *Cheilinus trilobatus*; G11-G20, *Cheilinus quinquecinctus* G21-G30

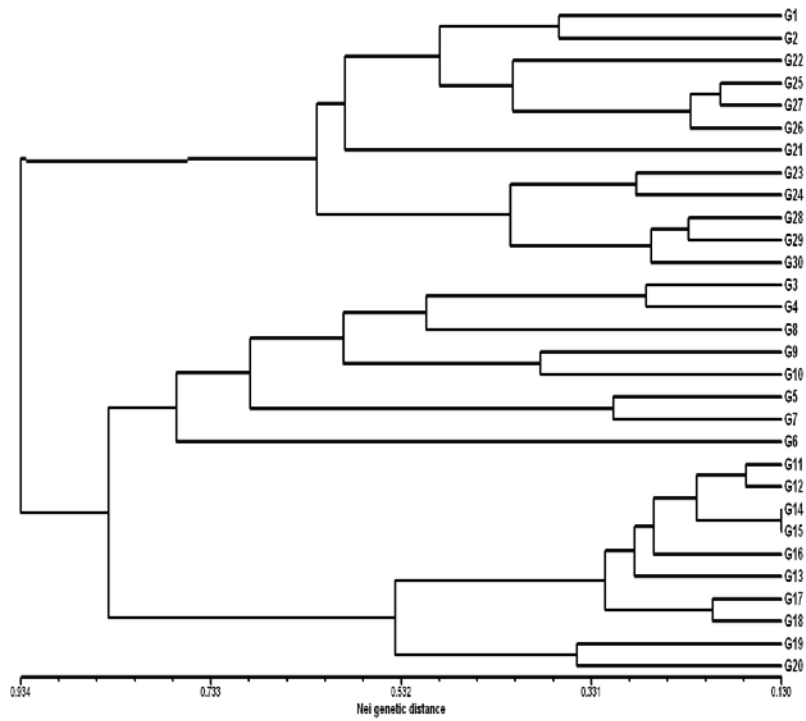


Figure S2. UPGMA phylogenetic tree based on SCoT of the parrotfish species. *Chlorurus sordidus*; G1-G10, *Cheilinus trilobatus*; G11-G20, *Cheilinus quinquecinctus* G21-G30.

Fungal Endophytes from *Tabernaemontana heyneana* Wall. (Apocynaceae), their Molecular Characterization, L-asparaginase and Antioxidant Activities

Naguvanahally S. Bhavana¹, Harischandra S. Prakash² and Monnanda S. Nalini^{1,*}

¹Department of Studies in Botany, ²UGC-BSR Fellow, Department of Studies in Biotechnology, University of Mysore, Manasagangotri, Mysore – 570 006, Karnataka, India

Received: December 24, 2019; Revised: January 19, 2020; Accepted: February 1, 2020

Abstract

Endophytic fungi are an interesting group of microorganisms associated with the healthy tissues of medicinal plants used in folk medicines for health benefits. Fifteen fungal endophytes were isolated from the plant parts of the ethnomedicinal plant of Western Ghats, *Tabernaemontana heyneana* Wall., and evaluated for their L-asparaginase and antioxidative potentials. They were identified by rDNA sequencing of the ITS region and characterized as strains of *Fusarium*, *Colletotrichum*, *Curvularia*, *Nigrospora*, *Plectospharella*, *Neocosmospora*, *Trichoderma* and *Endomelanconiopsis*. *Trichoderma hamatum* and *Fusarium* sp., colonized the bark, leaf and stem tissue fragments. Secondary metabolites from the endophytic strains were extracted in ethyl acetate and evaluated for total phenolic content and antioxidant activity. The total phenolic content of the extracts from all the fungal strains ranged from 17.29±12.92 to 90.41±4.56 mg Gallic acid equivalent/g (mg GAE/g) dry extract and IC₅₀ values in DPPH radical scavenging activity ranged from 51.64±8.91 µg/ml to 764.05±27.67 µg/ml. Eleven strains were positive for L-asparaginase enzyme activity in the range of 1.44 to 3.42 IU/ml. *Fusarium tricinctum* (MK752630) strain potentially produced high enzyme activity of 3.423 IU/ml. The highest total phenolic content (90.14±4.56 mg GAE/g dry extract) and scavenging activity (IC₅₀ value of 51.64±8.91 µg/ml) were detected in *F. tricinctum*.

Keywords: Endophytic fungi; L-asparaginase; *Fusarium tricinctum*; total phenolic content, DPPH radical scavenging, Western Ghats

1. Introduction

Plants are known to harbor endophytic fungi that reside in internal tissues without showing any disease symptoms (Frohlich and Hyde, 1999). The infected host tissues are transiently symptomless, and the microbial colonization can be demonstrated through histological means, by isolation from strongly surface disinfected tissue, or, most recently, through the direct amplification of fungal nuclear DNA from colonized plant tissue (Stone *et al.*, 2000). Fungal endophytes represent an important component of fungal biodiversity and are known to have mutualistic association with host plants (Selim *et al.*, 2012). Endophytes are known to influence population dynamics, plant community diversity and ecosystem functions (Saikkonen *et al.*, 1998). This group of microbes not only synthesizes metabolites to compete first with epiphytes and then with pathogens in order to colonize the host, but also regulates metabolism of the host in a balanced association (Schulz *et al.*, 2002). Once inside host tissue, they assume a quiescent state either for the whole time or for an extended period of time until environmental conditions are favorable for the fungus or the ontogenetic state of the host changes to the advantage of the fungus (Sieber, 2007).

Endophytic fungi are known to have profound effects on plant ecology, fitness, evolution (Brundett, 2006) and play vital roles in host plants being chemical synthesizers

inside plants (Owen and Hundley 2004), producing phytohormones (Schulz and Boyle, 2005), withstanding environmental stress (Malinowski and Belesky, 2000) and providing protection against pathogens (Akello *et al.*, 2007). In recent years, endophytes from medicinal plants have demonstrated the ability to produce bioactive compounds which are potential sources of novel natural products (Nalini *et al.*, 2019).

Asparaginase is widely distributed in nature from bacteria to mammals and plays a central role in the amino acid metabolism and utilization. L-asparaginase (EC 3.5.1.1.) belongs to the group of homologous amidohydrolases family, which catalyses the hydrolysis of the amino acid L-asparagine to L-aspartate and ammonia. L-asparaginase is the first enzyme with anti-leukemic activity studied thoroughly in human beings (Savitri *et al.*, 2003). Asparaginase is used in food industry to prevent the formation of acrylamide when foods are processed at high temperatures (Cachumba *et al.*, 2016).

Naturally occurring phenolic compounds are plant secondary metabolites which are good electron donors since their hydroxyl groups can directly contribute to antioxidant action. Currently, there is a great interest in finding natural antioxidants from endophytes associated with plant species. Plant-endophyte interaction and endophyte-endophyte interaction studies provide understandings of metabolite production by fungi. Endophytes are the repository of natural products

* Corresponding author e-mail: nmsomaiah@gmail.com.

displaying broad spectrum of biological activities like anticancer, antibacterial, antiviral, anti-diabetic, antioxidant and anti-inflammatory (Rajamanikyam *et al.*, 2017).

Tabernaemontana heyneana Wall., is endemic to southern Western Ghats and is listed as lower risk/ near threatened species in the "IUCN Red List of Threatened Species" (World Conservation Monitoring Centre, 1998). *T. heyneana* possess antimicrobial and anthelmintic properties against skin venereal, respiratory and nervous disorders (Duraipandiyar *et al.*, 2006) and get used in the traditional Indian system of medicine as a cure for cancer (Baskar *et al.*, 2012). The medicinal plants inhabiting Western Ghats are major sources of traditional pharmaceuticals and therapeutics of significant potentialities. Therefore, we have investigated the endophytic fungi residing in *T. heyneana*, their molecular identification and evaluation of their L-asparaginase and antioxidative capacities by *in vitro* methods.

2. Materials and methods

2.1. Collection of host plant

Healthy plant samples of *T. heyneana* Wall., were collected in the forests of Kodagu district, in the Talacauvery area of Western Ghats (12°17' to 12°27' N and 75°26' to 75°33' E), Karnataka, India, during the month of June 2014. The habit of plant and collection locality is shown in Figure 1. A total of five leaves, stem and bark samples were collected separately from five plants. Bark samples from the trunk were cut 1.5 m above the ground level with help of sterile machete. The samples were placed in pre-sterilized zip-lock polythene bags, stored at 4°C and transported to the laboratory. Fresh plant materials were used for the isolation of fungal endophytes to reduce the chance of contamination. Thus collected plant materials were subjected to surface sterilization within few hours after sampling.

2.2. Surface sterilization and isolation of fungal endophytes

The leaf, stem and bark samples were rinsed gently in running tap water to remove dust and debris. Before surface sterilization, the cleaned stems were cut into pieces of 5 cm length and bark samples were halved. Samples were first immersed in 70% (v/v) ethanol for one minute, 3.5% (v/v) Sodium hypochlorite for two minutes. The samples were rinsed three times with sterile distilled water and dried on sterile blotters under laminar airflow to ensure complete drying (Schulz *et al.*, 1993). Bits of 1.0X0.1 cm size were excised with the aid of sterilized blade. 200 segments of leaf, stem and bark were evenly placed on water agar (WA) medium (15 g/L). The Petri dishes were sealed using Parafilm™ and incubated at 27±2° C in a light chamber with 12 hours of light followed by 12 hours of dark cycles for 4-6 weeks. The Petri dishes were monitored periodically to check the growth of endophytic fungal colonies from the segments. The hyphal tips which grew out from the segments were transferred separately onto fresh Potato Dextrose Agar (PDA) slants with a sterile fine tipped needle under stereo binocular microscope and incubated at 27±2° C for 10-15 days and pure cultures were maintained at 4° C for further use.

2.3. Identification of endophytic fungi

Morphological identification was done by inoculating the endophytic fungi on PDA plates followed by seven days of incubation and observation of colony and spore morphology. The slides of each fungal endophytes were prepared by tease mount method using lactophenol cotton blue staining [NICE, Kerala, India] and observed under the light microscope (Quasmo, Haryana, India) with 400X magnification. The identification was based on the observation of mycelia, fruiting bodies, conidial characters according to the standard identification manuals (Domsch *et al.*, 1980; Singh *et al.*, 1991; Barnett and Hunter, 1998; Mathur and Kongsdal, 2003).

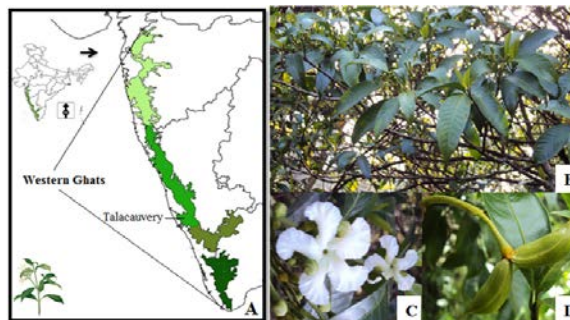


Figure 1. A. Map showing the location of plant sample collection from Talacauvery site of Western Ghats; B. *Tabernaemontana heyneana* Wall. habit; C-Flowers; D- A pair of follicles.

2.4. Molecular characterization of fungal endophytes

Hyphal tips from 15 morphologically different endophytic fungi, each representing individual morphospecies, were inoculated into conical flask containing Potato Dextrose Broth (PDB, Hi Media, Mumbai, India) and incubated at 27±2 °C for 7-10 days. The resulting mycelia were separated and placed in polythene zip lock covers. The mycelia were then freeze dried before being ground in a pestle and mortar containing liquid nitrogen. The powdered mycelia were stored at -20 °C until required. The genomic DNA was extracted using cetyltrimethylammonium bromide (CTAB) method with minor modifications (Ausubel *et al.*, 1994). The DNA concentration was measured using Nanodrop Spectrophotometer (Thermo Fischer 2000c, Bangalore, India) at 260 and 280 nm.

PCR amplification in ITS rDNA region of isolates was conducted using PCR 18 kit (Chromous Biotech Pvt. Ltd. Bangalore, India). The target ITS 1, ITS 2 regions and 5.8s gene were amplified using ITS 1 (5'-TCCGTAGGTGAACCTGCG - 3') and ITS 4 (5'-TCCTCCGCTTATTGATATGC - 3') primers. Amplification reactions were performed in a thermal cycler (Master cycler gradient, Eppendorf, Germany) with the following cycling conditions 94°C for 2 min (Initial denaturation), 35 cycles of 94°C for 1 min (Denaturation), 47°C for 15 sec (Primer annealing), 72°C for 30 sec (Primer extension), followed by 10 min of final extension at 72°C. Following amplification, the PCR products were analyzed by horizontal agarose gel electrophoresis through 1% agarose gel supplemented with ethidium bromide along with 100bp DNA marker. DNA bands on the gel were visualized under UV light trans-illuminator (Geldoc XRT, BioRad USA) and documented.

The PCR products were sent to Chromous Biotech Pvt. Ltd., Bangalore, India for purification and sequencing. Sequencing similarity searches were achieved for the obtained fungal sequences and compared with ITS sequence data from strains available in the database GenBank (National Centre for Biotechnology Information website; <http://www.ncbi.nlm.nih.gov/>) by using the BLAST sequence match routines.

2.5. Data Analysis

The relative colonization frequency (%CF) was calculated as the number of segments colonized by a fungal divide by total number of segments plated x 100.

2.6. L-asparaginase activity of fungal endophytes

Fifteen fungal endophytes isolated from leaf, stem and bark of *T. heyneana* were subjected to rapid screening of primary plate assay method using modified Czapek Dox (MCD) agar medium using phenol red as an indicator (Gulati *et al.*, 1997). The composition of the prepared medium was as follows: glucose- 2.0 g/l, L-asparagine- 10 g/l, potassium dihydrogen phosphate (KH_2PO_4)- 1.52 g/l, potassium chloride (KCl)- 0.52 g/l, magnesium sulphate ($\text{MgSO}_4 \cdot 7\text{H}_2\text{O}$)-0.52 g/l, copper nitrate ($\text{CuNO}_3 \cdot 3\text{H}_2\text{O}$)-0.001 g/l, zinc sulphate ($\text{ZnSO}_4 \cdot 7\text{H}_2\text{O}$)-0.001 g/l, ferrous sulphate ($\text{FeSO}_4 \cdot 7\text{H}_2\text{O}$)- 0.001 g/l and agar 20g/l. 2.5% (w/v) stock solution of the phenol red dye was prepared and MCD medium was supplemented with 0.009% phenol red dye indicator to check the ability of test fungi that grow in the medium. Final pH of the medium was adjusted to 6.2. The control plates were prepared with KNO_3 -0.001 g/l as the nitrogen source and lacking in phenol red dye indicator. The prepared media was autoclaved and poured into pre-sterilized plates and marked into four quadrants. Mycelial plugs from four different endophytic fungi were inoculated and incubated at $27 \pm 2^\circ\text{C}$ for five days. The colonies showing pink zones were inoculated individually on MCD agar plates to approve the activity of enzyme.

2.7. Quantitative assay for enzyme production

For the production of L-asparaginase under liquid state, the mycelial discs from positive agar plates were inoculated into modified Czapek Dox's broth and incubated at 30°C in orbital shaker (GeNei™, Bangalore) for 5 days at 120 rpm. The crude enzyme sample was extracted by centrifugation and supernatant that contained the enzyme used for further analysis by Nesslerization. The reaction mixture consisting of 0.5 ml of 0.04 M L-asparagine, 0.5 ml of 0.5 M TrisHCl buffer (pH 8.2), 0.5 ml of enzyme was obtained from the culture filtrate and 0.5 ml of distilled water. The samples were incubated for 30 min at 27°C . To stop the enzymatic reaction, 0.5 ml of 1.5 M trichloroacetic acid (TCA) was added. This was followed by pipetting 0.1 ml of the mixture into fresh tubes containing 3.7 ml of distilled water and 0.2 ml of Nessler's reagent and incubated at 27°C for 20 minutes, after which the absorbance of the samples was measured at 450 nm using UV-Visible spectrophotometer (TPL Technology

Pvt. Ltd., Bangalore). Blank was prepared by adding TCA followed by enzyme sample. One international unit (IU) of L-asparaginase was expressed as the amount of enzyme that catalyzes the formation of $1\mu\text{mol}$ of ammonia per minute at 27°C (Imada *et al.*, 1973).

2.8. Submerged fermentation and extraction of secondary metabolites

The sequential steps involved in fermentation and extraction of secondary metabolites is represented in Figure 2. At first the endophytic fungi were cultivated by inoculating the actively growing mycelia from 7-days-old pure culture into Erlenmeyer flask containing 500 ml of Potato Dextrose Broth. The flasks were then incubated for 21 days at $27 \pm 2^\circ\text{C}$. After incubation, the culture filtrates were filtered through muslin cloth to separate mycelia. To the culture filtrate, equal volume of ethyl acetate was added and mixed well for 10 minutes and kept for 5 minutes till two clear immiscible layers formed. The upper layer of the solvent containing extracted compounds was then separated, evaporated and dried in Rotary flash evaporator (Superfit Model PBU-6D, India). The dry solid residue was dissolved in ethanol and stored as crude extract in glass vials.

2.9. Determination of total phenolic content

The total phenolic content of ethyl acetate extracts of endophytic fungi was estimated using Folin-Ciocalteu (FC) reagent based assay using Gallic acid standard (Liu *et al.*, 2007). One ml of FC reagent and two ml of (20%, w/v) Na_2CO_3 was mixed with methanolic crude extracts. The mixture was incubated at room temperature in the dark for 45 minutes, and the absorbance of the developed color was recorded at 765 nm using UV-vis spectrophotometer (DU 730 "Life sciences", Beckman Coulter). Gallic acid was used as a reference standard for plotting the calibration curve. The TPC of the extracts was expressed as mg of Gallic acid equivalent (GAE)/ g of the dry extract.

2.10. Determination of antioxidant capacity by DPPH (2, 2-diphenyl-1-picrylhydrazyl) assay

The antioxidant activity of endophytic fungal extracts was determined by free radical scavenging activity of DPPH by the method of Pannangpetch *et al.* (2007) with slight modifications. A total of two ml of DPPH solution (DPPH, Sigma-Aldrich, Bangalore, India) (0.001 mM) was added into the endophytic fungal extracts and incubated for 20 minutes at room temperature in the dark. After incubation, the absorbance was measured at 517 nm. Ascorbic acid was used as reference antioxidant compound. The scavenging activity was expressed as inhibitory concentration 50% (IC_{50}) ($\mu\text{g}/\text{ml}$). The scavenging activity was calculated using the following equation:

$$\% \text{ Scavenging} = \frac{\text{Ac} - \text{As}}{\text{Ac}} \times 100$$

Ac= Absorbance of control; As= Absorbance of test sample

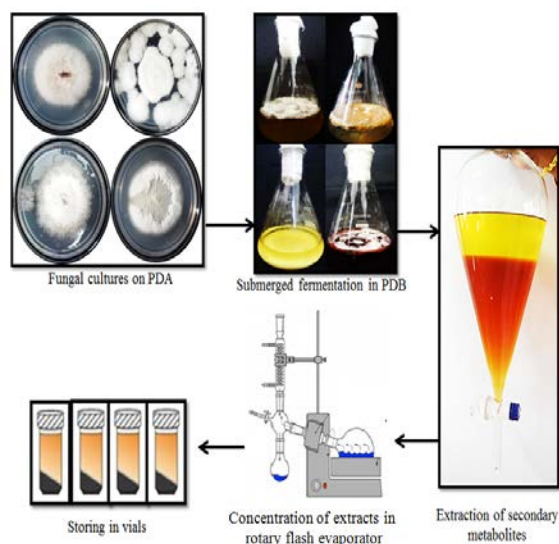


Figure 2. Fermentation and extraction of secondary metabolites from the fungal endophytes of *T. heyneana*

3. Results

3.1. Isolation and the identification of fungal endophytes

A total of 600 tissue segments yielded 477 isolates were obtained, which were distributed in 15 endophytic species. The results revealed that leaf fragments were colonized by more number of fungal endophytes (186) followed by stem (171) and bark segments (120). The analysis of distribution frequencies of endophytes indicated that the fungal communities in the host contained a few frequent genera and some infrequent species.

The isolates were identified using morphological and microscopic characteristics with the support of molecular analysis. 15 endophytic species belonged to Sordariomycetes (87%) and Dothideomycetes (13%) were obtained. Molecular characterization of isolated endophytic fungi with GenBank accession numbers, the closest match of ITS sequence in the NCBI database and their sequence similarity is depicted in Table 1. Among the isolated endophytic fungi, seven different species of *Fusarium* and two species of *Colletotrichum* were recovered. Five species of *Fusarium* viz., *Fusarium begoniae*, *Fusarium commune*, *Fusarium culmorum*, *Fusarium tricinctum*, *Fusarium babinda* were associated with the stem segments. In addition, *Nigrospora sphaerica* and *Curvularia coicis* were also recovered from the stem segments.

Neocosmospora haematococca, *Plectosphaerella cucumerina*, *Colletotrichum fruticola* exhibited tissue specificity by colonizing the leaf segments, while *Fusarium petroliphilum*, *Endomelanconiopsis endophytica* were isolated from bark segments. *Colletotrichum gloeosporioides* colonized both leaf and the stem fragments, whereas *Fusarium* sp. and

Trichoderma hamatum showed colonization in all plant segments. The percent colonization frequency of endophytic fungi in bark, leaf and stem parts along with their isolation code are represented in Table 2. The highest percent colonization was exhibited by *Fusarium* sp. (15.3) followed by *T. hamatum* (14.7) whereas *F. commune* showed the least percent colonization of 2.0. All endophytes from *T. heyneana* were assembled into eight different genera and assigned to Nectriaceae, Glomerallaceae, Plectosphaerellaceae, Hypocreaceae, Pleosporaceae, Botryosphaeriaceae and Trichosphaeriaceae.

3.2. Qualitative analysis of endophytic fungi for L-asparaginase activity

Of the 15 fungal endophytes screened for enzyme activity by preliminary plate assay method, 11 could grow on MCD agar producing pink zone with phenol red, a dye indicator that changes from yellow to pink (acidic to alkaline condition). The formation of pink zone around each fungal colony specified variations in pH due to the accumulation of ammonia in the medium.

3.3. Quantitative analysis by Nesslerization

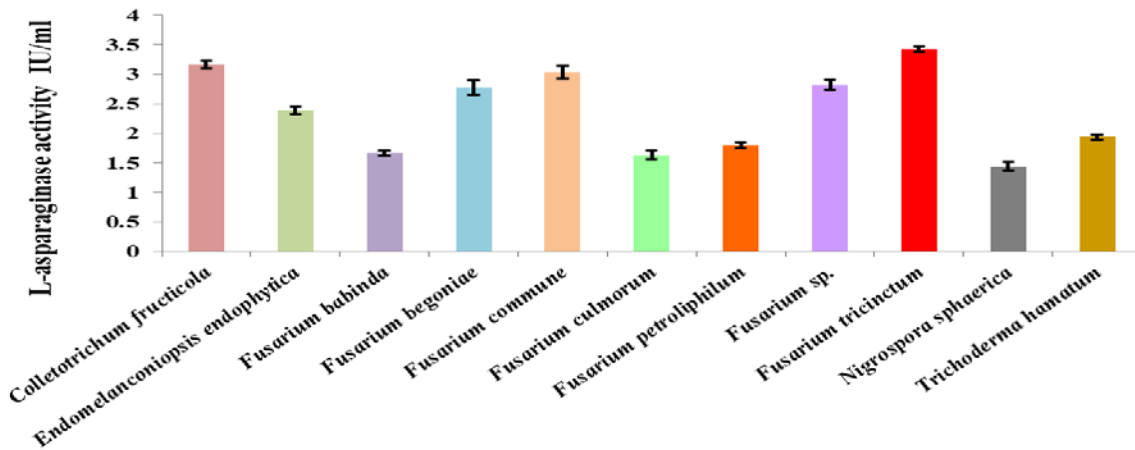
Positive isolates from preliminary screening were further evaluated by Nesslerization using spectrophotometric methods. Eleven positive isolates exhibited asparaginase activity in the range of 1.448 ± 0.07 to 3.423 ± 0.05 IU/ml (Figure 3). *F. tricinctum* from stem showed highest asparaginase activity among all the tested endophytic fungi with 3.423 ± 0.05 IU/ml of enzyme. *C. fruticola* from stem and *F. commune* from leaf also demonstrated high asparaginase activity of 3.166 ± 0.07 and 3.036 ± 0.11 IU/ml respectively. *Fusarium* sp., *F. begoniae* and *E. endophytica* showed moderate L-asparaginase activity in the range of 2.827 ± 0.09 – 2.388 ± 0.06 IU/ml of enzyme.

3.4. Determination of total phenolic content

Total phenolic content of all the fungal extracts ranged from 18.14 ± 8.62 to 90.41 ± 4.56 mg GAE/g dry extract (Table 3). The extracts of *F. tricinctum* displayed highest TPC (90.41 ± 4.56 mg GAE/g dry extract) followed by *C. coicis* (88.99 ± 38.75 mg GAE/g dry extract) and *N. sphaerica* (87.52 ± 34.44 mg GAE/g dry extract).

3.5. Antioxidant activity

The antioxidant activity of the endophytic extracts was determined following DPPH radical scavenging activity. The free radical scavenging activity is represented as 50% scavenging activity (IC_{50}) and is depicted in Table 3. The fungal extracts indicated IC_{50} values ranging from 51.64 ± 8.91 μ g/ml to 764.05 ± 27.67 μ g/ml. *F. tricinctum* extract depicted high scavenging activity with 51.64 ± 8.91 μ g/ml, followed by *F. commune* (124.16 ± 9.12) and *N. haematococca* (129.20 ± 15.12 μ g/ml).



Endophytic fungal isolates

Figure 3. L-asparaginase producers of endophytic fungal species isolated from *T. heyneana*.

Data are reported as mean±SD of three independent analyses (n=3).

Table 1. Molecular characterization of fungal endophytes isolated from *T. heyneana* with GenBank accession numbers, ITS sequence match in the NCBI database and their percent sequence similarity

Fungal endophytes	Isolate code	GenBank accession number	Closest match ITS	Sequence length (bp)	Sequencing similarity
<i>Colletotrichum gloeosporioides</i>	TH-WG-03	MK767027	KU682216	441	441/441 (100%)
<i>Colletotrichum fructicola</i>	TH-WG-11	MK976025	MK041495	516	507/517 (98%)
<i>Curvularia coicis</i>	TH-WG-12	MK976026	MG589634	555	532/553 (96%)
<i>Endomelanconiopsis endophytica</i>	TH-WG-13	MK991793	MK075024	527	527/527 (100%)
<i>Fusarium tricinctum</i>	TH-WG-04	MK752630	MK102656	504	495/504 (98%)
<i>Fusarium sp.</i>	TH-WG-06	MK776870	MH935958	293	290/290 (100%)
<i>Neocosmospora haematococca</i>	TH-WG-07	MK911734	KX099641	512	459/464 (99%)
<i>Nigrospora sphaerica</i>	TH-WG-15	MN066344	MF380852	493	484/500 (97%)
<i>Plectosphaerella cucumerina</i>	TH-WG-08	MK940863	MH063586	499	485/487 (99%)
<i>Trichoderma hamatum</i>	TH-WG-09	MK940897	MK304047	551	553/553 (100%)
<i>Fusarium babinda</i>	TH-WG-10	MK940898	MH862578	404	381/406 (94%)
<i>Fusarium begoniae</i>	TH-WG-01	MK720625	KM577645	483	475/483 (98%)
<i>Fusarium commune</i>	TH-WG-02	MK723994	KX878889	473	473/473 (100%)
<i>Fusarium culmorum</i>	TH-WG-05	MK767026	KU375665	468	468/468 (100%)
<i>Fusarium petroliphilum</i>	TH-WG-14	MN066343	LS999414	506	501/509 (98%)

Table 2. Colonization frequency of endophytic fungi associated with *T. heyneana*

Endophytic strains	Isolate code	Plant parts						Total % CF
		Bark*		Leaf*		Stem*		
		I	% CF	I	% CF	I	% CF	
<i>Colletotrichum gloeosporioides</i>	TH-WG-03	-	-	29	14.5	3	1.5	5.3
<i>Colletotrichum fructicola</i>	TH-WG-11	-	-	17	8.5	-	-	2.9
<i>Curvularia coicis</i>	TH-WG-12	-	-	-	-	17	8.5	2.9
<i>Endomelanconiopsis endophytica</i>	TH-WG-13	35	17.5	-	-	-	-	5.9
<i>Fusarium tricinctum</i>	TH-WG-04	-	-	-	-	36	18	6.0
<i>Fusarium sp.</i>	TH-WG-06	8	4.0	75	37.5	9	4.5	15.3
<i>Neocosmospora haematococca</i>	TH-WG-07	-	-	18	9.0	-	-	3.0
<i>Nigrospora sphaerica</i>	TH-WG-15	-	-	-	-	19	9.5	3.1
<i>Plectosphaerella cucumerina</i>	TH-WG-08	-	-	15	7.5	-	-	2.5
<i>Trichoderma hamatum</i>	TH-WG-09	49	24.5	32	16	7	3.5	14.7
<i>Fusarium babinda</i>	TH-WG-10	-	-	-	-	27	13.5	4.5
<i>Fusarium begoniae</i>	TH-WG-01	-	-	-	-	13	6.5	2.1
<i>Fusarium commune</i>	TH-WG-02	-	-	-	-	12	6.0	2.0
<i>Fusarium culmorum</i>	TH-WG-05	-	-	-	-	24	12	4.0
<i>Fusarium petroliphilum</i>	TH-WG-14	28	14.0	-	-	-	-	4.7

* 200 segments were plated from bark, leaf and stem respectively for frequency analysis. I: Number of isolates; CF-Colonization frequency; '-': Not detected

Table 3. Estimation of total phenolic content and radical scavenging potentials of *T. heyneana* endophytes

Fungal strains	Total phenolic content (mg GAE/ g dry extract)	DPPH radical scavenging capacity (IC ₅₀ µg/ml)
<i>C. gloeosporioides</i>	37.82±25.82	145.48±14.73
<i>C. fruticola</i>	33.51±16.02	413.36±26.40
<i>C. coicis</i>	88.99±38.75	374.15±30.50
<i>E. endophytica</i>	64.77±11.39	736.04±31.65
<i>F. babinda</i>	25.30±3.01	175.25±21.35
<i>F. begoniae</i>	37.87±3.44	138.68±5.71
<i>F. commune</i>	76.84±16.20	124.16±9.12
<i>F. culmorum</i>	35.96±21.52	378.04±17.48
<i>F. petroliphilum</i>	78.35±3.80	764.05±27.67
<i>F. tricinctum</i>	90.41±4.56	51.64±8.91
<i>Fusarium</i> sp.	18.14±8.62	336.03±22.71
<i>N. haematococca</i>	17.29±12.92	129.20±15.12
<i>N. sphaerica</i>	87.52±34.44	155.26±33.71
<i>P. cucumerina</i>	31.25±3.88	670.37±26.51
<i>T. hamatum</i>	68.65±12.62	481.24±17.99

Abbreviations: DPPH – 1,1-diphenyl-2-picrylhydrazyl; IC₅₀ – Inhibitory concentration 50%. Data are reported as mean ± SD of three independent analyses.

4. Discussion

The Western Ghats of India has an exceptionally high level of biological diversity and is recognized as one of the world's 'hot spots' of biological diversity. *T. heyneana* is one of the medicinally important species of apocynaceae known to possess active pharmacological principles. This study has aimed to isolate endophytic fungi from *T. heyneana* and evaluate their L-asparaginase activity, total phenolic content and antioxidant activity.

Fifteen endophytic fungal strains such as species of *Fusarium*, *Colletotrichum*, *Neocosmospora*, *Plectosphaerella*, *Trichoderma*, *Curvularia*, *Endomelanconiopsis* and *Nigrospora* were identified using ITS sequencing method. The occurrence of seven different *Fusarium* species is remarkable as these have adapted to a range of geographical sites, climatic conditions, ecological habitats and host plants. Researchers suggest that there are similar positive interactions of endophytic *Fusarium* species with plants (Blok and Bollen, 1995). *Fusarium* sp. and *Colletotrichum* sp. are also reported as endophytes from earlier studies in *T. heyneana* (Manasa and Nalini, 2014). In our quest to identify fungal endophytes from medicinal species of *Rauvolfia*, both *Fusarium* and *Colletotrichum* spp. were documented as endophytes (Bhavana *et al.*, 2019). Preceding findings also reveal the evaluation of *T. divaricata* for the isolation of endophytes like *Colletotrichum*, *Gliocladium*, *Mycelia sterilia*, *Phoma*, *Phomopsis*, *Xylaria* sp. (Huang *et al.*, 2008) as well as for arbuscular mycorrhizal and dark septate endophyte fungal associations (Debnath *et al.*, 2015).

It was interesting to document that some of the fungal genera such as *Plectosphaerella*, *Trichoderma*, *Curvularia*, *Endomelanconiopsis* and *Nigrospora* were not previously reported from *T. heyneana*. The variation in the colonization potential of the endophytic fungi shows that, each endophyte exhibited different degrees of affinity

towards different tissues of the plant. *Fusarium* sp., and *Trichoderma* showed colonization in leaf, stem and bark tissues while the remaining endophytes were specific to tissue types.

Of the 15 fungal endophytes, the highest percent colonization was recorded in *Fusarium* sp. (15.3) followed by *T. hamatum* (14.7) whereas *F. commune* showed low percent colonization (2.0). *Fusarium* spp. as endophytes are documented from *T. heyneana* (Manasa and Nalini, 2014), *Catharanthus roseus* (Ayob and Simarani, 2016), Himalayan Yew plants (Garyali *et al.*, 2013) and from Malaysian anticancer plants (Chow and Ting, 2015). Similarly, *Trichoderma* spp. as endophytes have been recorded from three medicinal plants ie., *Solanum surattense* (Ikram *et al.*, 2019), *Salvia miltiorrhiza* (Zhou *et al.*, 2019) and *Elettaria* (Munir *et al.*, 2019).

The fungal strains were investigated for L-asparaginase production, total phenolic content and antioxidative potentials. *T. heyneana* revealed the presence of diverse endophytic fungal species with L-asparaginase activity. Of the 15 endophytic strains screened, 11 were positive for L-asparaginase. *F. tricinctum* isolated from stem fragments showed high asparaginase activity among all the tested fungi (3.423±0.05 IU of enzyme).

Fusarium endophytes differ in their ability to produce L-asparaginase. *F. verticilloides* from *T. heyneana*, showed considerably less enzyme activity of 1.136 IU/ml (Manasa and Nalini (2014). *Fusarium* spp. are known producers of L-asparaginase. *F. oxysporum* with 27.10 units/gram dry substrate (Pallem, 2019), *F. equiseti* with 8.51 IU (Hosamani and Kaliwal, 2011), *F. culmorum* with 7.21 units/gram dry substrate (Meghavam and Janakiraman, 2017), *Fusarium* sp. with 11.4 U/min/ml (Gonçalves *et al.*, 2016), *F. solani* and *F. oxysporum* with 0.04 IU/ml and 0.08 IU/ml respectively were also reported for their asparaginase activity (Gulati *et al.*, 1997). Our results are on par with the original work of Theantana *et al.* (2009), wherein quantitative activity for 53 positive/82 strains of endophytes ranged from 0.014 to 1.5 Units/ml. It is interesting to note that *Trichosporon asahii* IBBLA1 isolated from soil and moss samples from Schirmacher hills, Antarctica regions exhibited significant enzyme activity of 20.57 IU/ml (Ashok *et al.*, 2019).

In the present investigation, high TPC of 90.41± 4.56 mg GAE/g dry extract, was detected in *F. tricinctum*. *T. heyneana* is a well-known Indian medicinal plant with various phytochemicals. The total phenolic contents of fresh leaf extract of *T. heyneana* contained 11.4± 0.17 mg GAE/g dry extract (Sathishkumar and Baskar, 2012), whereas in the methanol extract, the TPC was 14.0± 0.45 mg GAE/g dry extract (Manasa and Chandrashekar, 2015). On the basis of these observations, it can be opined that the phenolic content of endophytic fungal extracts are high in comparison with the host plants.

Because of their capability to secrete bioactive metabolites, endophytic fungi can also reduce the oxidative stress (Khan *et al.*, 2017). The anti-oxidative function of endophytic fungi is due to the secretion of phenolic compounds. Of the 15 endophytic fungal strains screened for the antioxidant activity, *F. tricinctum* was found have high antioxidative potentials with IC₅₀ value of 51.64 ± 8.91 µg/ml., whereas the DPPH radical scavenging activity of *T. heyneana* carried out by Baskar *et al.* (2012), Sathishkumar and Baskar (2012) showed IC₅₀ values of

340.17 ±26.04 µg/ml and 507 µg/ml respectively, lesser in comparison with the current study.

Endophytic *F. tricinctum* with unique bioactivity from several medicinal species are reported viz., *Taxus baccata* (Vasundhara *et al.*, 2016) *Salicornia bigelovii* (Zhang *et al.*, 2015), *Aristolochia paucinervis* (Wätjen *et al.*, 2009) *Fritillaria unibracteata* var. *wabuensis* (Pan *et al.*, 2017a), *F. cirrhosa* (Pan *et al.*, 2017b), grasses (Przemieniecki *et al.*, 2019) and *Paris polyphylla* var. *yunnanensis* (Zhang *et al.*, 2011).

5. Conclusion

This study explores the endophytic fungi from *T. heyneana* and their L-asparaginase, total phenolic content and antioxidative potentials. The increasing importance of L-asparaginase in recent years due to its anti-carcinogenic applications encouraged us to screen the extracts of endophytes for L-asparaginase activity. *F. tricinctum* displayed significant L-asparaginase activity with remarkable total phenolic content and antioxidative capacities. Our study has shown that fungal endophytes from *T. heyneana* have potential bioactivities. The extracts are being evaluated for their anti-proliferative potentials in *in vitro* cancer cell lines.

Conflict of interest

The authors declare that there is no conflict of interest

Funding

This work was partially funded by the Department of Backward Classes Welfare, Government of Karnataka, India to the first author

Acknowledgements

The authors thank the Institution of Excellence (IOE) Biodiversity & Sustainable Development, Vijnan Bhawan, and the University of Mysore for providing the necessary facilities to carry out the present study.

References

Akelo J, Dubois T, Gold CS, Coyne D, Nakavuma J and Paparu P. 2007. *Beauveria bassiana* (Balsamo) Vuillemin as an endophyte in tissue culture banana (*Musa* spp.). *J Invertebr Pathol.*, **96**: 34–42. <http://doi.org/10.1016/j.jip.2007.02.004>.

Ashok A, Doriya K, Rao JV, Qureshi A, Kumartiwar A and Kumar DS. 2019. Microbes producing L-asparaginase free of glutaminase and urease isolated from extreme locations of Antarctic soil and moss. *Sci rep.*, **9**: 1423. <https://doi.org/10.1038/s41598-018-38094-1>

Ausubel FM, Brent R, Kingston RE, Moore DD, Seidman JG, Smith JA and Struhl K. 1994. **Current Protocols in Molecular Biology**. Wiley, New York.

Ayob FW and Simarani K. 2016. Endophytic filamentous fungi from a *Catharanthus roseus*, identification and its hydrolytic enzymes. *Saudi Pharm J.*, **24**(3): 273-278.

Barnett HL and Hunter BB. 1998. **Illustrated Genera of Imperfect Fungi**. APS Press, Minnesota, Minn, USA, 4th edition.

Baskar AA, Al Numair KS, Alsaif MA and Ignacimuthu S. 2012. *In vitro* antioxidant and antiproliferative potentials of medicinal plants used in traditional Indian medicine to treat cancer. *Redox Rep.*, **17**(4): 145-156. DOI: 10.1179/1351000212Y.0000000017

Bhavana NS, Prakash HS and Nalini MS. 2019. Antioxidative and L-asparaginase potentials of fungal endophytes from *Rauvolfia densiflora* (Apocynaceae), an ethnomedicinal species of the Western Ghats. *Czech Mycol* **71**(2): 187–203. DOI: <https://doi.org/10.33585/cmy.71205>

Blok WJ and Bollen GJ. 1995. Fungi on roots and stem bases of *Asparagus* in the Netherlands species and pathogenicity. *Eur J Plant Pathol.*, **101**(1): 15-24. DOI:<https://doi.org/10.1007/BF01876090>

Brundrett MC. 2006. Understanding the roles of multifunctional mycorrhizal and endophytic fungi. In: Schulz BJE, Boyle CJC, Sieber TN (eds.), **Microbial Root Endophytes**. Berlin, Germany: Springer-Verlag, PP. 281–293.

Cachumba JJ, Antunes FA, Peres GF, Brumano LP, Santos JC and Da Silva SS. 2016. Current applications and different approaches for microbial L-asparaginase production. *Braz J Microbiol.*, **47**(1): 77-85.

Chow YY and Ting ASY. 2015. Endophytic L-asparaginase producing fungi from plants associated with anticancer properties. *J Adv Res.*, **6**(6): 869-876. DOI:10.1016/j.jare.2014.07.005

Debnath A, Karmakar P, Debnath S, Roy Das A, Saha AK and Das P. 2015. Arbuscular mycorrhizal and dark septate endophyte fungal association in some plants of Tripura, North-East India. *Curr Res Environ Appl Mycol.*, **5**(4): 398-407.

Domsch KH, Gams W and Anderson T. 1980. **Compendium of soil fungi**. Academic Press, New York, NY, USA.

Duraipandiyan V, Ayyanar M and Ignacimuthu S. 2006. Antimicrobial activity of some ethnomedicinal plants used by Paliyar tribe from Tamil Nadu, India. *BMC Complement Altern Med.*, **6**: 35-41. DOI:10.1186/1472-6882-6-35

Fröhlich J and Hyde KD. 1999. Biodiversity of palm fungi in the tropics: are global fungal diversity estimates realistic?. *Biodivers Conserv.*, **8**: 977–1004

Garyali S, Kumar A and Sudhakara Reddy M. 2013. Taxol production by an endophytic fungus *Fusarium redolens*, isolated from Himalayan Yew. *J Microbiol Biotechnol.*, **23**(10): 1372-1380.

Gonçalves AB, Maia ACF, Rueda JA and Vanzela APFC. 2016. Fungal production of the anti-leukemic enzyme L-asparaginase: from screening to medium development. *Acta Sci Biol Sci.*, **38**(4): 387-394.

Gulati R, Saxena RK and Gupta R. 1997. A rapid plate assay for screening L-asparaginase producing microorganisms. *Lett Appl Microbiol.*, **24**: 23-26.

Hosamani R and Kaliwal BB. 2011. L-asparaginase an antitumor agent production by *Fusarium equiseti* using solid state fermentation. *Int J Drug Discov.*, **3**(2): 88-99.

Huang WY, Cai YZ, Hyde KD, Corke H and Sun M. 2008. Biodiversity of endophytic fungi associated with 29 traditional Chinese medicinal plants. *Fungal Divers.*, **33**: 61–75.

Ikram M, Ali N, Jan G, Hamayun M, Jan FG and Iqbal A. 2019. Novel antimicrobial and antioxidative activity by endophytic *Penicillium roqueforti* and *Trichoderma reesei* isolated from *Solanum surattense*. *Acta Physiol Plant.*, **41**(164): 1-11.

Imada A, Igarasi S, Nakahama K and Isono M. 1973. Asparaginase and glutaminase activities of micro-organisms. *J Gen Microbiol.*, **76**(1): 85-99.

Khan AL, Gilani SA, Waqas M, Al-Hosni K, Al-Khiziri S, Kim YH, Ali L, Kang SM, Asaf S, Shahzad R, Hussain J, Lee IJ and Al-Harrasi A. 2017. Endophytes from medicinal plants and their potential for producing indole acetic acid, improving seed germination and mitigating oxidative stress. *J Zhejiang Univ Sci B.*, **18**(2): 125–137.

- Liu X, Dong M, Chen X, Jiang M, Lv X and Yan G. 2007. Antioxidant activity and phenolics of an endophytic *Xylaria* sp. from *Ginkgo biloba*. *Food Chem.*, **105**(2): 548-554.
- Malinowski DP and Belesky DP. 2000. Adaptations of endophyte-infected cool-season grasses to environmental stresses: mechanisms of drought and mineral stress tolerance. *Crop Sci.*, **40**: 923-940. DOI: 10.2135/cropsci2000.404923x.
- Manasa C and Nalini MS. 2014. L-Asparaginase activity of fungal endophytes from *Tabernaemontana heyneana* Wall. (Apocynaceae), endemic to the Western Ghats (India). *Int Sch Res Notices.*, 1-7. Article ID 925131, <http://dx.doi.org/10.1155/2014/925131>
- Manasa DJ and Chandrashekar KR. 2015. Antioxidant and antimicrobial activities of *T. heyneana* Wall. And endemic plant of Western Ghats. *Int J Pharm Pharm Sci.*, **7**(7): 311-315.
- Mathur SB and Kongsdal O. 2003. **Common laboratory seed health testing methods for detecting fungi**. International Seed Testing Association, Geneva, Switzerland.
- Meghavarman AK and Janakiraman S. 2017. Solid state fermentation: An effective fermentation strategy for the production of L-asparaginase by *Fusarium culmorum* (ASP-87). *Biocat Agri Biotech.*, **11**:124-130. DOI:10.1016/j.bcab.2017.06.001
- Munir E, Lutfia A and Yurnaliza 2019. Records of culturable endophytic fungi inhabiting rhizome of *Elettaria* in Hutan Sibayak, North Sumatera the 4th International Conference on Biological Sciences and Biotechnology. Pondicherry University, Kalapet, Pondicherry **305**: 1-6. DOI:10.1088/1755-1315/305/1/012004
- Nalini MS, Prakash HS and Tejesvi MV. 2019. Bioactive potentials of novel molecules from the endophytes of medicinal plants. In: Egamberdieva D and Tiezzi A (Eds.), **Medically Important Plant Biomes: Source of Secondary metabolites, Microorganisms for Sustainability 15**, Singapore, Springer Nature Singapore Pte Ltd, PP. 293-351. https://doi.org/10.1007/978-981-13-9566-6_13
- Owen NL and Hundley N. 2004. Endophytes-the chemical synthesizers inside plants. *Sci Pro.*, **87**: 79-99. <https://doi.org/10.3184/003685004783238553>.
- Pallem C. 2019. Solid-state fermentation of corn husk for the synthesis of asparaginase by *Fusarium oxysporum*. *Asian J Pharm Pharmacol.*, **5**(4): 678-681. DOI: <https://doi.org/10.31024/ajpp.2019.5.4.5>
- Pan F, Su TJ, Cai SM and Wu W. 2017a. Fungal endophyte-derived *Fritillaria unibracteata* var. *wabuensis*: diversity, antioxidant capacities *in vitro* and relations to phenolic, flavonoid or saponin compounds. *Sci Rep.*, **7**:42008. DOI: 10.1038/srep42008
- Pan F, Su TJ, Deng KL and Wu W. 2017b. Antioxidant activity and methanolic constituents of endophytic *Fusarium tricinctum* CBY11 isolated from *Fritillaria cirrhosa*. *Mycosystema.*, **36**(6): 752-765. DOI: 10.16333/j.1001-6880.2017.3.002
- Pannangpetch P, Laupatarakasem P, Kukonviriyapan V, Kukongriyapa C, Kongyinyoes B and Aromdee C. 2007. Antioxidant activity and protective effect against oxidative hemolysis of *Clinacanthus nutans* (Burm.f.)Lindau. *Songklanakarinn J Sci Technol.*, **29**(1): 1-9.
- Przemieniecki SW, Damszel M, Kurowski TP, Mastalerz J. and Kotlarz K. 2019. Identification, ecological evaluation and phylogenetic analysis of non-symbiotic endophytic fungi colonizing timothy grass and perennial ryegrass grown in adjacent plots. *Grass Forage Sci.*, **74**: 42-52. DOI: 10.1111/gfs.12404
- Rajamanikyam M, Vadlapudi V, Ramars amanchy and Upadhyayula SM. 2017. Endophytic fungi as novel resources of natural therapeutics. *Braz Arch Biol Technol.*, **60**: 1-26. <http://dx.doi.org/10.1590/1678-4324-2017160542>.
- Saikkonen K, Faeth SH, Helander M and Sullivan TJ. 1998. Fungal Endophytes: A continuum of interactions with host plants. *Annu Rev Ecol Syst.*, **29**(1): 319-343. <https://doi.org/10.1146/annurev.ecolsys.29.1.319>
- Sathishkumar T and Baskar R. 2012. Evaluation of antioxidant properties of *Tabernaemontana heyneana* Wall.leaves. *Ind J Nat Prod Resour.*, **3**(2): 197-207.
- Savitri, Asthana N and Azmi W. 2003. Microbial L-asparaginase a potent antitumor enzyme. *Ind J Biotech.*, **2**: 184-194.
- Schulz B and Boyle C. 2005. The endophytic continuum. *Mycol Res.*, **109**: 661-686. <https://doi.org/10.1017/S095375620500273X>
- Schulz BU, Wanke U, Drager S and Aust HJ. 1993. Endophytes from herbaceous plants and shrubs: effectiveness of surface sterilization methods. *Mycol Res.*, **97**: 1447-1450. [https://doi.org/10.1016/S0953-7562\(09\)80215-3](https://doi.org/10.1016/S0953-7562(09)80215-3)
- Schulz B, Boyle C, Draeger S, Römmert AK and Krohn K. 2002. Endophytic fungi: a source of novel biologically active secondary metabolites. *Mycol Res.*, **106** (9): 996-1004 <https://doi.org/10.1017/S0953756202006342>
- Selim KA, El-Beih AA, Abdel-Rahman TM and El-Diwany AI. 2012. Biology of endophytic fungi. *Curr Res Environ Appl Mycol.*, 31-82. DOI: 10.5943/cream/2/1/3
- Sieber TN. 2007. Endophytic fungi in forest trees: are they mutualists?. *Fungal Biol Rev.*, **21**(2-3): 75-89. <https://doi.org/10.1016/j.fbr.2007.05.004>
- Singh K, Frisvad JC, Thrane U and Mathur SB. 1991. **An illustrated manual on identification of some seed-borne Aspergilli, Fusaria, Penicillia and their mycotoxins**. Danish Government, Institute of Seed Pathology for Developing Countries, Hellerup, Denmark.
- Stone JK, Bacon CW and White JF. 2000. An overview of endophytic microbes: endophytism defined. In: Bacon CW and White JF (Eds.), **Microbial Endophytes**. Marcel Dekker, New York, PP. 3-29.
- Theantana T, Hyde KD and Lumyong S. 2009. Asparaginase production by endophytic fungi from Thai medicinal plants: cytotoxicity properties. *Int J Integr Biol.*, **7**(1): 1-8.
- Vasundhara M, Baranwal M and Kumar A. 2016. *Fusarium tricinctum*, an endophytic fungus exhibits cell growth inhibition and antioxidant activity. *Ind J Microbiol.*, **56**(4): 433-438. DOI: 10.1007/s12088-016-0600-x
- Wätjen W, Debbab A, Hohlfeld A, Chovolou Y, Kampkötter A, Edrada RA, Ebel R, Hakiki A, Mosaddak M, Totzke F, Kubbutat MH and Proksch P. 2009. Enniatins A1, B and B1 from an endophytic strain of *Fusarium tricinctum* induce apoptotic cell death in H4IIE hepatoma cells accompanied by inhibition of ERK phosphorylation. *Mol Nutri Food Res.*, **53**(4): 431-40. DOI: 10.1002/mnfr.200700428
- Zhang J, Liu D, Wang H, Liu T and Xin Z. 2015. Fusarictricina sesquiterpenoid ether produced by an endophytic fungus *Fusarium tricinctum* salicorn 19. *Eur Food Res Tech.*, **240**: 805-814. DOI:10.1007/s00217-014-2386-6
- Zhang Y, Zhao J, Wang J, Shan T, Mou Y, Zhou L and Wang J. 2011. Chemical composition and antimicrobial activity of the volatile oil from *Fusarium tricinctum*, the endophytic fungus in *Paris polyphylla* var. *yunnanensis*. *Nat Prod Commun.*, **6**(11): 1759-1762.
- Zhou J, Xu Z, Sun H and Zhang H. 2019. Smoke-isolated butenolide elicits tanshinone I production in endophytic fungus *Trichoderma atroviride* D16 from *Salvia miltiorrhiza*. *S Afr J Bot.*, **124**: 1-4. <https://doi.org/10.1016/j.sajb.2019.04.005>.

Responses of *Lantana Camara* Linn. Callus Cultures to Heavy Metals Added to the Culture Media

Reham W. Tahtamouni^{1,*}, Rida A. A .Shibli², Laila S.Younes³, Saida Abu-Mallouh⁴ and Tamara S. Al-Qudah⁴

¹ Department of Biotechnology, Faculty of Agricultural technology, Al Balqa- Applied University, Salt, Jordan.; ² Department of Horticulture and Crop Sciences, Faculty of Agriculture, University of Jordan, Amman, Jordan, ; ³ Agricultural and Animal Research Center, Tripoli, Libya, ; ⁴ Hamdi Mango Center for Scientific Research (HMCSR), University of Jordan, Amman, Jordan.

Received: October 30, 2019; Revised: January 8, 2020; Accepted: February 8, 2020

Abstract

Heavy metals represent a growing threat for ecosystems worldwide. In Jordan, several studies have searched the amounts of heavy metals in soils at roadsides of high ways and soils of litter dumps. The conducted studies found that these soils contained worrying levels of heavy metals that have exceeded in many cases the average world safe limit. For example, lead (Pb) level was 79 mg/ kg in soils closed to some highways while the world safe limit is only (25 mg/kg). In other studies, cadmium (Cd) concentration was (5.9 mg/kg) while the world safe limit for Cd is only (0.03 mg/kg). Also in some litter dumps in Jordan, soil chromium (Cr) average content was (6.9 mg/kg) while the world safe limit was only (0.1 mg/kg). *Lantana camara* Linn. is a flowering plant that has recently attracted the attention of researchers due to its novel phytoremediation powers against some heavy metals, which encouraged some countries to grow them in roadsides of highways and litter dumps. Tissue culture is an excellent approach for studying responses of *Lantana camara* to heavy metals without interference of other factors. In addition, tissue culture is the main method for producing elite plants lines from callus and cell suspension cultures with superior characteristics by genetic transformation. In this study, callus cultures were induced from leaf discs *in vitro*. Then, responses of *Lantana camara* callus cultures to different concentrations (0.0, 0.12, 0.2, 0.3 mg/L) of Cr, Pb, or Cd were monitored under *in vitro* environmentally controlled conditions to exclude the interference of any other factor. The obtained results revealed that callus growth and quality were found to decrease in response to adding heavy metals to the media at all concentrations. Meanwhile, all callus cultures recorded full survival rates (100%) by the end of the experiments and resumed growth after being transferred to normal growth conditions. Amounts of the three experimented heavy metals (Cr, Pb, and Cd) were found to reach the maximum in callus cultures (0.096, 0.109, 0.0193 mg/ kg), when pregrown on Murashige and Skoog media (MS media) supplemented with (0.3 mg/L), while maximum Biological Absorption Coefficient (BAC) values of (0.41, 0.6, 0.30) were recorded in callus cultures pregrown in media with (0.12 mg/L) of either Cr, Pb, or Cd, respectively. More work is still needed to improve BAC values obtained in *Lantana camara* callus cultures. Also, the produced callus cultures can be used in future research for preparing cell suspension cultures to be introduced to genetic transformation to produce *Lantana camara* plant lines with hyper accumulation powers against these contaminants.

Key words: *Lantana camara* Linn., Callus, *In vitro*, Heavy metals..

1. Introduction

Heavy metals act as natural components in the earth's crust (Laghlimi *et al.*, 2015). Meanwhile, due to the anthropogenic activities such as industrial effluents, fuel production, mining, and agricultural chemicals, heavy metals are presented nowadays as a major source of toxicity that threatens the health of more than 10 million people in many countries (Jadia and Fulekar, 2009). The problem with heavy metals is due to the fact that these elements cannot be degraded into non-toxic forms, so they would remain in the ecosystem for many years (Jabeen *et al.*, 2009, Wao *et al.*, 2014, Wao *et al.*, 2015.). Cd, Cr, Hg and Pb present the most common category of heavy metals, due to their presence in the in the ecosystems and

bioaccumulation in the food chain, which made them extremely dangerous to most biological systems (Jadia and Fulekar, 2009). In Jordan, several studies were conducted to investigate soil content of these contaminants in side roads of high ways and litter dumps. For example, El-Radaideh *et al.* (2018) found that Cr, Pb and Cd reached levels of 16, 11, 79 mg/kg respectively along Irbid-North Shooneh highway which are higher than world safe limit of each element (0.1, 5.9, 25.0 mg/kg, respectively). This was in agreement with Howari *et al.* (2004) who reported that soils along North Shuna— Aqaba Highway contained 5 mg/kg Cd and 79 mg/kg Pb. Additionally, Mashal *et al.* (2017) found that soils of roadsides of different sites of Al Hashmiyya City contained heavy metals (Pb, Zn, Cr and Cu) above threshold levels. Moreover, Daabes *et al.* (2013) reported in their study about soils of three litter dumps in

* Corresponding author e-mail: rehwt@bau.edu.jo.

Jordan (Ghabawi, Akaider and Russeifah) that the average concentrations of Cr (6.5 mg/ kg) and Cd (4.5 mg/ kg) were high and exceeded local and international standard limits.

Phytoremediation is a process where green plants remove pollutants from the environment before transforming them into biological forms (Doran, 2009). Via phytoremediation, pollutants are up taken by the plants before being translocated, and stored within plant biological systems (Subhashini, and Swamy 2013). Meanwhile, plant species differ in their phytoremediation potentials according to their root depth, type of contaminants, and regional climate (Laghlimi *et al.*, 2015).

For many years, studies were conducted in field or *in vivo* to investigate plant responses under environments contaminated with heavy metals, which was encountered by environmental, microflora and translocation barriers that made such studies very difficult (Doran, 2009). For this reason, plant tissue culture was presented as a reasonable and complementary approach for such studies, as via tissue culture most obstacles that might encounter such research types are eliminated, which would promote a deeper understanding for the mechanism of how plant cells detoxify such pollutants (Doran, 2009). Additionally, via *in vitro* techniques including callus and cell suspension cultures, it is possible to study genes responsible for their ability of accumulating heavy metals and to produce biotransformed plants with super phytoremediation powers that would present a revolutionary solution for heavy metals management strategies.

Lantana camara Linn. (also known as Wild Sage, Surinam Tea Plant and Spanish flag) is a widely spread flowering ornamental plant, and is a member of Verbenaceae family (Kalita *et al.*, 2012). Besides its aesthetic importance, *Lantana camara* Linn. has recently attracted the attention of researchers due to its novel phytoremediation powers against many types of heavy metals (Jusselme *et al.*, 2012; Mkumbo *et al.*, 2012; Waoo *et al.*, 2014; Waoo *et al.*, 2015). For example, in Mkumbo *et al.*, (2012) study, phytoremediation potential was investigated in *L. camara* plants grown in soil artificially contaminated soil with 500 or 1000 mg of Pb mg/ kg soil, where *Lantana camara* was found to be very promising as it was able to uptake 10% of 1000 mg/ kg of Pb per year. Additionally, Waoo *et al.* (2014) confirmed phytoremediation potential of *Lantana camara* plants collected from polluted areas in India, as these plants were found to be able to accumulate and tolerate high concentrations of different heavy metals types (Cd, Ni, Cr and Pb), mainly in their leaves and shoots. Moreover, Waoo *et al.* (2015) went more deep in their phytoremediation investigations about this plant, as they studied responses of *Lantana camara* microplants grown under *in vitro* conditions in MS medium supplemented with different concentrations of Cr, and they found that the microplants were able to maintain high survival rates in MS media up to 35 mg/L Chromium, while their survival and growth decreased drastically at higher concentrations. However, Waoo *et al.* (2015) had used only microplants as plant material in their research, and didn't measure the amount of Cr that had actually accumulated inside the *in vitro* grown microplants of *Lantana camara*.

From this prospective, our study aimed to investigate responses of *Lantana camara* callus cultures to addition of

Pb, Cr and Cd to the culture media. Moreover, for our knowledge this is the first research that uses callus cultures as a source of plant material for studying *Lantana camara*. responses to heavy metals, hoping that this approach would be a platform for future genetic and biotransformation studies at cell concentration that might produce *Lantana camara* plants with super accumulation powers.

2. Materials and Methods

2.1. *In vitro* establishment of plant material

Vegetative buds of *Lantana camara* Linn. were collected from a single plant growing at University of Jordan campus (Amman, Jordan). Buds were surface sterilized under running tap water before being soaked in tap water supplemented with few drops of a commercial detergent in addition to (1.0 g) of a fungicide (Benomyle) for 15 min. Next, the buds were washed again under running tap water and then soaked in 40% sodium hypochlorite for 20 min under the laminar air flow cabinet. Then, buds were rinsed with sterile distilled water and soaked in 70% ethanol (v/v) for 30 seconds before being rinsed again with sterile distilled water for three times. The buds were then inoculated in 4.4 g/L of MS (Murashige and Skoog, 1962) media premix (Sigma Aldrich Murashige and Skoog basal salt mixture) plus 1 ml/L MS vitamin mixture (Sigma Aldrich Murashige and Skoog Vitamin Powder 1000X) in addition to 0.1 M sucrose and 8.0 g/L bacto agar. The cultures were then kept under growth room consisting of a daily regime of 24 ± 1 °C and 16/8 (light/dark) photoperiod of $45\text{--}50 \mu\text{mol m}^{-2}\text{s}^{-1}$ irradiance. Subculturing was performed every four weeks to fresh MS media till enough plant material was obtained for the experiments.

2.2. Callus Establishment:

Callus was induced from leaf discs excised from the *in vitro* grown microshoots of *Lantana camara* Linn (5.0 mm diameter). The leaf discs were sub-cultured into Petri dishes containing solid MS media supplemented with either of (0.0, 1.0, 2.0 mg/ L) thidiazuron (TDZ) or 2,4-dichlorophenoxy acetic acid (2,4-D). Each treatment consisted of 10 replications with 2 leaf discs/ replicate. Cultures were then maintained under complete dark condition at 24 ± 1 °C. Data on callus formation and development were collected after two months including: callusing percentage, callus fresh weight, color and texture.

2.3. Callus Multiplication

Induced calli were transferred into Petri dishes containing fresh hormone free MS solid media for 5 days under dark to remove any hormonal carryover effect. Then, calli (0.7 mg) were transferred into MS media + 0.1 M sucrose and 2.0 mg/L 2,4-D (2,4-dichlorophenoxy acetic acid) in combination with different concentrations (0.5, 1.0 mg/L) of either Kinetin or Benzylaminopurine (BAP). The control treatment consisted of callus establishment media that yielded best callus establishment results in section (2.2) which consisted of a solid MS media plus 0.1 M sucrose and (2.0 mg/ L) 2,4-D. Each treatment consisted of 10 replications with 2 calli/ replicate. Data was collected after one month for callus fresh weight, color and texture.

2.4. Heavy Metals Experiments

Before heavy metals experiments, calli were transferred into fresh hormone free MS solid media for 5 days under dark to remove any hormonal carryover effect as described earlier in section 2.3. Next, callus multiplication media (control) that yielded best callus multiplication results in section (2.3) [MS media supplemented + 0.1 M sucrose + 2.0 mg/L 2, 4-D + 1.0 mg/L Kinetin] was prepared and poured into 250 ml glass bottles before being autoclaved. After media sterilization, each heavy metal type (chromium (Cr), lead (Pb) and cadmium (Cd) at concentrations of (0.0, 0.12, 0.2, 0.3 mg/L) was infiltrated aseptically into each media bottle, under continuous stirring before being poured into sterile Petri dishes. Next, calli (0.7 mg) were transferred into each treatment with ten replications/ treatment with two calli/ replicate. Data was collected after one month for callus fresh weight, color and texture. Also, samples of calli (0.7 mg) were transferred into to the control multiplication media with ten replications/ treatment and two calli/ replicate, to see if there were any carry over effect on callus growth resulting from preexposure to the experimented heavy metals, and data for fresh weight was taken after one month.

For heavy metals analysis, acid digestion of dried calli was carried out according to Jones (1984), where 20 samples were taken from each treatment, and 0.5g of each callus sample was heated with 5 ml of 70% HNO₃ and 1.5 ml of 60% HClO₄ until the brown fumes disappeared. Next, the solution was cooled down and 1:1 diluted with 5ml HCl (density 1.18 g/ml). The diluted solution was then filtered and diluted with distilled water up to 25ml.

Determination of Cr, Cd and Pb were done by Inductively Coupled Plasma–Optical Emission Spectrometry (ICP-OES) equipped with 40.68 MHz operating frequency generator, 1,800 L/mm t67 holographic grating which allows a wide range analysis from 160–800 nm and up to 6 pm resolution. This method meets the EN655011, IEC801-2, IEC801-3 and IEC801-4 EMC standards. The minimal detection limits and the R² for standard curves are listed in the Table 1. Then, data was recorded for concentration of each heavy metal absorbed in the callus cultures, while plant ability to uptake heavy metals from the media (Biological Absorption Coefficient (BAC) was determined as a ratio of element concentration in callus to element concentration in the growth media (Cheraghi *et al.*, 2011).

Table 1. The minimal detection limits and the R² for standard curves of Cr, Pb, and Cd using Inductively Coupled Plasma–Optical Emission Spectrometry (ICP-OES) technique

Element	Detection limit (ppb)	R ²
Cr	2	0.9918
Cd	0.5	0.9996
Pb	10	0.9980

2.5. Experimental Design

Treatments of the experiments were arranged in a completely randomized design (CRD) and each treatment was replicated ten times with 2 explant/ replicate.

Data recorded from each treatment was analyzed separately according to the analysis of variance (ANOVA) using (SPSS, version 17) analysis system. Means were separated and standard errors (SE) were extracted according to the Tukey's HSD test (Honest Significant Difference 22T) at a probability concentration of 0.05.

3. Results and Discussion

3.1. Callus Establishment

The obtained results indicated that, callus establishment was a function of growth regulator type and concentration in the culture media. In leaf discs treated with TDZ under complete dark conditions, callusing responded positively to increasing concentration of TDZ to reach maximum callusing rate (70%) and fresh weight (1.465 g) at concentration of 2.00 mg/L (Table 2). Meanwhile, the quality of the resulted callus was poor, as the callus was brown with a hard texture (Table 2). On the other hand, using 2,4-D, as a source of growth regulator enhanced all callus induction parameters (Table 2, Figure 1 B). Full callusing rate and maximum fresh weight (2.05 g) were obtained at concentration of 2.00 mg/L 2, 4-D under complete dark conditions (Table 2, Figure 1B). This was a combined with high quality of white friable callus. Successful callus induction from leaf discs and shoot tips of *Lantana camara* L. was reported by (Saxena *et al.*, 2013), where greenish compacted callus was obtained when the explants were treated with 0.02 mg/L 2, 4-D under light. Also, Veraplakorn (2016) was able to induce callusing from *Lantana camara* leaf discs using 40.0 µmol/L of 1-naphthalene acetic acid (NAA) combined with 40.0 µmol/L BA under light. So, our approach for successful callusing in *Lantana camara* Linn. leaf discs was completely different from the previous study, as 2.00 mg/L 2,4-D was used for callus induction under complete dark conditions.

Table 2: Effect of growth regulator type and concentration on *in vitro* establishment of *Lantana camara* Linn. callus cultures from leaf discs under complete dark conditions.

Concentration (mg/L)	Callus %	Fresh weight (g)	Color	Texture
Thidiazuron (TDZ)				
C* (0.0)	00.0±0.0	00.0±0.0 c	-	-
1.0	31.25±4.762	0.65±0.092 b	Brown	Hard
2.0	70±2.961	1.465±0.033 a	Brown	Hard
(2,4-D)				
C (0.0)	00.0±0.0	00.0±0.0 c	-	-
1.0	75±4.051	1.70±0.041 b	White	Friable
2.0	100.0±0.0	2.050.033 a	White	Friable

*C: represents control treatment (solid hormone free MS media+ 0.1 M sucrose). Values represent means ± standard error. Data for each growth regulator was statistically analyzed separately. Means within columns for each growth regulator having different letters are significantly different according to Tukey HSD at P≤0.05.

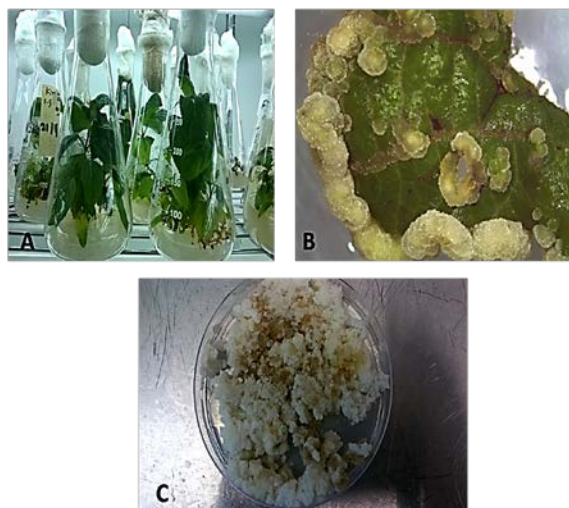


Figure 1. *In vitro* grown *Lantana camara* Linn. A: Microshoots grown in hormone free MS media + 0.1 M sucrose. B: Establishment of callus cultures from leaves discs in MS media + 2.0 mg/L 2,4-D + 0.1 M sucrose. C: Callus multiplication in MS media + 2.0 mg/L 2,4-D + 1.0 mg/L Kinetin + 0.1 M sucrose.

3.2. Callus growth

A tremendous increase in callus fresh weight was obtained on media supplemented with kinetin in combination with 2.0 mg/L 2, 4-D compared to those grown in either the control or BAP treatments (Table 3, Figure 1C). Also, our results revealed that the increase in fresh weight responded positively to the increase in kinetin concentration in the media to reach a maximum weight of (5.92 g) at kinetin concentration of 1.0 mg/L (Table 3). Moreover, quality of the resulted callus was excellent in kinetin treatment at all concentrations, as white friable callus was obtained, while callus turned brown when exposed to BAP treatments (Table 3, Figure 1C). Our results were in complete harmony with those reported by Raj *et al.* (2015) and Slazak *et al.* (2015), as kinetin in combination with 2,4-D were found to be excellent formula for callus growth in *Securinega suffruticosa* and *Viola uliginosa*. On the other hand, in Veraplakorn (2016) study, callus multiplication was best in *Lantana camara* L. when cultured on MS media supplemented with 40.0 $\mu\text{mol/L}$ (NAA) + 40.0 $\mu\text{mol/L}$ BA under light. Meanwhile, in another related study, Zatimeh *et al.* (2017) tried different hormones in combination with 2.0 mg/L 2, 4-D for multiplication of *Peganum harmala* L. callus cultures under dark conditions, where they found that (1.5 mg/L) TDZ in combination with 2.0 mg/L 2, 4-D was a great prescription for maximum callus diameter and fresh weight (3.98 cm, 2.88 g). This might lead to a conclusion that, despite using 2.0 mg/L 2, 4-D in combination with different hormones for callus multiplication, the response of callus cultures to these combinations is plant type dependent.

Table 3: Effect of growth regulator type and concentration in combination with 2,4-D on growth and quality of *Lantana camara* Linn. callus cultures.

Concentration (mg/L)	Fresh weight (g)	Color	Texture
Kinetin			
C*	2.03 ± 0.0194 c	White	Friable
0.5	4.65 ± 0.0133 b	White	Friable
1.0	5.92 ± 0.119 a	White	Friable
Benzylaminopurine (BAP)			
C	2.03 ± 0.019 b	White	Friable
0.5	2.21 ± 0.125 b	Brown	Friable
1.0	3.14 ± 0.179 a	Brown	Friable

*C: represents control treatment (solid MS media+ 0.1 M sucrose + 2, 2,4-D). Values represent means ± standard error. Data for each growth regulator was statistically analyzed separately. Means within columns for each growth regulator having different letters are significantly different according to Tukey HSD at $P \leq 0.05$.

3.3. Effect of Heavy Metals

3.3.1. Effect of Chromium

The obtained data revealed that growing callus cultures in media supplemented with Chromium (Cr) for one month had a negative impact on callus growth and quality. A significant decrease in callus fresh weight was recorded as Cr concentration increased in the media to reach a minimum record of (2.13 g) at Cr concentration of (0.3 mg/L) (Table 4). This was a combined with a decline in color quality, as cultures turned creamy compared with the whitish healthy callus obtained in the control treatment (Table 4, Figure 2A, B). Cr was reported to have inhibitory influence on plant growth even at low rates (Sundaramoorthy and Ganesh, 2015; Waoo *et al.*, 2015). This was attributed to the fact that Cr at high rates, like any other heavy metal, would interfere with metabolic reactions in plants and would lead to growth retardation or death (Schmidt 2003; Jadia and Fulekar 2009). Moreover, Waoo *et al.*, (2015) found that adding Cr in a form of Chromium Sulphate (CrSO_4) to the culture media had significantly decreased the shoot length and quality of *Lantana camara in vitro* grown plantlets, while survival was drastically declined when (CrSO_4) concentration exceeded 35 mg/L.

Meanwhile, full survival rates were obtained by the end of Cr experiment, and most callus cultures had recovered from the side effects of Cr one month after being subcultured into fresh control media, as an increase in fresh weight was recorded in all cultures (Table 4). This might indicate that *Lantana camara* L. callus cultures have the ability to withstand living under such contaminated environment without altering their survival and regrowth potentials. Moreover, Cr was detected in the dried callus cultures exposed to Cr at all concentrations and the maximum amount of Cr (0.069 mg/kg) was detected in cultures exposed to (0.3 mg/L) Cr (Table 4), which indicated that callus cultures were found to be able to accumulate Cr from chromium contaminated media without any losses in their survival rates (Table 4). Meanwhile, the biological absorption coefficient (BAC) decreased with increasing Cr concentration in the media to reach a minimum value of (0.23) in cultures pre-exposed to (0.3 mg/L) Cr compared to (0.41) recorded in callus

pretreated with (0.12 mg/L) Cr (Table 4), which implies that callus ability to uptake Cr from the media became more weak as Cr concentration increased in the culture media (Table 4). This would act as a defense mechanism adopted by living cells of plants growing in environment where high concentrations of heavy metals exist to prevent absorption of high amounts of heavy metals that would

enable the plant to avoid exposure to toxicity hazard or death. Meanwhile, according to Mkumbo *et al.* (2012), a plant with (BAC value > 1) is described as suitable for phytoextraction of heavy metals from soil, but this applies only at whole plant concentration and not at concentration of callus cultures as it is the case in our study.

Table 4. Effect of Chromium (Cr) concentrations on fresh weight, color and texture of *Lantana camara* Linn. callus cultures, in addition to phyto remediation potential of the plant material.

Concentration (mg/L)	FW1(g)*	Color	Texture	FW2(g)	Cr ^Y concentration (mg/ kg dry weight)	BAC ^Z
C *	5.86±0.081 a	White	Friable	5.94±0.072 a	-	-
0.12	3.58 ± 0.065 b	Creamy	Friable	4.82±0.151 b	0.0493± 0.012 b	0.41± 0. 051 a
0.2	2.60±0.058 c	Creamy	Friable	4.39±0.091 c	0.0687± 0.018 a	0.34± 0.016 b
0.3	2.13±0.044 e	Creamy	Friable	3.78 ±0.073 d	0.06948± 0.022 a	0.23± 0.012 c

*C: represents control treatment (solid MS media+ 0.1 M sucrose +1 mg/L kinetin + 2 mg/L 2,4-D). FW1: callus fresh weight recorded after growth for one month in media supplemented with each type and concentration of heavy metal. FW2: callus fresh weight recorded one month after being subcultured into control media. Y: concentration of the heavy metal in the callus cultures in dry weight bases. Z: BAC represents the Biological Absorption Coefficient. Values represent means ± standard error. Means within columns for each heavy metal type having different letters are significantly different according to Tukey HSD at P≤0.05.



Figure 2. Effect of heavy metals on growth and quality of *Lantana camara* L. callus cultures grown in either of A: control, B: 0.3 mg/L Cr, C: 0.3 mg/L Pb or D: 0.3 mg/L Cd.

3.3.2. Effect of Lead

Adding lead to the culture media resulted in a drastic decline in callus fresh weight and quality. The lowest fresh weight was recorded in callus exposed to (0.3 mg/L) Pb, while red spots appeared in all callus clumps treated with Pb at all concentrations (Table 5, Figure 2C). Although Pb is described as nonessential element in most vital biological reactions in plant cells, still it is reported as hazardous or lethal to most livings even when absorbed at very small amounts (Boonyapookana *et al.* (2005). At plant concentration, Pb was found to be responsible for necrosis, growth stunting and reduction in biomass

production in sunflower, tobacco, and vetiver plants grown in hydroponic environment supplemented with different concentrations of Pb (Boonyapookana *et al.* (2005), which agrees with our results. Meanwhile, full survival rates were recorded in all callus cultures of our study, and they resumed growth after being subcultured into lead free fresh media but at a lower extent in those exposed to either (0.2 or 0.3 mg/L) Pb (Table 5). Moreover, amount of Pb detected in callus cultures increased with increasing Pb concentration in the media to reach the maximum (0.1095 mg/ kg) at Pb concentration of (0.3 mg/L). On the other hand, BAC values declined with increasing Pb concentration to reach the minimum (0.37) at (0.3 mg/L) Pb compared to (0.60) BAC recorded in cultures pretreated with (0.12 mg/L) Pb (Table 5). In another related study, Mkumbo *et al.* (2012) assessed phytoextraction potential of several plant species *in vivo* against Pb, where they found that *Lantana camara* seedlings recorded low BAC (0.4) compared to values recorded in *Tephrosia candida* and *Tagetes minuta* (L.) (2.55 and 1.0) respectively, which made these two species most suitable for phytoextraction of Pb in the gold mining areas of Tanzania. However, BAC value (0.4) recorded in *Lantana camara* seedlings grown in Pb polluted soil (318.9 mg/kg dry weight) in Mkumbo *et al.* (2012) study was so close to BAC (0.45) obtained in our study when callus was pregrown in media supplemented with (0.2 mg/L) Pb.

Table 5. Effect of Lead (Pb) concentrations on fresh weight, color and texture of *Lantana camara* Lin. callus cultures, in addition to phyto remediation potential of the plant material.

Concentration (mg/L)	FW1(g)	Color	Texture	FW2(g)	Pb ^Y concentration mg/kg dry weight)	BAC ^Z
C *	5.86±0.081 a	White	Friable	5.94±0.072 a	-	-
0.12	2.72 ± 0.083 b	Reddish white	Friable	3.97 ± 0.086 b	0.0716± 0.011 c	0.60± 0.016 a
0.2	1.97 ± 0.084 c	Reddish white	Friable	3.25 ± 0.081 c	0.0895± 0.013 b	0.45± 0.01 bc
0.3	1.83 ± 0.069 c	Reddish white	Friable	2.93 ± 0.099 c	0.1095± 0.015 a	0.37± 0.021 c

*C: represents control treatment (solid MS media+ 0.1 M sucrose +1 mg/L kinetin + 2 mg/L 2,4-D). FW1: callus fresh weight recorded after growth for one month in media supplemented with each type and concentration of heavy metal. FW2: callus fresh weight recorded one month after being subcultured into control media. Y: concentration of the heavy metal in the callus cultures in dry weight bases. Z: BAC represents the Biological Absorption Coefficient. Values represent means ± standard error. Means within columns for each heavy metal type having different letters are significantly different according to Tukey HSD at P≤0.05.

3.3.3. Effect of Cadmium

A significant decline in callus fresh weight was recorded in response to Cadmium addition to the media at all concentrations (Table 6). However, the decline in fresh weight was most severe at Cd concentration of (0.3 mg/L) where callus color turned brown (Table 6, Figure 2D). Meanwhile, all callus cultures were back to grow normally when transferred to normal heavy metal free culture media, but cultures precultured in either (0.2 or 0.3 mg/L) Cd supplemented media were still suffering from the negative impacts of preexposure to Cd (Table 6). Toxic concentrations of Cadmium were reported to interfere with most primary biological processes such as, photosynthesis, carbohydrate metabolism, in addition to enzymatic activities that would either decline growth or cause plant

Table 6. Effect of Cadmium (Cd) concentrations on fresh weight, color and texture of *Lantana camara* Lin. callus cultures, in addition to phyto remediation potential of the plant material.

Concentration (mg/L)	FW1(g)	Color	Texture	FW2(g)	Cd ^Y concentration (mg/ kg dry weight)	BAC ^Z
C*	5.86±0.081 a	White	Friable	5.94±0.073 a	-	-
0.12	3.07 ± 0.075 b	Creamy	Friable	4.37 ± 0.081 b	-	-
0.2	2.43 ± 0.066 c	Brown	Friable	3.82 ± 0.055 c	0.0587± 0.023 b	0.29± 0.028 a
0.3	1.79 ± 0.032 e	Brown	Friable	3.61 ± 0.066 c	0.0913± 0.011 a	0.30± 0.012 a

*C: represents control treatment (solid MS media+ 0.1 M sucrose +1 mg/L kinetin + 2 mg/L 2,4-D). FW1: callus fresh weight recorded after growth for one month in media supplemented with each type and concentration of heavy metal. FW2: callus fresh weight recorded one month after being subcultured into control media. Y: concentration of the heavy metal in the callus cultures in dry weight bases. Z: BAC represents the Biological Absorption Coefficient. Values represent means ± standard error. Means within columns for each heavy metal type having different letters are significantly different according to Tukey HSD at P≤0.05.

4. Conclusions

Callus induction and multiplication were obtained successfully from *Lantana camara* L. *in vitro* grown leaf disc. Successful callus induction would facilitate using this callus as a source of cells which can be used in future studies to study and to specify genes responsible for phyto remediation powers in *Lantana camara* plants and to produce genetically transformed cell lines with super accumulation capabilities. Also, the obtained results showed that, although exposing callus cultures to different types and concentrations of heavy metals (Cr, Pb, and Cd) had negatively affected callus growth and color, callus cultures were able to withstand the exposure of heavy metals at all concentrations, as they maintained their survival potential and resumed growth after being subcultured into normal growth media. Also, callus cultures were able to absorb and accumulate different amounts of the experimented heavy metals types from the culture media at all concentrations. This indicates that survival and accumulation powers of *Lantana camara* delicate callus cultures against the tested heavy metals can be introduced to further studies to be improved if proper *in vitro* breeding protocols are applied. However, more work is still needed to test the response of *Lantana camara* callus cultures to higher and even toxic concentrations of each heavy metal and to find ways to improve BAC values obtained in *Lantana camara* L. callus cultures. This can be achieved by means of plant genetic biotransformation, where callus can be used as a raw material for massive production of elite hyperaccumulators against such annoying contaminants.

death (Javed and Greger, 2011). Moreover, Cd was not detected in callus dried samples at concentration of (0.12 mg/L), while the highest records for Cd concentrations (0.0913 mg/ kg) and BAC values (0.30) were found in callus pregrown in (0.3 mg/L) Cd supplemented media. In another related study about evaluation of phytoremediation potential in several plant species grown in Cd contaminated soil, it was found that the highest values for bioconcentration factor (BCF: concentration of heavy metal in shoots / concentration of heavy metal in soil) in French marigold, Impatiens, Garden verbena, and Scarlet sage plants exceeded (1) and ranged from 1.75 to 5.68, which made these plants hyper accumulators for Cd (Lin *et al.*, 2010)

References

- Abu-Daibes M., Qdais H., Alsyouri H. 2013. Assessment of heavy metals and organics in municipal solid waste leachates from landfills with different ages in Jordan. *Journal of Environmental Protection*. Published Online. (<http://www.scirp.org/journal/jep>).
- Boonyapookana B., Parkpian P., Techapinyawat S., Delaune R.D., Jugsujinda A. 2005. Phytoaccumulation of lead by Sunflower (*Helianthus annuus*), Tobacco (*Nicotiana tabacum*), and Vetiver (*Vetiveria zizanioides*). *J. Environ. Science Health*, **40(1)**: 117-137.
- Cheraghi, M., Lorestani, B., Khorasani, N., Yousefi, N., Karami, M. 2011. Findings on the phytoextraction and phytostabilization of soils contaminated with heavy metals. *Biological Trace Element Research*, **144(3)**: 1133-1141
- Doran P. M. 2009. Application of Plant Tissue Cultures in Phytoremediation Research: Incentives and Limitations. *Biotechnology and Bioengineering*, **103(1)**: 60-76.
- El-Radaideh, N.M., Al-Taani, A.A.A. 2018. Geo-environmental study of heavy metals of the agricultural highway soils, NW Jordan. *Arab J Geosci* **11(787)**. <https://doi.org/10.1007/s12517-018-4099-9>
- Howari F.M. , Abu-Rukah Y., . Goodell P. C. 2004. Heavy metal pollution of soils along North Shuna— Aqaba Highway. *Int. J. Environment and Pollution*, **22(5)**: 597-607
- Jabeen R., Ahmad A., Iqbal M. 2009. Phytoremediation of heavy metals: physiological and molecular mechanisms. *Bot. Rev.*, **75(4)**: 339-364.
- Jadia C.D. and Fulekar M.H. 2009. Phytoremediation of heavy metals: Recent techniques. *African Journal of Biotechnology*, **8(6)**: 921-928.
- Javed M.T., Greger M. 2011. Cadmium triggers *Elodea Canadensis* to change the surrounding water pH and thereby Cd uptake. *International Journal of Phytoremediation*, **13(1)**: 95-106.

- Jusselme M.D., Poly F., Miambi E., Mora P., Blouin M., Pando A., Rouland-Lefèvre C. 2012. *Science of the Total Environment*, **416**: 200–207
- Kalita S., Kumar G., Karthik L., Venkata V., Rao B. 2012. A Review on Medicinal Properties of *Lantana camara* Linn. *Research J. Pharm. and Tech*, **5(6)**: 711-715
- Laghlimi M., Baghdad B., El Hadi H., Bouabdli A. 2015. Phytoremediation Mechanisms of Heavy Metal Contaminated Soils: A Review. *Open Journal of Ecology*, **5**: 375-388.
- Lin C. C., Lai H.Y., Chen Z.S. 2010. Cadmium hyperaccumulation of fresh marigold and impatiens. *International Journal of Phytoremediation*, **12**: 1-14.
- Mashal K., Salahat M., Al-Qinna M. and Ali Y. 2017. Assessment of Heavy Metals in Urban Areas of Al Hashmiyya City of Jordan. *Jordan Journal of Earth and Environmental Sciences*, **8 (2)**: 61 – 67
- Mkumbo S. Mwegoha W., Renman G. 2012. Assessment of the phytoremediation potential for Pb, Zn and Cu of indigenous plants growing in a gold mining area. *International journal of environmental sciences*, **2(4)**: 2425-2434
- Murashige T and Skoog F. 1962. A revised medium for rapid growth and bioassays with tobacco tissue cultures. *Physiol. Plant*, **15**:473-497.
- Raj D. Kokotkiewicz A. Drys A., Luczkiewicz M. 2015. Effect of plant growth regulators on the accumulation of indolizidine alkaloids in *Securinega suffruticosa* callus cultures. *Plant Cell Tiss Organ Cult.*, **123(1)**:39–45
- Saxena, M.K., Gupta, S.J., Singh, N. 2013. Allelopathic potential of callus extract of *Lantana camara*. *Int. J. Recent Sci. Res.*, **4**: 1628-1630.
- Schmidt U. 2003. Enhancing Phytoextraction: The effects of chemical soil manipulation on mobility, plant accumulation, and leaching of heavy metals. *J. Environ. Qual.*, **32**: 1939-1954.
- Slazak B., Sliwinska E., Saługa M., Ronikier M., Bujak J., Słomka A., Go'ransson U., Kuta E. 2015. Micropropagation of *Viola uliginosa* (Violaceae) for endangered species conservation and for somaclonal variation-enhanced cyclotide biosynthesis. *Plant Cell Tiss Organ Cult*, **120**:179–190
- Subhashini, V. and Swamy, A.V.V.S. 2013. Phytoremediation of Pb and Ni Contaminated Soils Using *Catharanthus roseus* (L.). *Universal Journal of Environmental Research and Technology*, **3(4)**: 465-472.
- Sundaramoorthy P. and Ganesh K.S. 2015. Influence of Chromium Treatment on Growth and Nutrient Accumulation of Paddy (*Oryza sativa* L.) Seedlings. *International Letters of Natural Sciences*. **4**: 7-13.
- Veraplakorn V. 2016. Micropropagation and callus induction of *Lantana camara* L.: A medicinal plant. *Agriculture and Natural Resources*, **50 (5)**: 338-344.
- Wao A.A., Khare S. and Ganguly s. 2014. Evaluation of Phytoremediation Potential of *Lantana camara* for Heavy Metals in an Industrially Polluted Area in Bhopal, India. *International Journal of Engineering and Applied Sciences*, **1(2)**: 1-3.
- Wao A.A., Khare S. and Ganguly s. 2015. *In vitro* Studies on Effect of Chromium on *Lantana camara*. *Climate Change*. **1(1)**: 45-48
- Zatimeh A. Shibli R.A., Tahtamouni R.W., Al-Qudah T.S., Abu Mallouh S., Younes L.S. and AL-Hawamdeh F.M. 2017. Experimenting the possibility of callus development and growth from *Peganum harmala* L. leaf discs and assessment of the antibacterial activities of callus extract against *Salmonella* sp. and *Bacillus subtilis*. *Journal of Food, Agriculture & Environment*. **15 (1)**: 28 – 33.

Synthesis and Characterization of Zinc Nanoparticles by Natural Organic Compounds Extracted from Licorice Root and their Influence on Germination of *Sorghum bicolor* Seeds

Mahmood A. S. Al-Shaheen¹, Mustafa N. Owaid^{2,3,*} and Rasim F. Muslim³

¹Department of Biology, College of Education for Pure Sciences, University Of Anbar, Ramadi, Anbar 31001, ²Department of Heet Education, General Directorate of Education in Anbar, Ministry of Education, ³Department of Environmental Sciences, College of Applied Sciences-Heet, University Of Anbar, Hit, Anbar 31007, Iraq

Received: December 26, 2019; Revised: January 17, 2020; Accepted: February 8, 2020

Abstract

This work aims to biosynthesize zinc nanoparticles (ZnNPs) from licorice (*Glycyrrhiza glabra*) root extract and to apply that on seeds germination of two *Sorghum bicolor* varieties (Enkath and Rabeih). Three concentrations of both licorice extract and colloidal solutions of ZnNPs (25%, 50%, and 75%) were tested on some features of planting seeds *in vitro* including Seeds germination percentage, shoot length, root length, seedlings length, and Root-Shoot Ratio. Along with that, characterization of ZnNPs was also done. AFM of the phyto-synthesized ZnNPs reached an average of 68.69 nm. Presenting of (-CH) group through FTIR confirmed finding compounds -CH₃ and -CH₂ in monosaccharides, disaccharides, polysaccharides and mono acidic saccharides. The exposure to ZnNPs showed remarkable effects on seed germination and other growth parameters of sorghum seedlings. The low concentration of 25% of ZnNPs exhibited the best shoot length compared with the high concentrations (50% and 75%). The two concentrations of 50% and 75% exhibited the presence of hairy roots in order to the smallness of roots. Thus, the low concentration (25%) of ZnNPs can be used as a material for *S. bicolor* seed priming in the field with low toxicity on this plant. The results of this work encourage using ZnNPs as an improver in agricultural applications.

Keywords: Agriculture, Biosynthesis, Licorice, Nanobiofertilizer, ZnNPs.

1. Introduction

Sorghum, *Sorghum bicolor* (L.) Moench, is a major crop of agriculture economically important cereals used as food for the humans in developing countries, and it is easily grown (Queiroz *et al.*, 2011). *S. bicolor* is produced in Iraq, and its total production was 50000 Million Ton in 2018 (IndexMundi, 2018). The world population is increasing rapidly, and the production is not sufficient to meet the requirements of the market. Thus, especially in developing countries, this can lead to severe challenges in food security (FAO, 2009). Sorghum ranks as the main cereal crop next to the wheat, rice and maize in the world (Soomro *et al.*, 2015).

Moreover, it has multiple usages and is included in the production of human and animal food, as well as alcohol and industrial products (Awika and Rooney, 2004). Cultivation of this crop is centered in tropical and subtropical regions, primarily in marginal areas that are more stress-prone (Reddy and Patil, 2015). These conditions of stress, especially abiotic ones, are the biggest causes of the reduction of sorghum yield (Souza *et al.*, 2015), although these are minimized owing to its higher tolerance to stress compared to other cereals (Mutisya *et al.*, 2009).

Micronutrients are chemical elements meaningful for plant growth. They are necessary at a small quantity and although their participation is small. The absence of essential micronutrients can lead to reducing the productivity of crops significantly (Malakouti, 2008). Micronutrient deficiencies are a common problem in soils of semi-arid regions, especially zinc, sulphur and boron (Sahrawat *et al.*, 2007). Thus, the reduction of the elements in the crop negatively affects human health (Tuomisto *et al.*, 2017). It has been assessed that many people throughout the world suffer from micronutrient malnutrition, the most common deficiencies of iron, zinc, and iodine, or vitamin A (Welch, 2002). Nowadays, nanomaterials priming of micronutrients is a new approach for the increase of seedling vigor and development of seed germination percentage (Dehkourdi and Mosavi, 2013; Ghafari and Razmjoo, 2013). Using nano-emulsion is significant to improve nutritional elements in plants called agricultural nanotechnology (Mostafa *et al.*, 2017).

Sorghum is the main cereal crop after wheat, rice and maize globally (Soomro *et al.*, 2015), and needs eco-friendly fertilizer to enhance its growth, and in this study, *Glycyrrhiza glabra* was selected to use in the biosynthesis of ZnNPs. *G. glabra* is one of the most traditional herbs used in medicine. It belongs to the family Leguminosae (Nomura *et al.*, 2002). However, *G. glabra* contains glycyrrhizin, liquiritin, liquiritin apioside, isoliquiritin,

* Corresponding author e-mail: mustafanowaid@gmail.com , mustafanowaid@uoanbar.edu.iq.

isoliquiritin apioside, liquiritigenin, isoliquiritigenin, licuraside, glycyrrhetic acid, glycycomarin, glabridin, licochalcone A licoricidin, *p*-hydroxybenzylmalonic acid (Li *et al.*, 2016), coumarins, flavonoids, triterpenoids, tannins, glabrol, kumatakenin, chalcones, licoricone, and phytosterols (Mostafa *et al.*, 2017). The root of *Glycyrrhiza* sp. is containing bioactivities such as antibacterial, antifungal, antimalarial, antiviral, anticancer, antioxidant, antiallergenic, immunostimulant, antiulcer, anti-inflammatory, antidiabetic, antithrombic, expectorant and estrogenic activities (Dong *et al.*, 2007; Renjie, 2008; Zore *et al.*, 2008; Al-Ani *et al.*, 2018).

There are many studies that have sought biosynthesis of metallic nanoparticles from organic compounds in plant (Al-Bahrani *et al.*, 2018) and fungi (Owaid and Ibraheem, 2017) such as greener zinc (Owaid *et al.*, 2019), silver (Owaid *et al.*, 2015, 2018) and gold nanoparticles (Owaid *et al.*, 2017). Green synthesis of ZnNPs is considered useful, safety/non-toxic and potential agent in different fields as has been produced from ginseng root extract (Owaid *et al.*, 2019). Hence, ZnNPs reduced the negative influence of drought action toward some plants (Taran *et al.*, 2017). Thus, in this study, licorice (*G. glabra*) root extract has been used to biosynthesize ZnNPs and tested their bioactivity in the agricultural field. This study aims to use ZnNPs synthesized using licorice extract for germination and feeding seeds of Sorghum (*S. bicolor*) *in vitro* in comparison with the aqueous extract of licorice alone. Seeds germination percentage, shoot length, root length, seedlings length, and Root-Shoot Ratio were investigated. Also, characteristics of the biosynthesized ZnNPs were studied.

2. Materials and Methods

2.1. Germination of Sorghum bicolor L. Moench Seeds

Two sorghum varieties Enkath and RabeH (*Sorghum bicolor* L. Moench) were obtained from the Department of Yellow and White Maize Research, General Authority for Agricultural Research in Iraqi Ministry of Agriculture in May 2017 to use in the effect of the extracts and zinc nanoparticles (ZnNPs) on their growth *in vitro*.

2.2. Extraction of Glycyrrhiza glabra licorice root

Licorice root powder was obtained from the local market in Hit city, Iraq. About 5 g powder was extracted in 100 ml D.W (distilled water) by the magnetic stirrer hotplate for 15 min until boiling. The extracted solution was put for cooling then filtrated using gauze and centrifuged 4000 rpm. The aqueous extract has been collected and stored in the freezer until future use.

2.3. Biosynthesis of ZnNPs

For the licorice-mediated synthesis of ZnNPs, 10 ml of 3×10^{-3} M $ZnSO_4 \cdot 7H_2O$ has been mixed with 3 ml aqueous extract of *Glycyrrhiza glabra* licorice root on the magnetic stirrer hotplate at 80 °C for 3 h until the change of color was seen.

2.4. Characterization of ZnNPs

The change of color, UV-Visible spectroscopy, FTIR (Fourier-transform infrared spectroscopy, Bruker), AFM (Atomic Force Microscopy), and Granularity Cumulation distribution have been achieved in Department of Chemistry at University of Baghdad (SPM AA300

Angstrom Advanced Inc., USA, AFM contact mode, with a suitable silicon tip by using IMAGER 4.31 software) to characterize ZnNPs formed using aqueous extract of *G. glabra* (licorice) root.

2.5. In vitro planting Sorghum bicolor seeds

Seeds were immersed in 5% sodium hypochlorite solution for 10 min to ensure surface sterility (U.S. Environmental Protection Agency, 1996). They were soaked in distilled water (DW) for 2 h, rinsed four times with DW, and then soaked in a series of the synthesized ZnNPs suspensions for approx. 2 h. Hence, ten seeds of *S. bicolor* were planted on the sterilized filter paper in 9 cm Petri dish and wetted by 5 ml of solutions separately for each concentration. All plates were put in the plant incubator at 25 °C for 10 days then harvested and the determinations were calculated. Seeds germination percentage, shoot length, root length, seedlings length, and Root-Shoot Ratio were recorded by using three concentrations of licorice root extract (25%, 50% and 75%) and three concentrations of colloidal solutions of ZnNPs (25%, 50% and 75%), while DW was used as control.

2.6. Statistical analysis

The data, in five replicates, has been subjected by its mean to Two-Way analysis of variance (ANOVA) using the SAS program, version 9. The significance of differences has been determined by using Duncan's Multiple Range Test, and the probability less than 0.05 was considered to be statistically significant.

3. Results and Discussion

The UV-Visible spectrum and the optical vision of zinc nanoparticles (ZnNPs) synthesized using the licorice extract were observed in Figure 1. The changing in the solution color from brown to the whitish bright brown (Pale yellow to pale white) recorded a lambda max reached 350 nm with the absorption of 4.200 au compared with the lambda max 350 nm for the extract which appeared because of the organic compounds at the absorption of 3.650 au. The results of the present study agree with results of (Tomaev *et al.*, 2019) who referred to the formation of ZnNPs in the range from 200-400 nm, and agrees with (Rajamanickam *et al.*, 2012) who synthesized polydispersed ZnNPs from Actinomycetes the lambda max reached 310 nm. The change of color is due to the excitement of surface Plasmon vibration in ZnNPs (Owaid *et al.*, 2019). The heating to 80 °C is more suitable than the low temperature for synthesizing ZnNPs from the extract of licorice roots due to increase of activation energy to reduce the organic biomolecules (Burda *et al.*, 2005).

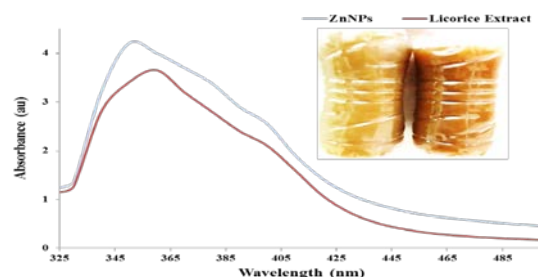


Figure 1. UV-Visible spectra and optical vision of the synthesized ZnNPs and the licorice extract .

Figure 2 exhibited AFM graphs (the three and lateral-dimensional graphs) to screen surface roughness of the licorice-assisted synthesis of ZnNPs at size image 1465.36 nm×1529.26 nm. The surface roughness analysis showed some functional parameters like roughness average of 2.92 nm, reduced core roughness depth of 10.3 nm, summit height of 0.91 nm, and reduced valley depth of 1.91 nm. Hybrid parameters were calculated such as surface area ratio reached 2.84, and mean summit curvature reached -1.0 nm^{-1} .

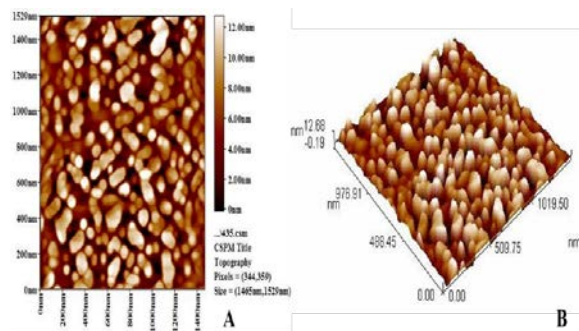
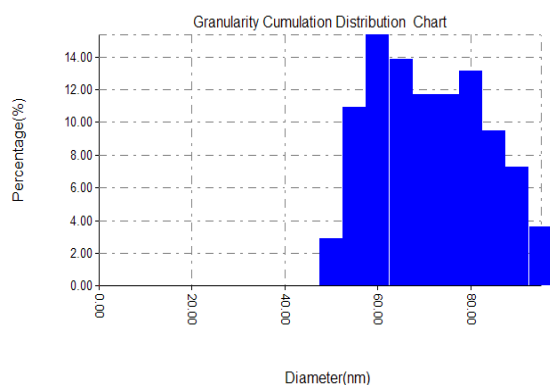


Figure 2. AFM of the biosynthesized ZnNPs, (A) 2D graph, (B) 3D graph

Figure 3 exhibited the histogram of the particle size distribution of the biosynthesized ZnNPs which reached to average 68.69 nm. The volume of ZnNPs of 65.00 nm was $\leq 50\%$ as in the AFM. The lower ZnNPs diameter was 50 nm whereas the higher diameter was 95 nm with volumes 2.92% and 3.65%, respectively. The higher amount was 15.33% for the ZnNPs with a diameter of 60 nm. Granularity Cumulation distribution of ZnNPs also has different accumulation according to their sizes as shown in Figure 3. The ZnNPs of 50 nm have the lowest accumulation of 2.92%, followed 13.87% and 29.20% for ZnNPs with diameters 55.00 and 60.00 nm respectively. The higher accumulation percentage is 100% for ZnNPs of 95.00 nm, followed 96.35% and 89.05% for the sizes 90.00 nm and 85.00 nm respectively.

Figure 3 Granularity Cumulation Distribution chart of ZnNPs



Figures 4A and 4B showed FTIR spectra of the licorice extract and ZnNPs, respectively. These figures showed two bands at 1369 cm^{-1} and 1417 cm^{-1} for the extract and 1375 cm^{-1} and 1421 cm^{-1} for ZnNPs related to symmetric and

asymmetric bending vibration for $-\text{CH}$ group. Absorption bands at 2926 cm^{-1} for the extract and 2894 cm^{-1} and 2938 cm^{-1} for ZnNPs return to symmetric and asymmetric extension vibration for $-\text{CH}$ group which refers to finding compounds of Alkane like $-\text{CH}_3$ (methyl) and $-\text{CH}_2$ (methylene) in monosaccharides, disaccharides, polysaccharides, proteins, amino acids and fatty acids. The presence of an absorption band evidence this at 1027 cm^{-1} for the extract and 1045 cm^{-1} for ZnNPs related to the single bond of C-C. The chemical composition of licorice may contain the protein, carbohydrates and fatty acids, and that agreed with the results of (Badr *et al.*, 2013).

Also, the spectra exhibited absorption bands at 1514 cm^{-1} for the extract, and at 1516 cm^{-1} for ZnNPs belong to extension vibration of C=C group for successive double bonds in the ring of aromatic compounds. On the other hand, the spectra exhibited absorption peaks at 3278 cm^{-1} for the extract and at 3277 cm^{-1} for ZnNPs return to the hydroxyl group ($-\text{OH}$) in amino acids and proteins (Silverstein *et al.*, 2005). Indications of the presence of fatty acids, amino acids and proteins are the presence of extension vibration of the broad absorption bands ranged from 2840 cm^{-1} to 3550 cm^{-1} for the extract and ranged from $2500\text{-}3500 \text{ cm}^{-1}$ for ZnNPs which belong to the hydrogen bonding of the hydroxyl (O-H) in the carboxyl group ($-\text{COOH}$). In addition, the absorption band due to the bending vibration of the hydroxyl group ($-\text{OH}$) and the band located at 1199 cm^{-1} for the extract due to the extension vibration of C-O group (Silverstein *et al.*, 2005; Mistry, 2009). The presence of carbonyl group (C=O) in extension vibration at 1591 cm^{-1} for the extract and at 1597 cm^{-1} for ZnNPs and band of bending vibration at 831 cm^{-1} for the extract and the clear vibration at 866 cm^{-1} may belong to hydroxyl group in carboxylic acids (Hayashi and Sudo, 2009), and flavonoids (Kondo *et al.*, 2007). The sharp absorption band in Figure 4B at 1045 cm^{-1} , two bands at 1375 cm^{-1} and 1421 cm^{-1} are clear evidence for the presence ZnNPs in the sample.

The FTIR spectrum of the extract contains the ZnNPs; Figure 4B is similar in the sites of the functional groups. Also, ZnNPs are expected to have a large surface area that allows all atoms with high electronegativity which contains pairs of non-co-electrons like oxygen and nitrogen to contribute them well. For example, the oxygen atom in the composition of monosaccharides, oligosaccharides and polysaccharides in the form of $-\text{OH}$ and in flavonoids in the form of ether ($-\text{O}-$) or in the form of carbonyl (C=O) and in the form of ($-\text{COOH}$). In amino acids, proteins and phenols are present in the form of ($-\text{OH}$); thus, the bond may be as follows: (Zn-O-R) where R is sugar, amino acids, or flavonoid. Another example of high electronegativity atoms is the nitrogen atom (N) in the amino acid composition ($-\text{NH}_2$) or ($=\text{NH}$) as in peptides. In protein, composition is in the form of ($-\text{NH}_2$); thus, it is likely that the bond may be as follows: (Zn-N-R) where R is an amino acid or protein. Finally, these organic compounds of the licorice extract reduced Zn ions to Zn atoms and covered them.

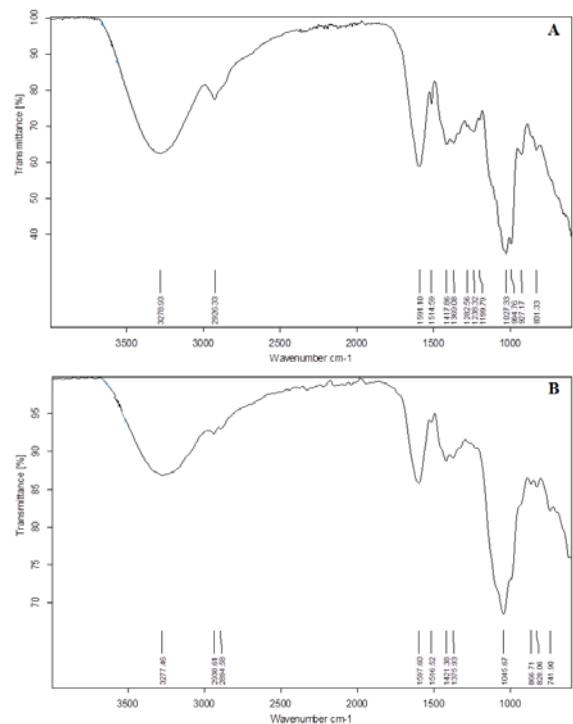


Figure 4 FTIR spectra of the licorice extract (A) and ZnNPs (B)

The germination percentage, shoot length, root length, seedlings length, and Root- Shoot Ratio of *Sorghum bicolor* seeds (Enkath and Rabeh varieties) were achieved *in vitro* for determination the influence of the licorice extract and the biosynthesized ZnNPs from licorice on the growth of *S. bicolor* seeds as in Table 1 and Figures 5 and 6. The germination percentage of Enkath seeds recorded germination percentage of 100%, while Rabeh showed 85% and 96% for the concentrations of extracts 25% and 50% respectively. The extract of 100%, and all concentrations of ZnNPs showed a percentage of seeds germination reached 100% as seen in Figure 5.

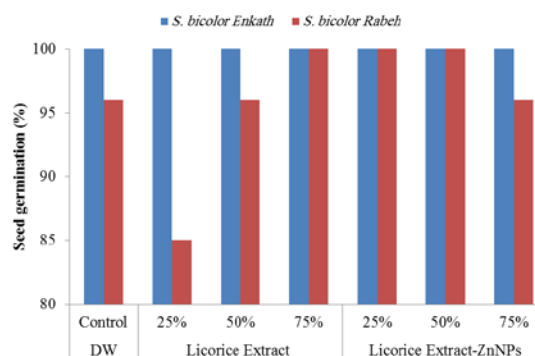


Figure 5 Percentages of Germination of *Sorghum bicolor* seeds

Rabeh variety significantly ($p<0.05$) recorded a high root length of 10.80 mm by using the extract of 50% compared to DW (Control) (9.06 mm), as shown in Table 1 and Figure 6. While the concentrations of 50% and 75% of ZnNPs led to root lengths reaching 3.14 mm and 5.10 mm respectively. Enkath showed a root length of 10.32 mm on DW followed by the extract of 25% (9.82 mm), while the shorter root was 5.18 mm on the 75% ZnNPs. Generally, shoot length was 5.43 mm by the extract of 50% while the ZnNPs (50%) decreased shoot length to 3.86 mm compared to 4.14 mm by DW. Rabeh recorded a more significant shoot length of 6.32 mm by the extract of 50% significantly ($p<0.05$) compared with 4.58 mm by DW, while the ZnNPs of 25% led to a shoot length of 3.74 mm.

In general, ZnNPs led to a decrease in the seedling length and root-shoot ratio of *Sorghum bicolor* plant *in vitro* compared with the licorice extract alone as in Figure 6. *Sorghum bicolor* Rabeh showed the best seedlings length in comparison with *S. bicolor* Enkath. Seedlings length of *S. bicolor* Rabeh has a more significant value 17.12 mm by the extract of 50% compared with 13.64 mm by DW, whereas the ZnNPs of 75% decreased the length of seedlings to 7.74 mm. *S. bicolor* Enkath recorded bigger seedlings length of 14.34 mm by the extract of 25% compared to 14.02 mm by DW, whereas ZnNPs of 50% decreased the length of seedlings to 9.62 mm. Generally, the Root-shoot ratio was 0.88 by ZnNPs (75%) but reached 2.03 by the extract (25%) as in Table 1. Hence, Figure 6 showed the increase in hairy roots in the higher concentrations of ZnNPs compared with the case of using licorice extract alone because of the increase of absorption mechanism in the hairy roots (Ghodake *et al.*, 2010).

Table 1 Properties of *Sorghum bicolor* seeds growth *in vitro*

Features	Germination of seeds (%)			root length (mm)			shoot length (mm)			seedlings length (mm)			Root- Shoot Ratio		
	Enkath	Rabeh	Mean	Enkath	Rabeh	Mean	Enkath	Rabeh	Mean	Enkath	Rabeh	Mean	Enkath	Rabeh	Mean
DW 1	100a	96b	98b	10.32a	9.06b	9.69a	3.70d	4.58c	4.14cd	14.02b	13.64b	13.83b	2.90a	2.00bcd	2.45a
E25%2	100a	85c	92.5c	9.82ab	9.02b	9.42a	4.52c	4.96cb	4.74b	14.34b	13.98b	14.16b	2.20bc	1.86cd	2.03b
E50%3	100a	96b	98b	9.00b	10.80a	9.90a	4.54c	6.32a	5.43a	13.54b	17.12a	15.33a	2.02bcd	1.74cd	1.88b
E75%4	100a	100a	100a	6.76dc	7.52c	7.14b	3.66d	4.62c	4.14cd	10.42de	12.14c	11.28c	1.86cd	1.64d	1.75bc
N25%5	100a	100a	100a	6.02de	7.10dc	6.56bc	5.42b	3.74d	4.58bc	11.44cd	10.84de	11.14c	1.12e	1.94bed	1.53c
N50%6	100a	100a	100a	6.74dc	5.10e	5.92c	2.88e	4.84bc	3.86d	9.62e	9.94e	9.78d	2.40b	1.04e	1.72bc
N75%7	100a	96b	98b	5.18e	3.14f	4.16d	4.76bc	4.60c	4.68bc	9.94e	7.74f	8.84e	1.08e	0.68e	0.88d
Means	100A	96.1B	98.07±0	7.69A	7.39A	7.54±0.81	4.21B	4.80A	4.51±0.56	11.90A	12.20A	12.05±0.89	1.94A	1.55B	1.74±0.35

Legend: Mean ±MSE (Mean Standard Error). The different small letters (a, b, c, etc.) show significant values ($p<0.05$) among each column, while the capital letters (A, B) exhibit a significant value ($p<0.05$) between means of Rabeh and Enkath in the row for each feature.

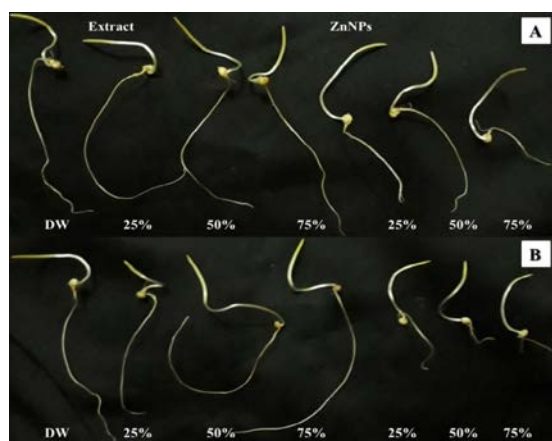


Figure 6. Planting *Sorghum bicolor* seeds (A) Enkath and (B) Rabeh *in vitro*

Table 2 exhibited significant ($p < 0.01$) negative correlation (-0.846) between shoot length and seedling length, while the positive correlation (0.312) was recorded between root length and germination of *Sorghum bicolor* seeds. The higher results of the indexes of seedlings in sorghum in the case using licorice extract possibly return to the significant bioactivity of licorice related with glycyrrhizin (Fenwick *et al.*, 1990; Karkanis *et al.*, 2018). The results of the current study agree with the results of recent works (Burman *et al.*, 2013; Raskar and Laware, 2014; Zafar *et al.*, 2016; Raigond *et al.*, 2017).

The lower concentrations of zinc oxide nanoparticles (ZnONPs) increased Seed germination of onion (Raskar and Laware, 2014). The variety of Enkath was best than Rabeh in some features that related to genotypic characteristics of Enkath variety and agreed with leaf area less than Rabeh but with high weight (Wuhaib *et al.*, 2017). The lower concentrations of ZnNPs exhibited a significant increase in seed germination features of *Macrotyloma uniflorum* compared with the higher concentration (Gokak and Taranath, 2015). Also, ZnNPs had adverse effects on the indexes of seedlings in wheat (Taran *et al.*, 2017). The lower results of seedling in sorghum in the case of using ZnNPs may be related to ZnONPs exerting adverse effects on length of root (Burman *et al.*, 2013). The sorter seedling may have higher biomass in order to the harmful effects of ZnNPs in comparison with the extract alone in the high concentration (Burman *et al.*, 2013). In the case of use of ZnNPs, the higher activity of antioxidative enzymes stabilized the content of photosynthetic pigments and increased relative water content in leaves (Taran *et al.*, 2017).

Table 2 Correlation of properties of *Sorghum bicolor* Planting

	Root length	Shoot length	Root- Shoot Ratio	Seedlings length	Germination of seeds
Root length	1.000				
Shoot length	0.000	1.000			
Root- Shoot Ratio	0.000	0.000	1.000		
Seedlings length	-0.066	-0.846**	-0.062	1.000	
Germination of seeds	0.312	-0.074	0.005	0.084	1.000

4. Conclusion

This work aims to biosynthesize zinc nanoparticles (ZnNPs) from licorice (*Glycyrrhiza glabra*) root extract and to apply that on seeds germination of two *Sorghum bicolor* varieties, (Enkath and Rabeh). The AFM of the biosynthesized ZnNPs reached an average of 68.69 nm. The FTIR confirmed finding -CH group which refers to finding compounds -CH₃ and -CH₂ in monosaccharides, disaccharides, polysaccharides and mono acidic saccharides. The exposure to ZnNPs showed remarkable effects on seed germination and other growth parameters of sorghum seedlings. The low concentration of 25% of ZnNPs exhibited the best shoot length compared with the high concentrations (50% and 75%). The two concentrations of 50% and 75% exhibited the presence of hairy roots in order to the smallness of roots. Thus, the low concentration (25%) of ZnNPs can be used as a material for *S. bicolor* seed priming in the field with low toxicity on this plant. The results of this work are essential to determine the compatibility of ZnNPs in agricultural applications in cereals enhancement and food production.

Acknowledgment

The authors thank the Department of Yellow and White Maize Research, General Authority for Agricultural Research in the Iraqi Ministry of Agriculture for obtaining sorghum seeds. The authors also thank the Department of Biology in College of Education for Pure Sciences, University of Anbar in Iraq for helping complete this work. Special thanks are due to Dr. Abdullah Khashaf for achieving FTIR spectra from Department of Chemistry. Thanks also go to Dr. Prof. Abdulkareem Al-Sammarraie for completing AFM analyses.

Conflict of Interest

None

References

- Al-Ani BM, Owaid MN, Al-Saeedi SSS. 2018. Fungal interaction between *Trichoderma* spp . and *Pleurotus ostreatus* on the enriched solid media with licorice *Glycyrrhiza glabra* root extract. *Acta Ecologica Sinica*, **38** (3): 268–273.
- Al-Bahrani RM, Muayad S, Majeed A, Owaid MN. 2018. Phyto-fabrication, characteristics and anti-candidal effects of silver nanoparticles from leaves of *Ziziphus mauritiana* Lam. *Acta Pharmaceutica Scientia*, **56** (3): 85–92.
- Awika JM, Rooney LW. 2004. Sorghum Phytochemicals and Their Potential Impact on Human Health. *Phytochemistry*, **65** : 1199–1221.
- Badr SE, Sakr DM, Mahfouz SA, Abdelfattah MS. 2013. Licorice (*Glycyrrhiza glabra* L.): Chemical Composition and Biological Impacts. *Research Journal of Pharmaceutical, Biological and Chemical Sciences*, **4** (3): 606–621.
- Burda C, Chen X, Narayanan R, El-Sayed MA. 2005. Chemistry and properties of nanocrystals of different shapes. *Chemical Rev.*, **105** : 1025–1102.

- Burman U, Saini M, Kumar P-. 2013. Effect of zinc oxide nanoparticles on growth and antioxidant system of chickpea seedlings. *Toxicological & Environmental Chemistry*, **95** (4): 605–612.
- Dehkourdi E, Mosavi M. 2013. Effect of anatase nanoparticles (TiO₂) on parsley seed germination (*Petroselinum crispum*) In Vitro. *Biological Trace Element Research*, **155** : 283–286.
- Dong S, Inoue A, Zhu Y, Tanji M, Kiyama R. 2007. Activation of rapid signaling pathways and the subsequent transcriptional regulation for the proliferation of breast cancer MCF-7 cells by the treatment with an extract of *Glycyrrhiza glabra* root. *Food Chem. Toxicol.*, **45** : 2470–2478.
- FAO. 2009. Food and Agricultural Organization
- Fenwick GR, Lutomski J, Nieman C. 1990. Liquorice, *Glycyrrhiza glabra* L.–Composition, uses and analysis. *Food Chemistry*, **38** (2): 119–143.
- Ghafari H, Razmjoo J. 2013. Effect of foliar application of nano-iron oxidase, iron chelate and iron sulphate rates on yield and quality of wheat. *International Journal of Agronomy and Plant Production*, **4** (11): 2997–3003.
- Ghodake G, Seo YD, Park D, Lee S. 2010. Phytotoxicity of carbon nanotubes assessed by *Brassica juncea* and *Phaseolus mungo*. *J Nanoelectronics and Optoelectronics*, **5** : 157–160.
- Gokak IB, Taranath TC. 2015. Seed germination and growth responses of *Macrotyloma uniflorum* (Lam.) Verdc. exposed to Zinc and Zinc nanoparticles. *International Journal of Environmental Sciences*, **5** (4): 840–847.
- Hayashi H, Sudo H. 2009. Economic importance of licorice. *Plant Biotechnol.*, **26** : 101–104.
- IndexMundi. 2018. Iraq Sorghum Production by Year.
- Karkanis A, Martins N, Petropoulos SA, Ferreira ICFR. 2018. Phytochemical composition, health effects, and crop management of liquorice (*Glycyrrhiza glabra* L.): A medicinal plant. *Food Reviews International*, **34** (2): 182–203.
- Kondo K, Shiba M, Nakamura R, Morota T, Shoyama Y. 2007. Constituent properties of licorices derived from *Glycyrrhiza uralensis*, *G. glabra*, or *G. inflata* identified by genetic information. *Biol. Pharm. Bull.*, **30** : 1271–1277.
- Li G, Nikolic D, Van Breemen RB. 2016. Identification and Chemical Standardization of Licorice Raw Materials and Dietary Supplements Using UHPLC-MS/MS. *Journal of Agricultural and Food Chemistry*, **64** : 8062–8070.
- Malakouti MJ. 2008. The effect of micronutrients in ensuring efficient use of macronutrients. *Turkish Journal of Agriculture and Forestry*, **32** (3): 215–220.
- Mistry BD. 2009. *A Handbook of Spectroscopic Data CHEMISTRY (UV, JR, PMR, JJCNR and Mass Spectroscopy)*. Oxford Book Company.
- Mostafa DM, Abd El-Alim SH, Kassem AA. 2017. *Nanoemulsions: A New Approach for Enhancing Phytonutrient Efficacy*. Elsevier Inc.
- Mutisya J, Sun C, Rosenquist S, Baguma Y, Jansson C. 2009. Diurnal Oscillation of SBE Expression in Sorghum Endosperm. *Journal of Plant Physiology*, **166** : 428–434.
- Nomura T, Fukai T, Akiyama T. 2002. Chemistry of phenolic compounds of licorice (*Glycyrrhiza* species) and their estrogenic and cytotoxic activities. *Pure Appl. Chem.*, **74** : 1199–1206.
- Owaid MN, Ibraheem IJ. 2017. Mycosynthesis of nanoparticles using edible and medicinal mushrooms. *European Journal of Nanomedicine*, **9** (1): 5–23.
- Owaid MN, Raman J, Lakshmanan H, Al-Saeedi SSS, Sabaratnam V, Ali IA. 2015. Mycosynthesis of silver nanoparticles by *Pleurotus cornucopiae* var. *citrinopileatus* and its inhibitory effects against *Candida* sp. *Materials Letters*, **153** : 186–190.
- Owaid MN, Al-Saeedi SSS, Abed IA. 2017. Biosynthesis of gold nanoparticles using yellow oyster mushroom *Pleurotus cornucopiae* var. *citrinopileatus*. *Environmental Nanotechnology, Monitoring and Management*, **8** : 157–162.
- Owaid MN, Muslim RF, Hamad HA. 2018. Mycosynthesis of Silver Nanoparticles using *Terminia* sp. Desert Truffle, Pezizaceae, and their Antibacterial Activity. *Jordan Journal of Biological Sciences*, **11** (4): 401–405.
- Owaid MN, Zaidan TA, Muslim RF. 2019. Biosynthesis, Characterization and Cytotoxicity of Zinc Nanoparticles Using *Panax ginseng* Roots, Araliaceae. *Acta Pharmaceutica Scientia*, **57** (1): 19–32.
- Queiroz VAV, Moraes EA, Schaffert RE, Moreira AV, Ribeiro SMR, Martino HSD. 2011. Potencial funcional e tecnologia de processamento do sorgo (*Sorghum bicolor* (L.) Moench), na alimentação humana. *Revista Brasileira de Milho e Sorgo*, **10** (3): 180–195.
- Raigond P, Raigond B, Kaundal B, Singh B, Joshi A, Dutt S. 2017. Effect of zinc nanoparticles on antioxidative system of potato plants. *Journal of Environmental Biology*, **38** : 435–439.
- Rajamanickam U, Viswanathan S, Muthusamy P. 2012. Biosynthesis of Zinc Nanoparticles Using Actinomycetes for Antibacterial Food Packaging. In *International Conference on Nutrition and Food Sciences IPCBEE IACSIT Press*: Singapore; 195–199.
- Raskar S V., Laware SL. 2014. Effect of zinc oxide nanoparticles on cytology and seed germination in onion. *International Journal of Current Microbiology and Applied Sciences*, **3** (2): 467–473.
- Reddy PS, Patil JV. 2015. *Genetic Enhancement of Rabi Sorghum*. Nikki Levy, Chennai.
- Renjie L. 2008. Orthogonal test design for optimization of the extraction of polysaccharides from *Phascolosoma esulenta* and evaluation of its immunity activity. *Carbohydr. Polym.*, **73** : 558–563.
- Sahrawat KL, Wani SP, Rego TJ, Pardhasaradhi G, Murthy KVS. 2007. Widespread deficiencies of sulphur, boron and zinc in dryland soils of the Indian semi-arid tropics. *Current Science*, **93** (10): 1428–1432.
- Silverstein R, Webster F, Kiemle D. 2005. *Spectrometric identification of organic compounds*. John Wiley and sons, Inc.: London, UK.
- Soomro AA, Shaikh TA, Chand L, Solangi M, Laghari GM. 2015. Comparative study on spent wash and water seed priming on germination and early growth traits of sorghum (*Sorghum bicolor* L.). *Sci. Int. (Lahore)*, **27** (5): 4409–4412.
- Souza AP, Cocuron JC, Garcia AC, Alonso AP, Buckeridge MS. 2015. Changes in Whole-Plant Metabolism during Grain-Filling Stage in *Sorghum bicolor* L. (Moench) Grown under Elevated CO₂ and Drought. *Plant Physiology*, **169** : 1755–1765.
- Taran N, Storozhenko V, Sviatlova N, Batsmanova L, Shvartau V, Kovalenko M. 2017. Effect of Zinc and Copper Nanoparticles on Drought Resistance of Wheat Seedlings. *Nanoscale Research Letters*, **12** : 60.
- Tomaev V V., Polishchuk VA, Vartanyan TA, Vasil'ev EA. 2019. Surface Plasmon Resonance in Zinc Nanoparticles. *Glass Physics and Chemistry*, **45** (3): 238–241.
- Tuomisto HL, Scheelbeek PFD, Chalabi Z, Green R, Smith RD, Haines A, Dangour AD. 2017. Effects of environmental change on population nutrition and health: A comprehensive framework with a focus on fruits and vegetables. *Wellcome open research*, **2** : 21.

U.S. Environmental Protection Agency (USEPA). 1996. Ecological effects test guidelines: Seed germination/root elongation toxicity test., OPPTS 850, 4200, EPA 712-C-96-154, Washington DC.

Welch RM. 2002. The impact of mineral nutrients in food crops on global human health. *Plant and Soil*, **247** (1): 83–90.

Wuhaib KM, Hadi BH, Hassan WA. 2017. Estimation of genetic parameters in sorghum under the effect of populations and planting seasons. *The Iraqi Journal of Agricultural Sciences*, **48** (2): 551–562.

Zafar H, Ali A, Ali JS, Haq IU, Zia M. 2016. Effect of ZnO Nanoparticles on Brassica nigra Seedlings and Stem Explants: Growth Dynamics and Antioxidative Response. *Frontiers in Plant Science*, **7** : 535.

Zore GB, Winston UB, Surwase BS, Meshram NS, Sangle VD, Kulkarni SS, Mohan Karuppaiyl S. 2008. Chemoprofile and bioactivities of Taverniera cuneifolia (Roth) Arn.: a wild relative and possible substitute of Glycyrrhiza glabra L. *Phytomedicine*, **15** : 292–300.

Assessment of Antimicrobial and Anticancer Activity of Radish Sprouts Extracts

Mahmoud Khalid¹, Reem Ayayda¹, Nameer Gheith¹, Zaidoun Salah¹, Saleh Abu-Lafi², Amal Jaber¹, Fuad Al-Rimawi³ and Ghassab Al-Mazaideh^{4,5,*}

¹Al Quds-Bard College, Al-Quds University, Abu Dies, Jerusalem, Palestine; ²Faculty of Pharmacy, Al-Quds University, P.O. Box 20002, Jerusalem, Palestine; ³Chemistry Department, Faculty of Science and Technology, Al-Quds University, P.O. Box 20002, Jerusalem, Palestine; ⁴Department of Pharmaceutical Chemistry, College of Pharmacy, University of Hafr Al-Batin, Hafr Al-Batin, Saudi Arabia; ⁵Department of Chemistry and Chemical Technology, Faculty of Science, Tafila Technical University, P.O. Box 179, Tafila 66110, Jordan;

Received: December 31, 2019; Revised: January 29, 2020; Accepted: February 8, 2020

Abstract

People have used plants as medications since the beginning of history. With the advancement in science, people headed more towards using synthetic drugs. However, with the rise of problems like the toxic side effects of these drugs as in the case of chemotherapy, and the origin of drug resistant bacteria, the need has come for developing new drugs. The safest source of developing new drugs is natural products from plants. In this study, antimicrobial and anticancer activity of radish sprouts extracts was tested. Radish seeds were planted and watered until they sprouted. Sprouts were then dried and grinded. Radish sprouts were soaked in three different solvents, (100% water, 100% ethanol, and 80% ethanol) for three hours with sonication, and then solvents were evaporated using rotary evaporator at 40 C°. Radish sprouts extracts were then tested for anticancer activity against MCF7 and HT29 cancer cells. Their antimicrobial activity for different types of positive and negative gram bacteria (*E. coli*, *S. pneumonia*, and *S. aureus*) was also tested using disk-diffusion method. Results showed that radish sprouts have anticancer activity against HT29 and MCF7. The most drastic effect was observed for radish sprouts extracted with 100% ethanol against MCF7 cells where 62% of cells were found dead compared to the control. No antimicrobial activity was observed for the radish sprouts extracts.

Keywords: Anticancer activity, Antimicrobial activity, Radish Sprouts

1. Introduction

Using plants as medicine has been known since ancient ages. Recently, there has been an increased interest in finding therapy for many diseases using natural products; especially the ones derived from plants. Medicinal activities of plants come from their secondary metabolites which include tannins, terpenoids, coumarins, alkaloids and flavonoids (Khamees, 2017). These secondary metabolites could be specifically useful for antimicrobial and antioxidant activity. In recent years, research has been focusing on sprouts and their therapeutic benefits. Sprouts have high nutritional value, and many possible health benefits. For example, mung beans sprouts are used especially in East Asian countries like China, since they have been known for their detoxification activities and are widely used to refresh mentality, ease heat stroke, and reduce swelling in the summer. They also regulate gastrointestinal upset and lipid metabolism (Tang *et al.*, 2014). Also, broccoli sprouts have shown chemoprotective effects, and they can reduce cholesterol or lipid levels. They also have a powerful preventative effect against *Helicobacter pylori* infections. In addition, broccoli

sprouts can possibly improve insulin resistance in type II diabetes (Paško *et al.*, 2018).

Radish is a member of the cruciferous family. Nutritional value of radish sprouts is attributed to the presence of many essential minerals and vitamins, carbohydrates, high content of fiber, and low content of fat. Radish is typically used in traditional medicine as a treatment for many infectious diseases. This made studying its antimicrobial activity of great interest to researchers (Jerjes *et al.*, 2016). Researchers who studied radish sprouts have found that they contain alkaloids, flavonoids, saponins, anthraquinones, tannins, steroids, and terpenoids (Angel *et al.*, 2019). This gave them strong antioxidant ability, as these compounds can act as radical scavengers for free radicals, which can sometimes cause cancer. It was also found that radish seeds have important antimicrobial activity against most of the tested microorganisms, most importantly *E. coli*, *S.aureas* and *P.aerugenosa*, with high zone of inhibition (Khamees, 2017).

Most of medicinal benefits of plants are a result of their production of secondary metabolites. Secondary metabolites are chemicals that are not required for the immediate survival of the plant, but they allow the plant to cope with its environment. For example, they are produced

* Corresponding author e-mail: gmazideh@ttu.edu.jo.

* **List of abbreviations:** MCF7: breast cancer cell line isolated in 1970 from a 69-year-old Caucasian woman. MCF-7 is the acronym of Michigan Cancer Foundation-7. HT29: human colon cancer cell line used extensively in biological and cancer research. PDA: Photodiode Array detector. MIC: Minimum Inhibitory Concentration. DMSO: Dimethyl sulfoxide

in response to pathogen attacks, herbivore induced damage, or nutrient deficiency. Secondary metabolites can be unique to specific species or genera, depending on the environment in which the plant grows and the environmental challenges it faces (Kennedy and Emma, 2011). Secondary metabolites are usually classified based on their biosynthetic pathways into alkaloids, terpenoids, and phenolics (Tiwari and Rana, 2015). Phenolics are widely spread in plants and include flavonoids, tannins, coumarins, quinones and anthocyanins (Shaik *et al.*, 2011).

An antioxidant is a molecule that is capable of neutralizing a free radical by donating an electron to it, which reduces the free radical capacity to damage. Free radicals can be Oxygen derived (ROS) or Nitrogen derived (RNS). Free radicals are normally produced as a result of normal cellular metabolism such as respiratory chain reactions in the mitochondria (Birben *et al.*, 2012). When ROS concentrations are at high level, oxidative stress is generated, which can result in damage to cell structures. Oxidative stress is a major cause of the development of chronic and degenerative diseases such as cancer, arthritis, aging, autoimmune disorders, cardiovascular and neurodegenerative diseases. Antioxidants production is one of the mechanisms that the body uses in order to counteract oxidative stress. Antioxidants are either naturally produced inside the body or provided externally through foods or supplements. Antioxidants support immune defenses and decrease the risk of cancer and degenerative diseases by acting as “free radical scavengers” that can prevent and repair damages caused by free radicals (Pham-Huy *et al.*, 2008).

Cancer is a widespread disease that causes the death of thousands of people every year. Unfortunately, there is no ultimate cure to treat cancer so far. One of the most used treatments is chemotherapy, where chemical anticancer drugs are used to target dividing cells. However, chemotherapy cannot differentiate between cancer cells and normal cells. This creates serious side effects for patients receiving this treatment. These side effects include fatigue, hair loss, easy bruising and bleeding, anemia, appetite changes, nausea and vomiting, and much more. That is why there has been increasing research trying to find a natural alternative to chemotherapy (Vichaya *et al.*, 2015).

Antibiotic resistance is currently another serious problem. Many types of bacteria, whether they were gram negative or gram positive, are now developing resistance to the known and commonly used antibiotics and can grow despite the presence of the drug. This might cause the spreading of dangerous diseases without any possible cure. Thus, new natural antibiotics need to be developed (Zaman *et al.*, 2017).

Plants have been used in therapy since ancient ages, and they can be the solution to all previously mentioned problems by using the different anticancer and antimicrobial products found naturally in plants. Many plants are known to exhibit antioxidant activity, and consuming them reduces the risk of free radicals. Also, plants that possess anticancer activity can be a safer replacement for chemotherapy with fewer side effects (Khamees, 2017; Tang *et al.*, 2014). As for antimicrobial resistance, many plants have antibacterial activity and can be used in the synthesis of new antibiotics (Zaman *et al.*, 2017). In this study, anticancer activity for radish sprouts

extract on colon cancer and breast cancer cell line will be tested; in addition, their antimicrobial activity will be tested on some types of both positive and negative grams bacteria.

2. Materials and Methods

2.1. Study design:

Radish seeds were sprouted for 3-4 weeks, then sprouts were collected, dried in shade, and extracted with water/methanol solvent, then the crude extract was obtained after evaporation of the solvent. The crude extract was then analyzed by HPLC and then its activity against bacteria and cancer was tested.

2.2. Sprouting

Radish seeds were purchased from the local market. The seeds were planted on cotton soaked with water and were put in an area with access to sun and air. Seeds were watered every two days until they became sprouts (around 5 cm tall), Figure 1. This process took approximately 3-4 weeks. After that, sprouts were collected and dried in the shade, since UV light from the sun can lead to the loss of active compounds that are present in sprouts.

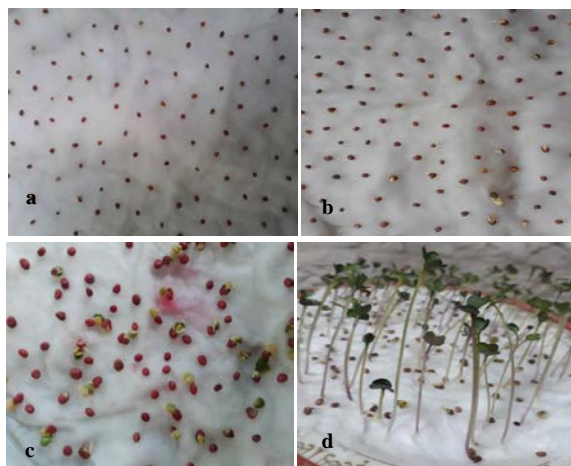


Figure 1. Sprouting process. (a) radish seeds- day 1. (b) radish seeds- day 3. (c) radish seeds- day 7. (d) radish sprouts ready to be collected- day 25.

2.3. Extraction

The dried sprouts were grinded and turned into powder. Five grams of the dried sprouts powder was added separately to 50 ml of three extraction solvents which are 100% water, 80% ethanol, and 100% ethanol. These solvents were then put in a water bath at 37 °C and waited for three hours with sonication. The extracts were then filtered. The filtrate was evaporated using rotary evaporator at 40 °C and reduced pressure. The resulting crude extract viscous extracts were stored at 4 °C.

2.4. HPLC conditions

The HPLC analysis of the extracts was run on ODS column of Waters (XBridge, 4.6 ID x 150 mm, 5 μm). The mobile phase used is a mixture of acetic acid in water (0.5%) (solvent A) and acetonitrile (solvent B) run in a linear gradient mode. 100% (solvent A) descended to 70% (solvent A) in 40 minutes, then to 40% (solvent A) in 20 minutes and finally to 10% (solvent A) in 2 minutes and stayed there for 6 minutes and then back to the initial

conditions in 2 minutes. The HPLC system was equilibrated for 7 minutes with the initial acidic water mobile phase (solvent A) before injecting the next sample. All the samples were filtered with a 0.45 μm PTFE filter. The PDA wavelengths range was from 210-500 nm. The flow rate was 1 ml/min. Injection volume was 20 μl and the column temperature were set at 25°C.

2.5. Antimicrobial Activity Testing

In order to test the antimicrobial activity of radish sprouts extracts, disk diffusion method was used. *E. coli*, a gram negative bacteria and *S. pneumonia* and *S. aureus*, which are gram positive bacteria were streaked on Mueller-Hinton agar plates using cotton swaps. After that, sterilized blank disks were dipped in the crude extracts for five minutes, and were then put on the plates using aseptic techniques. Also, antibiotic disks of novobiocin, penicillin, gentamycin, cefepime, and aztreonam were placed on the plates in order to compare the zone of inhibition of these antibiotics and the different sprouts extracts. Plates were then incubated for 24h at 37 °C before measuring the zone of inhibition (MIC) on these plates.

2.6. Anticancer Activity Testing

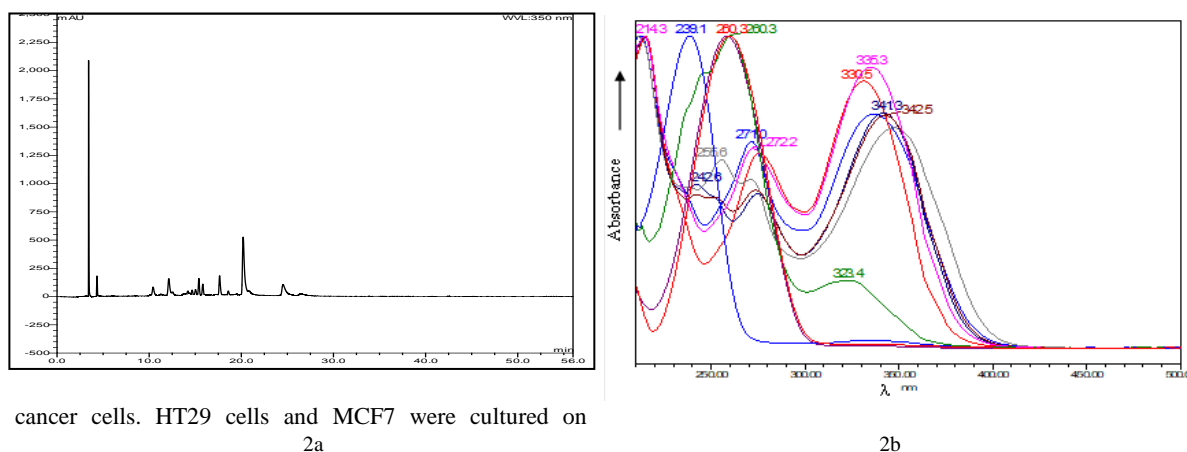
Radish sprouts extracts were tested for anticancer activity on HT29 colon cancer cells, and MCF7 breast

RPMI media and incubated for 24h before treatment with radish sprouts extracts. After that, 100 μl of the radish sprouts extracts were diluted with DMSO and added separately in four different concentrations 50 $\mu\text{g/ml}$, 100 $\mu\text{g/ml}$, 300 $\mu\text{g/ml}$, 500 $\mu\text{g/ml}$ and 1000 $\mu\text{g/ml}$. Cells were then incubated for 24h, and 48h after treatment.

3. Results and Discussion

3.1. HPLC-PDA profiles of the extracts

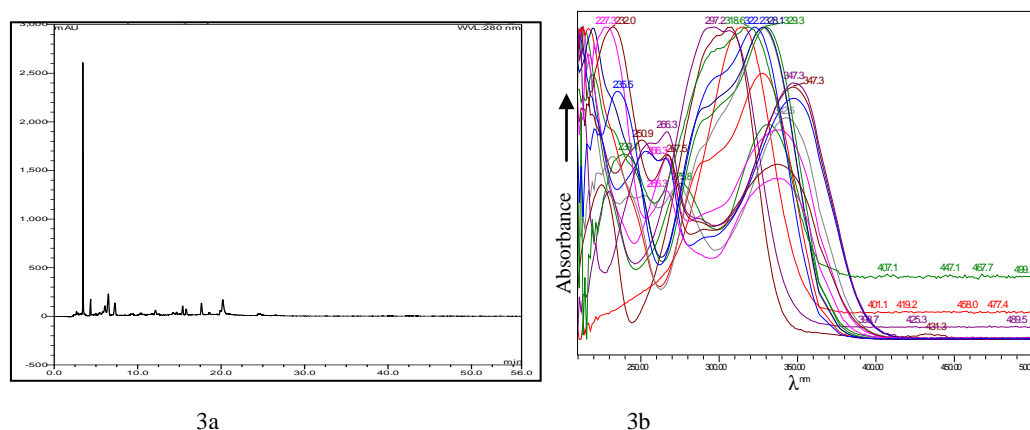
HPLC chromatogram at 350nm and 280nm of crude radish extracts was analyzed; it indicated the presence of polar and non-polar phenolic compounds. Crude radish extracts spectrum showed a maximum absorption at 350nm for the major seven peaks. The eluted compounds were detected in the range of 9-26 minutes; indicating polar and non-polar combination (Fig 2a). At 280nm, new peaks eluted at 5-7 minutes appeared, indicating the presence of polar compounds (Fig 3a). The UV-Vis ranges of these compounds were applied in the range of 220-360nm indicating flavonoids and phenolic compounds abundance (Al-Rimawi *et al.*, 2017; Al-Zereini *et al.*, 2018; Al-Rimawi *et al.*, 2018) (Fig 2b, 3b). Radish sprouts contain polar and non-polar compounds that could possibly possess antimicrobial and anticancer activity.



cancer cells. HT29 cells and MCF7 were cultured on
2a

2b

Figure 2. HPLC-PDA chromatogram of radish sprouts extracts at 350 nm (2a), and overlaid UV-Vis spectra at 350nm (2b).



In order to test the antimicrobial activity of radish sprouts extracts, disk diffusion method was used. Radish sprouts extracts illustrated no antimicrobial activity for any of the tested bacteria. *S. pneumonia* exhibited no zone of inhibition of any of the tested antibiotics, nor for radish extracts. *S. aureus* also demonstrated no zone of inhibition for any of the tested antibiotics and for radish extracts as well. *E. coli* showed a zone of inhibition for the antibiotics aztreonam and cefepime, but not for novobiocin; however, no zone of inhibition was detected for radish extracts. This indicates that radish sprouts extracts have no antimicrobial activity for any of the tested bacteria. This could possibly be due to the extraction method. Other extraction methods of radish sprouts could give antimicrobial activities as previous studies found that red and white radish seeds have antimicrobial activity against *E. coli*, *S. aureus* with a zone of inhibition ranging between 18mm and 34.2mm (Khamees, 2017).

3.3. Anticancer activity

Anticancer activity of radish sprouts extracts was assessed for HT29 colon cancer cells and MCF7 breast cancer cells. Radish sprouts exhibited anticancer activity against HT29 and MCF7 cells at the higher extract's concentrations. For HT29 cells, radish sprouts extract after 24h showed no effect at 100 µg/ml for any of the solvents (Fig 4d, 4g, 4j). Radish extracted with water demonstrated a change in cell morphology and cell number as there were some few dead cells at 500 µg, and 1000 µg (Fig 4e, 4f). Ethanol 100% extracts at 1000 µg resulted in change in cell morphology, and lowering the density of cells with the presence of few dead cells (Fig 4i). Radish extracts with 80% ethanol resulted in lowering the cells density at 500 µg/ml (Fig 4k), cell density was even lower at 1000 µg with the presence of few dead cells (Fig 4). Radish sprouts exhibit an anticancer activity for HT29 colon cancer cells

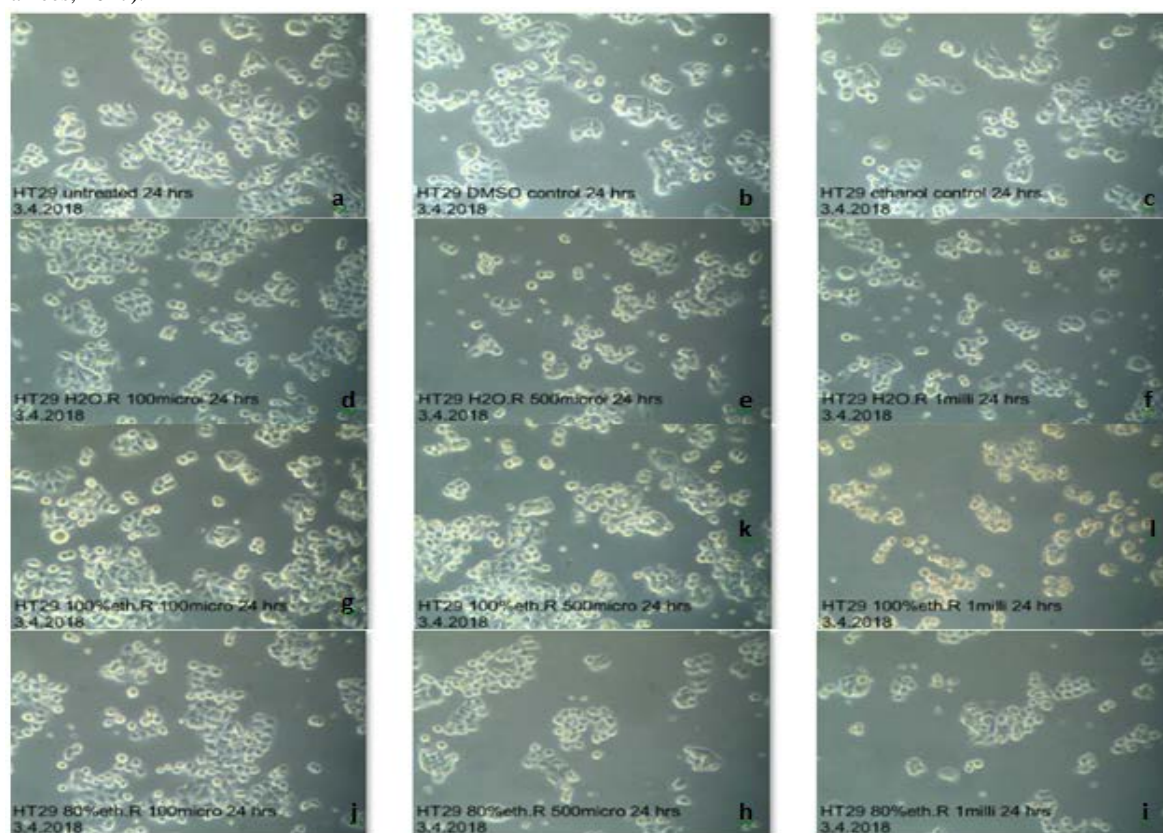


Figure 4. Anticancer activity of radish sprouts extracts against HT29 colon cancer cells. HT29 colon cancer cells cultured were on RPMI media and incubated for 24h at 37 C°. (a) Cells untreated. (b) DMSO control. (c) Ethanol control. (d) water radish extracts 100 µg/ml (e) water radish extract 500 µg/ml. (f) water radish extract 1000 µg/ml. (g) 100% ethanol radish extract 100 µg/ml. (h) 100% ethanol radish extract 500 µg/ml. (i) 100% ethanol radish extract 1000 µg/ml. (j) 80% ethanol radish extract 100 µg/ml. (k) 80% ethanol radish extract 500 µg/ml. (l) 80% ethanol radish extract 1000 µg/ml.

When anticancer activity of radish sprouts extracts was tested against MCF7 cells, it showed the presence of dead and floating cells at high extracts concentrations. After 24h of MCF7 cancer cells incubation and treatment with radish sprouts extracts, extracts in water resulted in a change in cell morphology, and lowering cell density with presence of floating cells at a concentration of 300 µg/ml. At 500 µg/ml, the effect was more drastic as most cells were round and floating. Yet, there was no effect for the extract at low concentrations of 50 µg/ml and 100 µg/ml (Fig 5). Radish extracts in 100% ethanol also showed no effect at

especially when extracted with water.

50 µg/ml, but there were very few floating cells at 100 µg/ml. At 300 µg/ml, there were more floating cells. At 500 µg/ml, most cells were floating and cells density became less, and less cells numbers were present as a result of cells death (Fig 6). The effect of 80% ethanol radish extracts was less than that of 100% ethanol at 300 µg/ml and 500 µg/ml, and no effect was observed at 100 µg/ml and 50 µg/ml (Fig 7). Radish sprouts possess a strong anticancer activity against MCF7 breast cancer cells.

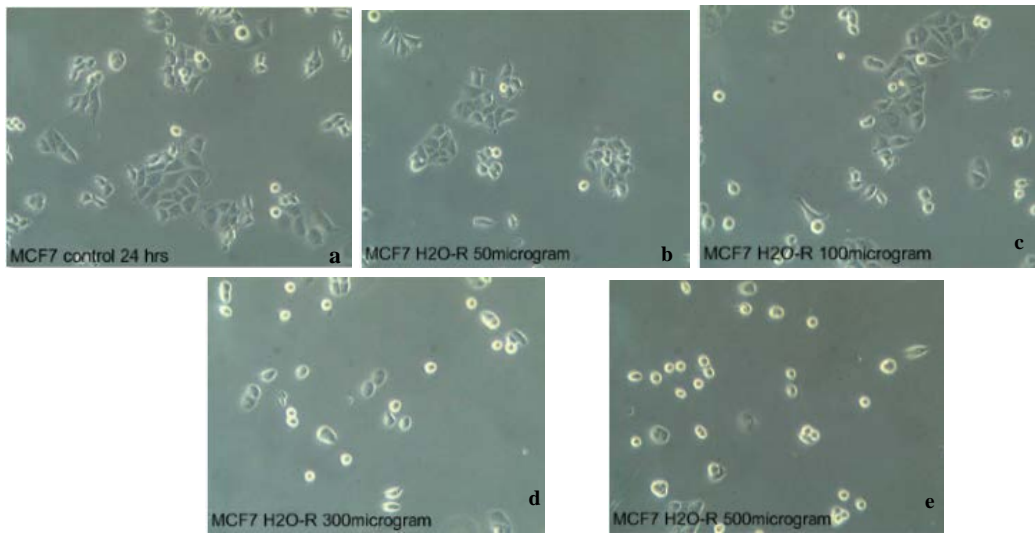


Figure 5. Anticancer activity of radish sprouts water extracts against MCF7 breast cancer cells after 24h of incubation. MCF7 breast cancer cells were cultured on RPMI media and incubated for 24h at 37 C°. (a) control. (b) water radish extracts 50 µg/ml. (c) water radish extract 100 µg/ml. (d) water radish extract 300 µg/ml. (e) water radish extract 500 µg/ml.

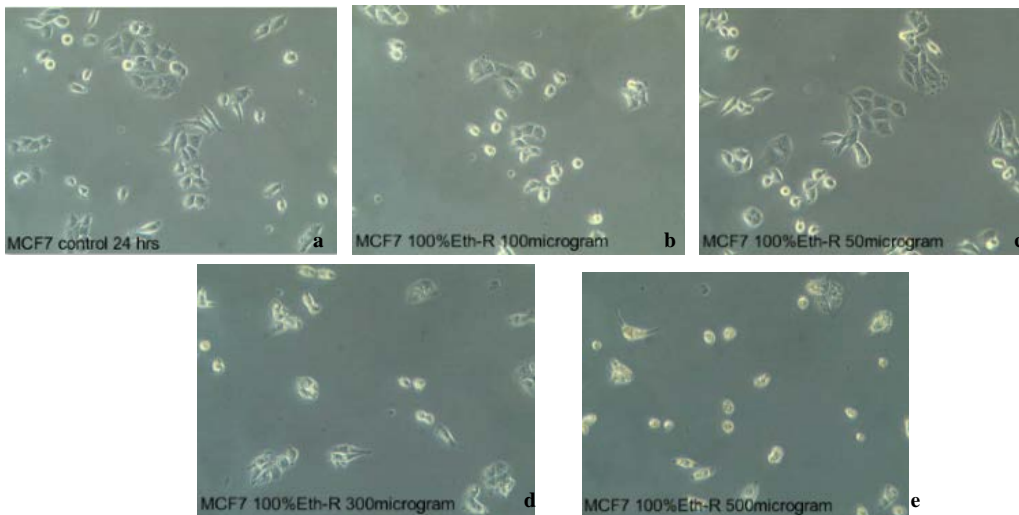


Figure 6. Anticancer activity of radish sprouts absolute ethanol extracts against MCF7 breast cancer cells after 24h of incubation. MCF7 breast cancer cells were cultured on RPMI media and incubated for 24h at 37 C°. (a) control. (b) 100% ethanol radish extract 50 µg/ml. (c) 100% ethanol radish extract 100 µg/ml. (d) 100% ethanol radish extract 300 µg/ml. (e) 100% ethanol radish extract 500 µg/ml.

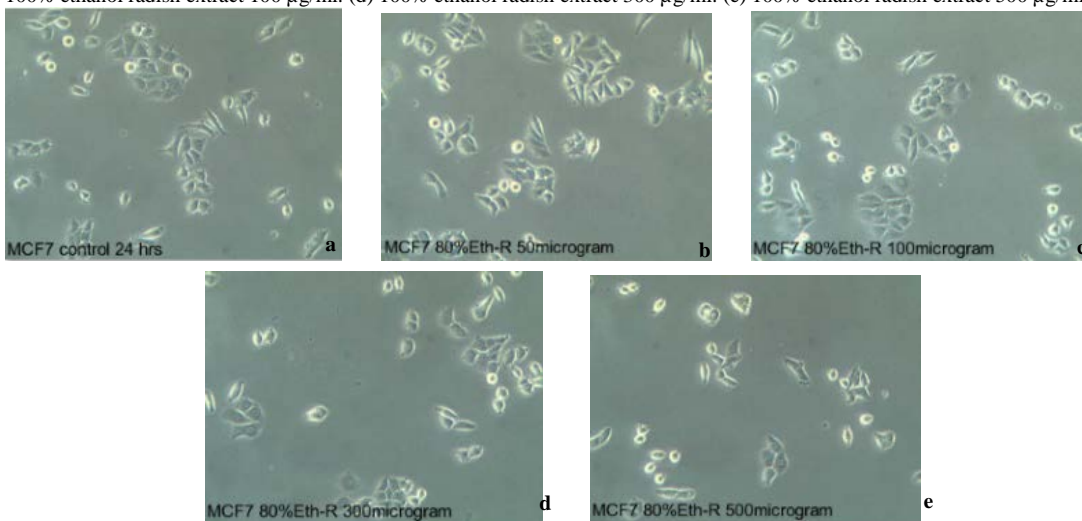


Figure 7. Anticancer activity of radish sprouts 80% ethanol extracts against MCF7 breast cancer cells after 24h of incubation. MCF7 breast cancer cells were cultured on RPMI media and incubated for 24h at 37 C°. (a) control. (b) 80% ethanol radish extract 50 µg/ml. (c) 80% ethanol radish extract 100 µg/ml. (d) 80% ethanol radish extract 300 µg/ml. (e) 80% ethanol radish extract 500 µg/ml.

In order to further examine anticancer activity of radish sprouts extracts, MCF 7 cells were incubated for 48h after treatment with the extracts. Upon doing that, stronger

effect of the extracts was spotted. Water extracts still showed no effect at 50 µg/ml, but few floated cells were observed at 100 µg/ml. A much stronger effect was

observed at 300 $\mu\text{g/ml}$, and 500 $\mu\text{g/ml}$ where cell count was noticeably lower than control, and existing cells were round and floating, and cell density was less, which indicates cell death (Fig 8). Cells treated with 100% ethanol showed no effect at 50 $\mu\text{g/ml}$ and 100 $\mu\text{g/ml}$; however, at concentrations of 300 $\mu\text{g/ml}$ and 500 $\mu\text{g/ml}$, radish sprouts extracts displayed the severest effect of all extracts, where most cells were dead (Fig 9), and cell death percentage was approximately 62% (Fig 11). 80% ethanol extracts also showed no effect at 50 $\mu\text{g/ml}$ and 100 $\mu\text{g/ml}$. There was a slight effect at 300 $\mu\text{g/ml}$ and 500 $\mu\text{g/ml}$ and a presence of few floating and few dead cells (Fig 10). Radish sprouts extracted with ethanol have a strong anticancer potential for breast cancer as they resulted in the death of more than half of MCF7 cells cultured on the plate.

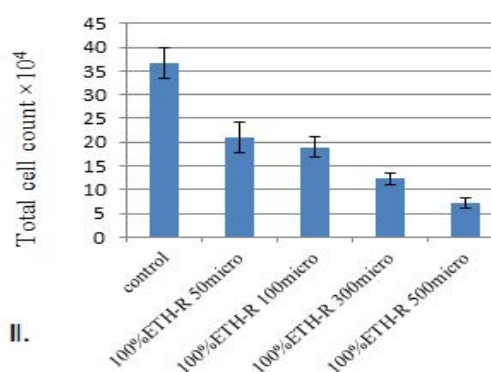
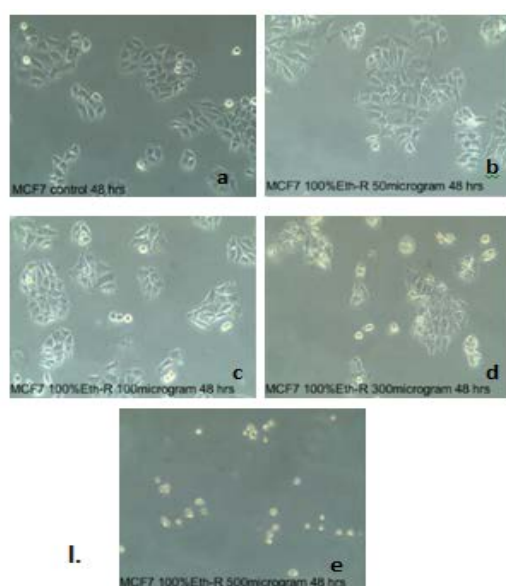


Figure 8. Anticancer activity of radish sprouts water extracts against MCF7 breast cancer cells after 48h of incubation. I. MCF7 breast cancer cells were cultured on RPMI media and incubated for 48h at 37 C° after extracts treatment. (a) control. (b) water radish extract 50 $\mu\text{g/ml}$. (c) water radish extract 100 $\mu\text{g/ml}$. (d) water radish extract 300 $\mu\text{g/ml}$. (e) water radish extract 500 $\mu\text{g/ml}$. II. Total cell count after treatment with water radish sprouts extracts for 48h.

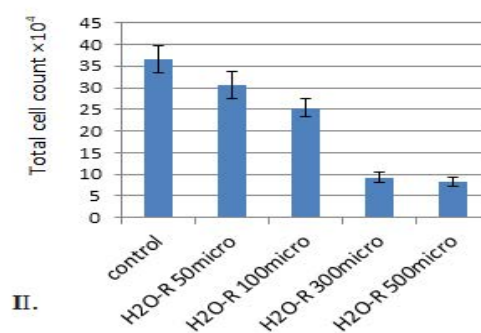
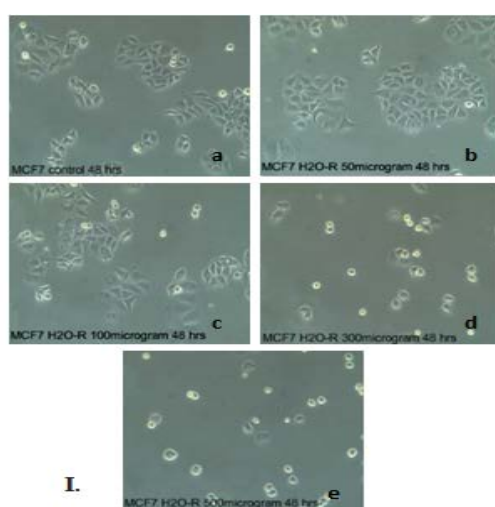


Figure 9. Anticancer activity of absolute ethanol extracts against MCF7 breast cancer cells after 48h of incubation. I. MCF7 breast cancer cells were cultured on RPMI media and incubated for 48h at 37 C° after extracts treatment. (a) control. (b) 100% ethanol radish extract 50 $\mu\text{g/ml}$. (c) 100% ethanol radish extract 100 $\mu\text{g/ml}$. (d) 100% ethanol radish extract 300 $\mu\text{g/ml}$. (e) 100% ethanol radish extract 500 $\mu\text{g/ml}$. II. Total cell count after treatment with 100% ethanol radish sprouts extracts for 48h.

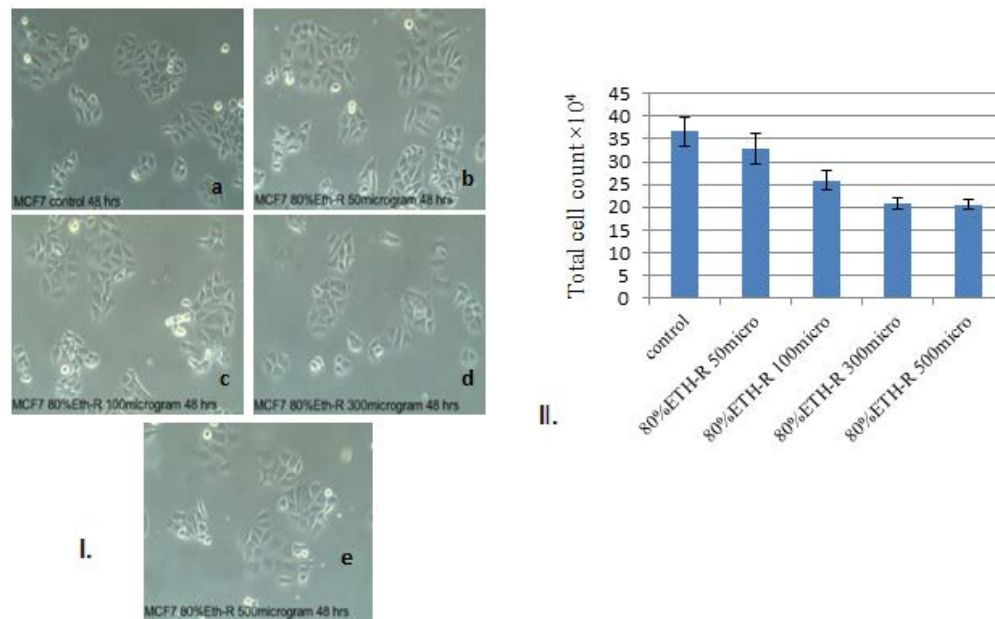


Figure 10. Anticancer activity of radish sprouts 80% ethanol extracts against MCF7 breast cancer cells after 48h of incubation. I. MCF7 breast cancer cells were cultured on RPMI media and incubated for 48h at 37 C° after extracts treatment. (a) control. (b) 80% ethanol radish extract 50 µg/ml. (c) 80% ethanol radish extract 100 µg/ml. (d) 80% ethanol radish extract 300 µg/ml. (e) 80% ethanol radish extract 500 µg/ml. II. Total cell count after treatment with 80% ethanol radish sprouts extracts for 48h.

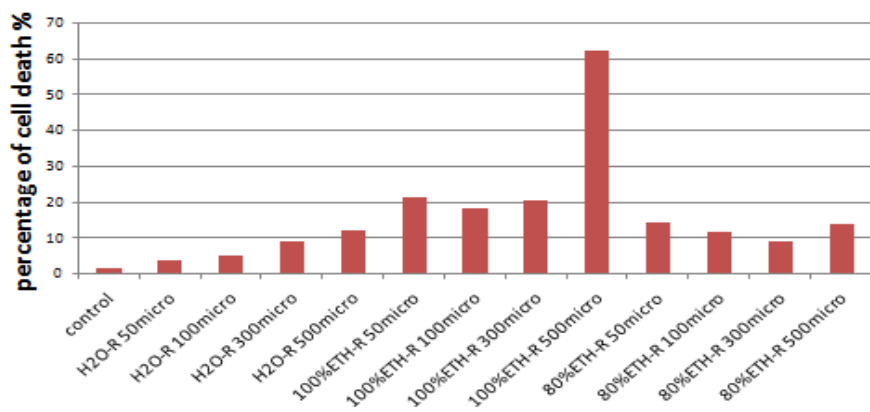


Figure 11. Percentage of MCF7 dead cells after 48h of being treated with different concentrations of radish sprouts extracts of water, 100% ethanol, and 80% ethanol.

4. Conclusion

Radish sprouts have anticancer activity against MCF7 breast- and of HT29 colon-cancer cell lines, especially when extracted with ethanol. Radish sprouts extracts exhibited stronger anticancer activity against MCF7 breast cancer cells than that of HT29 colon cancer cells. Ethanol extracts showed the fiercest effect against MCF7 cells, as 62% of cells were found dead after 48h of incubation. Radish sprouts have negative antibacterial activity against *E. coli*, *S. aureas* and *S. pneumonia*. In conclusion, radish sprouts extracts can be a possible target for developing anticancer drugs, especially for breast cancer.

Conflict of Interest

The authors have no conflicts of interest to declare.

References

- Al-Rimawi F, Abu-Lafi S, Abbadi J, Alamarneh A, Sawahreh R and Odeh I. 2017. Analysis of phenolic and flavonoids and wild of wild Ephedra alata plant extracts by LC/PDA and LC/MS and their antioxidant activity. *Afr J Tradit Compl Altern Med*, **14**:130-141.
- Al-Rimawi F, Alakhras F, Al-Zereini WA, Aldal'in HK, Abu-Lafi S, Al-Mazaideh GM and Ayyal Salman HJ. 2018. HPLC Analysis of chemical composition and their bioactive property of selected Jordanian medicinal plants. *Ori J Chem*, **34**: 2397-2403.
- Al-Zereini WA, Al-Rimawi F, Abu-Lafi S, Alakhras F, Al-Mazaideh GM, Ayyal Salman HJ and Jamhour R. 2018. Identification and antibacterial evaluation of selected Jordanian medicinal plants. *Ori J Chem*, **34**: 1-8.
- Angel A, Raul D, Diego AM. and Cristina G. 2019. Sorting out the Value of Cruciferous Sprouts as Sources of Bioactive Compounds for Nutrition and Health, *Nutrients*, **11**: 429-451.

- Birben E, Sahiner UM, Sackesen C, Erzurum S and Kalayci O. 2012. Oxidative stress and antioxidant defense. *World Allergy Organ J*, **5(1)**: 9-19.
- Jeries J, Ahmad Y, Salwa R, Amira R and Hassan AH. 2016. Identification of a New Antibacterial Sulfur Compound from *Raphanus sativus* Seeds. *Evidence-Based Compl Alter Med*, **2016**: 1-7.
- Kennedy DO and Emma LW. 2011. Herbal extracts and phytochemicals: plant secondary metabolites and the enhancement of human brain function. *Adv Nut*, **2(1)**: 32-50.
- Khamees A. 2017. Phytochemical and Pharmacological Analysis for Seeds of Two Varieties of Iraqi *Raphanus sativus*. *Inter J Pharm Sci Rev Res*, **43**: 237-242.
- Paško P, Krośniak M, Prochownik E, Tyszka-Czochara M, Folta M, Francik R, Sikora J, Malinowski M and Zagrodzki P. 2018. Effect of broccoli sprouts on thyroid function, haematological, biochemical, and immunological parameters in rats with thyroid imbalance. *Biomed Pharmacotherapy*, **97**: 82-90.
- Pham-Huy LA, He H and Pham-Huy C. 2008. Free radicals, antioxidants in disease and health. *Int J Biomed Sci*, **4(2)**:89-96.
- Shaik S, Singh N and Nicholas A. 2011. Comparison of the selected secondary metabolite content present in the cancer-bush *Lessertia (Sutherlandia) frutescens* L. Extracts. *Afri J Trad Compl Alter Med*, **8(4)**: 429-34.
- Tang D, Dong Y, Ren H, Li L and He C. 2014. A review of phytochemistry, metabolite changes, and medicinal uses of the common food mung bean and its sprouts (*Vigna radiata*). *Chem Cent J*, **8(1)**:4.
- Tiwari R and Rana C. 2015. Plant secondary metabolites: a review. *Inter J Eng Res Gen Sci*, **3(5)**: 661-670.
- Vichaya EG, Gabriel SC, Karen K, Tamara EL, Annemieke K, Robert D, Cobi JH and Adam KW. 2015. Mechanisms of chemotherapy-induced behavioral toxicities. *Front Neurosci*, **9**:131-147.
- Zaman SB, Hussain MA, Nye R, Mehta V, Mamun KT and Hossain N. 2017. A Review on Antibiotic Resistance: Alarm Bells are Ringing. *Cureus*, **9(6)**: e1403-1411.

Jordan Journal of Biological Sciences

An International Peer – Reviewed Research Journal

Published by the Deanship of Scientific Research, The Hashemite University, Zarqa, Jordan



Name: الاسم:

Specialty: التخصص:

Address: العنوان:

P.O. Box: صندوق البريد:

City & Postal Code: المدينة: الرمز البريدي:

Country: الدولة:

Phone: رقم الهاتف:

Fax No.: رقم الفاكس:

E-mail: البريد الإلكتروني:

Method of payment: طريقة الدفع:

Amount Enclosed: المبلغ المرفق:

Signature: التوقيع:

Cheque should be paid to Deanship of Research and Graduate Studies – The Hashemite University.

I would like to subscribe to the Journal

For

- One year
 Two years
 Three years

One Year Subscription Rates

	Inside Jordan	Outside Jordan
Individuals	JD10	\$70
Students	JD5	\$35
Institutions	JD 20	\$90

Correspondence

Subscriptions and sales:

The Hashemite University
P.O. Box 330127-Zarqa 13115 – Jordan
Telephone: 00 962 5 3903333
Fax no. : 0096253903349
E. mail: jjbs@hu.edu.jo

المجلة الأردنية للعلوم الحياتية
Jordan Journal of Biological Sciences (JJBS)

<http://jjbs.hu.edu.jo>

المجلة الأردنية للعلوم الحياتية: مجلة علمية عالمية محكمة ومفهرسة ومصنفة، تصدر عن الجامعة الهاشمية وبدعم من صندوق دعم البحث العلمي والإبتكار – وزارة التعليم العالي والبحث العلمي.

هيئة التحرير

رئيس التحرير

الأستاذ الدكتورة منار فايز عتوم
الجامعة الهاشمية، الزرقاء، الأردن

الأعضاء:

الاستاذ الدكتور زهير سامي عمرو
جامعة العلوم و التكنولوجيا الأردنية
الاستاذ الدكتور عبدالرحيم أحمد الحنيطي
الجامعة الأردنية

الأستاذ الدكتور جميل نمر اللحام
جامعة اليرموك
الأستاذ الدكتورة حنان عيسى ملكاوي
جامعة اليرموك

الاستاذ الدكتور خالد محمد خليفات
جامعة مؤتة

فريق الدعم:

المحرر اللغوي

الدكتور شادي نعامنة

تنفيذ وإخراج

م. مهند عقده

ترسل البحوث الى العنوان التالي:

رئيس تحرير المجلة الأردنية للعلوم الحياتية
الجامعة الهاشمية

ص.ب , 330127 , الزرقاء, 13115 , الأردن

هاتف: 0096253903333

E-mail: jjbs@hu.edu.jo, Website: www.jjbs.hu.edu.jo



المملكة الأردنية الهاشمية



المجلة الأردنية



للعلوم الحياتية

مجلة علمية عالمية محكمة

تصدر بدعم من صندوق دعم البحث العلمي و الابتكار



<http://jjbs.hu.edu.jo/>